

**Matrix Isolation Study of magnetically bistable
Diphenylmethane- and Fluorene-based
Carbenes**

Dissertation

To obtain the degree of
Doctor of natural science (Dr. rer. nat.)

by

Tobias Thomanek

from Hattingen

RUHR
UNIVERSITÄT
BOCHUM

RUB

Bochum 2020

Dedicated to my family and my friends

This work was carried out from November 2016 to May 2020 at the Faculty of Chemistry and Biochemistry, Chair of Organic Chemistry II, of the Ruhr-Universität Bochum under the supervision of Prof. Dr. Wolfram Sander. Part of the work reported in this thesis was performed in collaboration with Dr. Enrique Méndez Vega (Ruhr-Universität Bochum).

First Referee: Prof. Dr. W. Sander

Second Referee: Prof. Dr. S. Huber

Third Referee: Prof. Dr. F. Schulz

Day of submission: 04.05.2020

Publications

I. Trosien, E. Mendez-Vega, **T. Thomanek**, W. Sander, Conformational Spin Switching and Spin-Selective Hydrogenation of a Magnetically Bistable Carbene, *Angew. Chem. Int. Ed.*, **2019**, *58*, 14855-14859.

M. Maehara, I. Trosien, A. H. Raut, **T. Thomanek**, W. Sander, Reactions of Fluorenylidenes with Ammonia (in preparation).

T. Thomanek, W. Sander, The Magnetically Bistable [4-(Dimethylamino)phenyl]-phenylcarbene (in preparation).

Scientific Meetings

European Symposium on Organic Reactivity (ESOR), 08.-13.09.2019, Dubrovnik, Croatia (Poster).

International Symposium on “Confinement-Controlled Chemistry”, 16.-18.09.2019, Ruhr-Universität Bochum (Poster).

RESOLV (Ruhr Explores Solvation) Autumn Workshop, Area III, 26.11.2019, Ruhr-Universität Bochum

RESOLV (Ruhr Explores Solvation) Autumn Workshop, Area II, 03.12.2019, Ruhr-Universität Bochum

*“The most exciting phrase to hear in science,
the one that heralds new discoveries,
is not ‘Eureka’ but ‘That’s funny...’”*

- Isaac Asimov

Table of contents

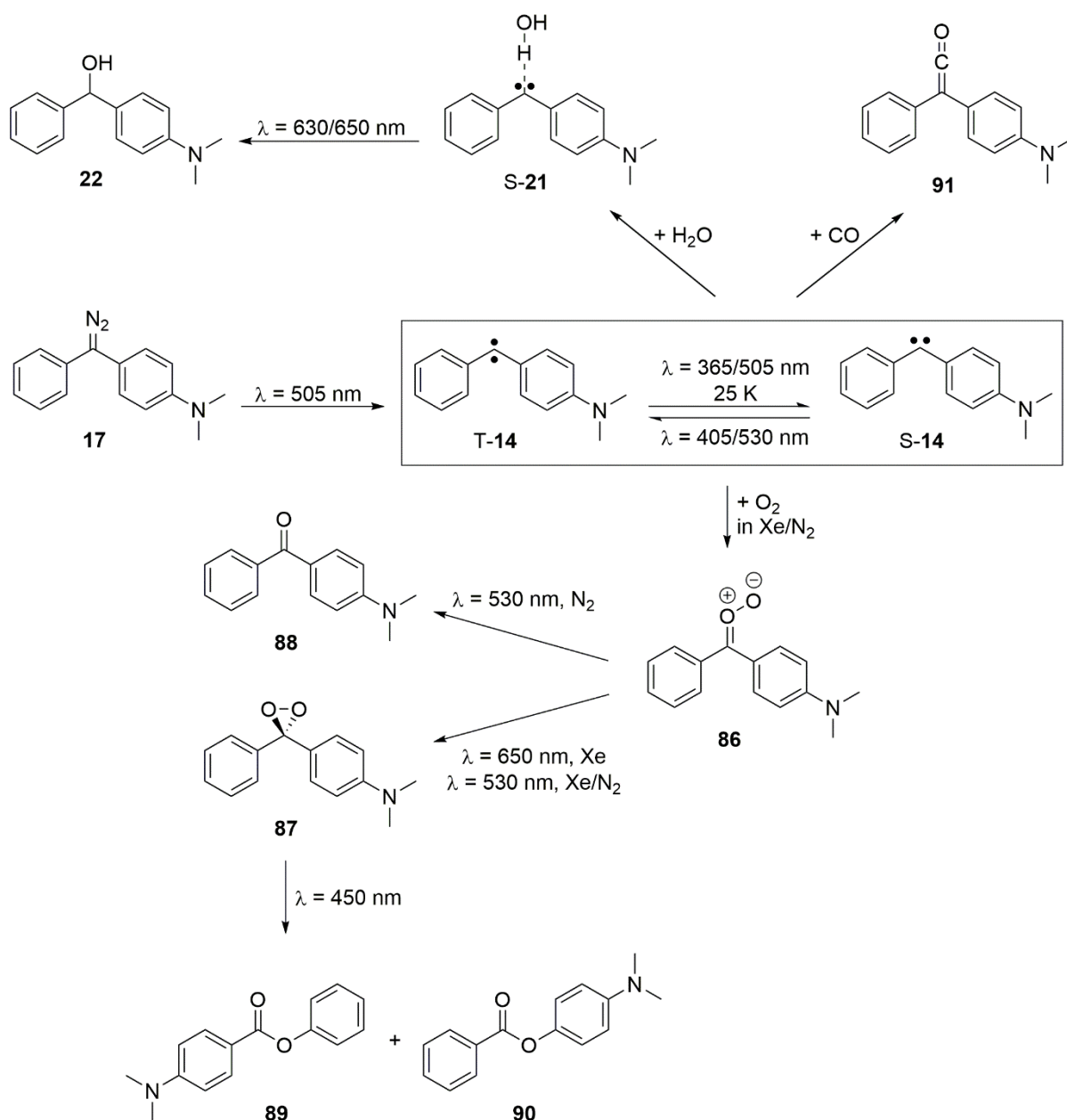
1. Summary	1
2. Introduction	6
2.1. Carbenes	6
2.2. Hydrogen bonds	11
2.3. Matrix isolation	13
2.4. EPR spectroscopy	17
2.5. Computational methods	22
3. Investigation of Diphenylcarbenes	24
3.1. Introduction	24
3.2. [4-(Dimethylamino)phenyl]phenylcarbene	28
3.2.1. Experiments in Ar, Xe and N ₂	28
3.2.2. Reaction with water	41
3.2.3. Computational Results	46
3.2.4. Conclusions	48
3.3. Further potential diphenylcarbenes with magnetic bistability	49
3.3.1. Bis[4-(dimethylamino)phenyl]carbene	49
3.3.2. (4-Aminophenyl)phenylcarbene	50
4. Investigation of Fluorenylidenes	54
4.1. Introduction	54
4.2. 3,6-Dimethoxy-9-fluorenylidene	57
4.2.1. Experiments in Ar and Xe	57
4.2.2. Reaction with water	64
4.2.3. Computational Results	67
4.2.4. Conclusions	71
4.3. 3-Hydroxy-9-fluorenylidene	72
4.3.1. Experiments in Ar, Xe and N ₂	72
4.3.2. Reaction with water	84
4.3.3. Experiments in Ar doped with dimethyl ether (DME)	88
4.3.4. Experiments in Ar doped with trimethyl amine	91
4.3.5. Computational Results	95
4.3.6. Conclusions	101

5. Reactions of Fluorenylidenes with Ammonia	103
5.1. Introduction	103
5.2. Reaction of 3,6-Dimethoxy-9-fluorenylidene with Ammonia	105
5.2.1. Experimental Results	105
5.2.2. Computational Results	111
5.3. Reaction of 3-Hydroxy-9-fluorenylidene with Ammonia	113
5.3.1. Experimental Results	113
5.3.2. Computational Results	120
5.4. Conclusions	123
6. Spin-dependent Reactions of Carbenes	125
6.1. Introduction	125
6.2. Reactions of [4-(Dimethylamino)phenyl]phenylcarbene	129
6.2.1. Experiments in O ₂ -doped Ar, Xe and N ₂	129
6.2.2. Experiments in CO-doped Argon	136
6.3. Reactions of 3-hydroxy-9-fluorenylidene with oxygen	138
6.4. Conclusions	143
7. Experimental part	145
7.1. Materials and methods	145
7.2. Syntheses	148
8. References	162
9. Acknowledgements	170
10. Appendix	172
10.1. IR Frequencies	172
10.2. Optimized geometries	208

1. Summary

In this work, the investigation of several diphenylcarbene and fluorenylidene species was conducted to obtain information about possible magnetic bistability. Furthermore, the reactivity of these carbenes towards different reagents was tested. For this investigation, the matrix isolation technique and IR, UV/Vis and EPR spectroscopy were applied. The experimental results were supported by quantum chemical calculations.

[4-(Dimethylamino)phenyl]phenylcarbene (**14**) was obtained in an argon, xenon and nitrogen matrix at 3 K after photolysis of its diazo precursor **17**. Since it formed as a mixture of its singlet state S-**14** and triplet state T-**14**, it is verified that this carbene is magnetically bistable. This is in agreement with DFT calculations at the B3LYP/def2-TZVP level of theory that predict a small singlet triplet energy gap (ΔE_{ST}) of 1.5 kcal/mol. Irradiation with 530 nm and 405 nm light resulted in a partial conversion from S-**14** to T-**14**, while 505 nm and 365 nm irradiation as well as annealing to 25 K (Ar) or 50 K (Xe) reversed this process. In a nitrogen matrix, the photochemical or thermal conversion from T-**14** to S-**14** was not observed. In addition to the experiments in pure noble gas matrices, the reactivity of **14** towards H₂O, O₂ and CO was tested to investigate the spin-specificity of these reactions. Experiments in a water-doped argon matrix showed the formation of singlet carbene-water complex S-**21** from both S-**14** and T-**14**, where T-**14** presumably converted to S-**14** first before interacting with water. Calculations (B3LYP/def2-TZVP) show that the singlet complex S-**21** is lower in energy than triplet complex T-**21** by 4.4 kcal/mol, which is in accordance with the experimental observation. The complex S-**21** was stable at 3 K but rearranged to the corresponding alcohol **22** when irradiated with 650 nm and 630 nm light. The reaction of **14** with oxygen proceeded by generating carbonyl oxide **86** when O₂ interacted with the carbene center. Since both S-**14** and T-**14** underwent this reaction, it is verified that this process is not spin-specific. In addition to that, this reaction was observed in an O₂-doped xenon and nitrogen matrix, but hardly any reaction was detected in an argon matrix. Irradiation of the photolabile carbonyl oxide **86** with light of 650 nm or 530 nm in a xenon matrix yielded the corresponding dioxirane **87**. In nitrogen, 530 nm irradiation led to dioxirane **87** and to small amounts of ketone **88**. Subsequently, irradiation with 450 nm light converted **87** to the ester compounds **89** and **90**. Experiments of carbene **14** in a CO-doped argon matrix verified that both S-**14** and T-**14** react partially to ketene **91** when annealed to 25 K. Thus, this reaction is not spin-specific.

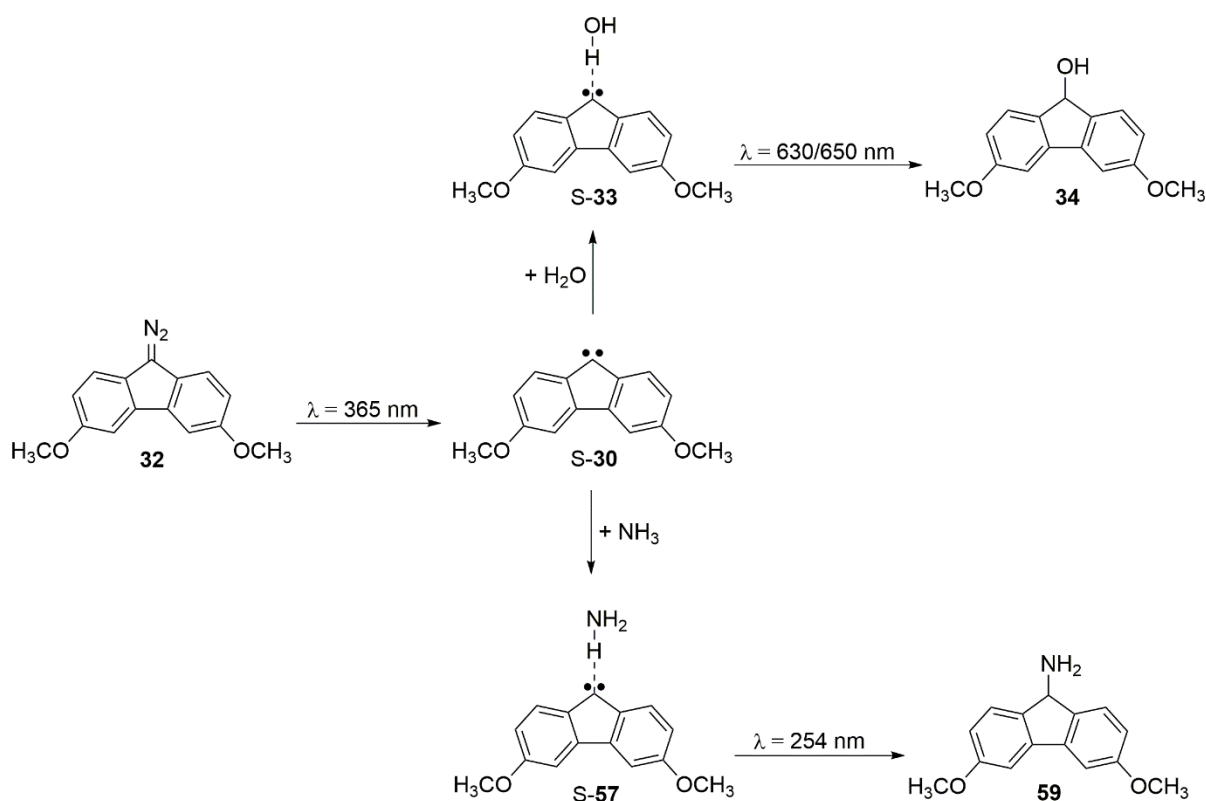


Scheme 1.1: Reactivity of the magnetically bistable carbene **14** with H_2O , CO and O_2 .

Apart from **14**, it was attempted to generate the two diphenylcarbene-based compounds bis[4-(dimethylamino)phenyl]carbene (**15**) and (4-aminophenyl)phenylcarbene (**16**) in an argon matrix. However, the matrix isolation of **15** was not successful and **16** was only formed as traces containing several impurities.

The second major project of this work was the investigation of 3,6-dimethoxy-9-fluorenylidene (**30**). This carbene was generated only in its singlet ground state as a conformer mixture in an argon and xenon matrix at 3 K from its diazo precursor **32**. Hence, magnetical bistability was excluded. DFT calculations at the B3LYP/def2-TZVP level of theory deliver a singlet-triplet energy gap of $-0.7 - 1.0 \text{ kcal/mol}$ (depending on the conformer). Interactions of **30** with water

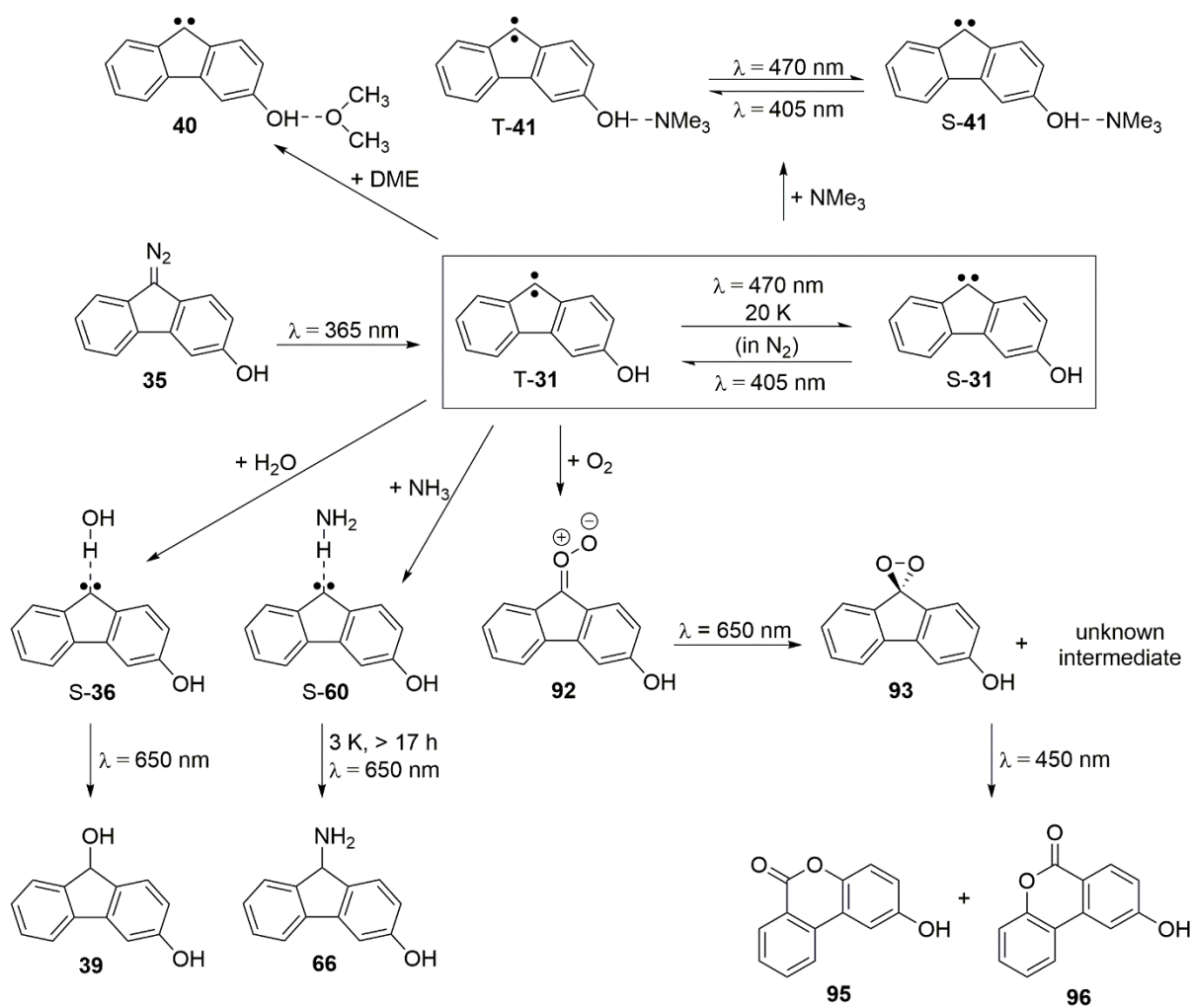
resulted in the formation of the corresponding singlet carbene-water complex **S-33**. DFT calculations (B3LYP/def2-TZVP) show that interactions of **30** with water further stabilize the singlet state, resulting in a singlet-triplet energy gap of $-6.0 - -7.9$ kcal/mol (depending on the conformer). This complex was stable at 3 K but rapidly converted to alcohol **34** when irradiated with 650 nm or 630 nm light. The reaction of **30** with ammonia demonstrated a similar behavior like the reaction with water by forming singlet carbene-ammonia complex **S-57** that was stable at 3 K. The rearrangement to the corresponding amine **59** was initiated by irradiation with 254 nm light. Via calculations at the B3LYP/def2-TZVP level of theory, a singlet-triplet gap of $-2.1 - -4.0$ kcal/mol (depending on the conformer) was calculated for the ammonia complex.



Scheme 1.2: Reactivity of singlet carbene **S-30** with H_2O and NH_3 .

As a second magnetically bistable carbene, 3-hydroxy-9-fluorenylidene (**31**) was generated by photolysis of diazo precursor **35** in argon, xenon and nitrogen matrices at 3 K as a mixture of its singlet state **S-31** and triplet state **T-31** and as a conformer mixture. In a nitrogen matrix, irradiation with 405 nm light resulted in a partial conversion from **S-31** to **T-31** while the reverse effect was observed after irradiation with 470 nm light or annealing from 3 K to 20 K. In argon or xenon matrices, singlet-triplet conversion was hardly occurring. These results were supported by DFT calculation at the B3LYP/def2-TZVP level of theory that yield a low singlet-triplet energy gap of $2.2 - 2.5$ kcal/mol (depending on the conformer) for carbene **31**. Coupled cluster calculations at the CCSD(T)/cc-PVDZ//B3LYP-D3/def2-TZVP level of theory deliver

an energy gap (for the favored conformer) of $\Delta E_{ST} = 0.7$ kcal/mol. Since DFT calculations also predict that the interaction of the hydroxy group of **31** with Lewis bases lowers the singlet-triplet gap, experiments in argon matrices doped with dimethyl ether or trimethyl amine were conducted to test the influence on the magnetic bistability. While no changes of the magnetically bistable behavior were observed after formation of ether complex **40**, trimethyl amine complex **41** exhibited distinct singlet-triplet conversion when irradiated with 405 nm and 470 nm light, which was not the case for carbene **31** in a pure argon matrix. Further investigations included the determination of the reactivity and spin-specificity of **31** with H₂O, NH₃ and O₂. Experiments in a water-doped argon matrix demonstrated that both S-**31** and T-**31** interacted with water to form the hydrogen bonded singlet complex S-**36**. DFT calculations (B3LYP/def2-TZVP) support this result by depicting that singlet complex S-**36** is 4.4 kcal/mol lower in energy than the corresponding triplet complex. Similar to triplet [4-(dimethylamino)phenyl]phenylcarbene (T-**14**), it is presumed that T-**31** first switches its spin state to singlet before forming complex S-**36**. The complex was stable at 3 K but converted to alcohol **39** when irradiated with light of 650 nm. The reaction of **31** with ammonia in an argon matrix resulted in the formation of singlet carbene-ammonia complex S-**60** from both S-**31** and T-**31**. DFT calculations (B3LYP/def2-TZVP) predict a singlet-triplet gap of -0.9 kcal/mol for complex **60** that proves that the singlet complex is lower in energy. This complex was metastable and slowly converted to the corresponding amine **66** in a timescale of more than 17 h at 3 K. Irradiation with 650 nm also resulted in the formation of **66**. Experiments in an argon matrix doped with oxygen indicated that both S-**31** and T-**31** reacted to carbonyl oxide **92** as the oxidation product. Thus, it is verified that this reaction is not spin-specific. Irradiation with 650 nm light resulted in the formation of dioxirane **94** and another intermediate with a strong IR signal at 1720 cm^{-1} that was not identified yet. The corresponding lactone compounds **95** and **96** were formed after irradiation with 450 nm. In summary, the experiments with H₂O, NH₃ and O₂ verified that the reaction of carbene **31** with these reagents was not spin-selective.



Scheme 1.3: Interaction behavior of the magnetically bistable carbene **31** with the Lewis bases DME and NMe_3 and reaction pathways with the reagents H_2O , NH_3 and O_2 .

2. Introduction

The content of several parts of the chapters 2.1, 2.3, 2.4 and 2.5 was adapted from chapter 2 of my master thesis.^[1]

2.1. Carbenes

In physical organic chemistry, the study of molecular properties, reactivities and the investigation of the process of chemical reactions are pivotal aspects for the understanding of reaction mechanisms.^[2] Past research showed that, rather than the reactants and products of a chemical reaction, the nature and the formation of reactive intermediates play important roles in the analysis of the key steps of chemical reaction mechanisms.^[3-4] In this context, the term “intermediate” is defined as a molecular structure with a notably longer lifetime than a molecular vibration, which forms from the reactant of a chemical reaction and is eventually converted to the reaction product.^[5] Several types of reactive intermediates were reported in literature, including carbenes, radicals, carbocations, carbanions, which have a high significance in synthetic chemistry.^[6-10] They take part in several types of reactions, including addition and rearrangement reactions.^[11-12] However, the use of these intermediates is limited due to their rather low stability which prevents the isolation under normal conditions. For instance, the lifetime of the benzophenone ketyl radical is only 2 ns in cyclohexane, and the lifetime of α -methylbenzylidenecarbene in acetonitrile is around 13.3 ps.^[13-14] Among these reactive intermediates, especially carbenes have various applications in the field of synthetic chemistry.^[15-16] One particular type of application is the use of *N*-heterocyclic carbenes as ligands for palladium catalysts in Heck-type coupling reactions.^[17]

The first carbene concept was reported by Nef in 1904.^[10] Based on the fact that the carbon atom in compounds like carbon monoxide or isonitriles is not tetravalent like in common organic compounds, he was speculating that there are other carbon-containing substances with an untypical valence at the carbon atom. In this connection, he described carbenes as compounds with an unsaturated, bivalent carbon atom. The IUPAC defines carbenes in a similar manner and depicts them as a species with a bivalent, electrically neutral carbon atom with two non-bonding electrons and the general structure $R_2C:$.^[5] An important aspect is the electron occupation of the orbitals of the carbene carbon center, given that this determines if the carbene is present in its singlet or triplet state (Figure 2.1).^[18]

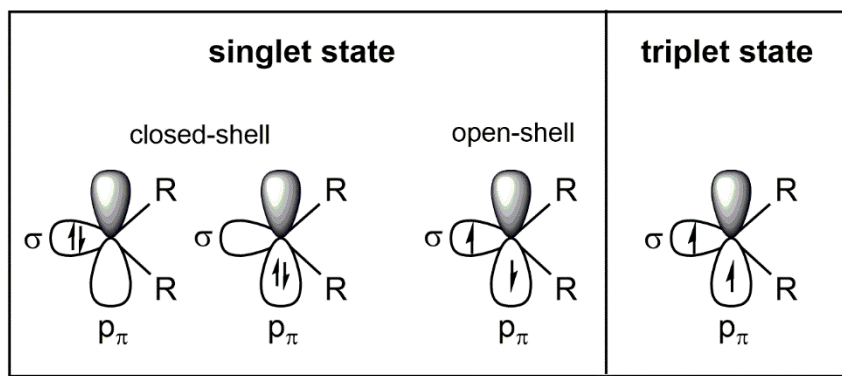


Figure 2.1: Possible electron configurations of singlet and triplet carbenes. While the triplet carbene can only exhibit one configuration, one open-shell and two-closed shell configurations are possible for the singlet carbene.^[19-21]

Since the geometry of the carbene influences the nature of its orbitals, it has a large effect on the orbitals electron occupation. In a linear carbene, the carbene center is sp -hybridized and two degenerate, non-bonding p -orbitals are present.^[19, 22] In such a case, the triplet state where both p -orbitals are occupied by one electron is the state with the highest spin multiplicity and most favored (as stated in Hund's rule).^[23] If the molecule is not linear but bent, the p -orbitals are not degenerate anymore and the carbene center gets an sp^2 -like hybridization. Compared to the remaining p -orbital (also: p_π), the corresponding σ -orbital is stabilized by additional s -character and is lower in energy. Therefore, both electrons being positioned in the σ -orbital is the favored electronic configuration, resulting in a singlet state.

However, the geometry of most carbenes differs in reality from the ideal linear triplet geometry or the ideal sp^2 -hybridized singlet geometry. Most triplet carbenes have bond angles between 130° and 150° , and most singlet carbenes have angles in the range of $100 - 110^\circ$.^[24] One example for such a carbene with neither a linear nor an ideal sp^2 -geometry is methylene as the simplest carbene. In several previous investigations of this carbene via electron paramagnetic resonance (EPR) spectroscopy (a spectroscopic method used to investigate substances with unpaired electrons), it was determined that the bond angle of methylene is $134 - 138^\circ$.^[25-28] This bond angle is closer to the typical 120° angle of sp^2 -hybridization than to a linear geometry, so that normally a singlet state would be expected for methylene. However, it was proven that this carbene is a triplet carbene with a singlet-triplet energy gap (ΔE_{S-T}) of 9 kcal/mol.^[29] This observation shows that the triplet state can also occur if the carbene center is not sp -hybridized and there are not two degenerate p -orbitals present. The crucial factor is the energy difference between the two orbitals σ and p_π .^[19] Hoffmann stated that a very low energy difference of less

than 1.5 eV is necessary to form the triplet ground state. On the other hand, the singlet ground state will occur if the σ - p_π energy gap is higher than 2 eV.^[30-31]

This energy difference as well as the singlet-triplet energy gap ΔE_{S-T} and therefore the spin ground state of the carbene are depending on multiple factors, i.e. steric and electronic effects. As mentioned before, an increased s -character stabilizes the σ -orbital while the p_π -orbital remains relatively unchanged, resulting in a singlet state (Figure 2.2). Then again, an increased p -character stabilizes both the σ - and the p_π -orbital so that they are close in energy, resulting in a triplet state.^[32]

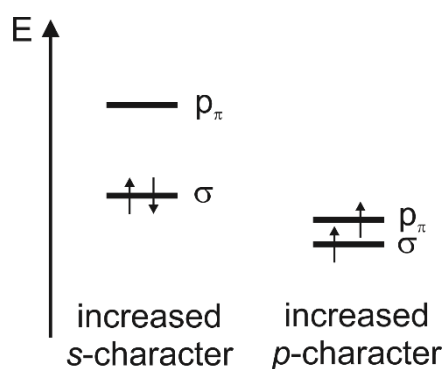


Figure 2.2: Orbital occupation of a carbene with higher s -character (singlet state) and with higher p -character (triplet state).^[21, 32]

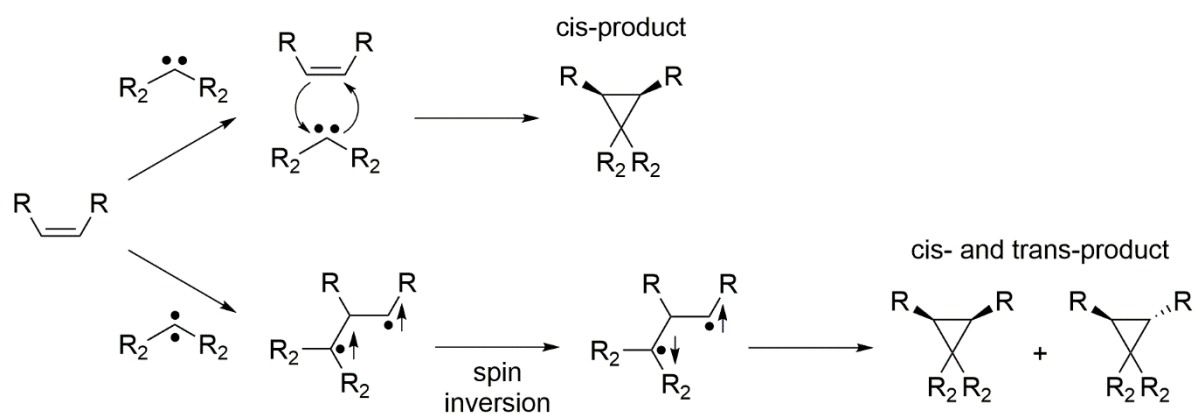
The first factor that has an influence on the carbene ground state are the steric properties of the substituents. While bulky substituents stabilize carbenes kinetically, increased steric demands lead to an increased bond angle. The resulting decrease of s -character of the σ -orbital favors the triplet ground state.^[19, 32] The second factor are the electronic properties of the substituents next to the carbene center. If substituents with a higher electronegativity than carbon are bound to the carbene center, this leads to an electron-withdrawing effect towards the substituent. Because the ionization potential of p -orbitals is lower than for s orbitals, the p -character of the non-bonding σ -orbital decreases while its s -character increases.^[33] This results in a favored singlet state. Contrary, substituents with a lower electronegativity show the inverted effect and favor the triplet state.^[32] Harrison studied this behavior and investigated the ground state of multiple carbenes with different substituents. By showing that a carbene with electronegative fluorine substituents has a singlet ground state while electropositive lithium substituents lead to the triplet state, he confirmed the aspects mentioned before.^[34-35] Another important factor that influences the carbene ground state are hyperconjugation and mesomeric effects. If the carbene has substituents with free electron pairs like $-OR$, $-NR_2$ or halogens, these electron pairs can donate π -electron density towards the carbene center.^[19, 32] This effect results in an

increased energy of the p_{π} -orbital due to interactions with the lone pairs, while the σ -orbital remains relatively unchanged. The increased σ - p_{π} gap leads to a favored singlet state.

In summary, it was shown that the singlet ground state is favored if the carbene center has electronegative substituents, substituents with free electron pairs and/or low steric demands. The triplet ground state is favored if the carbene has bulky and/or electropositive substituents. Furthermore, it has been shown by EPR spectroscopy that most carbenes with aromatic substituents have a triplet ground state.^[21, 36]

The spin ground state of carbenes has a major impact on the reactivity. In general, carbenes can undergo addition reactions to olefins as well as insertion reactions into C–H bonds or similar bonds.^[22] The difference concerning reactivity is that triplet carbenes react in the manner of a diradical, and the reaction mechanism often contains 1,3-diradical intermediates. Singlet carbenes have two paired electrons and an empty p_{π} -orbital, so that they show an electrophilic behavior and react in a similar way like other electrophiles.

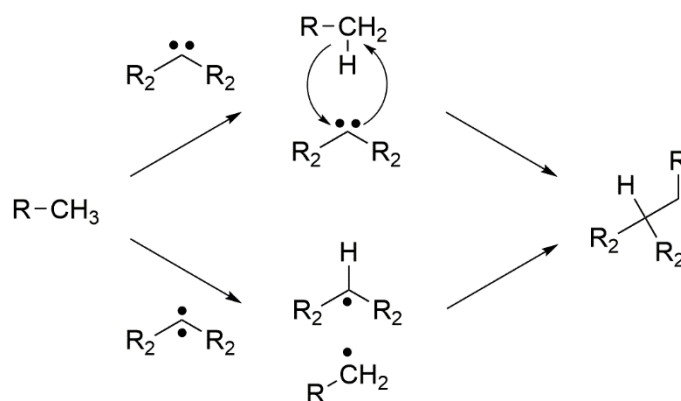
Early attempts to investigate the addition reaction of carbenes with olefins were reported by Skell and Garner.^[37-38] They stated that dihalogencarbenes like dibromocarbene (a singlet carbene) undergo addition reactions via a concerted reaction mechanism, yielding cyclopropane derivatives as the cis-addition product. Similar experiments were conducted several years later by Houk and Singleton.^[39] They tested the reaction behavior of dichlorocarbene with olefins and obtained similar addition products like Skell and Garner, confirming their results. For the addition reaction of triplet carbenes to olefins, a different reaction mechanism that leads to products with different stereochemistry is described.^[22, 24] Due to its diradical character, one of the electrons of the triplet carbene attacks the double bond of the olefin and forms a 1,3-diradical species (Scheme 2.1). The following cyclopropane ring closure by the combination of both radicals can only occur if one of the electrons undergoes spin inversion beforehand.



Scheme 2.1: Mechanistic pathways of singlet (above) and triplet (below) carbenes and their addition reactions with olefins. While a concerted mechanism is described for singlet carbenes, the triplet carbene reacts via a diradical intermediate.^[24]

Because this spin inversion is a rather slow process, the lifetime of this intermediate is long enough to enable C–C bond rotation that results in the changing of the stereochemistry. Thus, the addition product will form as a conformer mixture.^[37-38]

A similar difference in reaction mechanisms of singlet and triplet carbenes is described for insertion reactions into C–H bonds. While singlet carbenes insert into a C–H bond in a concerted manner, triplet carbenes react via a radical intermediate (Scheme 2.2).^[22, 24] However, insertion reactions of this type have only rarely been observed for triplet carbenes.



Scheme 2.2: Insertion reactions of a singlet and triplet carbene into a C–H bond. The singlet carbene (above) is undergoing a concerted reaction mechanism while the triplet carbene (below) forms a radical intermediate that converts to the product.^[22]

An important difference resulting from these two reaction mechanisms is the stereochemistry of the products (similar to the olefin addition reaction). Singlet carbenes react under retention of the stereochemistry. An example was shown by Cane who applied C–H-insertion in a stereoselective way during the synthesis of pentalenolactones.^[40] In the case of triplet carbenes,

it is assumed that the stereochemistry of the product is randomized due to the occurrence of an intermediate state. However, a solid proof for this assumption has not been reported yet. Beside the C–H insertions, there were also examples of O–H insertions reported which occurred after the formation of complexes of a carbene with a hydrogen-bond-donor.^[41]

2.2. Hydrogen bonds

A hydrogen bond is a term that was first mentioned by Rodebush and Latimer while they investigated the interactions between amines or several acids with water.^[42] They described this phenomenon as a weak “bond” or as some kind of ionic complex. Modern definitions of a hydrogen bond depict it as an attractive non-covalent interaction between the hydrogen atom of a group X–H and an electron-rich atom (Y) or molecule (Y–Z).^[43-44] The atom or group X has to be more electronegative than the hydrogen atom so that this group can act as the hydrogen bond donor, while Y or Y–Z acts as a hydrogen bond acceptor. In general, such a kind of interaction can be written as X–H ··· Y–Z, where the dotted line represents the hydrogen bond. The interaction between hydrogen bond donor and acceptor can consist of several different interaction types. The main interactions are electrostatics (acid/base), polarization (hard/soft), van der Waals interactions (dispersion/repulsion) and covalency (charge transfer).^[45]

Hydrogen bonds can be divided into several classes, depending on their bond strength: Strong bonds, moderate bonds and weak bonds.^[46] Additionally, there are very weak interactions that stand on the borderline between a hydrogen bond and a weak van der Waals interaction.^[45] These classes have different properties concerning bond energy, bond length and bond angle. Furthermore, the type of intermolecular force of the hydrogen bond correlates with the strength of the bond. Strong hydrogen bonds tend to have a strongly covalent character that results in a high directionality of the bond. They primarily exhibit almost linear bond angles of 170–180° and have a bond energy between 15–40 kcal/mol.^[46] The formed hydrogen bond with a rather short H ··· Y distance of 1.2–1.5 Å leads to an elongation of the X–H bond by 0.08–0.25 Å. Moderate hydrogen bonds are mainly determined by electrostatic interactions. This leads to only moderate directionality with bond angles larger than 130°, and bond energies of 4–15 kcal/mol. Because of the lower bond energy, the H ··· Y distance is longer (2.5–3.2 Å) which results in a smaller X–H bond elongation of 0.02–0.08 Å.^[46] For weak hydrogen bonds, the main interaction forces are dispersion and electrostatic forces. Due to the low bond energies

of less than 4 kcal/mol, they only express a weak directionality and bond angles of more than 90° . With a H- -Y bond length of more than 3.2 Å, the hydrogen bond distance is even longer than for moderate bonds, and the elongation of the X-H bond is even shorter (< 0.02 Å).^[46] The strength of the bonds as well as the symmetry can further be explained by diagrams that show the relation between the distance of the heteroatoms X- -Y in a hydrogen bond and the resulting energy (Figure 2.3).

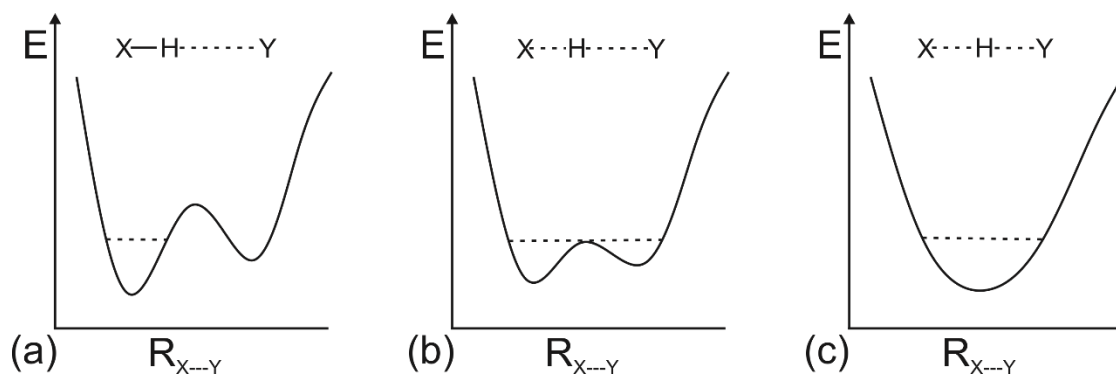


Figure 2.3: Potential energy diagrams of different hydrogen bonds as a function of the distance between the atoms X and Y. (a) Energy diagram of a weak hydrogen bond. The energy barrier is too high and broad to allow atom H to be separated from atom X, resulting in a covalent X-H bond. (b) Diagram of a strong hydrogen bond. The energy barrier is much lower compared to a weak bond, so that atom H can be placed at this barrier (or slightly above it). (c) Diagram of a very strong hydrogen bond. Because of the absence of an energy barrier, atom H is equally bound to both atom X and atom Y.^[47]

For all hydrogen bonds, it has to be noted that stronger hydrogen bonds lead to larger redshifts of the X-H bond in the infrared spectrum due to its elongation.^[44, 48]

Several examples have been reported for hydrogen bonds of different strengths. In the field of strong hydrogen bonds, Del Bene conducted numerous computational calculations on hydrogen-bonded complexes consisting of small molecules like H_2O , NH_4^+ and OH^- to obtain the bonding energies.^[49] Some of these complexes, like the strongly hydrogen-bonded complex $HOH\cdots OH^-$, had symmetrical structures with a hydrogen atom being “trapped” between two identical small groups. In addition to that, organic molecules have been reported that “trap” hydrogen atoms in a similar manner and form very strong hydrogen bonds (Chart 2.1, I).^[47, 50] Strong or moderate bonds typically include bonds between alcohol or amino groups as the hydrogen bond donor and ketones or other alcohol groups as the hydrogen bond acceptor.^[45] Jeffrey and Takagi presented examples of these bonds by showing different hydrogen bonds in crystals of methyl α -glucopyranoside (II) (Chart 2.1).^[51]

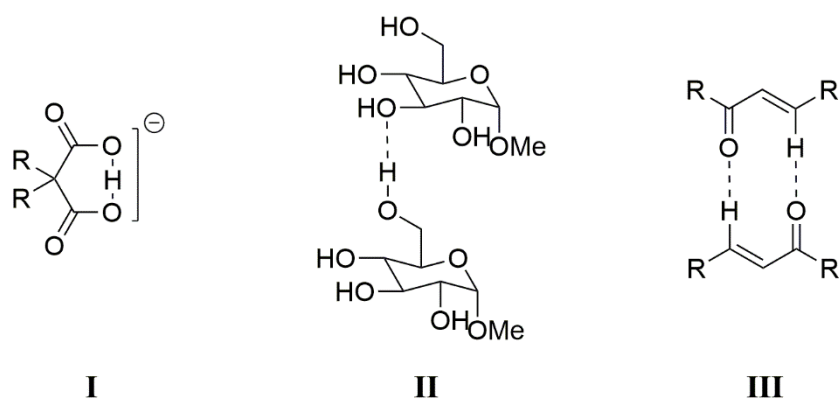


Chart 2.1: Examples for hydrogen-bonded complexes of different bond strengths. (I) Very strong hydrogen bond. (II) Strong/moderate hydrogen bond. (III) Weak hydrogen bonds.^[47, 50-52]

Concerning weak hydrogen bonds, several articles have been reported by Desiraju.^[45, 52] Typical hydrogen bond donors in weak hydrogen bonds are C–H groups at an sp^2 -hybridized center. They can form bonds with ketones or alcohol groups (e.g. in complex III).

Among the examples mentioned in Chart 2.1, the complexes II and III are from the field of crystal engineering, which is one of the topics of supramolecular chemistry. In supramolecular chemistry, hydrogen-bonded self-assembly systems and the cooperativity of hydrogen bonds plays a major role.^[48] Further applications of hydrogen bonds can be found in the biochemical field, since they occur in peptides and majorly influence the structure of biologic macromolecules like proteins.^[53]

2.3. Matrix isolation

The nature and reactivity of reaction intermediates is an important aspect for the research of chemical reactions.^[3] However, intermediates like carbenes, radicals, carbenium ions and nitrenes cannot be investigated under normal conditions because of their short lifetime preventing the successful isolation.^[54] There are two methods reported which enable the investigation of short-living compounds. The first method is ultrafast time-resolved spectroscopy, which is fast enough to detect transient species, e.g. carbenes, before they decompose.^[55] The other method deals with the isolation of single molecules of the intermediate in a frozen medium at cryogenic temperatures, and is called “matrix isolation”. The main advantage of this method is that it stabilizes the reactive intermediates and extends the lifetime to a timescale in which ordinary spectroscopic methods can be used.^[54] The matrix

isolation technique can be conducted by either trapping the sample in frozen organic solutions (organic glass) at 77 K or frozen gas cages at even lower temperatures.^[54, 56] However, the disadvantages of organic glasses are that they are more reactive than gas matrices of e.g. noble gases, and that they often absorb light in wide regions of the infrared range as well as parts of the UV range, which is inconvenient for spectroscopic investigations.^[56]

The first attempts of matrix isolation in a gas matrix were presented by Pimentel, Dows and Whittle in 1954.^[57] They performed experiments in which they tried to trap sample compounds like NH_3 , HN_3 , NO_2 or NH_4N_3 in frozen gas matrices of CCl_4 , CO_2 , xenon or methylcyclohexane at 66-115 K to test the effectivity of different matrix cages concerning the prevention of reactions. Surprisingly, Norman and Porter developed the method to isolate reactive compounds in organic glass at around the same time in 1954.^[58] In the following research, Pimentel and Becker attempted matrix isolation experiments with inert gases, namely nitrogen, argon and xenon, as the matrix materials.^[59] Using the sample compounds NO_2 , HBr , HCN , HN_3 , NH_3 and H_2O , they again investigated the ability of the matrix materials to prevent reactions. In the same article, they also described the matrix isolation technique in more detail and mentioned necessary properties that the used matrix materials need to include:

Because the main purpose of the matrix isolation is the prevention of reactions, the first necessary property of the matrix has to be its inertness. In general, the use of noble gases is ideal for this purpose.^[59] Depending on the sample compound, also other matrix materials like hydrocarbons or nitrogen with a “relative” inertness can be used. However, hydrocarbon matrices would be more preferable for the inhibition of hydrogen bonding but less useful in the presence of radicals, considering that they can react with all kinds of radicals. Also for nitrogen matrices, reactivity towards radicals is expected. Another important property of the matrix is its rigidity. For a successful matrix isolation, it is necessary to immobilize the trapped sample molecules so that diffusion through the matrix is inhibited. This way, intermolecular interactions and reaction are prevented.^[59] Additionally, it has to be taken into account that the structure of the matrix must be suitable for the sample to fit either into the lattice or into holes in the matrix. The combination of the matrix rigidity (and the resulting steric restraints) and the cryogenic temperatures forms an ideal environment for preventing intermolecular reactions. The third important property necessary for matrix isolation experiments is the volatility of the matrix material.^[59] The matrix material and the sample compound are mixed in the gas phase prior to the deposition and freezing on a cold spectroscopic window (more about this procedure is explained later in this chapter). This will only work sufficiently if the vapor pressure of the matrix substance is high at room temperature so that it can be handled as a gas in the matrix

apparatus. On the other hand, the vapor pressure of this substance has to be low at cryogenic temperatures. Because matrix isolation experiments are conducted under high vacuum, a low vapor pressure of the solid matrix is necessary to prevent matrix evaporation during the experiment. However, the matrix materials have temperature ranges in which the matrix is solid and stable. If the temperature will surpass the upper limit of this temperature range, the matrix will evaporate. For inert gases like xenon, argon and nitrogen, the reported temperature limits are 70 K, 35 K and 30 K, respectively.^[59] The next property of the matrix material that is especially important for spectroscopic analysis is its transparency. This means that it is crucial that the matrix does not have any absorptions in the spectral regions that are investigated during the matrix experiments. Additionally, it is necessary that the matrix does not scatter too much light. Therefore, the matrix must form a glassy structure instead of a crystalline one.

As mentioned before, the successful matrix isolation is achieved if a small amount of the gaseous sample compound is mixed with an excess of the matrix gas and subsequently co-deposited on a spectroscopic window at cryogenic temperatures. Using this method, it is ensured that single sample molecules are isolated.^[60] If the sample compound is solid or liquid, it is necessary to sublime the compound to get it into the gas phase. This is achieved either by connecting the sample to the high vacuum of the apparatus at room temperature, or by additional external heating under vacuum. The vacuum in the apparatus is not only convenient for the easier sublimation of the sample, but is also necessary to enable the generation of cryogenic temperatures by preventing temperature exchange of the cold spectroscopic window with surrounding atmosphere. Furthermore, surrounding gases or moisture would also be isolated as impurities in the matrix cage and interfere with the spectroscopic investigation.^[60] If the aim of the matrix isolation experiment is the investigation of reactive intermediates instead of stable compounds, there are three different methods on how to proceed (depending on the intermediate).^[56] The first method is the external generation of intermediates by pyrolysis prior to the isolation, the second method is the co-condensation of a precursor compound with a reagent that will undergo the reaction to the corresponding reactive intermediate. The third method is the *in situ* generation of reactive intermediates. For this method, the precursor substance is deposited in the matrix first, and subsequently the intermediate is generated by photolysis with light of different wavelengths. This method has the advantage that it is usually the easiest method to isolate intermediates. It can be used for the isolation of carbenes and nitrenes, which precursor synthesis is generally known in literature.^[61-63] The matrix isolation technique is also used to investigate interactions and reactions between sample compounds and smaller interacting molecules like H₂O, NH₃ or

oxygen.^[64-65] For this purpose, the matrix gas has to be doped with a small amount of this interacting compound and co-deposition with the sample compound must be conducted (in the same manner as mentioned before). Due to the rigidity of the matrix at low temperatures of around 10 K, diffusion of the isolated compounds through the matrix cannot occur. If the matrix is annealed to higher temperatures, the matrix gradually becomes softer and allows the diffusion of smaller molecules (Figure 2.4).^[64] This enables the interaction of smaller molecules with the sample compounds.

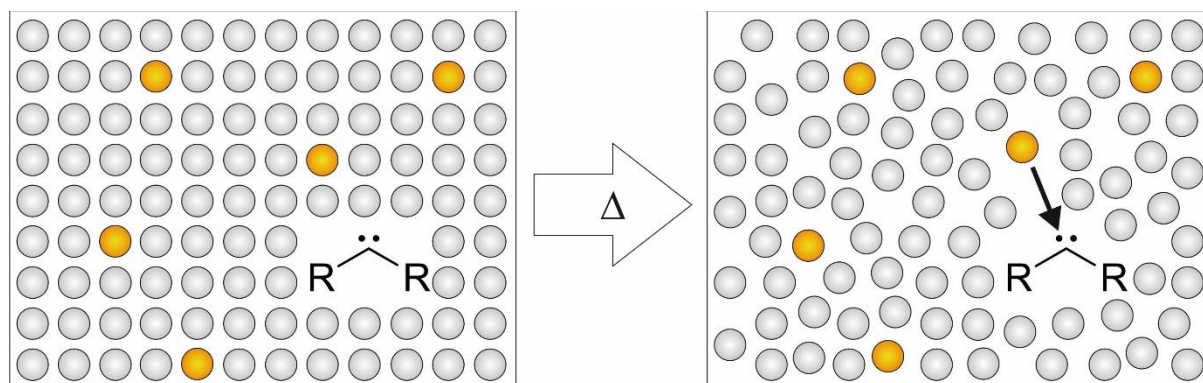


Figure 2.4: Matrix isolation of a carbene in a matrix doped with small amounts of a small molecule (orange circles). Annealing of the matrix to elevated temperatures results in the softening of the matrix (right), which allows diffusion of smaller molecules. The molecules can now interact with the isolated carbene.^[54]

The technical set-up of a matrix isolation apparatus is build up by multiple important elements. The matrix deposition occurs on a spectroscopic window that is made of cesium iodide (IR) or sapphire (UV/Vis).^[56, 60] This window is cooled to cryogenic temperatures by a closed-cycle helium cryostat. Furthermore, a radiation shield around the window protects it from radiative heat transfer (Figure 2.5). This shield is surrounded by the outer steel vacuum shroud that has several outer windows (cesium iodide or potassium bromide) for either spectroscopy or irradiation. The advantage of this shroud is that it is rotatable, so that it is possible to switch between the matrix head orientation suitable for spectroscopy and the one suitable for irradiation. The matrix isolation apparatus also includes a flow controller to control the matrix gas flow during the deposition. An oil diffusion pump connected to the system generates the high vacuum of around 10^{-6} mbar. If necessary, a sublimation or pyrolysis oven can additionally be attached to the matrix head, enabling sublimation of the sample compounds at higher temperatures.^[56, 60] The spectroscopic investigation of the sample compounds is mostly conducted via IR and UV/Vis spectroscopy.^[66] Especially IR spectroscopy is a useful tool for the identification of substances, since the signals of matrix-isolated compounds are very sharp and narrow compared to IR spectra at room temperature. These sharp signals occur because the

rigid environment of the matrix and the cold temperatures largely inhibit rotations of the molecules, leading to strongly simplified spectra.^[56, 60]

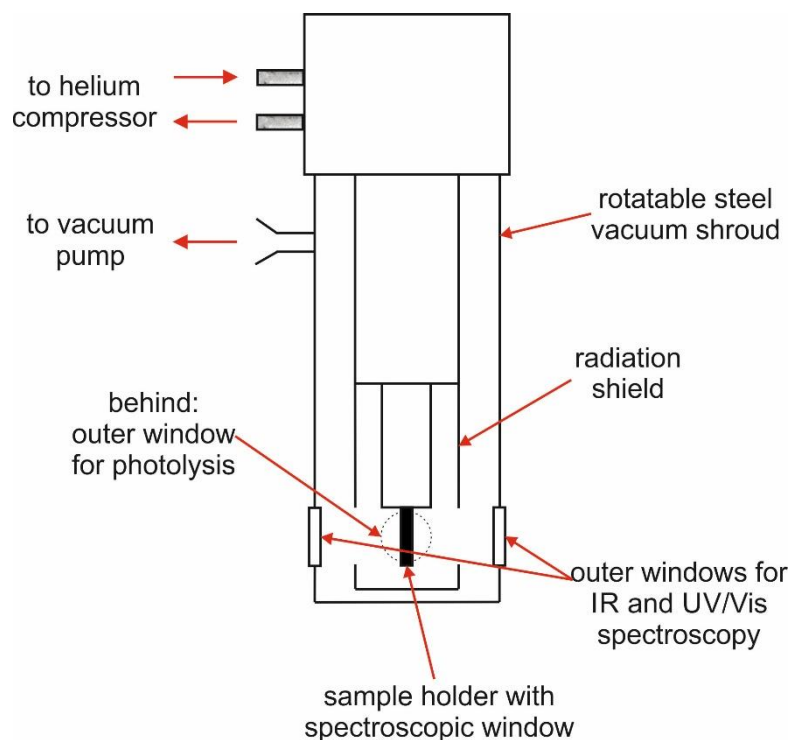


Figure 2.5: Technical set-up of the cold head of a matrix isolation apparatus.^[56, 60]

2.4. EPR spectroscopy

An important spectroscopic method to investigate reactive intermediates that are paramagnetic (they have unpaired electrons and a permanent magnetic moment)^[67] is the electron paramagnetic resonance (EPR) spectroscopy which was first introduced by Zavoisky in 1945.^[68] The main aspect of this method is the interaction of the magnetic moment of electrons with a magnetic field.^[69]

The general principle of EPR spectroscopy is based on the spin of an electron which has a spin quantum number of either $+\frac{1}{2}$ or $-\frac{1}{2}$. Due to the spin of an electron, a magnetic moment is arising that is proportional to the spin and can adopt values of $M_s = \pm\frac{1}{2}$.^[70] While both energy levels are degenerate in the absence of an external magnetic field, an increasing magnetic field results in a linearly increasing energy level separation (Figure 2.6). The reason for this effect, called Zeeman effect,^[71] is the orientation of the electrons spin angular momentum in an external magnetic field. A parallel orientation of the spin angular momentum towards the

magnetic field results in $M_s = +1/2$ (α electron spin state), an antiparallel orientation leads to $M_s = -1/2$ (β electron spin state).^[69]

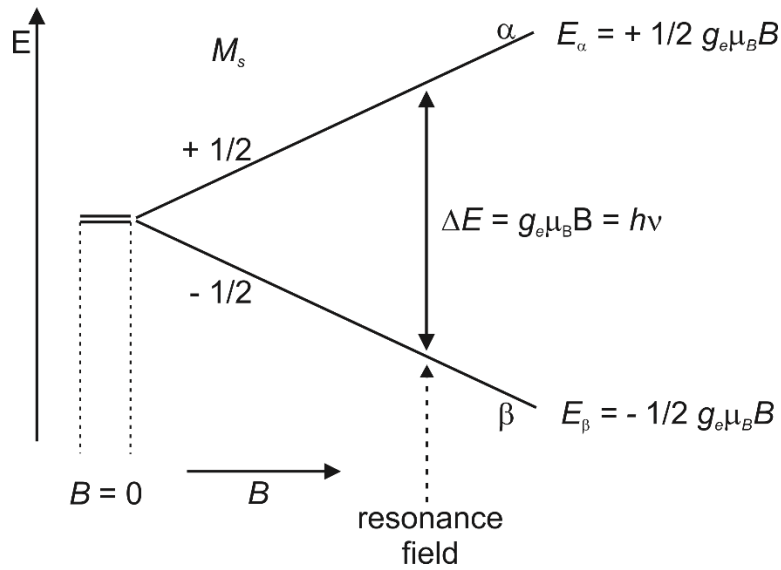


Figure 2.6: Zeeman effect: the two energy levels $M_s = +1/2$ and $M_s = -1/2$ of a single electron are degenerate at an external magnetic field $B = 0$, but an increasing field B linearly increases the energy difference ΔE between both levels. Resonant absorption occurs if the energy of a light source is equal to the energy splitting ΔE at the resonance magnetic field.^[69-70]

The energy E of these energy levels in a magnetic field B is given by the equation

$$E = g_e \mu_B B M_s \quad (2.1)$$

where the factor g_e describes the so-called Landé factor, which is also called the g-factor. The g-factor is a constant for a free electron and describes its magnetic environment, having a value of $g_e = 2.002319$.^[69, 72] The factor μ_B is the Bohr magneton, which is the atomic unit of the magnetic moment.

In an external magnetic field, it is possible to induce a transition between the two spin states α and β by irradiation. However, it has to be noted that transitions only occur if the energy of the electromagnetic irradiation equals the energy difference ΔE between these states.^[70] To apply this effect for EPR spectroscopy, either the wavelength of the irradiation or the magnetic field in the EPR spectrometer must be adjusted to induce transitions. In most EPR spectrometers, a constant radiation energy of 9.5 GHz ($\lambda = 32$ mm) is used while the magnetic field is modulated until the resonance field is reached.

In the case of a single electron, the transition between its two spin states is visible in an EPR spectrum as a single peak (Figure 2.7). However, spectra with higher complexity are observed

if the electron is located at a nucleus having a nuclear spin.^[69-70] Similar to the case of electrons, nuclear spins also develop a permanent magnetic moment. Hence, the electron spins can interact with the nuclear spins, and this spin coupling results in further splitting of the spin states $M_s = +\frac{1}{2}$ and $M_s = -\frac{1}{2}$. This effect is called hyperfine splitting and is independent of an external magnetic field. For nuclei with a nuclear spin of $I = \frac{1}{2}$ (e.g. a proton), each of the energy levels resulting from the Zeeman splitting is split into two separate sub-levels $M_I = +\frac{1}{2}$ and $M_I = -\frac{1}{2}$ (Figure 2.7).

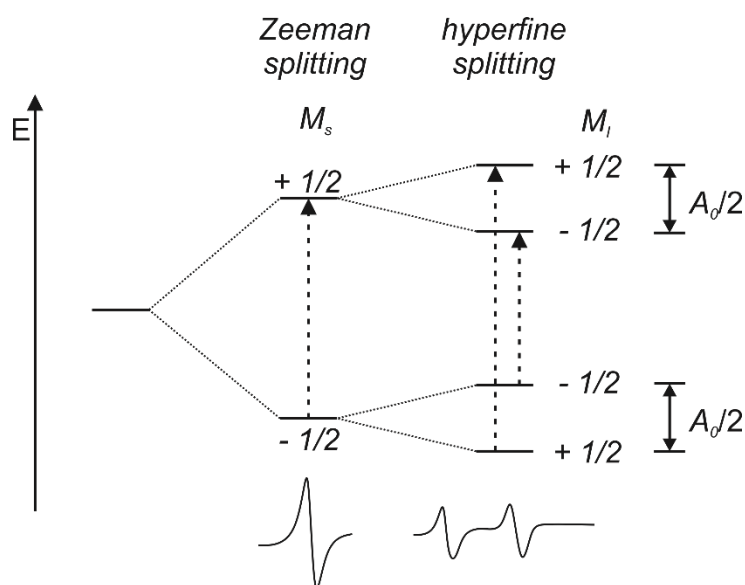


Figure 2.7: Hyperfine splitting of an unpaired electron in the proximity of a nucleus with a spin of $I = \frac{1}{2}$. The energy levels $M_s = +\frac{1}{2}$ and $M_s = -\frac{1}{2}$ deriving from the Zeeman splitting in an external magnetic field are each split into two sublevels due to the interaction of the electron spin with the nuclear spin. The hyperfine splitting leads to two transitions between the energy levels, resulting in two signals in the EPR spectrum. The energy difference between two energy levels with the same electron spin is half of the isotropic hyperfine splitting constant A_0 .^[69-70]

If the nuclear spin is different or the number of nuclei is higher, also the number N of sublevels resulting from the hyperfine splitting changes. This is described by the equation:

$$N = 2I + 1 \quad (2.2)$$

If more than one nucleus is present, the nuclear spins of these nuclei are added. According to equation 2.2, a system with one electron and two nuclei ($I = \frac{1}{2}$) will exhibit three energy sublevels N due to hyperfine splitting.^[70] Concerning the possible transitions, there are selection rules that describe which transitions are allowed. These rules depict that transitions are allowed if the nuclear spin is maintained and the electron spin changes, hence $\Delta M_s = \pm 1$ and $\Delta M_I = 0$. According to these selection rules, the system in Figure 2.7 exhibits two allowed while a system with one electron and two nuclei with $I = \frac{1}{2}$ has three transitions.^[69-70]

In systems with more than one unpaired electron, another type of splitting can be observed.^[73] This splitting is based on the interaction between the magnetic moments of the different electrons that is similar to the interaction between an electron spin and a nuclear spin mentioned before. Due to the independence of an external magnetic field, this phenomenon is called zero-field splitting.^[69, 74] It can be explained by taking a deeper look to the energy states and geometry of such molecules.

In a system with two free electrons like a carbene, the spins of these electrons can be either antiparallel or parallel, resulting in a singlet or triplet state. While only one energy state is present for singlet carbenes with the spin $S = 0$, triplet carbenes with $S = 1$ have three energy states.^[69, 73] Since singlet carbenes do not have unpaired electrons and therefore do not exhibit an EPR spectrum, only the three states of the triplet carbene are important for zero-field splitting. The energetic position of these states is highly dependent on the geometry of the molecule, i.e. the geometry along the magnetic x-, y- and z-axis (Figure 2.8). Therefore, the three energy states can be denoted as T_x , T_y and T_z .^[75]

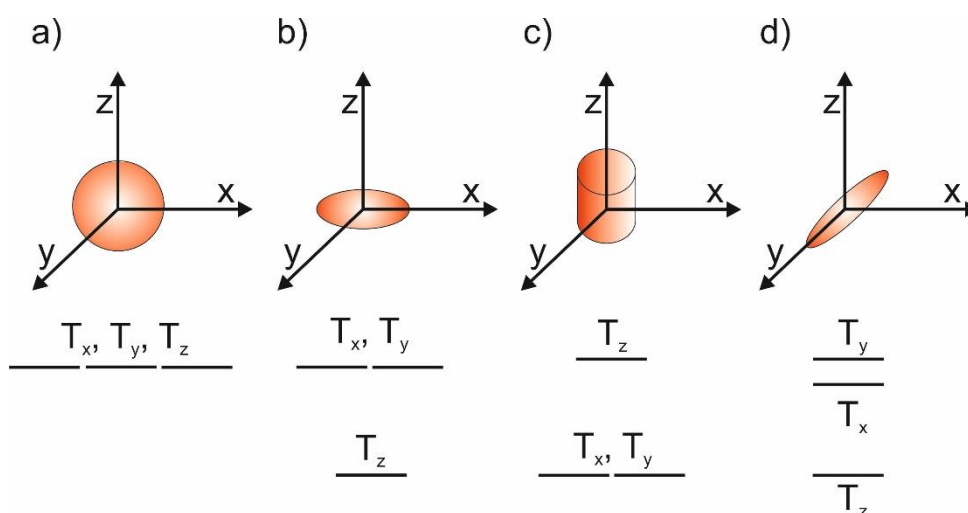


Figure 2.8: Zero-field splitting of triplet state organic molecules with different geometries. (a) Molecules with a spherical geometry have degenerate energy levels T_x , T_y and T_z . (b) A triplet state molecule with a flattened geometry in z-direction, resulting in a T_z state which is lower in energy. (c) A molecule with an elongated geometry in z-direction and an equally shortened geometry in x- and y-direction. The state T_z is higher in energy while both states T_x and T_y are equally lowered. (d) Different symmetry in x-, y- and z-direction results in different energies of all three states.^[75]

Since most of the organic molecules have different geometries in x-, y- and z-direction, the corresponding energy states are mostly not degenerate. To describe the energetic separation between these states in absence of an external magnetic field, the zero-field splitting (zfs) parameters D and E are used.^[74] The parameter D shows the energy gap between the energy

level T_z and the center of the two states T_x and T_y , where T_z is set as the state with the highest distance to the other states (Figure 2.8). Parameter E describes half of the distance between the states T_x and T_y . For a molecule with spherical geometry, these zfs parameters are both zero because all three energy states are degenerate. Molecules with a flattened geometry in z -direction (like excited triphenylene)^[76] have degenerate T_x and T_y states but a lowered T_z state, which results in $D \neq 0$ and $E = 0$. It is important to note that zfs parameters that are both not zero do only occur for systems that have different geometries in x -, y - and z -direction (like e.g. excited triplet naphthalene)^[74, 76] and hence non-degenerate energy levels T_x , T_y and T_z .^[70]

While zero-field splitting is not dependent on an external magnetic field, triplet state organic molecules that underwent this splitting are still influenced by Zeeman splitting if an external magnetic field is applied. The alignment of the axes x , y and z along the external magnetic field influences the extent of the Zeeman splitting. More precisely, the energy level assigned to the axis that is aligned parallel to the magnetic field does not change in energy.^[70, 74, 76]

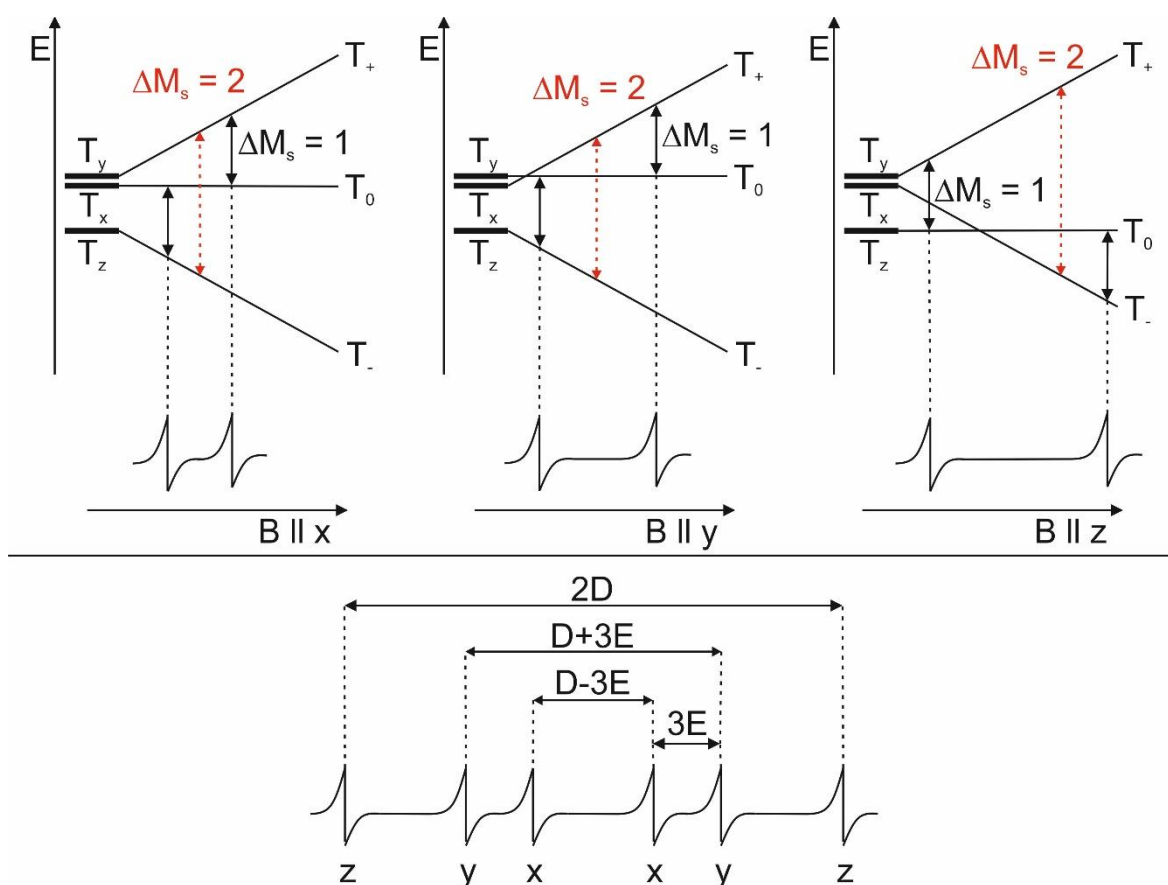


Figure 2.9: Organic triplet molecules that undergo zero-field splitting are additionally influenced by Zeeman splitting in an external magnetic field. The splitting is different if the magnetic field is aligned parallel to the x -axis (left), y -axis (middle) or the z -axis (right). Transitions occur between energy levels with $\Delta M_s = 1$, while transitions with $\Delta M_s = 2$ (red lines) are forbidden. The combination of all three alignments results in the EPR spectrum displayed below.^[70, 73-74, 77]

On the other hand, the energy levels of the other two axes are either stabilized or destabilized, depending on if their spin angular momentum is aligned parallel or antiparallel to the magnetic field (as mentioned in the section about the Zeeman effect). Since the magnetic field can be aligned parallel to all three axes, the Zeeman splitting results in three different configurations of the energy levels (figure 2.9). Based on the selection rules that $\Delta M_s = \pm 1$ transitions are allowed and $\Delta M_s = \pm 2$ transitions are forbidden, the resulting EPR spectrum for compounds of this type will exhibit six signals.^[70]

2.5. Computational methods

In modern research, the support of experimental results via computational methods is steadily increasing. Since computer hardware and software development was improving majorly in recent years, it is not only possible to perform quantum chemical calculations on smaller molecules but also on larger compounds with up to 50–100 atoms.^[78] These calculations deliver e.g. theoretical properties of substances as well as molecular structures.

Computational calculation methods are based on the topic of quantum mechanics, in which the Schrödinger equation

$$H\Psi = E\Psi \quad (2.3)$$

plays an essential role. With this equation, the energy eigenvalues E of a system are obtained by solving the equation.^[78-79] Here, Ψ is the wavefunction of an electron which describes its behavior in an atom or molecule. The operator H is the Hamiltonian that represents the sum of all kinetic and potential energies of a system. An important approximation that is included for solving the Schrödinger equation is the Born-Oppenheimer approximation.^[80] It states that the movement of electrons is considerably faster than the movement of nuclei, so that these nuclei can be assumed to be fixed. Hence, the electronic and nuclear terms in the Schrödinger equation can be separated, enabling the solving of this equation for fixed nuclei while the electronic energy can be calculated for different internuclear distances.^[78, 80]

While exact solutions are only obtainable for simple systems like the particle in a box or the hydrogen atom, more complex systems require the use of computational calculation methods to obtain appropriate results. The simplest ab initio method that can be used for this purpose is the Hartree-Fock self-consistent field (HF-SCF) method.^[81-85] However, this method has the

disadvantage that it neglects any kind of electron correlation, i.e. repulsive interactions between electrons, so that the precision of this calculation method is limited. A more progressive approach was presented by Hohenberg and Kohn in 1964.^[86] They described a theory in which the electronic energy of the ground state is completely determined by the electron density of a molecule, giving rise to the density functional theory (DFT). This theory was improved later by the so-called Kohn-Sham equations that are denoted as “self-consistent equations including exchange and correlation effects”.^[87]

For practical applications, hybrid SCF-DFT functionals are often used.^[78] One important hybrid functional is the B3LYP functional, consisting of the Becke 3-parameter (B3) exchange functional^[88] and the Lee, Yang and Parr (LYP) correlation functional.^[89] The advantage of this method is the high precision of the results while it is only slightly more computationally demanding than the HF-SCF method. For this DFT calculation method (as well as for other calculation methods), several basis sets can be used which contribute a combination of different Gaussian functions to the Schrödinger equation.^[78] A frequently used base set like 6-311++G** which adds d functions and diffuse functions to second row elements (N, O, C etc.) usually delivers sufficient results. The base set def2-TZVP presented by Weigend is even more improved.^[90-91] The abbreviation “def” indicates default basis sets of split valence (SV) and triple zeta valence (TZV) quality that were tested for the chemical elements from hydrogen to astatine. Furthermore, “def2” basis sets are series of newer and more improved basis sets. For def2-TZVP the parameter “P” additionally includes 1p-sets for hydrogen, 1f-sets for d-elements and partially reduced sets for s-elements.^[90-91] In addition to these DFT methods mentioned above, advanced coupled cluster methods are also an important tool in computational chemistry.^[92]

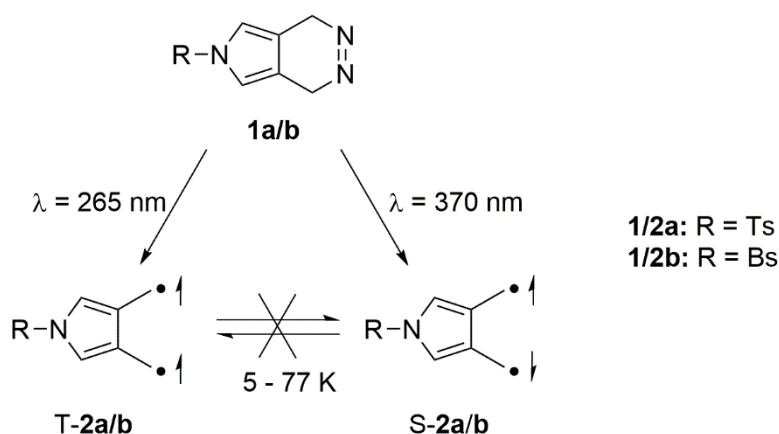
For all quantum chemical calculation methods, a geometry optimization of the molecular geometry has to be conducted beforehand. In this step, the geometry of a molecule is continuously changed until the energy of this molecule is at its minimum.^[78] Based on the optimized geometry, energies and molecular properties like molecular vibrations and IR frequencies (determined by calculating the second derivative of the energy with respect to the force constants) are obtained which can be compared to experimental data.

3. Investigation of Diphenylcarbenes

3.1. Introduction

Paramagnetism and diamagnetism are properties that have been observed for different transition metal complexes, dependent on the nature of the metal and the ligands.^[93] These properties are connected to the spin state of the system, which can either exhibit a high spin or low spin state. Among these complexes, several examples have been reported that are able to undergo spin switching from the high spin to the low spin state or vice versa under different conditions like irradiation, pressure or electric control by applying voltage.^[94-96] It has to be noted that this spin change is often induced by the conformational change of the ligands of the complex.

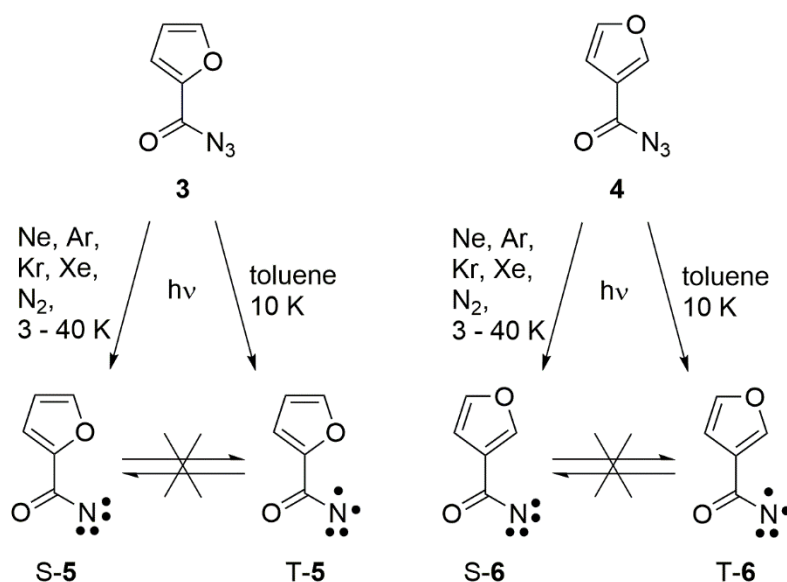
For pure organic molecules without metal atoms, a similar spin isomerism has only rarely been observed. The first examples for an organic compound that can be formed in both the singlet and triplet state was presented by Berson and coworkers.^[97-98] They tried to tune the singlet-triplet energy gap of several 3,4-dimethylpyrrole biradical species by adding different electron-withdrawing substituents to the nitrogen atom in the ring. According to quantum chemical calculations, this should result in singlet-triplet gaps that are close to zero.^[99] For these species, the biradicals **2a/b** are formed from the corresponding dihydropyrrolo[3,4-*d*]pyridazines **1a/b** via photolysis (Scheme 3.1), with the wavelength used for photolysis determining whether the biradical is formed in its singlet or triplet state.



Scheme 3.1: Spin-selective wavelength-dependent formation of the biradicals **2a/b** by photolysis of the respective precursors **1a/b**.^[97-98]

While photolysis with 265 nm light results in an EPR-active triplet biradical, the use of 370 nm light is forming the biradical in its singlet state. An important aspect about these biradicals is

that they do not undergo spin interconversion between the singlet and triplet state (at 5–77 K), compared to the metal complexes mentioned above. Similar examples were presented by Abe and Zheng.^[100] They generated the two acylnitrenes **5** and **6** both in inert gas matrices and in frozen toluene (Scheme 3.2). Compared to the results of Berson, the decisive factor if the nitrenes were produced in their singlet or triplet state is not the photolysis wavelength, but the nature of the matrix material.

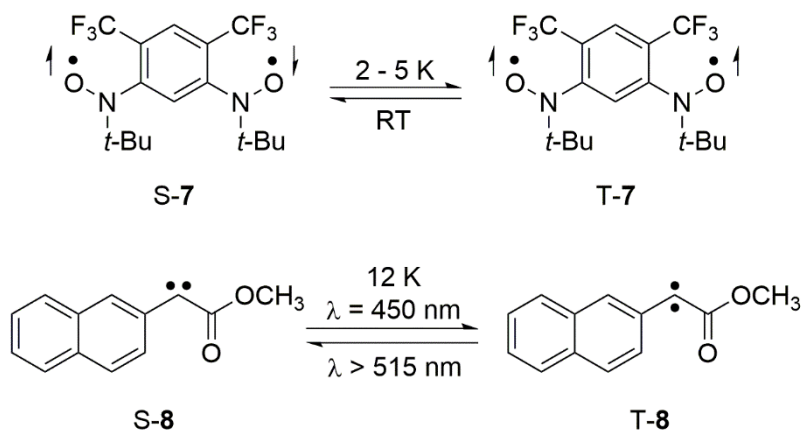


Scheme 3.2: Photolysis of azides **3/4** to form the corresponding nitrenes **5/6**.^[100]

In a matrix of inert gases like Ne, Ar, Kr, Xe or N₂, photolysis of the azide precursors yielded exclusively the singlet nitrenes S-**5** and S-**6**. Contrary, the same experiment in a matrix of frozen toluene at 10 K formed the nitrenes in their triplet states. These nitrenes did not undergo any conversion between the singlet and triplet state via irradiation or annealing to higher temperatures. Instead, irradiation with UV light or visible light led to the Curtius rearrangement to the corresponding furyl isocyanates.

The first magnetically bistable organic molecule in which singlet-triplet conversion was observable was presented by Rajca and coworkers.^[101] They generated the 1,3-phenylene-based bis(aminoxyl) diradical **7** in its singlet state which slowly converted to the triplet state when cooled down to cryogenic temperatures of 5 K or below (Scheme 3.3). A system with similar behavior was reported by Bally and McMahon.^[102] They formed the bistable 2-naphthyl-(carbomethoxy)carbene (**8**) primarily in its triplet state after photolysis which can be converted to its singlet state when irradiated with light of a wavelength greater than 515 nm. At 12 K, the singlet carbene slowly converts back to its triplet state, which can also be induced by irradiation

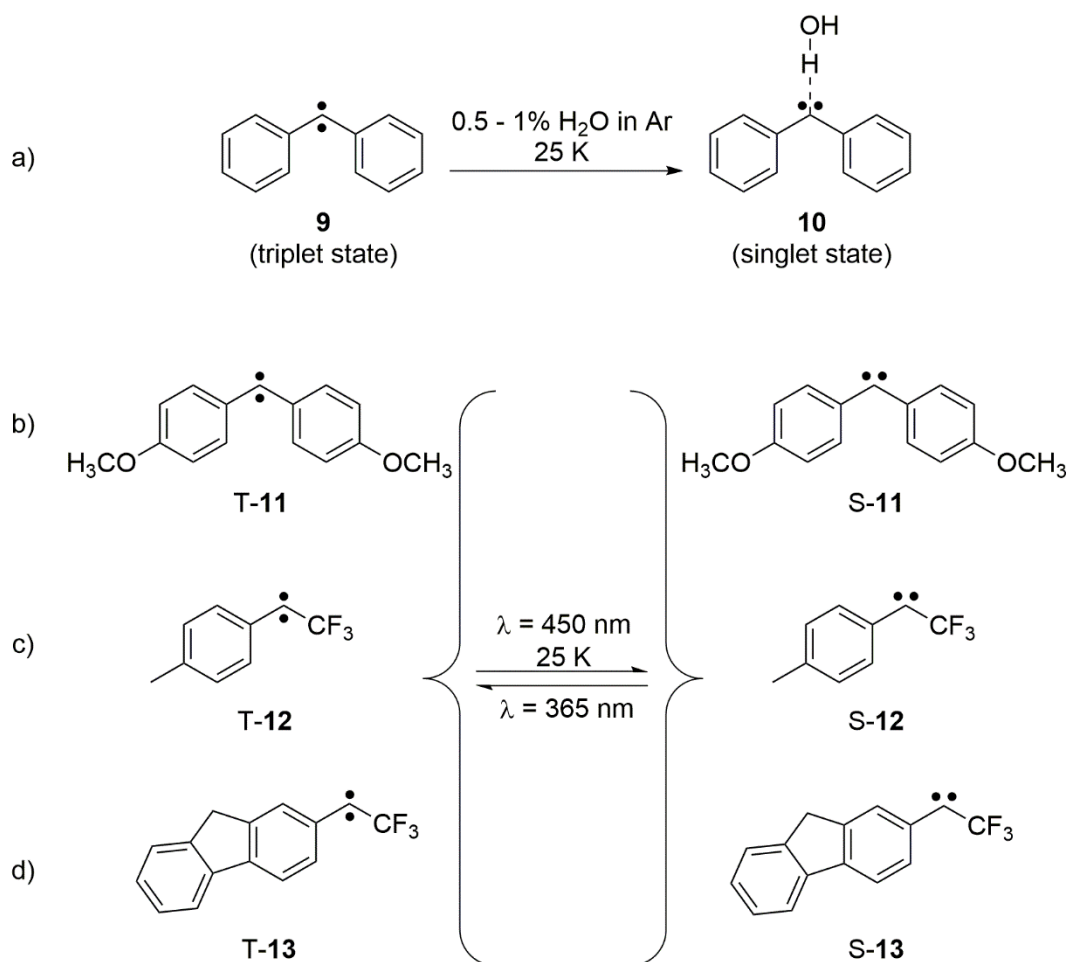
with $\lambda = 450$ nm. This molecule is the first example of a carbene for which magnetic bistability was observed.



Scheme 3.3: Magnetically bistable organic compounds presented by Rajca (diradical **7**) and by Bally and McMahon (carbene **8**).^[101-102]

While both the systems of Rajca and of Bally and McMahon are bistable organic compounds, the main difference consists in the singlet-triplet interconversion that occurred thermally for diradical **7** but also photochemically for carbene **8**.^[101-102]

Regarding spin switching in carbenes, several investigations have been conducted by Sander and coworkers on switching the spin state of diphenylcarbene systems. The parent diphenylcarbene **9** is a triplet ground state carbene with a singlet-triplet energy gap of approximately 3 kcal/mol.^[41] While magnetic bistability and hence thermal or photochemical singlet-triplet interconversion was not observed for this carbene, interactions with single water molecules result in the switching of the ground state from triplet to singlet by forming a strong hydrogen bond (Scheme 3.4). Investigations of the related bis(*p*-methoxyphenyl)carbene (**11**) showed that two additional methoxy substituents at the 4- and 4'-position have an electron-donating effect towards the carbene center, resulting in a favored singlet ground state carbene with a very low singlet-triplet gap of 0.3 kcal/mol.^[103] Due to this small energy gap, this carbene exhibits magnetic bistability where, unlike the carbene of Bally and McMahon, both spin states of **11** are coexisting indefinitely at cryogenic temperatures of 3 K. Irradiation of **11** with 365 nm light leads to conversion from the singlet to the triplet state, while irradiation with 450 nm light or annealing to 25 K results in singlet carbene formation. However, 100 % conversion to either the singlet or triplet state was not obtained.^[103] Besides carbene **11**, further magnetically bistable carbenes with different structural motifs but similar properties have been discovered by Sander (Scheme 3.4).^[104]



Scheme 3.4: Singlet-triplet conversion of diphenylcarbene and several bistable carbene compounds presented by Sander et al. (a) Triplet diphenylcarbene forms a singlet water complex when annealed to 25 K in a water-doped argon matrix. (b-d) Carbenes **11-13** are formed as a mixture of singlet and triplet. Via thermal or photochemical methods, switching between the singlet and triplet state is induced.^[41, 103-104]

In the following chapters, the investigation of other diphenylcarbene systems (Chart 3.1) and their properties concerning magnetic bistability are investigated.

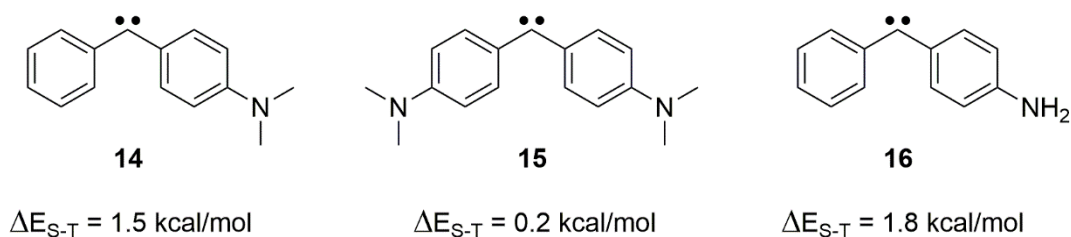


Chart 3.1: Diphenylcarbene-based carbenes with low calculated singlet-triplet energy gaps (B3LYP/def2-TZVP) and thus potential for magnetic bistability.

These carbene systems **14-16** have the advantage that compared to e.g. bis(*p*-methoxyphenyl)-carbene **11**, the substituents do not lead to different conformers which simplifies the analysis

of the spectroscopic data. While carbene **16** is a molecule that has not been researched in previous works yet, the carbenes **14** and **15** were already investigated in organic glass via EPR spectroscopy by Humphreys and Arnold.^[105-106] They stated that both compounds exhibit an EPR spectrum and thus most likely triplet ground states. In addition to that, UV/Vis investigations of **15** were also conducted in organic glass by Ware and Ono.^[107] However, these previous investigations did not include any analysis concerning magnetic bistability.

3.2. [4-(Dimethylamino)phenyl]phenylcarbene

3.2.1. Experiments in Ar, Xe and N₂

IR Experiments

To investigate the properties and the magnetically bistable behavior of the reactive intermediate [4-(dimethylamino)phenyl]phenylcarbene (**14**), several experiments were conducted in different inert gas matrices (Ar, Xe, N₂) with IR spectroscopy as the primary investigation method. Prior to these experiments, the carbene precursor **17** was synthesized according to literature.^[108] For the first experiment, the synthesized diazo compound **17** was sublimed at 55 °C via a sublimation oven and matrix-isolated at 3 K by co-deposition with an excess of argon. The experimental IR spectrum shows an intense signal at 2042 cm⁻¹ which is assigned to the N=N stretching vibration of the diazo group (Figure 3.1), indicating the successful deposition of diazo compound **17**. Furthermore, the experimental spectrum is in good accordance with the theoretical spectrum calculated at the B3LYP/def2-TZVP level of theory.

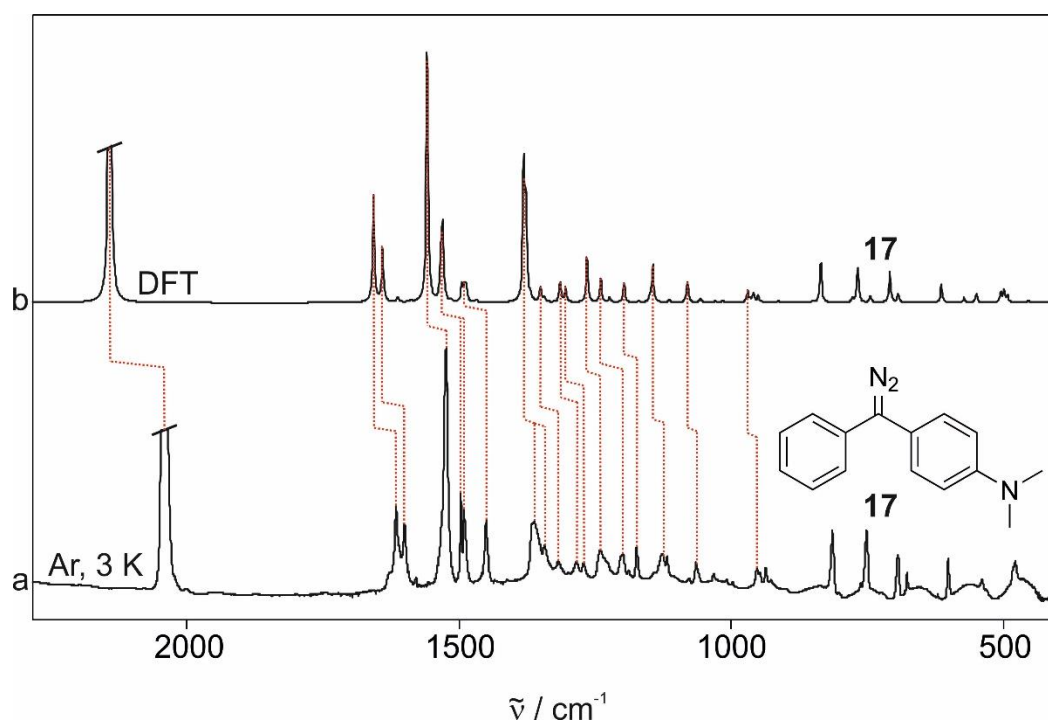


Figure 3.1: Comparison of the experimental and calculated IR spectra of diazo compound **17**. (a) Experimental IR spectrum in an argon matrix at 3 K. (b) Theoretical spectrum of **17** calculated at the B3LYP/def2-TZVP level of theory.

Subsequent photolysis was conducted with LED light of 505 nm or 530 nm for three hours, with the use of 505 nm light proceeding more efficiently. The disappearing of the diazo band at 2042 cm^{-1} after the irradiation indicate the decomposition of diazo precursor **17**, while the concomitantly signals can be assigned to carbene **14** (Figure 3.2). While this carbene does not exhibit different conformers like the related bis(*p*-methoxyphenyl)carbene (**11**),^[103] the rather high flexibility of the system leads to the formation of broader signals due to the presence of multiple rotamers. Since DFT calculations show that **14** has a low singlet-triplet energy gap, it is assumed that this carbene is magnetically bistable and forms as a mixture of its singlet and triplet state. However, the overlapping of multiple signals in the IR spectrum of this carbene prevent the proper assignment of singlet and triplet signals with the help of calculated spectra.

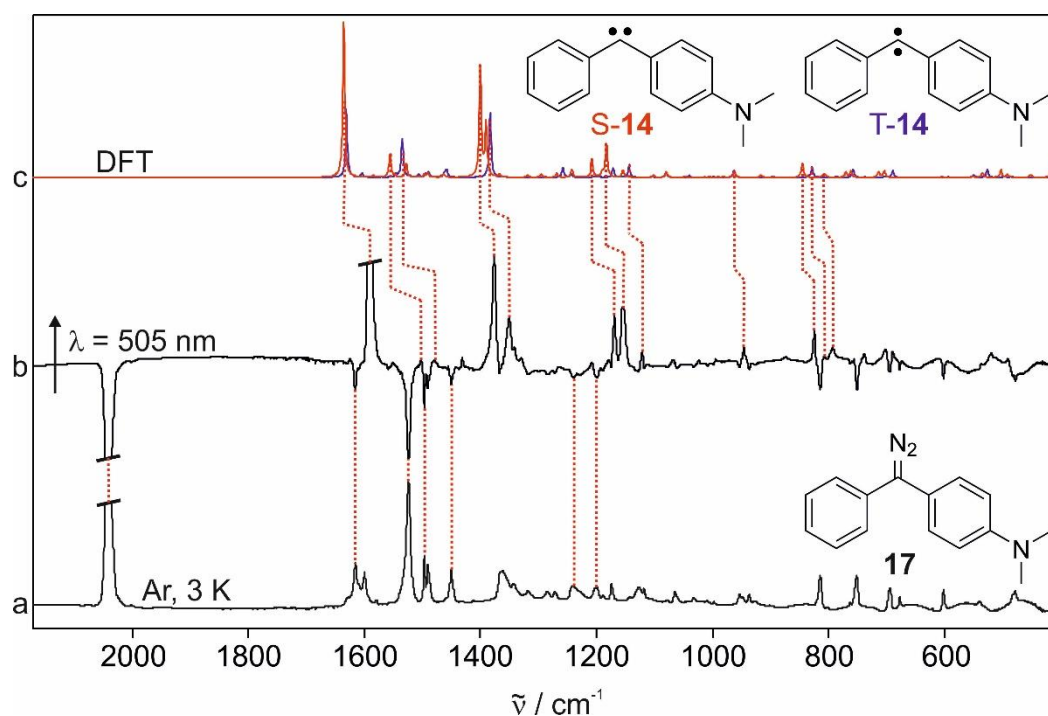


Figure 3.2: Comparison of the IR spectra of diazo compound **17** and the spectrum obtained after irradiation with 505 nm light. The disappearance of the intense diazo band and the appearance of new signals indicate the formation of carbene **14**. (a) Deposition spectrum of diazo precursor **17** in argon at 3 K. (b) Difference spectrum after irradiation with 505 nm LED light. The bands pointing upwards are assigned to carbene **14**, the bands pointing downwards to diazo precursor **17**. (c) Theoretical IR spectra of singlet carbene S-**14** (red) and triplet carbene T-**14** (blue) calculated at the B3LYP/def2-TZVP level of theory.

It was tested if the carbene undergoes singlet-triplet interconversion in the same manner as the bistable carbenes **11**, **12** and **13**.^[103-104] Therefore, irradiation with LED light in the range of 365–650 nm was conducted. It was observed that after irradiation with 505 nm or 365 nm light, the intensity of several signals in the IR spectrum increased while it decreased for other signals (Figure 3.3). Upon irradiation with 530 nm or 405 nm light, this process was reversed. Comparison of the increasing and decreasing signals with theoretical spectra of singlet carbene S-**14** and triplet carbene T-**14** calculated at the B3LYP/def2-TZVP level of theory show that several similarities are present. The increasing signals after irradiation with 505 nm or 365 nm light are assigned to singlet carbene S-**14**. On the other hand, the signals increasing after irradiation with 530 nm or 405 nm light are assigned to triplet carbene T-**14** (Figure 3.3). Therefore, it is confirmed that irradiation led to reversible singlet-triplet conversion, which is in agreement with the calculated small singlet-triplet energy gap.

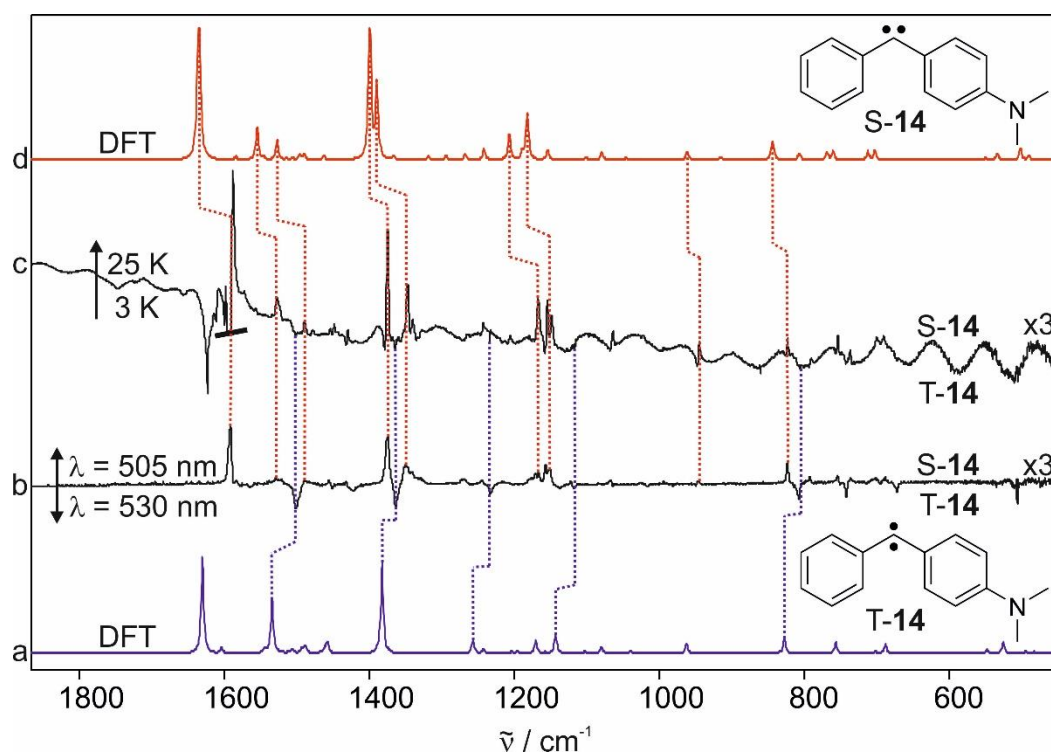


Figure 3.3: Comparison of the experimental difference spectra of **14** after irradiation with 530 nm and 505 nm light and after annealing from 3 K to 25 K with calculated spectra of S-**14** and T-**14**. (a) Theoretical spectrum of triplet carbene T-**14** calculated at the B3LYP/def2-TZVP level of theory. (b) Experimental difference spectrum after irradiation, with the signals pointing upwards being assigned to singlet carbene S-**14**, the signals pointing downwards to triplet carbene T-**14**. (c) Difference IR spectrum after annealing to 25 K. The signals pointing upwards increase at 25 K and are assigned to S-**14** while the decreasing signals pointing downwards are assigned to T-**14**. (d) Theoretical spectrum of singlet carbene S-**14** calculated at the B3LYP/def2-TZVP level of theory.

To test if an increase of temperature also results singlet-triplet conversion, annealing of the matrix to 25 K was conducted. After 10 minutes, changes in the spectrum were detected which were similar to the observed changes after irradiation with 505 nm light (Figure 3.3). Therefore, it was shown that annealing results in formation of S-**14**. However, additional other changes were detected which did not occur during the irradiation experiments before and which could not be assigned to any molecule. It is suggested that these additional changes in the spectrum after annealing were caused by matrix effects or possible traces of oxygen impurities.

In the case of the formation of the triplet carbene, it was observed that the irradiation with 405 nm and with 530 nm light showed slight deviations in the difference spectra (Figure 3.4). In general, the increasing triplet signals are more intense after irradiation with 530 nm. Especially the triplet carbene signals at 1234 cm^{-1} and 1365 cm^{-1} show a much higher intensity. Furthermore, a few peaks exhibit small shift differences, depending on the wavelength used for triplet carbene formation. The triplet signals at 816 cm^{-1} and 1520 cm^{-1} (formed after 405 nm

irradiation) are shifted to 809 cm^{-1} and 1503 cm^{-1} , respectively, when T-**14** is formed after 530 nm irradiation. Since both signals are assigned to C–H deformation vibrations, it is assumed that the deviations in the difference spectra are caused by small geometric distortions of the phenyl rings between the possible conformers **14a** and **14b** (Chart 3.2).

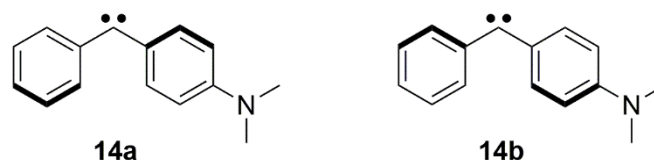


Chart 3.2: Different possible geometric orientations of the phenyl rings of carbene **14**.

Calculations at the B3LYP/def2-TZVP level of theory show that the theoretical zero-point energies are nearly identical ($\Delta E < 0.1\text{ kcal/mol}$) as well as the theoretical IR spectra of **14a/b** (singlet/triplet). Comparison of the experimental and theoretical IR spectra does not yield any conclusive results about the assumed shifting of the phenyl ring orientation. Therefore, it cannot be verified if irradiation with 405 nm and 530 nm light leads to any kind of conversion between **14a** and **14b**.

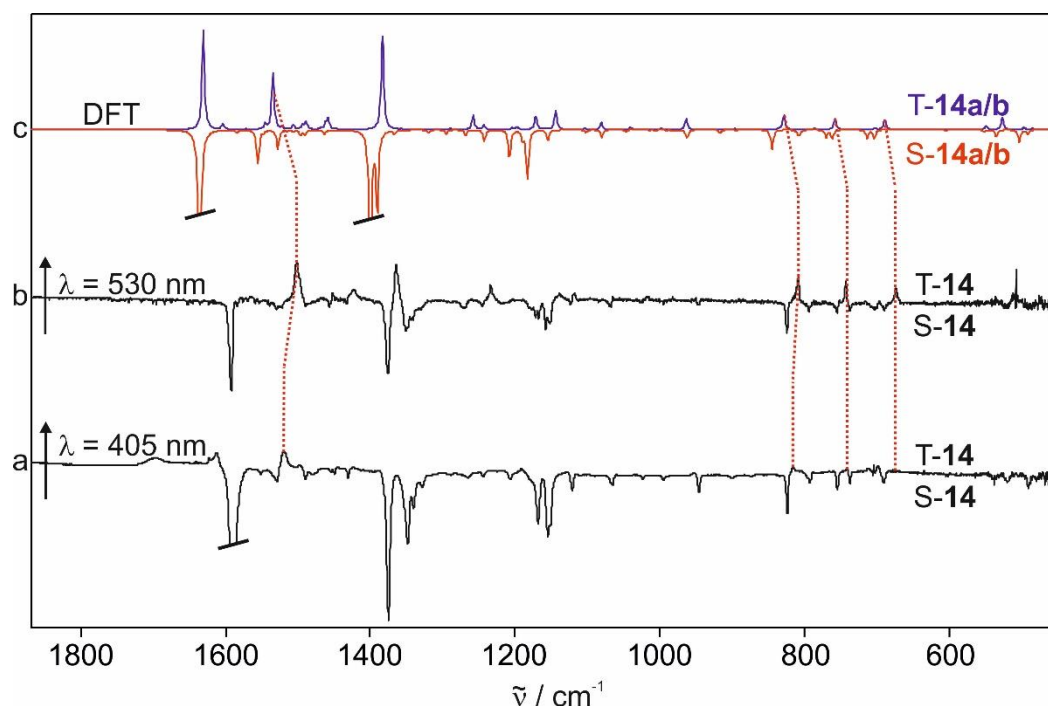
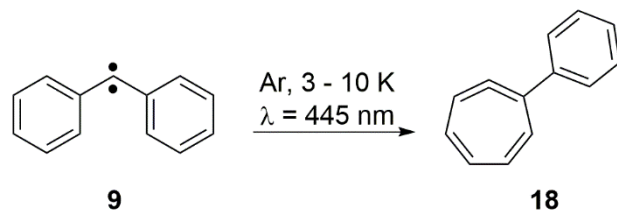


Figure 3.4: Triplet formation after irradiation with 405 nm and 530 nm light. (a-b) Difference IR spectra after irradiation of **14** in argon at 3 K with (a) 405 nm or (b) 530 nm light. The signals pointing upwards are assigned to triplet carbene T-**14**, the signals pointing downwards to singlet carbene S-**14**. (c) Theoretical difference spectrum of T-**14a/b** (blue) and S-**14a/b** (red) calculated at the B3LYP/def2-TZVP level of theory.

Regarding the differences in the IR difference spectra after 530 nm and 405 nm irradiation, it was tested if these were caused by possible side reactions. In previous research, Costa and Sander showed that irradiation of unsubstituted diphenylcarbene with a 445 nm diode laser led to 1-phenyl-1,2,4,6-cycloheptatetraene as a ring expansion product (Scheme 3.5).^[110]



Scheme 3.5: Formation of the ring expansion product **18** by laser irradiation of diphenylcarbene **9**.^[110]

Therefore, it was tested if overnight irradiation of carbene **14** with light of 405 nm would lead to any kind of ring expansion. Prior to this experiment, theoretical IR spectra of the assumed ring expansion products **19** and **20** were calculated at the B3LYP/def2-TZVP level of theory. Both calculated spectra show characteristic bands at 1836 cm^{-1} (product **19**) and 1854 cm^{-1} (product **20**) which are assigned to the allene $\text{C}=\text{C}=\text{C}$ stretch (Figure 3.5). The experimental IR spectra after the overnight irradiation with light of 405 nm were compared to the calculated spectra. No new signals in the range of $1700\text{--}1800 \text{ cm}^{-1}$ were detected which would have been expected for the characteristic allene stretch of the ring expansion products. Thus, the formation of **19** and **20** as side products during the experiments of carbene **14** is excluded.

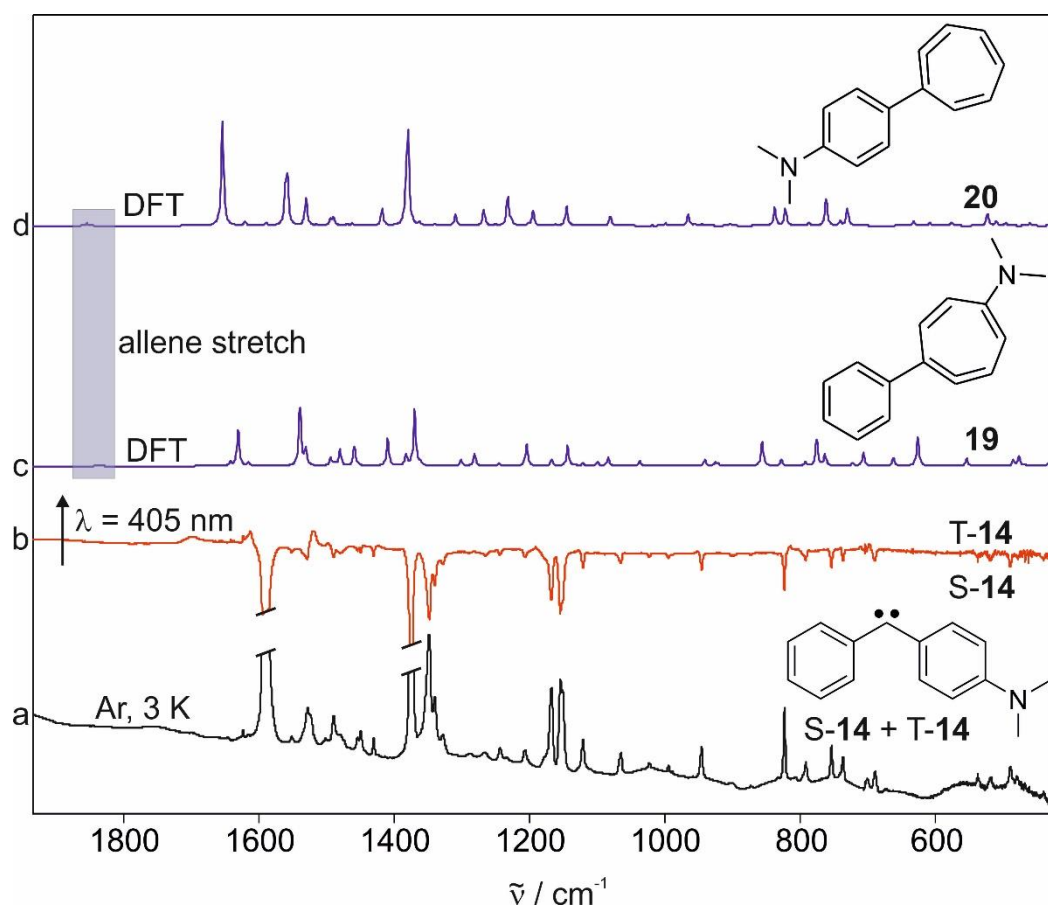


Figure 3.5: IR spectra of carbene **14** before and after overnight irradiation with 405 nm light. The formation of any ring expansion product was not observed, indicated by the missing signal of the allene C=C=C stretch which would be expected at around 1800 cm^{-1} . (a) IR spectrum of **14** before irradiation with 405 nm light. (b) Difference IR spectrum of **14** before and after 405 nm light irradiation. The signals pointing upwards are assigned to T-**14**, the signals pointing downwards to S-**14**. (c-d) Theoretical IR spectra (B3LYP/def2-TZVP) of the ring expansion products **19** and **20**, respectively.

Quantitative investigation of the singlet-triplet ratios and the amount of singlet-triplet conversion via integration of the IR signals of **14** shows that after photolysis of diazo precursor **17** with 505 nm light, an excess of singlet carbene S-**14** was formed with an amount of 91%. Photolysis of **17** was also tested with 405 nm and 470 nm light, but only around 74% S-**14** were formed under these conditions. Further irradiation with 505 nm light in combination with annealing to 25 K increased the singlet amount, resulting in a maximum singlet amount of 96% (Table 3.1). In addition to the singlet maximization, it was attempted to maximize the amount of T-**14**. Thus, irradiation with 405 nm light for at least 16 hours was conducted to decrease the singlet amount to 63%, hence resulting in a maximum triplet amount of 37%. Subsequently, it was tested if the initial singlet amount after the precursor photolysis could be obtained again. Irradiation with 505 nm light while annealing to 25 K increased the singlet amount again by 9% (Table 3.1). However, the initial singlet amount could not be regenerated under any

experimental conditions in an argon matrix. To test if more of S-**14** forms under different experimental conditions, irradiation with 470 nm light was conducted. For similar carbene systems, it was reported that the triplet carbene absorption band was in the range near 470 nm (450–480 nm, depending on the type of carbene).^[41, 103, 109] Therefore, it was assumed that irradiation of **14** with this wavelength would result in larger triplet decrease and singlet increase. However, the results showed that 470 nm irradiation led to a much smaller increase of S-**14** than the irradiation with 505 nm.

Table 3.1: Singlet-triplet ratios and maximization of the amounts of S-**14** and T-**14** in matrices of argon, xenon and nitrogen.

Experiments	S-T Ratio (Ar)	S-T Ratio (Xe)	S-T Ratio (N ₂)
after precursor photolysis (505 nm)	91% / 9%	70% / 30%	71% / 29%
$\lambda = 505$ nm + 25 K (Ar) / 50 K (Xe) / 20 K (N ₂)	96% / 4%	82% / 18%	71% / 29%
$\lambda = 405$ nm	63% / 37%	42% / 58%	44% / 56%
$\lambda = 505$ nm + 25 K / 50 K / 20 K (again)	72% / 28%	70% / 30%	44% / 56%

The quantitative investigation of the singlet-triplet amounts of **14** was also conducted for experiments in a xenon matrix. It is detected that the changes in the IR spectrum caused by singlet-triplet shift are much more distinct than in argon (Figure 3.6). After photolysis of **17** with 505 nm light, a singlet amount of only 70% was obtained, which is 21% lower than in argon (Table 3.1). After subsequent annealing of **14** to 50 K, the singlet amount increased by 12%. Irradiation with 405 nm light overnight led to a large singlet decrease (S-T ratio: 42/58). When the matrix was annealed to 50 K again, the initial singlet amount of 70% was regenerated. The major differences concerning the singlet-triplet ratios of **14** in argon and xenon are that the triplet amount after photolysis and the achievable maximum triplet amount were much larger in xenon than in argon. Furthermore, more singlet carbene was formed in xenon via annealing directly after the photolysis of **17**. The last important difference is that after photochemical triplet formation, the initial singlet amount could not be regenerated in argon, but it was possible in xenon.

In a nitrogen matrix, photolysis of diazo precursor **17** led to a singlet-triplet ratio of 71/29, which is similar to the results in xenon. Annealing to 20 K did not result in any observable changes in the IR spectrum, indicating that no spin interconversion occurred. It is supposed that the starting singlet amount of 71% was already the maximum amount obtainable in N₂, so that no further singlet carbene could be formed. Irradiation with 405 nm led to singlet decrease and accordingly to triplet increase, resulting in a singlet-triplet ratio of 44/56 (Table 3.1).

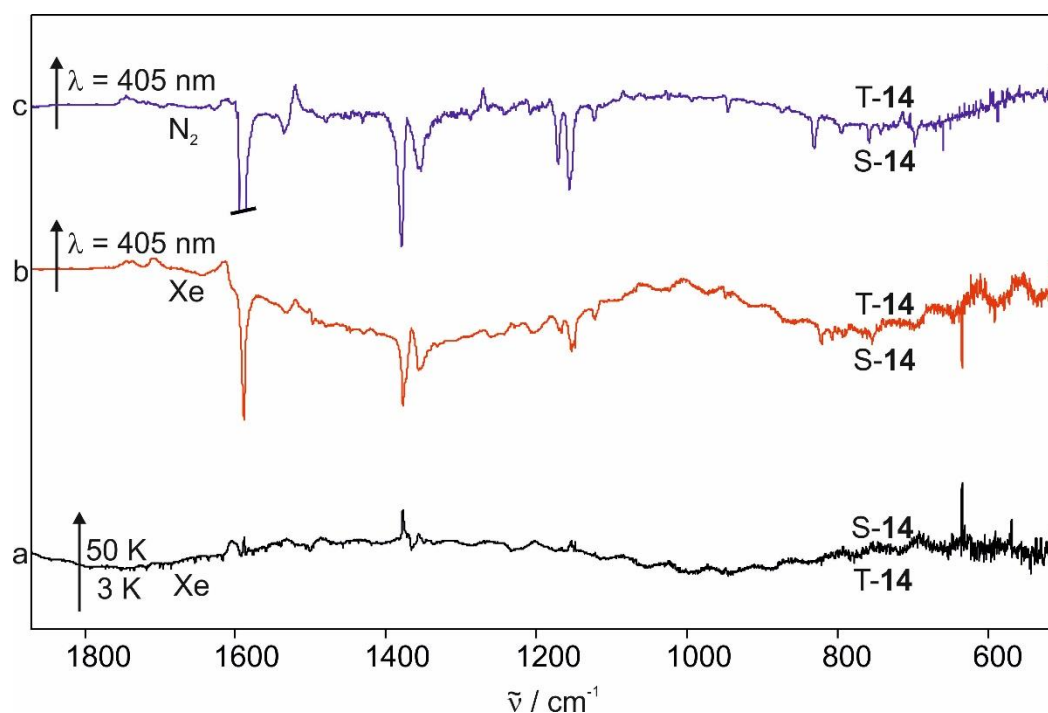


Figure 3.6: Singlet-triplet switching of carbene **14** in a xenon and nitrogen matrix. (a) IR difference spectrum after annealing **14** to 50 K in a xenon matrix for ten minutes. The signals pointing upwards are assigned to singlet carbene S-**14**, the signals pointing downwards to T-**14**. (b) IR difference spectrum after irradiation of **14** with 405 nm light in a xenon matrix. The peaks pointing upwards are assigned to triplet carbene T-**14**, the peaks pointing downwards to S-**14**. (c) IR difference spectrum of **14** after irradiation with 405 nm light in a nitrogen matrix. The signals are assigned according to spectrum b.

Compared to the experiments in argon and xenon, the signals of T-**14** in the IR difference spectrum in N₂ are very distinct and sharp (Figure 3.6). However, subsequent irradiation with 505 nm light or annealing to 20 K did not result in the regeneration of the singlet carbene. More precisely, no changes were observed anymore. Therefore, it was discovered that photochemical conversion from S-**14** to T-**14** is possible in nitrogen matrices, but this process is not reversible.

UV/Vis Experiments

To support the IR experiments, matrix isolation UV/Vis experiments were conducted. First, diazo precursor **17** was deposited in an argon matrix at 8 K and photolyzed with 505 nm light to generate carbene **14**.

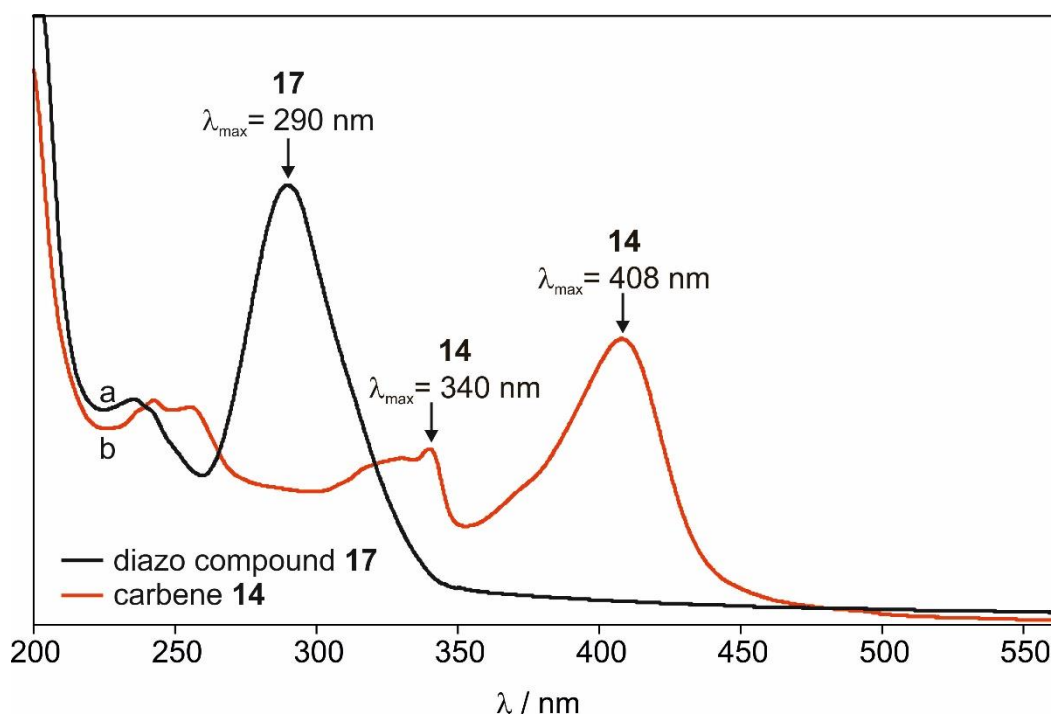


Figure 3.7: UV/Vis spectra of diazo compound **17** and carbene **14** obtained after photolysis with 505 nm light in an argon matrix at 8 K. (a) UV/Vis spectrum of diazo compound **17**. (b) UV/Vis spectrum of carbene **14** obtained in its singlet and triplet state.

Diazo compound **17** exhibits an intense signal at 290 nm (Figure 3.7). Photolysis for three hours led to the complete disappearance of this peak while two new signals at 340 nm and 408 nm appeared that are assigned to carbene **14**. Since the IR investigation showed that this carbene is magnetically bistable, it was assumed that one of these signals belonged to singlet carbene S-**14** while the other one belonged to triplet carbene T-**14**. Irradiation with 405 nm and 505 nm light was conducted in the same manner as for the IR investigations to observe singlet-triplet interconversion. It was found that 405 nm light irradiation resulted in a decrease of the signal at 408 nm while the signal at 340 nm increased (Figure 3.8). The irradiation with 505 nm light reversed this effect. Based on these results and those of the previous IR experiments, the signal at 408 nm is assigned to S-**14**, the signal at 340 nm to T-**14**.

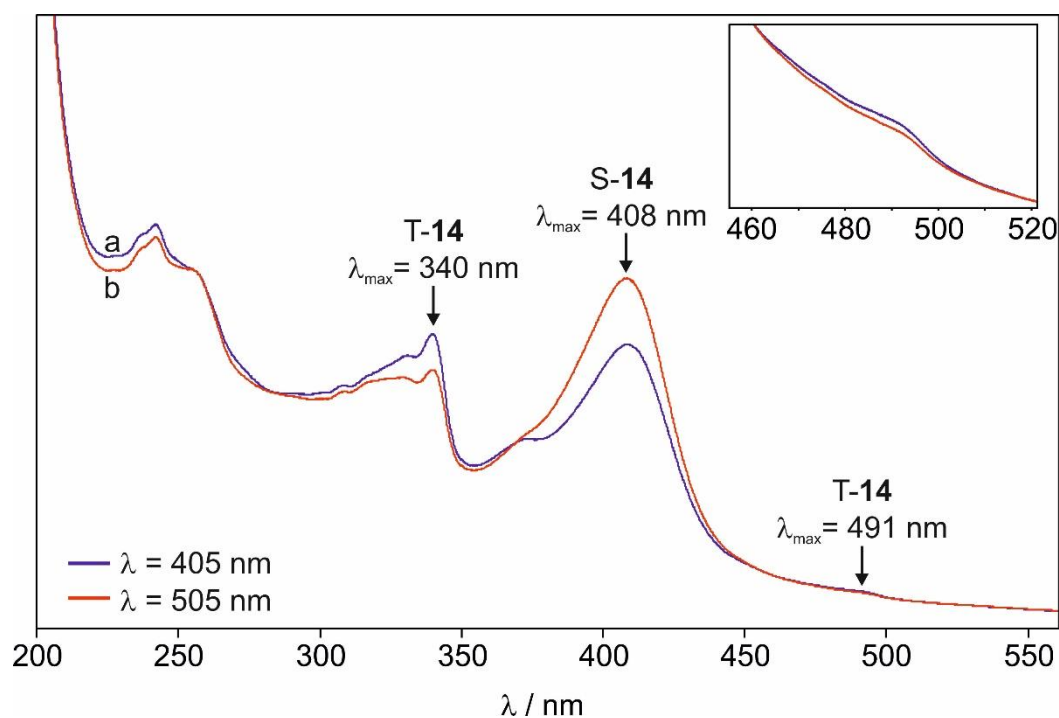


Figure 3.8: UV/Vis spectra of carbene **14** showing its singlet-triplet interconversion after irradiation with light of 405 nm and 505 nm. (a) Spectrum after irradiation with 505 nm light. (b) Spectrum after irradiation with 405 nm light.

Further investigation of the spectra shows that another small signal is present at 491 nm that increases when irradiated with 405 nm and decreases if 505 nm light is used. Hence, this signal is also assigned to triplet carbene T-14. Comparison with literature data of the related bis(*p*-methoxyphenyl)carbene (**11**) confirms these results. Although the signals of carbene **11** are shifted by 8–24 nm compared to **14**, they appear roughly in the same wavelength range (singlet **11**: 384 nm, triplet **11**: 316 nm, 483 nm).^[103] Subsequently, the matrix was annealed to 25 K for ten minutes to investigate the thermal singlet-triplet conversion. It was observed that the triplet signal at 340 nm decreased while the singlet signal at 408 nm increased (Figure 3.9). Due to a slight baseline increase, it is not possible to determine with certainty if the small triplet signal at 491 nm underwent any changes.

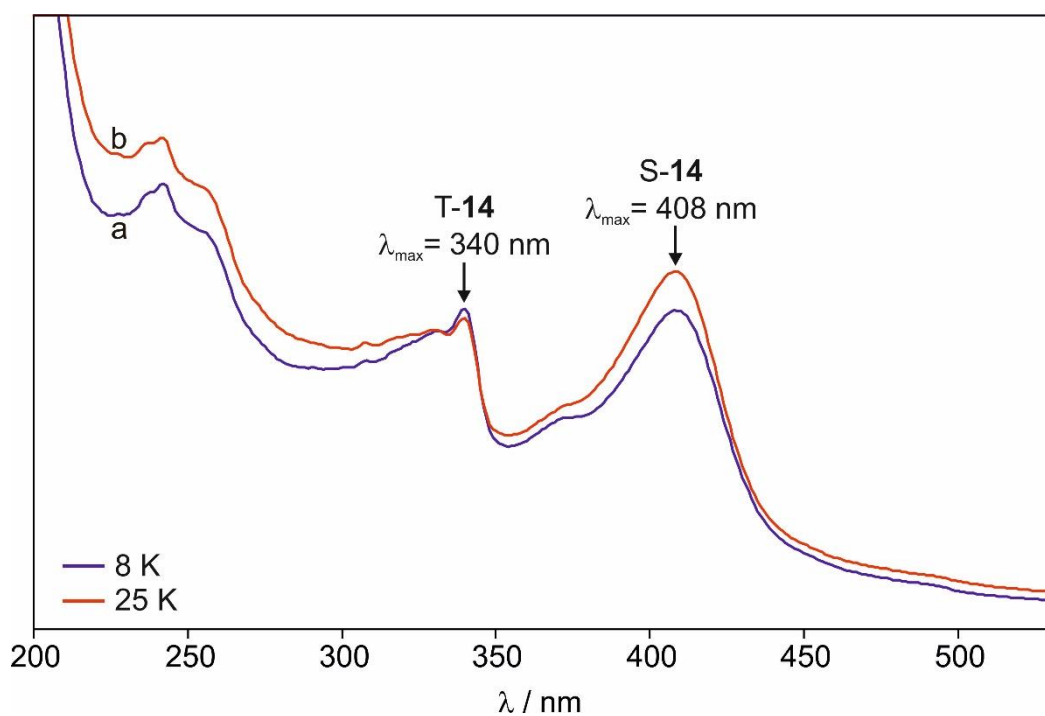


Figure 3.9: UV/Vis spectra of carbene **14** before and after annealing to 25 K. The increase of the signal at 408 nm and the decrease of the peak at 340 nm indicated conversion from the triplet to the singlet state. (a) UV/Vis spectrum at 8 K. (b) UV/Vis spectrum at 25 K.

After cooling down to 8 K again, this process was not reversed. In general, the results of the IR investigation showing that annealing to elevated temperatures induces conversion of T-**14** to its singlet state are verified. Based on the results of the irradiation and annealing experiments, the singlet-triplet ratio was investigated quantitatively. It was observed that the S-T ratios of the UV/Vis experiments are in accordance with the previously shown IR experiments. UV/Vis experiments in xenon or nitrogen matrices were not conducted yet, so that the singlet-triplet ratios of **14** in these matrices were not determined.

EPR Experiments

Since triplet carbenes exhibit two unpaired electrons, the behavior of this species in magnetically bistable carbenes can directly be observed via EPR spectroscopy. This method further corroborates the influence of irradiation and annealing on the S-**14**/T-**14** ratios. After deposition of diazo precursor **17** and photolysis with 505 nm light, several small signals appeared in the EPR spectrum (Figure 3.10), which indicated that triplet carbene T-**14** was present. Due to non-optimized deposition conditions, the EPR signals only had a very low intensity. Furthermore, IR and UV/Vis experiments indicated that photolysis with 505 nm light

formed an excess of EPR-silent singlet carbene S-**14**, so that the EPR signals of T-**14** are presumably rather small in general. The intensity of the Z_2 peak is so low that it is not observed in the spectrum.

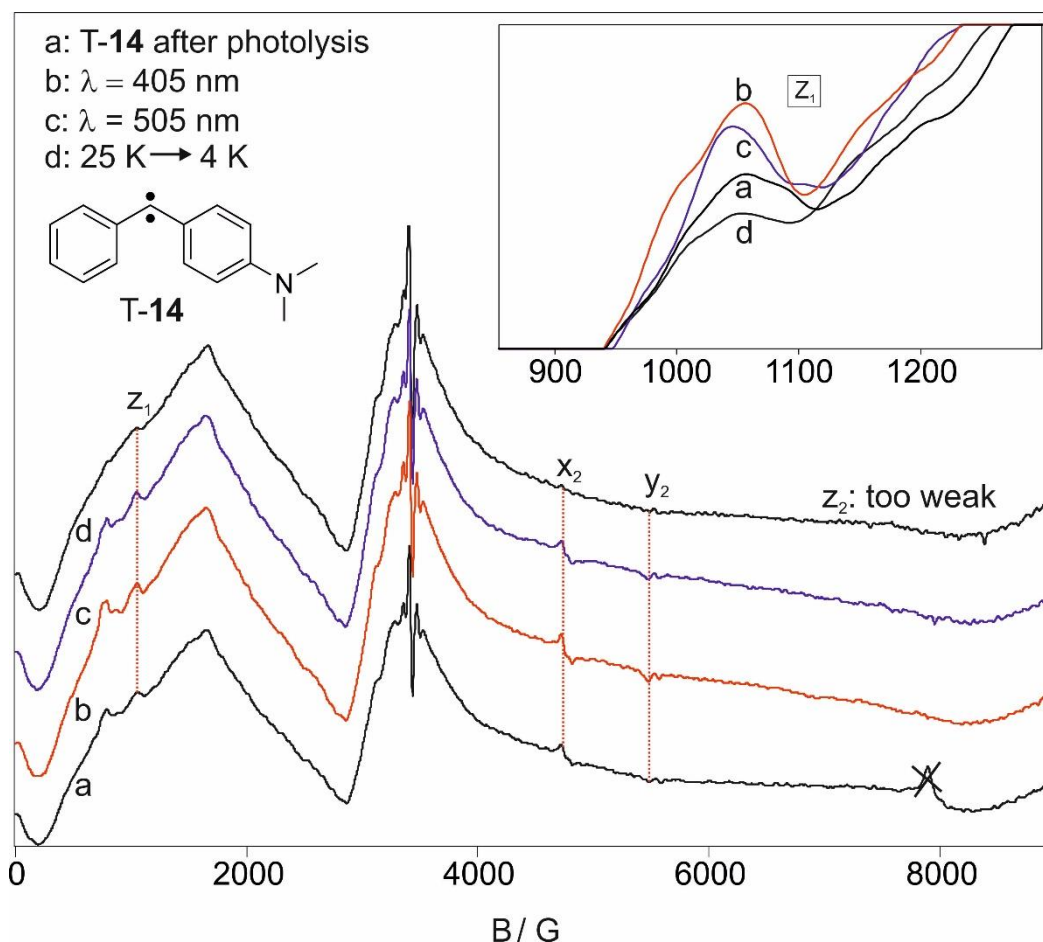


Figure 3.10: EPR spectra of triplet carbene T-**14** after irradiation and annealing. Due to the low intensity, the Z_2 peak is not observable. (a) EPR spectrum of T-**14** directly after precursor photolysis with 505 nm light. The signal at around 8000 G is not assigned to the carbene. (b) EPR spectrum after subsequent irradiation with 405 nm light. (c) EPR spectrum after subsequent irradiation with 505 nm light. (d) EPR spectrum after subsequent annealing to 25 K and cooling down again.

Since the low intensity results in rather indistinct signals and the Z_2 peak is not visible, the values of the zero-field splitting parameters D and E cannot be determined. Irradiation with light of 405 nm showed only slight changes of the spectrum. However, integration of the signals verifies that 405 nm irradiation led to an increase of all the signals and therefore to an increase of triplet carbene T-**14**. By subsequent irradiation with 505 nm light, the signal intensity decreased again. This indicates the conversion of **14** from its triplet to its singlet state. Annealing of carbene **14** to 25 K and cooling back to 4 K led to a major decrease in signal intensity. It is not clear if this decrease was only caused by singlet-triplet conversion or by a

partial loss of the matrix. Because **14** undergoes thermal singlet-triplet interconversion, it is not possible to prepare a Curie-Weiss plot to give hints about the possible spin ground state of this carbene.^[111] By taking a closer look to the Z_1 peak in the EPR spectrum, the photochemically and thermally induced singlet-triplet conversion is observed more clearly (Figure 3.10), in accordance with the results from the IR and UV/Vis investigations.

3.2.2. Reaction with water

IR Experiments

The interaction and reaction behavior of carbenes with water have been studied for several different carbenes in previous research.^[41, 109] For the unsubstituted diphenylcarbene (**9**), it was shown that interactions with water switch the ground state from triplet to singlet by forming a hydrogen-bonded complex. Subsequently, this complex can be converted to the corresponding alcohol by photochemical methods. Since carbene **14** is a magnetically bistable carbene where the singlet and triplet state are coexisting, it was tested which spin state preferably interacts with water, or if both states interact. Furthermore, it was investigated if potential interactions with water might have an influence on the singlet-triplet switching in this carbene system. After isolating carbene **14** in an argon matrix doped with 1% water, the matrix was annealed to 25 K.

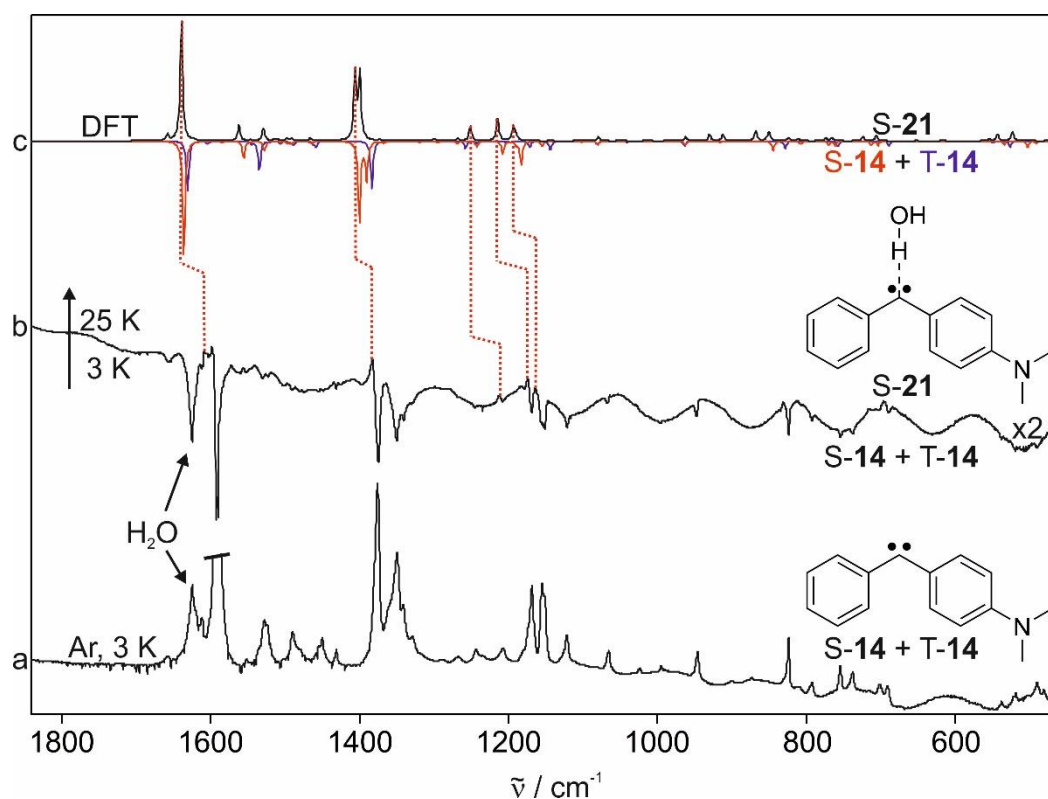


Figure 3.11: IR spectra of the annealing experiments to 25 K in an argon matrix doped with 1 % water. **(a)** IR spectrum of carbene **14** at 3 K, before the annealing. **(b)** Difference spectrum after annealing to 25 K. The signals pointing upwards are assigned to singlet carbene-water complex **S-21**, the signals pointing downwards to singlet and triplet carbene **S-14** and **T-14**. **(c)** Theoretical IR difference spectrum. The signals pointing upwards belong to singlet complex **S-21**, the signals pointing downwards to **S-14** (red) and **T-14** (blue).

After ten minutes of annealing, the water signals at around 1600 cm^{-1} as well as the signals of both **S-14** and **T-14** in the range of 500 cm^{-1} to 1700 cm^{-1} decreased (Figure 3.11). At the same time, several new signals increased. Comparison with theoretical spectra calculated at the B3LYP/def2-TZVP level of theory verify that these new signals belong to the newly formed singlet carbene-water complex **S-21**. Additionally, calculations at the same level of theory show that the singlet water complex is energetically more favored than the triplet complex, which is in agreement with the experimental results. Integration of the peaks of **S-14** and **T-14** before and after annealing shows that the intensity of both species decreased. However, it was determined that the decrease of **S-14** is much higher. While the **S-14/T-14** ratio before annealing was 81:19, a ratio of 73:27 was detected after formation of water complex **S-21**. This result is in contrast to the expectation that due to both thermal conversion to **S-14** and interaction with water, the decrease of **T-14** would be higher. It can be assumed that this was observed because the thermal conversion from the triplet to the singlet state only barely occurs when the triplet amount is already low. In this case, the interaction of **S-14** with water at 25 K possibly happens faster than the singlet-triplet interconversion, so that the singlet carbene amount decreases

faster than the triplet carbene amount. To test if carbene **14** behaves differently when a larger amount of triplet carbene is present before annealing, short irradiation with 405 nm light was conducted beforehand, resulting in a singlet-triplet ratio of 72/28. After annealing to 25 K, the triplet ratio decreased again by 3%. Therefore, the decrease of T-**14** was higher than the decrease of S-**14** due to increased thermal spin switching and additional spin switching due to the interaction of water molecules with T-**14**. In summary, it was observed that the singlet carbene decrease was higher when a low triplet amount is present, while the triplet carbene decrease is higher when the triplet amount is increased before annealing.

Cooling down again to 3 K and keeping complex S-**21** in the dark at this temperature for 15 h did not result in any changes in the spectrum. Hence, an insertion reaction from S-**21** to the corresponding alcohol **22** was not observed. To induce this insertion reaction, irradiation with LED light of several wavelengths was tested. Irradiation with 650 nm and 630 nm light resulted in decreasing signals of complex S-**21** while several new signals with a low intensity appeared (Figure 3.12).

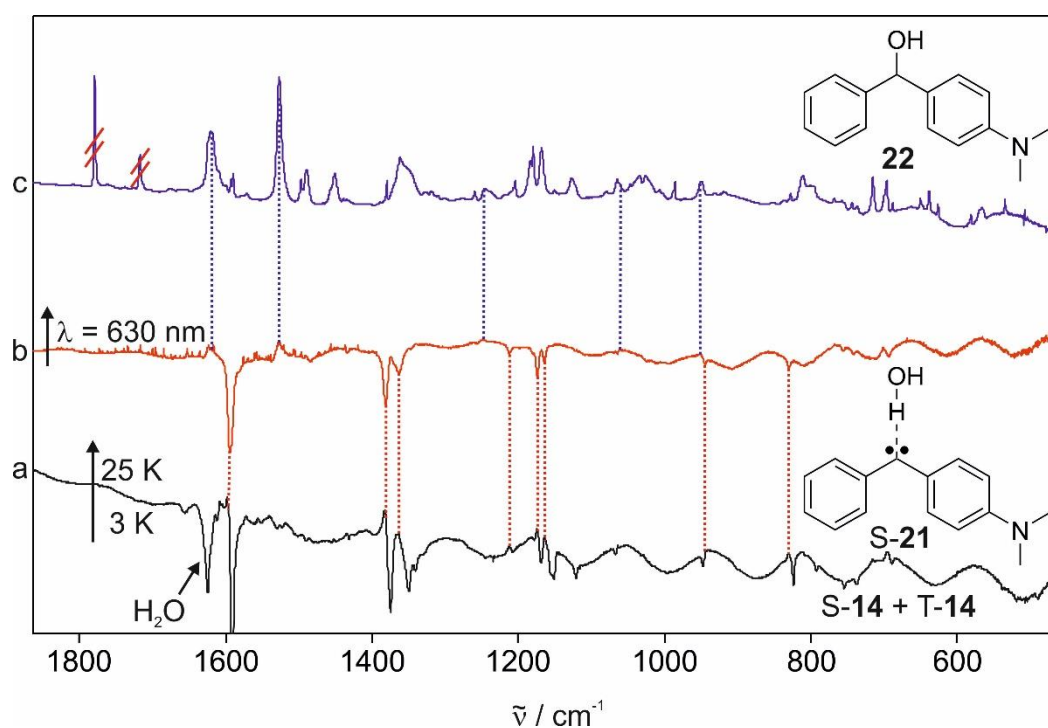


Figure 3.12: Formation of alcohol **22** after irradiation of S-**21** with 630 nm light. (a) Difference spectrum after annealing of the argon matrix doped with 1% water to 25 K. The signals pointing upwards are assigned to singlet-water-complex S-**21**, the signals pointing downwards to both S-**14** and T-**14**. (b) Difference spectrum after irradiation with 630 nm LED light. The signals pointing upwards are assigned to alcohol **22**, the signals pointing downwards to water complex S-**21**. (c) IR spectrum of alcohol **22** in an argon matrix at 3 K. The signals above 1650 cm^{-1} are ketone impurities.

Comparison of these new signals with the experimental IR spectrum of alcohol **22** as a reference verifies that the irradiation of complex S-**21** formed the alcohol. This is especially proven by the two intense signals at 1527 cm^{-1} and 1620 cm^{-1} . Furthermore, calculations at the B3LYP/def2-TZVP level of theory show that the smaller signal at 1244 cm^{-1} belongs to the CO–H deformation vibration of the formed alcohol group.

UV/Vis Experiments

To complement the results of the IR experiments in water-doped argon matrices, the same experiments were investigated via UV/Vis spectroscopy. Diazo precursor **17** was deposited in an argon matrix doped with 2% water and photolyzed with 505 nm light. Subsequently, the matrix was annealed to 25 K.

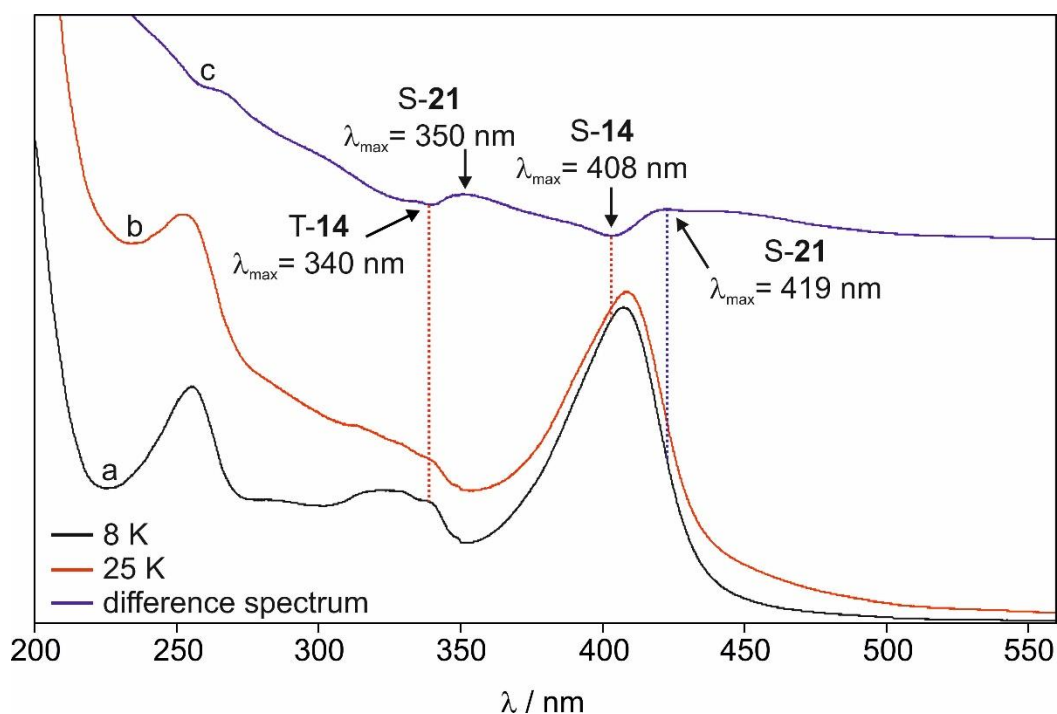


Figure 3.13: UV/Vis spectra of carbene **14** before and after annealing to 25 K in an argon matrix doped with 2% water. (a) UV/Vis spectrum at 8 K. (b) UV/Vis spectrum at 25 K. (c) Difference UV/Vis spectrum after annealing to 25 K. The broad bands pointing downwards are assigned to T-**14** and S-**14**, the broad signals pointing upwards to water complex S-**21**.

Annealing primarily led to baseline shifts (Figure 3.13). While the UV/Vis spectra at 8 K and 25 K do not show distinct signal changes, the UV/Vis difference spectrum exhibits two broad decreasing signals at 340 nm and 408 nm that are assigned to T-**14** and S-**14**, respectively. In

addition to that, two small and broad increasing bands at 350 nm and 419 nm are observed that are assigned to water complex S-21. Comparison with the UV/Vis spectrum of the similar molecule fluorenylidene in a water-doped argon matrix shows that the singlet water-fluorenylidene complex exhibits a signal at 416 nm,^[109] which is in the same range as the signal of S-21 at 419 nm. Complex S-21 was kept in the dark at 8 K for 24 h. Similar to the IR experiments, no changes were observed.

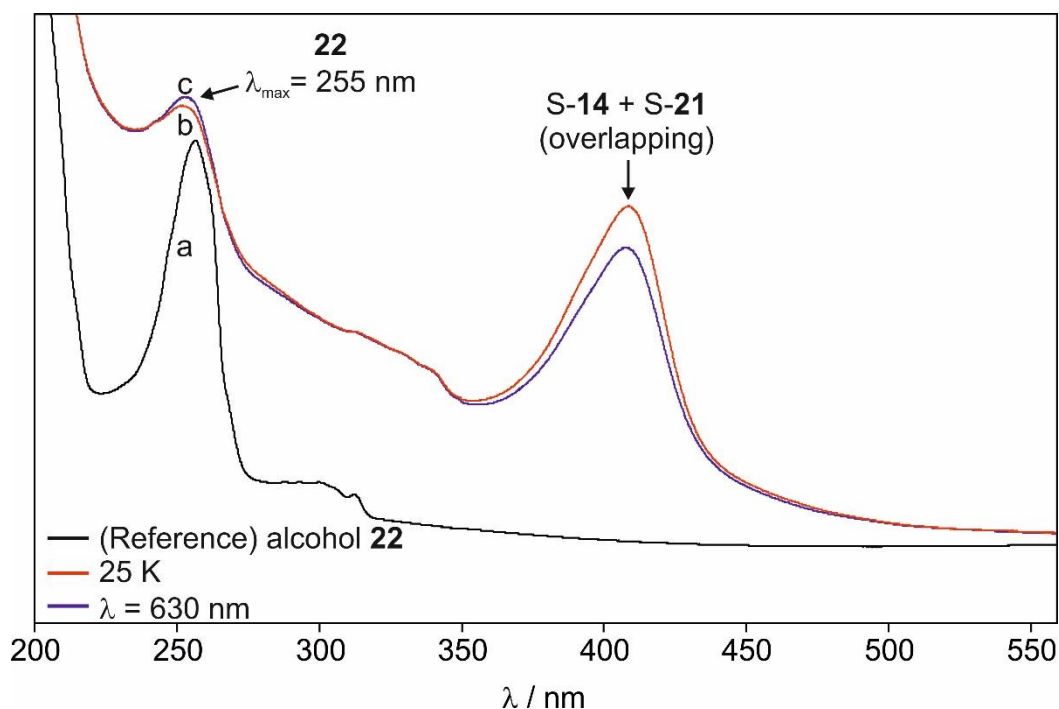


Figure 3.14: UV/Vis spectra of carbene **14** with small amounts of water complex S-21 that formed after annealing of the matrix to 25 K. (a) UV/Vis spectrum of alcohol **22** in an argon matrix as a reference spectrum. (b) UV/Vis spectrum of carbene **14** at 25 K after formation of water complex S-21. (c) UV/Vis spectrum after irradiation with 630 nm light.

Subsequent irradiation with 630 nm light resulted in the decrease of the broad signal at 408 nm (Figure 3.14). Since the experiments in pure argon matrices verified that irradiation with 630 nm light did not induce singlet-triplet interconversion, it can be excluded that the decrease of this signal was caused by this effect. Additionally, the triplet signal at 340 nm did not increase, which confirms this assumption. It is assumed that the signal at 408 nm decreased due to a signal overlap with the decreasing signal of water complex S-21 at 419 nm. As shown in the IR investigations, 630 nm light converts this complex to the corresponding alcohol **22**. This is verified in the UV/Vis spectrum by the increase of a band at 255 nm that is assigned to this alcohol. In summary, the results of the UV/Vis experiments of carbene **14** in a water-doped argon matrix are in accordance with the results of the IR experiments.

3.2.3. Computational Results

To support the experimental data of the matrix isolation experiments of **14**, several quantum mechanical calculations were conducted. For this carbene, calculations at the B3LYP/def2-TZVP level of theory deliver a low singlet-triplet energy gap of 1.5 kcal/mol. This gap is notably lower than the singlet-triplet gap of the parent diphenylcarbene which is 3.3 kcal/mol (calculated at the same level of theory),^[41] which nicely demonstrates the electron-donating effect of the dimethylamino substituent. The different orientation of the phenyl rings, like in the two structures of **14a** and **14b** mentioned in chapter 3.2.1, results in only very small energy differences for this system. While for the triplet carbene, the energy difference between these two structures is only 3.1 cal/mol, the energy difference for the singlet carbene is zero. Hence, these small differences can be neglected.

Further calculations have been conducted to support the experiments of **14** in water-doped matrices. It is shown that the interaction with water switches the ground state of carbene **14** from triplet to singlet (Figure 3.15), since the stabilization of singlet carbenes with water is considerably higher than the stabilization of triplet carbenes (Table 3.2) It is determined that the singlet state of this complex is 4.4 kcal/mol below the triplet state.

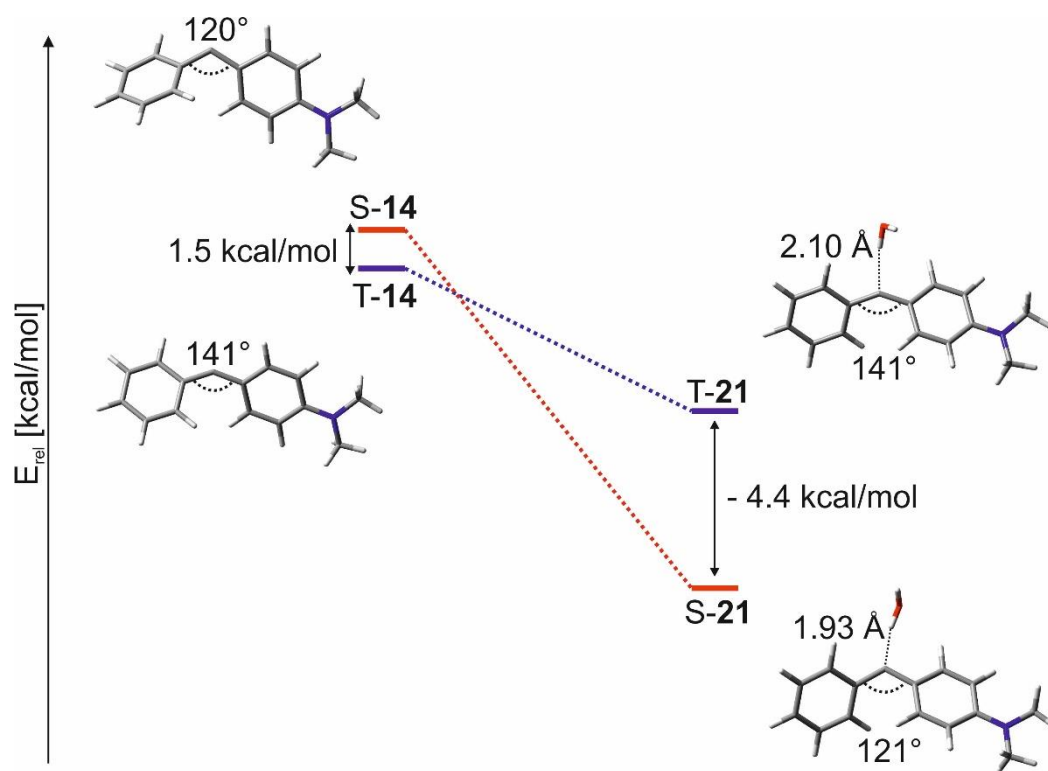


Figure 3.15: Singlet-triplet energy gaps of carbene **14** and carbene-water-complex **21** calculated at the B3LYP/def2TZVP level of theory.

Table 3.2: Stabilization energies (ΔE_s) and singlet-triplet gaps (ΔE_{ST}) of water complex **21** calculated at the B3LYP/def2-TZVP level of theory. The energies are given in kcal/mol.

ΔE_s (S- 21)	ΔE_s (T- 21)	ΔE_{ST}
- 10.5	- 4.6	- 4.4

For the insertion reaction of complex S-**21** to alcohol **22**, the intrinsic reaction coordinate (IRC) was calculated at the B3LYP/def2-TZVP level of theory. The IRC shows that the conversion to **22** occurs via a transition state that is 7.4 kcal/mol higher in energy than the water-complex S-**21** (Figure 3.16).

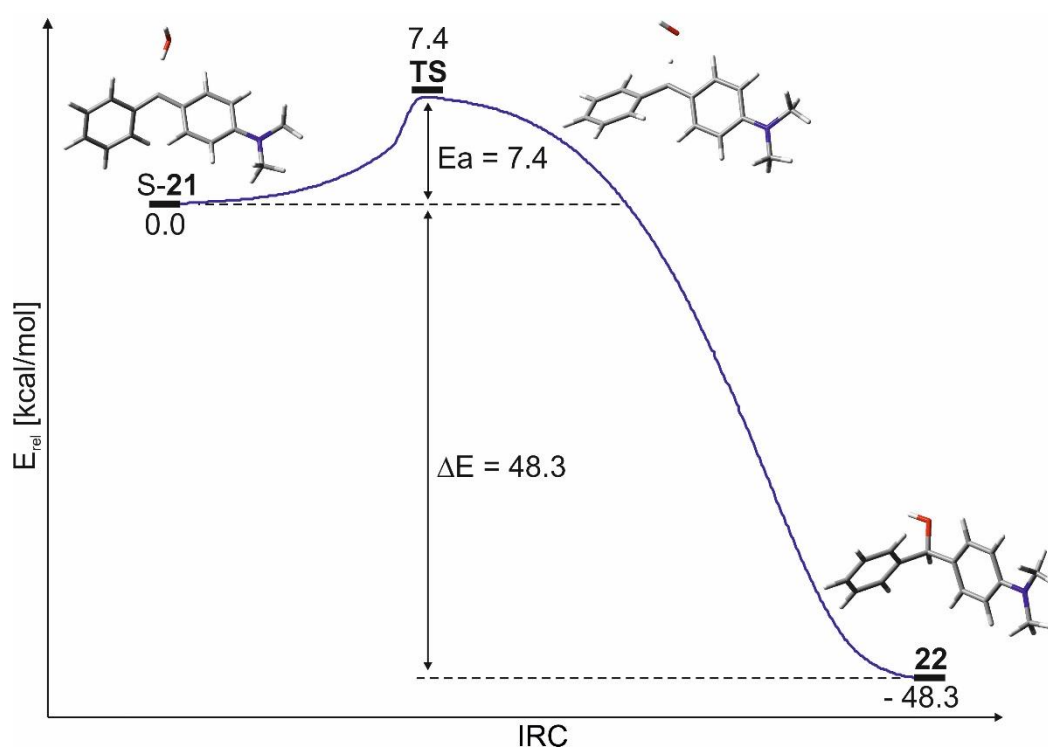
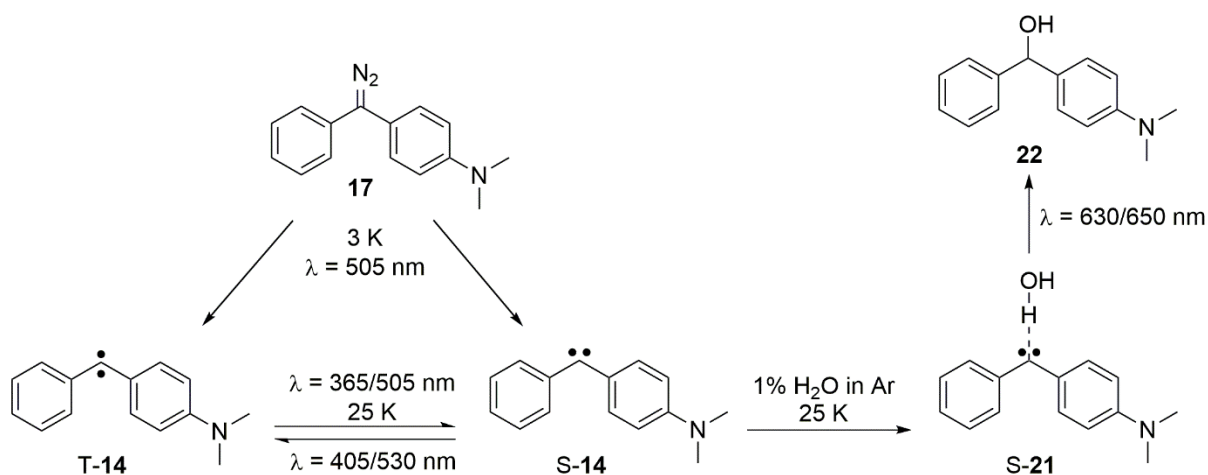


Figure 3.16: IRC of the rearrangement of water-complex S-**21** to alcohol **22**. The energies are given in kcal/mol and were calculated at the B3LYP/def2-TZVP level of theory.

3.2.4. Conclusions

The reactive intermediate [4-(Dimethylamino)phenyl]phenylcarbene (**14**) was generated in matrices of solid argon, xenon and nitrogen as well as in water-doped argon and was investigated via IR, UV/Vis and EPR spectroscopy. It was detected that this carbene **14** is magnetically bistable under these conditions and that both the singlet and triplet state are coexisting. Quantum chemical calculations at the B3LYP/def2-TZVP level of theory corroborated this notion by predicting a small singlet-triplet energy gap of 1.5 kcal/mol. In argon and xenon, it was possible to reversibly switch the spin state by photochemical or thermal methods. Irradiation with 530 nm or 405 nm light converted singlet carbene S-**14** into its triplet state, while irradiation with 505 nm or 365 nm light as well as annealing to 25 K converted the triplet carbene T-**14** back into its singlet state. In N₂ matrices, it was possible to generate T-**14** under the same conditions, but this process was not reversible. In all matrices, complete conversion to 100% singlet or triplet carbene could not be obtained.

In water-doped argon matrices, carbene **14** formed the hydrogen bonded singlet water complex S-**21** after annealing to 25 K. Calculations showed that this complex formation resulted in a change of the spin ground state from triplet to singlet, with an energy gap between T-**21** and S-**21** of -4.4 kcal/mol. Both the amount of S-**14** and T-**14** decreased. While the decrease of S-**14** occurs due to interactions with water, it is not clear if the decrease of T-**14** is also resulting from carbene-water interactions (by water switching the spin-state of T-**14** to singlet before complex formation) or only from thermal conversion to the singlet state. Irradiation with light of 650 nm or 630 nm converted complex S-**21** to alcohol **22** as the insertion product.

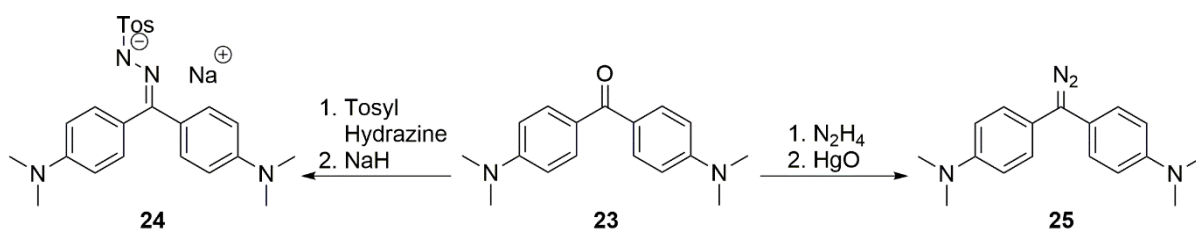


Scheme 3.6: Formation of carbene **14** in both its singlet and triplet state, and the reaction pathway with water to the corresponding alcohol **22**.

3.3. Further potential diphenylcarbenes with magnetic bistability

3.3.1. Bis[4-(dimethylamino)phenyl]carbene

Another research project concerning magnetically bistable carbenes is the investigation of bis[4-(dimethylamino)phenyl]carbene (**15**). For this carbene, a triplet ground state with a singlet-triplet gap of 0.2 kcal/mol was calculated at the B3LYP/def2-TZVP level of theory. Due to this low energy gap, it is assumed that this carbene is bistable and forms as a mixture of its singlet and triplet states. As mentioned before, *Humphreys* and *Arnold* stated that **15** exhibits an EPR spectrum and thus concluded that it is most likely a triplet ground state carbene.^[105-106] However, investigations concerning the magnetic bistability have not been conducted yet. To investigate this topic, the carbene precursors **24** and **25** were synthesized to be used in matrix isolation experiments.



Scheme 3.7: Synthetic pathway to synthesize the compounds **24** and **25** as the precursors of bis[4-(dimethylamino)phenyl]carbene. For the synthesis of sodium salt **24**, ketone **23** was converted to the corresponding tosyl hydrazone and deprotonated with sodium hydride. Diazo compound **25** was obtained after **23** was converted to a hydrazone and oxidized with yellow mercury oxide.^[112-113]

The attempts to deposit **24** or **25** in an argon matrix at 3 K were not successful. Instead, these compounds decomposed during the sublimation at 50–100 °C in high vacuum and dimerized. As an alternative to the isolation of these compounds in gas matrices, experiments in organic glass will be tested in future research. For this method, sublimation of carbene precursor compounds is not necessary, so that temperature-induced decomposition will not occur. Via IR, UV/Vis and EPR spectroscopy, it will be investigated if bis[4-(dimethylamino)phenyl]carbene (**15**) can be formed from the precursor and proves to be a magnetically bistable carbene.

3.3.2. (4-Aminophenyl)phenylcarbene

Since for the carbene [4-(dimethylamino)phenyl]phenylcarbene (**14**) magnetically bistable properties were detected, it was tested if carbenes with similar structural and electronic properties exhibit a similar behavior. Therefore, the similar (4-aminophenyl)phenylcarbene (**16**) was investigated in an argon matrix. For this carbene, a triplet ground state with a singlet-triplet energy gap of 1.8 kcal/mol was calculated at the B3LYP/def2-TZVP level of theory. This energy gap is only 0.3 kcal/mol higher than the calculated gap of **14**, so that it is assumed that **16** would also be magnetically bistable.

At the beginning of the matrix isolation experiments, diazo precursor **26** was sublimed at 55 °C and deposited in an argon matrix at 3 K. The intense N=N stretch vibration of the diazo group at 2044 cm⁻¹ indicates that **26** has been successfully deposited in the matrix (Figure 3.17). However, an additional signal at 1805 cm⁻¹ as well as several undefined signals in the fingerprint region show that large amounts of impurities have also been deposited.

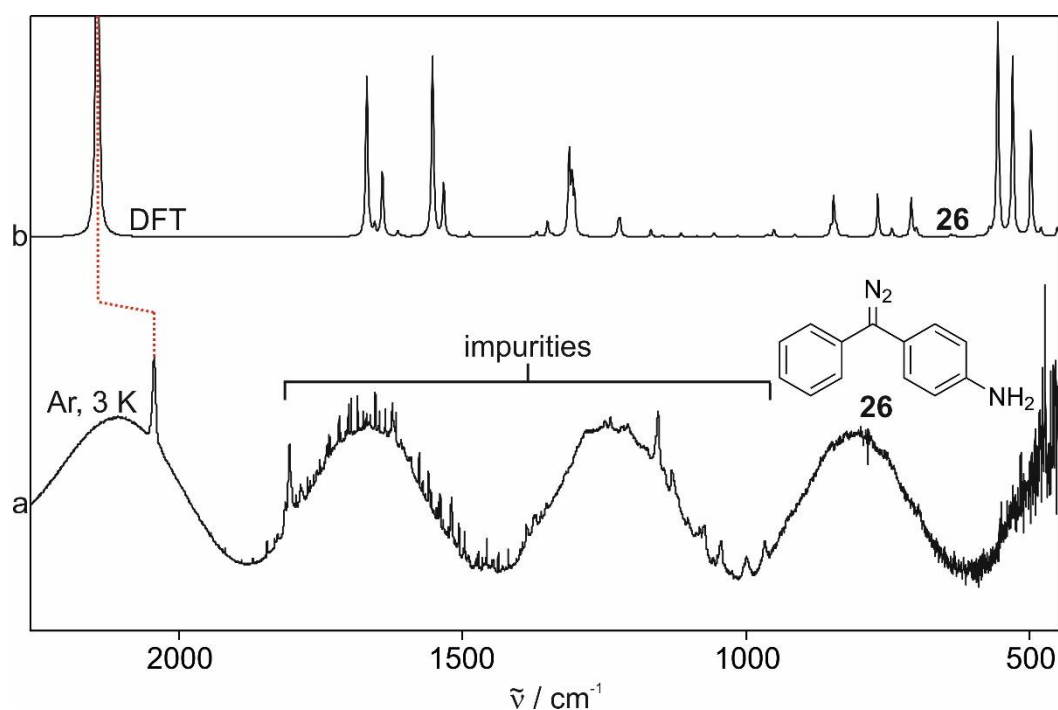


Figure 3.17: Experimental and calculated IR spectra of diazo compound **26**. The intense band at 2044 cm⁻¹ indicates the successful deposition in an argon matrix at 3 K. (a) Experimental IR spectrum in an argon matrix at 3 K. Large amounts of impurities and noise are detected. (b) Theoretical IR spectrum of **26** calculated at the B3LYP/def2-TZVP level of theory.

It is assumed that these impurities consist of the corresponding ketone and decomposition products of diazo compound **26**. Since the diazo compound is rather sensitive and

decomposition occurs already during the synthesis and purification, it was not possible to remove these impurities after the synthesis. Furthermore, it is possible that thermal decomposition occurred during the sublimation of **26** at 55 °C. Due to the low intensity of the signals of **26** as well as due to the impurity signals and the presence of noise in the range of 1500–1600 cm^{-1} , it is not possible to properly compare the experimental and theoretical IR spectrum calculated at the B3LYP/def2-TZVP level of theory. However, the diazo group signal indicates the presence of compound **26**.

Subsequent irradiation with 505 nm LED light for two hours resulted in the vanishing of the diazo signal (Figure 3.18). The difference IR spectrum shows that several small new signals appeared that were assigned to carbene **16**.

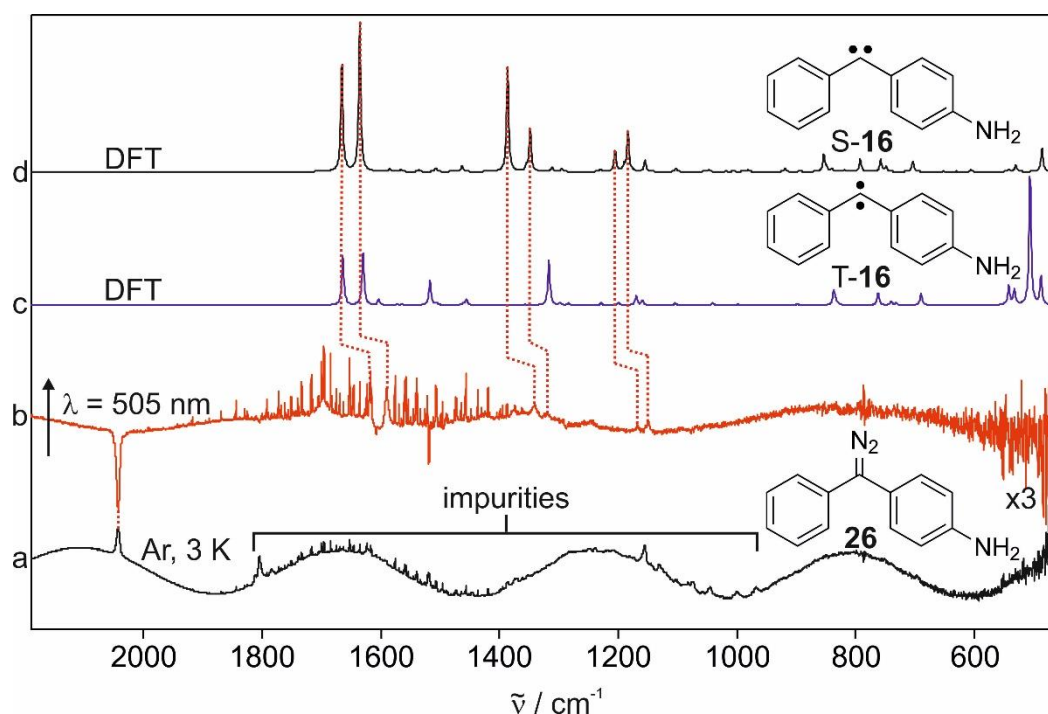


Figure 3.18: Formation of carbene **16** after photolysis of diazo precursor **26**. (a) IR spectrum of diazo compound **26** at 3 K. Large amounts of impurities and noise are detected. (b) IR difference spectrum after photolysis with 505 nm light. The signals pointing upwards are assigned to carbene **16** (except for the noise between 1500–1600 cm^{-1}), the signals pointing downwards to **26**. (c-d) Theoretical IR spectra of triplet carbene T-**16** (spectrum c) and singlet carbene S-**16** (spectrum d) calculated at the B3LYP/def2-TZVP level of theory.

Since the new appearing signals have a low intensity, the assignment of the signals is challenging to conduct. However, comparison with theoretical spectra of the singlet and triplet carbene S-**16** and T-**16** calculated at the B3LYP/def2-TZVP level of theory shows that the new signals are similar to the calculated spectrum of S-**16**. No signals can be assigned to T-**16** due to low overall intensities, so that it is still unclear if triplet signals are present. Subsequent

irradiation experiments indicated that irradiation with light of 505 nm and 405 nm resulted in small changes in the spectrum (Figure 3.19). Irradiation with 505 nm led to an increase of several signals that showed similarities to the theoretical IR spectrum of singlet carbene S-16. The following irradiation with 405 nm light reversed this effect and resulted in a decrease of the same signals. For both irradiation wavelengths, no increase or decrease of signals is observed that shows similarities to the theoretical spectrum of triplet carbene T-16. Therefore, it is not clear if the observed changes resulted from singlet-triplet interconversion. Furthermore, annealing to 25 K led to small changes in the spectrum, but these changes differ from the changes after irradiation and cannot be assigned to any molecule. Hence, it is assumed that these changes were caused by impurities like oxygen.

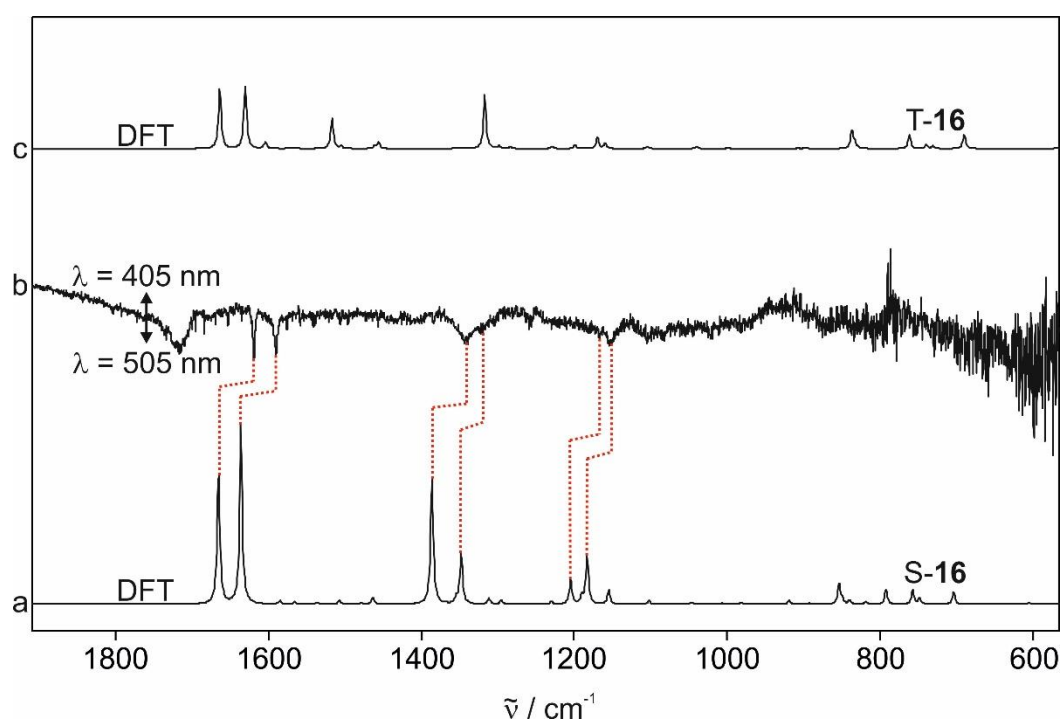


Figure 3.19: Irradiation of carbene **16** with light of 505 nm and 405 nm. (a) Theoretical IR spectrum of S-16 calculated at the B3LYP/def2-TZVP level of theory. (b) IR difference spectrum of carbene **16** after irradiation with different wavelengths. The signals pointing upwards increased after irradiation with 405 nm light and decreased when 505 nm light was used, the signals pointing downwards showed the opposite behavior. (c) Theoretical IR spectrum of T-16 calculated at the B3LYP/def2-TZVP level of theory.

In summary, magnetical bistability has not been detected for carbene **16** yet. To optimize the experimental conditions, it is necessary to find methods to increase the purity of the used diazo precursor **26** and optimize the deposition conditions to increase the signal intensity. In future research, it will furthermore be attempted to obtain more information about the possible magnetically bistable character of this carbene by UV/Vis and especially EPR investigations. While UV/Vis spectroscopy can be used to detect the characteristic singlet and triplet bands of

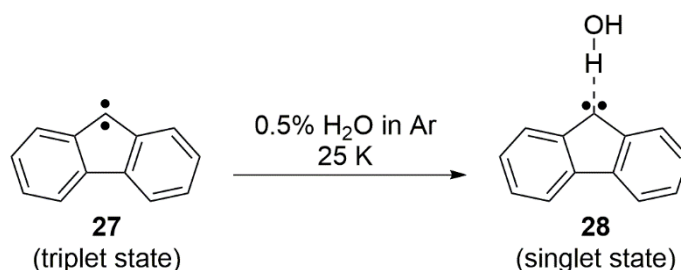
the molecule (which might be in the same range as for carbene **14**), EPR spectroscopy is useful to detect traces of triplet carbene T-**16** that were not visible during the IR investigation. Furthermore, singlet-triplet interconversion can directly be observed via this spectroscopic method.

4. Investigation of Fluorenylidenes

4.1. Introduction

Several of the magnetically bistable carbenes recently reported undergo singlet-triplet interconversion when irradiated with light of different wavelengths or annealed to elevated temperatures.^[102-104] All of these carbenes have in common that their structure is rather flexible. Therefore, the thermal or photochemical switching of the spin state generally includes an appreciable change of geometry, since triplet carbenes favor a larger central C–C–C bond angle than singlet carbenes (Chapter 2.1).^[19, 22] On the other hand, rather rigid carbenes that would potentially exhibit spin bistability have rarely been reported.

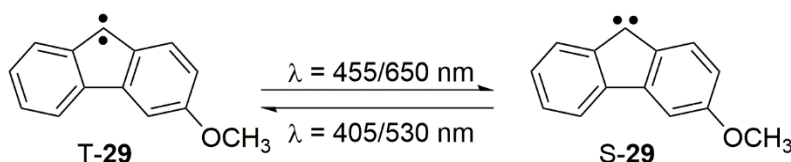
Fluorenylidene (**27**) is a rigid carbene that has thoroughly been investigated in past research concerning reactivity and spin equilibration.^[114-117] Like other arylcarbenes, **27** is initially formed in its singlet state after photolysis but quickly converts to its triplet ground state by intersystem crossing.^[118-119] Magnetical bistability has not been observed for this carbene due to its singlet-triplet energy gap ($\Delta E_{S-T} = 3.4$ kcal/mol, CCSD(T)/cc-pVDZ//B3LYP-D3/def2-TZVP level of theory)^[109] that is larger than the gaps of the reported bistable carbenes. However, experiments in water-doped argon matrices showed that, similar to diphenylcarbene (**9**),^[41] single water molecules switch the spin ground state of **27** from triplet to singlet by forming a hydrogen-bonded complex.^[109]



Scheme 4.1: Formation of a hydrogen-bonded water complex **28** by annealing **27** to 25 K in a water-doped argon matrix. The interaction with water switches the spin ground state from triplet to singlet.

The spin ground state of arylcarbenes can also be tuned by adding electron-donating substituents like methoxy groups, e.g. in bis(p-methoxyphenyl)carbene (**11**) that has a lower singlet-triplet gap than **9**.^[103] This effect was also predicted by Sheridan as well as by Humphreys and Arnold.^[120-121] In addition, the orientation of the methoxy group was found to selectively stabilize a particular spin state in 3-methoxy-9-fluorenylidene (**29**), as reported by

Sander and coworkers. It was shown that this carbene is magnetically bistable and is formed as a mixture of its singlet and triplet state.^[122] Similar to the bistable diphenylcarbene-based carbenes, irradiation with light of different wavelengths influenced the singlet-triplet ratio (Scheme 4.2). Irradiation with 405 nm or 530 nm light switched the spin state from singlet to triplet, whereas light of 455 nm or 650 nm light reversed this process. Thermally induced singlet-triplet interconversion was not observed for this carbene.



Scheme 4.2: Singlet-triplet interconversion of carbene **29** by irradiation with light of different wavelengths.

Since the geometry at the carbene center of **29** is rather rigid, the conversion from the singlet to the triplet state or vice versa results only in a C–C–C bond angle difference of 10°. However, the spin inversion is accompanied by a major geometry change at the methoxy substituent. In the singlet state, the methoxy group is orientated towards the carbene center (conformer *u*) while in the triplet state, the group is oriented towards the opposite direction (conformer *d*). It is assumed that this geometry change is also affecting the singlet-triplet interconversion, since a change of the conformer also results in the change of the spin. Such conformational spin switching is possible because the energy differences (and the energy barriers) between the different conformers and spin states are rather low (Chart 4.1).

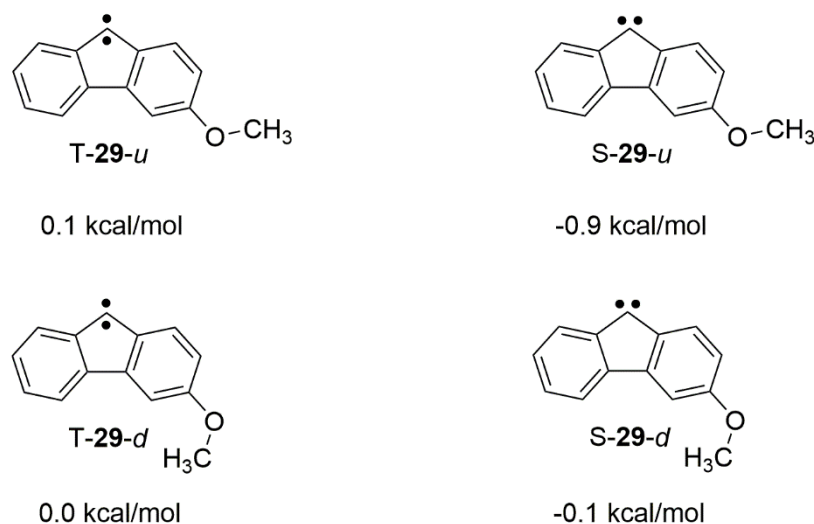


Chart 4.1: Different conformers of **29** in its singlet and triplet state. The energies relative to conformer T-29-*d* were calculated at the CCSD(T)/cc-pVTZ//B3LYP/def2-TZVP level of theory.^[122]

So far, carbene **29** is the only reported bistable carbene with a rigid structure at the carbene center. The following chapters will describe recent experiments and calculations about two further rigid fluorenylidene-based carbenes. Both the carbenes 3,6-dimethoxy-9-fluorenylidene (**30**) and 3-hydroxy-9-fluorenylidene (**31**) have small singlet-triplet energy gaps and exhibit different conformers due to different orientations of the substituents (Chart 4.2).

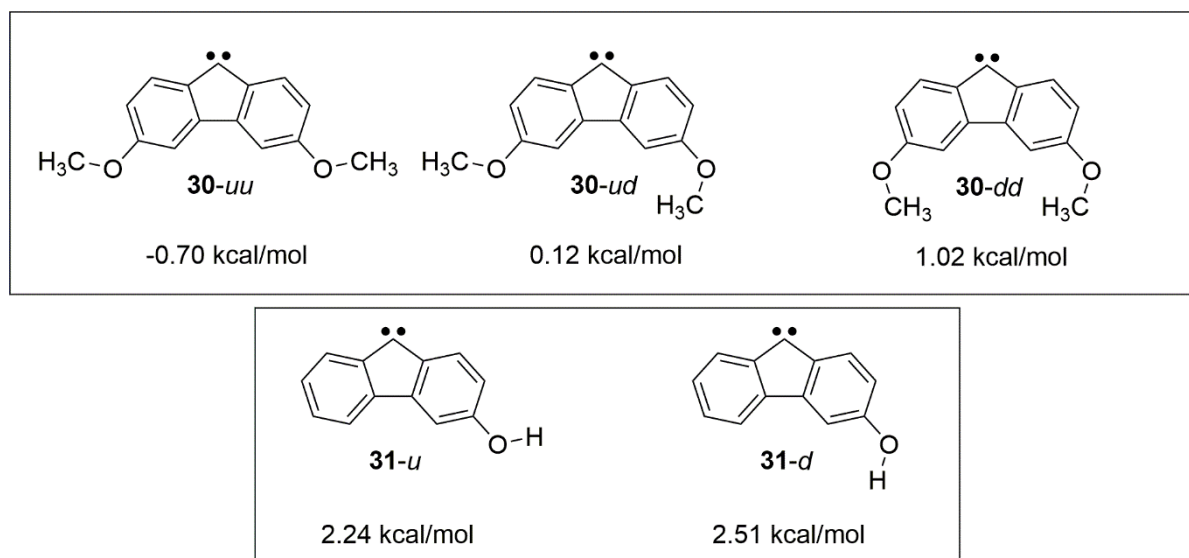


Chart 4.2: Fluorenylidene-based carbenes **30** and **31** and their different conformers. The energies below the molecules correspond to the singlet-triplet energy gaps of the conformer, calculated at the B3LYP/def2-TZVP level of theory.

Carbene **30** has already been investigated via UV/Vis and EPR spectroscopy in organic glass at 77 K by Schuster.^[123] It was detected that the EPR spectrum of **30** did not show any signals, hence it was assumed that this carbene is present in only its singlet state. Calculations as well as experimentally obtained singlet-triplet energy gaps confirmed this assumption, delivering an experimental singlet-triplet gap of approximately -2.7 kcal/mol.^[124] Therefore, 3,6-dimethoxy-9-fluorenylidene was reported as the first known singlet ground state carbene without a heteroatom directly attached to the carbene center. Previously reported singlet carbenes included e.g. phenylhalocarbenes with halogen atoms next to the carbene center.^[125] It was shown in previous research that fluorenylidene and other triplet state arylcarbenes tend to react with hydrocarbons.^[126-128] Therefore, it is possible that traces of **30** in its triplet state would have reacted with the organic glass material in the experiments of Schuster, preventing the detection of triplet carbene in the EPR spectrum. Hence, matrix isolation and spectroscopic characterization of carbene **30** as well as its reaction with water is described in the next sections.

Substitution of the OCH₃ group in carbene **29** by an OH group would enhance its functionality due to potential confinement in molecular networks. Since the structures of 3-hydroxy-9-fluorenylidene (**31**) and carbene **29** are very similar, similar properties are expected. Furthermore, it is assumed that photochemical switching of the conformer of **31** would also result in singlet-triplet interconversion. In this context, Reva and Fausto reported that it is possible to induce conformational switching via vibrational excitation of NH or OH groups.^[129] Accordingly, calculations indicate that excitation of the OH group in **31** might result in singlet-triplet interconversion of the carbene.

However, it is possible that the rotamerization of the OH group occurs through H-atom tunneling. Recent investigations by Räsänen and Fausto already showed that conformational hydrogen tunneling rather readily occurs at OH groups of organic molecules (e.g. formic acid).^[130-131] If this kind of hydrogen tunneling would also influence possible spin interconversion of carbene **31**, then the investigation of this phenomenon would be challenging. To prevent or slow down this type of tunneling process, two possible methods were reported: First, it was shown that this hydrogen tunneling is slowed down if the compound is isolated in a nitrogen matrix.^[132-134] Second, several attempts were conducted to “trap” one of the conformers via hydrogen bonding. To fix the conformer and prevent tunneling, either water molecules were used or the formation of dimers (e.g. formic acid) that form intermolecular hydrogen bonds was conducted.^[135-137] It was observed that this method indeed stabilized one of the conformers and slows down the tunneling.

4.2. 3,6-Dimethoxy-9-fluorenylidene

4.2.1. Experiments in Ar and Xe

IR Experiments

The properties, reactivity and potential spin bistability of 3,6-dimethoxy-9-fluorenylidene (**30**) were investigated in an argon matrix. Prior to the matrix isolation experiments, the carbene precursor 3,6-dimethoxy-9-diazofluorene (**32**) was prepared from 4,4'-dimethoxybenzophenone with the methods presented in literature [123] and [138]. The synthesized diazo precursor was subsequently sublimed at 85 °C and deposited in an argon matrix at 3 K.

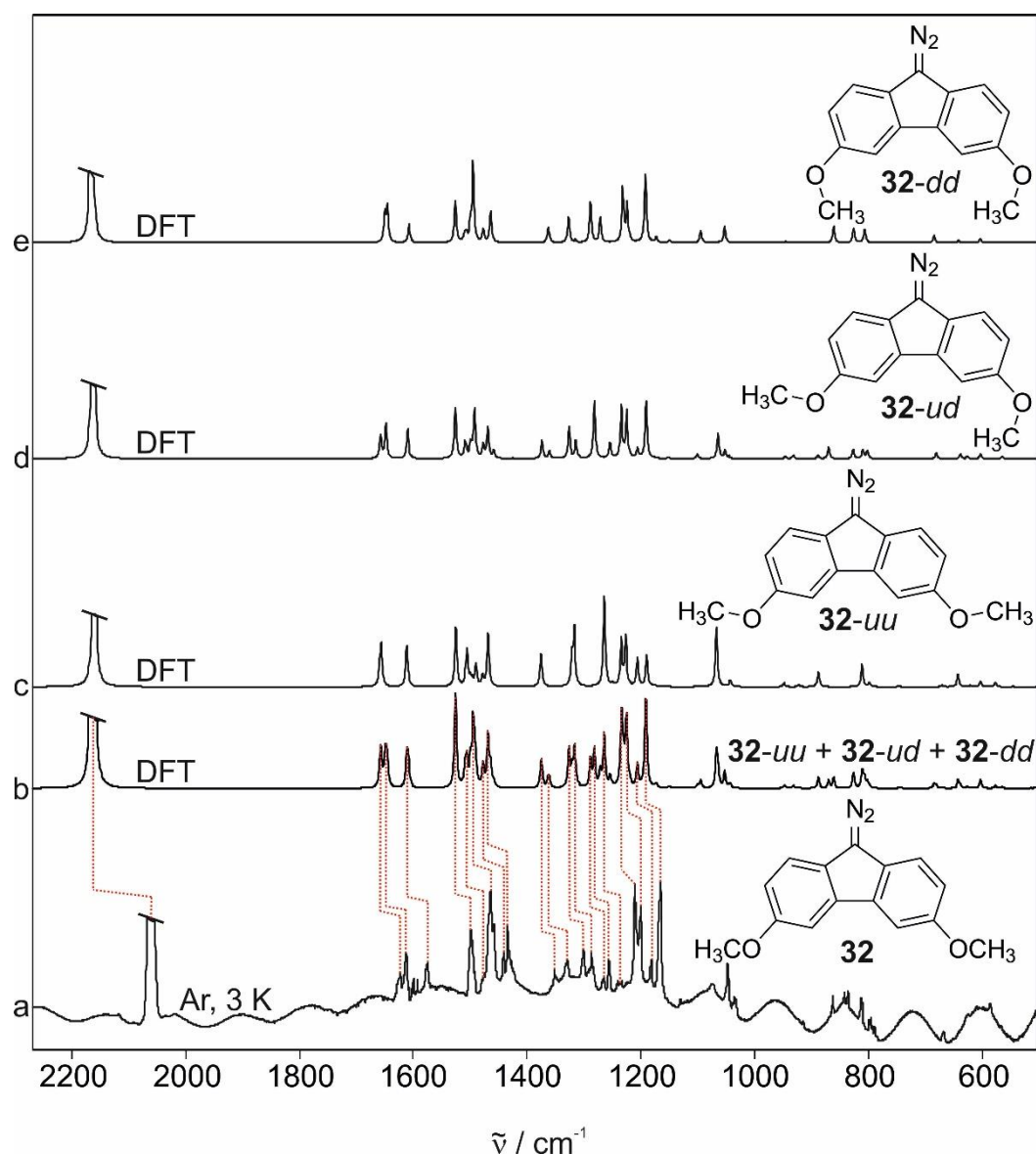


Figure 4.1: Comparison of the experimental and calculated IR spectra of 3,6-dimethoxy-9-diazo fluorene (**32**). (a) Experimental IR spectrum of **32** in an argon matrix at 3 K. (b) Theoretical spectrum of a mixture of the conformers **32-uu**, **32-ud**, and **32-dd** calculated at the B3LYP/def2-TZVP level of theory. (c-e) Theoretical spectra of each conformer **32-uu**, **32-ud** and **32-dd** calculated at the B3LYP/def2-TZVP level of theory.

The experimental IR spectrum shows an intense signal at 2058 cm^{-1} which is assigned to the diazo N=N stretch. Likewise, the other signals match in position and intensity with those calculated at the B3LYP/def2-TZVP level of theory, verifying the successful deposition of **32** (Figure 4.1). However, it was detected that a mixture of three different conformers was present, depending on the orientation of the methoxy substituents. While the signal at 837 cm^{-1} was assigned to only conformer **32-uu**, the signal at 843 cm^{-1} was assigned to **32-ud** and the signal at 863 cm^{-1} to **32-uu**. Integration yields a *uu/ud/dd* ratio of 34/30/36 which is not in accordance with the expected results, since DFT calculations (B3LYP/def2-TZVP) predict that **32-uu** is the lowest-energy conformer and hence was expected to have the highest population.

Subsequent photolysis with 365 nm LED light led to the decomposition of precursor **32** and the formation of 3,6-dimethoxyfluorenylidene (**30**), indicated by the vanishing of the diazo band at 2058 cm^{-1} and the appearance of multiple new signals (Figure 4.2).

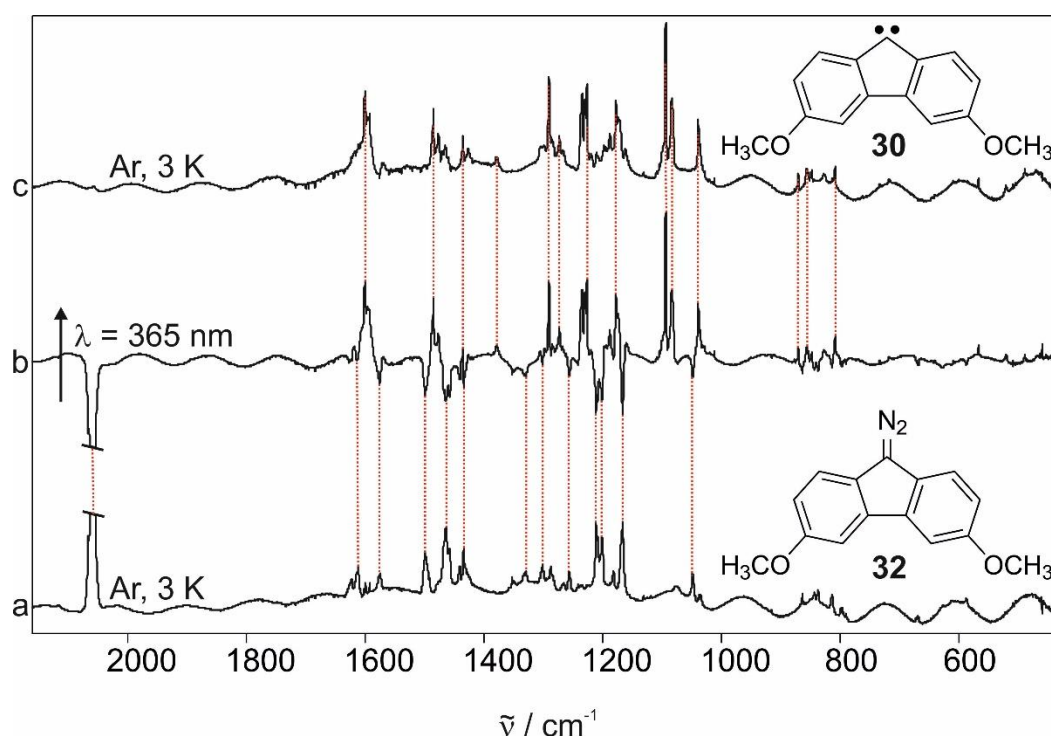


Figure 4.2: Formation of carbene **30** after photolysis of diazo precursor **32** with 365 nm light. (a) Deposition spectrum of diazo precursor **32** in argon at 3 K. (b) Difference IR spectrum after irradiation with 365 nm light. The bands pointing upwards were assigned to **30**, the bands pointing downwards to diazo precursor **32**. (c) IR spectrum of carbene **30** formed after photolysis.

The IR spectra indicate that carbene **30** was obtained only in its singlet state (Figure 4.3), which is in agreement with the UV/Vis and EPR investigations of Schuster.^[123] Similar to the precursor **32**, most of the IR signals of carbene **30** are split into several components, indicating the presence of several conformers. The signals at 1094 cm^{-1} and 870 cm^{-1} are assigned to conformer **30-uu**, the signals at 1285 cm^{-1} , 1234 cm^{-1} and 856 cm^{-1} to **30-ud** and the peak at 1231 cm^{-1} was assigned to only conformer **30-dd**. Furthermore, comparison of the observed and calculated IR spectra as well as signal integration indicate that the mayor product is conformer **30-uu**, giving a conformer ration of $uu/ud/dd = 41/29/30$. In agreement, DFT calculations predict **30-uu** to be the lowest energy conformer.

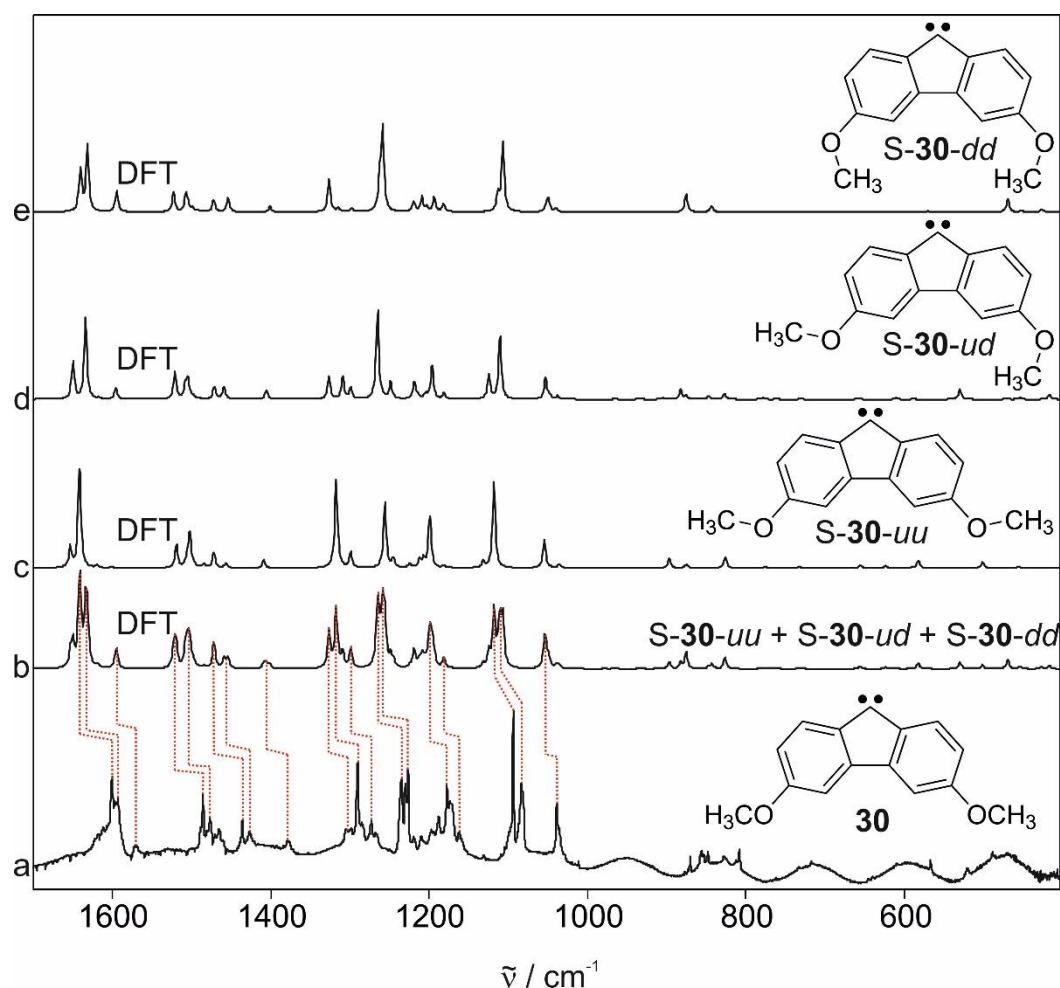


Figure 4.3: Comparison of the experimental and calculated IR spectra of carbene **30**. (a) Experimental IR spectrum of **30** in an argon matrix at 3 K. (b) Theoretical IR spectrum of a mixture of the singlet carbene conformers S-**30-uu**, S-**30-ud**, and S-**30-dd** calculated at the B3LYP/def2-TZVP level of theory. (c-e) Theoretical spectra of each conformer S-**30-uu**, S-**30-ud** and S-**30-dd** calculated at the B3LYP/def2-TZVP level of theory.

In the following experiments, irradiation was conducted to test if light of different wavelengths might induce singlet-triplet conversion. It was observed that LED light with wavelengths of 650 nm and 505 nm led to reversible changes in the IR spectrum (Figure 4.4). However, EPR signals were not observed under the same conditions, indicating that S-T interconversion did not occur, but rather just minor photo-induced conformational changes. Irradiation with 650 nm light resulted in an increase of conformer **30-uu**, while irradiation with 505 nm light formed the other two conformers **30-ud** and **30-dd**. This observation shows similarities to 3-methoxy-9-fluorenylidene (**29**) that also undergoes photochemical conformer switching of the methoxy group.^[122] It is also assumed that for carbene **30**, the conformer switch is possible due to low energy differences between the conformers, as shown by calculations at the B3LYP/def2-TZVP level of theory.

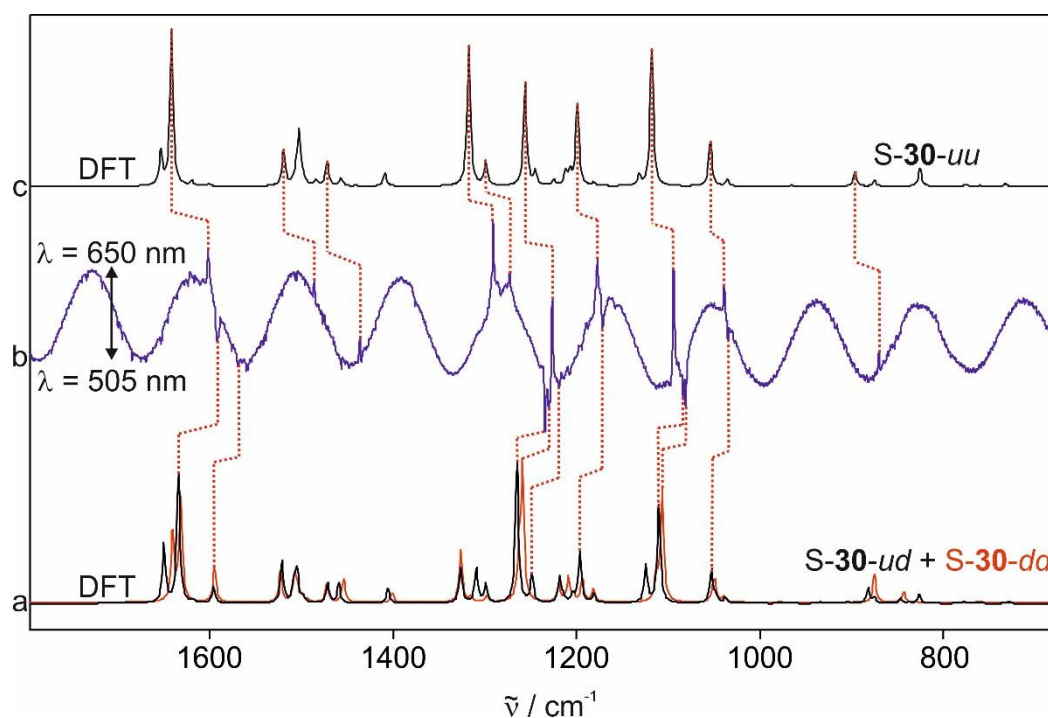


Figure 4.4: Difference IR spectrum of carbene **30** after irradiation with 650 nm and 505 nm light. (a) Theoretical IR spectrum of a mixture of the conformers S-30-ud (black spectrum) and S-30-dd (red spectrum) calculated at the B3LYP/def2-TZVP level of theory. (b) Experimental IR difference spectrum. The signals pointing upwards were assigned to S-30-uu, the signals pointing downwards to S-30-ud and S-30-dd. (c) Theoretical IR spectrum of conformer S-30-uu calculated at the B3LYP/def2-TZVP level of theory.

Further experiments included the annealing of the matrix to temperatures between 13 K and 25 K to test if this showed similar changes in the spectrum or induced singlet-triplet conversion. During the annealing and subsequent re-cooling to 3 K, only matrix effects were detected in the spectra but no distinct changes. Therefore, it was observed that slight annealing to elevated temperatures did not lead to singlet-triplet conversion or conformer changes.

The irradiation and annealing experiments were repeated in a xenon matrix to test if any differences to the argon matrix could be determined. The results of the experiments in xenon were in accordance with the results in argon and no differences were detected. Even while annealing to 50 K (instead of 25 K, like in argon) only matrix effects were observable.

UV/Vis Experiments

In addition to the IR experiments, further characterization via UV/Vis spectroscopy was conducted. The deposition of diazo precursor **32** as well as the subsequent photolysis were performed under the same conditions as for the IR experiments.

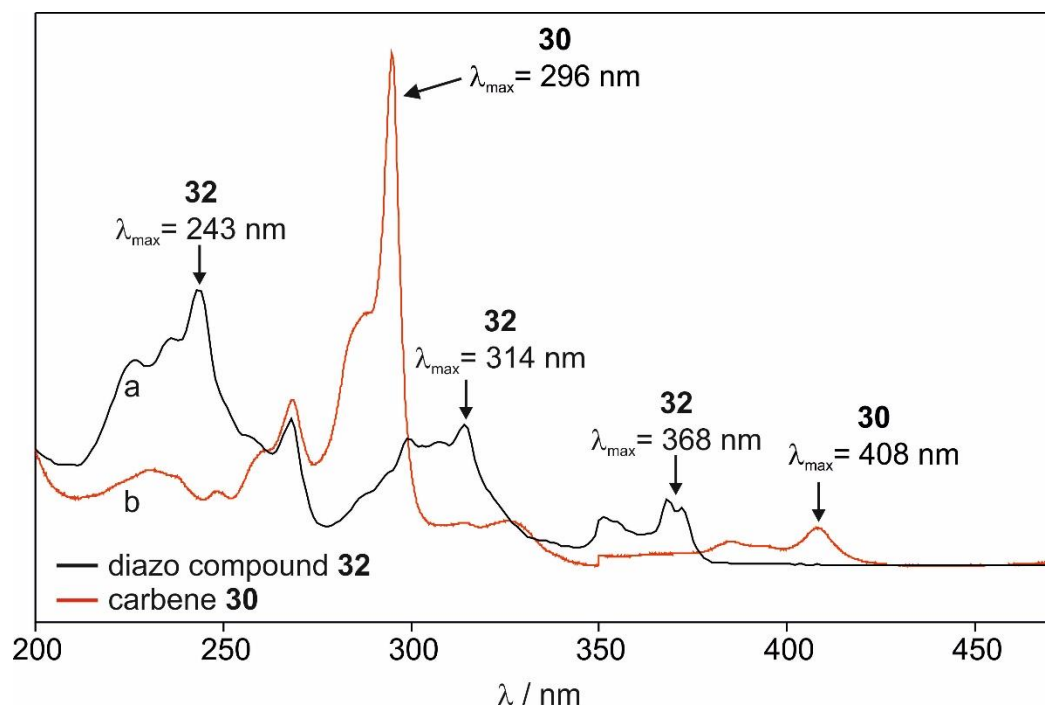


Figure 4.5: UV/Vis spectra of diazo precursor **32** and carbene **30** obtained after photolysis with 365 nm LED light. (a) Deposition spectrum of compound **32** in argon at 8 K. (b) UV/Vis spectrum of carbene **30** obtained in its singlet state after photolysis.

Diazo precursor **32** shows absorption maxima at 234, 314 and 368 nm (Figure 4.5). Irradiation with 365 nm LED light led to a decrease of these signals and to the formation of new intense bands with absorption maxima at 296 and 408 nm. These new signals are assigned to singlet carbene **30**. Comparison with the UV/Vis spectrum of 3-methoxy-9-fluorenylidene confirms this result by showing that its singlet bands are approximately in the same range at 276 and 410 nm.^[122] After 20 minutes of irradiation, the signals of diazo precursor **32** had completely vanished. Upon subsequent irradiation with LED light of 650 nm, it was observed that the most intense peak at 296 nm increased slightly while a smaller shoulder of this peak at 292 nm decreased (Figure 4.6). Irradiation with 505 nm light reversed this effect.

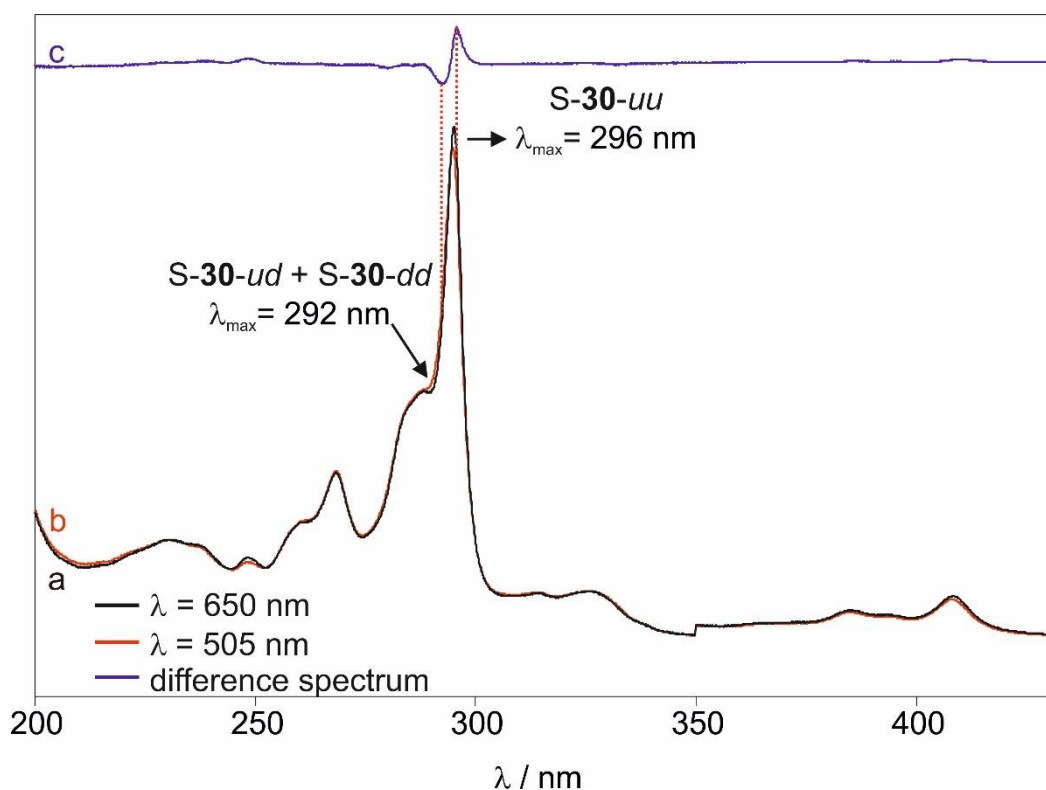


Figure 4.6: UV/Vis spectra of the irradiation experiments of carbene **30**. (a) UV/Vis spectrum after irradiation of **30** with 650 nm light. (b) UV/Vis spectrum after irradiation with 505 nm light. (c) Difference UV/Vis spectrum after irradiation with 650 nm light. The signal pointing upwards was assigned to conformer **S-30-uu**, the signal pointing downwards to the conformers **S-30-ud** and **S-30-dd**.

Considering the result of the IR measurements, the signal at 296 nm is assigned to the carbene conformer **S-30-uu** while the signal at 292 nm is assigned to the two conformers **S-30-ud** and **S-30-dd**. Subsequently conducted annealing experiments to temperatures between 13 K and 25 K showed no distinct changes in the spectra, similar to the IR experiments. In xenon matrices, the irradiation and annealing experiments were repeated and showed results which were in accordance with the experiments in argon.

4.2.2. Reaction with water

IR Experiments

Experiments of 3,6-dimethoxy-9-fluorenylidene with 1%, 2% and 3% water in an argon matrix were conducted to investigate the reactivity of this carbene towards water. After the formation of **30** by photolysis, the matrix was annealed to 25 K. At this temperature, the water molecules diffused through the matrix to the isolated molecules of **30**. The IR difference spectrum shows that the signals of the carbene decreased as well as the intense water signals at approximately 1600 cm^{-1} while several new bands appeared (Figure 4.7). The largest changes in the spectrum are observed when a matrix doped with 3% H_2O is used.

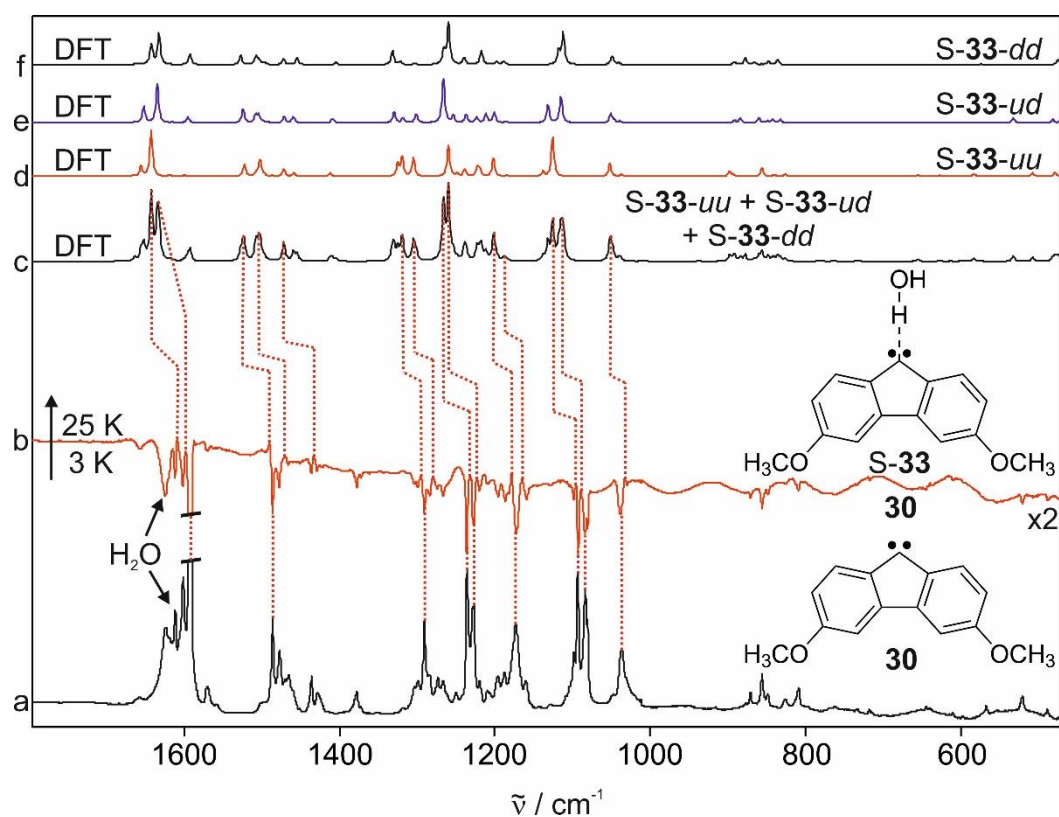


Figure 4.7: Formation of the singlet water complex S-33 by annealing carbene **30** in an argon matrix doped with 3% H_2O . (a) IR spectrum of carbene **30** in an argon matrix doped with 3% H_2O at 3 K. (b) IR difference spectrum after annealing to 25 K. The signals pointing upwards were assigned to singlet water complex S-33, the signals pointing downwards to carbene **30**. (c) Theoretical IR spectrum of a mixture of all three conformers of S-33 calculated at the B3LYP/def2TZVP level of theory. (d-f) Theoretical IR spectra of the different singlet-water-complex conformers S-33-uu, S-33-ud and S-33-dd.

Comparison with theoretical spectra calculated at the B3LYP/def2-TZVP level of theory verifies that these new signals belong to the singlet water-carbene complex S-33. This is in accordance with calculated results that the singlet complex is lower in energy than the triplet complex. Similar to diazo compound **32** and carbene **30**, also water complex S-33 exhibits three conformers. However, multiple signal overlaps complicate the assignment of single signals to the corresponding conformers. The signals at 1302 cm^{-1} and 1280 cm^{-1} are assigned to conformer S-33-*uu*, the signals at 1271 cm^{-1} and 1102 cm^{-1} to S-33-*ud* and the signals at 1375 cm^{-1} and 1427 cm^{-1} to S-33-*dd*. After cooling down again to 3 K, the water complex was kept in the dark for 24 h to test if any insertion of the complex to the corresponding alcohol **34** occurs. However, no changes were observed, excluding any reaction. Irradiation of water-complex S-33 with light of 650 nm and 630 nm led to observable changes in the IR spectrum (Figure 4.8). While the signals of water complex S-33 decreased, new signals increased that were assigned to alcohol **34** by comparison with a reference spectrum.

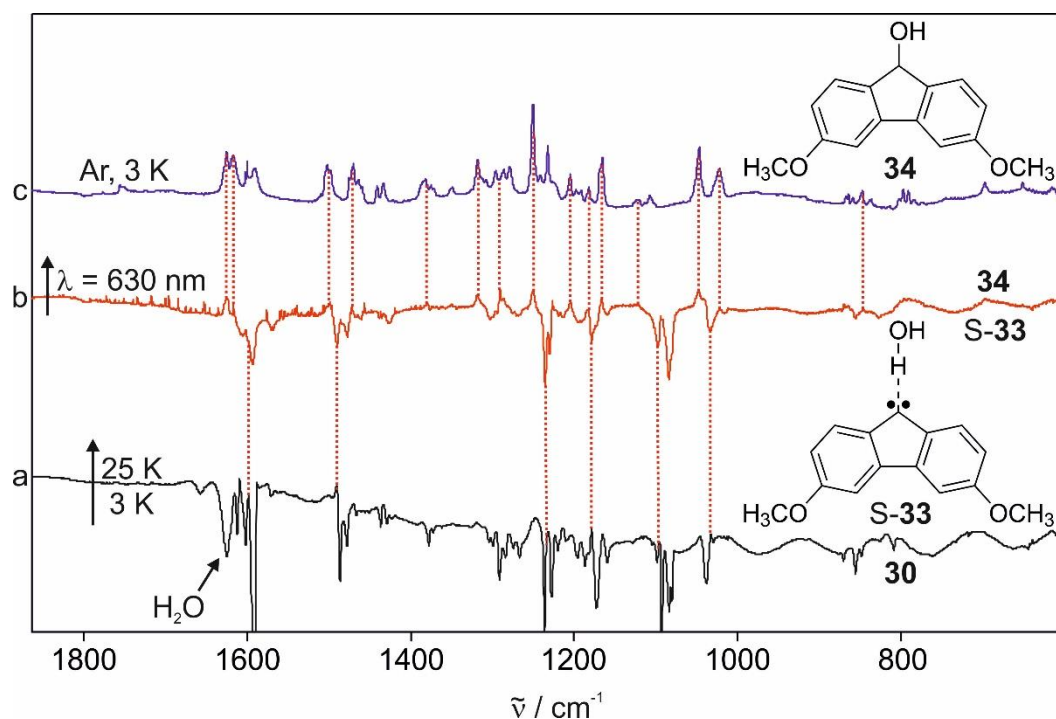


Figure 4.8: Photochemical conversion from water complex S-33 to alcohol **34**. (a) IR difference spectrum after annealing **30** in a water-doped argon matrix to 25 K. The signals pointing upwards were assigned to complex S-33, the signals pointing downwards to singlet carbene **30**. (b) IR difference spectrum after irradiation with 630 nm light. The signals pointing upwards were assigned to alcohol **34**, the signals pointing downwards to singlet water complex S-33. (c) Reference IR spectrum of alcohol **34** in argon at 3 K.

UV/Vis Experiments

The IR investigation of 3,6-dimethoxy-9-fluorenylidene and its interactions with water were supported by additional UV/Vis experiments. After deposition of the diazo precursor in argon doped with 3% H₂O, photolysis and annealing to 25 K for 10 minutes, it was observed that the carbene signals at 296 nm and 408 nm decreased while a new small peak at 421 nm appeared (Figure 4.9).

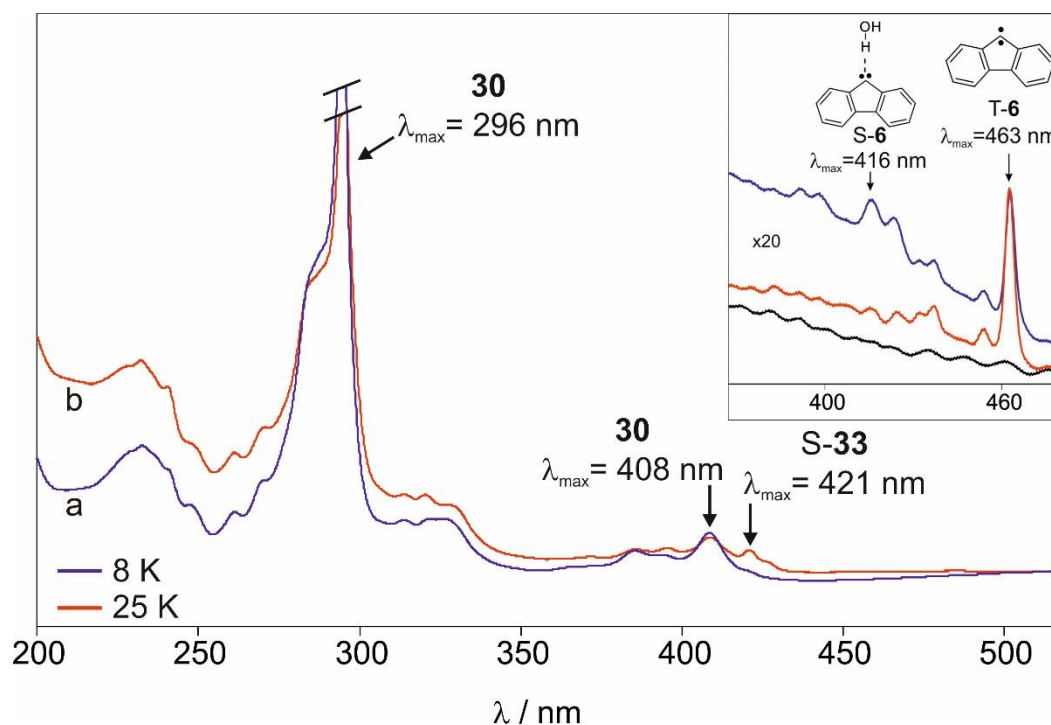


Figure 4.9: UV/Vis spectra of carbene **30** before and after annealing to 25 K in an argon matrix doped with 3 % water. The new appearing signal of water complex S-**33** at 421 nm is compared with the water complex signal of the parent fluorenylidene at 416 nm (reported by Sander and co-workers).^[109] (a) UV/Vis spectrum of carbene **30** at 8 K. (b) UV/Vis spectrum after annealing to 25 K.

Previous research showed that for the unsubstituted fluorenylidene, the signal of the water complex was found in a similar wavelength range at 416 nm.^[109] Hence, the observed signal at 421 nm is assigned to the water complex S-**33**. The matrix was cooled down to 8 K and the water complex was kept in the dark for 24 hours. During this time, no changes in the spectra were observable, in agreement to the IR experiments. After irradiation with LED light of 630 nm for ten minutes, the small signal of the complex S-**33** at 421 nm vanished completely while three new bands at 320, 241 and 232 nm increased (Figure 4.10). Comparison with the UV/Vis reference spectrum of alcohol **34** synthesized by the reduction of 4,4'-dimethoxybenzophenone shows that the increasing peaks after irradiation belong to this alcohol.

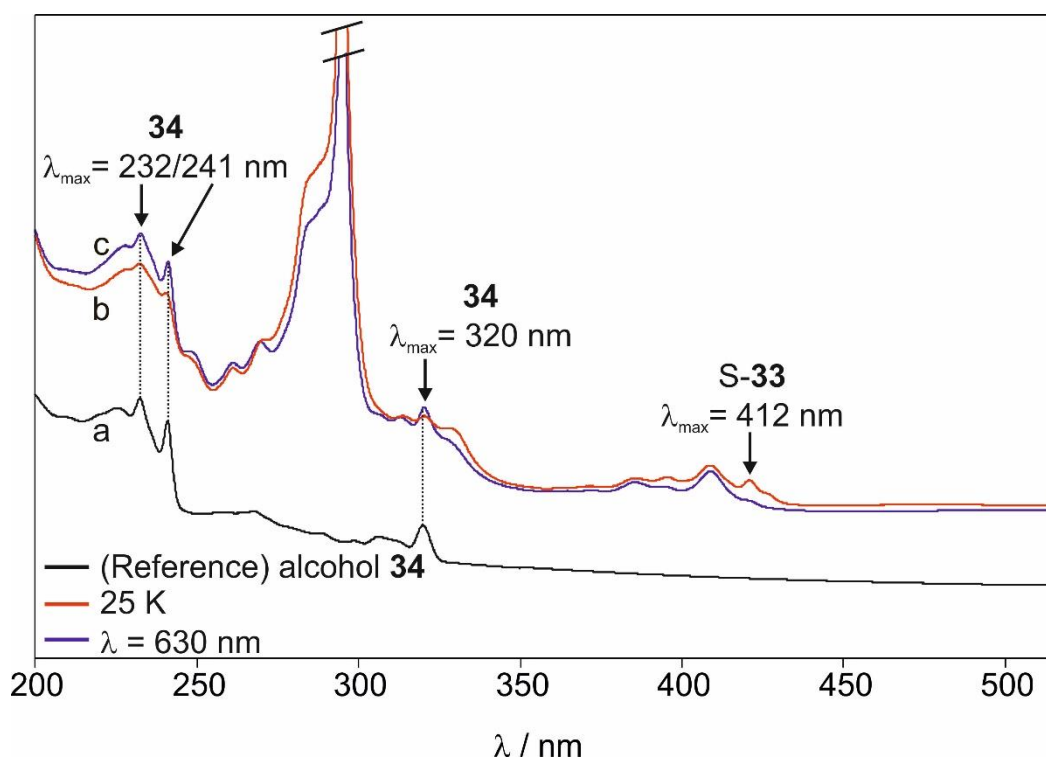


Figure 4.10: UV/Vis spectra of singlet-water complex S-33 before and after irradiation with 630 nm light. Comparison with the reference spectrum of alcohol **34** shows that the irradiation led to the conversion of S-33 to **34**. (a) UV/Vis reference spectrum of alcohol **34**. (b) UV/Vis spectrum at 25 K, after formation of water complex S-33. (c) UV/Vis spectrum after irradiation of S-33 with 630 nm light.

4.2.3. Computational Results

The results of the spectroscopic measurements were supported by quantum chemical calculations at the B3LYP/def2-TZVP level of theory. It is shown that for the most favored conformer **30-uu** of the carbene 3,6-dimethoxy-9-fluorenylidene, a singlet-triplet energy gap of -0.7 kcal/mol is obtained. For the other conformers, singlet-triplet gaps of 0.1 kcal/mol (**30-ud**) and 1.0 kcal/mol (**30-dd**) are obtained. Likewise, the calculated energy differences are considerably larger for the singlet carbene than for the triplet carbene. For S-**30**, the energy differences in relation to the lowest-energy conformer S-**30-uu** are 0.8 kcal/mol (S-**30-ud**) and 1.8 kcal/mol (S-**30-dd**). Triplet carbene T-**30** exhibits energy differences of 0.1 kcal/mol (T-**30-uu**) and 0.2 kcal/mol (T-**30-dd**), in relation to the most favored conformer T-**30-ud**.

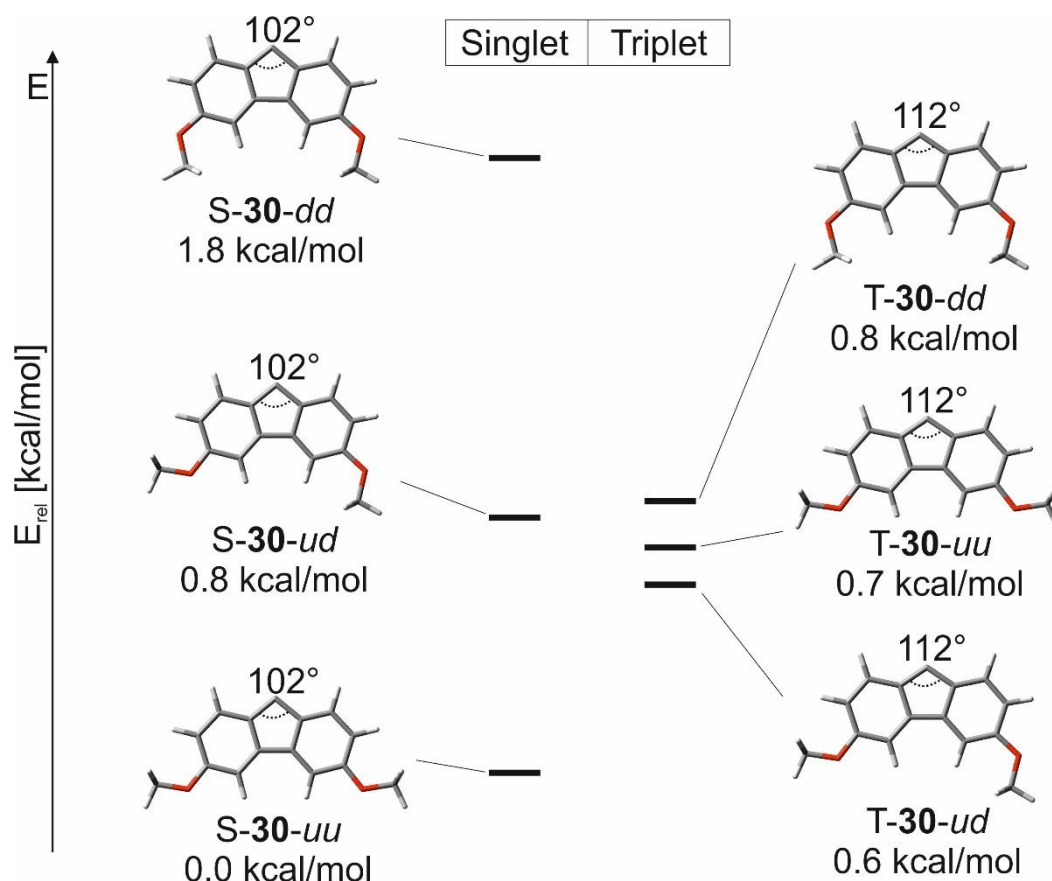


Figure 4.11: Theoretical energy differences of the different conformers of carbene **30** relative to the most stable conformer S-30-uu. It is observed that the energy differences between the singlet carbene conformers were larger than for the triplet carbene conformers due to the larger dipole moments. The energies were calculated at the B3LYP/def2-TZVP level of theory.

This result can be explained by the different dipole moments of singlet and triplet carbene **30**. Singlet carbene S-30 exhibits dipole moments of 3.8 D (S-30-uu), 5.8 D (S-30-ud) and 7.1 D (S-30-dd) while triplet carbene T-30 shows lower values of 0.5 D (T-30-uu), 2.6 D (T-30-ud) and 3.5 D (T-30-dd). Since the singlet carbene is much more polar, the orientation of the methoxy substituent has a larger influence on the dipole moment, the charge separation and hence on the energetic ordering of the conformers.

Calculations of **30** with water show that the formation of a hydrogen-bonded complex with single water molecules favors the singlet state, resulting in a singlet triplet gap that is even more negative than for **30** (Figure 4.12). For the lowest-energy conformer S-33-uuu of the complex, a singlet-triplet gap of -7.9 kcal/mol is calculated at the B3LYP/def2-TZVP level of theory.

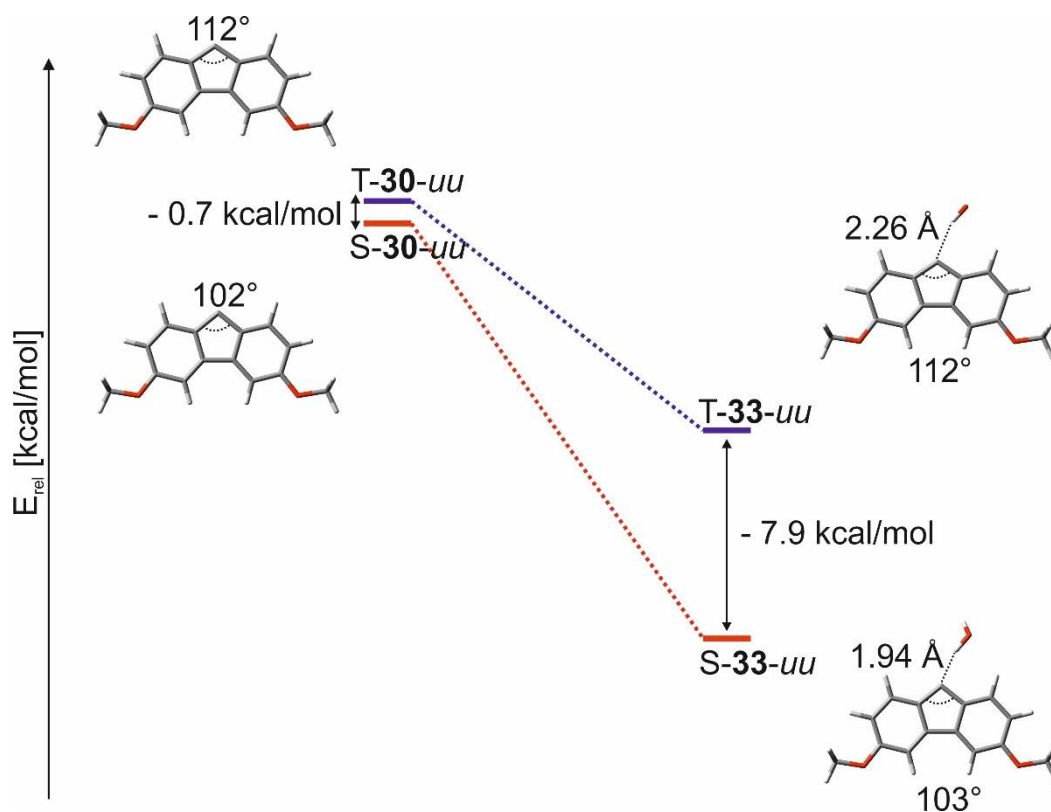


Figure 4.12: Singlet-triplet energy gaps of carbene **30** and carbene-water-complex **33** in their *uu*-conformer, calculated at the B3LYP/def2TZVP level of theory.

The other conformers of the complex exhibit singlet-triplet energy gaps of -7.1 kcal/mol (**33-ud**) and -6.0 kcal/mol (**33-dd**). Since S-**30** is a better hydrogen bond acceptor than T-**30**, the stabilization energy of water complex S-**33** is $7.0 - 7.2$ kcal/mol larger than for T-**33** (Table 4.1). The conformer “*dd*” is slightly less stabilized for both the singlet and triplet complex.

Table 4.1: Stabilization energies (ΔE_s) of singlet and triplet water complex **33** calculated at the B3LYP/def2-TZVP level of theory. The energies are given in kcal/mol.

complex	ΔE_s (singlet)	ΔE_s (triplet)
33-uu	- 10.8	- 3.6
33-ud	- 10.8	- 3.6
33-dd	- 10.5	- 3.5

The calculation of the IRC of the reaction to alcohol **34** shows that the conversion from complex S-**33** to alcohol **34** is proceeding via a transition state that is 6.1 kcal/mol above S-**33** (Figure 4.13). Since this activation barrier can presumably not be overcome at a temperature of 3 K, photoexcitation of complex S-**33** was necessary during the experiments.

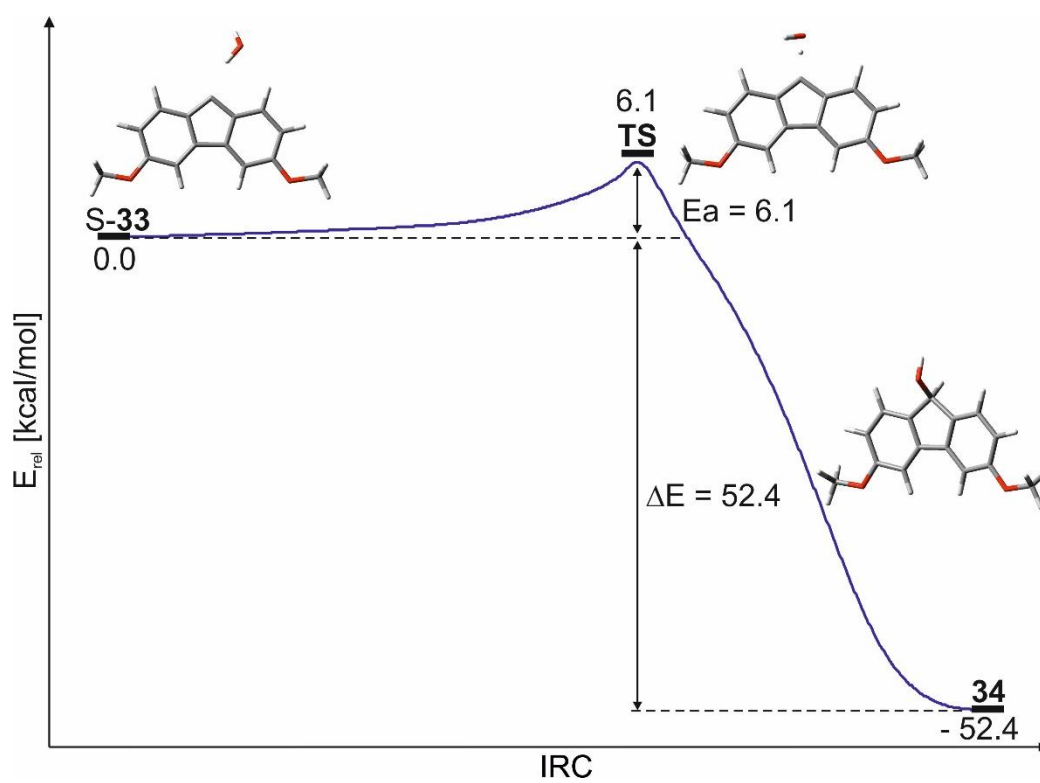
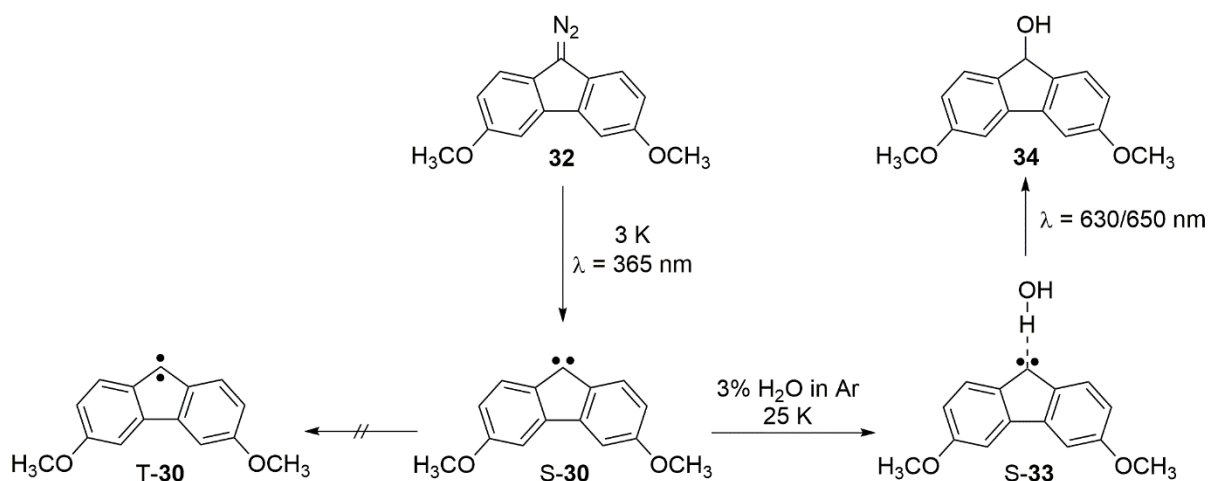


Figure 4.13: IRC of the reaction from water-complex **S-33** to alcohol **34**. The energies calculated at the B3LYP/def2-TZVP level of theory are given in kcal/mol.

4.2.4. Conclusions

3,6-dimethoxy-9-fluorenylidene (**30**) was successfully isolated in argon, xenon or water-doped argon matrices at cryogenic temperatures. It was demonstrated by EPR spectroscopy that **30** exhibits a singlet ground state and experiments with IR and UV/Vis spectroscopy showed that singlet-triplet interconversion does not occur. Therefore, it was verified that this carbene is not magnetically bistable. It was found that **30** is present as a mixture of three conformers, with a singlet-triplet gap of $-0.7 - 1.0$ kcal/mol (depending on the conformer) calculated at the B3LYP/def2-TZVP level of theory. Via irradiation with 650 nm light, a conformer switch to the conformer **30-uu** was induced, while 505 nm irradiation resulted in the conversion to **30-ud** and **30-dd**.

In water-doped argon matrices, the carbene formed the corresponding water complex S-**33** that is also present as a mixture of three conformers. Interactions with water via hydrogen-bonding stabilized the singlet state further and increased the singlet triplet gap to $-6.0 - -7.9$ kcal/mol (depending on the conformer). The water complex was stable under the applied conditions and did not undergo any thermal reaction at 3 – 10 K. The formation of the corresponding alcohol **34** was induced by irradiation with light of 650 or 630 nm.



Scheme 4.3: Generation of carbene **30** in its singlet state under matrix isolation conditions. Conversion to triplet carbene **T-30** is not possible. Interactions with single water molecules formed water complex **S-33** that converts to the corresponding alcohol **34** after irradiation with 630 nm or 650 nm light.

4.3. 3-Hydroxy-9-fluorenylidene

4.3.1. Experiments in Ar, Xe and N₂

IR Experiments

Another carbene system for which magnetic bistability can be envisioned is 3-hydroxy-9-fluorenylidene (**31**). Previously conducted calculations at the B3LYP/def2-TZVP and CCSD(T)/cc-PVDZ//B3LYP-D3/def2-TZVP level of theory predicted a low singlet-triplet energy gap for this system. Due to this low energy gap and a similar structure to 3-methoxy-9-fluorenylidene (**29**), carbene **31** is expected to show a similar behavior to **29** when irradiated or annealed.^[122] To investigate **31**, the carbene precursor **35** was synthesized analogous to the synthesis of diazo precursor **32** according to literature [123] and [138]. Compound **35** was subsequently sublimed at 70 °C and deposited in an argon matrix at 3 K.

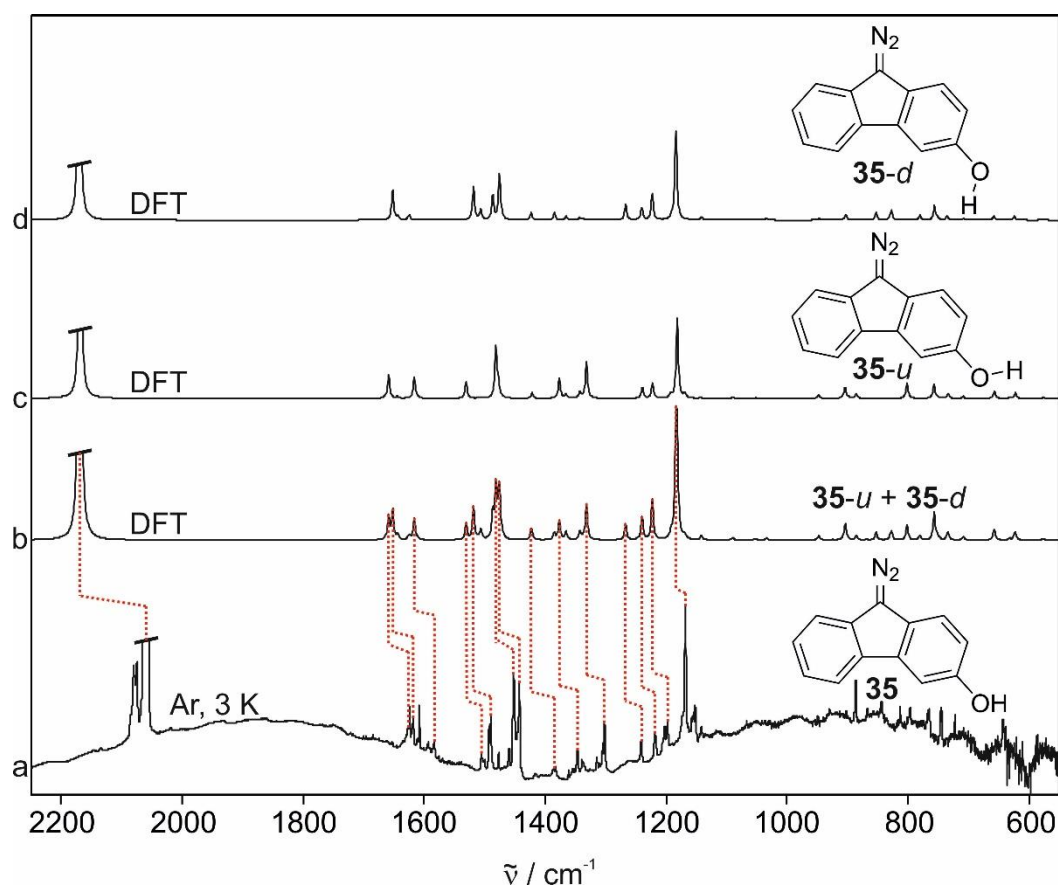


Figure 4.14: Experimental and calculated IR spectra of 3-hydroxy-9-diazo fluorene (**35**). (a) IR spectrum of **35** in an argon matrix at 3 K. (b) Theoretical spectrum of a mixture of the conformers **35-u** and **35-d** calculated at the B3LYP/def2-TZVP level of theory. (c-d) Theoretical spectra of each conformer **35-u** and **35-d** calculated at the B3LYP/def2-TZVP level of theory.

The intense signal at 2058 cm^{-1} which is assigned to the N=N stretch vibration indicates the successful deposition of precursor **35** (Figure 4.14). Furthermore, the signals in the region between 1100 cm^{-1} and 1650 cm^{-1} are in good accordance with the theoretical spectrum. Detailed comparison of the experimental spectrum with the calculated spectra of both conformers shows that several signals can only be assigned to one of the conformers. The signals at 1303 cm^{-1} and 1506 cm^{-1} are assigned to only **35-u**, while the signals at 1242 cm^{-1} and 1490 cm^{-1} are assigned to only **35-d**. This is in agreement with calculations at the B3LYP/def2-TZVP level of theory that predict a very low energy difference between the conformers **35-u** and **35-d**. Photolysis with 365 nm light for 30 minutes led to the decrease of the diazo precursor and to the formation of several new bands that are assigned to **31**.

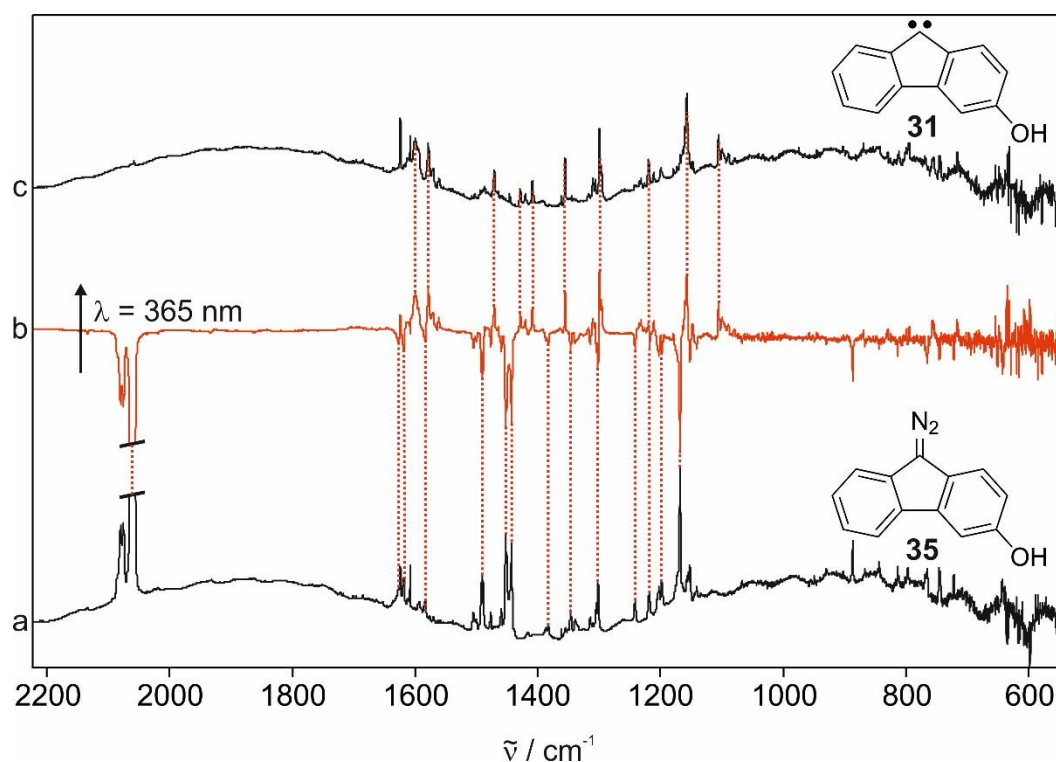


Figure 4.15: Photolysis of diazo precursor **35** with 365 nm light to form carbene **31**. (a) IR spectrum of **35** after the deposition in an argon matrix at 3 K. (b) IR difference spectrum after the photolysis. The signals pointing upwards are assigned to carbene **31**, the signals pointing downwards to diazo precursor **35**. (c) IR spectrum of carbene **31** after photolysis.

The main evidence that the diazo precursor decomposed is the vanishing of the intense diazo stretch signal (Figure 4.15). To investigate if the carbene forms in its singlet or triplet state and as a conformer mixture, theoretical IR spectra calculated at the B3LYP/def2-TZVP level of theory are compared with the experimental spectrum after photolysis (Figure 4.16).

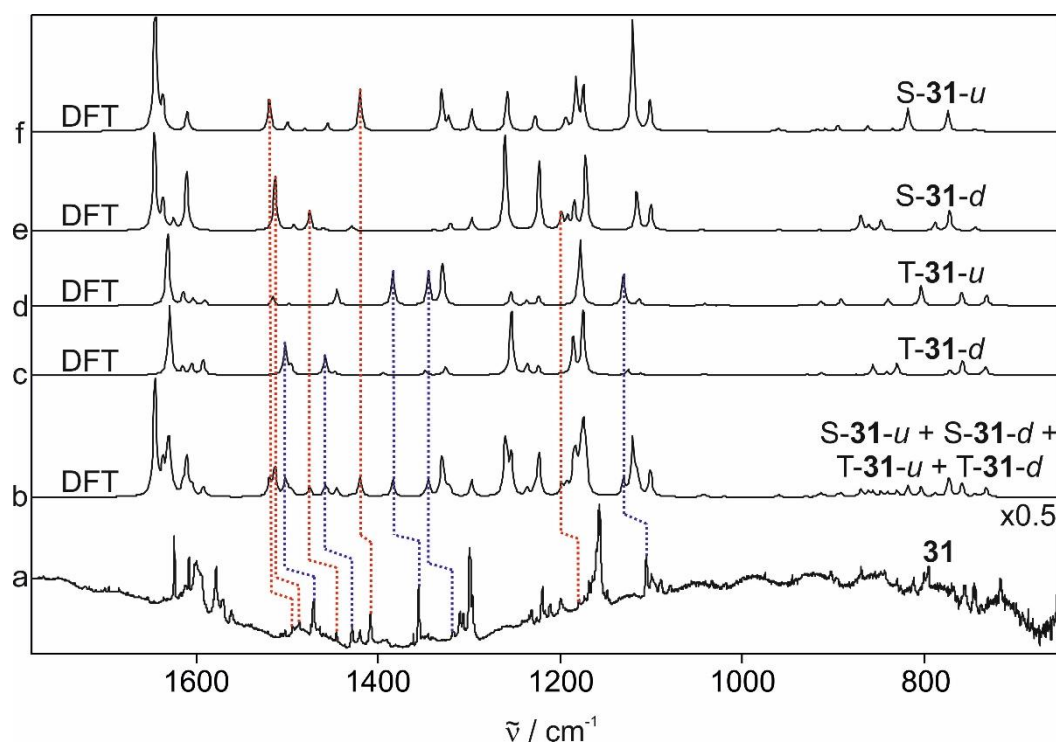


Figure 4.16: Comparison of the IR spectrum of carbene **31** with theoretical spectra of the different singlet carbene conformers **S-31-*u*** and **S-31-*d*** and the triplet carbene conformers **T-31-*u*** and **T-31-*d*** calculated at the B3LYP/def2-TZVP level of theory. The blue dotted lines mark triplet carbene signals, the red dotted lines singlet carbene signals. (a) IR spectrum of carbene **31**. (b) Theoretical IR spectrum of a mixture of **S-31** and **T-31** in its different conformers. (c-f) Theoretical IR spectra of the carbene species **T-31-*d***, **T-31-*u***, **S-31-*d*** and **S-31-*u***, respectively.

Carbene **31** is present as a mixture of its singlet and triplet state. The small signals at 1179, 1487 and 1494 cm^{-1} are assigned to only **S-31**, while the signals at 1106, 1357 and 1561 cm^{-1} are assigned to only **T-31**. This observation is assisted by theoretical calculations that predict a small singlet-triplet gap for **31**. Concerning the intensity of the singlet and triplet signals, it is observed that the relative intensity of the triplet carbene peaks is more intense than the intensity of the singlet carbene peaks. Integration of the signals shows that the singlet-triplet ratio after photolysis is 31/69. In summary, magnetic bistability was detected for carbene **31**. In addition to that, the theoretical IR spectra show that for both **S-31** and **T-31**, both conformers are present. The signals appearing at 1408 cm^{-1} and 1494 cm^{-1} are assigned to conformer **S-31-*u***, the signals at 1179 cm^{-1} and 1487 cm^{-1} to **S-31-*d***. The *u/d* ratio for the singlet carbene was 75/25. Furthermore, the peaks at 1106 cm^{-1} and 1357 cm^{-1} were assigned to **T-31-*u*** while conformer **T-31-*d*** exhibits significant signals at 1430 cm^{-1} and 1471 cm^{-1} . Triplet carbene signal integration delivers a *u/d* ratio of 69/31, so that it is shown that both **S-31** and **T-31** exhibit an excess of the *u*-conformer. These results are in contrast to the similarly structured 3-methoxy-9-fluorenylidene (**29**) that only exhibits the conformers **S-29-*u*** and **T-29-*d***.^[122] To investigate the photochemistry of **31** and to test if possible singlet-triplet interconversion or conformer

switching (like in the case of **14** or **30**) occurs, carbene **31** was irradiated with light in the range of 254 – 650 nm. While no changes in the spectrum were observed after irradiation with light in the range of 365 – 650 nm, 254 nm irradiation led to a decrease of both the signals of S-**31** and T-**31** and to the formation of several new, small signals (Figure 4.17).

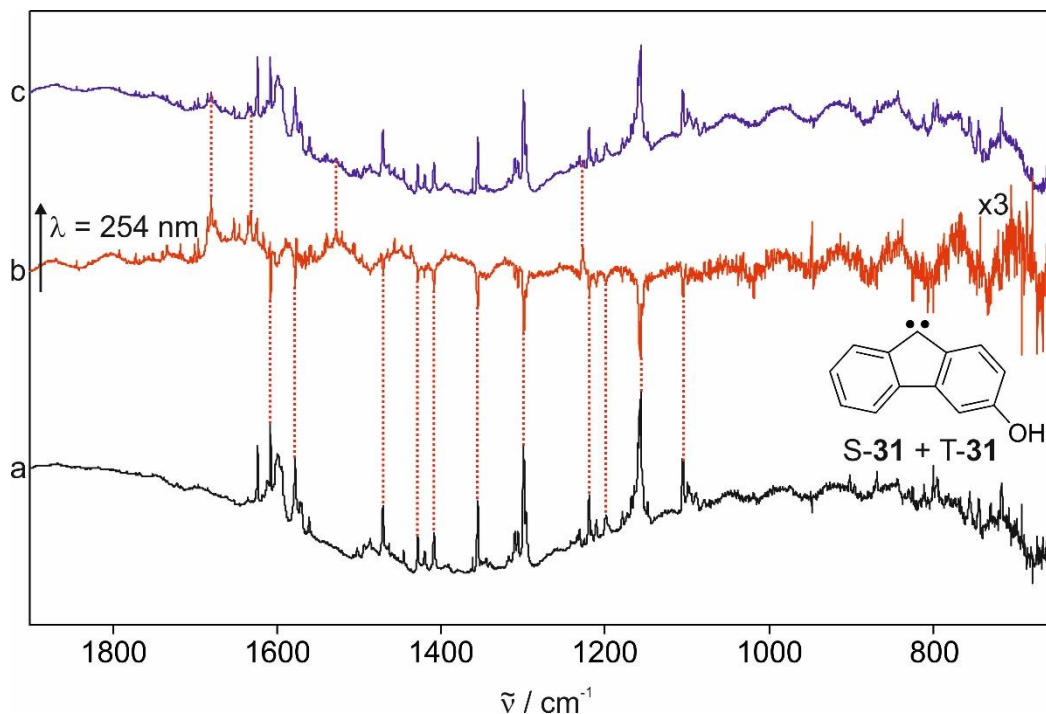


Figure 4.17: Irradiation of carbene **31** with 254 nm light. The decrease of the carbene as well as the formation of several new, unknown signals is observed. (a) IR spectrum of **31** in argon at 3 K. (b) IR difference spectrum after irradiation with 254 nm light. The signals pointing upwards cannot be assigned to any known compound, the signals pointing downwards are assigned to both S-**31** and T-**31**. (c) IR spectrum of **31** after irradiation with 254 nm light.

It is not possible to assign these new signals to S-**31**, T-**31** or any other known compound. Since aromatic hydrocarbons like fluorene-based systems have UV/Vis absorption bands in the UV-region around 249 nm, it is assumed that irradiation with 254 nm into these absorption bands might have induced several side reactions.^[139] However, a solid proof for this assumption has not been obtained yet. In summary, spin interconversion from the singlet to the triplet state or vice versa was not observed. Annealing to 25 K and cooling back down to 3 K did not result in any singlet-triplet switching either.

To test if the matrix material has an influence on the magnetic bistability, the irradiation and annealing experiments were repeated in a xenon matrix. After photolysis of diazo precursor **35**, the carbene **31** was obtained as a mixture of its singlet and triplet state with a singlet-triplet ratio of 48/52. Annealing up to 50 K did not result in any changes. However, irradiation with

450/365 nm light or 405/395 nm light resulted in minimal changes in the IR spectrum that were most distinct for the singlet signal at 1093 cm^{-1} and the triplet signal at 1103 cm^{-1} (Figure 4.18).

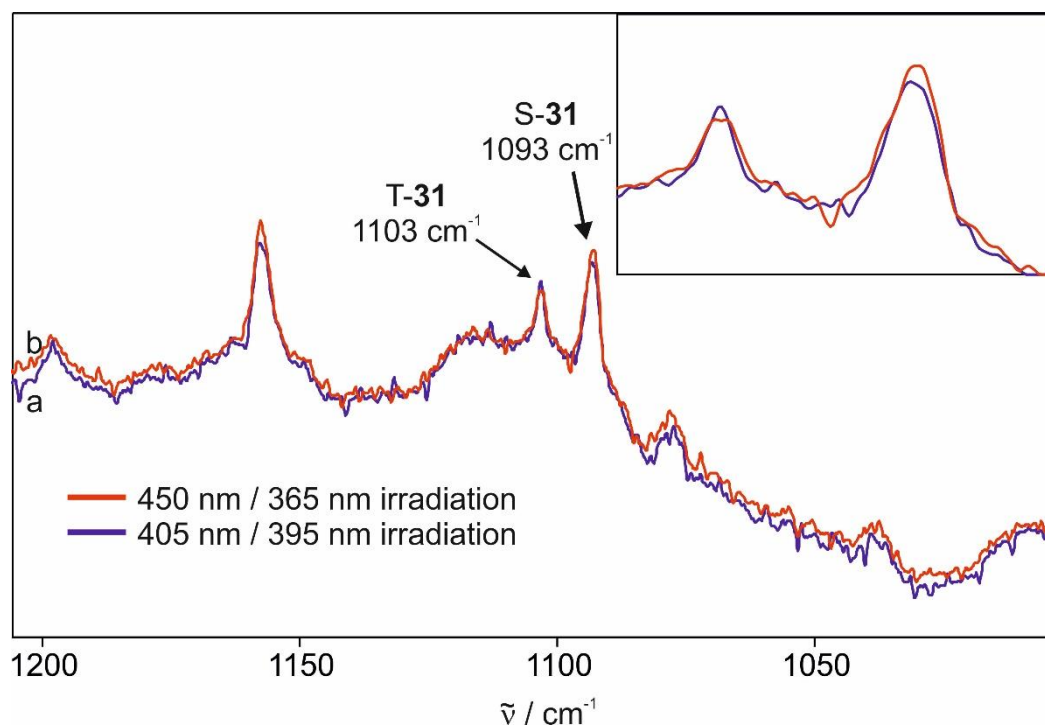


Figure 4.18: Irradiation experiments of carbene **31** in a xenon matrix. (a) IR spectrum after irradiation with 405 nm or 395 nm light. (b) IR spectrum after 450 nm or 365 nm irradiation.

450 nm or 365 nm light resulted in a small increase of the singlet signal at 1093 cm^{-1} while the triplet signal at 1103 cm^{-1} decreased slightly. Irradiation with 405 nm or 395 nm reversed this process. Since the used irradiation wavelengths are in the same range as the typical absorption bands of singlet and triplet fluorenylidene systems, it was assumed that the small changes in the spectrum of **31** might be singlet-triplet interconversion.^[109, 122] However, integration of the peaks leads to the result that the intensity of these two peaks nearly did not change. Hence, it is assumed that either almost no singlet-triplet interconversion occurred, or that the observed changes are only matrix effects.

Subsequently, experiments in a nitrogen matrix were conducted. After the carbene **31** was obtained from its diazo precursor by photolysis, it was observed that it also formed as a mixture of its singlet and triplet state and as a conformer mixture (Figure 4.19).

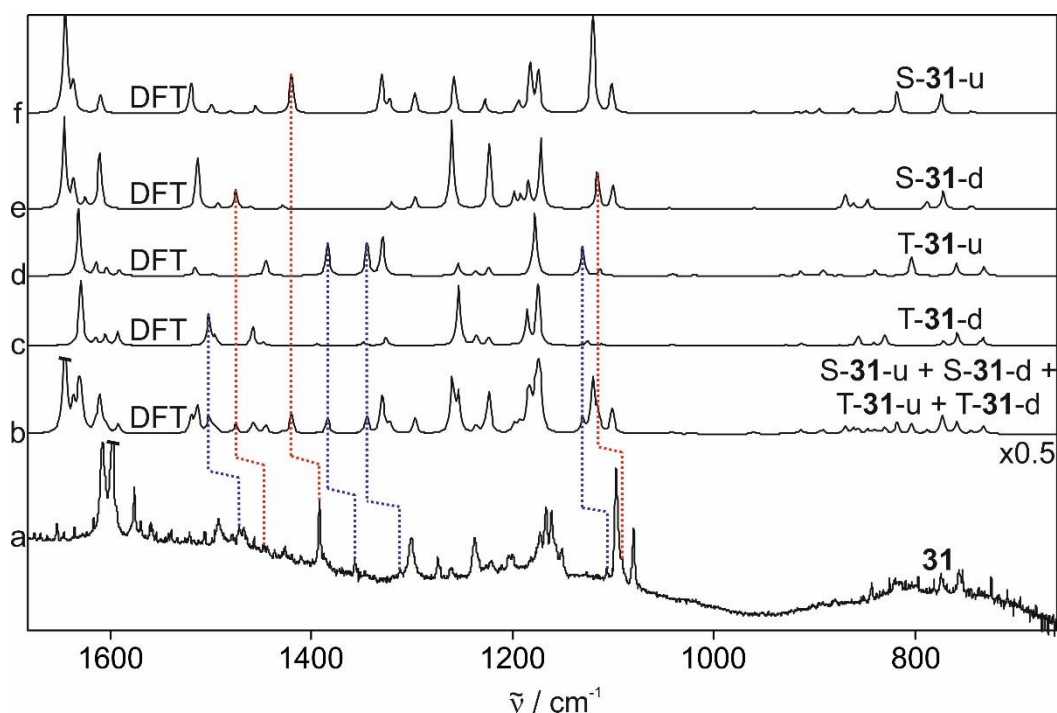


Figure 4.19: IR spectrum of carbene **31** isolated in a nitrogen matrix at 9 K and comparison with theoretical spectra of the different singlet and triplet carbene conformers calculated at the B3LYP/def2-TZVP level of theory. The blue dotted lines mark triplet carbene signals, the red dotted lines singlet carbene signals. (a) IR spectrum of carbene **31**. (b) Theoretical IR spectrum of a mixture the different conformers of S-**31** and T-**31**. (c-f) Theoretical IR spectra of the carbene species T-**31-d**, T-**31-u**, S-**31-d** and S-**31-u**, respectively.

The singlet carbene signal at 1392 cm^{-1} is assigned to conformer S-**31-u**, while the signals at 1092 cm^{-1} and 1447 cm^{-1} belong to S-**31-d**. For these conformers, a u/d ratio of 61/39 is determined. For the triplet carbene signals, the peaks at 1106 cm^{-1} , 1309 cm^{-1} and 1357 cm^{-1} are assigned to T-**31-u** and the signal at 1471 cm^{-1} to conformer T-**31-d**. The u/d ratio for the triplet carbene was 29/71.

Table 4.2: Conformer ratios of S-**31** and T-**31** in matrices of argon and nitrogen.

Carbene	u/d ratio (Ar)	u/d ratio (N ₂)
S- 31	75% / 25%	61% / 39%
T- 31	69% / 31%	29% / 71%

Irradiation and annealing experiments of **31** in nitrogen showed clear differences to the experiments in argon and xenon. While no changes after irradiation with 365 – 650 nm were observed for an argon matrix, 405 nm and 470 nm light led to distinct changes in the IR spectrum of **31** in a nitrogen matrix (Figure 4.20).

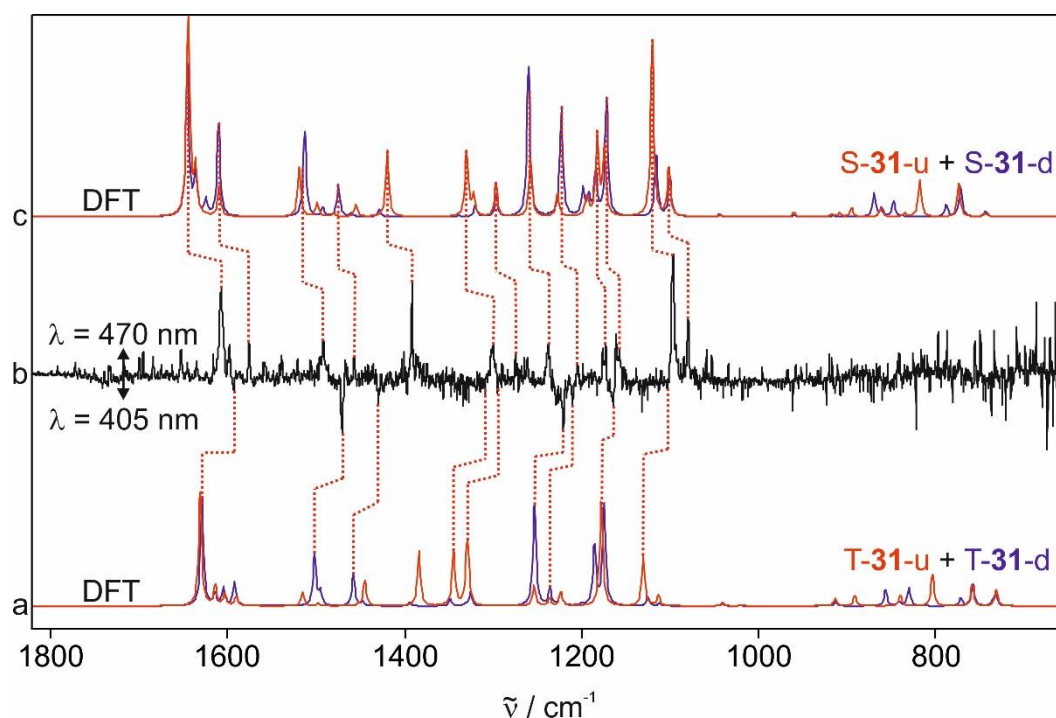


Figure 4.20: Irradiation experiments of carbene **31** in a nitrogen matrix. (a) Theoretical IR spectrum of a mixture of the triplet conformers T-**31-u** (red spectrum) and T-**31-d** (blue spectrum) calculated at the B3LYP/def2-TZVP level of theory. (b) Experimental IR difference spectrum of **31**. The signals pointing upwards are assigned to S-**31**, the signals pointing downwards to T-**31**. (c) Theoretical IR spectrum of a mixture of the conformers S-**31-u** and S-**31-d** calculated at the B3LYP/def2-TZVP level of theory.

470 nm irradiation light to the increase of several signals that are assigned to singlet carbene S-**31** while multiple other signals decreased that are assigned to T-**31**. The same behavior was observed after annealing to 20 K. Light of 405 nm resulted in the opposite effect and led to triplet increase and singlet decrease. The singlet-triplet ratio of 81/19 obtained directly after photolysis of diazo precursor **35** changed to a ratio of 88/12 when **31** was irradiated with 470 nm light, indicating singlet carbene formation. 405 nm light shifted the ratio to 73/27, verifying triplet carbene formation and singlet carbene degradation.

Table 4.3: Singlet-triplet ratios of S-**31** and T-**31** in matrices of argon, xenon and nitrogen.

Experiments	S-T Ratio (Ar)	S-T Ratio (Xe)	S-T Ratio (N ₂)
after precursor photolysis (365 nm)	31% / 69%	48% / 52%	81% / 19%
$\lambda = 470$ nm	31% / 69%	48% / 52%	88% / 12%
$\lambda = 405$ nm	31% / 69%	48% / 52%	73% / 27%

Further analysis of the different conformers during the irradiation experiments shows that the increase or decrease of S-**31** included both conformers, as seen by the increasing/decreasing signals at 1392 cm^{-1} (S-**31-u**) and 1447 cm^{-1} (S-**31-d**). However, the changes of the signals of S-**31-d** are considerably smaller, indicating that this conformer undergoes less spin interconversion. For triplet carbene T-**31**, the changes of the signals of conformer T-**31-d** at 1430 cm^{-1} and 1471 cm^{-1} are rather distinct, compared to the signals of the other conformer at 1106 cm^{-1} and 1309 cm^{-1} that only show minimal changes. This indicates that the spin interconversion occurs mainly for conformer T-**31-d** but only barely for T-**31-u**. In summary, these results show similarities to the spin interconversion behavior of 3-methoxy-9-fluorenylidene that only switches between the two species S-**29-u** and T-**29-d**.^[122] However, carbene **31** also exhibits small traces of spin interconversion of the two conformers S-**31-d** and T-**31-u**.

Since **31** undergoes distinct spin interconversion in N_2 but not in argon or xenon matrices, it is assumed that the property of N_2 to slow down tunneling processes plays a major role for this topic.^[132-134] If the spin state of this carbene would be dependent on the conformer (similar to carbene **29**),^[122] then possible hydrogen tunneling between two conformers would have an enormous effect on the spin interconversion. Hence, it is possible that this tunneling and therefore the spin switch would be too fast in argon and xenon to be observed. In nitrogen, the possible decreased tunneling rate could have enabled the observation of the spin interconversion. However this assumption is not verified yet.

UV/Vis Experiments

Further investigation of carbene **31** was conducted by using UV/Vis spectroscopy. At the beginning of the UV/Vis experiments, diazo precursor **35** was isolated in an argon matrix at 8 K and photolyzed by 365 nm light to form the carbene.

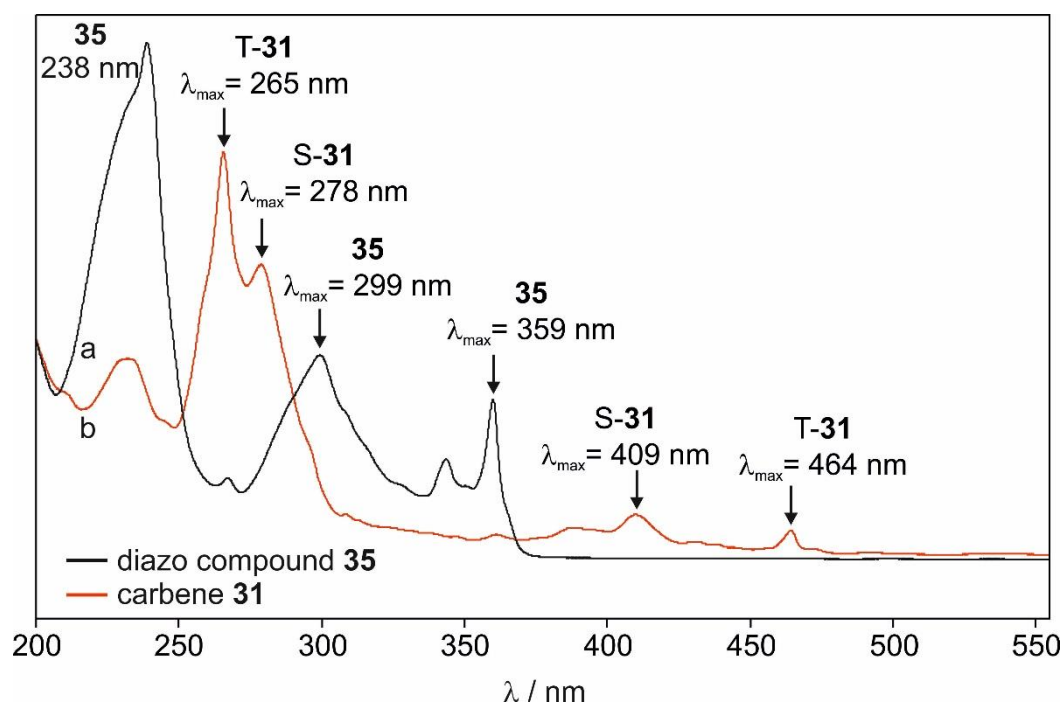


Figure 4.21: UV/Vis spectra of diazo compound **35** and carbene **31** generated in its singlet and triplet state after photolysis in an argon matrix at 8 K. (a) Spectrum of **35**. (b) Spectrum of carbene **31**.

After the photolysis, the signals at 238, 299 and 359 nm of the diazo compound vanished. Furthermore, new signals at 265, 278, 409 and 464 nm appeared that were assigned to carbene **31** (Figure 4.21). Comparison with the UV/Vis spectrum of the bistable fluorenylidene **29** verifies that the signals at 265 nm and 464 nm belong to triplet carbene T-**31** and the signals at 278 nm and 409 nm to singlet carbene S-**31**, since the singlet and triplet signals of **29** are in the same wavelength ranges (267 nm and 461 nm for T-**29**, 277 nm and 410 nm for S-**29**).^[122] Annealing to 25 K did not result in any observable changes. On the other hand, irradiation with 470 nm and 405 nm light led to minimal differences in the spectrum. By comparison with a difference UV/Vis spectrum before and after irradiation, it is observed that 470 nm light led to a slight increase of the singlet peak at 278 nm while the triplet signal at 265 nm decreased (Figure 4.22). 405 nm light resulted in the opposite effect.

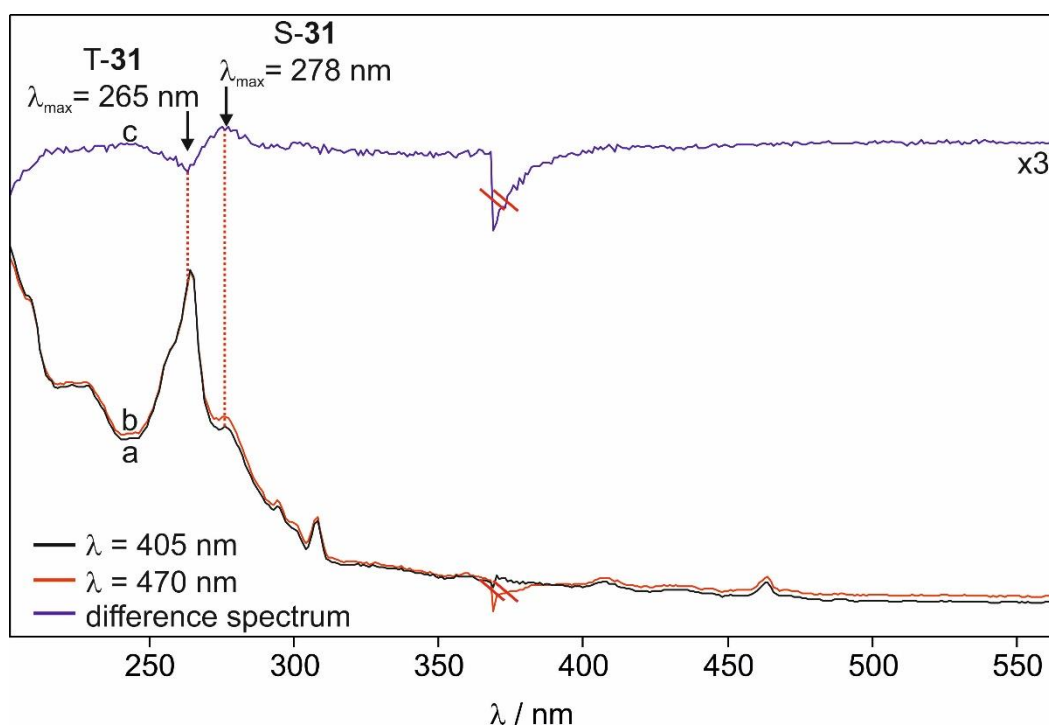


Figure 4.22: UV/Vis spectra of carbene **31** after irradiation with 470 nm and 405 nm light. (a) UV/Vis spectrum after irradiation with 405 nm light. (b) UV/Vis spectrum after 470 nm light irradiation. (c) Difference UV/Vis spectrum after 470 nm light irradiation. The band pointing upwards is assigned to S-**31**, the band pointing downwards to T-**31**.

Integration of the signals yields a singlet-triplet ratio of 27/73 directly after photolysis of precursor **35** that is similar to the ratio obtained at the IR experiments. After irradiation with 470 nm light, the singlet increase resulted in a ratio of 28/72. Furthermore, 405 nm irradiation changed the ratio to 26/74. Since the changes in the UV/Vis spectrum are very small, it is possible that the same changes occurred during the IR experiments but were just not observable. However, UV/Vis measurements verified that carbene **31** undergoes a minimal reversible singlet-triplet interconversion in an argon matrix.

In a nitrogen matrix, irradiation with 470 nm light resulted in a distinct increase of the singlet carbene signals at 276 nm and 408 nm, while the triplet carbene peaks at 265 nm and 462 nm decreased (Figure 4.23). Annealing to 20 K showed the same result, but the observed changes were weaker. Irradiation with 405 nm light reversed this effect and formed T-**31** while S-**31** decreased. These changes in the spectrum caused by singlet-triplet interconversion are considerably larger than in an argon matrix.

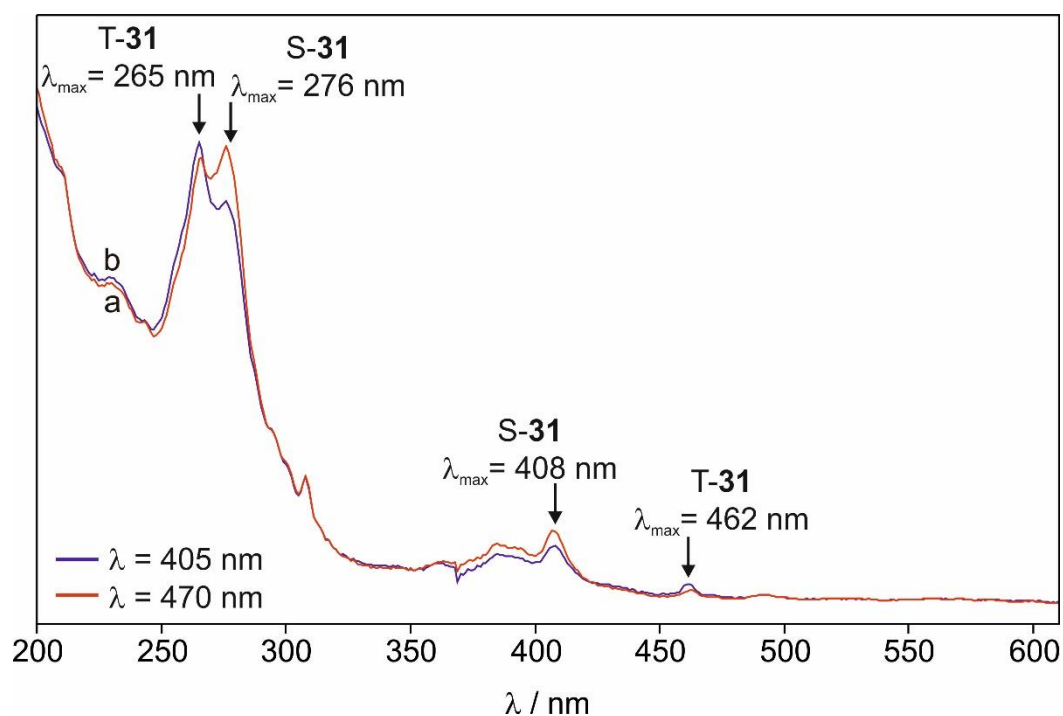


Figure 4.23: Irradiation of carbene **31** in a nitrogen matrix with 405 nm and 470 nm light. (a) UV/Vis spectrum after irradiation with 470 nm light. (b) UV/Vis spectrum after irradiation with 405 nm light.

After diazo precursor photolysis, a singlet-triplet ratio of 55/45 was obtained. Irradiation with 405 nm light changed this ratio to 49/51, indicating conversion from S-**31** to T-**31**. Using 470 nm light, the starting ratio of 55/45 was obtained again. In summary, **31** is a magnetically bistable carbene that undergoes photochemically or thermally induced singlet-triplet interconversion, as demonstrated by IR and UV/Vis spectroscopy.

EPR Experiments

In addition to the IR and UV/Vis experiments in argon, carbene **31** was investigated via EPR spectroscopy. After deposition of **35** in an argon matrix at 4 K and photolysis with 365 nm, several signals appeared that were characteristic for a triplet carbene (Figure 4.24). Comparison of the EPR spectrum with the spectra of fluorenylidene (**27**) and 3-methoxy-9-fluorenylidene (**29**) shows that the EPR spectra are almost identical, indicating the successful formation of carbene **31**.^[109, 122, 140]

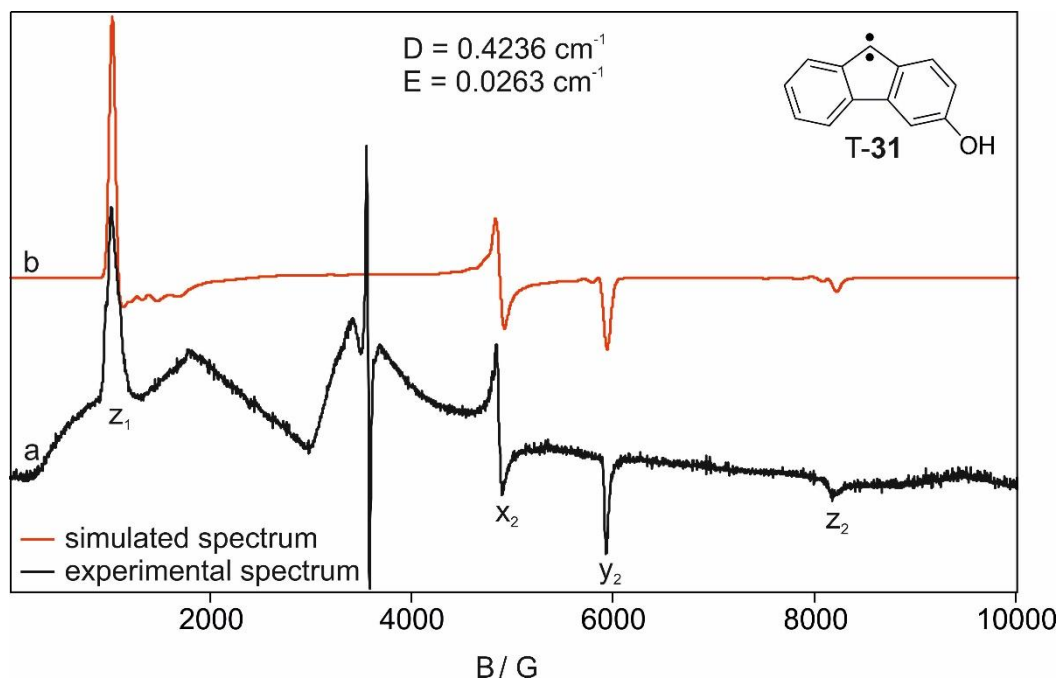


Figure 4.24: EPR spectrum of triplet carbene T-31 in argon at 4 K. The spectrum shows similarities to other triplet carbene EPR spectra.^[109, 122, 140] (a) Experimental EPR spectrum of T-31. (b) Simulated EPR spectrum.

The simulated EPR spectrum of carbene T-31 delivers zfs parameters of $D = 0.4236 \text{ cm}^{-1}$ and $E = 0.0263 \text{ cm}^{-1}$ that are similar to the zfs parameters of the similarly structured 3-methoxy-9-fluorenylidene ($D = 0.4235 \text{ cm}^{-1}$, $E = 0.0261 \text{ cm}^{-1}$). The observation of strong EPR signals at 4 K indicates that either the triplet state is the ground state or that the singlet-triplet energy gap is very small, so that the excited triplet state is accessible at such low temperatures. However, unambiguous determination of the spin ground state can be achieved by performing a Curie-Weiss plot which will be conducted in the future. Furthermore, irradiation and annealing experiments will be conducted in a nitrogen matrix to directly verify the increase and decrease of T-31.

4.3.2. Reaction with water

IR Experiments

To investigate the interactions of **31** with water, several experiments in water-doped argon matrices were conducted and analyzed via IR spectroscopy. It is expected that single water molecules do not only interact with the carbon carbene center but will also form hydrogen bonds with the free hydroxy group. One question arising from the possibility to form the latter kind of hydrogen bond is if these interactions have an influence on the singlet-triplet gap or on the reactivity of the carbene with water.

Compound **35** was isolated in an argon matrix doped with 2% water and photolyzed. After annealing of **31** to 25 K, several changes in the spectrum were observable. Both the signals of S-**31** (1429 cm⁻¹, 1271 cm⁻¹, 1097 cm⁻¹) and T-**31** (1356 cm⁻¹, 1106 cm⁻¹) decreased as well as the water signals at around 1600 cm⁻¹, indicating that the water molecules interacted with both types of carbenes (Figure 4.25). The singlet-triplet ratio after photolysis (39/61) did not change after annealing, which indicates that equal parts of both carbene species interacted with water. On the other hand, several new small signals appeared that were assumed to be a mixture of several water complexes. Calculations at the B3LYP/def2-TZVP level of theory show that for possible water complexes **36**, **37** and **38**, the singlet state is more favored. Comparison of the experimental IR spectrum of **31** after annealing with theoretical spectra of these complexes in their singlet state depict that all three complexes have formed. The signals at 1339 cm⁻¹ and 1204 cm⁻¹ are exclusively assigned to complex S-**38-u**, and the signal at 1251 cm⁻¹ is assigned to the other conformer S-**38-d**. The complex S-**37-d** exhibits a signal at 1216 cm⁻¹, but for the other conformer, no characteristic peak is assignable due to signal overlaps. Several peaks are assigned to conformer S-**36**, but all of these signals also show overlaps with signals of the other complexes. In general, the proper assignment of all the peaks to different conformers of all the possible complexes S-**36**, S-**37** and S-**38** is not possible due to several signal overlaps and rather small signal intensities in the experimental IR spectrum. Furthermore, it is not excluded that other water complexes formed that were not considered in the spectrum analysis.

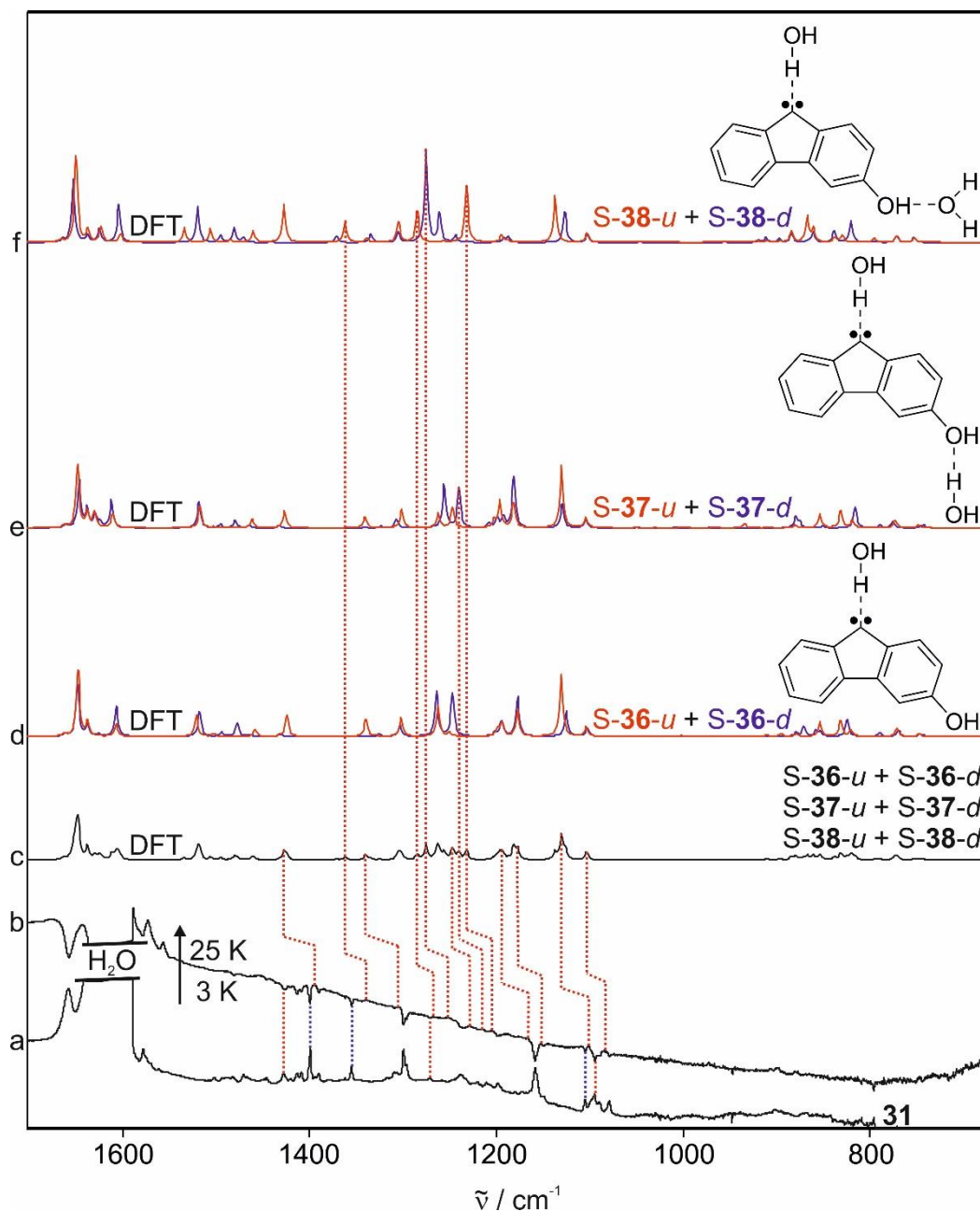


Figure 4.25: Annealing experiments of carbene **31** in an argon matrix doped with 2% H₂O. (a) IR spectrum of **31** in both its singlet and triplet states at 3 K. (b) IR difference spectrum after annealing to 25 K. The signals pointing downwards are assigned to S-**31** (red dotted line) and T-**31** (blue dotted line), the signals pointing upwards to the water complexes S-**36**, S-**37** and S-**38** as a mixture of their conformers. (c) Theoretical IR spectrum of a mixture of the complexes S-**36-u**, S-**36-d**, S-**37-u**, S-**37-d**, S-**38-u** and S-**38-d** calculated at the B3LYP/def2-TZVP level of theory. (d-f) Calculated IR spectra of each water complex S-**36**, S-**37** and S-**38** (respectively) in their conformer “u” (red spectra) and “d” (blue spectra).

The water complexes were left in the dark at 3 K for 23 hours whereupon no changes in the spectrum were observed. After irradiation of the water complexes with 650 nm light, it was observed that the signals of the water complexes decreased while several new, smaller signals appeared (Figure 4.26). By comparison with a reference spectrum of **39** (also measured in a

water-doped argon matrix), it is verified that these new signals belong to the alcohol. Due to the small signal intensity, it is not observable if the alcohol formed as a mixture of both possible conformers.

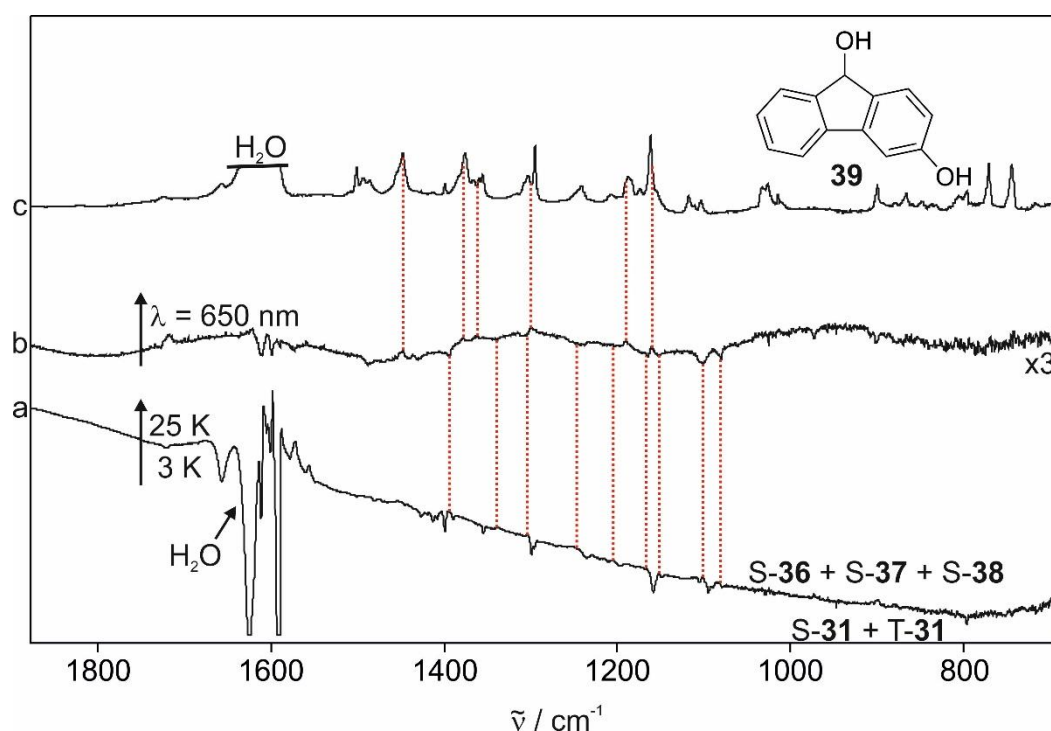


Figure 4.26: IR spectra showing the conversion of the water complexes S-36, S-37 and S-38 to the corresponding alcohol **39**. (a) Difference IR spectrum after annealing of **31** to 25 K. The signals pointing upwards are assigned to singlet water complexes S-36, S-37 and S-38, the signals pointing downwards to both the carbene species S-31 and T-31. (b) Difference IR spectrum after irradiation of the water complexes with 650 nm light. The signals pointing upwards are assigned to alcohol **39**, the signals pointing downwards to the water complexes S-36, S-37 and S-38. (c) IR spectrum of alcohol **39** in an argon matrix doped with 2% water at 3 K.

UV/Vis Experiments

For the UV/Vis investigation, carbene **31** was generated in a water-doped argon matrix and annealed to 25 K whereupon several small changes occurred in the spectrum (Figure 4.27). Both the signals of singlet carbene S-31 at 278 nm and 409 nm and the signals of triplet carbene T-31 at 265 nm and 464 nm decreased. On the other hand, two new small signals at 398 nm and 421 nm appeared that are assigned to water complex S-36. Since other water complexes most likely have absorptions in the same range, it is assumed that these two signals also belonged to the water complexes S-37, S-38 and other possible complexes. Comparison with the UV/Vis spectra of fluorenylidene (**27**) and 3,6-dimethoxy-9-fluorenylidene (**30**)

(Figure 4.9) shows that for these two systems, the water complex signals are in the same range (fluorenylidene: 416 nm, 3,6-dimethoxy-9-fluorenylidene: 421 nm).^[109] Therefore, it is verified that the new signal at 421 nm after annealing of **31** belongs to water complex S-36.

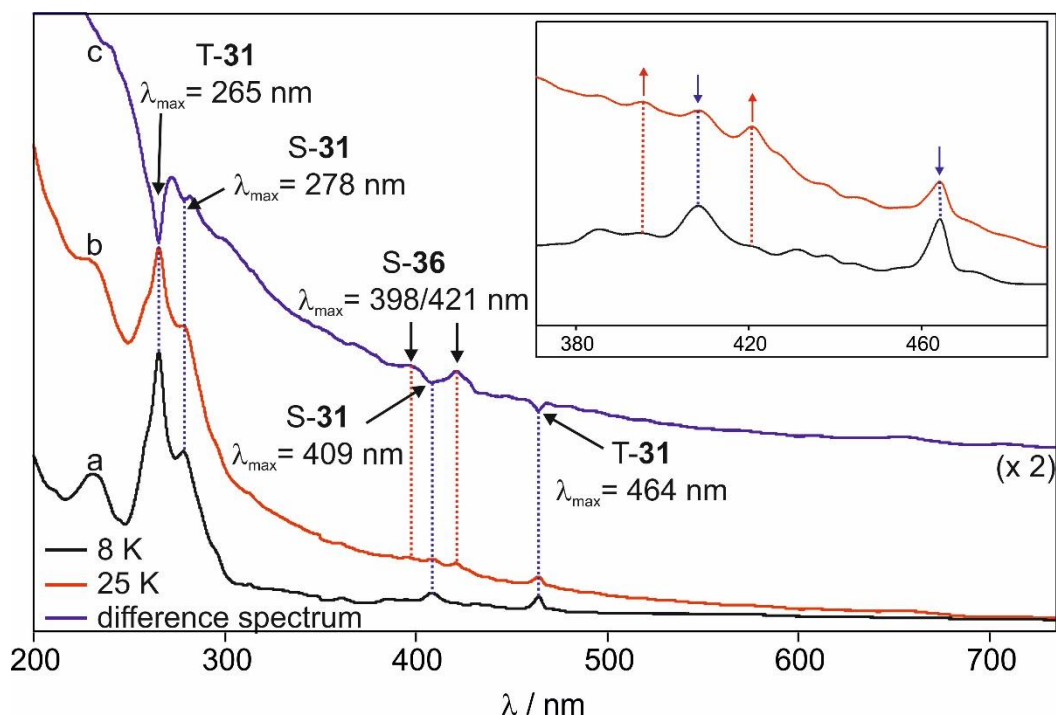


Figure 4.27: UV/Vis spectra of carbene **31** before and after annealing to 25 K in an argon matrix doped with 2% water. (a) UV/Vis spectrum of S-31 and T-31 at 8 K. (b) UV/Vis spectrum after annealing to 25 K. (c) Difference UV-Vis spectrum after annealing to 25 K. The bands pointing upwards are assigned to water complex S-36 (red dotted lines), the bands pointing downwards to singlet and triplet carbene S-31 and T-31 (blue dotted lines).

The complex was left in the dark for 23 hours whereupon no changes in the spectrum were observed, verifying that no reaction occurred. To form alcohol **39** from complex S-36, irradiation with 650 nm light was conducted (according to the IR experiments). The water complex signals at 421 nm and 398 nm decreased while two small signals at 240 nm and 313 nm increased (Figure 4.28). Comparison with a reference UV/Vis spectrum of alcohol **39** verifies that the new increasing signals belong to this alcohol, which is in agreement with IR investigations.

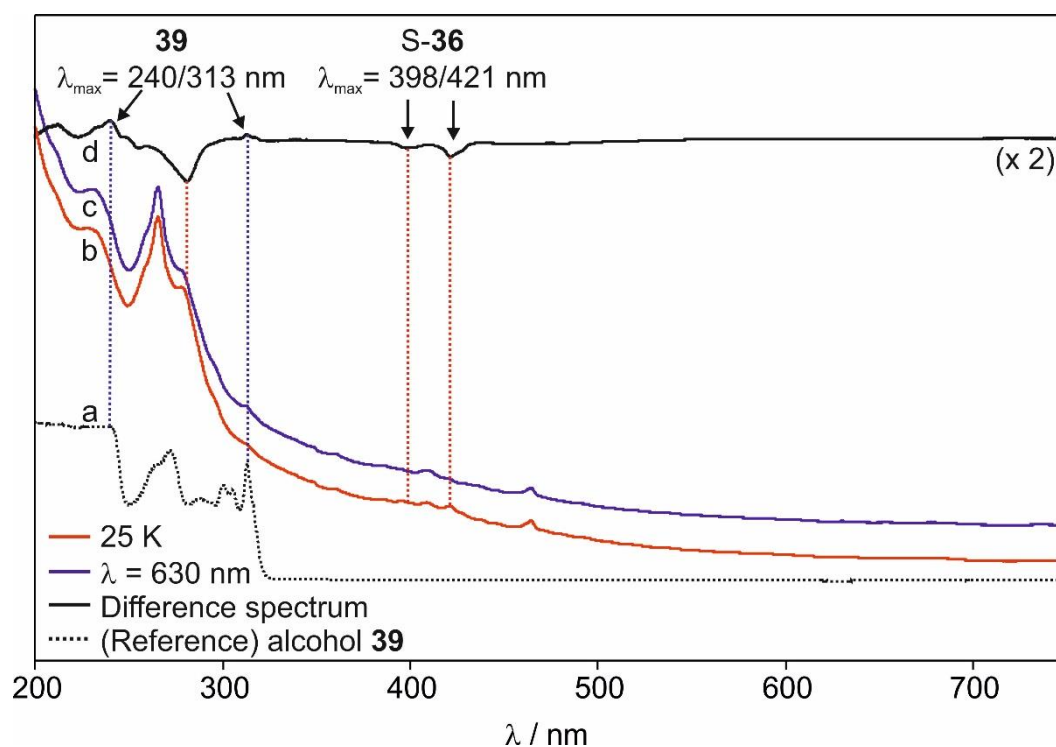


Figure 4.28: Irradiation experiments of water complex S-36 that has formed after annealing of carbene **31** in a water-doped argon matrix. (a) UV/Vis reference spectrum of alcohol **39**. (b) UV/Vis spectrum before irradiation, after leaving water complex S-36 in the dark for 23 h. (c) UV/Vis spectrum after irradiation of S-36 with 650 nm light. (d) Difference spectrum after irradiation with 650 nm light. The bands pointing upwards are assigned to alcohol **39** (blue dotted lines), the bands pointing downwards to water complex S-36 (red dotted lines).

4.3.3. Experiments in Ar doped with dimethyl ether (DME)

Since the magnetically bistable 3-hydroxy-9-fluorenylidene shows hardly any spin interconversion in an argon matrix, it was tested if it is possible to lower the singlet gap via interactions with smaller molecules, i.e. Lewis bases. Calculations at the B3LYP/def2-TZVP level of theory show that the formation of a hydrogen bond between the hydroxy group of carbene **31** and a single molecule of dimethyl ether (DME) results in a significantly lowered singlet-triplet gap. Since a lower energy gap could lead to enhanced singlet-triplet interconversion, experiments of carbene **31** in DME-doped argon were tested. After the formation of the carbene by photolysis of its diazo precursor, the matrix was annealed to 25 K for several minutes. It was observed that the carbene signals slightly decreased while several new signals increased that are assigned to the hydrogen-bonded DME complex **40** (Figure 4.29). However, the changes were only small, so that the annealing did only barely result in the formation of new intermolecular interactions.

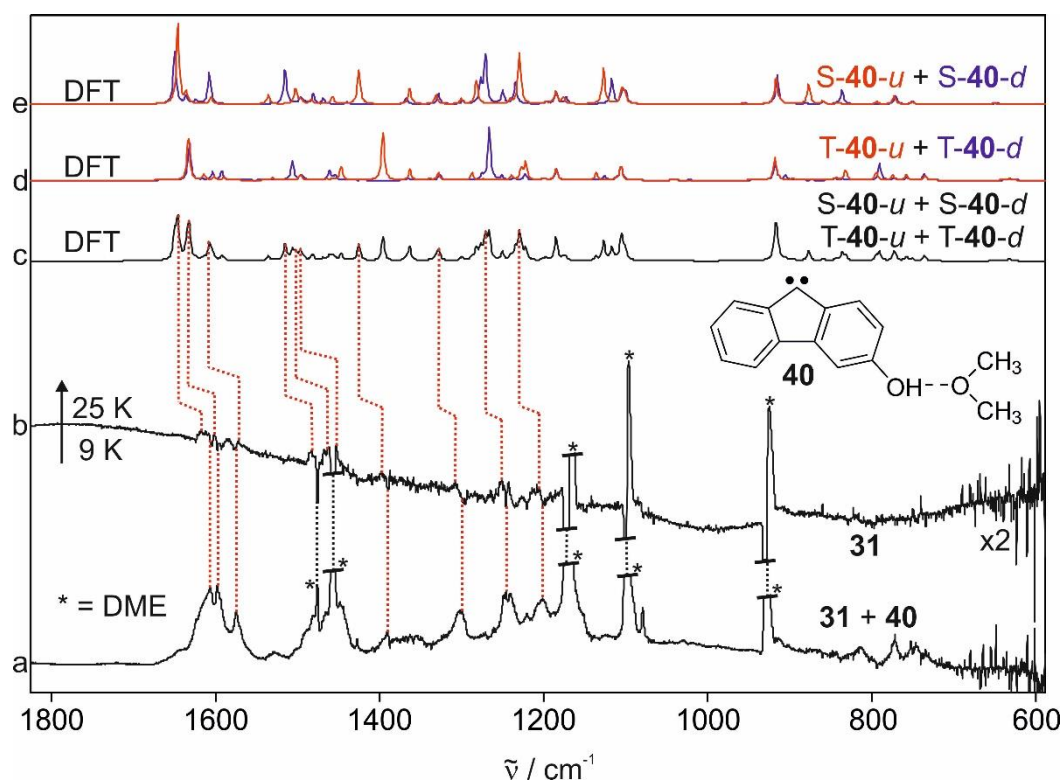


Figure 4.29: Annealing experiments of carbene **31** in an argon matrix doped with 5% DME. (a) IR spectrum of carbene **31** in an argon matrix doped with 5% of DME at 9 K. The signals marked with an asterisk correspond to dimethyl ether. (b) IR difference spectrum after annealing to 25 K. The signals pointing upwards are assigned to DME complex **40**, the signals pointing downwards to carbene **31**. Signals of DME are marked with an asterisk. (c) Theoretical IR spectrum of a mixture of the DME complex species S-**40-u**, S-**40-d**, T-**40-u** and T-**40-d** calculated at the B3LYP/def2-TZVP level of theory. (d-e) Theoretical IR spectra of each DME complex T-**40** and S-**40** (respectively) in their conformers “u” (red spectra) and “d” (blue spectra).

Furthermore, it is not possible to determine if **40** was formed as a conformer mixture since several peaks are overlapping, which prevents the proper assignment of the signals to the single conformers. Nevertheless, it is detected that **40** formed as a mixture of its singlet and triplet state. The signal at 1398 cm^{-1} is assigned to only singlet complex S-**40**, while the signal at 1602 cm^{-1} corresponds to the triplet complex T-**40**. In addition to that, it is observed that the carbene signals before annealing are rather broad compared to the signals in argon, xenon or nitrogen. This leads to the assumption that interactions between **31** and DME were already formed during the deposition due to the use of a high amount of DME (5% in Ar). To avoid this problem, lower amounts of DME will be used in future experiments.

Calculations at the B3LYP/def2-TZVP level of theory show that complex **40** exhibits intense signals at 3402 cm^{-1} (up conformer, singlet state, S-**40-u**), 3412 cm^{-1} (down conformer, singlet state, S-**40-d**), 3484 cm^{-1} (up conformer, triplet state, T-**40-u**) and 3488 cm^{-1} (down conformer, triplet state, T-**40-d**) in the theoretical spectra that are assigned to the RO-H---O(CH₃)₂ stretch.

Hence, the experimental IR spectra are reviewed to search for bands in the corresponding range. The difference spectrum after annealing to 25 K does not show any distinct changes in this area, which again indicates that annealing barely produces the complex (Figure 4.30). However, it is detected that the IR spectrum before annealing already exhibits two broad bands at around 3215 cm^{-1} and 3353 cm^{-1} that are not present in the IR spectra in pure argon and are assigned to the singlet and triplet complexes S-40 and T-40, respectively.

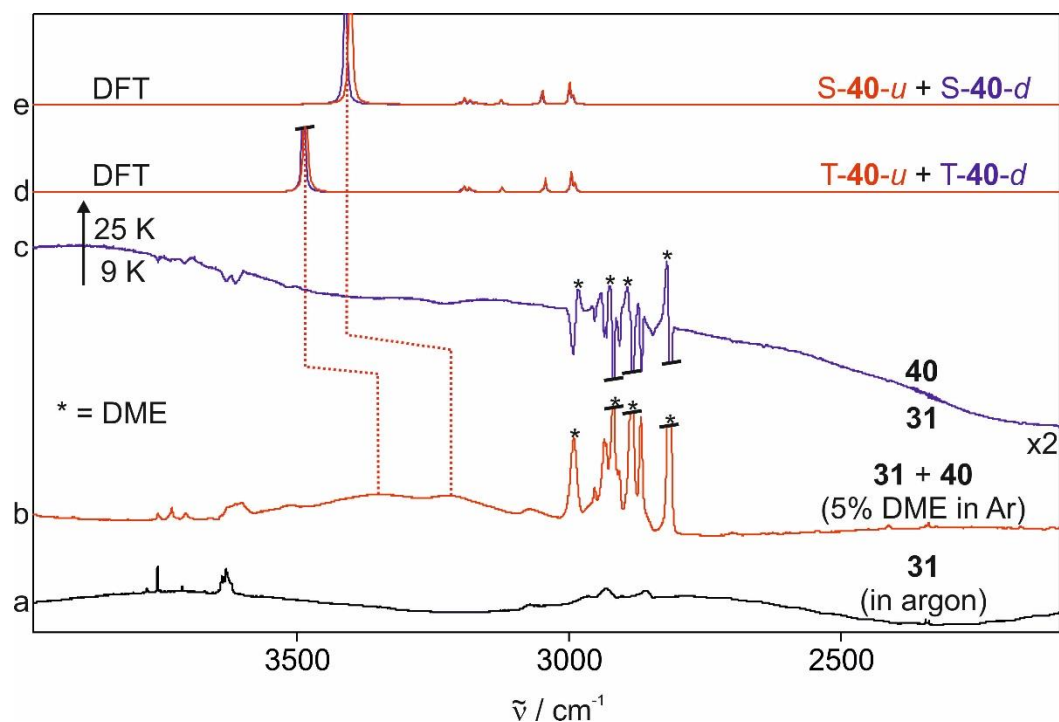


Figure 4.30: Comparison of the IR spectra (range: $2000 - 4000\text{ cm}^{-1}$) of carbene **31** in pure argon and in argon doped with 5% DME. (a) IR spectrum of carbene **31** in an argon matrix. (b) IR spectrum of **31** in an argon matrix doped with 5% DME. Due to interactions of the carbene with DME, a certain amount of complex **40** is present. (c) IR difference spectrum after annealing **31** in a DME-doped argon matrix to 25 K. (d) Theoretical IR spectra of triplet complexes T-40-*u* (red spectrum) and T-40-*d* (blue spectrum) calculated at the B3LYP/def2-TZVP level of theory. (e) Theoretical spectra of singlet complexes S-40-*u* (red spectrum) and S-40-*d* (blue spectrum).

Subsequent irradiation and annealing experiments were conducted to test if singlet-triplet interconversion was observable. Light in the range of 365 – 650 nm as well as annealing to 25 K did not result in any observable changes in the spectrum. Thus, it is assumed that spin interconversion did not occur or is too weak to be observed. To further investigate this topic, UV/Vis and EPR investigations will be conducted to test if the complexation with DME has any influence on the magnetic bistability.

4.3.4. Experiments in Ar doped with trimethyl amine

IR experiments

Aside from dimethyl ether, trimethyl amine was used as another Lewis base to form a hydrogen-bonded complex with the hydroxy group of carbene **31**. Calculations at the B3LYP/def2-TZVP level of theory show that the singlet-triplet gap of the NMe₃ complex **41** is even smaller than of the similar DME complex **40**. At the beginning of the experiment, carbene **31** was annealing to 25 K in an argon matrix doped with 4% of NMe₃ whereupon no changes in the IR spectrum were observable (Figure 4.31). Similar to the experiments in DME, the signals in the spectrum are much broader than in a pure argon matrix due to the high amount of NMe₃ in the gas mixture that already interacted with **31** during the deposition, forming complex **41**.

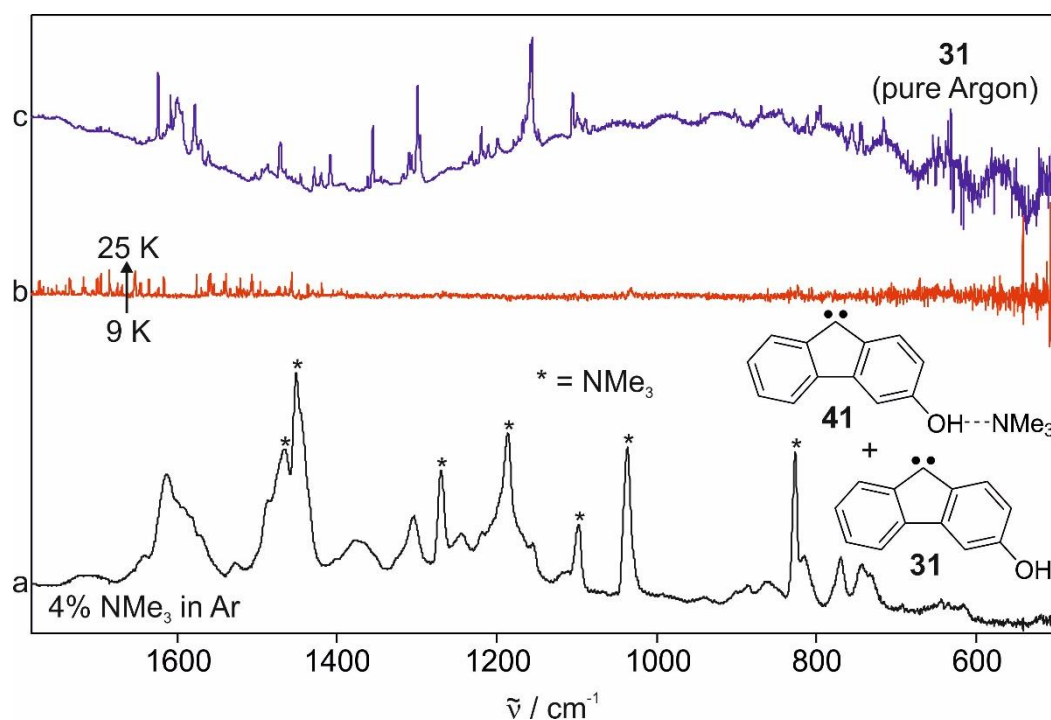


Figure 4.31: Annealing experiment of carbene **31** in an argon matrix doped with 4% of trimethyl amine. (a) IR spectrum of **31** in an argon matrix doped with 4% NMe₃ at 9 K. The signals marked with an asterisk correspond to trimethyl amine. (b) IR difference spectrum after annealing to 25 K. (c) IR spectrum of **31** in an argon matrix (for comparison).

Irradiation experiments with light in the range of 365 – 650 nm were conducted. It was shown that light of several wavelengths (e.g. 530 nm, 405 nm) resulted in small broad signal changes that were reversible when 650 nm or 505 nm light was used (Figure 4.32). Theoretical IR spectra of **41** calculated at the B3LYP/def2-TZVP level of theory do not reproduce the spectral

changes. Therefore, investigations via other spectroscopic methods (UV/Vis and EPR) are necessary to identify if these photochemically induced changes corresponding to singlet-triplet interconversion.

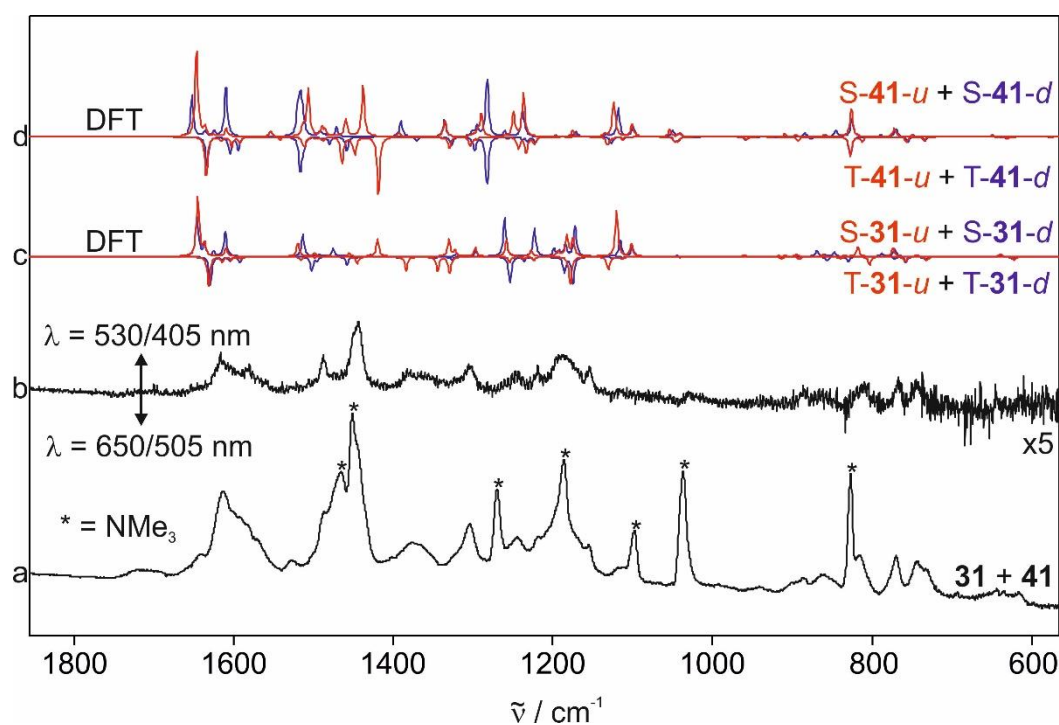


Figure 4.32: Irradiation experiments of carbene **31** and NMe₃ complex **41** in an argon matrix doped with 4% NMe₃. (a) IR spectrum of a mixture of **31** and **41** at 9 K. (b) IR difference spectrum after irradiation with 530 nm or 405 nm light. The changes in the spectrum are not properly assignable to the carbene or the NMe₃ complex. (c) Theoretical IR difference spectrum of carbene **31**. The signals pointing upwards correspond to the singlet conformers S-**31**-*u* (red spectrum) and S-**31**-*d* (blue spectrum), the signals pointing downwards to the triplet carbene conformers T-**31**-*u* (red spectrum) and T-**31**-*d* (blue spectrum). (d) Theoretical IR difference spectrum of NMe₃ complex **41**. The signals pointing upwards belong to S-**41**-*u* (red spectrum) and S-**41**-*d* (blue spectrum), the signals pointing downwards to T-**41**-*u* (red spectrum) and T-**41**-*d* (blue spectrum).

UV/Vis experiments

Carbene **31** was generated in an argon matrix doped with 4% NMe₃ analogue to the IR experiments. Annealing to 25 K resulted in a decrease of both the signals of the singlet carbene S-**31** (278 nm, 409 nm) and the triplet carbene T-**31** (265 nm, 464 nm) while two broad bands in the UV region increased that are not assigned to **31** or the complex **41** (Figure 4.33). The decrease of the carbene signals indicates that interactions with NMe₃ occurred while it is assumed that the absorption bands of **41** are in the same range as the bands of the carbene, so that signal overlaps would be observed.

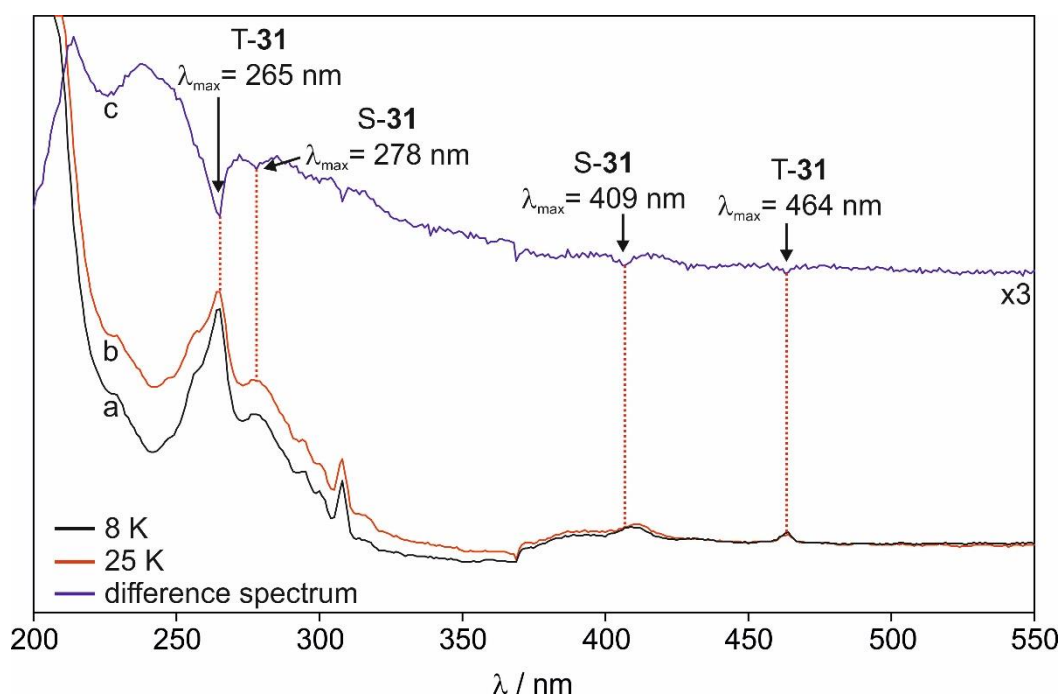


Figure 4.33: Annealing of carbene **31** to 25 K in an argon matrix doped with 4% of NMe₃. (a) UV/Vis spectrum of carbene **31** in an argon matrix doped with 4% NMe₃ at 8 K. (b) UV/Vis spectrum at 25 K. (c) Difference UV/Vis spectrum after annealing to 25 K.

Subsequent irradiation experiments showed that light of 405 and 470 nm induced small changes. Via preparation of a difference spectrum and comparison with the UV/Vis spectra before and after irradiation, it is verified that 405 nm light results in the increase of the signal at 265 nm that corresponds to triplet carbene T-**31** and complex T-**41** (Figure 4.34). Additionally, the signals at 278 and 409 nm decreased that are assigned to S-**31** and S-**41**. Irradiation with 470 nm light resulted in the opposite effect.

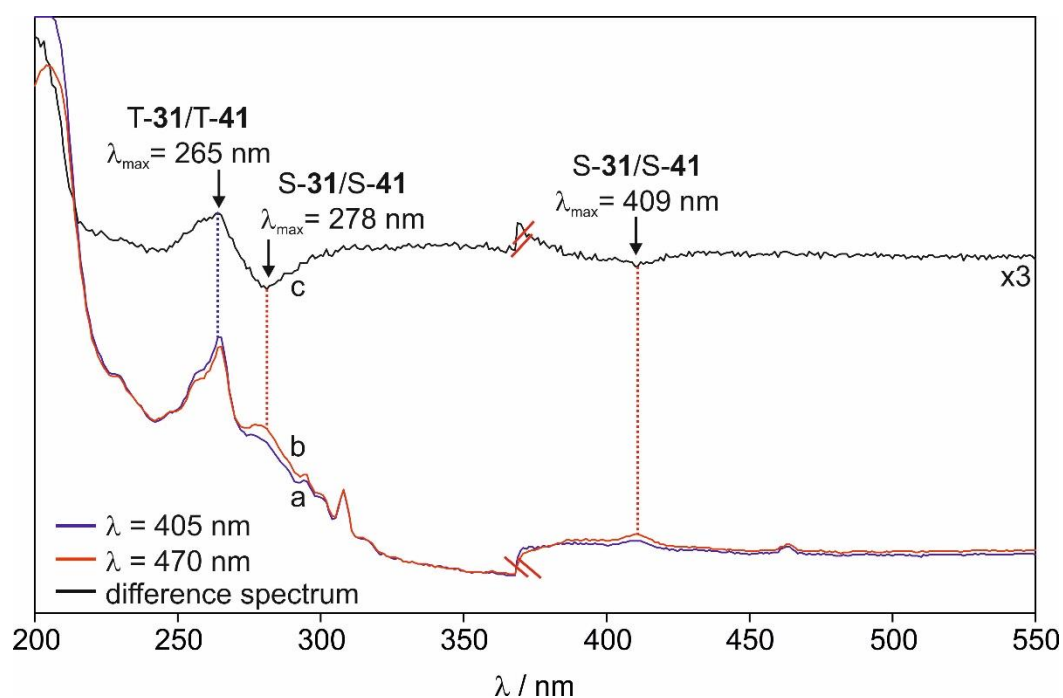


Figure 4.34: Singlet-triplet interconversion between the singlet carbene species S-**31** and S-**41** and the triplet carbene species T-**31** and T-**41**. (a) UV/Vis spectrum after irradiation with 405 nm light. (b) UV/Vis spectrum after 470 nm light irradiation. (c) Difference UV/Vis spectrum after irradiation with 405 nm light. The signal pointing upwards is assigned to T-**31** and T-**41**, the signals pointing downwards to S-**31** and S-**41**.

Since calculations predict a lower singlet-triplet energy gap for complex **41** than for the non-complexed carbene **31**, a higher amount of singlet-triplet interconversion is expected in this experiment compared to experiments in a pure argon matrix. Integration of the signals and comparison of the singlet-triplet ratios in pure argon and NMe₃-doped argon confirm this assumption. In NMe₃-doped argon, the starting singlet-triplet ratio (after photolysis of diazo precursor **35**) of 36/64 changed to a ratio of 29/71 when irradiated with 405 nm light. In comparison, the starting ratio in pure argon (27/73) only changed to 26/74 under the same irradiation conditions. These results clearly show that the amount of triplet formation in NMe₃-doped argon is considerably higher, which indicates that also triplet complex T-**41** has formed. However, subsequent irradiation with 470 nm light resulted only in a small singlet formation for both matrices (singlet-triplet ratios: argon = 28/72, NMe₃-doped argon = 30/70). In summary, it was observed that complexation of carbene **31** with trimethyl amine results in a favored singlet-triplet interconversion.

4.3.5. Computational Results

The calculations at the CCSD(T)/cc-PVDZ//B3LYP-D3/def2-TZVP of theory were performed by Dr. Enrique Mendez Vega.

Computational methods were used to calculate the corresponding singlet-triplet energy gaps of the compounds that were investigated via matrix isolation spectroscopy. For 3-hydroxy-9-fluorenylidene, calculations at the B3LYP/def2-TZVP level of theory provide a singlet-triplet gap of 2.2 kcal/mol for the energetically favored conformer **31-u**, while the other conformer **31-d** has an energy gap of 2.5 kcal/mol. Furthermore, calculations with the more advanced method CCSD(T)/cc-PVDZ//B3LYP-D3/def2-TZVP show a singlet-triplet gap of 0.7 kcal/mol for the favored conformer **31-u**, which is rather close to zero. The energy differences between the different conformers of **31** calculated at the B3LYP/def2-TZVP level of theory are 0.5 kcal/mol (singlet state) and 0.2 kcal/mol (triplet state).

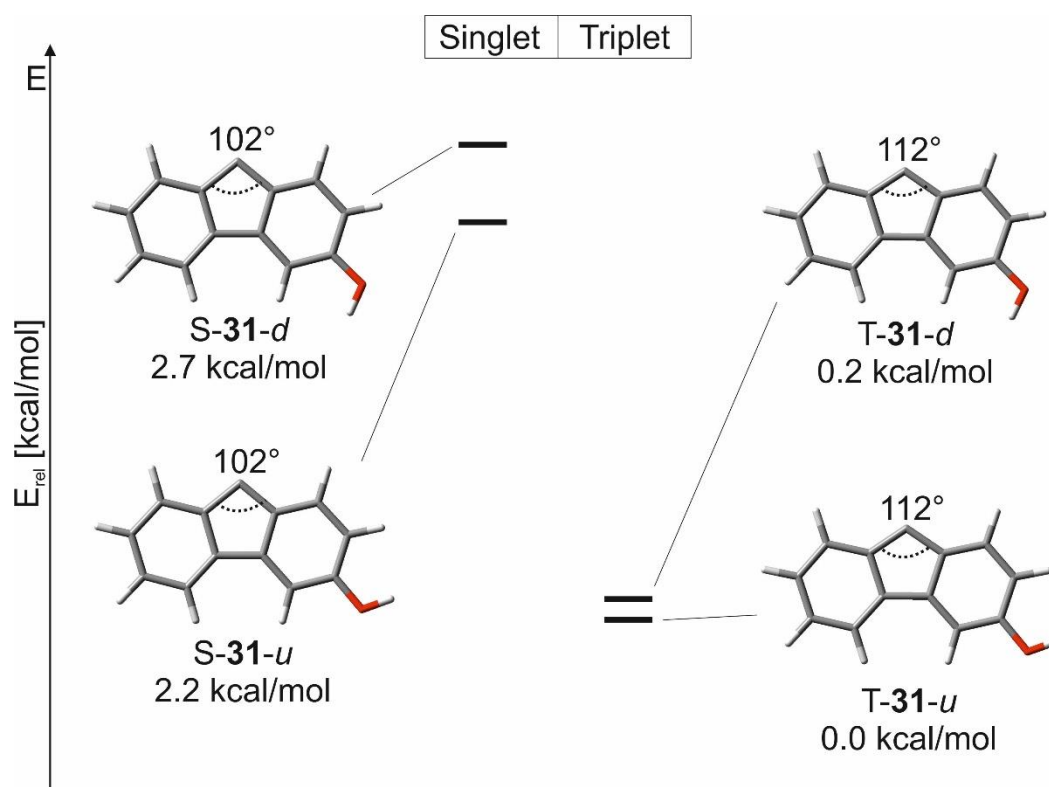


Figure 4.35: Theoretical energy differences of the different singlet and triplet carbene conformers of **30** relative to the most stable conformer T-**31-u**, calculated at the B3LYP/def2-TZVP level of theory. Since the singlet carbene S-**31** has a larger dipole moment, the energy difference between the two conformers is larger than for T-**31**.

Similar to 3,6-dimethoxy-9-fluorenylidene, it is detected that the conformer energy difference of **S-31** is higher than the energy difference of **T-31**. Again, this can be explained by the dipole moments of the carbene species. The singlet carbene conformers have dipole moments of 3.7 D (**S-31-u**) and 5.0 D (**S-31-d**), while the triplet carbene conformers have significantly smaller dipole moments of 1.5 D (**T-31-u**) and 1.9 D (**T-31-d**). Since the singlet carbene is more polar, the lone electron pair of the oxygen atom has an important impact on the global dipole moment, and hence the charge separation and the relative stability, similar to carbene **30**. To support the experiments in water-doped argon matrices, calculations at the B3LYP/def2-TZVP level of theory show that interactions of carbene **31** with single molecules of water switches the ground state from triplet to singlet by forming a hydrogen bond. The singlet-triplet energy gap for water complex **36** (containing only one water molecule) is -4.8 kcal/mol for the favored conformer **S-36-u** (Figure 4.36). Adding another molecule of water to the hydroxy group of the carbene has an influence on the singlet-triplet gap, depending on the type of hydrogen bond. In complex **37**, the additional hydrogen bond lowers the S-T gap to -4.4 kcal/mol (up conformer), while the additional bond in complex **38** stabilizes the singlet state even more and results in an increased energy gap of -6.1 kcal/mol (up conformer).

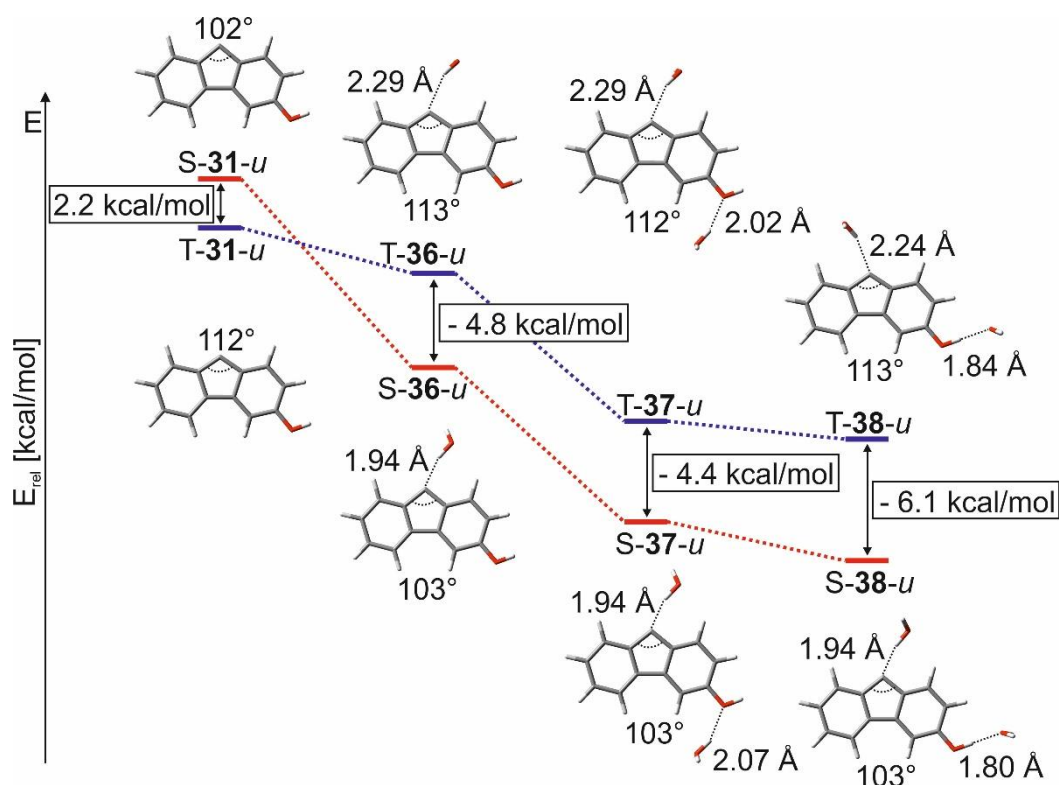


Figure 4.36: Singlet-triplet energy gaps of carbene **31** and the corresponding carbene-water-complexes **36-38** in their up-conformer. It is observed that an additional water molecule at the hydroxy group has an influence on the S-T gap of the complex. The energies were calculated at the B3LYP/def2-TZVP level of theory.

The singlet-triplet energy gaps of the down-conformer complexes are 4.4 kcal/mol (**36-d**), 3.7 kcal/mol (**37-d**) and 5.5 kcal/mol (**38-d**). Regarding the stabilization energy of the complexes, it is shown that the complexes **37** and **38** that contain two water molecules are considerably more stabilized due to additional hydrogen bond formation at the hydroxy group than complex **36** with only one water molecule (Table 4.4). The hydrogen bond at the hydroxy group in complex **38** is stronger than the corresponding bond in complex **37**, which results in a larger stabilization for both the singlet and triplet complex.

Table 4.4: Stabilization energies (ΔE_s) of the singlet and triplet water complexes **36** – **38** calculated at the B3LYP/def2-TZVP level of theory. The energies are given in kcal/mol.

complex	ΔE_s (singlet)	ΔE_s (triplet)
36-u	- 10.5	- 3.5
36-d	- 10.3	- 3.4
37-u	- 14.2	- 7.6
37-d	- 13.3	- 7.1
38-u	- 18.8	- 10.5
38-d	- 18.6	- 10.6

The IRC of the conversion from the water complex to alcohol **39** is only determined for water complex S-**36** and calculated at the B3LYP/def2-TZVP level of theory. It is shown that the reaction proceeds via a transition state with an activation barrier of 5.5 kcal/mol (Figure 4.37). The barrier is slightly lower than the barrier of the rearrangement of water complex S-**33** to alcohol **34** (6.1 kcal/mol), which is presumably because the electron donation capacity from the OH group is less compared to the methoxy group, resulting in a more electrophilic singlet carbene complex that is more reactive. A similar reaction behavior to complex S-**33** was expected for this system, which is in accordance with the experimental results.

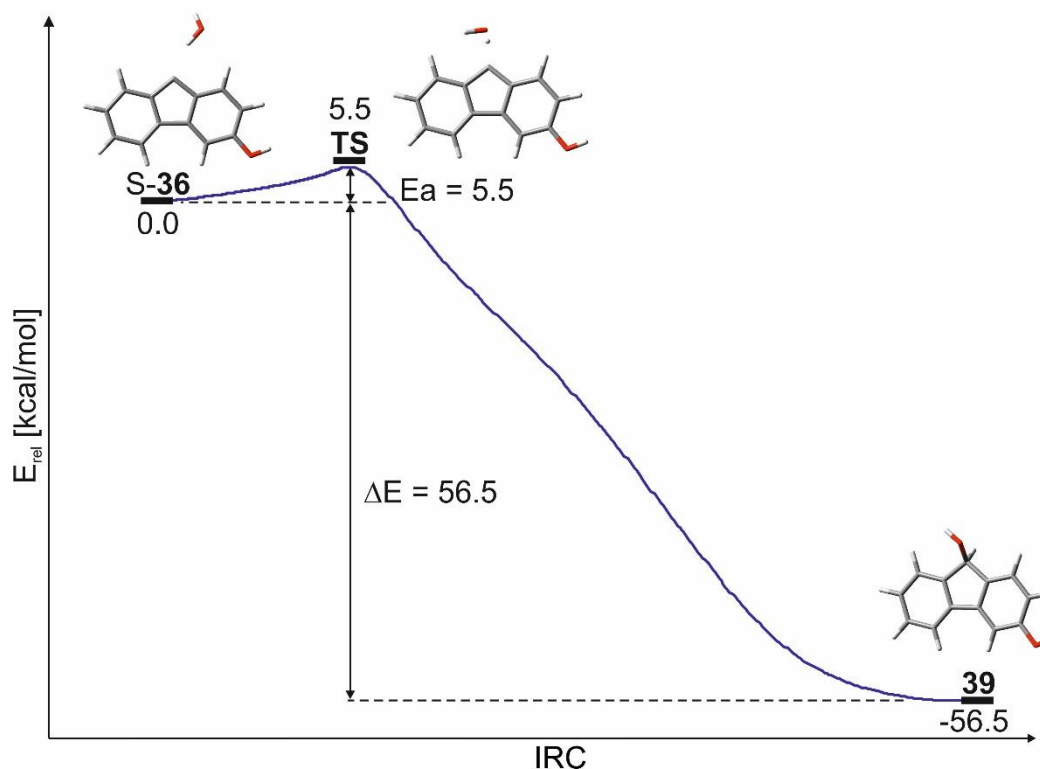


Figure 4.37: IRC of the rearrangement of water-complex S-36 to alcohol 39 via the displayed transition state. The energies are given in kcal/mol and were calculated at the B3LYP/def2-TZVP level of theory.

For the interactions of carbene **31** with different Lewis bases, it is calculated how the formation of hydrogen bonds at the hydroxy group of the carbene influences the singlet-triplet energy gap. For the interacting solvents dimethyl ether, diethyl ether, trimethyl amine, triethyl amine and acetone, it is observed that the formation of hydrogen bonds significantly lowers the singlet-triplet gap of **31** (Chart 4.3).

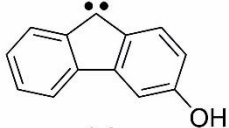
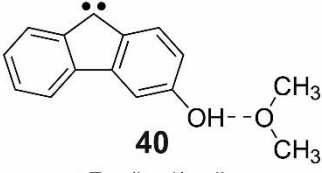
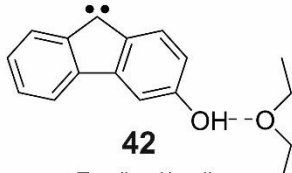
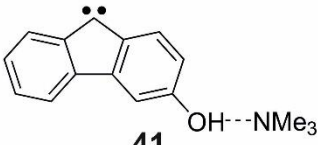
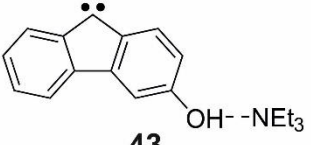
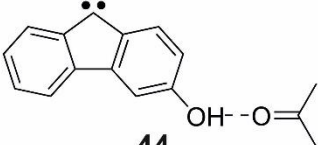
 <p>31</p> ΔE_{S-T} (kcal/mol): 2.2 (up) 2.5 (down)	 <p>40</p> ΔE_{S-T} (kcal/mol): 1.2 (up) 1.5 (down)	 <p>42</p> ΔE_{S-T} (kcal/mol): 1.2 (up) 1.5 (down)
 <p>41</p> ΔE_{S-T} (kcal/mol): 0.7 (up) 1.1 (down)	 <p>43</p> ΔE_{S-T} (kcal/mol): 0.7 (up) 1.1 (down)	 <p>44</p> ΔE_{S-T} (kcal/mol): 1.2 (up) 1.6 (down)

Chart 4.3: Theoretical singlet-triplet energy gaps of carbene **31** and several hydrogen-bonded carbene-Lewis base complexes **40-44**. The energies were calculated at the B3LYP/def2-TZVP level of theory for both the “up” and “down” conformer.

Carbene-DME complex **40** exhibited singlet-triplet energy gap values of 1.2 kcal/mol (**40-u**) and 1.5 kcal/mol (**40-d**). Analysis of the energies of the different conformers of **40** showed that the conformer energy differences are even lower than for the non-complexed carbene **31** (S-**40**: 0.3 kcal/mol ; T-**40**: < 0.1 kcal/mol).

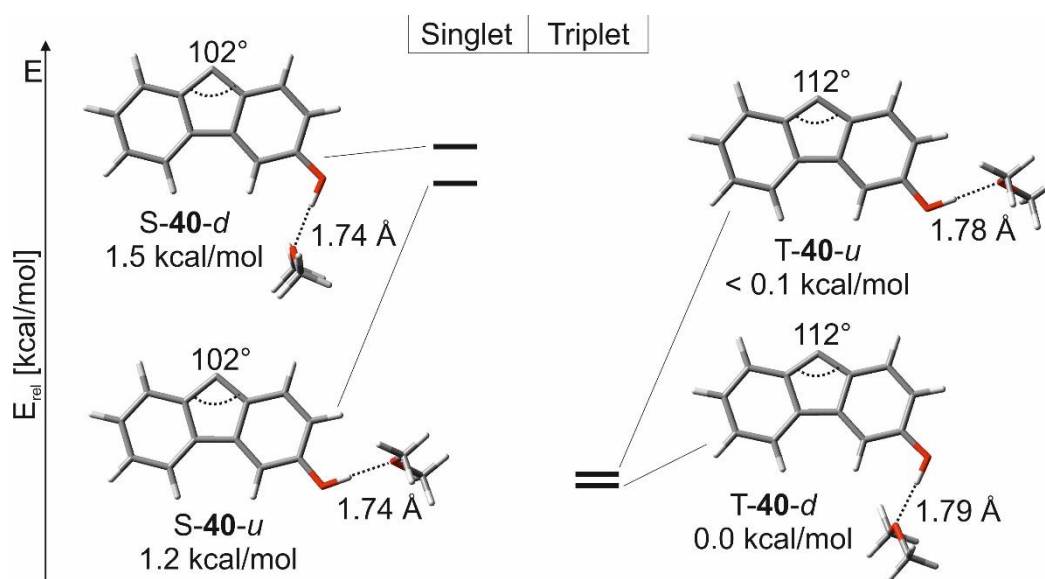


Figure 4.38: Theoretical energies of the different conformer and spin state species of DME complex **40** relative to the most stable conformer T-**40-d**. The energies were calculated at the B3LYP/def2-TZVP level of theory.

The DME complex **40** exhibits an increased steric bulkiness in the matrix cage. Hence, the rigid matrix probably prevents the switch of the conformer, which would be similar to the observations of Khriachtchev who prevented conformer switching of formic acid by forming hydrogen bonds with water.^[135-136]

The formation of a hydrogen-bonded complex of **31** with trimethyl amine results in a lowering of the singlet-triplet gap to 0.7 kcal/mol (**41-u**) and 1.1 kcal/mol (**41-d**). Like in the case of DME complex **40**, the energy differences between the conformers are lower than for carbene **31**. The singlet complex **S-41** exhibits a conformer energy difference of 0.3 kcal/mol, and the energy difference for **T-41** is 0.1 kcal/mol.

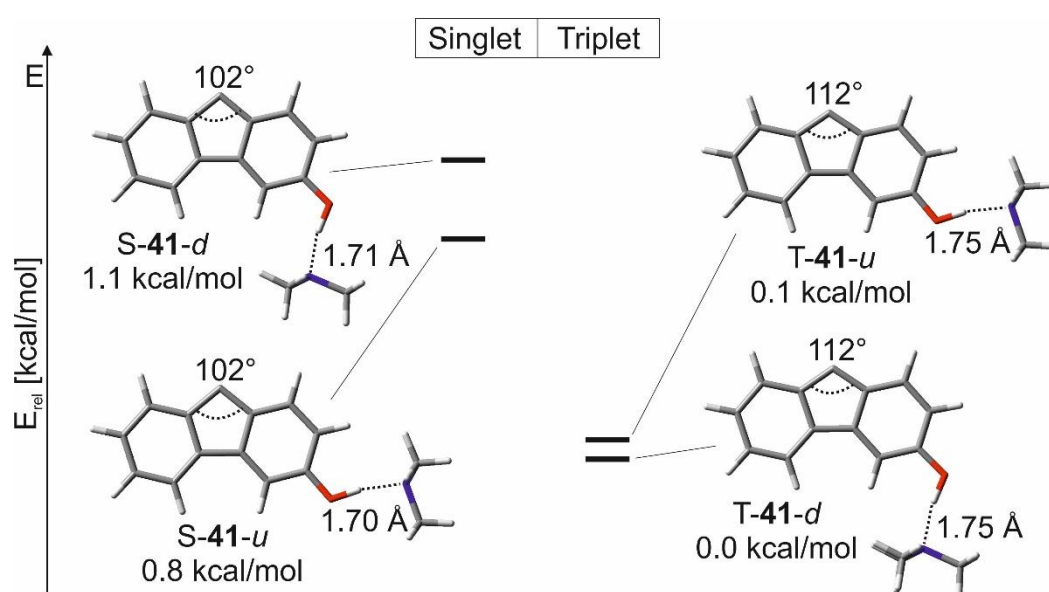
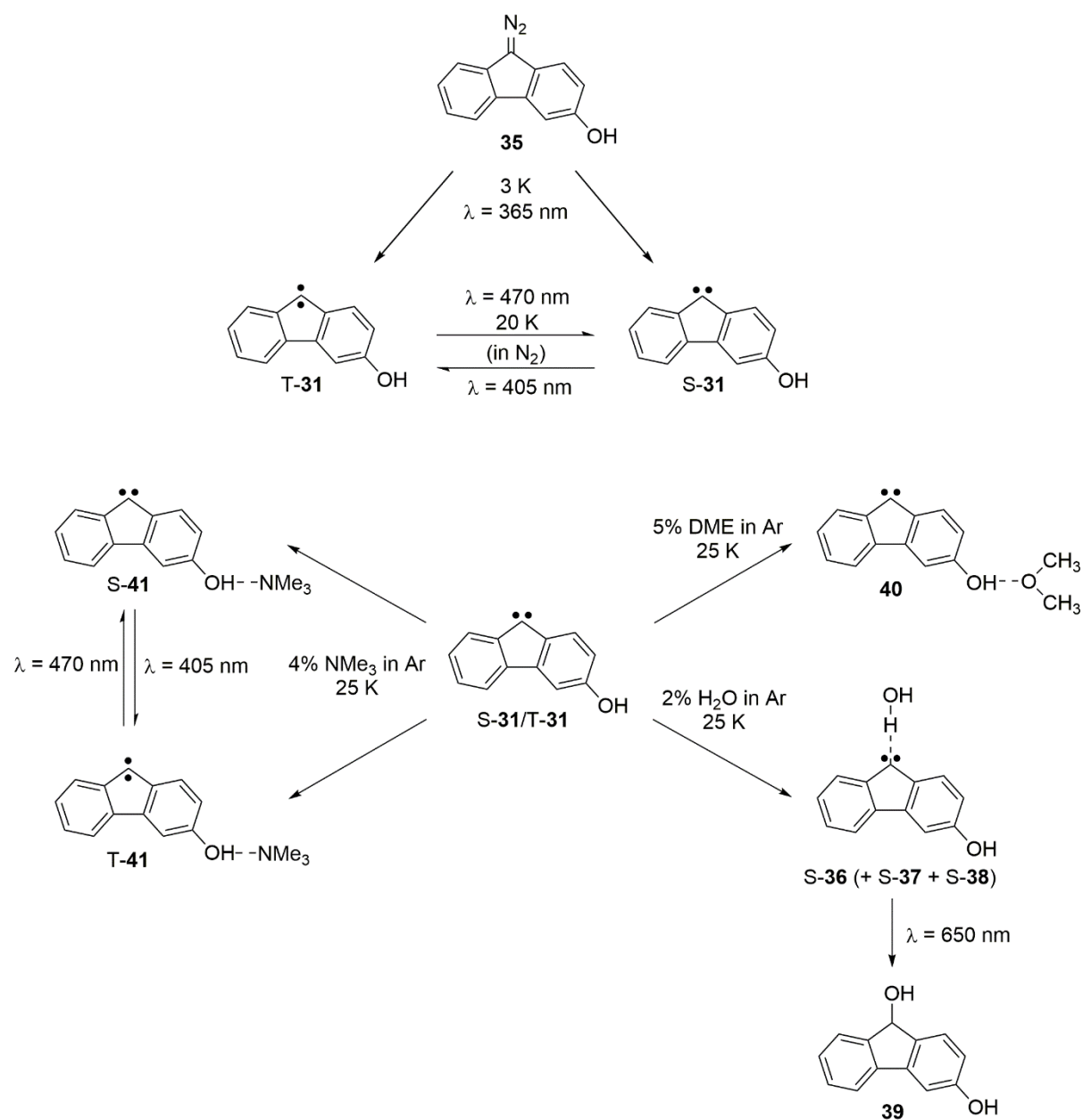


Figure 4.39: Energies of the “up” and “down” conformers of singlet and triplet NMe₃-carbene complex **41** relative to the most stable species T-41-d. The energies were calculated at the B3LYP/def2-TZVP level of theory.

Since the trimethyl amine molecule in **41** is even more sterically demanding than dimethylether in **40**, it is assumed that, despite the low conformer energy differences, no conformer switching is possible for this system. In addition to that, it is determined that the hydrogen bond length in **41** is slightly shorter than in complex **40**, which indicates that this hydrogen bond is marginally stronger.

4.3.6. Conclusions

The reactive intermediate 3-hydroxy-9-fluorenylidene (**31**) was successfully generated in matrices of argon, xenon and nitrogen. Carbene **31** is found to exhibit magnetic bistability, since both the singlet and triplet states coexist indefinitely in matrices, as demonstrated by IR, UV/Vis and EPR spectroscopy. Computational calculations at the B3LYP/def2-TZVP level of theory deliver a low singlet-triplet energy gap of 2.2 kcal/mol (**31-u**) and 2.5 kcal/mol (**31-d**), and calculations with the method CCSD(T)/cc-PVDZ//B3LYP-D3/def2-TZVP yield a singlet-triplet gap of 0.7 kcal/mol (**31-u**). In argon, the singlet-triplet conversion of carbene **31** was not efficient after irradiation with 405 nm and 470 nm light. However, a significantly higher amount of S-T conversion was observed under the same condition in a nitrogen matrix. Carbene **31** formed in a singlet-triplet ratio of 81/19, and irradiation with 405 nm light increased the amount of triplet carbene and decreased the singlet ratio. Irradiation with 470 nm light and annealing to 20 K reversed this effect. Furthermore, it was observed that both S-**31** and T-**31** formed as a conformer mixture. Since the singlet-triplet conversion of the similar compound 3-methoxy-9-fluorenylidene (**29**) was linked to the change of the conformer, it was assumed that this is also the case for carbene **31**.^[122] However, the low conformer energy differences of **31** of almost zero (S-**31**: 0.5 kcal/mol ; T-**31**: 0.2 kcal/mol) led to the assumption that hydrogen tunneling between the two conformers occurs, which has already been observed for other OH-containing organic systems with low conformer energy differences.^[130-131] Hence it is possible that in an argon matrix, the S-T interconversion was barely observable due to fast conformational hydrogen tunneling. In nitrogen matrices, the tunneling process is significantly slower,^[132-134] which could have resulted in the higher observable S-T interconversion. To proof these assumptions, experiments of deuterated carbene **31** with an OD group will be conducted in future investigations to test if the kinetic isotope effect^[3] has an influence on potential tunneling. By conducting experiments in argon matrices doped with the Lewis bases dimethyl ether or trimethyl amine, the complexes **40** and **41** were formed that exhibit lower singlet-triplet energy gaps than the non-complexed carbene **31** (according to calculations). For complex **41**, increased singlet-triplet conversion was observed after irradiation with 405 nm and 470 nm light. Doping of the matrix with water resulted in the formation of the corresponding singlet state water complexes **36-38** and probably other water complexes that have not been further investigated. It was observed that both S-**31** and T-**31** interacted with water. The complexes were stable under matrix isolation conditions at 3-10 K, but converted to the corresponding alcohol **39** via an insertion reaction when irradiated with light of 650 nm.



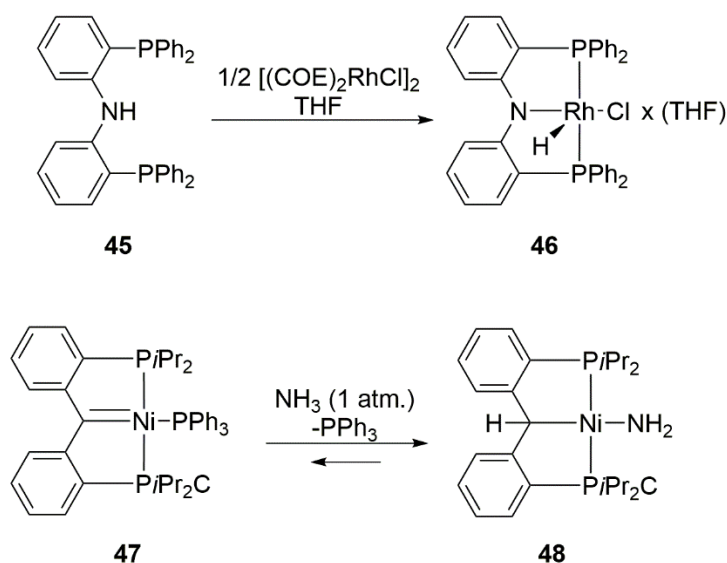
Scheme 4.4: Formation of the magnetically bistable carbene **31** in both its singlet and triplet state. Via thermal and photochemical methods, singlet-triplet interconversion is induced (especially in a nitrogen matrix). Carbene **31** interacts with NMe₃ to form the corresponding complex **41** that can also undergo S-T conversion when irradiated with 470 nm or 405 nm light. With DME, complex **40** is formed that does not show spin interconversion. Interactions with water formed several water complexes in their singlet state, including S-36, S-37 and S-38. Irradiation with 650 nm light converted these complexes to alcohol **39**.

5. Reactions of Fluorenylidenes with Ammonia

5.1. Introduction

In the field of synthetic organic chemistry, the activation of small molecules is an important topic for the production of new profitable compounds.^[141] For instance, this topic has a grave importance in the utilization of solar energy via solar fuel cells by activating hydrogen and water molecules.^[142] Mostly, transition metal complex compounds are used to enable the activation of small molecules. While the activation of molecules like H₂ has thoroughly been investigated in previous research, the activation of ammonia, i.e. the N–H bond, by metal complexes was observed to be rather challenging.^[143-145] The metal-based N–H activation is very limited, since transition metals complexes and ammonia tend to favor reactions in which Lewis acid-base complexes are formed by interactions with the lone electron pair of the nitrogen of NH₃. This observation was already shown by Werner who presented a range of several metal-ammonia complexes.^[146] One of the possible reasons is that the N–H bond in ammonia is rather strong (107.4 kcal/mol)^[147], so that activation of this bond requires too much energy.

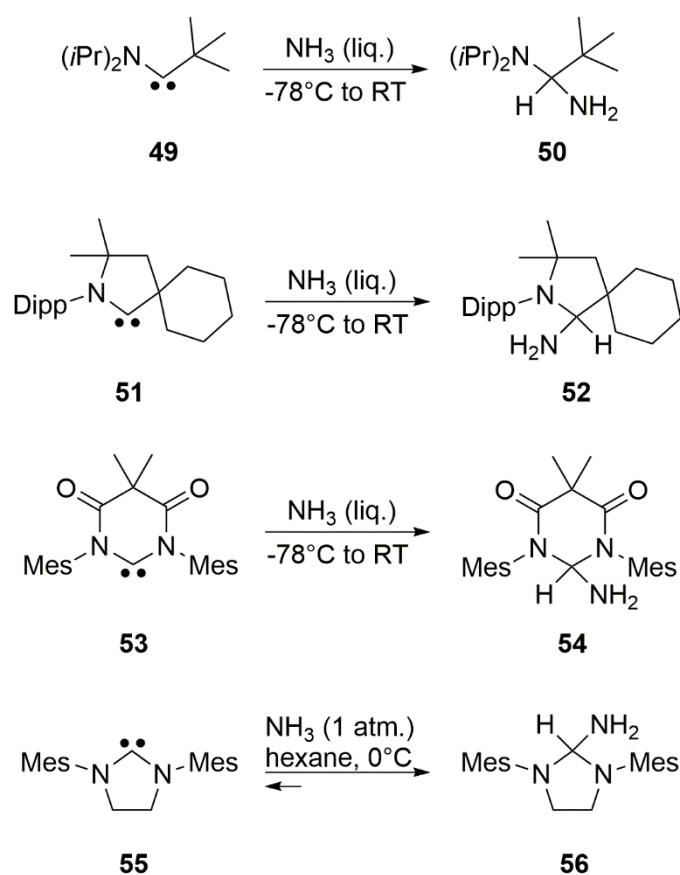
In recent years, several examples of metal complexes were reported that were able to activate the N–H bond of amines. These complexes mostly incorporate strongly σ -donating ligands into pincer-type ligand systems.^[143]



Scheme 5.1: N–H bond activation of amines by pincer-type transition metal complexes presented by Mayer and Kaska (**45** + **46**) and by Piers (**47** + **48**).^[143, 148]

An examples was presented by Mayer and Kaska for a transition metal complex that activates an N–H bond chelate-assisted in an intramolecular fashion, while another complex was presented by Piers that showed the intermolecular activation of ammonia by a nickel pincer complex (Scheme 5.1).^[143, 148]

Compared to the activation of ammonia by transition metal complexes, the metal-free activation has only rarely been reported. Bertrand and co-workers presented the first example of metal-free ammonia activation by singlet (alkyl)(amino)carbenes.^[149] Since singlet carbenes have a vacant orbital and a filled nonbonding orbital, they show similarities to the metal center of transition metal complexes.^[144] Two similar singlet carbene systems that also feature heteroatoms next to the carbene center and have the ability to activate ammonia were later reported by Bielawski and co-workers (Scheme 5.2).^[150-151]



Scheme 5.2: Activation of ammonia under rather mild conditions by different singlet carbenes presented by Bertrand (**49** – **52**) and by Bielawski (**53** – **56**).^[149-151]

Regarding the reaction mechanism of carbenes with amines, several investigations have been conducted in the past. In early research, it was shown that carbenes can react with an amine like pyridine under formation of an ylide.^[152] However, this amine did not include N–H bonds, so that this observation is not a reliable prognosis for the reaction behavior of ammonia with

carbenes. Bethell studied the reaction behavior of diphenylcarbene with *n*- and *t*-butylamines in presence of acetonitrile to investigate the reaction mechanisms.^[153] Since he did not observe a kinetic isotope effect after using a non-deuterated and a deuterated amine, he was assuming that the reaction intermediate must be an *N*-ylide. The following investigation of Schuster included laser spectrophotometric analysis of the reaction between fluorenylidene and *t*-butylamine, where he also concluded that the intermediate of this reaction was probably the corresponding ylide.^[154] However, both Bethell and Schuster only predicted the ylide since they were not able to isolate and hence directly observed it.

Since recent investigations of the reaction between different carbenes and water verified that this reaction proceeds via a hydrogen-bonded intermediate,^[41, 109] it is assumed that the reaction between amines and carbenes possibly proceeds in a similar manner. The following chapters describe the investigation of the two carbene 3,6-dimethoxy-9-fluorenylidene (**30**) and 3-hydroxy-9-fluorenylidene (**31**) and their reactivity towards ammonia to find out more details about the reaction mechanism and possible reaction intermediates.

5.2. Reaction of 3,6-Dimethoxy-9-fluorenylidene with Ammonia

5.2.1. Experimental Results

IR Experiments

The reaction behavior of the carbene 3,6-dimethoxy-9-fluorenylidene (**30**) with ammonia was investigated to identify the nature of the reaction mechanism. It was assumed that the interaction of **30** with ammonia leads either to the formation of the singlet-ammonia complex **S-57** or the corresponding ylide **58**. Calculations at the B3LYP/def2-TZVP show that the singlet ammonia complex **S-57** is considerably lower in energy than triplet complex **T-57**, so that the formation of the triplet complex is not expected. Ylide **58** is even lower in energy than the singlet or triplet complex. To determine which of the possible ammonia-carbene interaction products forms, experiments in argon matrices doped with 1 – 3% of ammonia were conducted. After photolysis of the diazo precursor, the matrix was annealed from 3 K to 25 K. It was observed that the signals of the carbene decreased while several new signals with low intensity appeared (Figure 5.1).

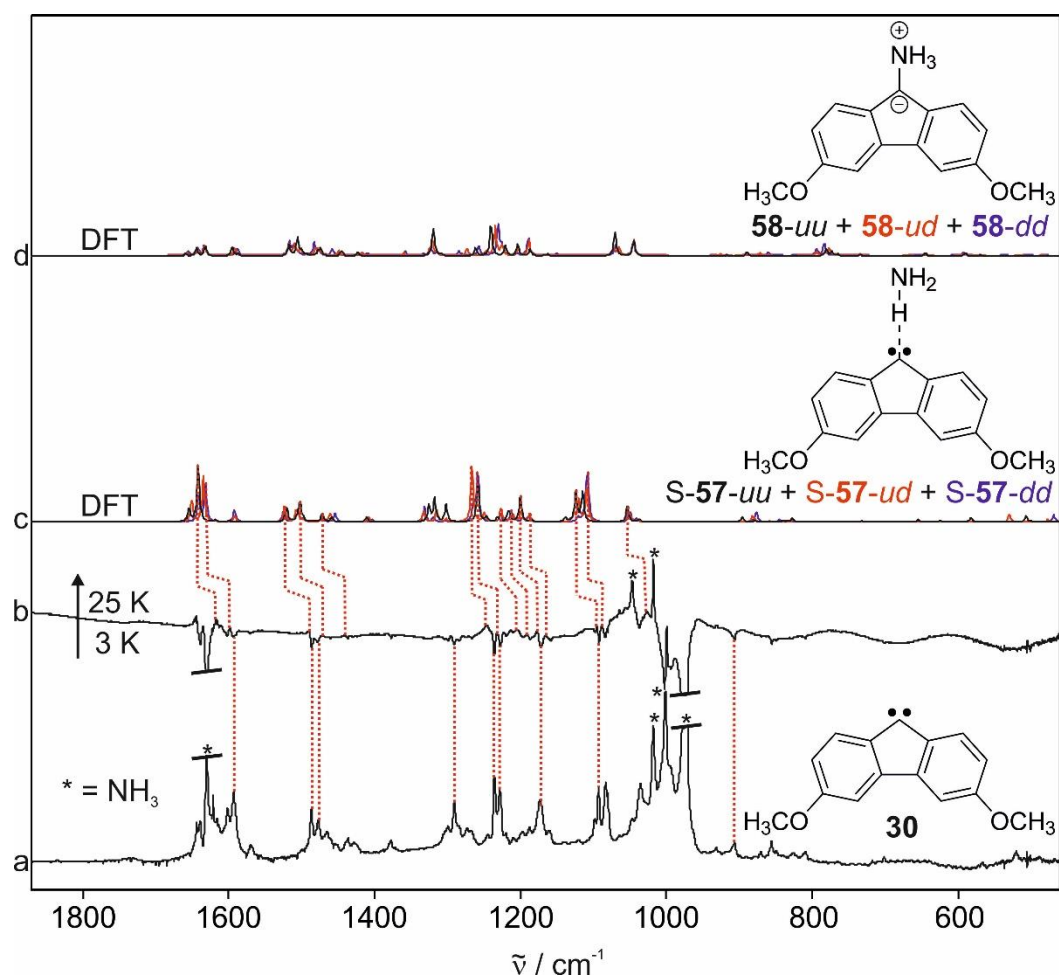


Figure 5.1: Annealing experiments of carbene **30** in an argon matrix doped with 3% ammonia. The signals marked with an asterisk correspond to ammonia and its aggregation products. (a) IR spectrum of **30** in an argon matrix doped with 3% ammonia at 3 K. (b) IR difference spectrum after annealing to 25 K. The signals pointing upwards are assigned to singlet complex S-57, the signals pointing downwards to singlet carbene **30**. (c) Theoretical IR spectra of the singlet ammonia complex conformers S-57-uu (black spectrum), S-57-ud (red spectrum) and S-57-dd (blue spectrum) calculated at the B3LYP/def2-TZVP level of theory. (d) Theoretical IR spectra of the ylide conformers 58-uu (black spectrum), 58-ud (red spectrum) and 58-dd (blue spectrum).

It was detected that the most distinct changes appeared when 3% of NH_3 were used. The new appearing signals and especially the shifts between these are compared with theoretical spectra of singlet ammonia complex S-57 and ylide **58** (B3LYP/def2-TZVP) to observed that they show the highest accordance with the theoretical spectrum of singlet complex S-57. For the theoretical spectra of the ylide **58**, several mismatches are detected in the region of around $1080 - 1150 \text{ cm}^{-1}$ and at $1200 - 1250 \text{ cm}^{-1}$. Hence, it is verified that the reaction of carbene **30** with ammonia does not proceed via an ylide intermediate but a hydrogen-bonded complex, which is in contrast to the predictions of Bethell and Schuster who presumed an ylide intermediate for reactions between amines and carbenes.^[153-154] The IR spectra show a conformer mixture of the conformers “uu”, “ud” and “dd” which is agreement with theoretical

calculations (B3LYP/def2-TZVP) that predict small energy differences between these conformers. To investigate if any reaction of complex **S-57** to the corresponding amine **59** occurs, the complex was left in the dark for 67 hours, but only very small changes were observed (Figure 5.2). Conducting of the same experiment in an ammonia-free argon matrix resulted in the same changes, which excludes that these were caused by conversion to the amine. Irradiation with 650 nm light (for both matrices) resulted in similar changes that are assigned to the conformer switch from **S-30-ud** and **S-30-dd** to conformer **S-30-uu**. Hence, it is proven that the changes after 67 h in the dark correspond to conformer switching to **30-uu**.

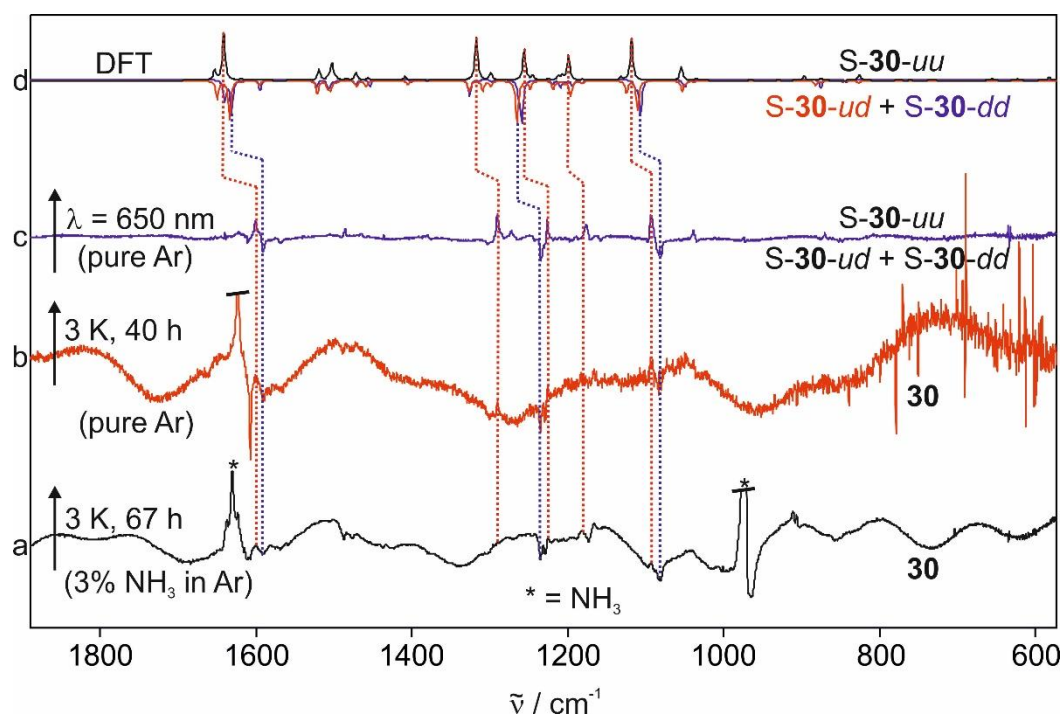


Figure 5.2: Carbene **30** after annealing to 25 K and subsequently keeping in the dark at 3 K for several hours. (a) Difference IR spectrum in an argon matrix doped with 3% NH_3 after 67 hours at 3 K in the dark. The ammonia signals are marked with an asterisk. Signals pointing upwards are assigned to **S-30-uu**, the signals pointing downwards to both **S-30-ud** and **S-30-dd**. (b) Difference IR spectrum in an argon matrix after 40 hours at 3 K in the dark. (c) IR spectrum of carbene **30** in an argon matrix after irradiation with 650 nm light. The signals pointing upwards and downwards are assigned according to spectrum a. (d) Theoretical IR difference spectrum calculated at the B3LYP/def2-TZVP level of theory. The signals pointing upwards correspond to **S-30-uu**, the signals pointing downwards to **S-30-ud** (red spectrum) and **S-30-dd** (blue spectrum).

In the following experiments, it was tested if the conversion to amine **59** is achievable via photochemistry. Irradiation of the ammonia complex **S-57** with LED light in the range of 650 – 365 nm for several minutes did not result in any significant changes aside of conformer shifts. After irradiation with 254 nm light, it was observed that the signals of the ammonia complex **S-57** decreased while several new signals increased (Figure 5.3). Comparison of these

signals with a reference IR spectrum verifies the formation of amine **59** via 254 nm irradiation. Since the calculated energy differences (B3LYP/def2-TZVP) between the different conformers of **59** are small, it is expected that this amine forms as a conformer mixture.

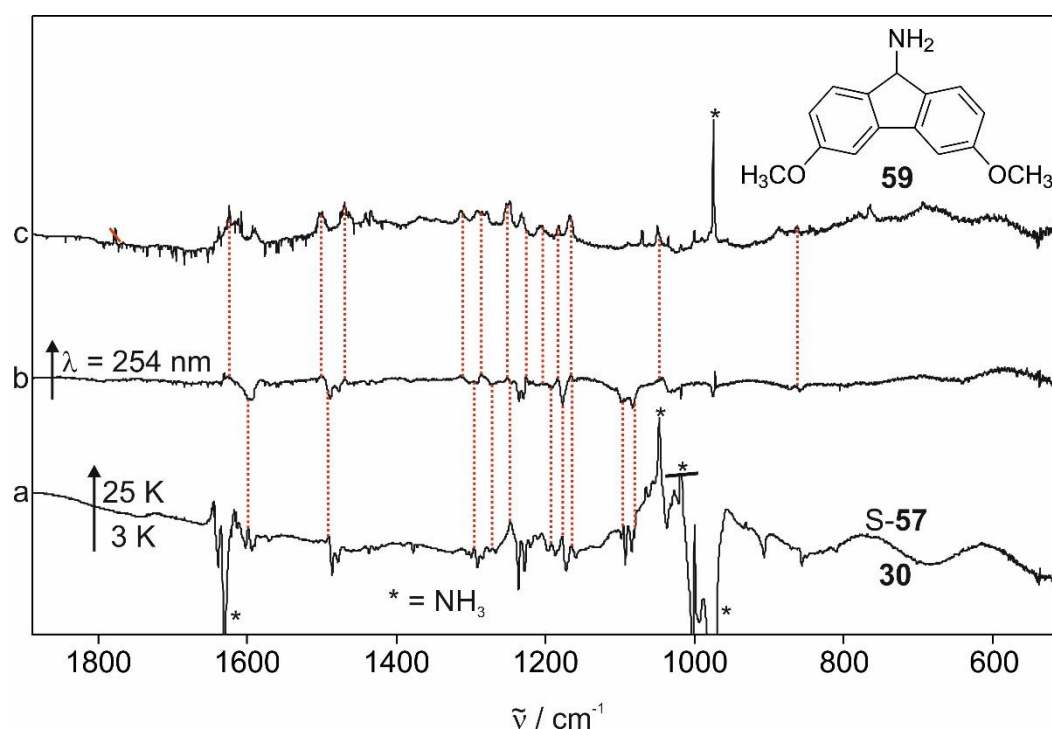


Figure 5.3: IR spectra showing the photochemical conversion from ammonia complex S-57 to amine **59**. The peaks of ammonia are marked with an asterisk. (a) IR difference spectrum after annealing of carbene **30** to 25 K in an ammonia-doped argon matrix. The signals pointing upwards are assigned to complex S-57 the signals pointing downwards to **30**. (b) Difference spectrum after irradiation with 254 nm light. The signals pointing upwards are assigned to amine **59**, the signals pointing downwards to S-57. (c) IR reference spectrum of amine **57** in an argon matrix at 3 K.

UV/Vis and EPR Experiments

To further analyze the reaction behavior of carbene **30** with ammonia and obtain more clarity about the results of the IR investigation, the experiments were additionally characterized via UV/Vis spectroscopy. Carbene precursor **32** was photolyzed in an argon matrix doped with 3% of ammonia at 8 K and the resulting carbene **30** was annealed to 25 K. It was observed that after annealing, the intensity of the carbene signal at 296 nm decreased while a new peak at 321 nm and another broad signal at 418 nm increased (Figure 5.4). The signal at 418 nm is assigned to the singlet ammonia complex S-57, which is in the same area as the signals of the water complexes of **30** (S-33: 412 nm) and 3-hydroxy-9-fluorenylidene **31** (S-36: 421 nm).

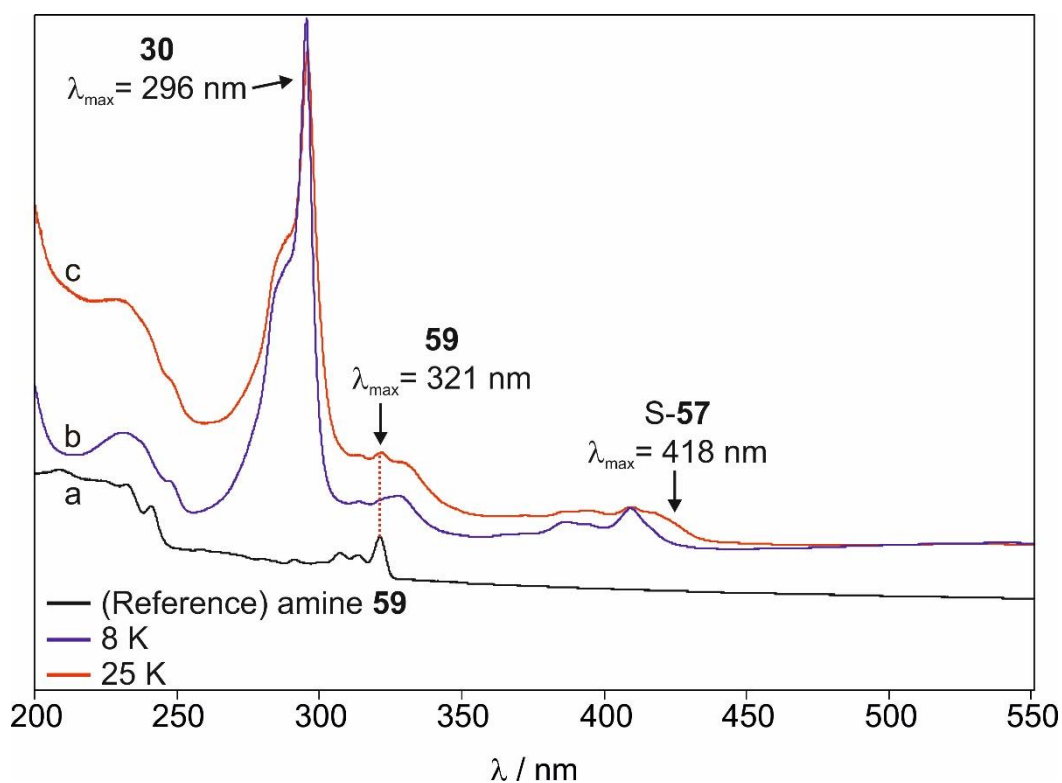


Figure 5.4: UV/Vis spectra of carbene **30** in an argon matrix doped with 3% ammonia before and after annealing to 25 K. (a) UV/Vis reference spectrum of amine **59** in argon at 8 K. (b) UV/Vis spectrum of carbene **30** at 8 K. (c) UV/Vis spectrum of carbene **30** after annealing to 25 K.

Comparison with a reference UV/Vis spectrum of amine **59** verifies that the new signal at 321 nm corresponded to traces of the amine. This was not observed during the IR investigation, presumably because the IR signals of the formed amine **59** are too small to be observable. In summary, it is shown that annealing of carbene **30** in an ammonia-doped argon matrix formed both the singlet complex S-**57** and the amine **59**.

Similarly to the IR experiments, there was no reaction observed after the sample was left in the dark for 66 h or irradiated with light in the range of 650 – 365 nm. Irradiation of the matrix with 254 nm light caused the signals of the ammonia complex S-**57** and carbene **30** to decrease, while the signal at 321 nm increased and new signals appeared at 241 and 232 nm (Figure 5.5). Comparison with the UV/Vis reference spectrum of amine **59** verifies that these increasing signals belong to the amine.

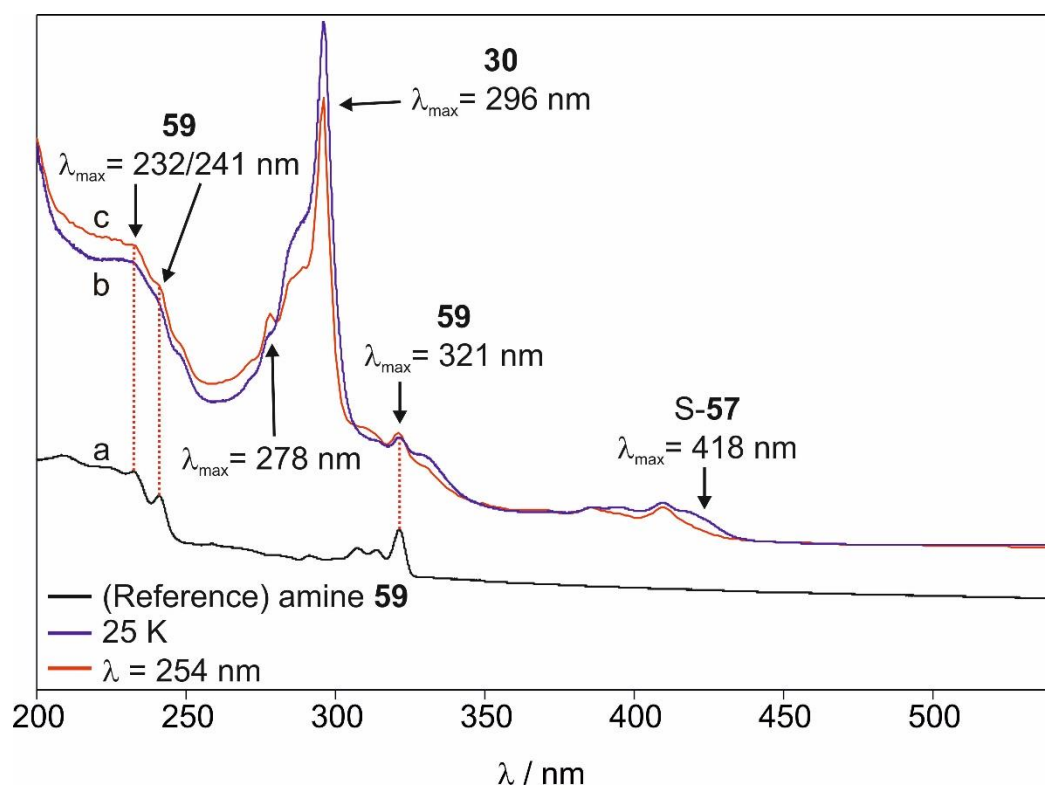


Figure 5.5: Irradiation experiments of ammonia complex S-57 that has formed after annealing of carbene **30** in an argon matrix doped with 3% ammonia. (a) UV/Vis reference spectrum of amine **59** in an argon matrix at 8 K. (b) UV/Vis spectrum after annealing to 25 K. (c) UV/Vis spectrum after irradiation with 254 nm light.

An additional new signal at 278 nm is observed that is not assigned to the compounds **30**, S-57 or **59**, so that further analysis has to be conducted in future research. It is assumed that this signal results from small traces of a side-reaction product. Since fluorene systems show absorptions in the range of 249 nm, it is possible that 254 nm irradiation could have induced side-reaction.^[139] However, this assumption was not confirmed yet.

Subsequently, the experiments of carbene **30** with ammonia were investigated by EPR spectroscopy to examine if any radical-like intermediate forms in the course of the reaction. However, the resulting EPR spectra did not exhibit any distinct signal during the whole experiment, which indicates that no paramagnetic species had formed.

5.2.2. Computational Results

The study to investigate the interactions and reaction behavior of carbene **30** with ammonia was supported by computational methods. Calculations at the B3LYP/def2-TZVP level of theory show that the complex formation between **30** and ammonia increases the singlet-triplet energy gap from -0.7 kcal/mol to -4.0 kcal/mol (for conformer “*uu*”, Figure 5.6). For the other conformers, singlet-triplet gaps of -3.1 kcal/mol (**57-ud**) and -2.1 kcal/mol (**57-dd**) are determined. The corresponding ylide **58** is even lower in energy than the singlet ammonia complex by 16.1 kcal/mol (**58-uu**), 17.9 kcal/mol (**58-ud**) and 19.7 kcal/mol (**58-dd**). However, experiments showed that the ylide did not form as an intermediate under matrix isolation conditions.

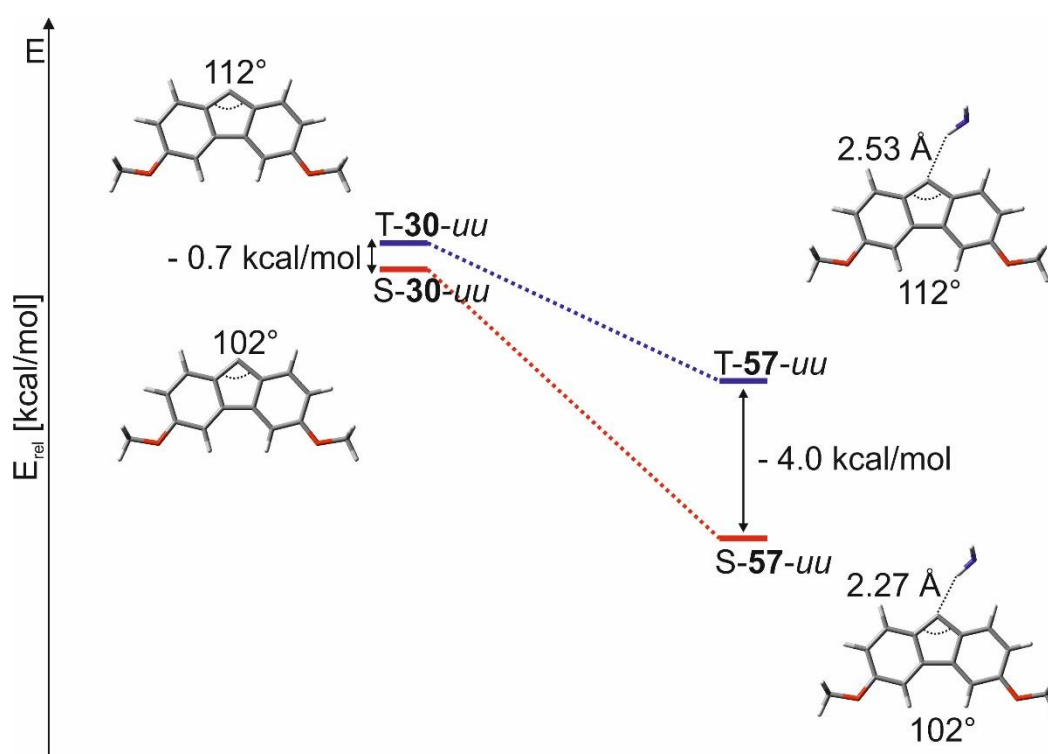


Figure 5.6: Singlet-triplet energy gaps of the energetically most favored conformer “*uu*” of carbene **30** and carbene-ammonia complex **57**. The energies were calculated at the B3LYP/def2-TZVP level of theory.

Regarding the energy differences between the different conformers complex **57**, it is observed that the conformer energy differences of **T-57** are significantly lower than those of **S-57** (Table 5.1) Similarly to the non-complexed carbene **30**, this result can be explained by the smaller dipole moment of triplet carbenes, as explained in Chapter 4.2.3.

Table 5.1: Energy differences between the different conformers of S-**57** and T-**57** in relation to the lowest-energy conformer. The energies are given in kcal/mol and were calculated at the B3LYP/def2-TZVP level of theory.

Conformer	S- 57	T- 57
<i>uu</i>	0.0	0.0
<i>ud</i>	1.0	< 0.1
<i>dd</i>	2.0	0.2

The calculated bond length of the hydrogen bond between the carbene center and the hydrogen of ammonia is slightly elongated compared to the hydrogen bond length in the water complex **33**. For the ammonia complex, the hydrogen bond is longer by 0.33 Å (S-**57**) and 0.27 Å (T-**57**). This indicates that the hydrogen bond in the ammonia complex **57** is slightly weaker than the hydrogen bond in the water complex **36** due to water being a better hydrogen bond donor.^[46] This weaker hydrogen bonding also explains the stabilization energies of **57** that are smaller than the energies of the corresponding water complex (Table 5.2). The stabilization energy of singlet water complex S-**36** is approximately 5.0 kcal/mol larger than for S-**57**, while the energy of complex T-**36** is around 1.1 kcal/mol larger compared to T-**36**.

Table 5.2: Stabilization energies (ΔE_s) of singlet and triplet ammonia complex **57** calculated at the B3LYP/def2-TZVP level of theory. The energies are given in kcal/mol.

complex	ΔE_s (singlet)	ΔE_s (triplet)
57-uu	- 5.8	- 2.5
57-ud	- 5.6	- 2.4
57-dd	- 5.6	- 2.4

The IRC of the insertion reaction from singlet ammonia complex S-**57** to the corresponding amine **59** is calculated at the B3LYP/def2-TZVP level of theory (Figure 5.7). A transition state is determined with an activation barrier of 6.3 kcal/mol that converts to amine **59**. Since the activation barrier of the reaction from the corresponding water complex complex S-**33** to alcohol **34** has a similar height (6.1 kcal/mol) and width, a similar reactivity is expected.

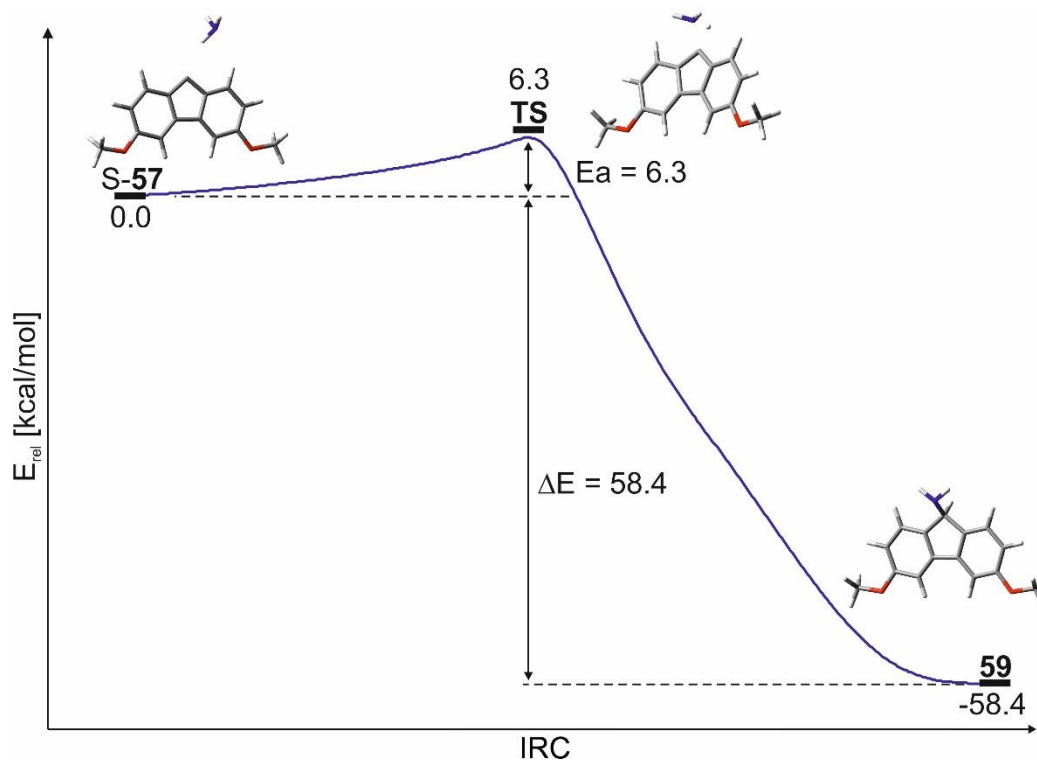


Figure 5.7: IRC of the formation of amine **59** from the singlet state ammonia complex **S-57**. The energies are given in kcal/mol and were calculated at the B3LYP/def2-TZVP level of theory.

5.3. Reaction of 3-Hydroxy-9-fluorenylidene with Ammonia

5.3.1. Experimental Results

IR Experiments

The reactivity of 3-hydroxy-9-fluorenylidene (**31**) with ammonia was investigated to study the reaction mechanism. For this purpose, diazo precursor **35** was isolated in an argon matrix doped with 1% ammonia at 3 K and photolyzed using 365 nm light. The matrix was annealed to 25 K, whereupon the signals of both singlet carbene **S-31** and triplet carbene **T-31** decreased (Figure 5.8). The singlet-triplet ratio of **31** changed from 50/50 to 30/70 after annealing of the matrix. This altered ratio indicates a higher singlet carbene decrease, and therefore it is observed that preferably **S-31** interacted with ammonia compared to **T-31**. In addition to the carbene signals, the intense signal of the ammonia monomers at around 950 cm^{-1} decreased while several new signals appeared. Theoretical calculations at the B3LYP/def2-TZVP level of theory show that the singlet ammonia complexes are energetically more favored than the

corresponding triplet complexes, so that the formation of triplet ammonia complexes is excluded. Comparison of the experimental IR spectra with theoretical spectra of the singlet ammonia complexes S-60 – S-62 and the ylide species 63 – 65 verified that interaction of carbene 31 with ammonia forms the corresponding singlet complexes (Figure 5.8, Figure 5.9).

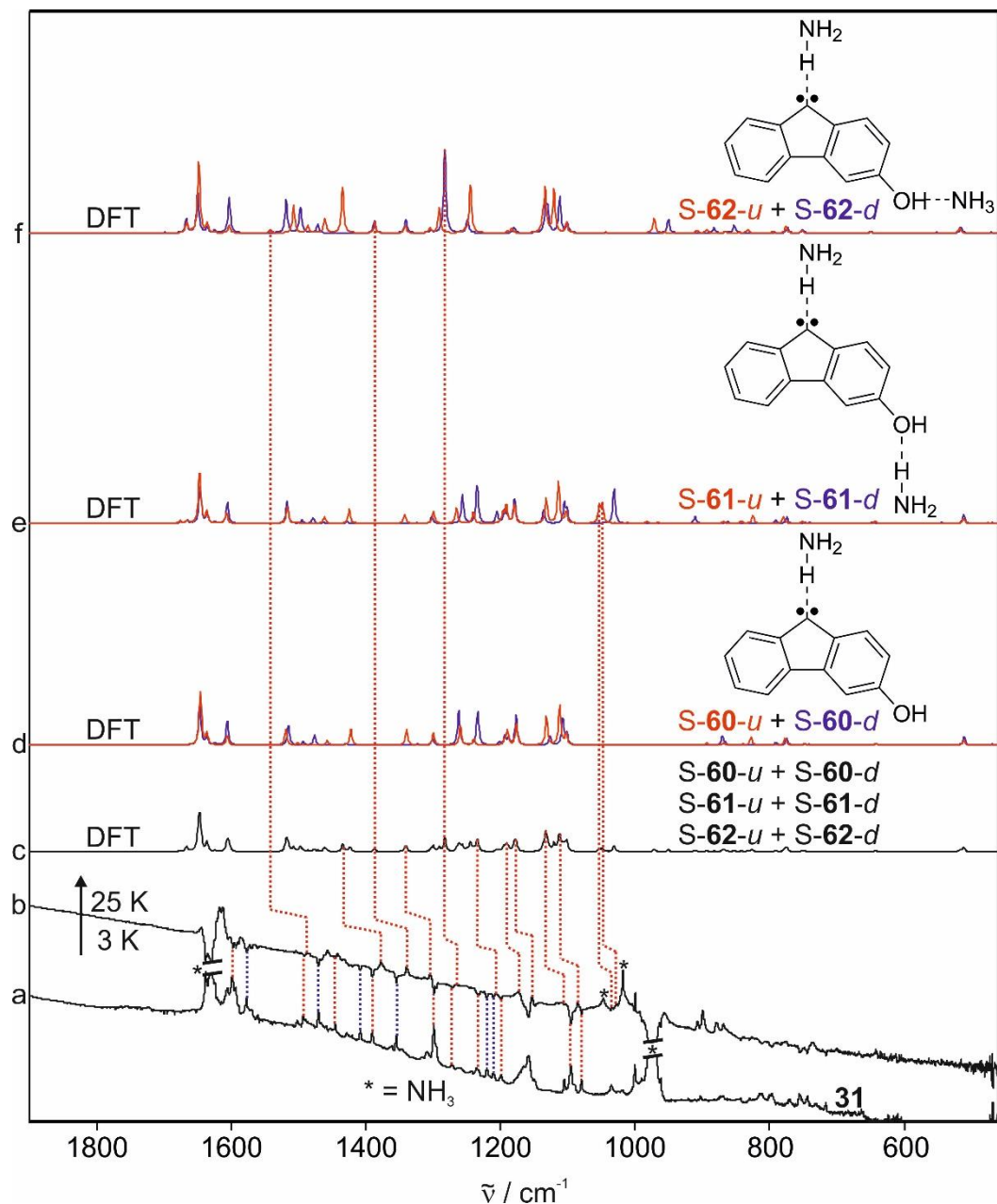


Figure 5.8: Annealing experiments of carbene 31 in an argon matrix doped with 1% ammonia. (a) IR spectrum of 31 in an argon matrix doped with 1% ammonia at 3 K. (b) IR difference spectrum after annealing to 25 K. The peaks pointing upwards were assigned to the singlet ammonia complexes S-60, S-61 and S-62, the signals pointing downwards to carbene S-31 (red dotted lines) and T-31 (blue dotted lines). (c) Theoretical IR spectrum (B3LYP/def2-TZVP) of a mixture of the ammonia complexes S-60, S-61 and S-62 in their “u” and “d” conformers. (d-f) Theoretical IR spectra of the singlet ammonia complexes S-60, S-61 and S-62 (respectively) in their “u” (red spectra) and “d” (blue spectra) conformers.

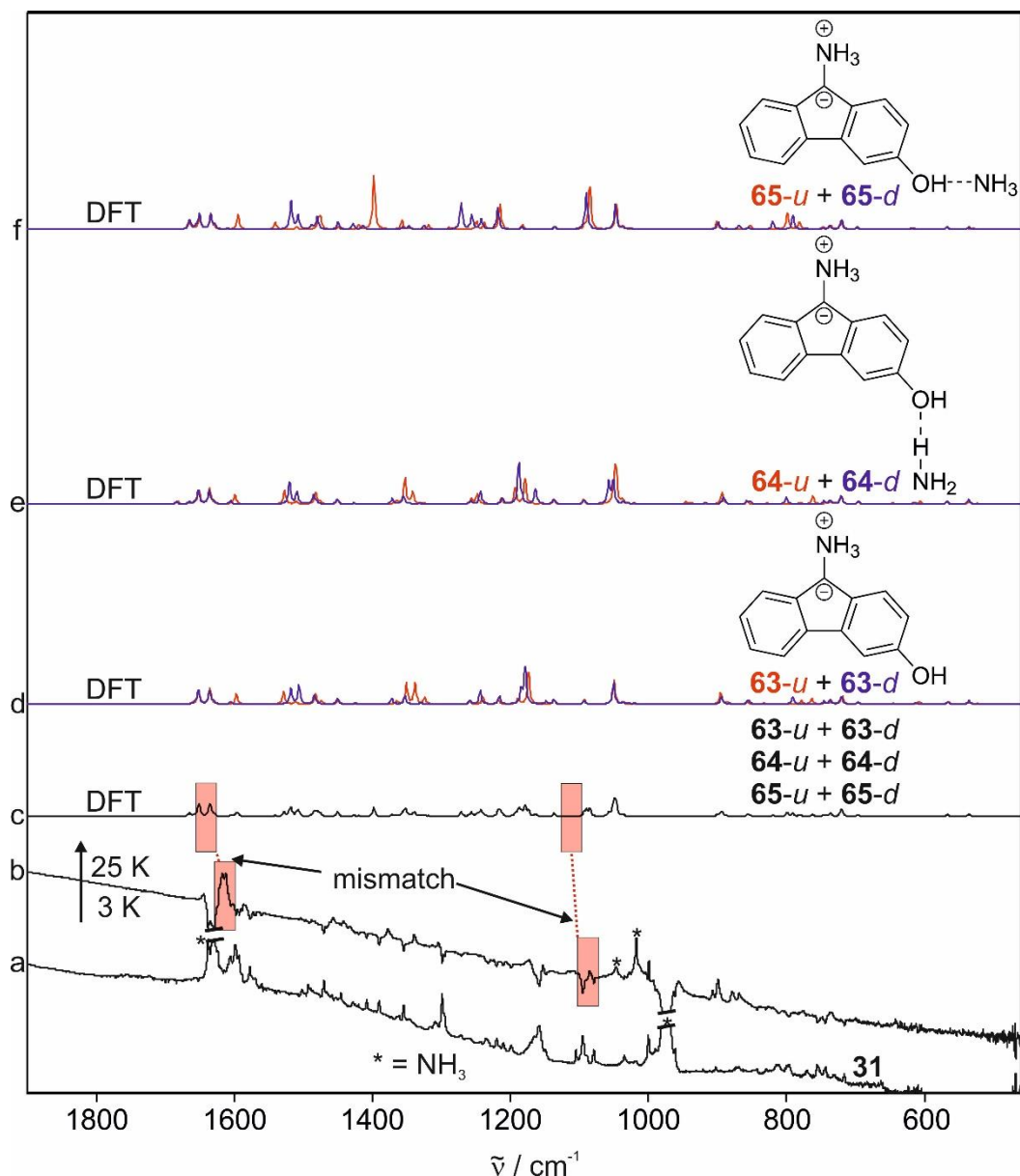


Figure 5.9: Comparison of the IR difference spectrum after annealing carbene **31** to 25 K in an ammonia-doped argon matrix with theoretical spectra of different complexes of ylide **63**. (a) IR spectrum of **31** at 3 K in an argon matrix doped with 1% ammonia. (b) IR difference spectrum after annealing to 25 K. The signals pointing upwards are assigned to the ammonia complexes S-**60**, S-**61** and S-**62**, the signals pointing downwards to both S-**31** and T-**31**. (c) Theoretical IR spectrum (B3LYP/def2-TZVP) of a mixture of the ylide complexes **63** – **65** in their “u” and “d” conformers. (d-f) Theoretical spectra of the ylide complexes **63**, **64** and **65** (respectively) in their conformers “u” (red spectra) and “d” (blue spectra).

The theoretical spectra of the ylide complexes showed several mismatches with the experimental IR spectrum in the range of 1080 – 1140 cm^{-1} and 1620 – 1670 cm^{-1} . Hence, the formation of the ylide as an intermediate in the reaction of **31** with ammonia was excluded. Furthermore, the comparison with the theoretical spectra of the singlet carbene ammonia complexes S-**60** – S-**62** shows that assumably all three complexes have formed after annealing. The signals at 1265, 1340 and 1450 cm^{-1} are assigned exclusively to complex S-**62**, while the

two signals at 1028 and 1035 cm^{-1} are assigned to only S-**61**. The signals assigned to S-**60** are all overlapping with signals of S-**61** and S-**62**, so that the assignment of characteristic signals of S-**60** is challenging. In addition to that, it is not excluded that several other ammonia complexes could have formed that have not been considered in the calculations. Concerning the different conformers of the complexes, it is expected that a conformer mixture is present, since the calculated energy gaps (B3LYP/def2-TZVP) between the conformers “*u*” and “*d*” of S-**60** – S-**62** are rather small.

The ammonia complexes were left in the dark for around 17.5 hours whereupon slight changes in the spectrum appeared (Figure 5.10). It is observed that several signals decreased that belong to the ammonia complexes S-**60** – S-**62** while several new small signals appeared. Irradiation with 650 nm light resulted in the same changes in the spectrum, but with a much higher intensity. Comparison with a reference spectrum of amine **66** and with theoretical spectra of the two amine conformers **66-*u*** and **66-*d*** verifies that the new increasing signals correspond to the amine. However, the comparison with the reference spectrum is challenging since the reference compound decomposed during the sublimation and matrix isolation, resulting in small signals and large amounts of ammonia formed after the decomposition of **66** (Figure 5.10). It is detected that the amine was formed as a conformer mixture because the signals at 1234 cm^{-1} (**66-*d***) and 1363 cm^{-1} (**66-*u***) were assignable to only one of the conformers. Concerning the conversion of S-**60** – S-**62** to amine **66** after 17.5 h at 3 K, it is assumed that this is a process occurring via quantum chemical tunneling.^[155] To verify this assumption, kinetic investigations at different temperatures have to be conducted in future research to indicate if this reaction is temperature-independent.

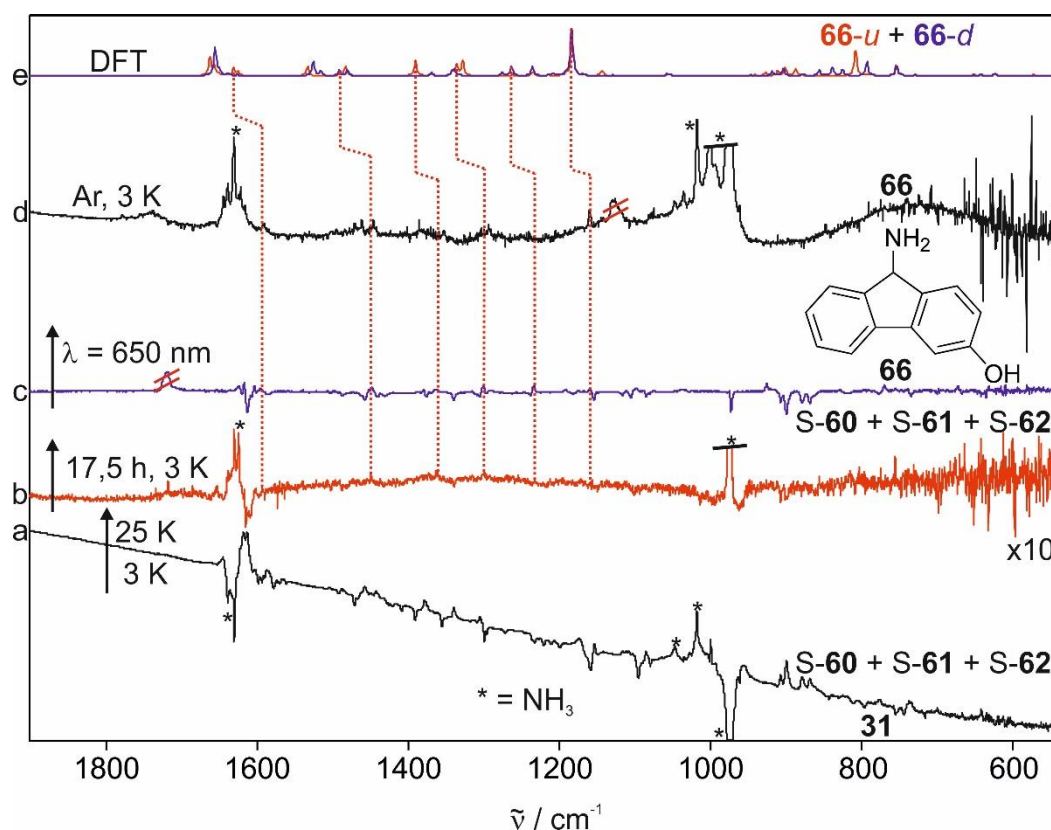


Figure 5.10: Formation of amine **66** after leaving the ammonia complexes S-**60** – S-**62** at 3 K for 17.5 h or irradiating with 650 nm light. (a) IR difference spectrum after annealing carbene **31** from 3 K to 25 K in an argon matrix doped with 1% ammonia. The signals pointing upwards are assigned to the singlet ammonia complexes S-**60**, S-**61** and S-**62**, the signals pointing downwards to S-**31** and T-**31**. (b) IR difference spectrum after leaving the ammonia complexes at 3 K for 17.5 h. The signals pointing upwards were assigned to amine **66**, the signals pointing downwards to the complexes S-**60** – S-**62**. (c) Difference spectrum after irradiation with 650 nm light. The peaks pointing upwards and downwards were assigned according to spectrum b. The signals at 1700 cm^{-1} is assigned to side products caused by possible oxygen impurities. (d) IR reference spectrum of amine **66** in argon at 3 K. Ammonia signals caused by partial decomposition of **66** are marked with an asterisk. The broad signal at around around 1250 cm^{-1} is not assigned to the amine. (e) Theoretical IR spectra of the alcohol conformers **66-u** (red spectrum) and **66-d** (blue spectrum) calculated at the B3LYP/def2-TZVP level of theory.

UV/Vis Experiments

For the UV/Vis investigation, diazo precursor **35** was deposited in an argon matrix doped with 1% ammonia and photolyzed to generate carbene **31**. After annealing to 25 K, slight changes in the UV/Vis spectrum were observed (Figure 5.11). It was detected that the signals of S-**31** at 278 nm and 409 nm and the signals of T-**31** at 265 nm and 464 nm decreased slightly, while new signals increased.

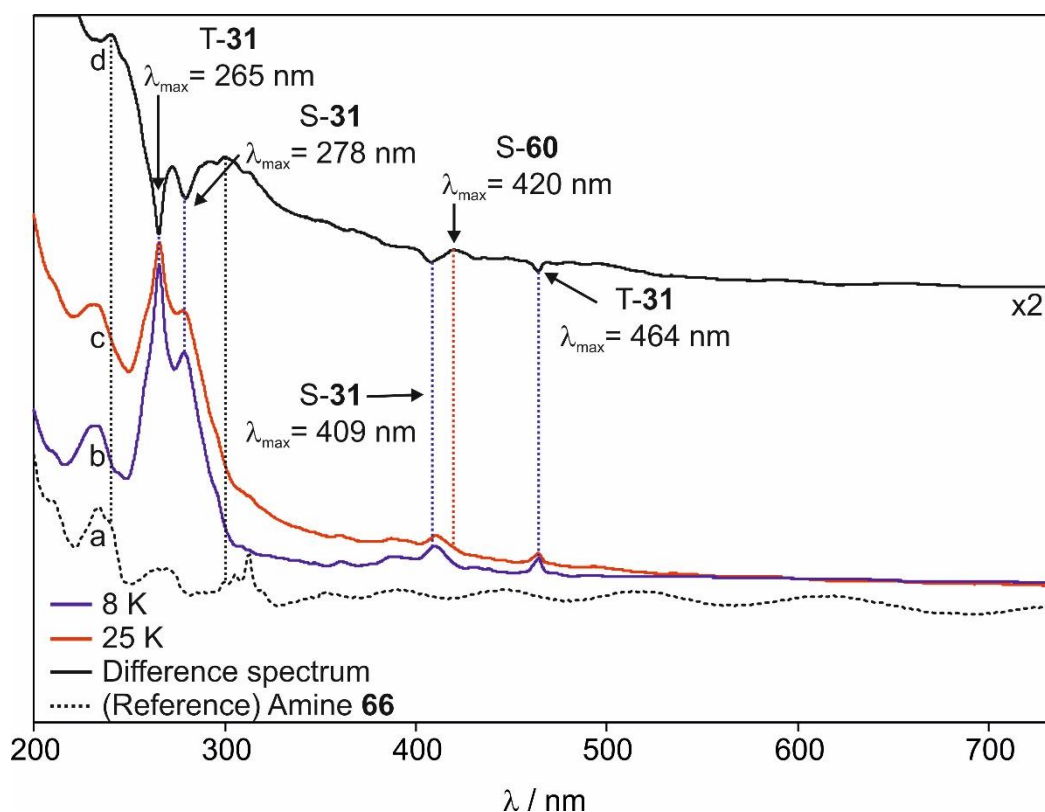


Figure 5.11: Annealing experiment of carbene **31** in an ammonia-doped argon matrix. (a) UV/Vis reference spectrum of amine **66** in argon at 8 K. (b) UV/Vis spectrum of carbene **31** in argon doped with 1% ammonia at 8 K. (c) UV/Vis spectrum after annealing to 25 K. (d) UV/Vis difference spectrum after annealing to 25 K. The signals pointing upwards are assigned to ammonia complex **S-60** and amine **66**, the signals pointing downwards to **S-31** and **T-31**.

At 420 nm, a small increase of a signal was observed that is assigned to ammonia complex **S-60**. Considering that other ammonia complexes likely have absorptions in the same area, it is expected that this signal also belong to the ammonia complexes **S-61**, **S-62** and other possible complexes. Aside of that, two small signals at 240 nm and 300 nm increased that were assigned to amine **66** after comparison with a reference spectrum (Figure 5.11). In summary, it is shown that annealing of **31** in an ammonia-doped matrix did not only result in the formation of ammonia complex **S-60**, but it also led to the formation of traces of **66**.

After cooling back down to 8 K, complex **S-60** was kept in the dark for 68.5 h which resulted in several changes in the spectrum (Figure 5.12).

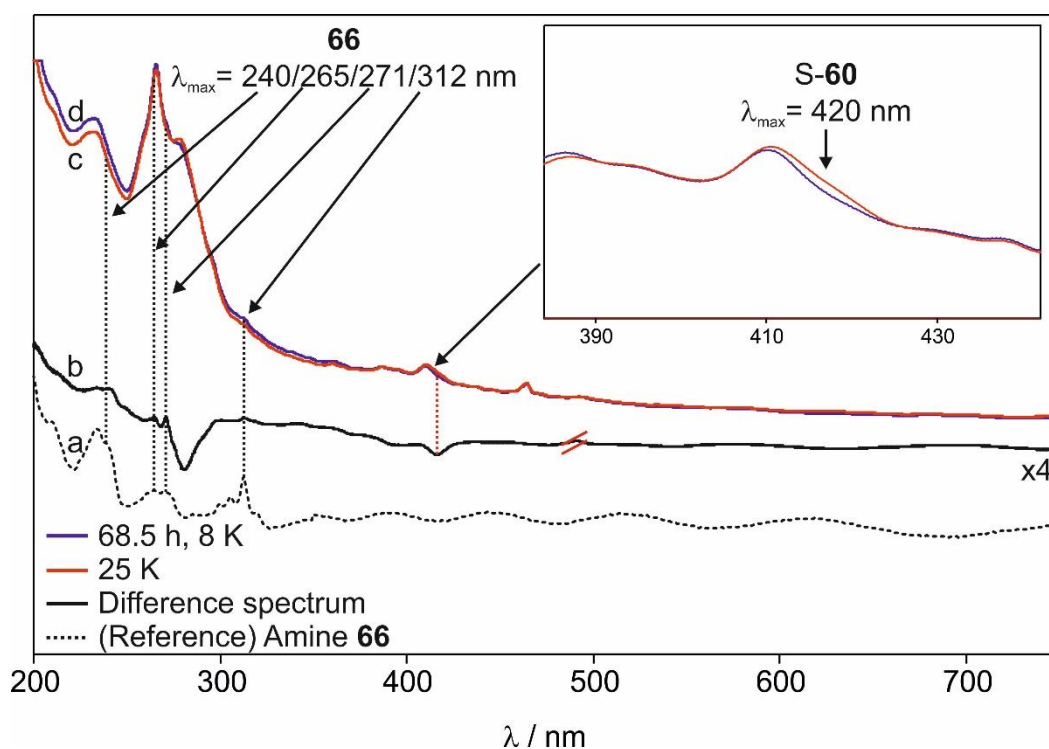


Figure 5.12: Investigation of the reaction behavior of ammonia complex S-60 by keeping it in the dark for several hours. (a) UV/Vis reference spectrum of amine **66** in argon at 8 K. (b) Difference spectrum after keeping ammonia complex S-60 in the dark for 68.5 hours. The signals pointing upwards are assigned to amine **66**, the signals pointing downwards to ammonia complex S-60. The small signal at 495 nm was not assigned to any known product. (c) UV/Vis spectrum after annealing carbene **31** to 25 K in an ammonia-doped matrix, forming singlet complex S-60 and traces of amine **66**. (d) UV/Vis spectrum after keeping ammonia complex S-60 in the dark for 68.5 h.

It was observed that the peak of ammonia complex S-60 at 420 nm decreased while several small signals at 240, 265, 271 and 312 nm increased that were assigned to amine **66** after comparison with a reference spectrum. Irradiation with 650 nm light also resulted in formation of **66**, which is in agreement with the IR experiments. As already stated, to obtain more information about this process and about a possible tunneling reaction, kinetic investigations will be conducted in future research to obtain the rate constant of this reaction to amine **66**.^[155]

5.3.2. Computational Results

Several calculations at the B3LYP/def2-TZVP level of theory were conducted to support the experimental investigation of the reaction between 3-hydroxy-9-fluorenylidene (**31**) and ammonia. Calculation show that similar to the formation of the water complex **36**, the interaction of **31** with ammonia and the resulting formation of the hydrogen-bonded complex **60** switches the ground state of the carbene from triplet to singlet (Figure 5.13, Table 5.3). For the energetically most favored conformer, the singlet-triplet energy gap of **31-*u*** (2.2 kcal/mol) changed to a value of -0.9 kcal/mol for ammonia complex **60-*u*** (containing one molecule of ammonia). Addition of an extra ammonia molecule to the hydroxy group of **31** and the resulting hydrogen bond lead to changes in the singlet triplet gap. While the additional hydrogen bond in complex **61-*u*** hardly changes the gap, the hydrogen bond in complex **62-*u*** (where the additional ammonia acts as a hydrogen bond acceptor) increases the gap to -2.5 kcal/mol.

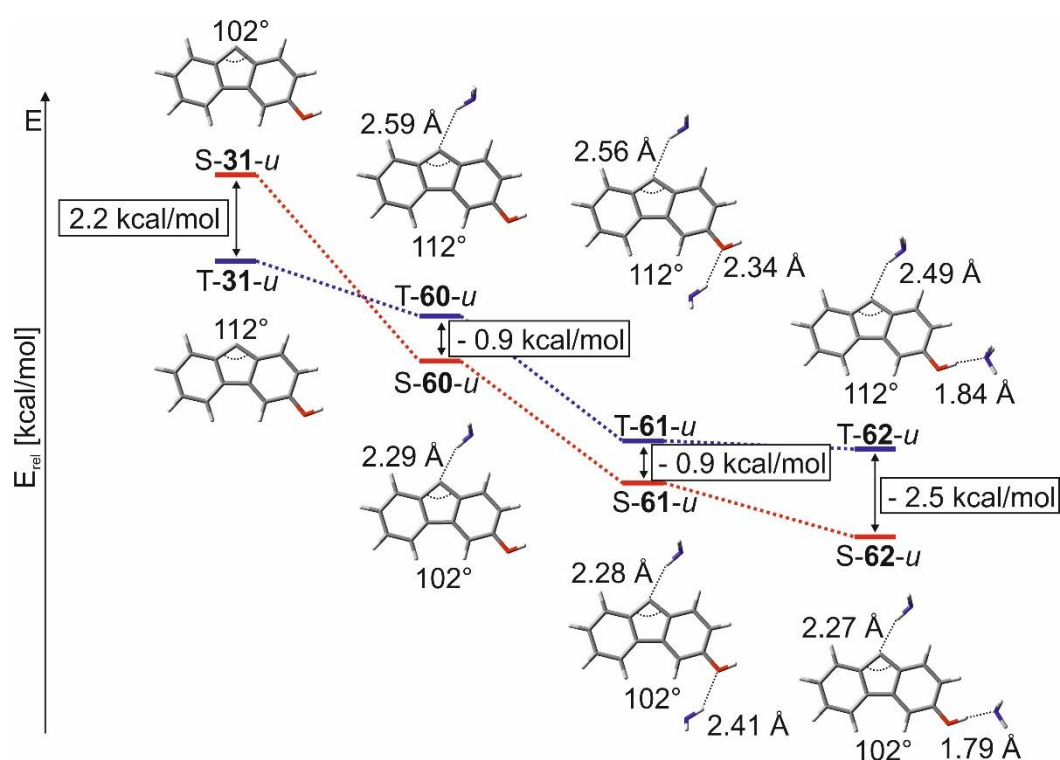


Figure 5.13: Singlet-triplet energy gaps of carbene **31-*u*** and the corresponding ammonia complexes **60-*u***, **61-*u*** and **62-*u*** calculated at the B3LYP/def2-TZVP level of theory.

Table 5.3: Singlet-triplet energy gaps of carbene **31** and the different ammonia complexes **60** – **62** considering both conformers. The energies are given in kcal/mol and were calculated at the B3LYP/def2-TZVP level of theory.

Conformer	31	60	61	62
<i>u</i>	2.2	-0.9	-0.9	-2.5
<i>d</i>	2.5	-0.6	-0.4	-2.0

Similar to the non-complexed carbene **31**, the energy differences between the different conformers of the ammonia complexes are rather small (Table 5.4). For all complexes, the conformer “*u*” is energetically favored.

Table 5.4: Energy differences between the different conformers of the ammonia complexes **60** – **62** in their singlet and triplet states. The energies are given in kcal/mol and were calculated at the B3LYP/def2-TZVP level of theory.

Spin state	60	61	62
singlet	0.7	1.4	0.9
triplet	0.3	0.9	0.3

Concerning the hydrogen bond lengths of the complexes, it is observed that the hydrogen bonds between the carbene center and the hydrogen atom of the ammonia molecule are longer than in the water complexes **36-38**. Complex **60** shows hydrogen bonds that are elongated by 0.35 Å (S-**60**) and 0.30 Å (T-**60**) compared to water complex **36**. Interactions with a second ammonia molecule results in a minimal shortening of the bond. While the hydrogen bond at the carbene center of ammonia complex **61** is 0.34 Å (S-**61**) and 0.27 Å (T-**61**) longer than the same bond of water complex **37**, this hydrogen bond of complex **62** is 0.33 Å (S-**62**) and 0.25 Å (T-**62**) longer compared to water complex **38**. This observation indicates that these hydrogen bonds in the ammonia complexes are weaker than in the corresponding water complexes. Furthermore, it is shown that the other hydrogen bond in complex **61** (where the hydroxy group acts as the hydrogen bond acceptor) is elongated by 0.34 Å (S-**61**) and 0.32 Å (T-**61**) compared to the same bond in water complex **37**. However, the additional hydrogen bonds in the complexes **62** and **38** (where the hydroxyl group acts as the hydrogen bond donor) have approximately the same length. Similar to ammonia complex **57** of 3,6-dimethoxy-9-fluorenylidene, the stabilization energies of the complexes **60** – **62** are smaller than the energies of the corresponding water complexes **36** – **38** due to ammonia being a weaker hydrogen bond donor than water (Table 5.5). Furthermore, complex **61** and especially complex **62** are additionally stabilized by the hydrogen bond between the hydroxy group and a second molecule of ammonia.

Table 5.5: Stabilization energies (ΔE_s) of the singlet and triplet ammonia complexes **60** – **62** calculated at the B3LYP/def2-TZVP level of theory. The energies are given in kcal/mol.

complex	ΔE_s (singlet)	ΔE_s (triplet)
60-u	- 5.8	- 2.6
60-d	- 5.6	- 2.5
61-u	- 8.7	- 5.6
61-d	- 7.8	- 4.9
62-u	- 16.7	- 11.9
62-d	- 16.3	- 11.8

To support the investigation of the amine formation, the IRC of the conversion from singlet ammonia complex S-**60** to amine **66** is calculated at the B3LYP/def2-TZVP level of theory. It is shown that the reaction proceeds via a transition state that is 4.4 kcal/mol higher in energy than the ammonia complex (Figure 5.14). Compared to the IRC of water complex **36** (Figure 4.37) that shows an energy barrier of 5.5 kcal/mol, this energy barrier is lower and less broad. Hence, it is assumed that a different reaction behavior of the ammonia complex is possible. This assumption is in accordance with the experimental results that show that S-**60** slowly converted to amine **66** after several hours at 3 K in the dark, while water complex S-**36** was stable under these conditions.

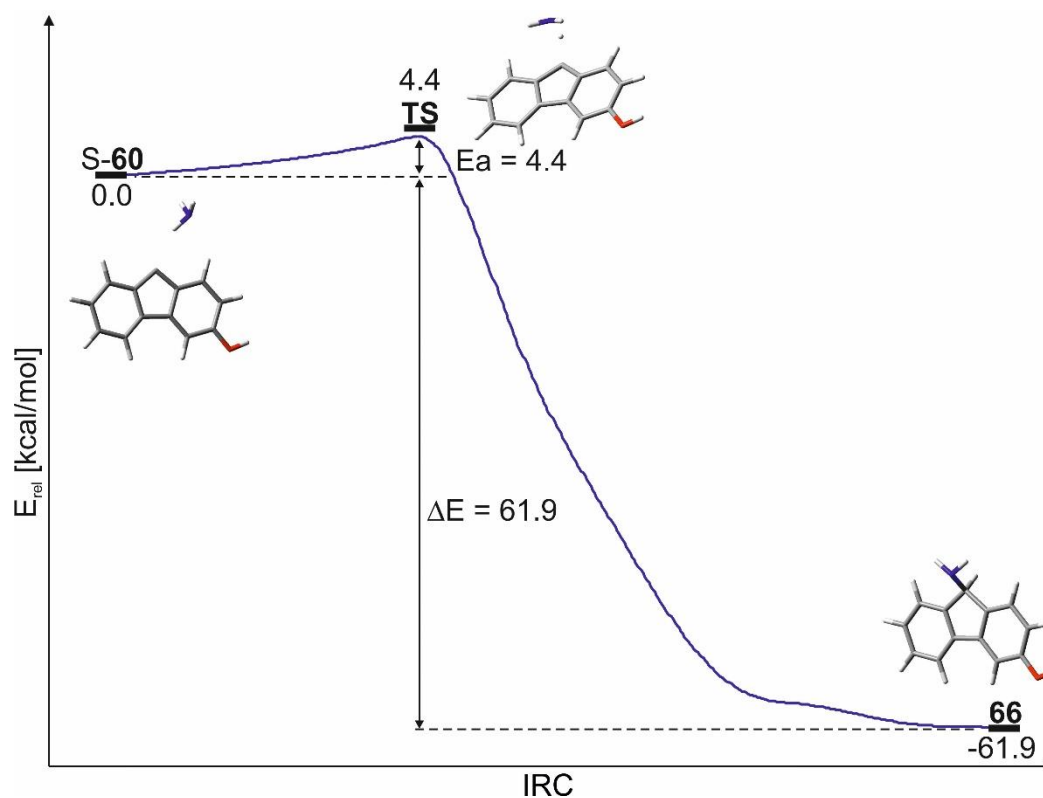
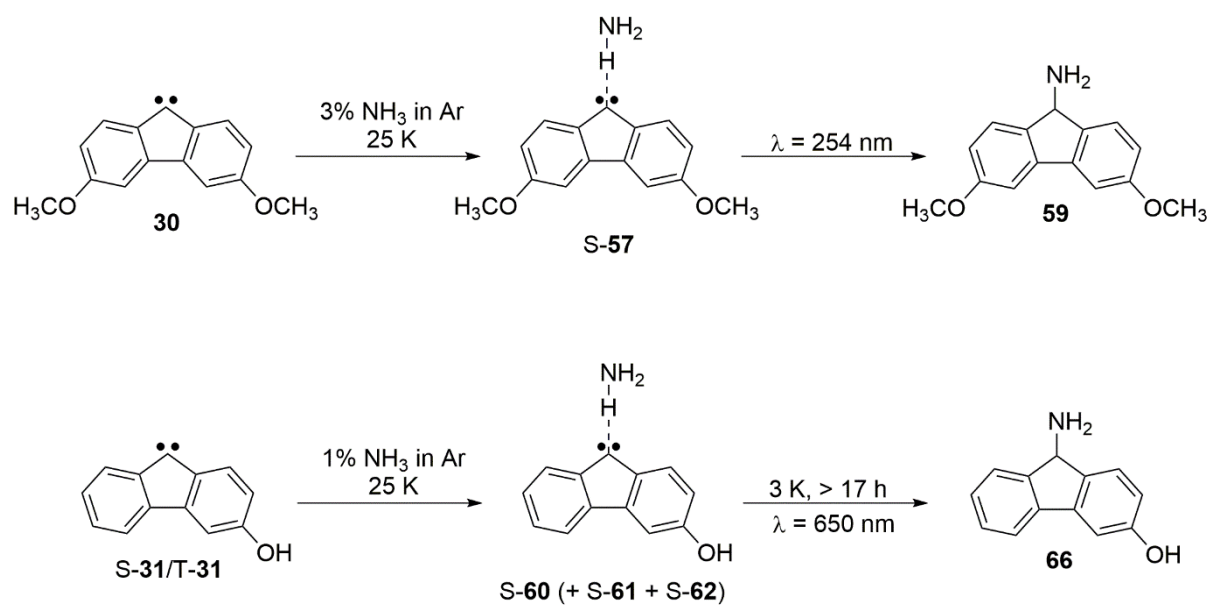


Figure 5.14: IRC of the reaction from the singlet state ammonia complex S-**60** to the corresponding amine **66**. The energies were calculated at the B3LYP/def2-TZVP level of theory.

5.4. Conclusions

The reactions of the two carbenes 3,6-dimethoxy-9-fluorenylidene (**30**) and 3-hydroxy-9-fluorenylidene (**31**) with ammonia have been successfully investigated using the matrix isolation technique combined with IR as well as UV/Vis spectroscopy. It was detected that for both carbenes, the reaction intermediate is a hydrogen-bonded complex, which is contrary to the prediction of Bethell and Schuster who assumed an ylide-type intermediate in the reaction of carbenes with ammonia.^[153-154] For the magnetically bistable carbene **31**, both the singlet and triplet carbene interacted with ammonia, forming the singlet state ammonia complexes S-**60** – S-**62** that were detected in the IR spectrum. While S-**31** directly interacted with ammonia, it is assumed that T-**31** switches its spin from triplet to singlet before interacting. Since the singlet-triplet ratio of **31** changed from 50/50 to 30/70 after the formation of the hydrogen-bonded complexes, it was indicated that higher amounts of S-**31** reacted with ammonia compared to T-**31**. According to calculations at the B3LYP/def2-TZVP level of theory, the interaction of ammonia switches the ground state of **31** from triplet to singlet. The resulting singlet-triplet energy gaps were -0.9 kcal/mol (**60-*u***), -0.9 kcal/mol (**61-*u***) and -2.5 kcal/mol (**62-*u***) for the different complexes and similar values for the other conformer. For the singlet ground state carbene **30**, the singlet-triplet energy gap increased to -4.0 kcal/mol (“*uu*”), -3.1 kcal/mol (“*ud*”) and -2.1 kcal/mol (“*dd*”) when the ammonia complex **57** was formed. While the ammonia complex of 3,6-dimethoxy-9-fluorenylidene (S-**57**) is stable at 3 K, the ammonia complexes S-**60** – S-**62** of 3-hydroxy-9-fluorenylidene slowly converted to the corresponding amine **66** under the same conditions within a few days. However, it is not known yet if this conversion occurs via quantum chemical tunneling.^[155] To investigate this question, kinetic measurements will be conducted in future research to test the temperature dependency of this reaction. If the rate constant of this reaction does not change with increasing temperature, it would be an indication for quantum chemical tunneling, since tunneling reactions are temperature-independent. The formation of the amine was additionally achieved by photochemical methods. Irradiation of ammonia complex S-**57** with 254 nm light converted it to amine **59**, while 3-hydroxy-9-aminofluorene (**66**) formed from the ammonia complexes S-**60**, S-**61** and S-**62** after irradiation with 650 nm light.

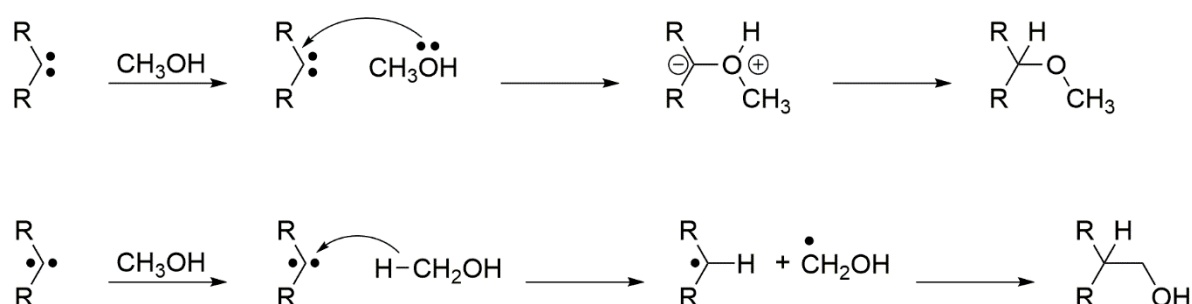


Scheme 5.3: Reactions of the carbenes **30** and **31** with ammonia to form the corresponding amines **59** and **66**.

6. Spin-dependent Reactions of Carbenes

6.1. Introduction

Carbenes are reactive intermediates that can undergo a number of different reactions.^[22] A relevant factor concerning the reactivity is given by the spin state that determines the general reaction behavior. Investigation showed that for reactions with alcohols or olefins, the reactivity between singlet and triplet state carbenes differs considerably.^[156] While triplet carbenes react with alcohols via a two-step radical reaction mechanism by first abstracting one hydrogen atom from the alcohol and subsequent radical recombination, singlet carbenes form a zwitterionic intermediate by interactions of one lone electron pair of the oxygen from the alcohol with the empty p orbital of the carbene (Scheme 6.1). From this intermediate, the reaction product is formed via a hydrogen shift. For reactions with olefins, triplet carbenes react via a radical reaction mechanism by first forming a diradical species with the double bond and recombination of the two radicals in the next step to form the cyclopropane product. Singlet carbenes undergo this reaction in a concerted mechanism (Chapter 2: Scheme 2.1).^[24]



Scheme 6.1: Reaction mechanisms of a singlet carbene (above) and a triplet carbene (below) with methanol. The singlet carbene forms a zwitterionic intermediate that forms the corresponding ether via hydrogen shift, while the triplet carbene abstracts one hydrogen atom to form two radicals that recombine in the next step.^[156]

Furthermore, it was shown in past research that triplet carbenes have the ability to abstract hydrogen atoms from organic hydrocarbon compounds, forming radical pairs.^[36] Due to these spin-specific properties, the reactivity towards small molecules is also highly spin-dependent. In recent research, it was stated that molecules such as HCl and CO are typically reacting with singlet carbenes, while O₂ and H₂ preferably react with triplet carbenes.^[36, 120]

As mentioned, HCl is frequently used for trapping experiments to verify the formation of singlet carbenes.^[36] Sheridan presented a range of singlet carbenes in past research that were able to interact with HCl to form the corresponding chloride compounds (Chart 6.1).^[157-160] Furthermore, he showed that the singlet ground state *p*-methoxyphenyl(trifluoromethyl)-carbene (**71**) reacts with HCl, while the similar triplet ground state compound *m*-methoxyphenyl(trifluoromethyl)carbene did not undergo any reaction.^[120]

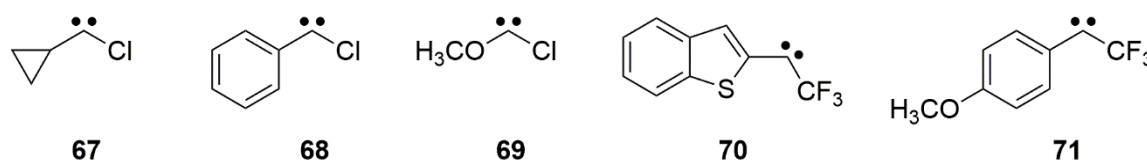
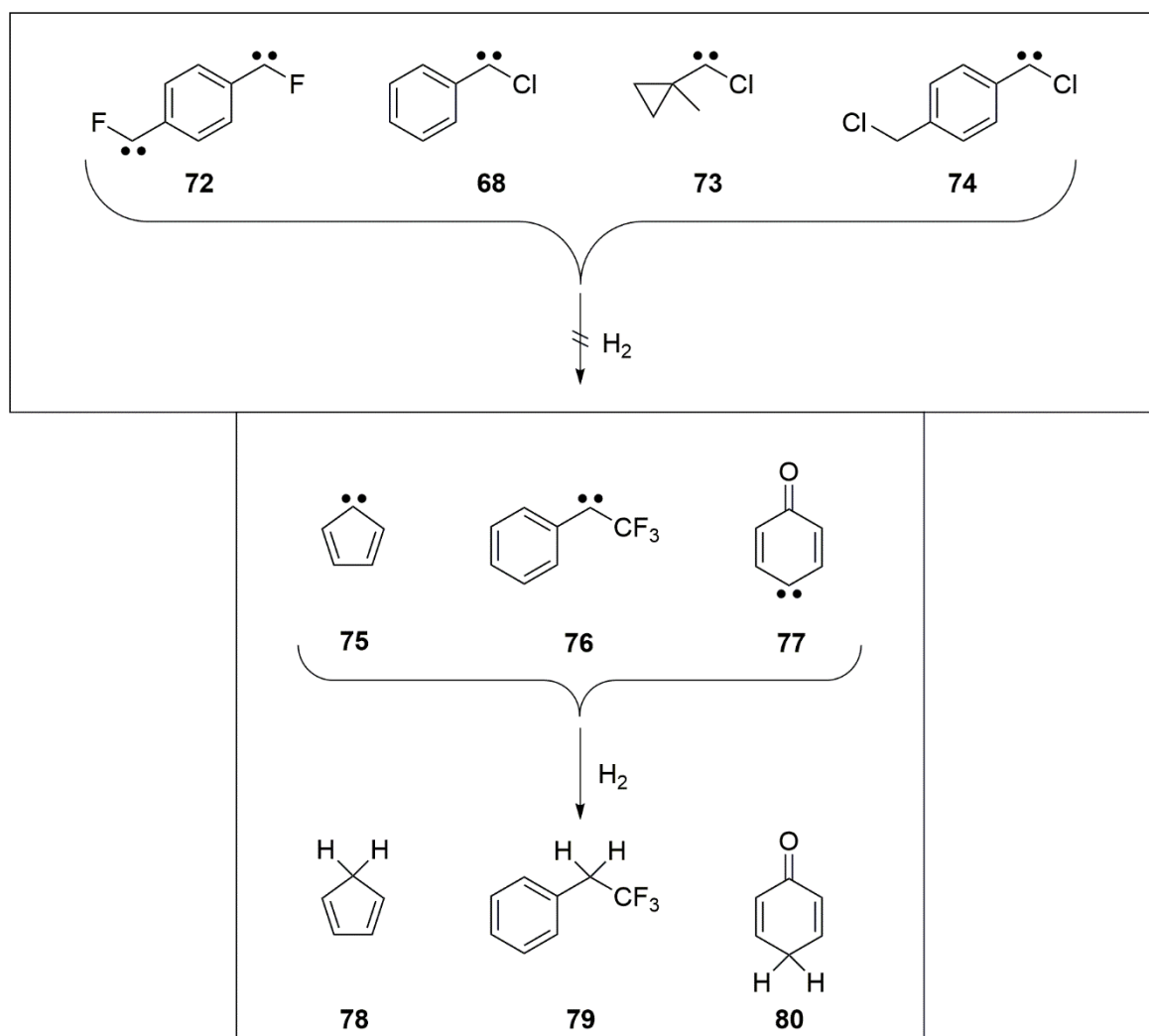


Chart 6.1: Different singlet carbenes presented by Sheridan that react with HCl to afford the corresponding chloride compounds.^[120, 157-160]

The reactivity of singlet carbenes towards CO is reported to be spin-allowed and hence expected to be faster than the reaction with triplet carbenes.^[36] However, in past research several examples of reactions between triplet carbenes and CO were observed, delivering ketene products with an intense signal in the range of 2000–2200 cm^{-1} .^[161-163] On the other hand, only a few examples of singlet carbenes that react with CO have been reported.^[164-165] Hence, carbon monoxide is a reagent that cannot be used to precisely determine the ground state of a carbene, since it reacts with both singlet and triplet carbene. However, it is still assumed that the spin-forbidden reaction with triplet carbenes is significantly slower than the reaction with singlet carbenes.

The reactions of carbenes with H_2 have been thoroughly investigated in past research. Early experiments with hydrogen have been conducted by Bass and Murrells.^[166-167] Bass generated methylene by flash photolysis and investigated its reaction behavior with hydrogen via kinetic spectroscopy, while Murrells investigated the interactions between the carbene CF_2 (also generated by flash photolysis) and hydrogen via time-resolved UV spectroscopy. Later investigations included the use of the matrix isolation technique to further analyze the carbene-hydrogen reactivity.^[163, 165] Concerning the reactivity of hydrogen towards singlet and triplet carbenes, early theoretical calculations suggested that the reaction of H_2 with singlet methylene is nearly barrierless and proceeds via an insertion reaction into the H–H bond.^[168] The reaction of H_2 with triplet methylene is assumed to proceed via hydrogen abstraction and subsequent recombination of the two formed radicals, having an activation barrier of approximately 15 kcal/mol.^[169] However, Sheridan stated that, contrary to these calculations, the reaction with hydrogen is more usual for triplet carbenes than for singlet ground state carbenes.^[170] He

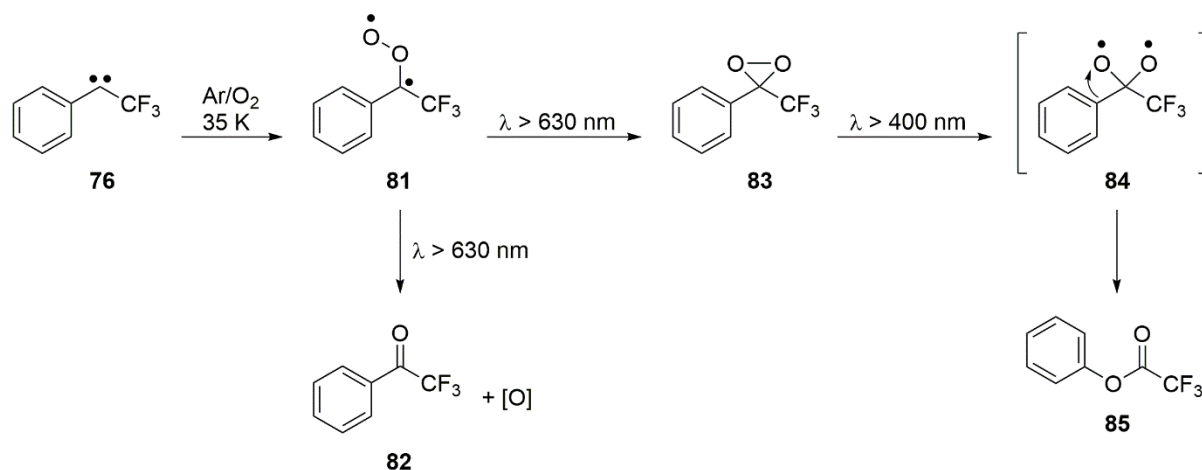
investigated the reactivity of carbenes with H_2 and showed several singlet carbenes that were unreactive towards hydrogen under matrix isolation conditions (Scheme 6.2). He additionally displayed multiple triplet ground state carbenes that readily underwent a reaction.



Scheme 6.2: Several singlet carbenes (above) and triplet carbenes (below) and their reaction behavior with molecular hydrogen described by Sheridan. While the singlet carbenes did not show any reaction, the triplet carbenes reacted with hydrogen to the corresponding products **78-80**.^[170]

These results clearly show that triplet carbenes react preferably with hydrogen. This observation is in accordance with more current observations that show that the activation barrier of the reaction between triplet carbenes and hydrogen can be overcome by quantum chemical tunneling.^[171] In contrast to this, the same behavior was not observed for singlet carbenes. However, Sander and coworkers reported several exceptions by describing a number of singlet ground state carbenes reactive towards hydrogen.^[165, 171]

Reactions of carbenes and other organic compounds with oxygen or ozone have been known for some time. In 1949, Criegee and Wenner reported the ozonization of 9,10-octalin for which they proposed a carbonyl oxide intermediate which was later referred to as the “Criegee-intermediate”.^[172] In later investigations, Bartlett and Murray provided evidence of the formation of this intermediate by using trapping experiments.^[173-174] However, direct spectroscopic observation of the carbonyl oxide had not been achieved at that time. The first isolation and direct spectroscopic observation of this intermediate was reported by Chapman and Hess who investigated reactions of carbenes with oxygen using the matrix isolation technique.^[175-176] Several years later, Dunkin conducted the first IR investigation of carbonyl oxides and showed the characteristic O–O IR band of this intermediate at around 1000 cm^{-1} .^[177] In several reports, Chapman and Hess as well as Dunkin investigated the possible reaction mechanism of cyclopentadienylidene (**75**) with oxygen and the formation of the reaction products.^[175, 178-179] They stated that the first observable intermediate is the carbonyl oxide, which converts to either the corresponding dioxirane, dioxetane or ketone upon irradiation with visible light. Further irradiation resulted in the formation of lactones and ketones as the oxidation products. Later, Sander presented a similar mechanism for the reaction of triplet ground state phenyl(trifluoromethyl)carbene (**76**) with O_2 (Scheme 6.3).^[180]



Scheme 6.3: Reaction pathway of carbene **76** in an oxygen-doped argon matrix, as reported by Sander.^[180] Annealing of the matrix to 35 K forms carbonyl oxide **81**, that converts to ketone **82** (by splitting off oxygen) and dioxirane **83** after irradiation with light of $> 630\text{ nm}$. Subsequent irradiation with light of $> 400\text{ nm}$ converts the dioxirane to ester **85** via diradical intermediate **84**.

Sander stated that during the annealing of the matrix, chemiluminescence was observed that resulted from the oxygen atoms formed during the conversion of **81** to **82**. Interactions of these oxygen atoms with carbene molecules generate ketones in their excited triplet state.^[180-181]

Concerning the spin selectivity of reactions between carbenes and O₂, both Sander and Sheridan reported that the reaction of triplet carbenes with oxygen is favored over the reaction with singlet carbenes.^[36, 120] Sander depicted that the reaction of singlet carbenes is considerably slower than the reaction with triplet carbenes, since the reaction between O₂ and triplet carbenes is spin allowed.^[182] In addition to that, Sheridan presented *p*-methoxyphenyl-(trifluoromethyl)carbene (**71**) as a singlet carbene that did not react with oxygen, while the similar triplet carbene *m*-methoxyphenyl(trifluoromethyl)carbene reacted rapidly to the corresponding carbonyl oxide. However, Sheridan also reported singlet carbenes like phenylchlorocarbene (**68**) that readily reacts with oxygen to form the carbonyl oxide.^[158]

In the next chapters, the reactivity of the magnetically bistable carbenes [4-(dimethylamino)phenyl]phenylcarbene (**14**) and 3-hydroxy-9-fluorenylidene (**31**) with O₂ and CO is described. One pivotal topic is whether only one or both of the carbene spin states react with these small molecules to elucidate if these reactions are spin selective.

6.2. Reactions of [4-(Dimethylamino)phenyl]phenylcarbene

6.2.1. Experiments in O₂-doped Ar, Xe and N₂

To test the interactions of the magnetically bistable carbene [4-(dimethylamino)phenyl]phenylcarbene (**14**) with oxygen, diazo precursor **17** was isolated in an argon matrix doped with 1% oxygen at 9 K. Subsequent photolysis with 505 nm light formed carbene **14** in a singlet-triplet ratio of 28/71 with a higher triplet amount than in pure argon (91/9). Subsequent irradiation with 405 nm light increased the amount of triplet carbene even further to a S-T ratio of 10/90. During the annealing of the matrix to 25 K, thermal conversion from the triplet to the singlet state was not observed. Instead, both the singlet carbene signals at 1155 cm⁻¹ and 1375 cm⁻¹ as well as the triplet carbene signals at 1217 cm⁻¹ and 1270 cm⁻¹ decreased slightly in equal parts, which led to the assumption that both species interacted with oxygen (Figure 6.1). However, the formation of any new signal was not observed after annealing. It is expected that interactions with oxygen would form the corresponding carbonyl oxide **86** which would exhibit an intense signal of the O–O stretching in the range of 900–1000 cm⁻¹.^[36] Additionally, the theoretical IR spectrum calculated at the B3LYP/def2-TZVP level of theory predicts the signal of the O–O stretching at 925 cm⁻¹. Nonetheless, the experimental spectrum did not exhibit any new signals in this area (900–1000 cm⁻¹) after annealing to 25 K. Based on this observation, it

is assumed that either carbene **14** did not react with oxygen and the decrease of the carbene signals resulted from minor matrix loss, or that the signals of the possibly formed carbonyl oxide **86** are too small to be observed. Further experiments about the carbonyl oxide formation will be conducted in future research using UV/Vis spectroscopy.

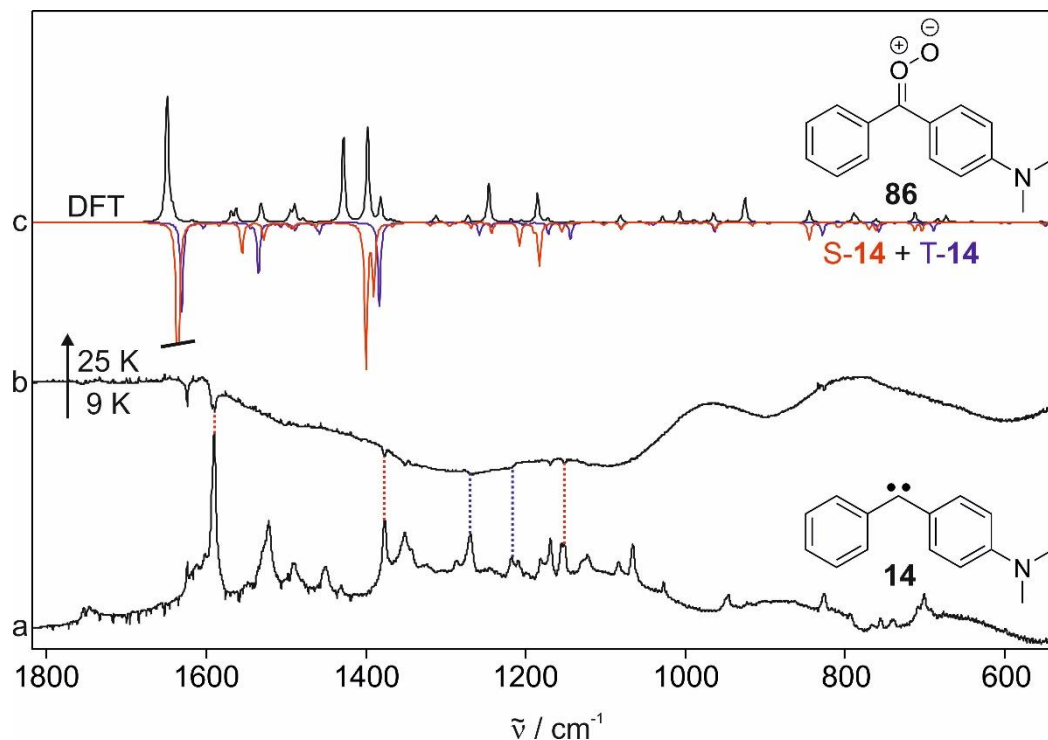


Figure 6.1: Annealing experiments of carbene **14** in an oxygen-doped argon matrix. (a) IR spectrum of **14** in an argon matrix doped with 1% O₂ at 9 K. (b) IR difference spectrum after annealing to 25 K. No distinct increasing signals is observed. The signals pointing downwards are assigned to S-**14** (red dotted lines) and T-**14** (blue dotted lines). (c) Theoretical IR spectra (B3LYP/def2-TZVP) of carbonyl oxide **86** (signals pointing upwards), S-**14** (signals pointing downwards, red spectrum) and T-**14** (signals pointing downwards, blue spectrum).

After 13 h in the dark at 9 K, no changes in the spectrum were observed, indicating that no reaction occurred. Subsequent irradiation experiments with light of 405–650 nm did not show any significant changes concerning dioxirane, ketone or ester formation. Irradiation with 455 nm light led to the conversion from S-**14** to T-**14**. However, it was detected that the amount of conversion is significantly lower after annealing to 25 K and cooling back to 3 K than before. Considering that thermal singlet-triplet conversion was inhibited during this experiment, it is assumed that the oxygen-doped argon matrix influences the spin conversion, since both annealing and irradiation with 455 nm light results in significantly larger changes in a pure argon matrix. This assumption will be investigated in future research.

A potential influence of the matrix material on the reaction of **14** with O₂ was tested by performing the same experiment in different hosts. In the following experiment, diazo precursor **17** was isolated in a Xe matrix doped with 1% O₂ and irradiated with 505 nm light to afford carbene **14**. Further irradiation with 405 nm and 505 nm light induced spin interconversion, resulting in a singlet-triplet ratio of 61/39. The subsequent annealing to 50 K led to a decrease of both singlet and triplet carbene signals, while several new signals appeared (Figure 6.2). Comparison with the theoretical spectra calculated at the B3LYP/def2-TZVP level of theory verifies that these signals belong to carbonyl oxide **86**.

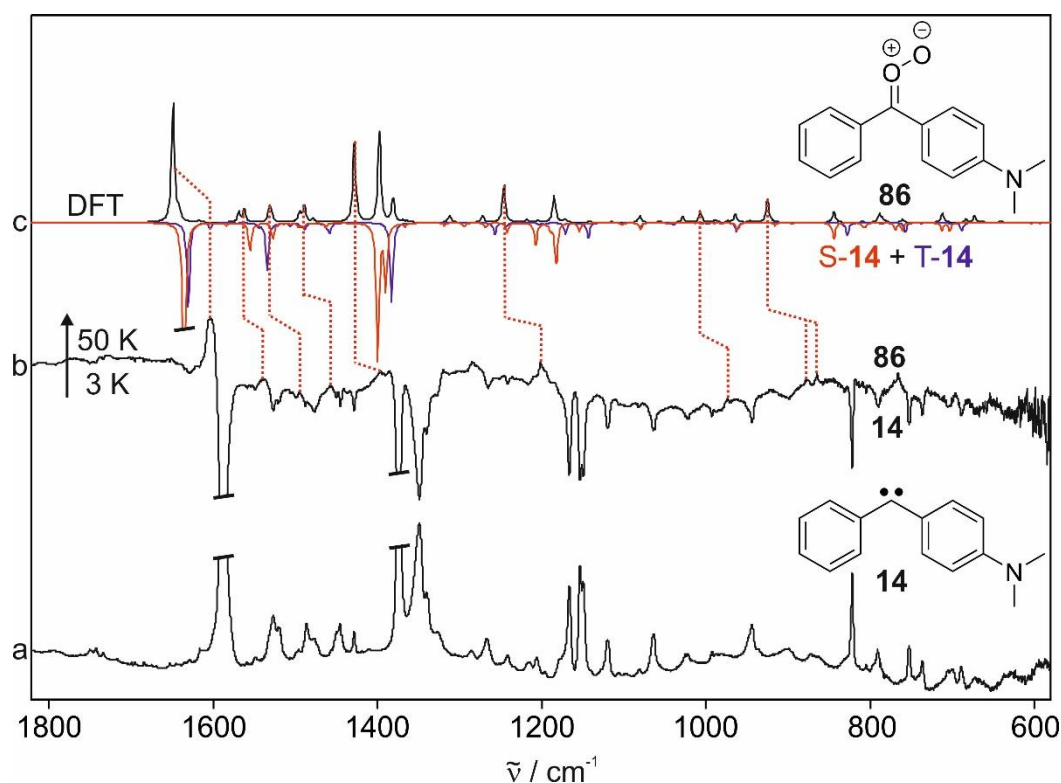


Figure 6.2: Annealing of carbene **14** in a xenon matrix doped with 1% O₂. (a) IR spectrum of **14** in a xenon matrix doped with 1% O₂ at 3 K. (b) IR difference spectrum after annealing to 50 K. The peaks pointing upwards are assigned to carbonyl oxide **86**, the peaks pointing downwards to both singlet carbene S-**14** and triplet carbene T-**14**. (c) Theoretical IR difference spectrum calculated at the B3LYP/def2-TZVP level of theory. The signals pointing upwards correspond to **86** while the peaks pointing downwards belong to S-**14** (red spectrum) and T-**14** (blue spectrum).

Especially the signals of the O–O stretching at 865 cm⁻¹ and 877 cm⁻¹ indicate the successful formation of compound **86**. Contrary to the expectation, two signals for this stretch are observed. It is assumed that these two signals result from two possible conformers, since the O–O group can be directed towards the dimethylamino group or away from this group. Further calculations will be conducted in future research to check this assumption. The determined singlet-triplet ratio of carbene **14** after the annealing was 35/65, which shows that the decrease

of S-**14** was considerably higher than the decrease of T-**14**. This leads to the assumption that in a xenon matrix, the reaction between S-**14** and oxygen is more favored than the reaction with T-**14**, which contradicts the previous results of Sander and Sheridan.^[36, 120] Since both S-**14** and T-**14** decreased, it is not possible to determine if thermally induced singlet-triplet interconversion occurs.

Subsequent irradiation with 650 nm light resulted in a decrease of the signals of carbonyl oxide **86** and the appearance of several new signals. Further irradiation with 530 nm led to the same results, but with considerably higher intensity (Figure 6.3). Comparison with theoretical spectra calculated at the B3LYP/def2-TZVP level of theory verifies that these new signals correspond to dioxirane **87**.

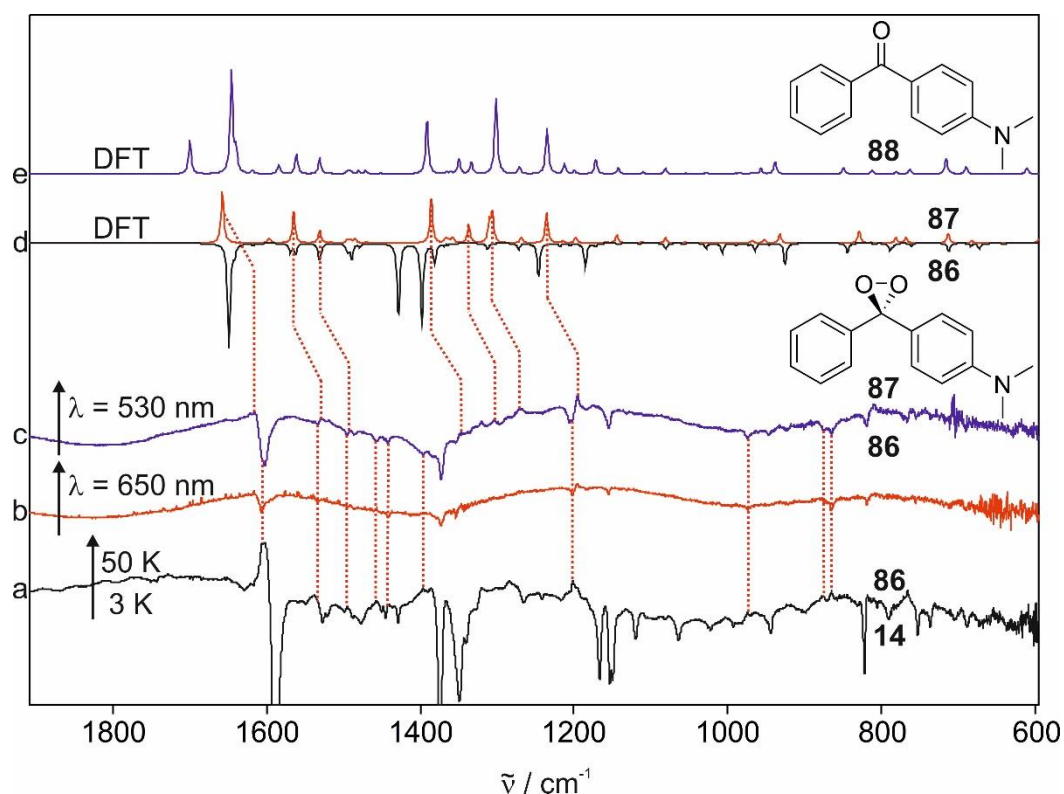


Figure 6.3: Irradiation experiments of carbonyl oxide **86** with 650 nm and 530 nm light. (a) IR difference spectrum after annealing carbene **14** in a xenon matrix doped with 1% O₂ to 50 K. The signals pointing upwards are assigned to carbonyl oxide **86**, the signals pointing downwards to carbene **14** (singlet and triplet). (b-c) Difference spectra after irradiating **86** with light of 650 nm and 530 nm, respectively. The signals pointing upwards are assigned to dioxirane **87**, the signals pointing downwards to **86**. (d) Theoretical IR difference spectrum calculated at the B3LYP/def2-TZVP level of theory. The signals pointing upwards correspond to dioxirane **87**, the signals pointing downwards to carbonyl oxide **86**. (e) Theoretical IR spectrum of ketone **88**.

At 1270 cm⁻¹, two signals are overlapping that are assigned to the asymmetric C–C–C stretching between the two phenyl rings (DFT: 1306 cm⁻¹) and the C–O stretch of the dioxirane

(DFT: 1310 cm^{-1}). Moreover, comparison with the theoretical IR spectrum of ketone **88** indicates that this ketone was not formed since the characteristic C=O stretching expected to appear at around 1700 cm^{-1} (as shown by calculations at the B3LYP/def2-TZVP level of theory) is not observed. Subsequent irradiation with 450 nm light resulted in the loss of the matrix, so that the possible formation of any ester as the reaction product was not observed. However, a small broad signal at around 1740 cm^{-1} was observed during the whole experiment that is assumed to belong to traces of a possible ester product formed after photolysis of precursor **17**.

Apart from the experiments in argon and xenon matrices, the reactivity of carbene **14** towards oxygen was also investigated using nitrogen as the host. Diazo precursor **17** was deposited in a nitrogen matrix doped with 1% O₂ and photolyzed with 505 nm light to obtain carbene **14** with a S-T ratio of 58/42. Subsequent irradiation with 405 nm light led to partial spin conversion from singlet to triplet, lowering the S-T ratio to 40/60. Annealing of the matrix to 20 K resulted in minimal changes in the spectrum that indicated the conversion from carbene **14** to the corresponding carbonyl oxide **86** (Figure 6.4).

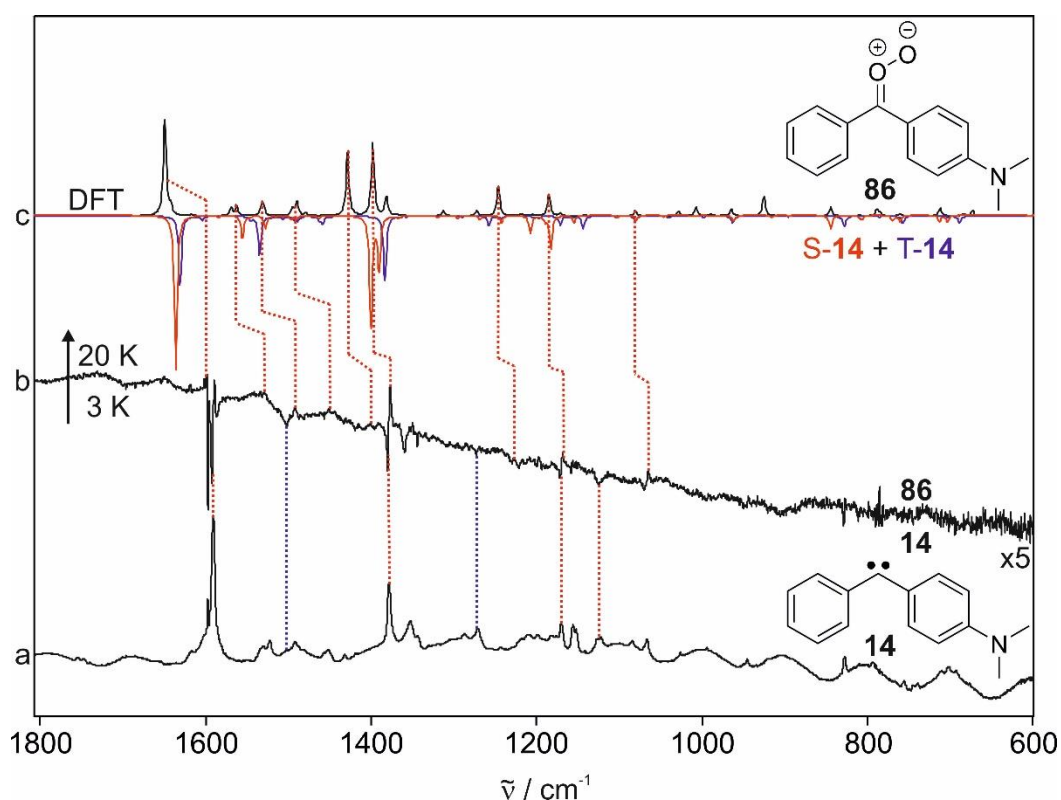


Figure 6.4: Annealing of carbene **14** in a nitrogen matrix doped with oxygen. (a) IR spectrum of carbene **14** in a nitrogen matrix doped with 1% O₂ at 3 K. (b) IR difference spectrum after annealing to 20 K. The signals pointing upwards are assigned to **86**, the signals pointing downwards to both S-**14** (red dotted lines) and T-**14** (blue dotted lines). (c) Theoretical IR difference spectrum calculated at the B3LYP/def2-TZVP level of theory. The signals pointing upwards correspond to carbonyl oxide **86**, the signals pointing downwards to S-**14** (red spectrum) and T-**14** (blue spectrum).

At 20 K, the signals of singlet carbene S-**14** at 1380 cm^{-1} and 1591 cm^{-1} and of triplet carbene T-**14** at 1271 cm^{-1} and 1502 cm^{-1} decreased slightly. In addition, several new signals appeared that match the theoretical spectrum of carbonyl oxide **86** (B3LYP/def2-TZVP). However, the significant signal of the O–O stretching at approximately 870 cm^{-1} (in xenon: 865 cm^{-1} and 877 cm^{-1}) is not observed. Since this signal is also rather weak in an oxygen-doped xenon matrix (Figure 6.2), it is assumed that the intensity in nitrogen is too low to be observable. Regarding the singlet-triplet ratio after annealing, it is detected that the ratio exhibited almost no change (3 K: 40/60, 25 K: 39/61), similar to the experiments in an O₂-doped argon matrix. Hence, it is proved that S-**14** and T-**14** reacted with oxygen in equal parts, indicating that the reaction is not spin-specific in a nitrogen matrix.

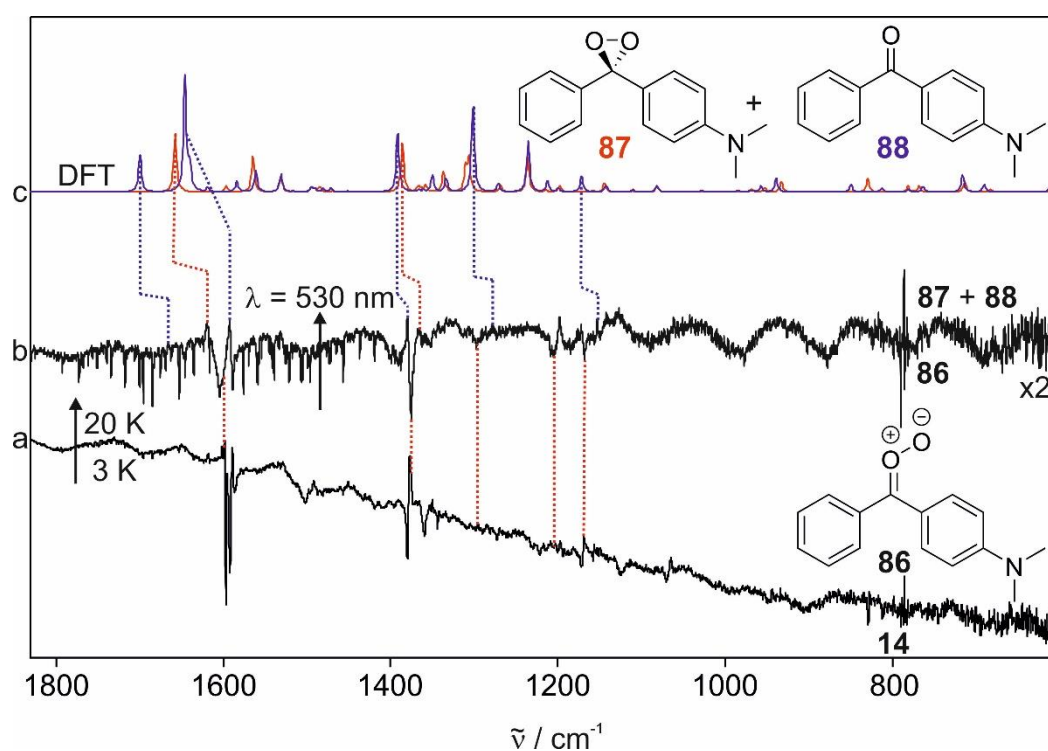


Figure 6.5: Irradiation experiments of carbonyl oxide **86** with 530 nm light in an oxygen-doped nitrogen matrix. The formation of both dioxirane **87** and ketone **88** was observed. (a) IR difference spectrum after annealing carbene **14** to 20 K in an N₂ matrix doped with 1% O₂. The signals pointing upwards are assigned to **86** the signals pointing downwards to carbene **14**. (b) Difference spectrum after irradiation with 530 nm light. The signals pointing downwards are assigned to carbonyl oxide **86**, the signals pointing upwards to dioxirane **87** (red dotted lines) and ketone **88** (blue dotted lines). (c) Theoretical IR spectra (B3LYP/def2-TZVP) of dioxirane **87** (red spectrum) and ketone **88** (blue spectrum).

Subsequently, irradiation experiments with light of different wavelengths were conducted. Contrary to the experiments in xenon, irradiation with 650 nm light did not result in any changes in the spectrum and hence no conversion of carbonyl oxide **86** to other products was observed. However, irradiation with 530 nm light led to a decrease of the carbonyl oxide peaks

(Figure 6.5) and the appearance of several small signals that are assigned to both dioxirane **87** and ketone **88**. Photochemically induced singlet-triplet interconversion of carbene **14** was not observed. The signals at 1367 cm^{-1} and 1620 cm^{-1} are characteristic of dioxirane **87** and are assigned to it, together with a small signal at 1277 cm^{-1} that belongs to the C–O stretching as well as the C–C–C stretch between the phenyl rings present in **87**. Ketone **88** is characterized by the signals at 1380 cm^{-1} , 1593 cm^{-1} and the C=O stretch at 1666 cm^{-1} . However, the signal of the C=O stretch is rather broad and exhibits a lower intensity than expected. The following irradiation with 450 nm light resulted in a major spin interconversion of the carbene **14** from singlet to triplet, verified by the decreasing peaks of S-**14** and the increasing peaks of T-**14** (Figure 6.6). In addition to that, the two signals at 1198 cm^{-1} and 1620 cm^{-1} decreased that are not assigned to S-**14** but to the dioxirane **87**. Additionally to the increasing signals of the triplet carbene T-**14**, a set of small overlapping bands in the area between $1734\text{--}1754\text{ cm}^{-1}$ are detected. Comparison with theoretical spectra of the two possible ester products **89** and **90** calculated at the B3LYP/def2-TZVP level of theory verifies that the bands in this area correspond to the C=O stretch of the esters. Detailed analysis of this band shows that also the different conformers “*u*” and “*d*” were present in the matrix (Figure 6.6). The signals of the two conformers **89-*u*** and **89-*d*** are found at 1734 cm^{-1} and 1748 cm^{-1} , respectively. The signal at 1740 cm^{-1} is assigned to ester conformer **90-*u*** and the signal at 1754 cm^{-1} to **90-*d***. In summary, it was observed that irradiation with 450 nm light converted the dioxirane **87** to the corresponding ester compounds **89** and **90**.

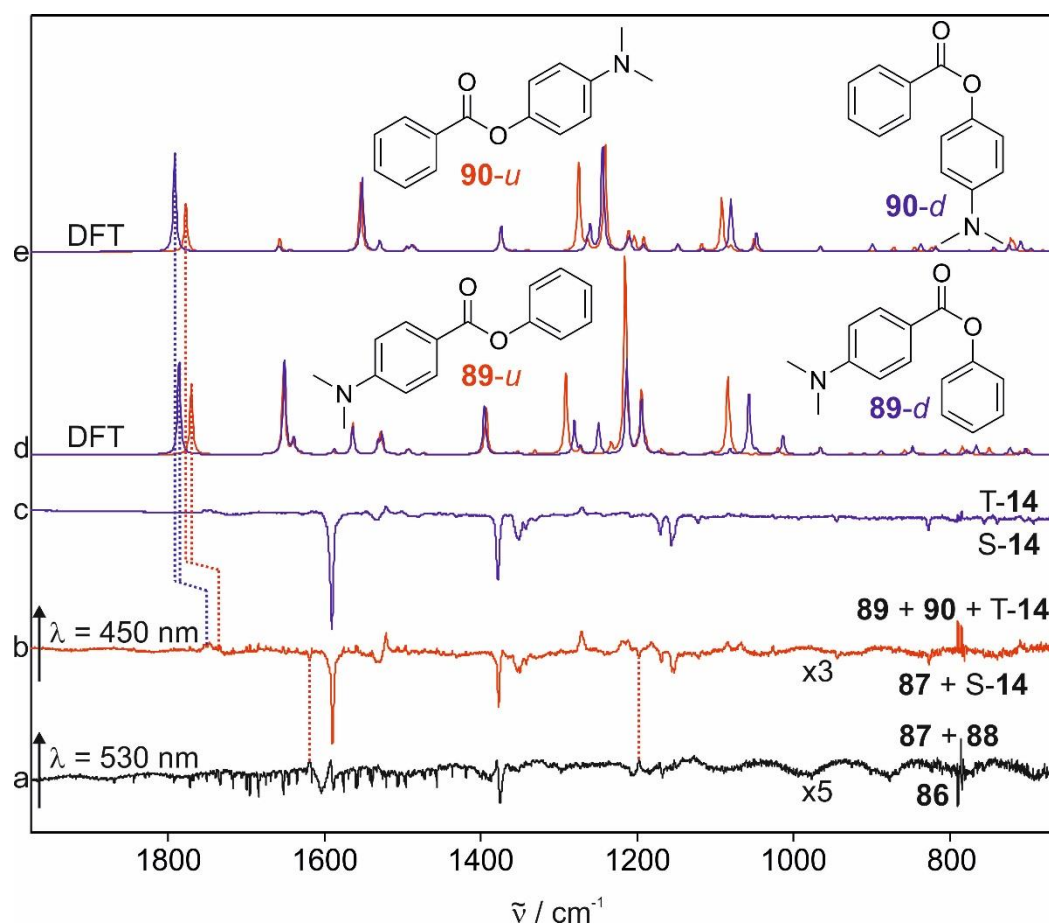


Figure 6.6: Irradiation of dioxirane **87** and ketone **88** with 450 nm in a nitrogen matrix doped with 1% O₂. (a) Difference IR spectrum after irradiation of carbonyl oxide **86** with 530 nm light. The signals pointing upwards are assigned to dioxirane **87** and ketone **88**, the signals pointing downwards to **86**. (b) Difference spectrum after irradiation with 450 nm light. The signals pointing upwards are assigned to the “u” conformers of the ester compounds **89** and **90** (red dotted lines), the corresponding “d” conformers (blue dotted lines) and to triplet carbene T-14, the signals pointing downwards to **87** (red dotted lines) and singlet carbene S-14. (c) Reference difference spectrum that shows the conversion from S-14 (peaks pointing downwards) to T-14 (peaks pointing upwards). (d) Theoretical IR spectra (B3LYP/def2-TZVP) of ester compounds **89-u** (red spectrum) and **89-d** (blue spectrum). (e) Theoretical IR spectra of **90-u** (red spectrum) and **90-d** (blue spectrum).

6.2.2. Experiments in CO-doped Argon

The reactivity of the carbene [4-(dimethylamino)phenyl]phenylcarbene (**14**) towards CO was investigated using the matrix isolation technique. One key aspect of this investigation lies in the possible spin-specificity of the reaction of **14** with CO. This is especially relevant considering that the reaction of singlet carbenes with CO was previously reported as spin-allowed, and therefore supposed to be faster than the reaction with triplet carbenes.^[36] To test this proposition, diazo compound **17** was isolated in an argon matrix doped with 1% of CO and

photolyzed using 505 nm light to afford the bistable carbene **14** with an S-T ratio of 79/21. An additional small peak is observed at 2103 cm^{-1} (Figure 6.7). Comparison with the theoretical IR spectrum of ketene **91** calculated at the B3LYP/def2-TZVP level of theory verifies that this peak belongs to traces of this ketene. This indicates that directly after the photolysis, small amounts of CO already reacted with carbene **14**. Presumably, this was due to small amounts of CO and the carbene precursor being already in close proximity after the matrix deposition.

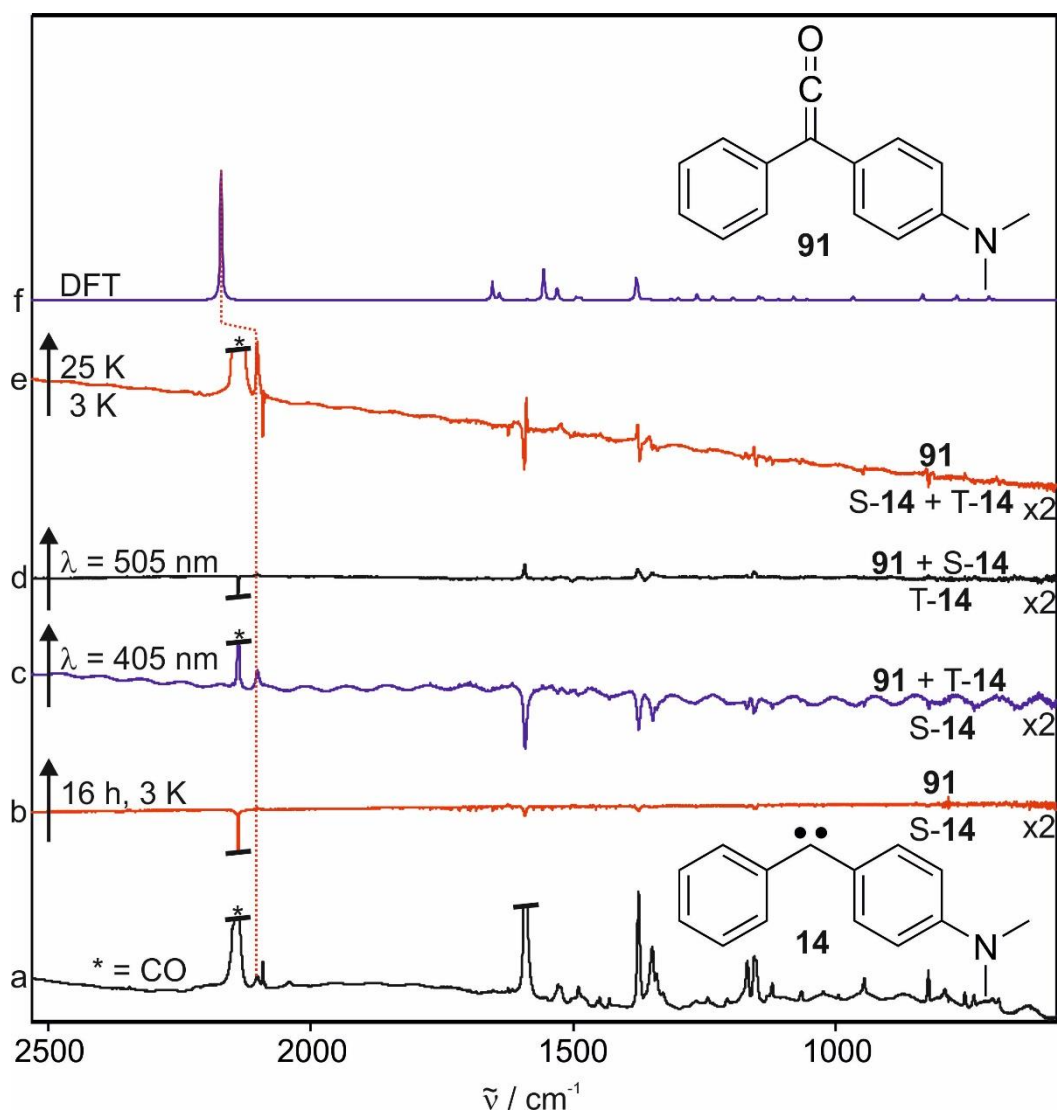


Figure 6.7: IR investigation of the reaction between matrix-isolated carbene **14** and CO. (a) IR spectrum of carbene **14** in an argon matrix doped with 1% CO at 3 K. (b) IR difference spectrum after 16 h in the dark at 3 K. The low-intensity band at 2103 cm^{-1} pointing upwards is assigned to ketene **91**, the signals pointing downwards to singlet carbene S-**14**. (c) Difference spectrum after irradiation with 405 nm. The signals pointing upwards are assigned to both **91** and T-**14**, the signals pointing downwards to S-**14**. (d) Difference spectrum after 505 nm light irradiation. The signals pointing upwards are assigned to ketene **91** and singlet carbene S-**14**, the signals pointing downwards to T-**14**. (e) Difference spectrum after annealing to 25 K. Matrix effects were observed in the range of 1100–1600 cm^{-1} . The signals pointing upwards are assigned to ketene **91**, the signals pointing downwards to both S-**14** and T-**14**. (f) Theoretical IR spectrum of **91** calculated at the B3LYP/def2-TZVP level of theory.

After 16 hours in the dark at 3 K, it was observed that a small amount of carbene **14** and carbon monoxide decreased while the ketene peak at 2103 cm^{-1} increased slightly, indicating further reaction with CO. This reaction is assumed to occur primarily due to pre-coordinated CO to the carbene, since diffusion of small molecules through the matrix is unlikely at 3 K. Analysis of the decreasing carbene peaks shows that only the singlet carbene S-**14** decreased while the amount of T-**14** stayed constant. This is in accordance with the expected results, since it was reported that singlet carbene reactions with CO are faster compared to triplet carbene reactions.^[36] Subsequent irradiation with 405 nm and 505 nm light showed the singlet-triplet spin interconversion of carbene **14**. 405 nm irradiation resulted in a S-T ratio of 72/28 by forming T-**14**, while 505 nm light shifted it back to 77/23 by generating S-**14**. In both cases, it was observed that the ketene peak at 2103 cm^{-1} slightly increased (Figure 6.7). Due to the simultaneous S-T interconversion, it is not possible to determine if both S-**14** and T-**14** or only one of them reacted with CO. Annealing to 25 K for 30 minutes continuously increased the ketene signal. In addition to that, signal integration clearly shows that the signals of both S-**14** and T-**14** decreased in almost equal parts, resulting in a S-T ratio of 76/24. This is contrary to the expected results, since annealing to 25 K results in thermal S-T conversion and should increase the amount of S-**14**. Hence, it is shown that the reaction of S-**14** with CO proceeds considerably faster, leading to the observed singlet carbene decrease.

6.3. Reactions of 3-hydroxy-9-fluorenylidene with oxygen

Besides the spin-dependent reactions of [4-(dimethylamino)-phenyl]phenylcarbene (**14**) with small molecules, the reactivity of another magnetically bistable carbene, 3-hydroxy-9-fluorenylidene (**31**), with oxygen was investigated. Since this carbene does barely undergo singlet-triplet interconversion when irradiated or annealed in an argon matrix, it is expected that it is less challenging to observe which spin state interacts with O₂ (compared to carbene **14**). Diazo precursor **35** was deposited in an argon matrix doped with 1% oxygen at 9 K, and subsequent photolysis formed the corresponding carbene **31** as a singlet-triplet mixture with an S-T ratio of 27/73. Annealing of the matrix to 25 K led to the decrease of both singlet and triplet carbene, as seen by the decreasing singlet signals at 1079 cm^{-1} and 1271 cm^{-1} (S-**31**) and the decreasing triplet signal at 1357 cm^{-1} (T-**31**), along with a set of increasing signals that are assigned to carbonyl oxide **92** (Figure 6.8). Clear evidence of this is given by the two characteristic signals at 900 cm^{-1} and 973 cm^{-1} that are assigned to the O–O stretching.

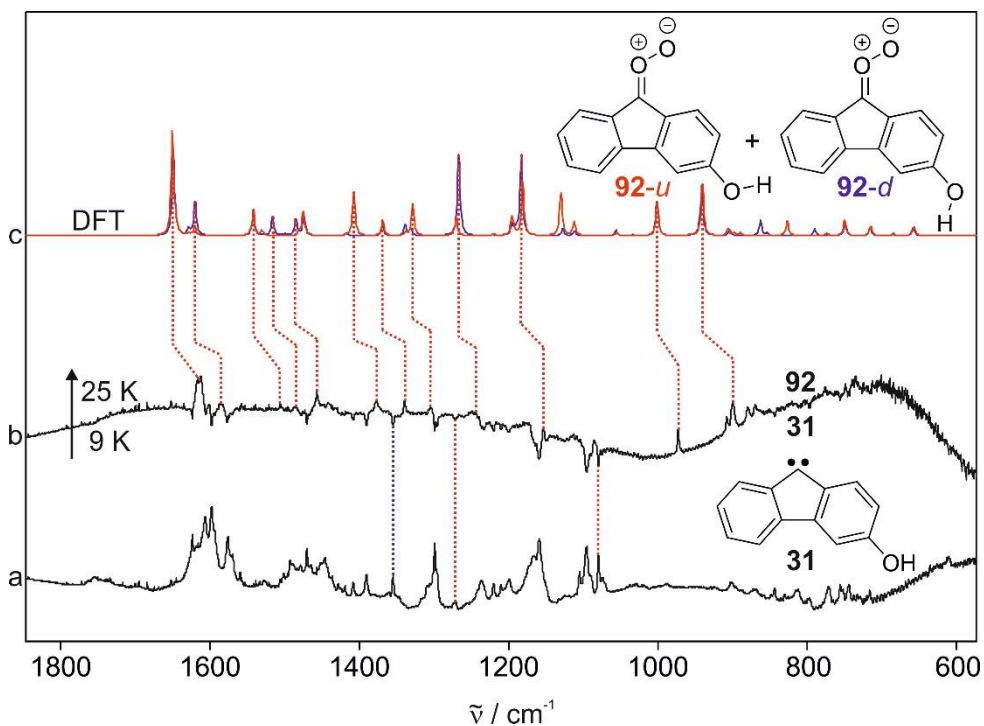


Figure 6.8: Annealing experiments of carbene **31** in an oxygen-doped argon matrix. (a) IR spectrum of carbene **31** in an argon matrix doped with 1% O₂ at 9 K. (b) IR difference spectrum after annealing to 25 K. The signals pointing upwards are assigned to carbonyl oxide **92**, the signals pointing downwards to both S-**31** (red dotted lines) and T-**31** (blue dotted lines). (c) Theoretical IR spectra of **92-u** (red spectrum) and **92-d** (blue spectrum).

Comparison with theoretical spectra (B3LYP/def2-TZVP) proves that **92** was present as a conformer mixture. While the signal at 1378 cm⁻¹ is assigned to only conformer **92-u**, the two signals at 1457 cm⁻¹ and 1586 cm⁻¹ are assigned to the other conformer **92-d**. Annealing to 25 K shifted the S-T ratio from 27/73 to 24/76. Since this indicates that the singlet carbene decrease is higher than the triplet carbene decrease, it is shown that the singlet amount reacting with oxygen was slightly higher than the triplet amount. This is contrary to the expectations, since it was stated in literature that oxygen reacts preferably with triplet carbenes.^[36, 120] In general, it is verified that the reaction of **31** with oxygen in an argon matrix is not spin-specific. After 16.5 h at 9 K in the dark, no changes were detected, which indicates that no reaction of the carbonyl oxide occurred. After irradiation with 650 nm light, the signals of carbonyl oxide **92** decreased while several new signals appeared (Figure 6.9). The comparison with theoretical spectra calculated at the B3LYP/def2-TZVP level of theory verifies that these signals correspond to the dioxirane **93**.

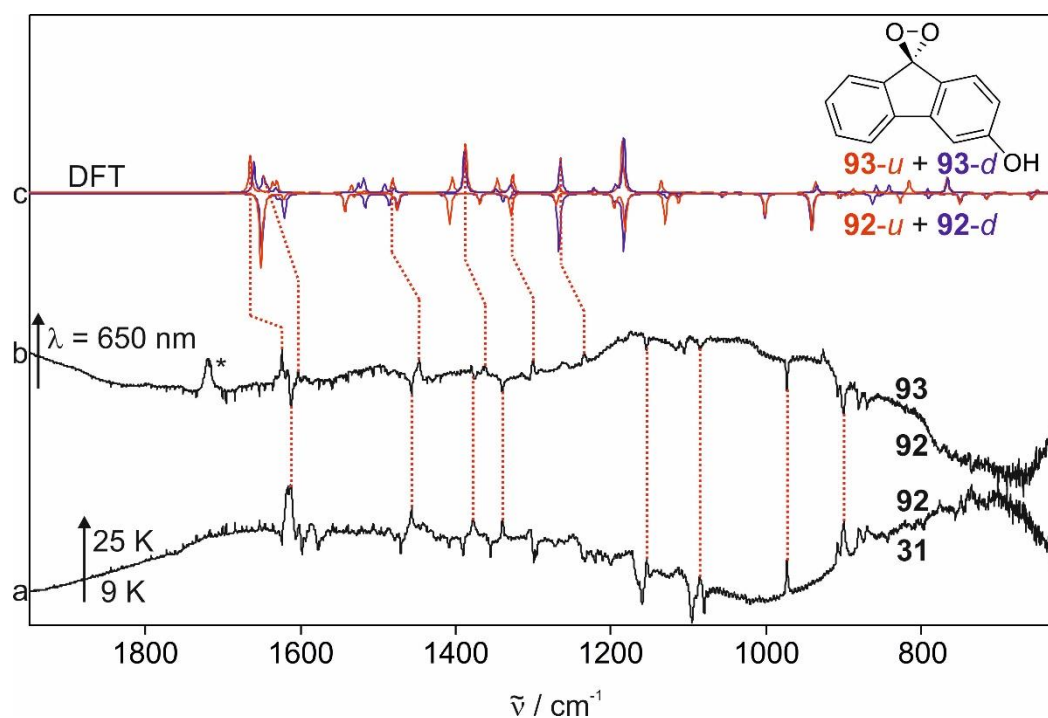


Figure 6.9: Irradiation experiments of carbonyl oxide **92** with 650 nm light. (a) IR difference spectrum after annealing carbene **31** to 25 K in an argon matrix doped with 1% O₂. The signals pointing upwards are assigned to **92**, the signals pointing downwards to singlet and triplet carbene **31**. (b) Difference spectrum after irradiation with 650 nm light. The signal at 1720 cm⁻¹ is not assignable to any product. The other signals pointing upwards are assigned to dioxirane **93**, the signals pointing downwards to carbonyl oxide **92**. (c) Theoretical IR difference spectrum calculated at the B3LYP/def2-TZVP level of theory. The signals pointing upwards correspond to the dioxirane conformers **93-u** (red spectrum) and **93-d** (blue spectrum), the signals pointing downwards to **92-u** (red spectrum) and **92-d** (blue spectrum).

Similar to carbonyl oxide **92**, dioxirane **93** also exhibits two conformers. The signals at 1316 cm⁻¹ and 1380 cm⁻¹ are assigned to only conformer **93-u**, and the signals at 1235 cm⁻¹ and 1604 cm⁻¹ are assigned to **93-d**. Additionally, another broad, intense signal at 1720 cm⁻¹ appeared after 650 nm irradiation that is not assigned to the dioxirane. Since this signal is observed in an area characteristic of a C=O stretching, the spectrum was compared to a reference spectrum of ketone **94** in pure argon (Figure 6.10). However, the C=O stretching in the reference spectrum is observed at 1670 cm⁻¹. Therefore, it is excluded that the intense band at 1720 cm⁻¹ formed after irradiation of carbonyl oxide **92** with 650 nm light belongs to ketone **94**. Yet, it is assumed that this unidentified compound also contains a C=O group. Further investigations via UV/Vis and EPR spectroscopy as well as further computational calculations will be conducted in future research to elucidate the structure of this unknown compound.

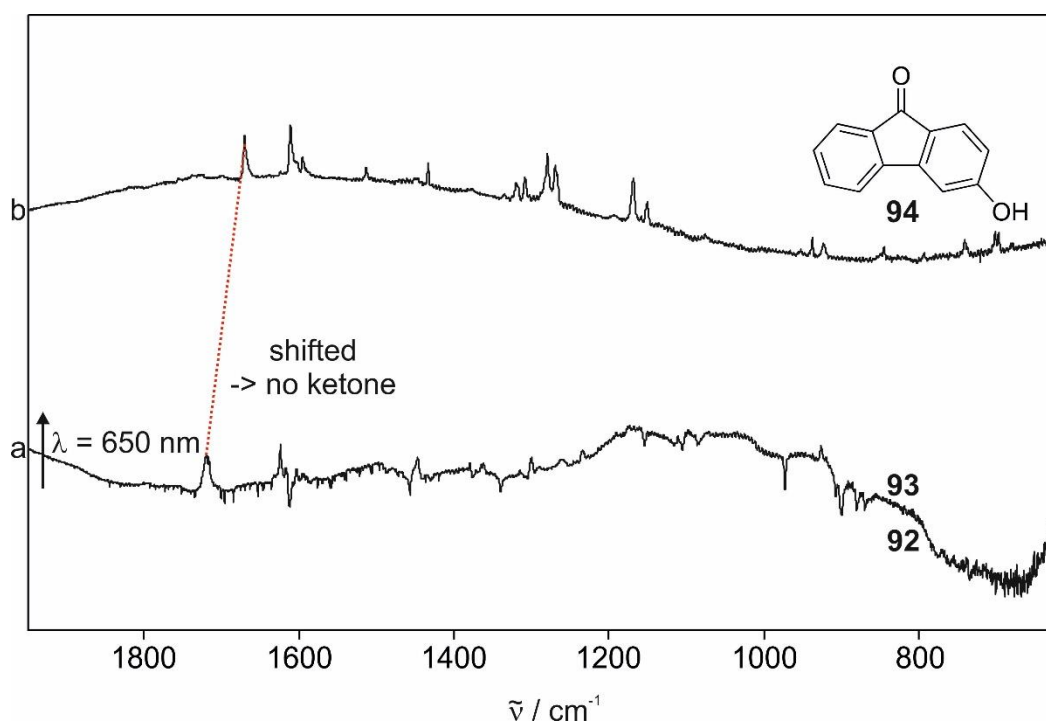


Figure 6.10: Comparison of the increasing signal at 1720 cm^{-1} after irradiation of carbonyl oxide **92** with the reference spectrum of the corresponding ketone **94**. (a) IR difference spectrum after irradiating **92** with 650 nm light. The signals pointing upwards are assigned to dioxirane **93** (except that at 1720 cm^{-1}), and those pointing downwards to **92**. (b) IR reference spectrum of an authentic sample of ketone **94**.

Subsequent irradiation with 450 nm light led to a decrease of the signals of dioxirane **93**, while several new small signals increased that are assigned to the lactone products **95** and **96**. The lactone formation is especially indicated by the formation of the broad band covering the two overlapping signals at 1748 cm^{-1} (**95**) and 1755 cm^{-1} (**96**) that are assigned to the lactone $\text{C}=\text{O}$ stretch (Figure 6.11). One surprising observation was that after irradiation with 450 nm light, the unidentified signal at 1720 cm^{-1} was also decreasing. Hence, it can be assumed that this unknown substance is also involved in the formation of the lactones.

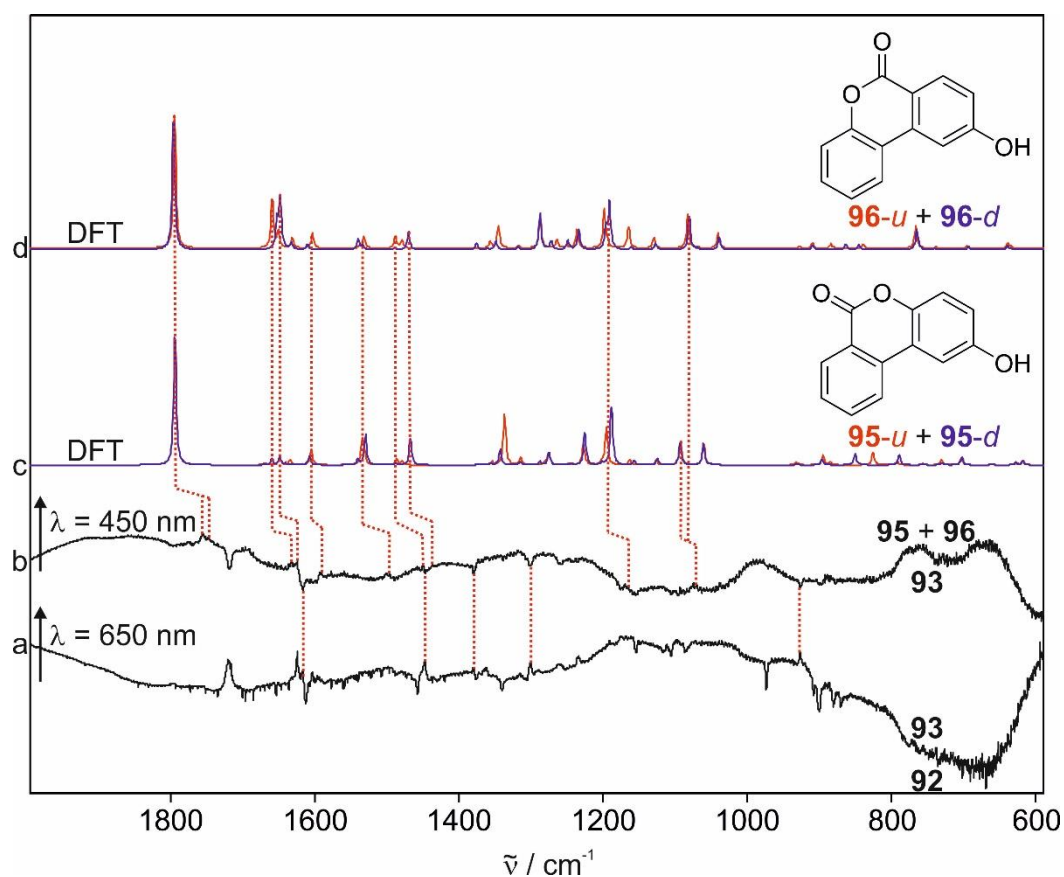


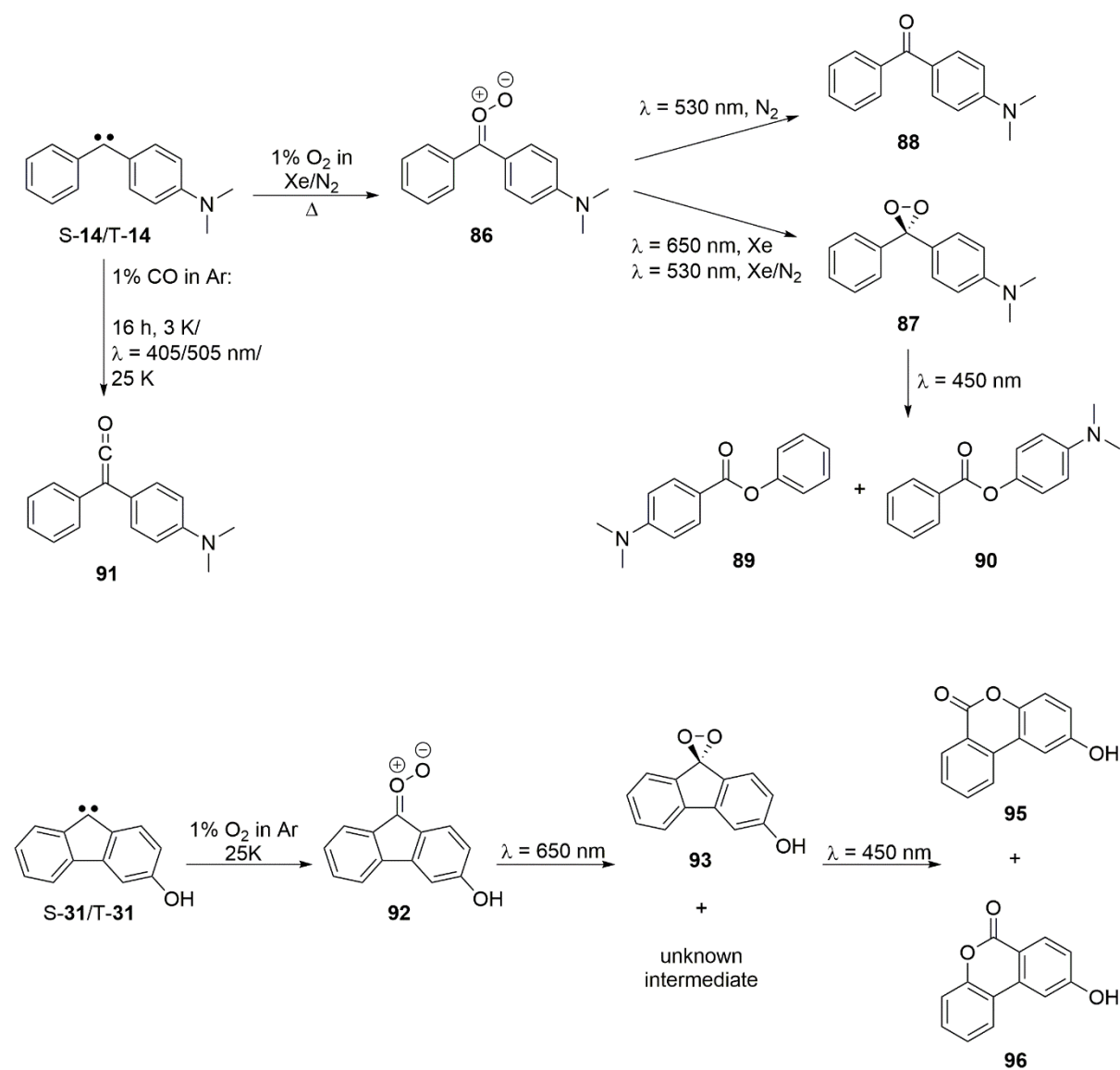
Figure 6.11: Irradiation of dioxirane **93** with 450 nm light to form lactone **95** and **96**. (a) IR difference spectrum after irradiating carbonyl oxide **92** with 650 nm light. The signals pointing upwards are assigned to dioxirane **93** (except that at 1720 cm⁻¹), the signals pointing downwards to **92**. (b) Difference spectrum after irradiation with 450 nm light. The signals pointing upwards are assigned to the lactones **95** and **96**, the signals pointing downwards to **93** (except that at 1720 cm⁻¹). (c-d) Theoretical IR spectra of the lactones **95** (spectrum c) and **96** (spectrum d) in their conformers “*u*” (red spectra) and “*d*” (blue spectra) calculated at the B3LYP/def2-TZVP level of theory.

6.4. Conclusions

The reactivity of the magnetically bistable carbenes [4-(dimethylamino)phenyl]-phenylcarbene (**14**) and 3-hydroxy-9-fluorenylidene (**31**) with oxygen as well as with carbon monoxide (carbene **14**) was successfully investigated via matrix isolation IR spectroscopy. Both the singlet and triplet states of **14** reacted with oxygen after annealing of the matrix to 20 K (N₂) or 50 K (Xe), forming the corresponding carbonyl oxide **86**. In an oxygen-doped argon matrix, the generation of **86** was not observed, so that it was unclear if the reaction with O₂ occurred. Since both S-**14** and T-**14** reacted with O₂ in equal parts in Xe and N₂, it was determined that the reaction is not spin-specific. Hence, the general tendency that oxygen preferably reacts with triplet carbenes compared to singlet carbenes^[36, 120] was not verified for carbenes **14**. The conversion from carbonyl oxide **86** to dioxirane **87** or ketone **88** was achieved after irradiation with light of 650 nm (Xe) or 530 nm (Xe, N₂). Carbonyl oxide **86** formed both dioxirane **87** and ketone **88** in N₂, but in xenon, only the dioxirane was observed. The formation of the ester compounds **89** and **90** from dioxirane **87** was observed after 450 nm irradiation. Regarding the reactivity of carbene **31** in an O₂-doped argon matrix, it was observed that both S-**14** and T-**14** reacted to carbonyl oxide **92**, so that this reaction was not spin-specific. However, slightly larger amounts of S-**14** reacted with O₂ compared to T-**14**. Irradiation with 650 nm light converted carbonyl oxide **92** to dioxirane **93** and another compound that was not identified yet but exhibited an intense signal at 1720 cm⁻¹. Comparison with the authentic sample showed that this peak does not belong to ketone **94**, it is still assumed that it contained a C=O group. To obtain more information about the nature of this unknown compound, UV/Vis and EPR investigations as well as further computational calculations will be conducted in the future. Irradiation with 450 nm light resulted in the generation of the lactones **95** and **96** from dioxirane **93**, but also in the decrease of the unidentified compound, which therefore is assumed to participate in the formation of the lactones.

Concerning the investigation of the reactivity of carbene **14** with carbon monoxide in argon, it was detected that the reaction with singlet carbene S-**14** is more favored. After 16 h at 3 K, small amounts of S-**14** reacted with pre-coordinated CO to ketene **91** while T-**14** did not react. Irradiation with 405 nm and 505 nm light resulted in further formation of small amount of ketene, accompanied by photochemical singlet-triplet spin interconversion. Annealing to 25 K led to the conversion from both S-**14** and T-**14** to ketene **91**. However, the singlet amount reacting with CO was higher, proving the favored reaction of carbene S-**14** with CO. This is in accordance with the literature that stated that the reaction of singlet carbenes with CO is spin-

allowed, and hence supposedly faster.^[36] In future investigations, the reactivity of the carbenes **14** and **31** with hydrogen and HCl will be conducted to test the spin-dependent behavior of these reactions. Furthermore, investigations of the reaction of **31** with CO will be conducted.



Scheme 6.4: Reaction scheme of the carbenes **14** and **31** and their reactions with O₂ and CO in different matrices.

7. Experimental part

7.1. Materials and methods

Chromatographic methods

Thin layer chromatography (TLC)

TLC was conducted using thin layer plates “Polygram Sil G/UV₂₅₄” (40 x 80 mm, 0.2 mm silica gel with fluorescence indicator) and “Polygram Alox N/UV₂₅₄” (40 x 80 mm, 0.2 mm aluminum oxide with fluorescence indicator) from *Macherey-Nagel*. The detection of the substance spots was conducted via an UV lamp from *CAMAG* (254 nm).

Column chromatography

For the stationary phase in column chromatography, either silica gel from *Acros Organics* (pore size: 60 Å, particle size: 35 – 70 µm) or aluminum oxide from *Acros Organics* (neutral, Brockmann activity I, pore size: 60 Å, particle size: 50 – 200 µm) was used. Prior to the use, aluminum oxide was deactivated to Brockmann activity II or III by adding 3 – 6% water. For the column chromatography of acid-sensitive compounds, the silica gel was basified with small amounts of triethyl amine in the solvent.

Reagents and solvents

The reagents for the syntheses were used without further purification and purchased from commercial suppliers. Reference alcohol fluorene-3,9-diol (**39**) was obtained from *abcr GmbH*. Technical grade solvents were used without distillation. Dry solvents were stored under molecular sieve and argon atmosphere.

Substance characterization methods

Nuclear magnetic resonance (NMR) spectroscopy

Characterization of the synthesized compounds was conducted by ^1H NMR spectra. These spectra were measured by the NMR spectrometers DPX-200 (200 MHz, *Bruker*) and AVIII 300 (300 MHz, *Bruker*). Chloroform- d_1 and DMSO- d_6 from *euriso-top* were used as deuterated solvents for the measurement. For the multiplicities, the following abbreviations were used: s (singlet), d (doublet), t (triplet), q (quartet), dd (doublet of doublets), dt (doublet of triplets), pd (pentet of doublets), m (multiplet).

IR spectroscopy

Infrared spectra at room temperature were measured with an “Equinox 55” FTIR spectrometer from *Bruker*, using potassium bromide as the matrix to form the product pellet. The signal intensities were described as follows: vw (very weak), w (weak), m (middle), s (strong), vs (very strong).

Mass spectrometry methods

Mass spectrometric analysis was conducted using a “VG Autospec” mass spectrometer for the electron ionization (EI) method. For the gas chromatography-mass spectrometry (GC-MS) method, the spectra were measured using a setup of *Hewlett Packard* with a 5890 Series II gas chromatograph and a 5972 series mass selective detector.

Matrix isolation spectroscopy

To conduct the matrix isolation, cryogenic temperatures of 3 K were generated by closed-cycle helium refrigerator systems by *Sumitomo Heavy Industries*. Temperatures of 8-10 K were generated by a close-cycle helium refrigerator system by *APD Cryogenics*. Inside the matrix apparatus, a pressure between 6×10^{-7} mbar and 2×10^{-6} mbar was generated by an oil diffusion

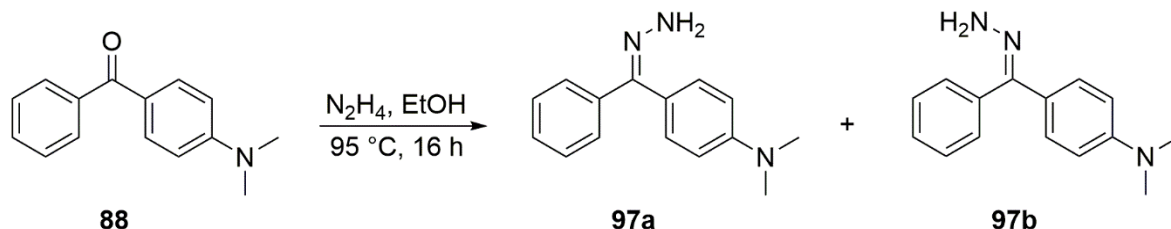
pump or a turbo pump. As the matrix gases, argon (99.999%), xenon (99.998%) and nitrogen ($\geq 99.8\%$) from *Air Liquide* were used as well as the gases carbon monoxide (*Messer*, 99.997%), oxygen (*Air Liquide*, 99.9995%), trimethyl amine (*Messer Griesheim*, $\geq 98\%$), ammonia (*Air Liquide*, 99.998%) and dimethyl ether (*Matheson Gas Products*) for doping the matrix. The gas deposition was conducted at a cesium iodide window (IR spectroscopy), a sapphire window (UV/Vis spectroscopy) and a copper rod (EPR spectroscopy). To control the gas flow during the deposition, a mass flow controller from *MKS* was used. Sample irradiation in the range of 650 – 365 nm was conducted by using custom-made LED lamps and for irradiation with light of 254 nm, a low-pressure mercury arc lamp (Pen-Ray) was used.

The spectroscopic characterization of the matrix-isolated compounds was conducted via IR, UV/Vis and EPR spectroscopy. The IR spectra were measured with the FTIR spectrometer IFS66, IFS 66v/S and Vertex 70v from *Bruker* with a resolution of 0.5 cm^{-1} in a range of $400 - 4000\text{ cm}^{-1}$. UV/Vis spectroscopy was conducted with a Cary 5000 and a Cary 1 spectrophotometer from *Varian*. The UV/Vis spectra were measured in the range from 200 – 800 nm with a resolution of 0.1 nm. Matrix isolation EPR spectroscopy was conducted with an Elexsys E500 X-band spectrometer from *Bruker*.

Calculation methods

The calculations of the vibrational frequencies, the intrinsic reaction coordinates and the geometry optimization were conducted with *Gaussian 09*.^[183] The functional B3LYP containing the three-parameter hybrid functional of Becke^[88] and correlation functional of Lee, Yang and Parr^[89] was applied in combination with the basis set def2-TZVP.^[90-91] In addition to that, the dispersion correction presented by Grimme was used.^[184] For the analysis of the EPR spectra, simulated EPR spectra were prepared using the *Easyspin* software (MATLAB).^[185]

7.2. Syntheses

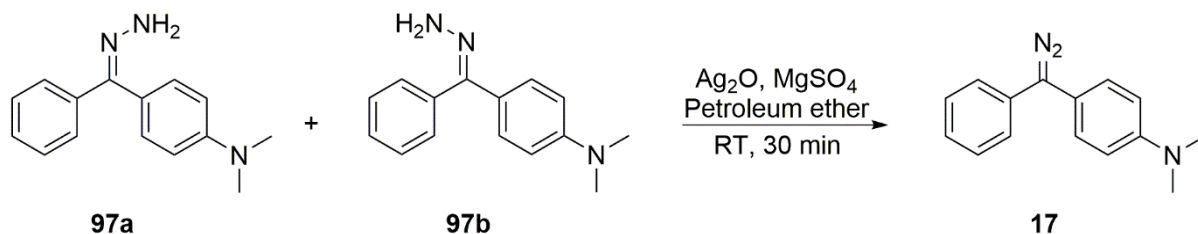
Synthesis of 4-(diazophenylmethyl)-*N,N*-dimethylbenzenamine (17)

According to Lit. [108]: To a mixture of 2.00 g (8.88 mmol) [4-(dimethylamino)phenyl]-phenylmethanone (**88**) in 11.0 mL absolute ethanol, 5.66 mL (117 mmol) hydrazine (64%) were added under argon. The mixture was stirred under argon and reflux at 95 °C for 16 hours. After cooling down, the solvent and the excess of hydrazine were removed *in vacuo* to obtain the crude product mixture. Subsequent purification via column chromatography on aluminum oxide (diethyl ether/pentane 1:2 \rightarrow ethyl acetate) yielded 1.74 g (7.27 mmol, 82%) of the hydrazone product **97** as a light-yellow solid.

¹H NMR (200 MHz, DMSO-*d*₆):

Conformer 97a: $\delta = 7.23 - 7.36$ (5 H, m, Ar-*H*), 7.03 (2 H, d, $J = 7.02$ Hz, Ar-*H*), 6.87 (2 H, d, $J = 8.92$ Hz, Ar-*H*), 6.15 (2 H, s, NH), 2.96 (6 H, s, NCH) ppm.

Conformer 97b: $\delta = 7.43 - 7.57$ (3 H, m, Ar-*H*), 7.14 - 7.20 (4 H, m, Ar-*H*), 6.64 (2 H, dd, $J = 9.07$ Hz, 3.07 Hz, Ar-*H*), 5.79 (2 H, s, NH), 2.88 (6 H, s, NCH) ppm.



According to Lit. [108]: A mixture of 212 mg (0.89 mmol) [4-(dimethylamino)phenyl]-phenylmethanone hydrazone (**97**), 5.83 mL petroleum ether and 50 - 80 mg MgSO₄ was prepared under argon. While stirring, 471 mg (2.03 mmol) silver (I) oxide were added under argon in the dark at room temperature. After 30 minutes of stirring, the intense purple solution

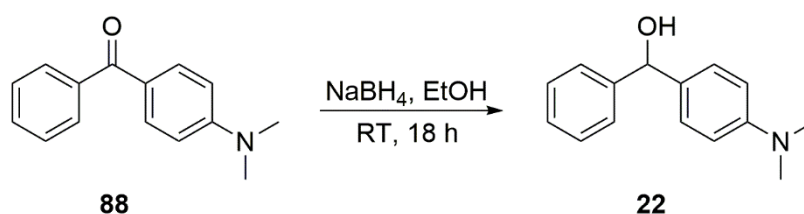
was filtrated and the solvent removed *in vacuo*. Purification via fast column chromatography (diethyl ether/pentane 1:2) on aluminum oxide yielded 135 mg (0.57 mmol, 64%) of a purple, crystalline solid.

¹H NMR (200 MHz, DMSO-d₆): δ = 7.39 (2 H, t, J = 7.53 Hz, Ar- H), 7.12 – 7.20 (5 H, m, Ar- H), 6.86 (2 H, d, J = 9.01 Hz, Ar- H), 2.93 (6 H, s, NCH) ppm.

IR (Ar, 3 K): $\tilde{\nu}$ = 2042 (vs), 1616 (m), 1600 (m), 1525 (s), 1497 (m), 1450 (m), 1362 (m), 1344 (w), 1318 (w), 1285 (w), 1272 (w), 1241 (w), 1201 (w), 1174 (w), 1124 (w), 1065 (w), 54 (w), 814 (m), 751 (m), 694 (m), 602 (w), 482 (w) cm⁻¹.

Synthesis of 4-(dimethylamino)- α -phenylbenzenemethanol (**22**)

This synthesis was conducted in collaboration with Luisa Weirich.



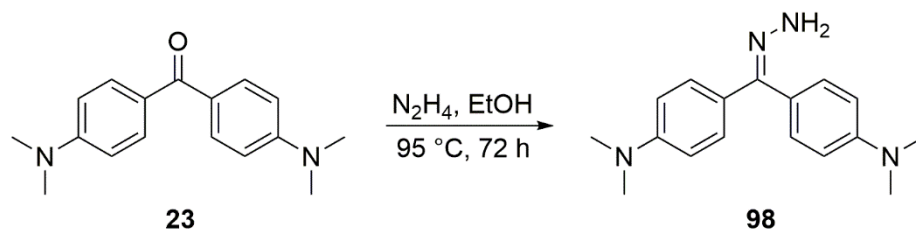
To a solution of 500 mg (2.22 mmol) 4-dimethylaminobenzophenone (**88**) in 10 mL absolute ethanol, 420 mg (11.09 mmol) sodium borohydride were added under argon. The solution was stirred at room temperature for 18 h and subsequently quenched with water. Extraction with small amounts of ethyl acetate for three times, drying with sodium sulfate and removal of the solvent *in vacuo* yielded 109 mg (0.48 mmol, 22%) of alcohol **22** as a white solid.

¹H NMR (200 MHz, DMSO-d₆): δ = 7.39 – 7.08 (7 H, m, Ar- H), 6.65 (2 H, d, J = 8.79 Hz, Ar- H), 5.59 (2 H, q, J = 4.01 Hz, OCH + OH), 2.83 (6 H, s, NCH) ppm.

MS (EI): m/z (%) = 227 [M]⁺, 225 [M – 2H]⁺, 211 [M – O]⁺, 210 [M – OH]⁺, 167, 165, 148, 134, 105, 77, 51.

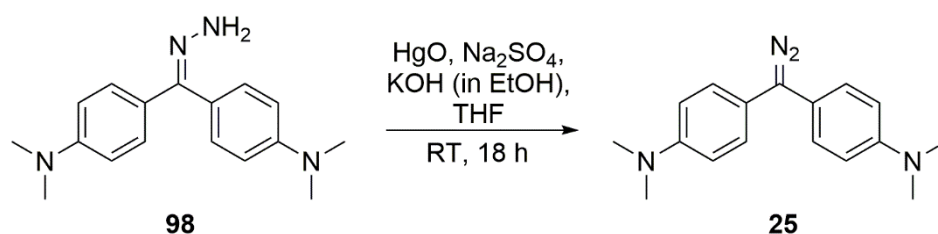
IR (Ar, 3 K): $\tilde{\nu}$ = 1620 (s), 1527 (vs), 1490 (m), 1451 (m), 1379 (w), 1362 (s), 1318 (vw), 1259 (vw), 1246 (w), 1204 (w), 1180 (m), 1168 (m), 1127 (w), 1065 (w), 1034 (w), 1026 (w), 950 (w), 811 (m), 768 (vw), 737 (vw), 715 (m), 697 (m), 638 (w), 567 (w) cm⁻¹.

Synthesis of bis[4-(dimethylamino)phenyl]diazomethane (**25**)



According to Lit. [112-113]: A mixture of 2.01 g (7.49 mmol) bis[4-(dimethylamino)phenyl]-methanone (**23**), 15 mL absolute ethanol and 5.50 mL (114 mmol) was stirred at $95\text{ }^\circ\text{C}$ under argon and reflux for 72 h. The solvent and hydrazine were removed *in vacuo* and to the remaining solid, 20 mL of isopropanol were added. Subsequent vacuum filtration yielded 1.79 g (6.34 mmol, 85%) of a yellowish solid.

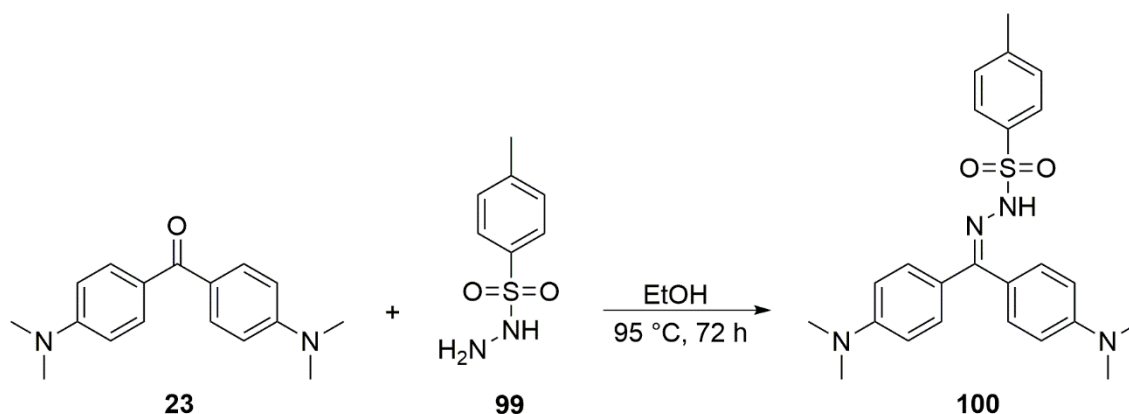
^1H NMR (200 MHz, DMSO- d_6): $\delta = 7.18$ (2 H, d, $J = 8.76$ Hz, Ar- H), 7.02 (2 H, d, $J = 8.56$ Hz, Ar- H), 6.83 (2 H, d, $J = 8.56$ Hz, Ar- H), 6.62 (2 H, d, $J = 8.76$ Hz, Ar- H) 5.76 (2 H, s, NH), 2.95 (6 H, s, NCH), 2.87 (6 H, s, NCH) ppm.



According to Lit. [112-113]: A mixture of 920 mg (4.25 mmol) thoroughly grinded, water-free mercury (II) oxide, 707 mg sodium sulfate and 6.00 mL KOH (10% in absolute ethanol) was slurried in 20.0 mL dry THF under argon. At $0\text{ }^\circ\text{C}$, 1.00 g (3.54 mmol) bis[4-(dimethylamino)phenyl]-methanone hydrazone (**98**) was added and the mixture was subsequently vigorously stirred at room temperature in the dark for 18 h. The mixture was filtered and the filter was washed with diethyl ether until the filtrate was colorless. The solvent was removed *in vacuo* and the remaining bluish solid was purified by column chromatography (hexane/ NEt_3 10:1 \rightarrow 20:1) on silica gel, yielding 302 mg (1.08 mmol, 31%) of light-blue crystals.

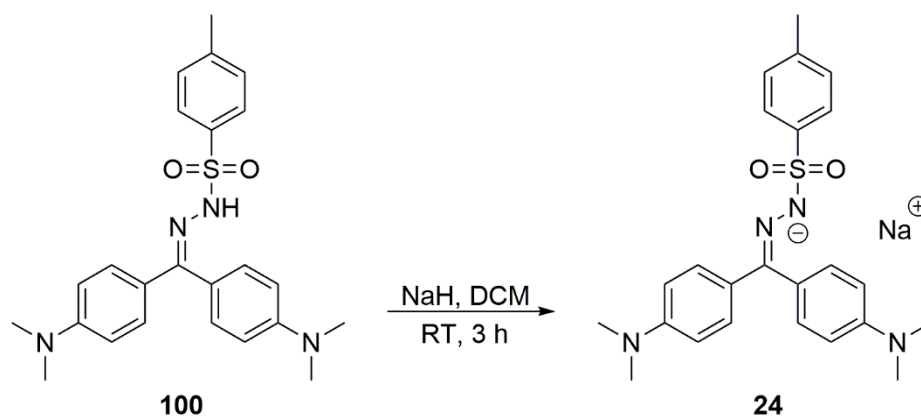
IR (KBr): $\tilde{\nu}$ = 2014 (s), 1613 (s), 1521 (s), 1479 (m), 1445 (m), 1351 (s), 1263 (m), 1229 (m), 1187 (m), 1165 (m), 1121 (w), 1091 (m), 1062 (m), 1023 (w), 946 (m), 814 (s), 592 (m) cm^{-1} .

Synthesis of the bis[4-(dimethylamino)phenyl]-methanone hydrazone sodium salt (**24**)



A solution of 1.00 g (3.73 mmol) bis[4-(dimethylamino)phenyl]-methanone (**23**) and 1.27 g (6.82 mmol) *p*-toluenesulfonyl hydrazide (**99**) in 5.10 mL absolute ethanol were heated to 95 °C under argon and reflux for 72 h. Subsequent removal of the solvent in vacuo and purification via column chromatography (diethyl ether/pentane 1:2 \rightarrow diethyl ether \rightarrow ethyl acetate) on aluminum oxide yielded 120 mg (0.27 mmol, 7%) of the product **100** as yellow-orange foam-like crystals.

^1H NMR (200 MHz, DMSO- d_6): δ = 9.79 (1 H, s, NH), 7.83 – 7.67 (1 H, m, Ar-*H*), 7.46 – 7.23 (3 H, m, Ar-*H*), 7.21 – 6.96 (4 H, m, Ar-*H*), 6.83 – 6.56 (4 H, m, Ar-*H*), 3.00 – 2.89 (12 H, m, NCH), 2.39 (3 H, s, Ar-*CH*) ppm.

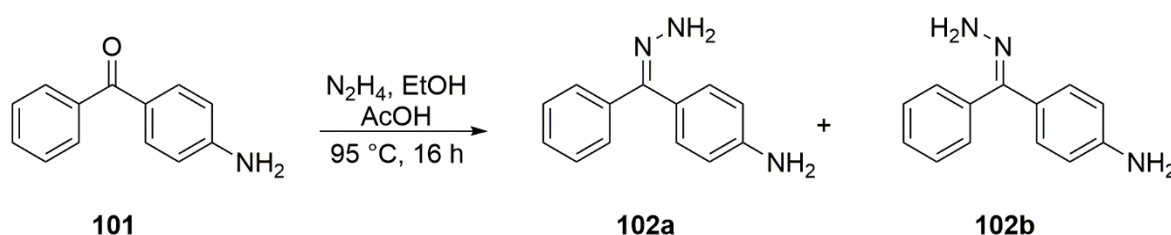


Sodium hydride (49.0 mg, 1.23 mmol, 60% in mineral oil) were washed with 1.70 mL dry pentane under argon. Subsequently, 0.90 mL dry dichloromethane were added and the solution was stirred. After the addition of 100 mg (0.23 mmol) bis[4-(dimethylamino)phenyl]-methanone tosylhydrazone (**100**), the mixture was stirred at room temperature for 3 h. Removal of the solvent *in vacuo* yielded 105 mg (0.23 mmol, 100%) of a dark brown solid that was not purified any further.

$^1\text{H NMR}$ (200 MHz, DMSO- d_6): δ = 7.63 – 7.48 (2 H, m, Ar-*H*), 7.34 – 7.03 (6 H, m, Ar*H*), 6.78 – 6.45 (4 H, m, Ar*H*), 2.98 – 2.80 (12 H, m, NCH), 2.29 (3 H, s, Ar-*CH*) ppm.

Synthesis of (*p*-aminophenyl)-phenyldiazomethane (**26**)

This synthesis was conducted in collaboration with Kseniya Gorbatenko.



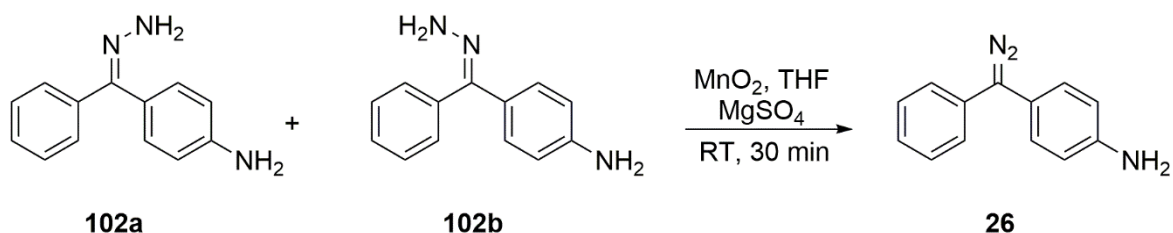
A solution of 2.00 g (10.1 mmol) 4-aminobenzophenone (**101**), 25.0 mL absolute ethanol, 5.80 mL (101 mmol) hydrazine (55%) and 0.60 mL acetic acid was stirred at 95 °C under argon and reflux for 16 h. After removal of the solvent and hydrazine *in vacuo*, the remaining solid was dissolved in ethyl acetate and washed several times with small amounts of water. Drying

of the organic phase with sodium sulfate, filtration and removal of the solvent yielded 2.10 g (9.94 mmol, 98%) of hydrazone **102** as an orange powder.

¹H NMR (200 MHz, DMSO-*d*₆):

Conformer 102a: $\delta = 7.32 - 7.11$ (5 H, m, Ar-*H*), 6.93 – 6.81 (2 H, m, Ar-*H*), 6.47 (2 H, dt, $J = 8.3$ Hz, 1.2 Hz, Ar-*H*), 5.68 (2 H, s, N-NH), 5.13 (2 H, s, Ar-NH) ppm.

Conformer 102b: $\delta = 7.63 - 7.31$ (5 H, m, Ar-*H*), 7.08 – 6.97 (2 H, m, Ar-*H*), 6.77 – 6.66 (2 H, m, Ar-*H*), 6.10 (2 H, s, N-NH), 5.29 (2 H, s, Ar-NH) ppm.

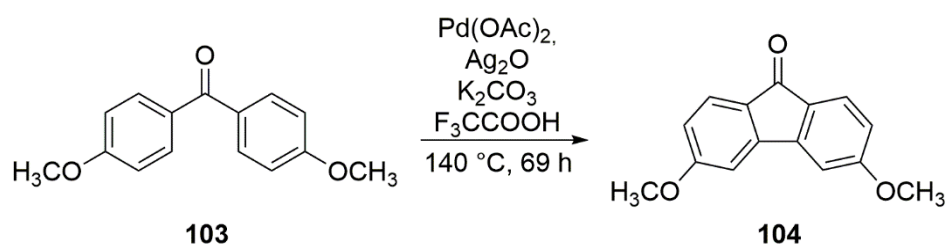


100 mg (0.47 mmol) 4-aminobenzophenone hydrazone (**102**) were dissolved in 5.00 mL dry THF and 500 mg magnesium sulfate and 80.0 mg (0.92 mmol) manganese (IV) oxide were added. The mixture was stirred for 30 minutes at room temperature und subsequently filtered through a celite pad. The celite was washed with 50 mL THF and the solvent was removed *in vacuo*. Purification of the resulting orange oil by column chromatography (diethyl ether/triethyl amine 10:1) on aluminum oxide yielded 32.0 mg (0.15 mmol, 32%) of diazo compound **26** as a purple oil.

¹H NMR (200 MHz, DMSO-*d*₆): $\delta = 7.75 - 7.24$ (3 H, m, Ar-*H*), 7.20 – 6.91 (4 H, m, Ar-*H*), 6.87 – 6.40 (2 H, m, Ar-*H*), 5.26 (2 H, s, NH) ppm.

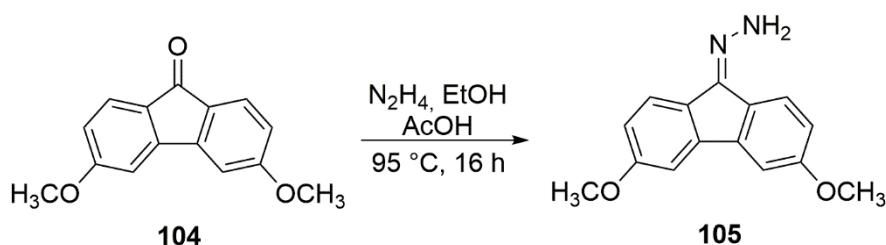
IR (KBr): $\tilde{\nu} = 2044$ (vs), 1609 (s), 1519 (s), 1496 (m), 1330 (m), 1289 (m), 1188 (w) cm^{-1} .

Synthesis of 3,6-dimethoxy-9-diazofluorene (**32**)



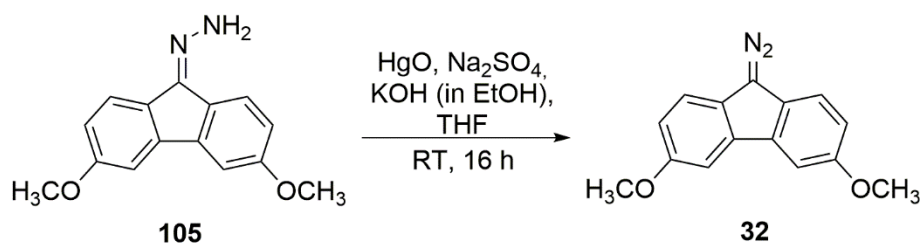
According to Lit. [138]: Under argon atmosphere, 1.20 g (4.95 mmol) 4,4'-dimethoxybenzophenone (**103**), 1.73 g (12.5 mmol) potassium carbonate, 101 mg (0.45 mmol) palladium (II) acetate and 1.74 g (7.51 mmol) silver (I) oxide were added into a pressure tube. At 0 °C, 12.5 mL trifluoroacetic acid were added dropwise and the pressure tube was closed. The mixture was stirred under argon for 69 h at 140 °C in the dark. After cooling down to room temperature, the solvent was evaporated *in vacuo* and the remaining black tar was purified by column chromatography (hexane/ethyl acetate 15:1) on silica gel to obtain 768 mg (3.20 mmol, 65%) of product **104** as a yellow powder.

¹H NMR (200 MHz, DMSO-*d*₆): δ = 7.54 – 7.46 (4 H, m, Ar-*H*), 6.87 (2 H, dd, J = 8.22 Hz, 2.29 Hz, Ar-*H*), 3.90 (6 H, s, OCH) ppm.



According to Lit. [123]: A solution of 768 mg (3.20 mmol) 3,6-dimethoxy-9-fluorenone (**104**), 2.04 mL (42.2 mmol) hydrazine (64%), 0.16 mL acetic acid and 19.2 mL absolute ethanol was heated to 95 °C under argon and reflux for 16 h. The solvent and hydrazine were removed *in vacuo* and the remaining solid was completely dissolved in ethyl acetate and washed with small portions of water for three times. The organic phase was dried with sodium sulfate, and evaporation of the solvent resulted in 744 mg (2.93 mmol, 92%) of hydrazone **105** as a light-yellow solid.

¹H NMR (200 MHz, CDCl₃): δ = 8.24 (1 H, d, J = 8.34 Hz, Ar-*H*), 7.90 (1 H, t, J = 8.76 Hz, Ar-*H*), 7.72 – 7.49 (1 H, m, Ar-*H*), 7.17 – 7.09 (1 H, m, Ar-*H*), 6.95 – 6.72 (2 H, m, Ar-*H*), 3.96 – 3.87 (6 H, m, OCH) ppm.



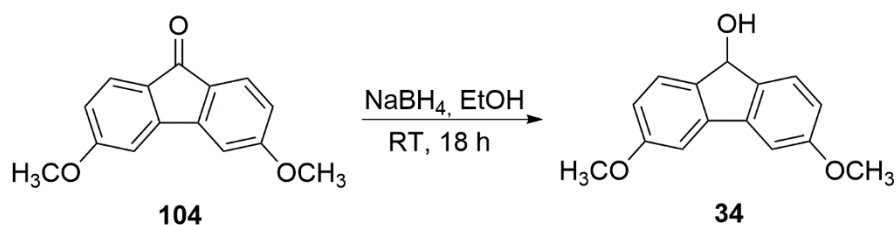
According to Lit. [123]: 134 mg (0.53 mmol) 3,6-dimethoxy-9-fluorenone hydrazone (**105**), 550 mg (2.54 mmol) water-free mercury (II) oxide (grinded) and 219 mg sodium sulfate were slurried in 31.3 mL very dry THF under argon. After the addition of 1 mL of KOH solution (10% in absolute ethanol), the mixture was vigorously stirred at room temperature in the dark for 16 h. The mixture was filtrated and the filter was washed several times with small amounts of diethyl ether. After removal of the solvent *in vacuo*, the resulting red oil was purified by column chromatography (diethyl ether/pentane 5:3) on aluminum oxide to obtain 92.0 mg (0.36 mmol, 68%) of diazo product **32** as light-purple crystals.

¹H NMR (200 MHz, DMSO-*d*₆): δ = 7.76 (2 H, d, J = 2.33 Hz, Ar-*H*), 7.57 (2 H, d, J = 8.53 Hz, Ar-*H*), 7.00 (2 H, dd, J = 8.53 Hz, 2.41 Hz, Ar-*H*), 3.86 (6 H, s, OCH) ppm.

IR (Ar, 3 K): $\tilde{\nu}$ = 2058 (vs), 1624 (m), 1615 (m), 1576 (m), 1497 (s), 1468 (s), 1441 (m), 1435 (m), 1350 (w), 1332 (w), 1301 (m), 1288 (w), 1266 (w), 1256 (m), 1238 (vw), 1211 (s), 1201 (s), 1182 (w), 1166 (s), 1076 (vw), 1048 (m), 1037 (w), 915 (vw), 863 (w), 843 (w), 837 (w), 813 (w), 797 (vw), 668 (vw), 627 (vw), 587 (vw) cm^{-1} .

Synthesis of 3,6-dimethoxyfluoren-9-ol (**34**)

This synthesis was conducted in collaboration with Luisa Weirich.



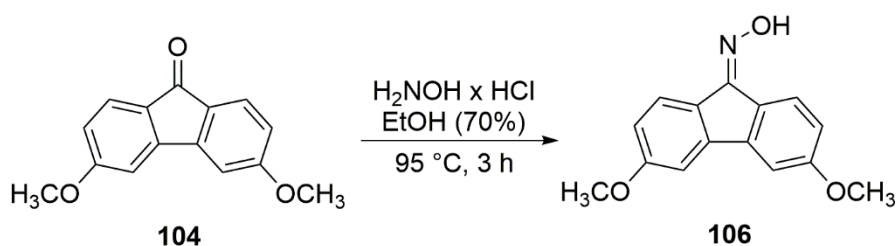
To a stirred solution of 130 mg (0.54 mmol) 3,6-dimethoxy-9-fluorenone (**104**) in 3 mL absolute ethanol, 102 mg (2.70 mmol) sodium borohydride were added and the mixture was

stirred under argon at room temperature for 18 h. The mixture was quenched with water and extracted with ethyl acetate for three times. Drying of the organic phase with sodium sulfate and evaporation of the solvent *in vacuo* yielded 44 mg (0.18 mmol, 33%) of alcohol **34** as a white solid.

¹H NMR (200 MHz, DMSO-*d*₆): δ = 7.49 – 7.37 (4 H, m, Ar-*H*), 6.84 (2 H, dd, J = 8.21 Hz, 2.53 Hz, Ar-*H*), 5.54 (1 H, d, J = 7.23 Hz, OH), 5.32 (1 H, d, J = 7.23 Hz, Ar-*CH*), 3.82 (6 H, s, Ar-O*CH*) ppm.

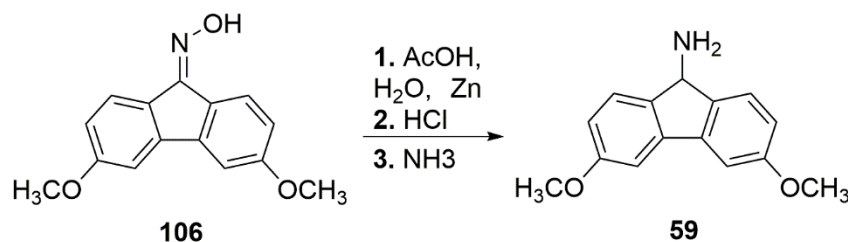
IR (Ar, **3 K):** $\tilde{\nu}$ = 1625 (s), 1617 (s), 1591 (s), 1502 (s), 1470 (s), 1441 (m), 1434 (m), 1381 (m), 1318 (s), 1296 (m), 1286 (m), 1278 (s), 1250 (vs), 1241 (m), 1232 (s), 1205 (m), 1197 (w), 1191 (w), 1182 (m), 1166 (s), 1123 (w), 1107 (m), 1046 (s), 1022 (s), 864 (w), 859 (w), 847 (m), 838 (w), 798 (w), 791 (w), 616 (w) cm⁻¹.

Synthesis of 3,6-dimethoxyfluoren-9-amine (**59**)



According to Lit. [186]: A solution of 201 mg (0.84 mmol) 3,6-dimethoxy-9-fluorenone (**104**), 1.51 mL ethanol (70%) and 153 mg (2.20 mmol) hydroxylamine hydrochloride was stirred at 95 °C under reflux for 3 h. After removal of the solvent *in vacuo*, the crude product was purified by washing with small amounts of diethylether and drying, yielding 179 mg (0.70 mmol, 83%) of oxime **106** as a white solid.

¹H NMR (200 MHz, DMSO-*d*₆): δ = 11.97 (1 H, s, OH), 8.21 (1 H, d, J = 8.47 Hz, Ar-*H*), 7.58 – 7.45 (3 H, m, Ar-*H*), 6.93 – 6.82 (2 H, m, Ar-*H*), 3.88 (3 H, s, O*CH*), 3.85 (3 H, s, O*CH*) ppm.

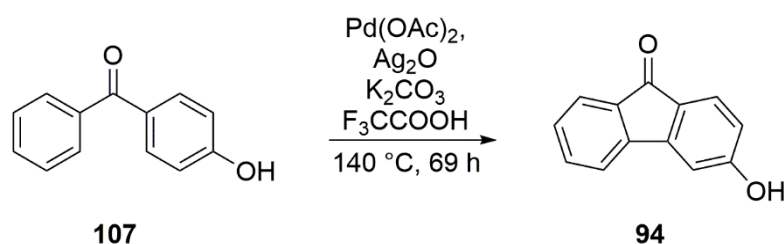


According to Lit. [186]: 179 mg (0.70 mmol) of 3,6-dimethoxy-9-fluorenone oxime (**106**) were dissolved in 2.28 mL acetic acid and 0.12 mL water. After heating the solution to 110 °C, 294 mg (4.50 mmol) zinc powder was added in small portions. The mixture was stirred at the same temperature under reflux for 1 h and subsequently filtrated. The filter was washed with diethyl ether until the filtrate was colorless, and the solvent of the filtrate was removed *in vacuo*. 3.22 mL (16.1 mmol) of 5 M hydrochloric acid were added at 0 °C, and the mixture was stirred at the same temperature for 10 h. The resulting solid was filtrated and washed with small amounts of concentrated ammonia. Subsequently, the solid was washed with water and again with ammonia, respectively. Recrystallization from diethyl ether yielded 34 mg (0.14 mmol, 20%) of amine **59** as a grey solid.

¹H NMR (200 MHz, DMSO-*d*₆): δ = 7.53 (2 H, d, J = 8.45 Hz, Ar-*H*), 7.44 (2 H, d, J = 2.17 Hz, Ar-*H*), 6.88 (2 H, dd, J = 8.21 Hz, 2.49 Hz, Ar-*H*), 4.74 (1 H, s, Ar-*CH*), 3.83 (6 H, s, *OCH*) ppm.

IR (Ar, 3 K): $\tilde{\nu}$ = 1639 (w), 1624 (m), 1590 (m), 1500 (m), 1469 (m), 1441 (w), 1434 (w), 1346 (vw), 1313 (w), 1285 (w), 1250 (m), 1233 (m), 1207 (w), 1191 (vw), 1182 (w), 1167 (m), 1050 (m), 1018 (vw), 887 (vw), 862 (vw), 846 (vw), 795 (vw), 764 (m) cm⁻¹.

Synthesis of 3-hydroxy-9-diazafluorene (**35**)



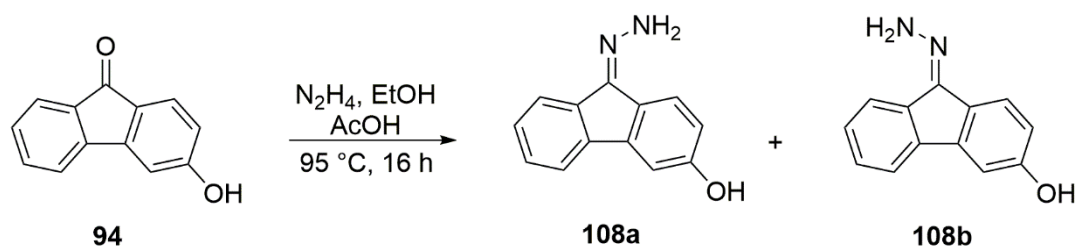
According to Lit. [138]: 1.21 g (6.10 mmol) 4-hydroxybenzophenone (**107**), 2.12 g (15.3 mmol) potassium carbonate, 125 mg (0.56 mmol) palladium (II) acetate and 2.13 g

(9.19 mmol) silver (I) oxide were added to a pressure tube under argon. At 0 °C, 15.3 mL trifluoroacetic acid were added dropwise and the tube was subsequently closed. The mixture was heated to 140 °C in the dark for 69 h. After cooling down to room temperature, the solvent was removed in vacuo and the dark brown residue was purified by column chromatography (hexane/ethyl acetate 15:1) on silica gel to obtain 450 mg (2.29 mmol, 38%) of a light-yellow powder.

¹H NMR (200 MHz, DMSO-*d*₆): δ = 10.70 (1 H, s, OH), 7.71 (1 H, d, J = 7.24 Hz, Ar-*H*), 7.61 – 7.44 (3 H, m, Ar-*H*), 7.35 (1 H, t, J = 7.24 Hz, Ar-*H*), 7.14 (1 H, d, J = 2.08 Hz, Ar-*H*), 6.70 (1 H, dd, J = 8.16 Hz, 2.06 Hz, Ar-*H*) ppm.

GC-MS: m/z (%) = 196 [M]⁺.

IR (KBr): $\tilde{\nu}$ = 1680 (vs), 1613 (s), 1590 (vs), 1448 (s), 1393 (s), 1336 (w), 1301 (s), 1267 (vw), 1207 (vs), 1155 (w), 1105 (s), 1026 (vw), 928 (m), 894 (vw), 871 (w), 831 (m), 799 (vw), 764 (m), 741 (m), 720 (w), 673 (m), 644 (vw), 614 (w), 557 (w), 521 (w), 481 (vw) cm⁻¹.



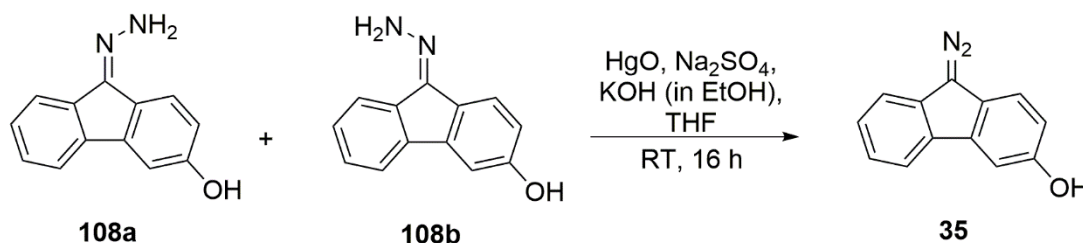
According to Lit. [123]: A mixture of 209 mg (1.07 mmol) 3-hydroxy-9-fluorenone (**94**), 0.68 mL (14.1 mmol) hydrazine (64%), 6.40 mL absolute ethanol and 0.05 mL acetic acid was stirred at 95 °C under argon and reflux for 16 h. The solvent and hydrazine were removed *in vacuo* and the remaining solid was dissolved in ethyl acetate and washed with small amounts of water for three times. The organic phase was dried with sodium sulfate, filtrated and the solvent was evaporated. An orange, foam-like solid with a mass of 189 mg (0.90 mmol, 84%) was obtained.

¹H NMR (200 MHz, DMSO-*d*₆):

Conformer 108a: δ = 9.88 (1 H, s, OH), 7.99 (1 H, d, J = 8.45 Hz, Ar-*H*), 7.63 – 7.55 (2 H, m, Ar-*H*), 7.32 – 7.21 (3 H, m, Ar-*H*), 6.75 (1 H, dd, J = 8.39 Hz, 2.24 Hz, Ar-*H*), 5.36 (2 H, d, J = 7.01 Hz, NH) ppm.

Conformer 108b: $\delta = 9.53$ (1 H, s, OH), 8.14 (1 H, d, $J = 7.34$ Hz, Ar-H), 7.80 (1 H, d, $J = 7.11$ Hz, Ar-H), 7.46 – 7.34 (3 H, m, Ar-H), 7.13 (1 H, dd, $J = 9.47$ Hz, 2.15 Hz, Ar-H), 6.70 - 6.65 (1 H, m, Ar-H), 5.60 (2 H, d, $J = 7.32$ Hz, NH) ppm.

MS (EI): m/z (%) = 210 $[M]^+$, 197, 181 $[M - 2N - H]^+$, 152 $[M - O - 2N - 2H]^+$, 151, 76.

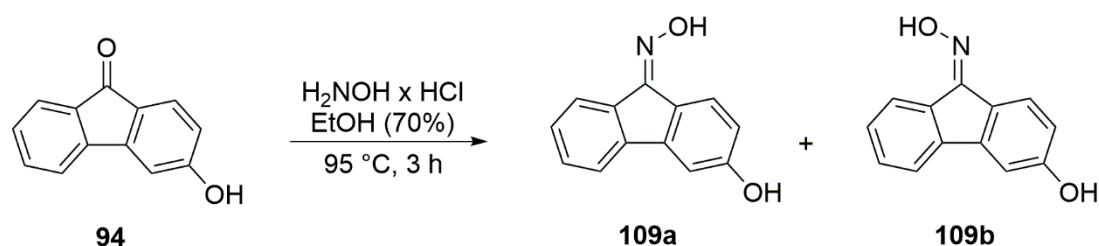


According to Lit. [123]: 610 mg (2.82 mmol) mercury (II) oxide were grinded several times and dried in vacuum at 80-90 °C for several minutes to remove traces of water. After cooling back to room temperature, 36.5 mL very dry THF, 269 mg sodium sulfate and 131 mg (0.62 mmol) 3-hydroxy-9-fluorenone hydrazone (**108**) were added under argon atmosphere. Ten drops of a KOH solution (10% in absolute ethanol) were added and the mixture was vigorously stirred at room temperature in the dark for 16 h. The black-reddish slurry was filtrated and the filter washed with diethyl ether until the solution was colorless. After removal of the solvent *in vacuo*, the resulting red oil was purified by column chromatography (diethyl ether/pentane 5:3 → diethyl ether) on silica gel to obtain 61.0 mg (0.29 mmol, 47%) of diazo product **35** as a pink solid.

¹H NMR (300 MHz, DMSO-d₆): $\delta = 9.49$ (1 H, s, OH), 7.96 (1 H, d, $J = 7.28$ Hz, Ar-H), 7.65 (1 H, d, $J = 7.61$ Hz, Ar-H), 7.51 – 7.25 (4 H, m, Ar-H), 6.88 (1 H, dd, $J = 8.45$ Hz, 2.27 Hz, Ar-H) ppm.

IR (Ar, 3 K): $\tilde{\nu} = 2058$ (vs), 1628 (m), 1619 (m), 1611 (w), 1591 (w), 1584 (w), 1506 (w), 1490 (m), 1477 (w), 1461 (w), 1452 (s), 1443 (s), 1386 (w), 1356 (vw), 1347 (w), 1339 (w), 1315 (w), 1303 (m), 1242 (w), 1219 (m), 1204 (w), 1198 (w), 1168 (s), 1154 (m), 887 (m), 866 (vw), 845 (w), 813 (w), 798 (w), 766 (m), 746 (m), 723 (w), 643 (m) cm⁻¹.

Synthesis of 3-hydroxyfluoren-9-amine (66)

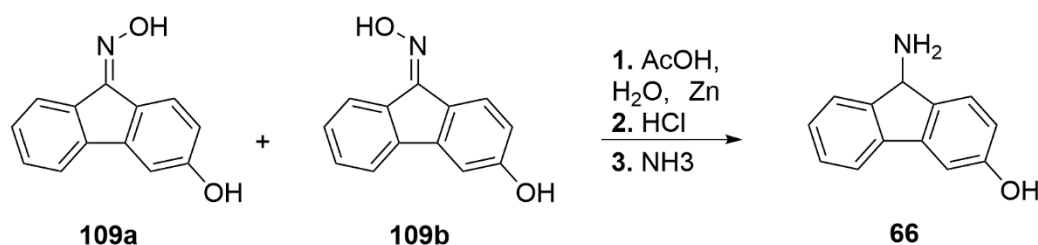


According to Lit. [186]: A mixture of 115 mg (0.59 mmol) 3-hydroxy-9-fluorenone (**94**), 107 mg (1.54 mmol) hydroxylamine hydrochloride and 1.50 mL ethanol (70%) was stirred at 95 °C under reflux for 3 h. The resulting brown solution was diluted with small amounts of water and the precipitate was filtrated and washed with water. The solid was dissolved in ethyl acetate, washed with water and the organic phase was dried with sodium sulfate. After filtration and removal of the solvent *in vacuo*, the product was further purified by dissolving in ethanol and re-precipitation by stepwise addition of water. Filtration and drying of the precipitate yielded 92.0 mg (0.44 mmol, 75%) of a light-brown solid.

¹H NMR (300 MHz, DMSO-*d*₆):

Conformer 109a: δ = 12.07 (1 H, s, NOH), 10.07 (1 H, s, Ar-OH), 8.14 (1 H, d, J = 8.35 Hz, Ar-H), 7.76 – 7.61 (2 H, m, Ar-H), 7.51 – 7.27 (2 H, m, Ar-H), 7.21 (1 H, d, J = 2.10 Hz, Ar-H), 6.74 (1 H, dd, J = 8.36 Hz, 2.29 Hz, Ar-H) ppm.

Conformer 109b: δ = 12.11 (1 H, s, NOH), 9.83 (1 H, s, Ar-OH), 8.30 (1 H, d, J = 7.47 Hz, Ar-H), 7.79 – 7.68 (2 H, m, Ar-H), 7.53 – 7.41 (2 H, m, Ar-H), 7.17 (1 H, d, J = 2.18 Hz, Ar-H), 6.72 (1 H, dd, J = 8.22 Hz, 2.23 Hz, Ar-H) ppm.



According to Lit. [186]: A mixture of 82.0 mg (0.39 mmol) 3-hydroxy-9-fluorenone oxime (**109**), 0.07 mL H₂O and 1.20 mL acetic acid was heated to 110 °C und stirring and reflux. 152 mg (2.32 mmol) zinc powder were added slowly at the mixture was stirred at the same

temperature for 1 h. The mixture was filtrated and the filter was washed with small portions of ethyl acetate. After removal of the solvent in vacuo, 2.00 mL (10.0 mmol) 5 M hydrochloric acid were added at 0 °C and it was stirred at the same temperature for 10 h. The precipitate was vacuum-filtrated and washed with a few mL of ammonia and subsequently with water. After drying, 23.0 mg (0.12 mmol, 31%) of a beige solid was obtained.

¹H NMR (300 MHz, DMSO-*d*₆): δ = 9.43 (2 H, s, *NH*), 9.39 (1 H, s, *OH*), 7.66 (1 H, d, J = 7.13 Hz, *Ar-H*), 7.60 (1 H, d, J = 7.13 Hz, *Ar-H*), 7.41 (1 H, d, J = 8.15 Hz, *Ar-H*), 7.30 (2 H, pd, J = 7.33 Hz, 1.47 Hz, *Ar-H*), 7.12 (1 H, d, J = 2.23 Hz, *Ar-H*), 6.71 (1 H, dd, J = 8.05 Hz, 2.26 Hz, *Ar-H*) ppm.

IR (Ar, 3 K): $\tilde{\nu}$ = 1592 (w), 1585 (vw), 1502 (vw), 1495 (vw), 1462 (w), 1446 (w), 1353 (w), 1301 (vw), 1293 (w), 1257 (vw), 1249 (vw), 1217 (vw), 1160 (m), 897 (vw), 813 (vw), 770 (w), 741 (w) cm⁻¹.

8. References

- [1] Thomanek, T. : *Investigation of the Bistability of 3-Methoxy-9-Fluorenylidene: A Matrix Isolation Study*, Master Thesis to obtain the degree of M. Sc., Ruhr-Universität Bochum, Faculty of Chemistry and Biochemistry, **2016**
- [2] Hammett, L. P. : *Physical Organic Chemistry; Reaction Rates, Equilibria and Mechanisms*, **1940**, First Edition, McGraw-Hill Book Company, Inc.
- [3] Carey, F. A. ; Sundberg, R. J. : *Advanced Organic Chemistry, Part A: Structure and Mechanisms*, **2007**, Fifth Edition, Springer
- [4] Hammond, G. S. : In: *Pure & Appl. Chem.*, **1997**, Vol. 69, No. 9, 1919-1922
- [5] Muller, P. : In: *Pure & Appl. Chem.*, **1994**, Vol. 66, No. 5, 1077-1184
- [6] Whitmore, F. C. : *J. Am. Chem. Soc.*, **1932**, 54, 3274-3283
- [7] Clarke, R. W. S. ; Lapworth, A. : *J. Chem. Soc.*, **1907**, 91, 694-705
- [8] Schlenk, W. ; Marcus, E. : *Berichte der Deutschen Chemischen Gesellschaft*, **1914**, 47, 1664-1678
- [9] Gomberg, M. : *Berichte der Deutschen Chemischen Gesellschaft*, **1900**, 33, 3150-3163
- [10] Nef, J. U. : *J. Am. Chem. Soc.*, **1904**, Vol. 26, No. 12, pp. 1549-1577
- [11] Meerwein, H. : *Justus Liebigs Annalen der Chemie*, **1914**, 405, 129-175
- [12] Bartmess, J. E. et al. : *J. Am. Chem. Soc.*, **1981**, 103, 1338-1344
- [13] Majima, T. et al. : *J. Phys. Chem. A*, **2004**, 108, 8147-8150
- [14] Phillips, D. L. ; Hadad, C. M. ; Thamattoor, D. M. et al. : *J. Phys. Chem. A*, **2018**, 122, 6852-6855
- [15] Fu, G. C. ; Eckhardt, M. : *J. Am. Chem. Soc.*, **2003**, 125, 13642-13643
- [16] Murakami, M. et al. : *Org. Lett.*, **2011**, Vol. 13, No. 7, 1666-1669
- [17] Herrmann, W. A. et al. : *Angew. Chem. Int. Ed. Engl.*, **1995**, 34, No. 21, 2371-2374
- [18] Crabtree, T. H. : *The Organometallic Chemistry of the Transition Metals*, **2005**, Fourth Edition, Wiley-Interscience
- [19] Bertrand, G. et al. : *Chem. Rev.*, **2000**, 100, 39-91
- [20] Borden, W. T. ; Hoffmann, R. et al. : *J. Am. Chem. Soc.*, **2013**, 135, 13954-13964
- [21] Tomioka, H. : *Acc. Chem. Res.*, **1997**, 30, 315-321
- [22] Carey, F. A. ; Sundberg, R. J. : *Advanced Organic Chemistry, Part B: Reactions and Synthesis*, **2007**, Fifth Edition, Springer
- [23] Hund, F. : *Zeitschrift für Physik*, **1927**, 42, 93-120
- [24] Clayden, J. ; Greeves, N. ; Warren, S. ; Wothers, P. : *Organic Chemistry*, **2000**, Oxford University Press

- [25] Bernheim, R. A. ; Wood, L. S. ; Skell, P. S. et al. : *J. Chem. Phys.*, **1976**, Vol. 64, No. 7, 2747-2755
- [26] Wasserman, E. et al. : *J. Am. Chem. Soc.*, **1970**, 92:25, 7491-7493
- [27] Bernheim, R. A. ; Wood, L. S. ; Skell, P. S. et al. : *J. Chem. Phys.*, **1971**, Vol. 54, 3223-3225
- [28] Wasserman, E. et al. : *J. Chem. Phys.*, **1971**, Vol. 54, No. 9, 4120-4121
- [29] McKellar, A. R. W. ; Evenson, K. M. ; Langhoff, S. R. et al. : *J. Chem. Phys.*, **1983**, 79(11), 5251-5264
- [30] Hoffmann, R. ; Zeiss, G. D. ; Van Dine, G. W. : *J. Am. Chem. Soc.*, **1968**, 90:6, 1485-1499
- [31] Gleiter, R. ; Hoffmann, R. : *J. Am. Chem. Soc.*, **1968**, 90:20, 5457-5460
- [32] Carter, E. A. ; Khodabandeh, S. : *J. Phys. Chem.*, **1993**, 97, 4360-4364
- [33] Carter, E. A. ; Goddard, W. A. : *J. Chem. Phys.*, **1988**, 88(3), 1752-1763
- [34] Harrison, J. F. : *J. Am. Chem. Soc.*, **1971**, 93:17, 4112-4119
- [35] Harrison, J. F. ; Liebman, J. F. ; Liedtke, R. C. : *J. Am. Chem. Soc.*, **1979**, 101:24, 7162-7168
- [36] Sander, W. ; Bucher, G. ; Wierlacher, S. : *Chem. Rev.*, **1993**, 93, 1583-1621
- [37] Skell, P. S. ; Garner, A. Y. : *J. Am. Chem. Soc.*, **1956**, Vol. 78, 3409-3411
- [38] Skell, P. S. ; Garner, A. Y. : *J. Am. Chem. Soc.*, **1956**, Vol. 78, 5430-5433
- [39] Houk, K. N. ; Singleton, D. A. : *J. Am. Chem. Soc.*, **1999**, 121, 3933-3938
- [40] Cane, D. E. ; Thomas, P. J. : *J. Am. Chem. Soc.*, **1984**, 106, 5295-5303
- [41] Sander, W. ; Sanchez-Garcia, E. et al. : *J. Am. Chem. Soc.*, **2014**, 136, 15625-15630
- [42] Rodebush, W. H. ; Latimer, W. M. : *J. Am. Chem. Soc.*, **1920**, 42, 1419-1433
- [43] Desiraju, G. R. ; Crabtree, R. H. et al. : *Pure Appl. Chem.*, **2011**, Vol. 83, No. 8, 1619-1636
- [44] Desiraju, G. R. ; Crabtree, R. H. et al. : *Pure Appl. Chem.*, **2011**, Vol. 83, No. 8, 1637-1641
- [45] Desiraju, G. R. : *Acc. Chem. Res.*, **2002**, 35, 565-573
- [46] Steiner, T. : *Angew. Chem. Int. Ed.*, **2002**, 41, 48-76
- [47] Frey, P. A. ; Whitt, S. A. ; Tobin, J. B. : *Science*, **1994**, Vol. 264, 1927-1930
- [48] Timmerman, P. ; Reinhoudt, D. N. ; Prins, L. J. : *Angew. Chem. Int. Ed.*, **2001**, 40, 2382-2426
- [49] Del Bene, J. E. : *J. Phys. Chem.*: **1988**, 92, 2874-2880
- [50] Perrin, C. L. ; Nielson, J. B. : *Annu. Rev. Phys. Chem.*, **1997**, 48, 511-544
- [51] Jeffrey, G. A. ; Takagi, S. : *Acc. Chem. Res.*, **1978**, 11, 264-270

- [52] Desiraju, G. R. : *Acc. Chem. Res.*, **1991**, *24*, 290-296
- [53] Tüchsen, E. ; Woodward, C. : *Biochemistry*, **1987**, *26*, 1918-1925
- [54] Dunkin, I. R. : *Chem. Soc. Rev.*, **1980**, *9*, 1-23
- [55] Eisenthal, K. B. ; Turro, N. J. et al. : *J. Am. Chem. Soc.*, **1980**, *102*, 6563-6565
- [56] Moss, R. A. ; Platz, M. S. ; Jones Jr., Maitland: *Reactive Intermediate Chemistry*, **2004**, *John Wiley & Sons, Inc.*
- [57] Pimentel, G. C. ; Dows, D. A. ; Whittle, E. : *J. Chem. Phys.*, **1954**, *22*, 1943
- [58] Norman, I. ; Porter, G. : *Nature*, **1954**, *Vol. 174*, 508-509
- [59] Pimentel, G. C. ; Becker, E. D. : *J. Chem. Phys.*, **1956**, *25*, 224-228
- [60] Schnöckel, H. ; Schunck, S. : *Chemie in unserer Zeit*, **1987**, *21. Jahrg.*, *Nr. 3*, 73-81
- [61] Patai, S. : *The chemistry of diazonium and diazo groups, Part 2*, **1978**, *John Wiley & Sons*
- [62] Gilchrist, T. L. ; Rees, C. W. : *Carbene, Nitrene und Dehydroaromaten*, **1972**, *Hüthig*
- [63] Bräse, S. et al. : *Angew. Chem. Int. Ed.*, **2005**, *44*, 5188-5240
- [64] Dunkin, I. R. : *Matrix-Isolation Techniques, A Practical Approach*, **1998**, *Oxford University Press*
- [65] Sander, W. ; Patyk, A. ; Bucher, G. : *J. Mol. Struct.*, **1990**, *222*, 21-31
- [66] Hesse, M. ; Meier, H. ; Zeeh, B. : *Spektroskopische Methoden in der organischen Chemie*, **2005**, Seventh Edition, *Thieme*
- [67] Dresselhaus, M. S. : *Solid State Physics, Part III: Magnetic Properties of Solids*, **2001**
- [68] Zavoisky, E. : *J. Phys. (Moscow)*, **1945**, *Vol. 9, No. 2*, 211-216
- [69] Brustolon, M. ; Giamello, E. : *Electron Paramagnetic Resonance, A Practitioner's Toolkit*, **2009**, *John Wiley & Sons*
- [70] Weil, J. A. ; Bolton, J. R. : *Electron Paramagnetic Resonance, Elementary Theory and Practical Applications*, **2007**, Second Edition, *Wiley-Interscience*
- [71] Zeeman, P. : *XXXII. On the influence of magnetism on the nature of the light emitted by a substance*, **1897**, *The London, Edinburgh and Dublin Philosophical Magazine and Journal of Science*, *43:262*, 226-239
- [72] Odom, B. et al. : *Phys. Rev. Lett.*, **2006**, *97(3)*, 030801(4)
- [73] Henkel, S. : *Matrix Isolation Studies of Azulenylcarbenes*, Dissertation to obtain the degree of Dr. rer. nat., Ruhr-Universität Bochum, Faculty of Chemistry and Biochemistry, **2014**
- [74] Wasserman, E. ; Snyder, L. C. ; Yager, W. A. : *J. Chem. Phys.*, **1964**, *41*, 1763-1772
- [75] El-Sayed, M. A. : *Pure Appl. Chem.*, **1970**, *24*, 475-493
- [76] Thomson, C. : *Q. Rev. Chem. Soc.*, **1968**, *22*, 45-74

- [77] Grote, D. : *Matrix ESR- und IR- spektroskopische Charakterisierung fluorierter Dehydrophenylnitrene und TR-ESR-Untersuchung an Alkoxy-carbonylradikalen*, Dissertation to obtain the degree of Dr. rer. nat., Ruhr-Universität Bochum, Faculty of Chemistry and Biochemistry, **2007**
- [78] Dines, T. J. ; Chowdhry, B. Z. ; Withnall, R. : *J. Chem. Educ.*, **2007**, *84*, No. 8, 1364-1370
- [79] Koch, W. ; Holthausen, M. C. : *A Chemist's Guide to Density Functional Theory*, **2001**, Second Edition, *Wiley-VCH*
- [80] Born, M. ; Oppenheimer, R. : *Ann. d. Phys.*, **1927**, *Vierte Folge, Band 84, No. 20*, 457-484
- [81] Hartree, D.R. : *Rep. Prog. Phys.*, **1947**, *11*, 113-143
- [82] Hartree, D. R. : *Math. Proc. Camb. Philos. Soc.*, **1928**, *24(1)*, 111-132
- [83] Hartree, D. R. ; Hartree, W. : *Proc. Royal Soc. Lond. A.*, **1935**, *150(869)*, 9-33
- [84] Fock, V. A. : *Z. Phys.*, **1930**, *61(1)*, 126-148
- [85] Fock, V. A. : *Z. Phys.*, **1930**, *62(11)*, 795-805
- [86] Hohenberg, P. ; Kohn, W. : *Phys. Rev.*, **1964**, *Vol. 136, Number 3B*, 864-871
- [87] Kohn, W. ; Sham, L. J. : *Phys. Rev.*, **1965**, *Vol. 140, Number 4A*, 1133-1138
- [88] Becke, A. D. : *J. Chem. Phys.*, **1993**, *98*, 5648-5652
- [89] Lee, C. ; Yang, W. ; Parr, R. G. : *Phys. Rev. B*, **1988**, *Vol. 37, No. 2*, 785-789
- [90] Weigend, F. ; Ahlrichs, R. : *Phys. Chem. Chem. Phys.*, **2005**, *7*, 3297-3305
- [91] Weigend, F. : *Phys. Chem. Chem. Phys.*, **2006**, *8*, 1057-1065
- [92] Sinanoglu, O. : *J. Chem. Phys.*, **1962**, *36*, 706-717
- [93] Cambi, L. ; Szegö, L. : *Berichte der Deutschen Chemischen Gesellschaft (Abteilung B)*, **1931**, *No. 10*, 2591-2598
- [94] Khusniyarov, M. M. : *Chem. Eur. J.*, **2016**, *22*, 15178-15191
- [95] Herges, R. ; Sander, W. ; Lohmiller, T. : *Nat. Commun.*, **2018**, *9*, 1-12
- [96] Herges, R. et al. : *Science*, **2011**, *Vol. 331*, 445-448
- [97] Berson, J. A. et al. : *J. Am. Chem. Soc.*, **1997**, *119*, 1416-1427
- [98] Berson, J. A. : *Acc. Chem. Res.*, **1997**, *30*, 238-244
- [99] Berson, J. A. ; Scaiano, J. C. et al. : *J. Am. Chem. Soc.*, **1997**, *119*, 1406-1415
- [100] Abe, M. ; Zheng, X. et al. : *J. Am. Chem. Soc.*, **2018**, *140*, 10-13
- [101] Rajca, A. et al. : *Chem. Commun.*, **1999**, *13*, 1249-1250
- [102] Bally, T. ; McMahon, R. J. et al. : *J. Am. Chem. Soc.*, **1999**, *121*, 2863-2874
- [103] Sander, W. ; Sanchez-Garcia, E. ; Savitsky, A. et al. : *J. Am. Chem. Soc.*, **2016**, *138*, 1622-1629

- [104] Sander, W. ; Sanchez-Garcia, E. : *J. Am. Chem. Soc.*, **2017**, *139*, 12310-12316
- [105] Humphreys, W. R. ; Arnold, D. R. : *Can. J. Chem.*, **1979**, *Vol. 57*, 2652-2661
- [106] Humphreys, W. R. ; Arnold, D. R. : *J. Chem. Soc. Chem. Commun.*, **1978**, *4*, 181-182
- [107] Ware, W. R. ; Ono, Y. : *J. Phys. Chem.*, **1983**, *87*, 4426-4433
- [108] Hüttel, R. et al. : *Chemische Berichte*, **1960**, *93*, pp. 1425-1432
- [109] Sander, W. ; Sanchez-Garcia, E. et al. : *Angew. Chem. Int. Ed.*, **2015**, *54*, 2656-2660
- [110] Costa, P. ; Sander, W. : *J. Phys. Org. Chem.*, **2015**, *28*, 71-74
- [111] Iwamura, H. ; Koga, N. ; Matsuda, K. : *Pure & Appl. Chem.*, **1998**, *Vol. 70, No. 10*, 1953-1960
- [112] Moloney, M. G. et al. : *Langmuir*, **2016**, *32*, 7917-7928
- [113] Moloney, M. G. et al. : *Macromol. React. Eng.*, **2014**, *8*, 170-180
- [114] Schuster, G. B. et al. : *J. Am. Chem. Soc.*, **1983**, *105*, 6833-6845
- [115] Schuster, G. B. ; Zupancic, J. J. : *J. Am. Chem. Soc.*, **1981**, *103*, 944-946
- [116] Schuster, G. B. ; Zupancic, J. J. ; Grasse, P. B. : *J. Am. Chem. Soc.*, **1981**, *103*, 2423-2425
- [117] Schuster, G. B. et al. : *J. Am. Chem. Soc.*, **1982**, *104*, 6814-6816
- [118] Schuster, G. B. ; Zupancic, J. J. : *J. Am. Chem. Soc.*, **1980**, *102*, 5958-5960
- [119] Eisenthal, K. B. ; Turro, N. J. et al. : *J. Am. Chem. Soc.*, *102*, 6565-6566
- [120] Sheridan, R. S. ; Song, M.G : *J. Am. Chem. Soc.*, **2011**, *133*, 19688-19690
- [121] Humphreys, R. W. R. ; Arnold, D. R. : *Can. J. Chem.*, **1977**, *Vol. 55*, 2286-2291
- [122] Trosien, I. ; Mendez-Vega, E. ; Thomanek, T. ; Sander, W. : *Angew. Chem. Int. Ed.*, **2019**, *58*, 14855-14859
- [123] Schuster, G. B. et al. : *J. Am. Chem. Soc.*, **1985**, *107*, 4238-4243
- [124] Schuster, G. B. ; Li, Y. Z. : *J. Org. Chem.*, **1988**, *53*, 1273-1277
- [125] Turro, N. J. ; Moss, R. A. : *J. Am. Chem. Soc.*, **1980**, *102*, 7578-7579
- [126] Gutsche, C. D. ; Baer, T. A. : *J. Am. Chem. Soc.*, **1971**, *93:20*, 5180-5186
- [127] Tomioka, H. et al. : *J. Chem. Soc., Perkin Transactions 2: Physical Organic Chemistry (1972-1999)*, **1980**, *4*, 603-609
- [128] Moss, R. A. ; Joyce, M. A. : *J. Am. Chem. Soc.*, **1978**, *100:14*, 4475-4480
- [129] Fausto, R. ; Reva, I. et al. : *J. Am. Chem. Soc.*, **2015**, *137*, 14240-14243
- [130] Räsänen, M. ; Fausto, R. ; Pettersson, M. et al. : *J. Chem. Phys.*, **2002**, *117*, 9095-9098
- [131] Khriachtchev, L. ; Räsänen, M. ; Fausto, R. et al. : *Phys. Chem. Chem. Phys.*, **2005**, *7*, 743-749
- [132] Khriachtchev, L. ; Räsänen, M. ; Fausto, R. et al. : *J. Chem. Phys.*, **2010**, *133*, 144507

- [133] Khriachtchev, L. ; Marushkevich, K. ; Räsänen, M. : *J. Phys. Chem. A*, **2010**, *114*, 10584-10589
- [134] Schreiner, P. R. ; Gerbig, D. ; Eckhardt, A. K. : *J. Phys. Chem. A*, **2018**, *122*, 1488-1495
- [135] Khriachtchev, L. : *J. Mol. Struct.*, **2008**, *880*, 14-22
- [136] Khriachtchev, L. ; Marushkevich, K. ; Räsänen, M. : *J. Phys. Chem. A*, **2007**, *Vol. 111*, No. 11, 2040-2042
- [137] Khriachtchev, L. ; Räsänen, M. : *J. Am. Chem. Soc.*, **2006**, *128*, 12060-12061
- [138] Shi, Z. J. et al. : *Org. Lett.*, **2012**, *Vol. 14*, No. 18, pp. 4850-4853
- [139] Jones, N. : *Chem. Rev.*, **1943**, *32*, *1*, 1-46
- [140] Wasserman, E. ; Murray, R. W. ; Trozzolo, A. M. : *J. Am. Chem. Soc.*, **1962**, *84*, *24*, 4990-4991
- [141] Kubas, G. J. : *J. Organomet. Chem.*, **2014**, *751*, 33-49
- [142] Lewis, N. S. ; Nocera, D. G. : *PNAS*, **2006**, *Vol. 103*, No. 43, 15729-15735
- [143] Piers, W. E. et al. : *J. Am. Chem. Soc.*, **2013**, *135*, 11776-11779
- [144] Van der Vlugt, J. I. : *Chem. Soc. Rev.*, **2010**, *39*, 2302-2322
- [145] Klinkenberg, J. L. ; Hartwig, J. F. : *Angew. Chem. Int. Ed.*, **2011**, *50*, 86-95
- [146] Werner, A. : *Z. Anorg. Chem.*, **1893**, *3*, 267-330
- [147] MacMillen, D. F. ; Golden, D. M. : *Ann. Rev. Phys. Chem.*, **1982**, *33*, 493-532
- [148] Mayer, H. A. ; Kaska, W. C. et al. : *J. Organomet. Chem.*, **2003**, *682*, 149-154
- [149] Schoeller, W. W. ; Bertrand, G. et al. : *Science*, **2007**, *Vol. 316*, 439-441
- [150] Bielawski, C. W. et al. : *Chem. Commun.*, **2010**, *46*, 4288-4290
- [151] Bielawski, C. W. et al. : *J. Am. Chem. Soc.*, **2013**, *135*, 18798-18801
- [152] Band, I. B. M. et al. : *Chem. Commun. (London)*, **1966**, 544
- [153] Bethell, D. ; Hayes, J. ; Newall, A. R. : *J. Chem. Soc., Perkin Trans.*, **1974**, *2*, 1307-1312
- [154] Schuster, G. B. et al. : *Tetrahedron*, **1985**, *Vol. 41*, No. 8, 1471-1478
- [155] McMahan, R. J. : *Science*, **2003**, *299 (5608)*, 833-834
- [156] Eisenthal, K. B. ; Moss, R. A. ; Turro, N. J. : *Science*, **1984**, *Vol. 225*, No. 4669, 1439-1445
- [157] Sheridan, R. S. ; Moss, R. A. ; Krogh-Jespersen, K. et al. : *J. Am. Chem. Soc.*, **1989**, *111*, 6875-6877
- [158] Sheridan, R. S. et al. : *J. Am. Chem. Soc.*, **1986**, *108*, 1517-1520
- [159] Sheridan, R. S. ; Kesselmayr, M. A. : *J. Am. Chem. Soc.*, **1986**, *108*, 99-107
- [160] Sheridan R. S. ; Wang, J. : *Org. Lett.*, **2007**, *Vol. 9*, No. 16, 3177-3180

- [161] Dunkin, I. R. ; Baird, M. S. ; Poliakoff, M. : *J. Chem. Soc. Chem. Commun.*, **1974**, 21, 904-905
- [162] Sander, W. ; Müller, W. ; Sustmann R. : *Angew. Chem.*, **1988**, 100, No. 4, 577-579
- [163] Sander, W. et al. : *Chem. Eur. J.*, **2000**, 6, No. 24, 4567-4579
- [164] Sheridan, R. S. ; Ammann, J. R. ; Subramanian, R. : *J. Am. Chem. Soc.*, **1992**, 114, 7592-7594
- [165] Sander, W. ; Kötting, C. : *Chem. Eur. J.*, **1999**, 5, No. 1, 24-28
- [166] Bass, A. M. ; Braun, W. ; Pilling, M. : *J. Chem. Phys.*, **1970**, 52, 5131-5143
- [167] Murrells, T. P. et al. : *J. Chem. Soc. Faraday Trans.*, **1996**, 92(18), 3305-3313
- [168] Schaefer, H. F. ; Ignatyev, I. S. : *J. Am. Chem. Soc.*, **1997**, 119, 12306-12310
- [169] Schaefer, H. F. et al. : *J. Am. Chem. Soc.*, **1976**, 98:11, 3072-3074
- [170] Sheridan, R. S. ; Zuev, P. S. : *J. Am. Chem. Soc.*, **2001**, 123, 12434-12435
- [171] Henkel, S. ; Sander, W. : *Angew. Chem. Int. Ed.*, **2015**, 54, 4603-4607
- [172] Criegee, R. ; Wenner, G. : *Justus Liebigs Ann. Chem.*, **1949**, 564, 9-15
- [173] Bartlett, P. D. ; Traylor, T. G. : *J. Am. Chem. Soc.*, **1962**, 84, 17, 3408-3409
- [174] Murray, R. W. ; Higley, D. P. : *J. Am. Chem. Soc.*, **1973**, 95:23, 7886-7888
- [175] Chapman, O. L. : *Pure & Appl. Chem.*, **1979**, Vol. 51, 331-339
- [176] Chapman, O. L. ; Hess, T. C. : *J. Org. Chem.*, **1979**, Vol. 44, No. 6, 962-964
- [177] Dunkin, I. R. ; Bell, G. A. : *J. Chem. Soc. Chem. Commun.*, **1983**, 1213-1215
- [178] Chapman, O. L. ; Hess, T. C. : *J. Am. Chem. Soc.*, **1984**, 106, 1842-1843
- [179] Dunkin, I. R. ; Shields, C. J. : *J. Chem. Soc. Chem. Commun.*, **1986**, 154-156
- [180] Sander, W. W. : *J. Org. Chem.*, **1988**, 53, 121-126
- [181] Sander, W. : *Angew. Chem.*, **1985**, 97, No. 11, 964-965
- [182] Sander, W. W. : *J. Org. Chem.*, **1989**, 54, 333-339
- [183] Frisch, M. J. ; Trucks, G. W. ; Schlegel, H. B. ; Scuseria, G. E. ; Robb, M. A. ; Cheeseman, J. R. ; Scalmani, G. ; Barone, V. ; Mennucci, B. ; Petersson, G. A. ; Nakatsuji, H. ; Caricato, M. ; Li, X. ; Hratchian, H. P. ; Izmaylov, A. F. ; Bloino, J. ; Zheng, G. ; Sonnenberg, J. L. ; Hada, M. ; Ehara, M. ; Toyota, K. ; Fukuda, R. ; Hasegawa, J. ; Ishida, M. ; Nakajima, T. ; Honda, Y. ; Kitao, O. ; Nakai, H. ; Vreven, T. ; Montgomery Jr., J. A. ; Peralta, J. E. ; Ogliaro, F. ; Bearpark, M. ; Heyd, J. J. ; Brothers, E. ; Kudin, K. N. ; Staroverov, V. N. ; Kobayashi, R. ; Normand, J. ; Raghavachari, K. ; Rendell, A. ; Burant, J. C. ; Iyengar, S. S. ; Tomasi, J. ; Cossi, M. ; Rega, N. ; Millam, N. J. ; Klene, M. ; Knox, J. E. ; Cross, J. B. ; Bakken, V. ; Adamo, C. ; Jaramillo, J. ; Gomperts, R. ; Stratmann, R. E. ; Yazyev, O. ; Austin, A. J. ; Cammi, R. ; Pomelli, C. ; Ochterski, J. W. ; Martin, R. L. ; Morokuma, K. ; Zakrzewski, V. G. ; Voth, G. A. ; Salvador, P. ; Dannenberg, J. J. ; Dapprich, S. ; Daniels, A. D. ; Farkas, Ö. ; Foresman, J. B. ; Ortiz, J.

- V. ; Cioslowski, J. ; Fox, D. J. ; Revision B.01 ed., Gaussian, Inc., Wallingford CT, **2010**
- [184] Grimme, S. et al. : *J. Chem. Phys.*, **2010**, *132*, 154104
- [185] Stoll, S. ; Schweiger, A. : *J. Magn. Res.*, **2006**, *178*, 42-55
- [186] Zhang, L. ; Liu, L. et al. : *Bioorg. Med. Chem. Lett.*, **2015**, *25*, 5682-5686

9. Acknowledgements

I would like to thank Prof. Dr. Wolfram Sander for giving me the opportunity to work on the highly interesting topic of magnetically bistable carbenes and to get an insight on the different fields in physical organic chemistry. Furthermore, I am thankful for the good support as well as for the productive discussions and ideas that helped me to successfully progress my work in this research field. I would also like to thank my second supervisor Prof. Dr. Stefan Huber for the support.

In addition to that, I would like to thank every past and present colleague from the OC II group, namely Arun, Nadja, Geneviève, Joel, Pritam, Paolo, Soumya, Yetsedaw, Iris, Sujan, Akshay, Enrique, Stefan, Tim, Adam, Linda, Mohamed, Nesli, Mika, Adrián, Julien, Ankit, Melania, Alex, Christian, Corina, Tino, Nora, Karoline, Kevin, Luisa, Daniel and Michael. Thank you for this amazing and relaxed working atmosphere all the nice discussions about scientific as well as completely non-scientific topics.

I am grateful for the help and tips I received from all my colleagues, especially Stefan, Iris and Enrique, concerning problems in computational calculations, matrix isolation and evaluation of spectroscopic data. I also thank Stefan, Paolo, Yetsedaw, Mohamed and Dirk for all their assistance during the EPR experiments. You helped me a lot with learning about the set-up, the measurement technique and the analysis of the EPR spectra.

I would also like to thank the technical and administrative staff, namely Catharina, Klaus, Robin, Thorsten, Elric, Sabine, Jacinta and Dirk. Klaus and Robin helped me out numerous times, whenever I needed new glassware or tips and tricks in the synthesis lab (or whenever the rotary evaporator broke again). I am especially thankful to Thorsten and Catharina who always assisted me with solving mechanical or electronic problems of the matrix isolation setup.

Furthermore, I want to thank my former in-depth practical students Luisa and Kseniya for helping me out in the synthesis lab. The in-depth practicals might probably not have been the funniest synthesis experience (the column chromatography of my compounds is a nightmare), but still I hope that you learned one or two things that will help you in your future scientific carrier.

I thank Tim, Julien, Mika, Adrián and Enrique for proofreading my thesis and giving me great tips on how to prepare better scientific reports.

I would like to thank Mika, Ankit, Melania, Adrián, Enrique and Anjali for the awesome time in Dubrovnik during the ESOR conference. The interesting scientific talks as well as the exploration of the historic old town made this excursion into a trip that I will always remember.

I am also thankful for Steffen and Robin who always picked me up for the lunch break and helped me to clear my head from work by talking about funny and amusing stuff, like absurd stories of the previous weekend, political satire and how Steffen investigates methods how to make the VFL Bochum win its soccer matches.

Special thanks goes to all my friends and my family for all their support. I especially want to thank my parents and Niki and Anne, as well as my nephews, the “Turbochefchen”, Lukas and Jonas for always brightening up my day and encouraging and motivating me. You always provided little moments of relaxation in stressful times.

10. Appendix

10.1. IR Frequencies

Table 10.1: Spectroscopic data of diazo compound **17**.

mode	ν/cm^{-1} (calc.) ^a	I_{rel} (calc.) ^a	ν/cm^{-1} (Ar) ^b	I_{rel} (Ar) ^b	ν/cm^{-1} (Xe) ^c	I_{rel} (Xe) ^c	ν/cm^{-1} (N ₂) ^d	I_{rel} (N ₂) ^d	assignment
21	498.9	1.7	478.8	1.4					skel. vibr.
22	505.2	1.5	482.5	1.2					C=N=N def.
25	613.9	2.6	601.9	2.7	601.2	3.4	602.1	2.6	C=N=N def.
29	708.7	4.5	694.0	4.3	695.3	6.7	697.2	3.8	C=C def. (oop)
31	767.8	5.0	751.1	6.3	752.8	5.8	756.8	6.3	C-H def. (oop)
34	835.4	5.8	814.4	6.5	812.5	4.6	819.8	6.3	C-H def. (oop)
41	969.8	1.8	953.7	1.6	953.6	1.4	949.0	2.5	methyl C-H def. (ip)
46	1080.5	3.0	1065.2	2.4	1065.6	2.0	1063.9	2.6	methyl C-H def. (ip)
49	1144.2	5.4	1123.8	4.4	1122.3	5.7	1128.3	4.8	methyl C-H def. (oop)
53	1197.3	2.8	1174.1	2.8	1174.3	2.9	1175.2	2.7	methyl C-H def. (ip)
55	1239.7	3.4	1201.3	4.6	1206.1	3.8	1201.5	3.3	C-H def. (ip)
56	1264.7	6.5	1240.9	9.4	1242.1	5.5	1230.0	7.0	methyl C-N str.
57	1304.4	2.2	1271.8	2.2	1268.0	1.0	1273.3	1.3	sym. C-C-C str.
58	1314.3	2.8	1285.2	3.0	1284.00	0.8	1284.9	1.5	asym. C-C-C str.
60	1350.5	2.1	1318.2	3.3	1317.0	2.0	1318.6	1.8	sym. C-C-C str.
62	1377.4	12.6	1343.6	7.1	1343.5	1.7	1343.8	4.7	C-H def. (ip)
63	1381.3	18.7	1361.8	17.5	1364.5	11.9	1358.9	16.0	ring C-N str.
68	1489.9	1.9	1450.5	6.8	1446.6	5.9	1450.6	6.0	methyl C-H def. (ip)
69	1494.4	2.5	1450.5		1452.9	1.5	1456.7	1.1	methyl C-H def. (oop)
71	1530.0	10.0	1490.9	7.5	1486.4	7.7	1490.7	7.8	methyl C-H def. (ip)
72	1533.1	5.0	1496.8	5.4	1496.1	6.6	1497.5	5.9	C-H def. (ip)
73	1558.7	36.5	1524.7	40.4	1520.9	41.6	1524.9	41.7	C-H def. (ip)
76	1640.7	8.0	1599.7	7.6	1599.5	5.8	1597.2	7.8	C=C str.
77	1657.1	15.2	1615.5	13.1	1613.8	12.6	1615.3	16.2	C=C str.
78	2141.7	100.0	2042.1	100.0	2036.3	100.0	2043.7	100.0	N=N str.

^aThe theoretical values were calculated at the B3LYP/def2-TZVP level of theory.

^bThe experimental values were obtained in an argon matrix at 3 K.

^cThe experimental values were obtained in a xenon matrix at 3 K.

^dThe experimental values were obtained in a nitrogen matrix at 9 K.

Table 10.2: Spectroscopic data of singlet carbene S-14.

mode	ν/cm^{-1} (calc.) ^a	I_{rel} (calc.) ^a	ν/cm^{-1} (Ar) ^b	I_{rel} (Ar) ^b	ν/cm^{-1} (Xe) ^c	I_{rel} (Xe) ^c	ν/cm^{-1} (N ₂) ^d	I_{rel} (N ₂) ^d	assignment
18	502.6	5.6	490.3	2.5			495.4	5.0	C=C def. (oop)
19	534.4	3.2	519.3	1.4			520.9	1.6	C=C def. (oop)
24	703.4	4.1	690.4	2.9			694.6	3.5	C-N def. (ip)
25	712.9	3.9	702.5	0.5			703.1	0.8	C=C def. (oop)
26	761.0	3.9	736.9	2.2			740.1	1.4	C=C def. (oop)
27	769.6	3.6	754.3	3.4	753.5	4.6	755.9	2.6	C=C def. (oop)
28	806.2	1.8	792.0	2.2	792.2	2.4	792.8	3.0	C=C def. (ip)
29	808.9	1.7	795.4	0.5	806.1	5.4	792.8		C=C def. (oop)
30	844.4	8.8	823.4	6.9	821.5	10.6	829.6	8.1	C-H def. (oop)
33	916.1	1.5	899.5	0.9			872.8	1.1	C-H def. (oop)
35	962.4	3.3	945.8	3.8	948.7	4.5	944.2	2.3	C-H def. (oop)
42	1079.8	3.5	1065.2	2.9	1068.1	1.8	1066.6	0.4	C-H def. (oop)
46	1154.6	4.6	1120.8	4.3	1122.4	12.1	1122.7	3.6	C-H def. (oop)
47	1182.6	21.8	1154.7	22.3	1151.5	42.6	1156.1	30.1	methyl C-H def. (ip)
48	1189.5	3.6	1154.7		1151.5		1156.1		methyl C-H def. (ip)
50	1207.6	12.0	1168.0	14.0	1167.1	15.5	1170.7	15.9	C-H def. (ip)
51	1242.4	5.3	1206.6	2.2	1206.9	3.11	1207.6	1.1	C-H def. (ip)
52	1268.3	2.6	1243.7	1.9	1242.8	5.0	1240.4	2.1	C-H def. (ip)
53	1295.1	1.9	1265.4	1.4	1261.1	5.8			C-H def. (ip)
54	1319.1	1.5	1288.7	0.8			1287.7	2.9	C-H def. (ip)
56	1367.0	1.6	1328.2	3.9	1330.9	3.7			methyl C-N str.
57	1390.3	34.5	1348.2	33.5	1353.6	40.3	1354.9	39.9	C-H def. (ip)
58	1400.0	70.7	1374.8	45.2	1377.2	54.1	1379.6	56.2	C-H def. (ip)
60	1463.4	2.2	1430.6	1.6	1429.5	2.8	1431.4	1.3	C-H def. (ip)
63	1490.5	2.5	1449.5	2.0	1447.3	1.8	1449.6	0.7	asym. C-C-C str.
64	1496.6	2.2	1454.3	1.4	1451.0	1.3	1458.0	0.6	ring C-N str.
67	1527.7	8.8	1489.7	4.7	1497.3	2.6	1487.7	4.4	C-H def. (ip)
69	1555.4	15.2	1529.0	7.8	1530.5	7.6	1536.3	8.9	methyl C-H def. (ip)
70	1584.7	1.4	1551.6	0.7			1550.5	1.2	methyl C-H def. (oop)
72	1635.8	100.0	1592.3	100.0	1588.5	100.0	1590.6	100.0	methyl C-H def. (ip)

^aThe theoretical values were calculated at the B3LYP/def2-TZVP level of theory.

^bThe experimental values were obtained in an argon matrix at 3 K.

^cThe experimental values were obtained in a xenon matrix at 3 K.

^dThe experimental values were obtained in a nitrogen matrix at 9 K.

Table 10.3: Spectroscopic data of triplet carbene T-14.

mode	ν/cm^{-1} (calc.) ^a	I_{rel} (calc.) ^a	ν/cm^{-1} (Ar) ^b	I_{rel} (Ar) ^b	ν/cm^{-1} (Xe) ^c	I_{rel} (Xe) ^c	ν/cm^{-1} (N ₂) ^d	I_{rel} (N ₂) ^d	assignment
19	526.1	11.9	511.3	6.6					C=C def. (oop)
24	688.7	9.8	673.5	10.1	674.5	51.7			C=C def. (oop)
27	757.4	11.4	742.8	14.3	740.2	30.3	711.6	27.9	C=C def. (oop)
30	828.0	14.4	814.7	18.7	803.8	7.4			C=C def. (oop)
37	963.1	10.4	951.9	6.1	952.7	58.8	949.7	5.3	methyl C-H def. (ip)
42	1080.4	7.1	1064.8	11.9	1064.6	100.0	1062.3	9.8	methyl C-H def. (ip)
45	1143.6	19.1	1117.4	15.2	1115.5	30.6	1084.4	26.7	methyl C-H def. (oop)
47	1171.3	13.4	1128.0	11.9					sym. C-C-C str.
52	1257.6	14.4	1234.2	10.6	1232.4	16.3	1270.9	53.1	methyl C-N str.
57	1383.2	94.4	1363.8	100.0	1365.3	44.3	1371.9	36.2	ring C-N str.
59	1458.2	11.0	1423.9	5.0	1416.1	21.4			asym. C-C-C str.
60	1461.8	5.5	1423.9		1416.1				C-H def. (ip)
63	1488.9	7.4	1445.8	3.7			1444.7	2.3	methyl C-H def. (ip)
64	1493.6	4.7	1452.0	16.6	1448.9	7.3	1453.7	0.1	methyl C-H def. (oop)
68	1534.6	57.8	1502.1	42.3	1501.1	39.0	1521.9	100.0	methyl C-H def. (ip)
69	1545.2	4.8			1521.4	97.1			C=C str.
71	1604.1	5.9	1565.3	7.1			1545.9	9.6	C=C str.
72	1630.8	100.0					1610.9	92.8	C=C str.

^aThe theoretical values were calculated at the B3LYP/def2-TZVP level of theory.

^bThe experimental values were obtained in an argon matrix at 3 K.

^cThe experimental values were obtained in a xenon matrix at 3 K.

^dThe experimental values were obtained in a nitrogen matrix at 9 K.

Table 10.4: Spectroscopic data of singlet water complex S-21.

mode	ν/cm^{-1} (calc.) ^a	I_{rel} (calc.) ^a	ν/cm^{-1} (Ar) ^b	I_{rel} (Ar) ^b	assignment
29	705.8	2.4	683.1	39.8	C=C def. (oop)
30	723.4	1.9	695.5	67.3	C=C def. (ip)
34	823.4	1.5	788.9	1.3	O-H--C def.
35	849.7	4.0	812.8	55.8	C-H def. (oop)
36	852.8	0.8	812.8		C-H def. (oop)
37	867.6	4.9	830.7	20.2	O-H def. (ip)
48	1079.1	1.8	1064.0	2.1	methyl C-H def. (ip)
53	1189.3	2.6	1164.1	22.5	C-H def. (ip)
54	1193.3	6.5	1164.1		C-H def. (ip)
56	1214.5	10.7	1174.3	36.5	C-H def. (ip)
57	1251.1	6.9	1212.5	22.3	C-H def. (ip)
58	1267.9	1.1	1233.5	4.6	methyl C-N str.
63	1399.5	31.5	1364.3	30.5	asym. C-C-C str.
64	1405.7	31.8	1382.7	100.0	ring C-N str.
66	1466.1	1.2	1434.7	14.0	C-H def. (ip)
69	1490.6	1.0	1477.4	1.4	methyl C-H def. (ip)
70	1497.4	1.2	1486.7	9.4	methyl C-H def. (oop)
73	1529.0	5.9	1518.0	45.5	methyl C-H def. (ip)
75	1561.9	7.1	1541.1	45.9	C-H def. (ip)
78	1639.1	54.6	1598.1	37.9	C=C def.
79	1657.8	2.8	1608.6	52.6	O-H def. (oop)

^aThe theoretical values were calculated at the B3LYP/def2-TZVP level of theory.

^bThe experimental values were obtained in an argon matrix at 3 K.

Table 10.5: Spectroscopic data of alcohol **22**.

mode	ν/cm^{-1} (calc.) ^a	I_{rel} (calc.) ^a	ν/cm^{-1} (Ar) ^b	I_{rel} (Ar) ^b	assignment
23	575.4	14.4	566.7	9.8	skel. vibr.
25	643.9	5.5	638.2	5.5	C=C def. (ip)
27	709.9	22.6	696.6	15.2	C=C def. (oop)
28	728.9	5.4	715.2	15.5	C=C def. (ip)
29	748.4	11.1	736.8	2.7	C=C def. (oop)
30	782.7	7.4	768.2	2.0	C-H def. (oop)
31	811.5	7.4	800.5	15.7	C-H def. (oop)
32	817.7	18.3	811.0	21.0	C-H def. (oop)
40	967.2	8.5	949.8	10.1	C-H def. (oop)
44	1046.0	26.6	1026.3	20.5	C-O str.
45	1055.3	12.0	1034.4	16.2	C-H def. (ip)
46	1079.5	10.9	1064.8	8.2	methyl C-H def. (ip)
49	1147.5	26.9	1126.9	20.2	methyl C-H def. (oop)
51	1184.7	35.7	1168.4	36.5	O-H def.
53	1198.8	6.0	1179.6	39.5	O-H def.
56	1234.6	5.7	1204.5	11.2	H-CO-H def.
57	1245.6	10.0	1236.5	7.9	C-H def. (ip)
58	1267.6	21.2	1246.2	7.3	methyl C-N-C str.
59	1302.9	8.2	1259.4	2.4	HOC-H def.
61	1354.8	5.1	1318.2	5.1	C-H def. (ip)
62	1363.3	8.7	1345.4	38.9	C-H def. (ip)
63	1371.9	100.0	1361.7	64.1	ring C-N str.
65	1400.9	14.4	1379.8	5.1	H-CO-H def.
69	1488.5	7.0	1451.1	20.2	methyl C-H def. (ip)
71	1494.2	8.8	1456.1	6.2	methyl C-H def. (oop)
73	1529.1	13.6	1489.6	21.2	C-H def. (ip)
74	1529.3	20.5	1497.4	7.6	methyl C-H def. (ip)
75	1560.5	92.3	1527.2	100.0	C-H def. (ip)
79	1661.6	56.5	1620.4	86.9	C=C def.

^aThe theoretical values were calculated at the B3LYP/def2-TZVP level of theory.

^bThe experimental values were obtained in an argon matrix at 3 K.

Table 10.6: Spectroscopic data of diazo compound **26**.

mode	ν/cm^{-1} (calc.) ^a	I_{rel} (calc.) ^a	ν/cm^{-1} (Ar) ^b	I_{rel} (Ar) ^b	assignment
46	1221.8	1.8	1188.3	9.3	C-H def. (ip)
47	1225.2	1.9	1188.3		C-H def. (ip)
48	1302.2	4.8	1288.7	5.0	sym. C-C-C str.
49	1307.0	6.2	1288.7		asym. C-C-C str.
50	1312.1	9.9	1288.7		C-N str.
52	1349.8	1.9	1329.6	4.1	C=N str.
57	1532.9	6.5	1496.4	1.1	C-H def. (ip)
58	1552.7	22.5	1518.5	16.1	C-H def. (ip)
61	1640.7	8.0	1608.7	23.2	C=C str.
63	1668.2	19.8	1630.9	1.2	N-H def. (ip)
64	2143.1	100.0	2043.5	100.0	N=N str.

^aThe theoretical values were calculated at the B3LYP/def2-TZVP level of theory.

^bThe experimental values were obtained in an argon matrix at 3 K.

Table 10.7: Spectroscopic data of singlet carbene S-16.

mode	ν/cm^{-1} (calc.) ^a	I_{rel} (calc.) ^a	ν/cm^{-1} (Ar) ^b	I_{rel} (Ar) ^b	assignment
21	748.1	3.3	729.2	9.4	C-H def. (oop)
22	757.1	7.9	735.8	17.0	C=C def. (oop)
23	791.9	8.3	772.7	14.4	C-H def. (oop)
26	848.9	2.3	833.3	38.4	C-H def. (oop)
27	853.5	11.5	833.3		C-H def. (oop)
40	1183.0	26.8	1149.1	25.0	sym. C-C str.
41	1190.0	4.5	1153.8	9.6	C-H def. (ip)
42	1204.7	14.3	1167.5	13.0	C-H def. (ip)
45	1311.6	3.2	1292.4	3.4	C-H def. (ip)
46	1347.8	28.4	1319.5	19.7	C-N str.
47	1354.3	3.1	1325.4	3.9	C-H def. (ip)
49	1386.1	70.4	1340.8	40.8	asym. C-C-C str.
57	1636.1	100.0	1590.5	100.0	C=C str.
58	1665.4	74.4	1619.1	68.6	N-H def. (ip)

^aThe theoretical values were calculated at the B3LYP/def2-TZVP level of theory.^bThe experimental values were obtained in an argon matrix at 3 K.**Table 10.8:** Spectroscopic data of diazo compound 32.

mode	uu: ν/cm^{-1} (calc.) ^a	uu: I_{rel} (calc.) ^a	ud: ν/cm^{-1} (calc.) ^a	ud: I_{rel} (calc.) ^a	dd: ν/cm^{-1} (calc.) ^a	dd: I_{rel} (calc.) ^a	ν/cm^{-1} (Ar) ^b	I_{rel} (Ar) ^b	ν/cm^{-1} (Xe) ^c	I_{rel} (Xe) ^c	assignment
25	603.8	1.2	604.1	1.1	604.4	1.1	586.9	0.9	586.0	0.7	C=C def. (oop)
27	643.5	2.8	638.9	1.0			627.4	0.5	626.4	0.6	C=C def. (ip)
29			682.0	1.3			667.8	0.4	667.2	0.6	C=C def. (ip)
29					685.8	1.7	669.3	0.7	669.0	0.9	C=C def. (ip)
33	799.4	0.9					789.9	0.5	787.7	0.3	C=C def. (ip)
33			802.8	2.0			793.2	0.3	789.5	0.3	C=C def. (ip)
33					807.4	3.4	794.9	0.3	792.6	1.2	C=C def. (ip)
34			810.7	2.1			796.9	0.8	795.1	0.4	C-H def. (oop)
35	812.0	4.8					799.7	0.6	797.9	0.1	C-H def. (oop)
35			827.4	2.2	826.5	3.6	813.4	3.1	810.9	2.7	C-H def. (oop)
36					862.1	4.0	837.2	1.4	835.7	2.0	C-H def. (oop)
36			870.9	2.8			843.4	0.8	840.8	0.9	C-H def. (oop)
36/37	888.7	3.4	889.8	0.8			863.1	1.0	860.8	0.7	C-H def. (oop)
39			932.5	0.9			915.4	0.3	915.9	0.5	C-H def. (ip)
42	1043.4	1.5					1034.0	0.9	1033.3	2.9	C-H def. (ip)
43			1053.3	2.0			1036.8	0.9	1035.9	0.2	C-H def. (ip)
43					1053.8	4.0	1039.3	0.3	1039.7	0.3	C-H def. (ip)
44	1067.9	13.1	1065.2	6.1			1048.3	5.3	1046.7	4.3	C-O str.
45			1101.0	1.2	1095.2	3.1	1075.7	2.2	1072.1	1.7	C-H def. (ip)
47					1173.5	1.2			1138.0	1.0	C-H def. (ip)
50	1190.1	6.8	1191.2	13.7	1192.3	16.8	1166.3	18.5	1164.4	17.9	C-H def. (ip)
51	1206.2	6.1	1206.0	2.4			1181.9	2.7	1180.9	1.9	OC-H def. (ip)
52	1227.3	11.1	1225.4	11.6	1224.5	9.7	1200.9	9.9	1199.3	9.9	OC-H def. (ip)
53					1232.3	13.6	1209.1	4.4	1208.3	8.3	C-H def. (ip)
53	1235.0	10.2	1234.8	12.7			1211.3	8.1	1211.1	3.0	C-H def. (ip)
54			1254.8	3.7			1233.9	0.3	1231.7	0.5	C-H def. (ip)
55	1264.7	20.1					1238.0	0.5	1235.5	1.3	C-H def. (ip)
54					1271.8	6.0	1241.5	0.6	1241.6	1.5	C-H def. (ip)
55			1281.9	13.7			1256.3	3.7	1255.0	3.3	C-H def. (ip)
55					1288.7	10.0	1265.8	1.7	1264.3	3.9	C-H def. (ip)
56			1314.5	4.4			1284.2	1.7	1284.0	1.1	C-H def. (ip)
56	1317.4	13.1					1287.5	2.3	1286.7	0.6	C-H def. (ip)
57	1321.8	6.7					1292.3	1.7	1289.6	0.7	C-H def. (ip)
57			1326.9	7.6	1327.6	6.4	1301.4	4.1	1299.6	3.3	C-H def. (ip)
58			1361.0	1.7	1361.4	0.9	1329.5	1.3	1330.2	3.7	C-H def. (ip)
59					1363.4	3.2	1332.1	1.4	1335.5	0.3	C-H def. (ip)
59			1374.1	4.3			1350.1	0.5	1349.4	0.9	C-H def. (ip)

59	1375.6	7.6					1352.6	0.7	1351.4	0.6	C-H def. (ip)
61			1458.7	1.9			1428.1	1.6	1425.4	1.7	C-H def. (ip)
62					1464.1	7.3	1431.0	1.2	1428.1	1.8	OC-H def. (ip)
62	1468.6	12.0	1469.0	7.4			1434.7	5.2	1432.4	2.1	OC-H def. (ip)
63	1478.3	2.2	1477.2	3.2	1477.0	3.1	1441.4	2.6	1437.6	1.7	OC-H def. (ip)
64	1489.8	4.9	1492.1	11.6			1458.7	6.8	1455.8	10.1	OC-H def. (ip)
64					1494.9	18.2	1464.6	12.8	1464.3	16.1	OC-H def. (ip)
66	1496.5	1.3			1496.0	1.3	1464.6		1464.3		OC-H def. (oop)
67	1500.1	1.8	1499.4	3.2	1500.0	3.7	1467.7	6.2	1464.3		OC-H def. (ip)
68	1506.2	7.9	1507.8	1.7	1507.3	2.1	1475.3	1.7	1471.8	1.5	OC-H def. (oop)
69			1509.7	3.0	1510.7	1.5	1480.3	0.7	1476.7	0.9	OC-H def. (oop)
70	1525.6	13.5					1495.7	3.1	1496.2	13.4	C-H def. (ip)
70			1526.6	12.6			1497.3	2.0	1496.2		C-H def. (ip)
70					1526.6	10.4	1498.9	7.9	1496.2		C-H def. (ip)
71	1608.6	1.2	1609.5	0.9	1607.6	4.6	1575.6	4.2	1571.9	2.3	C=C str.
72	1612.2	8.8	1610.3	6.4			1575.6		1575.9	1.1	C=C str.
73					1645.6	8.6	1612.4	3.8	1607.9	2.9	C=C str.
73			1648.2	8.3			1615.1	2.9	1611.8	3.4	C=C str.
74					1650.0	6.9	1617.3	1.7	1616.7	1.9	C=C str.
73	1656.3	9.0					1622.8	1.6	1623.6	2.7	C=C str.
74			1657.4	5.7			1623.8	1.0	1623.6		C=C str.
74	1659.2	3.1					1625.9	2.5	1623.6		C=C str.
75	2160.6	100.0	2162.7	100.0	2165.2	100.0	2058.3	100.0	2056.5	100.0	N=N str.

^aThe theoretical values were calculated at the B3LYP/def2-TZVP level of theory.

^bThe experimental values were obtained in an argon matrix at 3 K.

^cThe experimental values were obtained in a xenon matrix at 3 K.

Table 10.9: Spectroscopic data of singlet carbene **30**.

mode	uu: v/cm ⁻¹ (calc.) ^a	uu: I _{rel} (calc.) ^a	ud: v/cm ⁻¹ (calc.) ^a	ud: I _{rel} (calc.) ^a	dd: v/cm ⁻¹ (calc.) ^a	dd: I _{rel} (calc.) ^a	v/cm ⁻¹ (Ar) ^b	I _{rel} (Ar) ^b	v/cm ⁻¹ (Xe) ^c	I _{rel} (Xe) ^c	assignment
19	501.0	5.6					488.7	4.5	488.3	1.1	C=C def. (ip)
19			529.6	12.0			519.9	5.5	520.0	9.1	C=C def. (ip)
20	582.0	7.1					566.7	5.1	565.1	2.5	C=C def. (ip)
22	623.4	2.7					609.3	1.7	609.6	0.8	C=C def. (ip)
23	655.2	3.1					640.3	1.1	644.6	2.4	C=C def. (ip)
29	825.7	10.9	826.7	6.7			808.3	16.0	808.3	10.0	C-H def. (oop)
29					843.2	7.6	824.6	2.7	822.9	6.7	C-H def. (oop)
31			847.0	3.7			827.0	6.4	822.9		C-H def. (oop)
32	875.0	3.6	875.3	4.0	875.3	17.0	847.7	9.1	847.0	8.5	C=C def. (oop)
33					875.4	4.7	847.7		847.0		C=C def. (oop)
33			882.2	11.2			855.8	20.3	853.8	19.1	C-H def. (oop)
33	896.6	9.4					870.3	6.2	868.7	3.0	C-H def. (oop)
38	1035.7	4.0	1037.8	3.7	1039.5	4.2	1011.6	1.8	1015.0	7.8	C-H def. (ip)
39			1047.9	4.6	1049.2	15.1	1035.4	20.8	1028.3	12.3	C-H def. (ip)
40	1054.4	28.5	1053.1	24.2	1051.9	7.6	1039.2	42.0	1035.4	54.5	C-O str.
41					1106.7	85.9	1081.3	25.7	1080.3	45.0	C-H def. (ip)
41			1110.4	71.7			1083.6	63.9	1083.6	63.9	C-H def. (ip)
42					1113.1	20.6	1086.8	12.5	1090.9	34.5	C-H def. (ip)
41	1118.1	84.8					1093.8	81.0	1098.0	22.7	C-H def. (ip)
42			1124.6	27.9			1104.6	4.1	1102.8	4.4	C-H def. (ip)
42	1131.8	6.1					1109.7	1.8	1107.8	1.1	C-H def. (ip)
45	1181.6	1.9	1181.3	6.5	1181.9	9.8	1161.9	35.0	1157.5	17.3	C-H def. (ip)
46			1196.4	37.9	1193.8	17.7	1174.0	100.0	1170.4	27.5	OC-H def. (ip)
46	1199.1	50.5					1177.7	69.1	1174.0	34.9	OC-H def. (ip)
47	1207.0	8.1	1204.3	6.1	1203.0	5.1	1187.8	55.5	1186.0	15.7	sym. C-C-C str.
48	1212.0	8.1	1214.4	3.3	1209.1	18.4	1187.8		1186.0		C-H def. (ip)
49			1218.6	19.1			1194.0	10.1	1195.6	11.6	OC-H def. (ip)
49					1219.5	12.9	1197.2	29.1	1195.6		OC-H def. (ip)
49	1224.7	3.6							1206.3	7.4	C-H def. (ip)
50	1245.2	8.7					1217.2	5.4	1218.5	21.1	C-H def. (ip)
50			1248.7	19.2			1219.4	13.1	1218.5		C-H def. (ip)
51	1256.1	64.2					1226.6	41.3	1226.5	99.3	C-H def. (ip)

10. Appendix

50					1258.9	100.0	1230.7	56.7	1234.3	96.8	C-H def. (ip)
51			1265.2	100.0	1262.8	34.6	1234.9	91.2	1238.0	20.6	C-H def. (ip)
52	1299.2	15.3	1299.1	13.1	1298.0	4.4	1273.1	35.4	1271.0	33.0	C-H def. (ip)
53			1309.4	24.9			1284.8	30.0	1281.8	13.1	C-H def. (ip)
53	1317.0	10.4			1315.0	4.0	1290.3	82.2	1287.4	12.9	C-H def. (ip)
54	1317.6	81.2					1290.3		1289.5	21.6	C-H def. (ip)
54					1326.3	40.5	1298.6	22.5	1295.4	23.0	C-H def. (ip)
54			1326.5	26.0			1304.6	19.4	1301.4	23.4	C-H def. (ip)
55					1401.0	6.8	1374.9	2.1	1370.3	4.3	C-H def. (ip)
55			1405.6	10.5			1376.7	6.4	1377.6	7.8	C-H def. (ip)
55	1409.0	8.1					1378.8	8.5	1382.3	3.0	C-H def. (ip)
57	1456.9	4.9	1459.3	14.3	1454.0	17.6	1427.1	24.2	1426.1	11.9	C-H def. (ip)
58	1471.9	15.2	1471.3	13.9	1472.1	14.6	1436.3	20.4	1432.6	16.6	OC-H def. (ip)
59	1484.2	3.7					1465.5	26.6	1455.4	16.2	OC-H def. (ip)
61	1497.3	3.4			1498.9	4.1	1470.9	10.6	1463.2	36.0	OC-H def. (oop)
62	1502.3	33.1					1476.7	37.3	1472.1	9.4	OC-H def. (ip)
63	1505.1	7.2	1504.5	21.5	1504.5	6.8	1476.7		1476.2	45.9	OC-H def. (ip)
64	1508.1	2.9	1508.0	15.4	1507.3	21.3	1480.4	14.7	1485.3	47.4	OC-H def. (ip)
65	1519.4	22.7	1521.2	30.0			1485.8	39.5	1485.3		C-H def. (ip)
65					1523.0	23.6	1488.5	16.7	1485.3		C-H def. (ip)
66			1595.9	11.7	1594.8	25.9	1570.7	17.0	1569.6	20.9	C=C str.
67	1619.5	2.8							1582.7	11.3	C=C str.
68					1631.7	82.2	1592.9	66.6	1591.7	100.0	C=C str.
68			1634.1	90.7			1594.6	23.5	1591.7		C=C str.
69					1640.5	53.2	1596.9	35.2	1598.1	26.4	C=C str.
68	1641.6	100.0					1600.6	88.3	1603.6	35.1	C=C str.
69			1650.0	41.9			1610.9	13.8	1611.9	11.9	C=C str.
69	1653.4	20.9					1612.3	18.4	1616.5	9.2	C=C str.

^aThe theoretical values were calculated at the B3LYP/def2-TZVP level of theory.

^bThe experimental values were obtained in an argon matrix at 3 K.

^cThe experimental values were obtained in a xenon matrix at 3 K.

Table 10.10: Spectroscopic data of singlet water complex S-33.

mode	uu: v/cm ⁻¹ (calc.) ^a	uu: I _{rel} (calc.) ^a	ud: v/cm ⁻¹ (calc.) ^a	ud: I _{rel} (calc.) ^a	dd: v/cm ⁻¹ (calc.) ^a	dd: I _{rel} (calc.) ^a	v/cm ⁻¹ (Ar) ^b	I _{rel} (Ar) ^b	assignment
24	507.0	3.9					490.6	8.4	C=C def. (ip)
24			532.0	4.5			524.8	3.3	C=C def. (ip)
27	626.3	1.4					612.3	6.9	C=C def. (ip)
28	655.1	1.8					639.5	2.0	C=C def. (ip)
30	733.6	0.9					719.0	2.6	C=C def. (ip)
34			832.2	2.7	835.5	4.4	817.4	24.0	C-H def. (oop)
36	840.2	1.5	842.3	2.6			817.4		C-H def. (oop)
38	893.4	2.2	891.4	2.4	890.9	1.2	873.7	4.2	O-H def. (ip)
40					891.9	1.3	873.7		C-H def. (oop)
45			1046.6	1.6	1048.6	5.3	1032.5	3.6	C-H def. (ip)
46	1052.1	12.9	1050.8	8.1	1050.4	2.3	1032.5		methyl C-O str.
47			1114.7	22.3	1111.9	25.9	1089.2	0.5	C-H def. (ip)
48					1117.6	11.1	1089.2		C-H def. (ip)
47	1125.3	39.1					1095.7	2.6	C-H def. (ip)
48			1131.7	15.5			1102.6	45.6	C-H def. (ip)
51	1185.1	1.1	1185.5	1.3	1188.5	3.3	1165.2	7.5	methyl C-H def. (ip)
52	1201.7	18.0	1200.6	8.9	1197.3	2.5	1178.7	8.7	methyl C-H def. (ip)
53			1211.6	7.6			1183.4	2.9	methyl C-H def. (ip)
53	1219.7	7.1			1217.6	11.6	1191.4	5.7	C-H def. (ip)
54	1222.8	8.0	1223.6	4.7			1203.1	24.6	C-H def. (ip)
55	1238.7	7.4	1236.9	6.8	1239.3	5.7	1214.0	32.9	C-H def. (ip)
56	1248.6	2.5	1253.9	5.8			1223.5	6.0	C-H def. (ip)
57	1260.0	29.9			1259.8	33.7	1230.7	4.1	C-H def. (ip)
57			1266.4	37.5	1265.6	11.5	1232.6	6.8	C-H def. (ip)
58			1301.6	7.7			1271.5	100.0	C-H def. (ip)
58	1305.0	18.4			1303.5	1.2	1279.9	10.8	C-H def. (ip)
59	1319.4	18.7	1318.5	4.2	1321.7	2.4	1295.7	11.2	C-H def. (ip)
60	1325.1	12.2					1301.9	2.9	C-H def. (ip)
60			1330.0	9.3	1332.1	11.3	1308.9	13.1	C-H def. (ip)
61					1404.3	1.8	1375.1	4.0	C-H def. (ip)
61	1412.0	3.6	1408.9	3.6			1386.2	3.5	C-H def. (ip)
63					1455.2	5.4	1426.7	8.0	C-H def. (ip)
63	1459.2	3.5	1460.0	5.3			1433.5	13.7	C-H def. (ip)
64	1472.0	7.0	1471.4	5.0	1472.3	4.9	1442.0	19.8	methyl C-H def. (ip)
70	1508.2	2.3	1508.3	6.6	1507.9	7.0	1469.8	17.8	methyl C-H def. (ip)
71	1522.6	12.6	1524.4	11.7	1527.4	7.5	1490.6	73.0	C-H def. (ip)
72					1592.8	9.2	1566.0	11.8	C=C str.
74			1635.0	32.4	1632.9	25.9	1598.5	58.7	C=C str.
74	1642.8	46.0			1642.6	17.5	1609.3	8.5	C=C str.
75	1655.8	9.8	1652.2	14.0			1615.6	8.0	C=C str.

^aThe theoretical values were calculated at the B3LYP/def2-TZVP level of theory.^bThe experimental values were obtained in an argon matrix at 3 K.

Table 10.11: Spectroscopic data of alcohol **34**.

mode	uu: v/cm ⁻¹ (calc.) ^a	uu: I _{rel} (calc.) ^a	ud: v/cm ⁻¹ (calc.) ^a	ud: I _{rel} (calc.) ^a	dd: v/cm ⁻¹ (calc.) ^a	dd: I _{rel} (calc.) ^a	v/cm ⁻¹ (Ar) ^b	I _{rel} (Ar) ^b	assignment
19					478.5	5.2	460.4	1.5	C=C def. (ip)
25			625.4	7.9	623.6	6.9	611.9	3.9	C=C def. (ip)
25	628.5	8.8					615.6	6.4	C=C def. (ip)
32	805.2	10.6			804.2	9.0	791.2	11.8	C-H def. (oop)
32			815.3	19.8			797.5	14.5	C-H def. (oop)
32					816.9	8.9	802.4	8.1	C-H def. (oop)
34	850.2	6.0					836.4	3.4	C-H def. (oop)
34			857.9	5.2			838.4	3.8	C-H def. (oop)
35			871.0	6.8	869.6	32.1	847.5	15.6	C-H def. (oop)
36			875.0	18.6	874.1	4.4	858.9	5.0	C-H def. (oop)
35	879.5	4.2					864.2	3.1	asym. C-C-C str.
36	889.3	15.6					867.3	4.9	C-H def. (oop)
41	1034.6	20.1	1037.4	33.1	1038.0	44.5	1022.1	57.9	C-OH str.
43	1065.6	10.0	1061.4	10.1	1062.2	10.6	1047.0	76.0	C-H def. (ip)
44	1066.6	49.8	1066.5	37.0			1047.0		methyl C-O str.
45					1125.5	47.5	1107.1	16.6	C-H def. (ip)
45			1134.6	19.6			1113.8	2.3	C-H def. (ip)
45	1142.1	15.6	1147.1	9.7	1143.0	10.8	1122.7	11.7	C-H def. (ip)
49	1185.1	24.8	1188.8	45.1	1189.2	65.3	1165.6	63.2	methyl C-H def. (ip)
50			1191.3	17.9			1165.6		C-H def. (ip)
51	1203.5	14.3	1205.2	6.0			1181.9	15.5	O-H def. (oop)
52	1206.1	22.2	1206.4	9.4	1205.7	8.7	1181.9		methyl C-H def. (ip)
53			1221.2	7.9	1220.7	9.2	1191.4	9.4	methyl C-H def. (ip)
54					1224.4	16.4	1197.5	10.4	methyl C-H def. (ip)
54	1232.8	18.1	1231.0	22.1			1205.1	24.6	methyl C-H def. (ip)
55	1240.1	7.5	1251.5	56.5	1243.9	31.2	1223.7	24.5	H-CO-H def. (oop)
57	1259.7	100.0					1232.3	50.2	asym. C-O-C str.
56			1267.5	8.5			1241.4	22.1	H-CO-H def. (oop)
56					1272.2	25.0	1250.4	100.0	C-H def. (ip)
57			1278.8	100.0	1273.3	100.0	1250.4		H-CO-H def. (oop)
58	1314.2	36.4	1311.3	28.0			1278.5	35.6	C-H def. (ip)
59	1318.8	19.9					1286.2	34.2	C-H def. (ip)
59			1326.4	55.0			1295.8	28.4	C-H def. (ip)
59					1333.2	62.1	1307.6	13.4	C-H def. (ip)
60			1345.1	9.7			1313.6	12.1	H-CO-H def. (oop)
60	1347.1	46.9					1318.3	37.8	H-CO-H def. (oop)
61	1385.9	4.5					1371.7	6.2	C-C-C def. (ip)
62			1395.0	19.6			1374.9	10.1	H-CO-H def. (oop)
62	1400.4	8.2			1401.3	13.9	1381.9	38.3	H-CO-H def. (oop)
64	1470.6	13.8	1468.3	18.5	1461.4	16.9	1433.7	22.2	methyl C-H def. (ip)
65	1478.0	5.7	1478.0	9.0	1477.9	12.9	1441.1	12.8	methyl C-H def. (ip)
67	1496.3	5.0			1496.4	6.5	1459.4	11.0	methyl C-H def. (oop)
68	1497.7	11.8	1497.8	18.1			1463.9	23.3	methyl C-H def. (ip)
69			1506.4	22.2	1507.1	10.2	1470.0	43.9	methyl C-H def. (ip)
70	1506.7	22.2			1507.1	35.7	1470.0		methyl C-H def. (ip)
70			1508.1	10.0			1475.3	13.5	methyl C-H def. (ip)
72	1532.5	50.4	1534.0	58.8	1533.9	43.7	1502.2	91.8	C-H def. (ip)
74	1624.8	27.8	1623.1	27.0	1623.4	18.2	1590.6	38.1	C=C str.
74			1625.9	7.4	1626.9	11.2	1592.9	15.0	C=C str.
75			1649.2	49.7	1647.2	46.3	1617.4	78.4	C=C str.
76					1651.9	57.2	1617.4		C=C str.
75	1659.1	11.8					1625.1	61.4	C=C str.
76	1662.6	60.3	1662.4	54.4			1625.1		C=C str.

^aThe theoretical values were calculated at the B3LYP/def2-TZVP level of theory.

^bThe experimental values were obtained in an argon matrix at 3 K.

Table 10.12: Spectroscopic data of diazo compound 35.

mode	u: ν/cm^{-1} (calc.) ^a	u: I_{rel} (calc.) ^a	d: ν/cm^{-1} (calc.) ^a	d: I_{rel} (calc.) ^a	ν/cm^{-1} (Ar) ^b	I_{rel} (Ar) ^b	ν/cm^{-1} (Xe) ^c	I_{rel} (Xe) ^c	ν/cm^{-1} (N ₂) ^d	I_{rel} (N ₂) ^d	assignment
19	622.4	1.4	624.2	1.0	613.5	2.0	610.3	0.4	615.5	0.8	C=C def. (oop)
21	657.0	1.9	658.0	1.0	643.4	2.3	642.7	1.1	643.7	0.9	C=C def. (ip)
23	733.4	1.2	735.2	1.0	722.9	1.0	720.8	1.3	724.4	0.7	C=C def. (oop)
25	756.6	3.6	755.7	3.5	745.6	3.0	742.8	3.1	747.6	2.5	C=C def. (oop)
26			780.4	1.2	766.0	2.8	765.2	3.1	768.5	2.3	C=C def. (oop)
27	801.4	4.0			797.5	1.1	795.3	0.8	803.7	1.8	C-H def. (oop)
27			827.7	2.4	813.3	1.2	810.7	1.5	817.0	1.6	C-H def. (oop)
28			852.9	1.9	844.6	1.0	842.7	0.3	849.1	1.1	C-H def. (oop)
29	885.6	1.2			866.4	0.5	865.8	0.5	871.5	0.5	C-H def. (oop)
31	904.5	2.8	903.4	1.5	887.2	2.1	885.2	2.1	887.7	1.7	C=C def. (ip)
40	1181.3	20.4			1154.3	4.6	1152.5	6.0	1155.8	4.5	O-H def. (ip)
40			1183.6	23.1	1168.3	9.0	1166.5	2.3	1169.0	6.9	O-H def. (ip)
41	1192.5	0.9			1176.6	1.3	1169.1	5.0	1175.9	8.0	C-H def. (ip)
42	1222.3	3.8			1198.0	1.6	1199.4	3.4	1200.4	1.3	C-H def. (ip)
42			1222.8	6.6	1203.5	2.1	1199.4		1205.1	1.3	C-H def. (ip)
43	1239.5	2.8	1240.5	3.1	1218.5	2.0	1219.2	2.7	1219.7	2.0	C-H def. (ip)
44			1266.9	4.0	1242.0	1.3	1241.8	1.4	1243.2	1.6	C-H def. (ip)
45	1331.4	9.3			1302.6	4.6	1302.4	3.8	1304.2	4.7	C-H def. (ip)
46	1342.4	1.6			1314.8	0.8	1312.9	0.9	1316.0	1.3	C-H def. (ip)
47			1364.9	0.9	1337.2	0.5	1337.1	0.9	1338.2	1.0	C-H def. (ip)
47	1365.4	1.1			1339.5	0.4	1337.1		1338.2		asym. C-C str.
48	1376.5	5.2			1346.8	1.3	1345.3	1.1	1347.0	1.8	O-H def. (ip)
48			1384.8	1.8	1356.5	0.5	1352.1	0.7	1354.1	0.6	C-H def. (ip)
49	1421.8	1.3			1382.9	0.6	1382.6	1.1	1384.9	2.2	C=N str.
49			1423.3	1.9	1386.1	0.7	1387.1	0.5	1384.9		C=N str.
50			1475.2	11.3	1442.7	6.4	1441.8	8.1	1443.5	6.0	C-H def. (ip)
50	1476.9	3.8			1447.6	1.3	1444.9	1.8	1447.5	2.0	C-H def. (ip)
51	1481.2	12.6			1452.5	9.0	1450.9	9.4	1453.2	8.4	C-H def. (ip)
51			1486.4	6.2	1460.6	1.9	1456.7	1.1	1460.4	0.5	C-H def. (ip)
52			1506.7	2.5	1476.7	1.3	1476.4	1.4	1477.2	1.0	C-H def. (ip)
53			1518.1	8.2	1490.1	5.6	1489.1	4.3	1489.9	3.9	C-H def. (ip)
53	1530.6	4.1			1505.8	2.3	1502.6	2.7	1506.2	2.3	C-H def. (ip)
55	1616.7	5.4			1583.7	1.2	1580.4	1.9	1583.5	1.7	C=C str.
55			1624.9	1.2	1590.5	1.2	1586.8	1.3	1591.9	0.4	C=C str.
56			1643.5	0.9	1610.7	1.8	1604.6	1.3	1597.3	2.9	C=C str.
57			1652.3	7.6	1619.1	2.5	1616.9	2.6	1620.1	2.4	C=C str.
57	1659.1	5.8			1627.6	3.1	1625.4	3.1	1628.2	1.4	C=C str.
58	2168.6	100.0	2170.2	100.0	2058.2	100.0	2057.1	100.0	2064.3	100.0	N=N str.

^aThe theoretical values were calculated at the B3LYP/def2-TZVP level of theory.

^bThe experimental values were obtained in an argon matrix at 3 K.

^cThe experimental values were obtained in a xenon matrix at 9 K.

^dThe experimental values were obtained in a nitrogen matrix at 9 K.

Table 10.13: Spectroscopic data of singlet carbene S-31.

mode	u: ν/cm^{-1} (calc.) ^a	u: I_{rel} (calc.) ^a	d: ν/cm^{-1} (calc.) ^a	d: I_{rel} (calc.) ^a	ν/cm^{-1} (Ar) ^b	I_{rel} (Ar) ^b	ν/cm^{-1} (Xe) ^c	I_{rel} (Xe) ^c	ν/cm^{-1} (N ₂) ^d	I_{rel} (N ₂) ^d	assignment
20	773.6	14.9	771.8	20.2	755.5	13.2	749.4	13.8	756.6	15.1	C-H def. (oop)
21			788.0	7.9	769.9	13.2	768.4	11.7	773.3	9.4	C-H def. (oop)
22	817.6	16.6			797.6	27.7	794.7	25.7	799.2	2.5	C-H def. (oop)
23			847.1	10.2	829.9	5.8	827.1	5.9	829.3	2.3	C-H def. (oop)
24	861.6	4.0	860.6	5.5	847.5	6.6	846.8	11.3	843.6	11.8	asym. C-C-C str.
25			869.3	15.5	858.1	3.3			851.8	3.9	C-H def. (oop)
25	894.7	3.9			869.1	4.0	871.3	7.0			C-H def. (oop)
33	1101.3	21.3	1100.1	25.5	1079.4	7.3	1078.1	33.1	1079.8	28.4	C-H def. (ip)
34			1115.5	41.0	1090.1	2.4	1093.1	100.0	1091.6	8.6	C-H def. (ip)
34	1120.1	76.7			1097.3	14.3	1103.1	51.6	1097.0	87.4	C-H def. (ip)
35			1171.8	76.1	1148.1	8.1	1149.8	14.4	1151.1	10.1	O-H def. (ip)
35	1174.4	30.7			1156.5	64.0	1157.0	44.4	1161.3	43.6	O-H def. (ip)
36	1182.3	36.2			1159.8	37.8	1162.6	25.0	1168.2	4.8	asym. C-C-C str.
36			1184.2	28.3	1164.6	17.9	1165.3	12.3	1168.2		O-H def. (ip)
37			1191.8	12.1	1173.3	10.8	1171.6	13.3	1172.7	14.2	C-H def. (ip)
37	1193.5	7.4			1175.5	2.4	1177.5	10.7	1172.7		C-H def. (ip)
38			1198.4	17.8	1178.6	5.0	1180.5	6.1	1176.3	8.9	C-H def. (ip)
39	1227.4	10.6	1223.0	69.8	1199.4	18.5	1197.3	12.9	1202.1	13.1	asym. C-C-C str.
40	1258.0	26.8	1260.3	98.0	1232.3	10.7	1234.8	9.4	1238.2	32.3	C-H def. (ip)
41	1297.0	14.6	1296.8	12.7	1270.8	5.1	1268.1	7.5	1274.1	12.5	C-H def. (ip)
42	1322.3	9.6	1320.2	7.5	1296.4	30.9	1294.4	27.7	1296.7	3.6	C-O str.
43	1330.1	28.3			1299.5	21.1	1297.5	34.4	1301.6	32.4	O-H def. (ip)
44	1419.7	29.5			1391.0	16.1	1390.4	14.2	1392.3	32.8	C-H def. (ip)
44			1428.7	4.7	1408.5	31.2	1406.0	8.9	1410.0	2.5	C-H def. (ip)
45	1455.3	5.5			1428.6	15.2	1422.7	3.1	1426.2	5.7	C-H def. (ip)
46			1475.1	20.2	1446.1	8.0	1444.0	18.6	1446.6	9.1	C-H def. (ip)
47			1492.9	5.7	1459.1	8.6	1454.7	44.7	1457.2	8.9	C-H def. (ip)
47	1499.3	6.4			1465.0	9.5	1466.2	32.5	1467.2	9.8	C-H def. (ip)
48			1513.2	55.2	1486.7	24.0	1484.1	11.0	1492.3	14.3	C-H def. (ip)
48	1519.5	23.0			1493.7	11.0	1488.4	10.3	1496.2	5.1	C-H def. (ip)
49	1609.6	13.5	1610.3	60.7	1578.2	62.9	1575.4	16.6	1576.0	16.5	C=C str.
50			1624.8	10.1	1590.0	8.1	1589.2	11.7	1591.0	6.2	C=C str.
51	1636.5	20.7	1636.4	30.0	1599.7	100.0	1603.7	63.1	1598.5	19.0	C=C str.
52	1644.8	100.0	1645.7	100.0	1608.1	55.0	1616.0	71.9	1607.9	100.0	C=C str.

^aThe theoretical values were calculated at the B3LYP/def2-TZVP level of theory.

^bThe experimental values were obtained in an argon matrix at 3 K.

^cThe experimental values were obtained in a xenon matrix at 9 K.

^dThe experimental values were obtained in a nitrogen matrix at 9 K.

Table 10.14: Spectroscopic data of triplet carbene T-31.

mode	u: ν/cm^{-1} (calc.) ^a	u: I_{rel} (calc.) ^a	d: ν/cm^{-1} (calc.) ^a	d: I_{rel} (calc.) ^a	ν/cm^{-1} (Ar) ^b	I_{rel} (Ar) ^b	ν/cm^{-1} (Xe) ^c	I_{rel} (Xe) ^c	ν/cm^{-1} (N ₂) ^d	I_{rel} (N ₂) ^d	assignment
18	731.2	13.1	732.1	11.1	716.0	32.1	721.2	35.4	717.9	25.4	C=C def. (oop)
20	758.7	18.4	757.8	20.5	744.6	48.3	741.6	14.9	744.8	8.7	C-H def. (oop)
21			771.5	7.2	755.8	21.2	753.5	7.5	755.2	5.1	C-H def. (oop)
22	803.2	27.8			783.0	8.0	784.0	2.6	781.9	12.7	C-H def. (oop)
22			829.8	17.0	811.7	16.7	809.6	16.9	814.5	12.8	C-H def. (oop)
23	839.5	8.8			825.7	4.9	823.3	2.2	819.8	19.2	C=C def. (ip)
24			856.2	14.8	843.3	13.9	841.4	7.0	838.0	4.9	C-H def. (oop)
25	891.0	8.8			869.1	3.0	866.6	8.8			C-H def. (oop)
33	1113.0	8.8			1089.6	19.9	1093.0	95.8	1089.1	100.0	C-H def. (ip)
34			1125.3	7.7	1099.9	18.4	1106.0	13.8			C-H def. (ip)
34	1130.3	44.1			1105.7	54.7	1117.4	61.2	1106.4	57.3	C-H def. (ip)
35	1177.7	91.0	1174.6	96.2	1158.1	66.6	1157.9	36.2	1164.0	50.4	O-H def. (ip)
36			1185.4	55.5	1168.3	28.8	1168.3	16.6	1169.9	12.9	O-H def. (ip)
38	1223.5	12.3	1223.7	12.1	1199.4	27.8	1198.8	7.2			asym. C-C-C str.
39	1236.6	6.4	1236.0	15.0	1211.1	17.2	1209.1	2.0	1210.5	32.6	asym. C-C-C str.
40	1254.0	18.0	1253.5	96.4	1220.5	34.3	1218.4	7.1	1220.8	46.3	C-O str.
41			1326.0	11.9	1296.4	51.9	1294.4	30.1	1295.3	9.7	C-H def. (ip)
42	1329.4	55.0			1300.0	78.2	1297.7	32.0	1295.3		C-H def. (ip)
43	1344.6	48.6			1306.7	24.8	1307.8	14.6	1309.4	10.8	asym. C-C-C str.
44	1383.9	47.2			1355.5	67.4	1353.1	23.5	1356.8	12.9	C-H def. (ip)
45	1445.2	22.5			1420.0	29.4	1410.6	3.1	1419.7	22.3	C-H def. (ip)
46			1458.2	28.4	1428.9	25.2	1425.9	4.2	1429.8	34.9	C-H def. (ip)
47			1495.7	12.8	1464.5	10.0	1462.1	100.0	1464.7	13.5	C-H def. (ip)
48			1502.1	46.8	1471.7	68.1	1468.4	64.2	1471.4	72.2	C-H def. (ip)
48	1515.6	12.6			1481.8	19.5	1474.4	52.1			C-H def. (ip)
49	1590.5	8.0	1592.4	22.0	1560.6	15.8			1560.6	5.6	C=C str.
50	1603.4	10.4	1604.8	16.0	1570.1	45.4	1568.6	16.5	1570.2	13.7	C=C str.
51	1614.1	17.7	1614.6	10.5	1578.7	100.0	1576.9	12.1	1581.8	9.1	C=C str.
52	1631.3	100.0	1629.2	100.0	1594.2	59.8	1596.5	81.8	1593.8	27.4	C=C str.

^aThe theoretical values were calculated at the B3LYP/def2-TZVP level of theory.

^bThe experimental values were obtained in an argon matrix at 3 K.

^cThe experimental values were obtained in a xenon matrix at 9 K.

^dThe experimental values were obtained in a nitrogen matrix at 9 K.

Table 10.15: Spectroscopic data of singlet water complex S-36.

mode	u: v/cm ⁻¹ (calc.) ^a	u: I _{rel} (calc.) ^a	d: v/cm ⁻¹ (calc.) ^a	d: I _{rel} (calc.) ^a	v/cm ⁻¹ (Ar) ^b	I _{rel} (Ar) ^b	assignment
25	771.3	2.8	769.5	2.4	748.1	42.0	C-H def. (oop)
27	820.5	2.6	824.4	6.3	806.4	21.8	C---H-O def. (ip)
39	1103.7	3.6	1102.5	3.1	1083.8	69.4	C-H def. (ip)
40	1130.5	23.7	1125.1	9.3	1101.7	49.1	C-H def. (ip)
41	1177.2	9.8	1177.3	14.8	1152.8	10.0	O-H def. (ip)
42	1193.7	4.9	1193.6	2.8	1166.5	32.3	C-H def. (ip)
43	1198.6	2.7	1195.0	3.3	1166.5		C-H def. (ip)
44			1201.4	1.4	1170.2	11.6	C-H def. (ip)
45	1250.0	1.5	1246.8	16.0	1229.1	28.8	C-H def. (ip)
46	1262.4	11.7	1264.0	16.4	1243.4	42.5	O-H def. (ip)
47	1301.9	7.1	1303.2	4.1	1281.8	5.3	asym. C-C-C str.
48			1325.4	0.8	1292.3	24.8	C-H def. (ip)
49	1339.6	6.5			1304.4	29.5	C-H def. (ip)
50	1424.1	7.8	1431.6	0.9	1395.5	75.4	C-H def. (ip)
51	1458.3	2.5			1433.5	62.0	C-H def. (ip)
52			1477.2	4.9	1452.4	100.0	C-H def. (ip)
53	1502.4	1.1			1474.5	69.0	C-H def. (ip)
54	1521.1	7.6	1517.5	9.3	1489.3	53.3	C-H def. (ip)

^aThe theoretical values were calculated at the B3LYP/def2-TZVP level of theory.

^bThe experimental values were obtained in an argon matrix at 3 K.

Table 10.16: Spectroscopic data of singlet water complex S-37.

mode	u: v/cm ⁻¹ (calc.) ^a	u: I _{rel} (calc.) ^a	d: v/cm ⁻¹ (calc.) ^a	d: I _{rel} (calc.) ^a	v/cm ⁻¹ (Ar) ^b	I _{rel} (Ar) ^b	assignment
31	773.0	2.8	775.4	2.5	748.1	42.0	C-H def. (oop)
33	819.0	2.7	816.1	7.6	806.4	21.8	C---H-O def. (ip)
45	1104.1	3.9	1104.1	3.1	1083.8	69.4	C-H def. (ip)
46	1130.1	22.6	1129.4	9.0	1101.7	49.1	C-H def. (ip)
47	1181.5	9.3	1181.3	18.9	1152.8	10.0	O-H def. (ip)
48	1196.2	9.8	1192.4	3.8	1166.5	32.3	C-H def. (ip)
49			1199.0	3.4	1166.5		C-H def. (ip)
50	1202.3	2.6	1207.4	1.7	1170.2	11.6	C-H def. (ip)
51			1239.9	14.3	1216.5	67.4	Ar-C str.
51	1246.7	7.4			1229.1	28.8	Ar-C str.
52	1262.1	5.4	1255.7	16.1	1243.4	42.5	C-H def. (ip)
53	1301.3	6.6	1306.8	3.2	1281.8	5.3	asym. C-C-C str.
55	1340.5	4.2			1304.4	29.5	C-H def. (ip)
56	1426.7	6.2	1431.9	0.8	1395.5	75.4	C-H def. (ip)
57	1461.3	3.3	1464.1	0.9	1433.5	62.0	C-H def. (ip)
58			1479.3	2.8	1452.4	100.0	C-H def. (ip)
59			1495.2	1.2	1474.5	69.0	C-H def. (ip)
60	1517.1	7.7	1518.3	9.7	1489.3	53.3	C-H def. (ip)

^aThe theoretical values were calculated at the B3LYP/def2-TZVP level of theory.

^bThe experimental values were obtained in an argon matrix at 3 K.

Table 10.17: Spectroscopic data of singlet water complex S-38.

mode	u: v/cm ⁻¹ (calc.) ^a	u: I _{rel} (calc.) ^a	d: v/cm ⁻¹ (calc.) ^a	d: I _{rel} (calc.) ^a	v/cm ⁻¹ (Ar) ^b	I _{rel} (Ar) ^b	assignment
30	771.5	1.9	771.3	2.4	748.1	42.0	C-H def. (oop)
32			820.3	7.8	806.4	21.8	OH--O def. (oop)
37			897.2	1.2	880.3	42.2	C-H def. (oop)
38			911.4	1.7	899.6	89.1	C-H def. (oop)
39			919.0	0.8	906.1	48.0	C=C def. (ip)
45	1103.1	2.9	1102.2	2.8	1083.8	69.4	C-H def. (ip)
46			1126.6	10.9	1101.7	49.1	C-H def. (ip)
46	1137.0	14.7			1109.5	33.1	C-H def. (ip)
48	1194.5	2.2	1191.9	1.4	1166.5	32.3	C-H def. (ip)
43	1198.6	2.3	1195.0	3.0	1166.5		C-H def. (ip)
50	1231.8	17.7			1204.4	72.0	O-H def. (ip)
50			1243.5	2.6	1229.1	28.8	O-H def. (ip)
51			1260.6	10.0	1243.4	42.5	Ar-C str.
52			1275.1	31.7	1251.3	92.6	C-H def. (ip)
52	1284.6	10.2			1265.5	18.9	O-H def. (ip)
53	1304.6	6.5	1305.0	3.5	1281.8	5.3	asym. C-C-C str.
54	1338.8	1.2	1334.2	3.0	1304.4	29.5	C-O str.
55	1361.9	6.6			1339.2	57.3	O-H def. (ip)
56	1427.3	12.0			1395.5	75.4	C-H def. (ip)
57	1460.3	3.7			1433.5	62.0	C-H def. (ip)
57			1470.7	1.7	1441.9	64.6	O-H def. (ip)
58	1484.7	0.7	1480.5	5.4	1452.4	100.0	C-H def. (ip)
59	1505.9	4.2			1474.5	69.0	C-H def. (ip)
60			1519.6	12.5	1489.3	53.3	C-H def. (ip)
60	1533.8	4.5			1504.5	3.9	O-H def. (ip)

^aThe theoretical values were calculated at the B3LYP/def2-TZVP level of theory.

^bThe experimental values were obtained in an argon matrix at 3 K.

Table 10.18: Spectroscopic data of alcohol **39**.

mode	u: ν/cm^{-1} (calc.) ^a	u: I_{rel} (calc.) ^a	d: ν/cm^{-1} (calc.) ^a	d: I_{rel} (calc.) ^a	ν/cm^{-1} (Ar) ^b	I_{rel} (Ar) ^b	assignment
17	583.4	6.0			576.6	6.3	C=C def. (ip)
19	647.5	6.8			633.4	13.2	C=C def. (ip)
20	657.9	8.7	658.2	7.3	644.1	15.6	C=C def. (ip)
23	753.3	29.0	752.8	20.8	744.3	53.9	C-H def. (oop)
24			785.0	10.4	770.6	38.7	C-H def. (oop)
25	802.9	13.7			796.3	12.1	C-H def. (oop)
26	844.0	13.5			830.9	4.0	C-H def. (oop)
26			851.5	17.3	836.8	4.9	C-H def. (oop)
28			860.9	10.6	848.1	7.0	C-H def. (oop)
28	882.5	7.9			866.4	14.1	C-H def. (oop)
30	915.8	15.5	914.6	8.0	899.2	19.4	C=C def. (ip)
35	1046.5	37.1			1026.6	30.6	C-O str.
35			1047.8	37.2	1032.4	31.3	C-O str.
37			1125.4	6.2	1103.0	12.8	C-H def. (ip)
38	1140.1	32.1			1117.6	19.3	C-H def. (ip)
39	1180.7	100.0	1181.1	100.0	1161.7	93.4	Ar-O-H def. (ip)
40	1187.1	9.0	1187.7	30.6	1173.9	24.7	C-H def. (ip)
41	1192.1	19.5	1191.1	17.7	1173.9		C-H def. (ip)
42	1204.3	15.8	1202.4	18.8	1187.0	66.2	HOC-H def. (ip)
44	1234.0	6.4	1232.9	11.4	1207.6	15.5	C-H def. (ip)
45	1254.4	14.4	1256.1	39.2	1241.9	21.2	HCO-H def. (oop)
46			1274.9	10.4	1248.0	13.2	HOC-H def. (oop)
47	1326.6	51.8	1330.8	6.6	1295.3	39.0	C-H def. (ip)
48	1332.2	6.0			1295.3		HOC-H def. (oop)
49	1345.2	17.0	1346.0	10.2	1303.3	44.7	HOC-H def. (oop)
50	1386.5	8.0			1358.9	36.6	HOC-H def. (oop)
50			1387.5	7.6	1366.2	19.2	HOC-H def. (oop)
51	1398.7	35.8			1376.2	100.0	HOC-H def. (oop)
52	1482.7	28.1	1482.6	14.2	1448.2	68.1	C-H def. (ip)
53			1489.5	11.3	1455.8	19.9	C-H def. (ip)
54			1515.1	17.9	1486.3	20.1	C-H def. (ip)
55			1526.1	29.2	1494.0	18.9	C-H def. (ip)
55	1533.6	23.3			1501.7	21.9	C-H def. (ip)

^aThe theoretical values were calculated at the B3LYP/def2-TZVP level of theory.

^bThe experimental values were obtained in an argon matrix at 3 K.

Table 10.19: Spectroscopic data of singlet DME complex S-40.

mode	u: ν/cm^{-1} (calc.) ^a	u: I_{rel} (calc.) ^a	d: ν/cm^{-1} (calc.) ^a	d: I_{rel} (calc.) ^a	ν/cm^{-1} (Ar) ^b	I_{rel} (Ar) ^b	assignment
27			750.0	0.7	740.0	11.4	C-H def. (oop)
28	772.3	2.1	770.8	2.7	749.9	6.7	C-H def. (oop)
29	793.8	0.5			775.7	2.4	C=C def. (oop)
30			835.8	4.6	820.4	19.8	O-H def. (oop)
32	859.7	0.7			838.1	7.3	asym. C-C-C str.
33	876.6	5.0			859.9	5.2	O-H def. (oop)
36	916.2	5.8	915.2	1.6	906.4	16.0	sym. Me-O-Me str.
37	917.4	1.1	915.6	2.4	906.4		C=C def. (ip)
43	1100.7	2.8	1099.6	3.7	1083.8	44.1	C-H def. (ip)
44	1104.5	3.6	1103.6	4.8	1083.8		asym Me-O-Me str.
45	1126.8	9.2			1104.8	5.7	C-H def. (ip)
48	1185.0	3.0	1184.7	4.2	1177.7	13.1	Me-O-Me asym. str.
52	1229.4	13.5	1234.4	7.5	1210.8	100.0	O-H def. (ip)
53	1240.5	1.0			1210.8		C-H def. (ip)
53			1249.8	4.4	1226.5	30.0	O-H def. (ip)
54			1270.8	16.2	1251.2	77.2	C-H def. (ip)
55			1276.8	7.6	1258.3	17.1	DME C-H def. (oop)
55	1281.9	5.8			1264.7	15.6	O-H def. (ip)
57	1331.2	2.3	1328.2	3.4	1308.0	46.4	C-OH str.
58	1363.4	4.1	1367.7	2.0	1335.7	23.1	O-H def. (ip)
59	1425.5	9.1			1398.4	18.2	O-H def. (ip)
60	1457.7	1.7			1432.3	13.3	C-H def. (ip)
61			1468.9	1.6	1438.8	15.0	C-H def. (ip)
62	1483.4	0.9	1481.2	3.2	1452.9	42.9	C-H def. (ip)
64			1492.6	0.8	1462.3	42.3	C-H def. (ip)
65	1496.2	0.6			1462.3		DME C-H def. (ip)
66	1496.5	0.6	1496.5	0.9	1462.3		DME C-H def. (ip)
67			1496.9	1.1	1462.3		DME C-H def. (ip)
67	1502.6	3.8			1467.7	32.4	C-H def. (ip)
68			1512.5	0.8	1483.8	61.8	DME C-H def. (ip)
69			1515.6	11.5	1483.8		C-H def. (ip)
69	1536.0	2.2			1507.1	19.3	O-H def. (ip)
70	1605.7	1.6	1607.9	10.6	1572.5	20.7	C=C str.
71			1624.5	1.4	1586.8	44.6	C=C str.
72	1636.0	2.9	1636.0	2.7	1601.6	22.6	C=C str.
73	1646.3	20.7	1650.0	17.8	1615.2	79.2	C=C str.

^aThe theoretical values were calculated at the B3LYP/def2-TZVP level of theory.

^bThe experimental values were obtained in an argon matrix at 3 K.

Table 10.20: Spectroscopic data of triplet DME complex T-40.

mode	u: v/cm ⁻¹ (calc.) ^a	u: I _{rel} (calc.) ^a	d: v/cm ⁻¹ (calc.) ^a	d: I _{rel} (calc.) ^a	v/cm ⁻¹ (Ar) ^b	I _{rel} (Ar) ^b	assignment
28	757.6	1.7	756.5	1.6	740.0	11.4	C-H def. (oop)
29	774.0	1.5	772.0	1.0	749.9	6.7	C=C def. (oop)
30	793.8	2.6	789.9	7.6	775.7	2.4	O-H def. (oop)
31	831.5	3.1			820.4	19.8	C-H def. (oop)
32	842.7	0.8	844.6	1.0	820.4		asym. C-C-C str.
36	913.3	0.7			906.4	16.0	C=C def. (ip)
37	917.8	7.1	917.4	8.0	906.4		sym. Me-O-Me str.
43	1105.6	4.5	1105.4	6.5	1083.8	44.1	asym. Me-O-Me str.
44			1111.2	1.0	1083.8		C-H def. (ip)
45			1125.5	2.2	1104.8	5.7	C-H def. (ip)
48	1184.9	3.7	1184.4	5.1	1177.7	13.1	asym. Me-O-Me str.
51	1221.8	5.5	1222.5	2.8	1210.8	100.0	asym. C-C-C str.
52	1227.0	3.6			1210.8		O-H def. (ip)
53	1239.1	1.5			1210.8		C-H def. (ip)
53			1251.2	1.9	1226.5	30.0	C-H def. (ip)
54			1266.3	24.7	1243.0	49.4	O-H def. (ip)
55			1275.1	2.0	1258.3	17.1	DME C-H def. (oop)
55	1287.1	2.3			1264.7	15.6	O-H def. (ip)
56	1328.2	2.3	1326.6	2.7	1308.0	46.4	C-H def. (ip)
58	1363.0	3.4			1335.7	23.1	O-H def. (ip)
59	1396.0	15.0			1375.8	22.0	O-H def. (ip)
60	1447.0	4.3	1454.4	2.4	1432.3	13.3	C-H def. (ip)
61			1461.3	4.4	1438.8	15.0	C-H def. (ip)
65	1496.1	0.7	1495.8	1.2	1462.3	42.3	DME C-H def. (ip)
66	1496.7	0.8			1462.3		DME C-H def. (ip)
68			1506.5	9.5	1467.7	32.4	C-H def. (ip)
69	1530.9	0.8			1507.1	19.3	O-H def. (ip)
71	1602.0	1.1	1604.0	3.7	1572.5	20.7	C=C str.
72	1614.8	1.8			1586.8	44.6	C=C str.
73	1633.3	13.6	1632.1	16.9	1601.6	22.6	C=C str.

^aThe theoretical values were calculated at the B3LYP/def2-TZVP level of theory.

^bThe experimental values were obtained in an argon matrix at 3 K.

Table 10.21: Spectroscopic data of singlet ammonia complex S-57.

mode	uu: v/cm ⁻¹ (calc.) ^a	uu: I _{rel} (calc.) ^a	ud: v/cm ⁻¹ (calc.) ^a	ud: I _{rel} (calc.) ^a	dd: v/cm ⁻¹ (calc.) ^a	dd: I _{rel} (calc.) ^a	v/cm ⁻¹ (Ar) ^b	I _{rel} (Ar) ^b	assignment
35	827.4	6.8	826.6	5.3			812.7	1.1	C-H def. (oop)
37	840.1	3.2					817.3	5.0	C-H def. (oop)
35					844.7	4.6	821.9	2.3	C-H def. (oop)
38					876.3	18.1	859.0	0.3	C-H def. (oop)
38	878.1	3.1	878.3	3.2	878.6	3.8	859.0		C=C def. (ip)
39			882.0	11.2			861.7	0.2	C-H def. (oop)
39	895.7	9.6					873.2	0.6	C-H def. (oop)
45			1048.5	6.1	1049.5	16.9	1026.9	19.7	methyl C-O str.
46	1053.5	28.3	1052.5	22.1	1051.5	7.1	1026.9		methyl C-O str.
47			1109.1	59.5	1108.1	91.9	1081.8	1.5	N-H def. (ip)
48					1111.2	34.2	1081.8		C-H def. (ip)
47	1114.9	52.8					1088.9	10.1	N-H def. (ip)
48			1120.2	40.6	1121.1	9.4	1094.4	9.1	C-H def. (ip)
48	1124.3	54.7	1126.8	13.4			1094.4		C-H def. (ip)
49	1138.3	8.1					1106.4	43.7	C-H def. (ip)
52	1185.3	3.2	1187.6	15.0	1188.7	12.9	1164.1	5.8	methyl C-H def. (ip)
53	1200.3	46.9	1199.6	19.8	1196.5	9.7	1178.0	16.1	methyl C-H def. (ip)
54	1215.0	11.6	1209.8	11.2			1191.5	8.7	methyl C-H def. (ip)
55	1217.5	12.8	1216.1	2.4	1212.7	24.9	1191.5		C-H def. (ip)
56	1231.3	8.3	1226.6	23.5	1227.4	16.3	1204.2	40.6	C-H def. (ip)
57	1246.6	8.9	1249.5	17.0			1223.4	13.1	C-H def. (ip)
58	1258.5	67.0			1258.7	100.0	1233.0	9.0	C-H def. (ip)
58			1266.7	100.0	1264.5	36.7	1246.7	100.0	C-H def. (ip)
59	1302.3	31.8	1302.0	5.8	1303.0	3.7	1279.6	6.6	C-H def. (ip)
60	1317.9	41.8	1315.1	22.1	1319.3	9.7	1295.5	2.9	C-H def. (ip)
61	1325.6	30.3					1301.7	2.1	C-H def. (ip)
61			1333.0	18.8	1331.9	31.1	1309.2	10.5	C-H def. (ip)
62					1403.6	5.8	1374.7	1.7	C-H def. (ip)
62	1411.3	8.2	1407.8	8.7			1383.3	6.1	C-H def. (ip)
64					1454.8	18.4	1432.9	1.6	methyl C-H def. (ip)
64	1458.7	7.8	1461.1	15.9			1438.3	2.5	C-H def. (ip)
70	1505.2	7.1	1504.8	17.6	1504.6	8.3	1472.6	3.4	methyl C-H def. (ip)
71	1508.0	2.8	1508.0	15.3	1507.3	21.1	1472.6		methyl C-H def. (ip)
72	1520.8	25.9	1523.5	28.9	1525.4	22.8	1490.9	9.6	C-H def. (ip)
73			1592.1	11.6	1592.4	26.3	1565.7	1.2	C=C str.
75			1635.1	81.4	1632.2	79.0	1599.4	3.5	C=C str.
75	1642.0	100.0			1641.5	53.9	1616.5	36.9	C=C str.

^aThe theoretical values were calculated at the B3LYP/def2-TZVP level of theory.

^bThe experimental values were obtained in an argon matrix at 3 K.

Table 10.22: Spectroscopic data of amine **59**.

mode	uu: v/cm ⁻¹ (calc.) ^a	uu: I _{rel} (calc.) ^a	ud: v/cm ⁻¹ (calc.) ^a	ud: I _{rel} (calc.) ^a	dd: v/cm ⁻¹ (calc.) ^a	dd: I _{rel} (calc.) ^a	v/cm ⁻¹ (Ar) ^b	I _{rel} (Ar) ^b	assignment
31					791.3	8.9	764.4	33.9	C=C def. (ip)
32			793.6	11.1	793.2	10.6	764.4		C=C def. (oop)
34	818.3	42.1	817.1	38.9			794.9	4.1	C-H def. (oop)
34			833.2	43.1	832.9	61.3	813.1	5.1	C-H def. (oop)
35	854.1	4.5	854.8	11.6	855.8	11.6	830.1	5.8	C=C def. (ip)
36					862.4	47.1	841.0	11.0	C-H def. (oop)
36			871.1	37.5			845.5	6.2	C-H def. (oop)
36	887.0	24.4	889.7	9.9			862.5	18.1	C-H def. (oop)
38	903.1	7.8	906.5	20.6	911.5	19.6	886.6	43.6	N-H def. (oop)
43			1046.8	9.2	1047.5	20.1	1018.3	7.1	C-H def. (ip)
44	1067.2	56.2	1063.3	35.7			1049.7	42.8	methyl C-O str.
45			1071.1	33.8	1067.7	27.1	1049.7		methyl C-O str.
51	1188.5	14.2	1191.2	64.4	1194.5	62.7	1167.4	85.6	methyl C-H def. (ip)
52	1206.1	16.2	1206.3	14.9			1182.3	26.3	methyl C-H def. (ip)
53	1209.9	10.5					1182.3		HNC-H def. (ip)
54			1222.0	13.4	1219.9	12.4	1191.3	3.6	C-H def. (ip)
55	1232.7	26.9	1232.2	64.5	1233.1	56.8	1206.8	54.1	C-H def. (ip)
56			1254.5	95.5	1254.1	100.0	1232.6	49.6	C-H def. (ip)
57	1259.4	100.0	1264.8	51.4			1232.6		ring C-O str.
57					1272.6	43.9	1250.2	100.0	C-H def. (ip)
58			1285.2	78.7	1293.8	53.6	1250.2		C-H def. (ip)
59			1312.6	44.3			1278.8	28.1	C-H def. (ip)
59	1319.4	23.3					1285.0	19.4	C-H def. (ip)
60	1320.2	57.6					1285.0		C-H def. (ip)
60			1329.7	60.9	1331.1	30.8	1291.1	42.5	C-H def. (ip)
61	1340.0	10.6	1340.3	48.0	1343.0	91.7	1313.2	51.7	HNC-H def. (oop)
62	1375.9	28.2					1346.4	9.5	HNC-H def. (ip)
63	1382.1	7.4	1380.2	34.5			1346.4		C=C def. (ip)
65	1470.9	15.0	1468.2	30.8	1461.9	24.7	1433.6	19.7	methyl C-H def. (ip)
66	1478.1	5.8	1477.9	15.3	1478.0	19.5	1441.1	12.1	methyl C-H def. (ip)
68	1496.2	5.4			1496.2	9.9	1463.5	23.2	methyl C-H def. (oop)
69	1497.9	13.4	1497.9	29.2			1463.5		methyl C-H def. (ip)
70			1506.4	37.1	1507.3	58.8	1469.3	61.4	methyl C-H def. (ip)
71	1506.8	23.9	1508.2	15.9	1507.3	15.2	1469.3		methyl C-H def. (ip)
73	1533.3	56.5	1534.7	100.0	1535.0	71.3	1500.5	82.4	C-H def. (ip)
74			1621.6	47.3	1620.8	23.9	1589.6	55.4	C=C str.
75	1622.5	26.7			1625.9	11.6	1589.6		C=C str.
76	1654.0	21.7	1650.8	89.4	1648.9	81.4	1623.8	60.4	N-H def. (ip)
77			1655.1	23.8	1652.4	80.7	1623.8		N-H def. (ip)
78					1655.7	10.9	1623.8		N-H def. (ip)
77	1660.9	6.1					1638.5	25.1	C=C str.
78	1663.1	57.2	1661.9	75.5			1638.5		C=C str.

^aThe theoretical values were calculated at the B3LYP/def2-TZVP level of theory.

^bThe experimental values were obtained in an argon matrix at 3 K.

Table 10.23: Spectroscopic data of singlet ammonia complex S-60.

mode	u: ν/cm^{-1} (calc.) ^a	u: I_{rel} (calc.) ^a	d: ν/cm^{-1} (calc.) ^a	d: I_{rel} (calc.) ^a	ν/cm^{-1} (Ar) ^b	I_{rel} (Ar) ^b	assignment
25	748.6	2.9			737.1	77.2	C=C def. (oop)
27			791.0	4.8	776.6	32.9	C-H def. (oop)
28	827.6	13.5			819.3	40.7	C-H def. (oop)
39	1102.5	18.8	1101.3	19.1	1085.8	30.5	C-H def. (ip)
40	1112.2	63.7	1107.6	44.0	1085.8		NH3 def. (ip)
41	1131.8	46.6	1126.6	15.1	1109.3	79.8	C-H def. (ip)
42	1176.3	35.1	1176.8	49.2	1153.4	32.5	O-H def. (ip)
43	1190.1	23.4	1188.3	11.4	1173.9	75.0	C-H def. (ip)
44	1194.3	6.0	1193.6	14.2	1173.9		C-H def. (ip)
46			1234.0	54.8	1206.6	12.6	C-H def. (ip)
46	1239.6	10.3			1214.4	18.0	C-H def. (ip)
47	1259.9	30.4	1262.3	57.6	1242.8	16.3	C-H def. (ip)
48	1300.0	20.5	1301.1	11.2	1277.2	1.3	asym. C-C-C str.
49			1323.5	2.9	1293.5	3.5	C-H def. (ip)
50	1339.8	25.0			1305.3	35.4	C-H def. (ip)
51	1422.6	27.0	1430.0	3.3	1377.9	71.3	C-H def. (ip)
52	1458.0	7.6			1432.5	30.1	C-H def. (ip)
53			1476.7	16.7	1442.1	69.5	C-H def. (ip)
54	1501.6	3.5	1493.2	6.3	1457.5	100.0	C-H def. (ip)
55	1519.5	26.2	1515.5	33.2	1487.2	22.8	C-H def. (ip)
56	1606.5	16.2	1606.5	40.1	1586.0	47.3	C=C str.

^aThe theoretical values were calculated at the B3LYP/def2-TZVP level of theory.

^bThe experimental values were obtained in an argon matrix at 3 K.

Table 10.24: Spectroscopic data of singlet ammonia complex S-61.

mode	u: ν/cm^{-1} (calc.) ^a	u: I_{rel} (calc.) ^a	d: ν/cm^{-1} (calc.) ^a	d: I_{rel} (calc.) ^a	ν/cm^{-1} (Ar) ^b	I_{rel} (Ar) ^b	assignment
31	751.1	3.0	748.4	3.0	737.1	76.6	C=C def. (oop)
33			791.1	5.4	776.6	32.6	C-H def. (oop)
34	825.0	12.6			819.3	40.3	C-H def. (oop)
38			910.6	11.3	878.9	100.0	C-H def. (oop)
43			1031.3	56.7	1004.7	20.0	N-H def. (ip)
44	1048.7	27.4			1027.8	18.0	O---NH3 def. (ip)
45	1053.1	25.3			1034.7	19.5	O---NH3 def. (ip)
46	1102.5	17.8	1101.2	20.8	1085.8	30.2	C-H def. (ip)
47	1114.0	63.4	1105.3	32.0	1085.8		N-H def. (ip)
48	1132.0	38.2	1135.8	22.3	1109.3	79.2	C-H def. (ip)
49	1179.3	28.6	1179.4	40.7	1153.4	32.3	O-H def. (ip)
50	1191.4	27.5	1190.1	10.2	1173.9	74.4	C-H def. (ip)
51	1196.6	16.3	1194.2	20.6	1173.9		C-H def. (ip)
53			1234.8	61.4	1206.6	12.5	Ar-C str.
53	1240.4	17.4			1214.4	17.9	Ar-C str.
54			1256.8	48.0	1242.8	16.2	C-O str.
54	1265.7	24.1			1251.2	27.0	C-O str.
55	1299.8	18.8	1302.2	12.0	1277.2	1.3	asym. C-C-C str.
57	1342.5	13.7			1305.3	35.1	C-H def. (ip)
58	1425.3	22.0	1428.8	3.7	1377.9	70.8	C-H def. (ip)
59	1461.9	9.7			1432.5	29.9	C-H def. (ip)
60			1479.1	9.9	1442.1	69.0	C-H def. (ip)
61			1495.6	5.8	1457.5	99.2	C-H def. (ip)
62	1517.0	25.6	1517.5	37.8	1487.2	22.6	C-H def. (ip)
63	1607.7	15.8	1606.3	35.4	1586.0	46.9	C=C str.

^aThe theoretical values were calculated at the B3LYP/def2-TZVP level of theory.

^bThe experimental values were obtained in an argon matrix at 3 K.

Table 10.25: Spectroscopic data of singlet ammonia complex S-62.

mode	u: ν/cm^{-1} (calc.) ^a	u: I_{rel} (calc.) ^a	d: ν/cm^{-1} (calc.) ^a	d: I_{rel} (calc.) ^a	ν/cm^{-1} (Ar) ^b	I_{rel} (Ar) ^b	assignment
30	751.7	0.6	750.9	0.9	737.1	46.7	C=C def. (oop)
33	832.7	0.8			819.3	24.6	C-H def. (oop)
36			882.5	1.4	857.3	16.8	C-H def. (oop)
36	893.5	0.9			869.2	71.6	C-H def. (oop)
37	908.2	0.5			878.9	61.0	C-H def. (oop)
39			950.0	1.5	899.9	100.0	O-H def. (oop)
40			950.6	2.3	899.9		O-H def. (oop)
40	971.6	3.1			907.4	32.1	O-H def. (oop)
41	972.8	0.4			907.4		O-H def. (oop)
45	1101.9	2.2	1100.8	2.5	1085.8	18.5	C-H def. (ip)
46			1112.1	9.8	1085.8		N-H def. (ip)
46	1120.7	9.7			1103.2	6.0	N-H def. (ip)
47	1133.7	9.7	1129.8	5.4	1109.3	48.3	N-H def. (ip)
48	1137.6	2.5	1133.0	7.4	1109.3		C-H def. (ip)
49	1183.5	1.0	1179.9	1.5	1153.4	19.7	Ar-C str.
52	1244.7	10.7			1224.8	8.2	Ar-C str.
52			1249.2	3.8	1229.1	10.3	Ar-C str.
54	1291.2	5.7	1282.9	22.3	1265.1	9.7	O-H def. (ip)
55	1305.1	1.1	1303.8	0.7	1277.2	0.8	C-H def. (ip)
56	1341.8	1.6	1340.9	3.5	1305.3	21.4	O-H str.
57	1387.1	1.8	1387.8	3.2	1339.7	33.7	O-H def. (ip)
58	1434.9	10.0			1377.9	43.2	O-H def. (ip)
59	1461.4	3.3			1432.5	18.2	C-H def. (ip)
59			1471.8	2.2	1442.1	42.1	C-H def. (ip)
60	1486.8	1.7			1449.6	23.5	C-H def. (ip)
60			1492.7	0.5	1457.5	60.5	O-H def. (ip)
61			1497.7	6.9	1457.5		O-H def. (ip)
61	1507.7	6.1			1468.5	3.4	C-H def. (ip)
62			1518.9	9.1	1487.2	13.8	C-H def. (ip)
62	1542.3	0.8			1504.4	7.2	O-H def. (ip)
63	1603.9	1.6	1603.7	9.7	1586.0	28.6	C=C str.
68	1666.1	1.1	1667.2	1.4	1646.0	39.3	N-H def. (oop)
69	1667.1	1.3	1667.4	2.5	1646.0		N-H def. (oop)

^aThe theoretical values were calculated at the B3LYP/def2-TZVP level of theory.

^bThe experimental values were obtained in an argon matrix at 3 K.

Table 10.26: Spectroscopic data of amine **66**.

mode	u: ν/cm^{-1} (calc.) ^a	u: I_{rel} (calc.) ^a	d: ν/cm^{-1} (calc.) ^a	d: I_{rel} (calc.) ^a	ν/cm^{-1} (Ar) ^b	I_{rel} (Ar) ^b	assignment
23	754.4	28.3	753.6	21.1	740.8	35.3	C-H def. (oop)
25			793.1	29.3	770.0	18.8	N-H def. (oop)
27			838.9	17.3	812.8	11.8	C-H def. (oop)
31			918.4	8.9	897.2	8.1	C-H def. (oop)
41	1182.8	100.0	1183.6	100.0	1159.9	95.8	O-H def. (ip)
45	1235.0	9.9	1235.5	19.1	1216.8	23.3	C-O str.
46			1263.1	19.3	1249.5	48.2	C-H def. (ip)
47			1275.6	6.6	1256.7	19.6	C-H def. (ip)
48	1327.8	37.0			1292.6	67.6	C-O str.
49	1335.7	27.2	1338.7	12.4	1300.9	26.5	NC-H def. (oop)
50	1341.2	10.3	1341.9	8.4	1300.9		NC-H def. (oop)
52	1390.3	39.2			1353.5	61.5	C=C str.
53	1482.7	24.4	1480.2	12.2	1446.0	100.0	C-H def. (ip)
54			1490.9	11.5	1461.9	85.3	C-H def. (ip)
56			1525.4	30.0	1495.0	19.5	C-H def. (ip)
56	1533.1	23.6			1502.3	31.7	C-H def. (ip)
57	1624.9	9.7			1585.2	14.3	C=C str.
58	1630.9	20.7	1638.4	5.0	1591.8	56.7	C=C str.

^aThe theoretical values were calculated at the B3LYP/def2-TZVP level of theory.

^bThe experimental values were obtained in an argon matrix at 3 K.

Table 10.27: Spectroscopic data of carbonyl oxide **86**.

mode	ν/cm^{-1} (calc.) ^a	I_{rel} (calc.) ^a	ν/cm^{-1} (Xe) ^b	I_{rel} (Xe) ^b	ν/cm^{-1} (N ₂) ^c	I_{rel} (N ₂) ^c	assignment
27	673.2	5.2	655.0	16.8	659.4	30.2	C=C def. (oop)
29	712.3	8.0	696.5	15.4	700.3	11.8	C=C def. (oop)
31	784.9	2.7	766.5	20.3			C=C def. (oop)
32	788.8	7.1	766.5				C-H def. (oop)
34	844.4	9.2	818.6	3.9	826.9	6.3	C-H def. (oop)
36	925.3	20.0	865.4	12.2	863.9	8.6	O-O str.
38	964.7	7.2			944.0	16.4	sym. Me-N-Me str.
43	1007.1	9.1	974.1	4.2	979.2	13.1	O-O str.
45	1028.4	4.9	1003.1	10.8	1001.9	11.7	C=C def. (ip)
47	1080.9	5.5			1065.2	28.6	asym. Me-N-Me str.
51	1171.7	2.8			1149.9	14.1	C-H def. (ip)
52	1185.2	22.6			1168.1	29.4	sym. C-C-C str.
55	1218.5	2.5	1201.8	69.0	1197.5	20.1	C-H def. (ip)
56	1246.3	31.2	1210.0	12.6	1218.2	9.3	C-H def. (ip)
57	1272.2	5.7	1246.6	3.9	1235.5	9.1	asym. Me-N-Me str.
58	1312.5	5.9	1284.5	35.3	1285.1	18.9	asym. C-C-C str.
62	1381.5	19.6			1350.2	33.6	asym. C-C-C str.
63	1398.0	74.2			1377.7	100.0	C-N str.
64	1428.5	69.0	1396.8	30.8			C-O str.
66	1478.9	2.8	1441.8	3.0	1438.1	17.0	C-H def. (ip)
68	1489.4	14.4	1455.9	6.8	1444.3	21.6	methyl C-H def. (ip)
69	1494.6	5.4	1457.7	12.2	1450.8	28.5	methyl C-H def. (ip)
70	1495.6	3.0	1457.7		1450.8		methyl C-H def. (oop)
72	1530.0	6.8	1495.1	4.5	1491.9	26.5	methyl C-H def. (oop)
73	1531.9	11.1	1495.1		1491.9		C-H def. (ip)
74	1562.5	10.8	1537.8	12.7	1528.8	19.6	C-H def. (ip)
75	1569.1	8.1	1541.2	13.0	1534.0	11.6	C=C str.
77	1642.0	9.0	1603.0	100.0	1598.5	16.5	C=C str.
78	1649.3	100.0	1605.8	71.0	1601.5	15.2	C=C str.

^aThe theoretical values were calculated at the B3LYP/def2-TZVP level of theory.

^bThe experimental values were obtained in a xenon matrix at 3 K.

^cThe experimental values were obtained in a nitrogen matrix at 3 K.

Table 10.28: Spectroscopic data of dioxirane **87**.

mode	ν/cm^{-1} (calc.) ^a	I_{rel} (calc.) ^a	ν/cm^{-1} (Xe) ^b	I_{rel} (Xe) ^b	ν/cm^{-1} (N ₂) ^c	I_{rel} (N ₂) ^c	assignment
30	768.0	10.7	743.5	58.2	750.9	100.0	C=C def. (ip)
31	781.0	10.2	760.3	47.0	763.3	64.0	C-H def. (oop)
33	829.3	23.7	810.2	43.7	815.6	43.5	C-H def. (oop)
37	932.4	18.1	917.9	27.4			C-H def. (oop)
38	952.7	7.0	932.6	22.7			C-H def. (oop)
47	1081.2	10.6	1066.9	32.0	1061.1	24.6	asym. Me-N-Me str.
50	1144.3	15.9	1127.4	21.9	1128.7	31.0	methyl C-H def. (oop)
54	1197.7	11.9	1175.7	55.5	1172.2	18.4	methyl C-H def. (ip)
56	1235.9	59.0	1195.8	100.0	1198.3	54.8	C-H def. (ip)
57	1268.6	11.9	1251.2	4.4	1258.2	14.5	asym. Me-N-Me str.
58	1306.2	55.6	1270.7	86.2	1278.7	19.8	asym C-C-C str.
59	1310.2	38.7	1270.7		1278.7		C-O str.
60	1336.8	34.4	1304.6	35.3	1307.7	10.8	asym. C-C-C str.
61	1358.3	10.5	1320.8	36.0	1333.9	15.3	C-H def. (ip)
63	1366.7	8.9	1331.7	25.2	1343.5	12.1	C-H def. (ip)
64	1385.9	83.7	1347.8	24.1	1366.3	34.0	C-N str.
67	1484.7	8.0	1445.7	15.6	1453.5	10.6	C-H def. (ip)
69	1490.6	4.7	1449.5	18.4			methyl C-H def. (ip)
70	1494.9	6.6	1452.4	18.0			methyl C-H def. (oop)
72	1531.0	24.2	1490.8	45.4	1486.2	7.6	methyl C-H def. (ip)
74	1564.6	61.9	1527.7	37.1	1536.4	17.3	C-H def. (ip)
75	1596.5	10.3	1564.6	52.0	1563.9	12.0	C=C str.
78	1657.8	100.0	1616.4	76.9	1620.1	37.8	C=C str.

^aThe theoretical values were calculated at the B3LYP/def2-TZVP level of theory.

^bThe experimental values were obtained in a xenon matrix at 3 K.

^cThe experimental values were obtained in a nitrogen matrix at 3 K.

Table 10.29: Spectroscopic data of ketone **88**.

mode	ν/cm^{-1} (calc.) ^a	I_{rel} (calc.) ^a	ν/cm^{-1} (N ₂) ^b	I_{rel} (N ₂) ^b	assignment
25	690.0	6.7	679.9	27.7	C=C def. (ip)
28	763.2	4.8	750.9	100.0	C=C def. (oop)
30	812.0	3.1	805.5	29.8	C-H def. (oop)
44	1081.4	5.7	1061.1	24.6	asym. Me-N-Me str.
47	1142.5	6.1	1123.9	15.4	methyl C-H def. (oop)
49	1171.7	13.4	1153.1	27.9	sym. C-C-C str.
51	1199.4	3.0	1172.2	18.4	methyl C-H def. (ip)
52	1212.3	9.9	1176.5	15.5	C-H def. (ip)
53	1235.4	46.1	1198.3	54.8	C-H def. (ip)
54	1271.2	6.9	1258.2	14.5	asym. Me-N-Me str.
55	1301.4	78.1	1270.1	9.2	asym. C-C-C str.
56	1333.5	11.3	1303.2	8.3	asym. C-C-C str.
57	1350.0	14.2	1321.8	19.0	C-H def. (ip)
60	1391.4	53.6	1380.2	48.9	C-N str.
62	1471.1	3.4	1440.3	21.1	C-H def. (ip)
63	1480.7	2.8	1453.5	10.6	C-H def. (ip)
69	1531.1	15.7	1493.8	10.3	methyl C-H def. (ip)
70	1561.2	19.4	1531.8	28.0	C-H def. (ip)
71	1584.0	9.2	1552.1	31.5	C=C str.
73	1640.1	21.2	1593.4	31.9	C=C str.
74	1646.0	100.0	1593.4		C=C str.
75	1699.9	32.8	1666.4	3.5	C=O str.

^aThe theoretical values were calculated at the B3LYP/def2-TZVP level of theory.

^bThe experimental values were obtained in a nitrogen matrix at 3 K.

Table 10.30: Spectroscopic data of ester **89**.

mode	u: ν/cm^{-1} (calc.) ^a	u: I_{rel} (calc.) ^a	d: ν/cm^{-1} (calc.) ^a	d: I_{rel} (calc.) ^a	ν/cm^{-1} (N ₂) ^b	I_{rel} (N ₂) ^b	assignment
78	1770.8	36.1			1734.2	100.0	C=O str.
78			1786.5	100.0	1746.9	100.0	C=O str.

^aThe theoretical values were calculated at the B3LYP/def2-TZVP level of theory.

^bThe experimental values were obtained in a nitrogen matrix at 3 K.

Table 10.31: Spectroscopic data of ester **90**.

mode	u: ν/cm^{-1} (calc.) ^a	u: I_{rel} (calc.) ^a	d: ν/cm^{-1} (calc.) ^a	d: I_{rel} (calc.) ^a	ν/cm^{-1} (N ₂) ^b	I_{rel} (N ₂) ^b	assignment
78	1777.8	42.8			1739.7	100.0	C=O str.
78			1791.9	90.1	1754.0	100.0	C=O str.

^aThe theoretical values were calculated at the B3LYP/def2-TZVP level of theory.

^bThe experimental values were obtained in a nitrogen matrix at 3 K.

Table 10.32: Spectroscopic data of ketene **91**.

mode	ν/cm^{-1} (calc.) ^a	I_{rel} (calc.) ^a	ν/cm^{-1} (Ar) ^b	I_{rel} (Ar) ^b	assignment
29	708.5	3.3	693.9	8.4	C=C def. (oop)
31	770.1	3.7	754.8	4.1	C-H def. (oop)
34	835.3	4.5	817.2	8.7	C-H def. (oop)
41	967.7	2.4	945.2	2.2	sym. Me-N-Me str.
46	1080.7	2.4	1064.3	3.4	asym. Me-N-Me str.
49	1140.4	2.1	1125.5	2.7	sym. C-C-C str.
50	1147.1	2.5	1125.5		methyl C-H def. (oop)
53	1196.0	2.1	1171.6	3.9	methyl C-H def. (ip)
56	1264.7	4.5	1243.1	1.9	asym. Me-N-Me str.
57	1300.3	1.8	1276.1	1.4	asym. C-C-C str.
58	1314.0	1.1	1289.3	0.5	asym. C-C-C str.
60	1355.4	1.0	1334.1	2.3	C-H def. (ip)
62	1377.9	9.2	1356.5	14.7	C-N str.
63	1380.7	13.7	1356.5		C-N str.
66	1486.0	1.2	1448.8	2.5	C-H def. (ip)
68	1489.7	1.3	1448.8		methyl C-H def. (ip)
69	1494.4	2.0	1448.8		methyl C-H def. (oop)
71	1530.0	7.3	1490.4	4.6	methyl C-H def. (ip)
72	1532.2	3.8	1497.9	3.3	C-H def. (ip)
73	1556.4	23.9	1524.0	13.0	C-H def. (ip)
76	1640.9	5.3	1607.1	18.8	C=C str.
77	1654.2	13.9	1607.1		C=C str.
78	2170.6	100.0	2101.9	100.0	C=C=O str.

^aThe theoretical values were calculated at the B3LYP/def2-TZVP level of theory.

^bThe experimental values were obtained in an argon matrix at 3 K.

Table 10.33: Spectroscopic data of carbonyl oxide **92**.

mode	u: ν/cm^{-1} (calc.) ^a	u: I_{rel} (calc.) ^a	d: ν/cm^{-1} (calc.) ^a	d: I_{rel} (calc.) ^a	ν/cm^{-1} (Ar) ^b	I_{rel} (Ar) ^b	assignment
22	714.3	9.4	715.1	9.6	703.4	55.9	C=C def. (ip)
23	749.7	15.0	748.6	16.1	734.9	73.4	C-H def. (oop)
26			789.8	8.4	776.3	17.6	C-H def. (oop)
27	826.5	14.9			815.9	7.7	C-H def. (oop)
30			903.6	7.3	869.7	46.7	C-H def. (oop)
30	905.7	6.7			879.9	60.7	C-H def. (ip)
31	940.1	50.0			900.1	100.0	O-O str.
31			941.1	61.7	907.8	29.9	O-O str.
35	1000.8	31.3	1001.1	40.9	972.9	41.1	O-O str.
38	1112.3	14.2	1111.7	6.4	1085.0	12.1	C-H def. (ip)
39	1129.9	41.5	1127.5	8.6	1113.7	43.2	C-H def. (ip)
40	1181.1	51.5	1183.0	96.9	1153.6	6.7	O-H def. (ip)
42	1195.6	18.5	1195.4	12.8	1172.9	36.7	O-H def. (ip)
45	1270.4	17.8	1266.7	100.0	1249.1	38.5	O-H def. (ip)
46	1328.5	32.8	1331.3	9.3	1304.9	19.6	C-O def.
47			1338.7	12.7	1304.9		C-H def. (ip)
48	1368.8	15.3	1369.4	13.4	1339.9	21.2	asym. C-C-C str.
49	1407.6	44.9			1377.8	42.9	O-H def. (ip)
50	1475.4	24.2	1474.4	25.8	1442.4	32.7	C-H def. (ip)
51			1485.4	20.4	1457.5	48.3	C-H def. (ip)
53			1516.5	24.0	1486.7	13.6	C-H def. (ip)
54	1542.4	26.6	1542.4	27.4	1506.1	12.3	C=O str.
55	1621.2	9.1	1620.6	42.5	1586.3	17.3	C=C str.
57	1646.3	11.6	1646.6	9.8	1602.3	5.8	C=C str.
57			1649.8	98.8	1612.8	77.4	C=C str.
58	1650.9	100.0			1617.0	68.5	C=C str.

^aThe theoretical values were calculated at the B3LYP/def2-TZVP level of theory.^bThe experimental values were obtained in an argon matrix at 9 K.**Table 10.34:** Spectroscopic data of dioxirane **93**.

mode	u: ν/cm^{-1} (calc.) ^a	u: I_{rel} (calc.) ^a	d: ν/cm^{-1} (calc.) ^a	d: I_{rel} (calc.) ^a	ν/cm^{-1} (Ar) ^b	I_{rel} (Ar) ^b	assignment
24	766.1	30.9	765.3	26.5	754.5	42.8	C-H def. (oop)
25			790.9	6.6	770.7	37.5	C-H def. (oop)
29	887.0	8.3			877.2	17.7	C-H def. (oop)
32	935.5	22.3	933.5	13.3	920.3	54.7	asym. C-C-C str.
39	1134.9	22.9			1110.9	30.4	C-H def. (ip)
41	1184.8	100.0	1182.5	100.0	1174.3	30.3	O-H def. (ip)
43	1219.5	6.8	1221.9	9.8	1192.4	19.4	C-H def. (ip)
45	1266.7	11.9	1264.8	61.8	1234.6	56.9	O-H str.
46	1326.5	34.5	1328.3	13.6	1300.6	75.2	O-H str.
47	1330.0	5.5	1331.8	5.1	1300.6		C-H def. (ip)
48	1346.2	28.6	1348.0	6.2	1315.8	20.4	asym. C-C-C str.
49	1386.8	95.0	1388.4	77.3	1363.0	64.0	dioxirane C-O str.
50	1404.2	29.6			1379.8	21.4	O-H def. (ip)
51	1480.8	28.3	1479.0	7.8	1447.5	100.0	C-H def. (ip)
52			1491.4	16.7	1452.5	31.5	C-H def. (ip)
55	1630.8	22.0	1632.0	7.9	1595.2	48.5	C=C str.
56	1636.1	18.3	1643.3	10.3	1604.0	39.1	C=C str.
58	1665.0	71.2	1660.0	54.2	1631.6	41.5	C=C str.

^aThe theoretical values were calculated at the B3LYP/def2-TZVP level of theory.^bThe experimental values were obtained in an argon matrix at 9 K.

Table 10.35: Spectroscopic data of ketone **94**.

mode	u: v/cm ⁻¹ (calc.) ^a	u: I _{rel} (calc.) ^a	d: v/cm ⁻¹ (calc.) ^a	d: I _{rel} (calc.) ^a	v/cm ⁻¹ (Ar) ^b	I _{rel} (Ar) ^b	assignment
14			517.9	8.9	503.2	7.9	skel. vib.
18	655.6	3.8			638.0	7.1	C=C def. (ip)
19	687.7	8.3	688.6	8.2	680.1	7.7	C=C def. (oop)
22			754.6	15.6	737.2	6.3	C-H def. (oop)
22	755.8	18.7			740.9	16.9	C-H def. (oop)
23			791.6	7.6	778.3	3.3	C-H def. (oop)
24	808.6	8.8			793.6	7.7	C-H def. (oop)
26			865.2	12.3	845.2	20.5	C-H def. (oop)
29			937.5	18.0	923.4	25.8	asym. C-C-C str.
29	939.6	24.5			937.6	15.7	asym. C-C-C str.
36	1124.2	47.9	1122.4	14.7	1073.7	14.3	C-H def. (ip)
37	1175.0	24.9	1177.2	10.6	1151.6	38.1	C-H def. (ip)
38	1186.5	47.0	1180.6	73.8	1168.6	84.1	O-H def. (ip)
39			1194.1	11.4	1168.6		C-H def. (ip)
40			1211.1	10.0	1194.0	20.1	asym. C-C-C str.
43	1322.3	10.8	1321.0	23.0	1269.2	83.1	C-H def. (ip)
44	1326.1	23.2			1279.5	100.0	C-OH str.
45	1341.3	19.4			1308.4	35.1	O-H def. (ip)
46	1410.0	33.3			1377.0	17.1	O-H def. (ip)
47	1480.5	19.6	1475.9	7.6	1433.7	17.7	C-H def. (ip)
47			1488.5	9.9	1449.3	17.6	C-H def. (ip)
50	1527.3	5.1			1513.5	16.8	C-H def. (ip)
51	1631.0	27.2	1631.7	39.9	1595.0	30.2	C=C str.
52	1634.6	11.4	1634.9	24.3	1595.0		C=C str.
53	1639.3	20.9	1641.2	20.3	1602.8	19.1	C=C str.
54	1654.6	82.5	1651.2	60.1	1611.1	81.5	C=C str.
55	1775.3	100.0	1776.3	100.0	1670.3	76.9	C=O str.

^aThe theoretical values were calculated at the B3LYP/def2-TZVP level of theory.

^bThe experimental values were obtained in an argon matrix at 9 K.

Table 10.36: Spectroscopic data of lactone **95**.

mode	u: ν/cm^{-1} (calc.) ^a	u: I_{rel} (calc.) ^a	d: ν/cm^{-1} (calc.) ^a	d: I_{rel} (calc.) ^a	ν/cm^{-1} (Ar) ^b	I_{rel} (Ar) ^b	assignment
27	824.7	9.5			811.1	13.5	C-H def. (oop)
28			849.6	8.7	833.1	38.6	C-H def. (oop)
29	894.1	7.4	895.4	4.1	884.3	3.8	C=C def. (ip)
32	931.1	1.9			921.0	15.4	C=C def. (ip)
36	1059.7	16.9	1060.1	15.7	1037.6	33.6	OC-O str.
37	1092.0	18.2	1092.5	17.3	1075.1	46.1	OC-O str.
38	1125.8	3.6	1124.0	4.6	1092.8	22.0	C-H def. (ip)
39	1162.5	4.1	1156.5	2.8	1133.2	35.7	C-H def. (ip)
40	1194.7	29.0	1187.8	43.2	1169.4	57.7	O-H def. (ip)
41	1200.6	2.6			1169.4		C-H def. (ip)
47	1336.2	38.4	1342.3	11.7	1316.0	67.4	C-OH str.
47			1466.8	19.4	1437.0	29.2	C-H def. (ip)
51	1485.9	4.3			1450.0	62.7	C-H def. (ip)
52	1531.0	9.8	1529.0	22.7	1500.0	85.6	C-H def. (ip)
53	1533.9	17.4			1500.0		C-H def. (ip)
53			1539.8	4.3	1508.6	22.1	C-H def. (ip)
54	1604.7	12.2	1607.0	7.0	1591.8	21.9	C=C def.
56	1648.1	5.9	1648.0	6.0	1625.9	36.7	C=C def.
57			1659.0	4.4	1632.0	26.0	C=C str.
58	1793.5	100.0	1793.5	100.0	1747.8	100.0	C=O str.

^aThe theoretical values were calculated at the B3LYP/def2-TZVP level of theory.

^bThe experimental values were obtained in an argon matrix at 9 K.

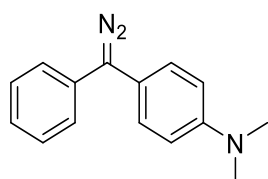
Table 10.37: Spectroscopic data of lactone **96**.

mode	u: ν/cm^{-1} (calc.) ^a	u: I_{rel} (calc.) ^a	d: ν/cm^{-1} (calc.) ^a	d: I_{rel} (calc.) ^a	ν/cm^{-1} (Ar) ^b	I_{rel} (Ar) ^b	assignment
25	765.3	17.4	763.6	15.3	751.8	48.8	C-H def. (oop)
30	908.7	3.9	908.3	3.3	888.8	6.4	C=C def. (ip)
35	1039.8	11.2	1038.4	9.7	1021.2	31.0	OC-O str.
37	1082.0	25.1	1079.8	25.0	1070.0	29.4	OC-O str.
38	1128.8	8.1	1126.5	4.6	1092.8	14.4	C-H def. (ip)
39	1164.0	15.9			1133.2	23.3	C-H def. (ip)
40	1193.3	3.5	1190.5	36.0	1169.4	37.7	C-H def. (ip)
41	1197.7	29.9	1195.3	14.5	1169.4		O-H def. (ip)
47	1344.7	17.2	1348.4	6.4	1316.0	44.0	C-OH str.
50			1469.5	13.6	1437.0	19.1	C-H def. (ip)
51	1487.7	9.2			1450.0	40.9	C-H def. (ip)
52	1531.3	9.3	1532.8	3.0	1500.0	55.8	C-H def. (ip)
53			1539.3	8.2	1508.6	14.4	C-H def. (ip)
54	1603.0	11.5	1609.5	3.5	1591.8	14.3	C=C str.
56	1650.1	12.3	1647.4	39.5	1625.9	23.9	C=C str.
57	1658.6	37.4			1632.0	17.0	C=C str.
58	1793.9	100.0	1795.5	100.0	1754.7	100.0	C=O str.

^aThe theoretical values were calculated at the B3LYP/def2-TZVP level of theory.

^bThe experimental values were obtained in an argon matrix at 9 K.

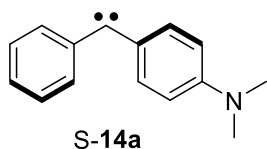
10.2. Optimized geometries



17

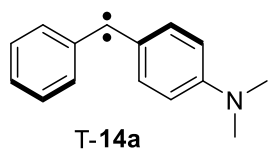
B3LYP/def2-TZVP
 E = -744.860042
 ZPVE = 0.268278

C	-4.61855000	-1.75238300	-0.29379000
C	-3.35385600	-2.11261900	-0.74676900
C	-2.28210900	-1.23999200	-0.62200000
C	-2.44893800	0.02025200	-0.02909800
C	-3.72940300	0.37184200	0.42526900
C	-4.79779500	-0.50187900	0.28912200
H	-5.45236100	-2.43500600	-0.39407300
H	-3.19938200	-3.07898100	-1.21087200
H	-1.30980300	-1.52882900	-0.99640700
H	-3.88969500	1.33361300	0.89686700
H	-5.77537500	-0.20635500	0.64944400
C	0.11816800	0.57655000	0.07151500
C	0.57934400	-0.57200900	0.72217700
C	1.07141700	1.36975800	-0.57264400
C	1.91901000	-0.91850900	0.72329500
H	-0.12534600	-1.21070200	1.23869200
C	2.41719900	1.04516700	-0.56548000
H	0.75629100	2.26125300	-1.10204900
C	2.88566800	-0.11011200	0.09098500
H	2.21108900	-1.82262300	1.23566500
H	3.10226200	1.69542100	-1.08790200
N	4.23072100	-0.43202400	0.12071100
C	5.15471700	0.29821800	-0.72453900
H	6.16314900	-0.07295300	-0.55637800
H	4.92328700	0.19455900	-1.79345600
H	5.15321200	1.36314900	-0.48066300
C	4.63906300	-1.73474900	0.60819500
H	5.72373400	-1.80633700	0.57180500
H	4.33655500	-1.87890000	1.64801800
H	4.21953200	-2.55903100	0.01534500
C	-1.31200000	0.94228900	0.08801100
N	-1.58695800	2.21077800	0.21610400
N	-1.82787300	3.31564200	0.31753900



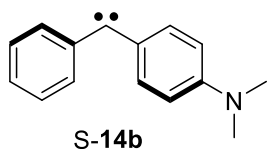
B3LYP/def2-TZVP
 E = -635.270093
 ZPVE = 0.257385

C	2.61497500	-0.01500500	-0.04250500
C	1.54309500	-0.86611400	-0.42095200
C	0.24551500	-0.41965500	-0.38796200
C	-0.09100500	0.91449800	-0.02434600
C	1.00055400	1.76260200	0.29887500
C	2.29888300	1.31990400	0.32453600
H	1.73986600	-1.87889700	-0.73955000
H	-0.54865200	-1.09371400	-0.68125800
H	0.77037600	2.79071900	0.54807500
H	3.08196800	2.00799500	0.60447400
C	-1.39631600	1.45532200	-0.01815800
C	-2.52614600	0.57838600	0.02138300
C	-3.62992900	0.82393000	-0.82775700
C	-2.64073800	-0.48801400	0.94610000
C	-4.74595200	0.00696400	-0.80254600
H	-3.57554200	1.66288800	-1.50965600
C	-3.79608200	-1.25192000	1.01713700
H	-1.82358600	-0.67777200	1.63043800
C	-4.84503100	-1.02629000	0.13064000
H	-5.56403600	0.19478600	-1.48747900
H	-3.87231500	-2.04214000	1.75472600
H	-5.73842200	-1.63617600	0.17576300
N	3.90332100	-0.45899900	-0.04740800
C	4.21259200	-1.82367200	-0.44249100
H	3.91711500	-2.02185500	-1.47738300
H	5.28380900	-1.98563900	-0.36066000
H	3.71068700	-2.55053700	0.20210400
C	4.99333900	0.43596400	0.30655400
H	4.88218100	0.81964200	1.32464400
H	5.93318400	-0.10644000	0.25285000
H	5.05358800	1.28874000	-0.37628600



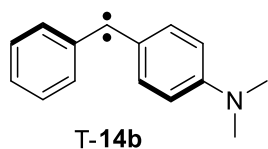
B3LYP/def2-TZVP
 E = -635.272537
 ZPVE = 0.256197

C	2.76413800	0.01157900	-0.01981900
C	1.79865300	0.94735800	0.41781900
C	0.46089800	0.62654500	0.47543400
C	-0.02205400	-0.65530100	0.09588700
C	0.95744500	-1.59306800	-0.31765400
C	2.29597200	-1.27564200	-0.37152700
H	2.09933800	1.93830700	0.72406600
H	-0.24554900	1.36657600	0.82872200
H	0.63687200	-2.58866800	-0.59688700
H	2.98939500	-2.03826100	-0.69296900
C	-1.37416000	-0.98498600	0.17477300
C	-2.63914800	-0.40840300	0.06048000
C	-3.78603900	-1.02462500	0.62847000
C	-2.83601800	0.80883600	-0.65285000
C	-5.03749100	-0.45365800	0.50020700
H	-3.66035900	-1.95393700	1.16901400
C	-4.09364900	1.37004800	-0.76377900
H	-1.98189300	1.28663900	-1.11473500
C	-5.20447000	0.74795900	-0.19098000
H	-5.89581900	-0.94295500	0.94429700
H	-4.21732300	2.29848600	-1.30844900
H	-6.18720300	1.19135700	-0.28560900
N	4.10156600	0.34061800	-0.10345900
C	4.56723200	1.60081800	0.44209500
H	4.39738500	1.67914000	1.52392700
H	5.63434100	1.69847400	0.25684300
H	4.07094000	2.44632600	-0.04021900
C	5.08103400	-0.69520600	-0.36907500
H	4.88763100	-1.18458400	-1.32660100
H	6.07010800	-0.24665400	-0.42450400
H	5.09705100	-1.46809400	0.41043700



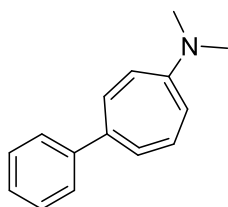
B3LYP/def2-TZVP
 E = -635.270093
 ZPVE = 0.257385

C	4.84503800	-1.02628200	0.13065500
C	4.74595400	0.00695300	-0.80255100
C	3.62992800	0.82391400	-0.82777900
C	2.52614600	0.57838300	0.02136700
C	2.64074200	-0.48800200	0.94610400
C	3.79609000	-1.25190200	1.01715500
H	5.73843200	-1.63616200	0.17578900
H	5.56403800	0.19476600	-1.48748800
H	3.57553600	1.66285700	-1.50969700
H	1.82358900	-0.67775100	1.63044300
H	3.87232600	-2.04210800	1.75475700
C	1.39631600	1.45531500	-0.01817300
C	0.09100300	0.91449700	-0.02434100
C	-1.00055500	1.76260000	0.29888200
C	-0.24551700	-0.41965600	-0.38795900
C	-2.29888300	1.31990300	0.32454000
H	-0.77037800	2.79071800	0.54808400
C	-1.54309800	-0.86611400	-0.42095500
H	0.54865000	-1.09371400	-0.68125600
C	-2.61497600	-0.01500800	-0.04250100
H	-3.08197100	2.00799300	0.60447000
H	-1.73986900	-1.87889400	-0.73956500
N	-3.90332300	-0.45900200	-0.04739600
C	-4.21259700	-1.82366900	-0.44249700
H	-5.28381100	-1.98564100	-0.36064500
H	-3.91714000	-2.02183400	-1.47739800
H	-3.71067500	-2.55054200	0.20207600
C	-4.99334100	0.43596400	0.30655300
H	-5.93318500	-0.10644500	0.25287400
H	-4.88217500	0.81966800	1.32463300
H	-5.05360300	1.28872500	-0.37630600



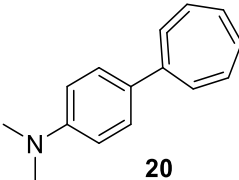
B3LYP/def2-TZVP
 E = -635.272532
 ZPVE = 0.256165

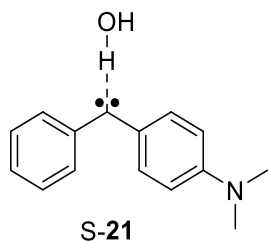
C	5.19305900	-0.76722200	0.22251100
C	5.04354700	0.44720900	-0.45005000
C	3.79729500	1.02700000	-0.58877800
C	2.63803100	0.40702400	-0.05066800
C	2.81699600	-0.82371000	0.64407200
C	4.06978200	-1.39343000	0.76580800
H	6.17185700	-1.21741600	0.32546000
H	5.91154800	0.93964300	-0.87128600
H	3.68522300	1.96630000	-1.11484900
H	1.95289500	-1.30516800	1.08306800
H	4.17977700	-2.33200000	1.29585800
C	1.37816000	0.99236200	-0.17504400
C	0.02290300	0.67031200	-0.12610800
C	-0.95634000	1.60303300	0.29947100
C	-0.46173300	-0.60088500	-0.53791100
C	-2.29763800	1.29401400	0.32432100
H	-0.63233800	2.58501000	0.61996700
C	-1.80234500	-0.91355000	-0.50943800
H	0.24681800	-1.34204200	-0.88457500
C	-2.77054900	0.02563800	-0.08509400
H	-2.98944500	2.04756700	0.66983200
H	-2.10306400	-1.90107000	-0.82663900
N	-4.11602300	-0.27793100	-0.08136400
C	-4.54781300	-1.63793200	-0.33859100
H	-5.63410800	-1.67960100	-0.31342600
H	-4.22825000	-1.97383100	-1.32822200
H	-4.15963900	-2.34841800	0.40275300
C	-5.06015000	0.64350700	0.52019400
H	-6.06706400	0.24867000	0.40775500
H	-4.87001400	0.80002000	1.58994600
H	-5.03126800	1.61763100	0.02574100

**19**

B3LYP/def2-TZVP
 E = -635.271094
 ZPVE = 0.257077

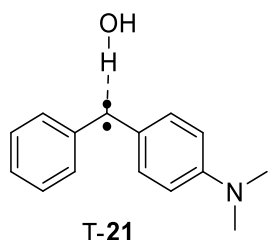
C	0.12910100	1.71317900	-0.45732800
C	0.71583400	0.54513600	-0.70630200
C	-0.16489800	-0.34044100	-1.47025400
C	-1.05903300	2.29405600	-0.29944900
C	-1.46636000	-0.50446900	-1.13688300
C	-2.11875100	1.49025600	0.23806400
C	-2.25665600	0.14874800	-0.08986200
H	0.22603500	-0.90651400	-2.31302500
H	-1.24183800	3.33072300	-0.56781900
H	-2.01676100	-1.22200300	-1.73371900
H	-2.86445900	1.96472600	0.86220800
C	2.03494200	0.11752000	-0.22353400
C	2.96706700	1.05453000	0.24287100
C	2.38862900	-1.23701500	-0.20270600
C	4.20063400	0.64850000	0.72684400
H	2.70971900	2.10572600	0.20704500
C	3.62980800	-1.64188500	0.27309100
H	1.67728000	-1.97996100	-0.54102400
C	4.54080100	-0.70244900	0.74169600
H	4.90696400	1.38800400	1.08378600
H	3.88295500	-2.69494000	0.28379500
H	5.50839000	-1.01749700	1.11154200
N	-3.27027800	-0.61017900	0.47068100
C	-4.29344200	0.03367700	1.26896400
H	-4.98510200	-0.71851000	1.64098900
H	-3.85740300	0.54515700	2.13178300
H	-4.86660400	0.77142700	0.69309600
C	-3.49836700	-1.98685200	0.07626700
H	-4.02016600	-2.08325400	-0.88621500
H	-2.55594200	-2.53072900	0.00868000
H	-4.10696900	-2.47604400	0.83522900

 <p>20</p> <p>B3LYP/def2-TZVP E = -635.274323 ZPVE = 0.257041</p>	C	2.52338600	-1.13870200	-0.43083200
	C	1.73499600	-0.07542200	-0.57996900
	C	2.50280100	1.13347400	-0.88464700
	C	3.69431100	-1.55871500	0.02913900
	C	3.61571400	1.44336100	-0.16894100
	C	4.35092200	-0.68304000	0.97790100
	C	4.28866700	0.67249700	0.84975900
	H	2.14119600	1.83538900	-1.63189100
	H	4.18839000	-2.46242700	-0.31462300
	H	4.05309500	2.42026900	-0.35581900
	H	4.98362600	-1.10193600	1.75605700
	H	4.90053600	1.25472700	1.53155400
	C	0.28563100	-0.05029500	-0.38014900
	C	-0.47312200	-1.22718300	-0.39154600
	C	-0.40188100	1.14628500	-0.15183800
	C	-1.83609900	-1.21860500	-0.16815200
	H	0.02475800	-2.16556600	-0.60302300
	C	-1.76823600	1.17360700	0.06789100
	H	0.14630500	2.07980100	-0.12220100
	C	-2.52780800	-0.01350100	0.08077300
H	-2.36813500	-2.15722900	-0.20476200	
H	-2.24137400	2.12839500	0.24066000	
N	-3.88765900	0.00151800	0.32714200	
C	-4.59552900	1.26649400	0.34131400	
H	-4.52439100	1.79995000	-0.61604000	
H	-5.64685100	1.08619700	0.55373900	
H	-4.21113100	1.92540700	1.12373500	
C	-4.66081200	-1.21131700	0.14705800	
H	-4.29155400	-2.01207000	0.79183300	
H	-5.69529900	-1.02034300	0.42358400	
H	-4.64321200	-1.57482900	-0.88936800	



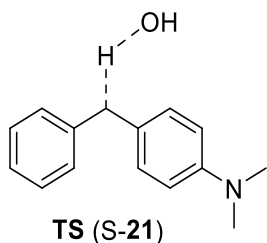
B3LYP/def2-TZVP
 E = -711.728919
 ZPVE = 0.281749

C	-2.73639800	-0.22843200	-0.04999300
C	-1.71051000	-1.15181600	-0.39283900
C	-0.39289100	-0.77574800	-0.37093900
C	0.01436300	0.54996200	-0.04474800
C	-1.03059000	1.47406300	0.23853200
C	-2.34956600	1.10133300	0.26516400
H	-1.96215200	-2.16140900	-0.68103400
H	0.36227500	-1.49975600	-0.64704900
H	-0.74966000	2.49898700	0.44937000
H	-3.09535100	1.84143200	0.51202900
C	1.34430500	1.01625100	-0.03621100
C	2.44282900	0.09483400	0.01147000
C	2.49159100	-1.00869300	0.89454900
C	3.57997200	0.33963200	-0.78955400
C	3.61435700	-1.81968000	0.96281700
H	1.65273800	-1.19036000	1.55397100
C	4.66709500	-0.51615700	-0.76797700
H	3.57759600	1.21011300	-1.43299700
C	4.69672400	-1.59353300	0.11759400
H	3.64196000	-2.64096900	1.66881000
H	5.51409300	-0.32650100	-1.41583600
H	5.56585800	-2.23761000	0.16182400
N	-4.04383700	-0.60246500	-0.04240500
C	-5.08650100	0.36341000	0.27126200
H	-6.05359900	-0.12981600	0.23228700
H	-4.95757500	0.77872900	1.27431900
H	-5.09688400	1.19041400	-0.44431900
C	-4.42668800	-1.96544900	-0.37795000
H	-5.50408500	-2.06735300	-0.28357400
H	-4.14966100	-2.22150200	-1.40496800
H	-3.95842500	-2.68868300	0.29487900
O	1.24782600	3.91952100	0.18433200
H	1.42234800	2.94262300	0.08985200
H	1.40621500	4.28289500	-0.69245100



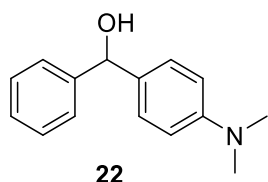
B3LYP/def2-TZVP
 E = -711.721985
 ZPVE = 0.279445

C	5.03735100	-1.31223600	0.12456100
C	3.89640100	-1.97209800	0.58499000
C	2.66575500	-1.34512300	0.56882100
C	2.52951900	-0.02003100	0.06403600
C	3.70562000	0.63334900	-0.39275500
C	4.92943100	-0.00627200	-0.35717900
H	5.99922200	-1.80782500	0.14611600
H	3.97553300	-2.98239400	0.96806300
H	1.78723700	-1.85346000	0.94415100
H	3.62746200	1.64577700	-0.76819000
H	5.81222700	0.51225700	-0.71033800
C	1.28878600	0.61702600	0.04353100
C	-0.07734800	0.34332900	0.05649600
C	-1.01916900	1.23624300	0.63018400
C	-0.61041400	-0.82389900	-0.55658600
C	-2.37014000	0.97669000	0.61504700
H	-0.66014600	2.15259600	1.08096900
C	-1.96044100	-1.08946200	-0.56246800
H	0.06855900	-1.51878000	-1.03361800
C	-2.88976400	-0.20369300	0.03267600
H	-3.03375200	1.69955600	1.06528300
H	-2.30067200	-1.99499700	-1.04242000
N	-4.23833100	-0.47826800	0.04475500
C	-4.75231000	-1.61808300	-0.68999000
H	-5.82650500	-1.68764800	-0.53762800
H	-4.56347000	-1.53931200	-1.76792300
H	-4.30705100	-2.55128500	-0.33543300
C	-5.17557300	0.51651300	0.53045800
H	-6.18299600	0.10998600	0.48836900
H	-4.96861400	0.78087900	1.57055700
H	-5.15232700	1.43735400	-0.06551000
O	1.47295700	3.62982800	-0.39564600
H	1.50767800	2.69700000	-0.12002600
H	0.91605000	3.61603600	-1.18146400



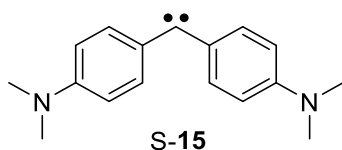
B3LYP/def2-TZVP
 E = -711.717141
 ZPVE = 0.278018

C	2.80101300	-0.18141400	-0.05350700
C	2.36311600	1.15512900	0.15007400
C	1.03518000	1.48125300	0.09030100
C	0.03148000	0.49381800	-0.13004100
C	0.47875900	-0.83932100	-0.33065000
C	1.81101200	-1.16587600	-0.31661300
H	3.07899000	1.93644400	0.35525600
H	0.69118600	2.49670600	0.26509100
H	-0.24153300	-1.60960200	-0.57073400
H	2.09878900	-2.18492800	-0.52597600
C	-1.30308400	0.92306600	-0.22955900
C	-2.46459800	0.07964100	-0.07559800
C	-3.64725900	0.49122700	-0.72050700
C	-2.51071000	-1.08206100	0.71978100
C	-4.80500100	-0.26425800	-0.63425600
H	-3.62642300	1.41248200	-1.28851000
C	-3.67773100	-1.82097700	0.82713600
H	-1.63578700	-1.37239300	1.28556100
C	-4.82166500	-1.42307700	0.13834700
H	-5.70086000	0.05553600	-1.15106200
H	-3.70389200	-2.70340800	1.45417400
H	-5.73149300	-2.00446800	0.22202700
N	4.12179800	-0.50596600	-0.00804900
C	4.55238800	-1.88280500	-0.19080600
H	5.62923200	-1.94127100	-0.05983900
H	4.08660300	-2.54613000	0.54272100
H	4.31077700	-2.25352600	-1.19193200
C	5.12876500	0.52540500	0.19337500
H	6.11523400	0.07115900	0.16657900
H	5.08355200	1.28720400	-0.58952800
H	5.00823400	1.02025700	1.16114800
O	-1.33078300	3.40379400	0.32661900
H	-1.46082900	2.11506000	-0.20997200
H	-2.03807900	3.59379900	0.95352100



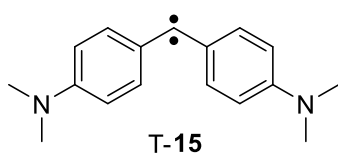
B3LYP/def2-TZVP
 E = -711.806000
 ZPVE = 0.286248

C	-4.22144500	-1.56147600	0.92579100
C	-3.38523500	-0.79112300	1.73183500
C	-2.48925900	0.09872900	1.15793900
C	-2.42031100	0.23914300	-0.22972800
C	-3.26285200	-0.52935900	-1.02773800
C	-4.15789900	-1.42968200	-0.45506000
H	-4.91750500	-2.25891400	1.37462700
H	-3.42948000	-0.89207600	2.80924900
H	-1.83009100	0.69055400	1.78039500
H	-3.21988700	-0.42374900	-2.10590400
H	-4.80628800	-2.02240300	-1.08836200
C	-0.00072300	0.81964600	-0.59721400
C	0.55786700	-0.24276500	-1.30295100
C	0.78889000	1.44233500	0.36287000
C	1.85268500	-0.67390400	-1.06823600
H	-0.03454500	-0.75883500	-2.05069100
C	2.08929000	1.02523200	0.61076900
H	0.38331700	2.27398800	0.92212200
C	2.66440000	-0.04023600	-0.10610900
H	2.22961000	-1.50655800	-1.64251300
H	2.65626800	1.54433400	1.36875000
N	3.97555300	-0.44029700	0.11208600
C	4.67931500	0.06341300	1.27480400
H	5.69113600	-0.33652200	1.28133100
H	4.75904000	1.15215000	1.24359500
H	4.19228000	-0.21356800	2.22051500
C	4.43183800	-1.69493000	-0.45245500
H	5.47831900	-1.84332200	-0.19440500
H	3.86032100	-2.55975500	-0.08680100
H	4.36382500	-1.68279600	-1.54243500
C	-1.43884100	1.22040700	-0.84952000
H	-1.60636800	1.22335900	-1.93475300
O	-1.64182100	2.54000900	-0.33527800
H	-2.59057300	2.70354000	-0.30708200



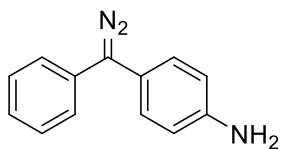
B3LYP/def2-TZVP
 E = -769.225207
 ZPVE = 0.330252

C	3.79284200	0.16039100	0.02458400
C	2.67332500	0.74612500	0.66069100
C	1.43628700	0.13997900	0.61854200
C	1.22898200	-1.12287900	0.00498200
C	2.38054200	-1.72824700	-0.55564700
C	3.60489700	-1.10259000	-0.58939600
H	2.77492300	1.68274700	1.18888800
H	0.60424500	0.61935700	1.11804000
H	2.26544800	-2.71479000	-0.98669800
H	4.43411600	-1.60762800	-1.06182600
C	0.00000000	-1.84118200	-0.00000300
C	-1.22898200	-1.12288100	-0.00498300
C	-2.38054200	-1.72824800	0.55564500
C	-1.43628700	0.13998000	-0.61853900
C	-3.60489800	-1.10259200	0.58939200
H	-2.26545000	-2.71479300	0.98669400
C	-2.67332500	0.74612500	-0.66069000
H	-0.60424300	0.61936000	-1.11803400
C	-3.79284200	0.16038900	-0.02458500
H	-4.43411700	-1.60763300	1.06181800
H	-2.77492200	1.68274800	-1.18888500
N	5.01792400	0.77997700	0.01978800
N	-5.01792500	0.77997500	-0.01979200
C	5.21052700	2.02001700	0.74700300
H	5.05166400	1.89753600	1.82526900
H	6.22722700	2.37249800	0.59191500
H	4.53032600	2.79838400	0.39122300
C	6.17964000	0.09589700	-0.51654000
H	6.03548900	-0.16810200	-1.56765700
H	7.04261400	0.75432500	-0.45600900
H	6.41072500	-0.82276100	0.03544200
C	-5.21052900	2.02001100	-0.74701300
H	-6.22723500	2.37248300	-0.59193900
H	-4.53033900	2.79838500	-0.39122800
H	-5.05165300	1.89752600	-1.82527500
C	-6.17963700	0.09590500	0.51655700
H	-7.04260400	0.75434400	0.45605300
H	-6.41074700	-0.82274600	-0.03542600
H	-6.03546400	-0.16810300	1.56766800



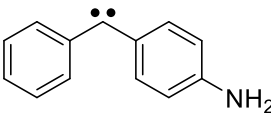
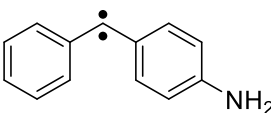
B3LYP/def2-TZVP
 E = -769.225447
 ZPVE = 0.328995

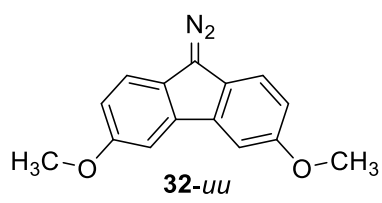
C	4.01696900	0.12957400	-0.03153700
C	2.96538300	0.89072900	0.52698500
C	1.66758500	0.42903600	0.53512800
C	1.31125900	-0.83053300	-0.02160200
C	2.37938700	-1.59420300	-0.55851500
C	3.67878500	-1.13743400	-0.55872200
H	3.16589600	1.85541300	0.96937600
H	0.89287400	1.03643500	0.98542600
H	2.15981600	-2.56860700	-0.97630300
H	4.44321800	-1.77409900	-0.97863000
C	0.00000000	-1.30097900	0.00000300
C	-1.31125800	-0.83052900	0.02160800
C	-2.37938800	-1.59419900	0.55852000
C	-1.66758300	0.42904100	-0.53511900
C	-3.67878400	-1.13742800	0.55873100
H	-2.15981700	-2.56860600	0.97630300
C	-2.96538100	0.89073500	-0.52697100
H	-0.89287400	1.03643900	-0.98542000
C	-4.01696700	0.12958400	0.03155500
H	-4.44321800	-1.77409600	0.97863300
H	-3.16589200	1.85541900	-0.96936500
N	5.31654400	0.60632100	-0.06819900
N	-5.31654200	0.60634000	0.06823300
C	5.65891300	1.79606000	0.68609600
H	5.50516200	1.67176500	1.76687900
H	6.70556500	2.03864400	0.51562100
H	5.06669700	2.65283000	0.35744700
C	6.39416200	-0.29472100	-0.42727500
H	6.25027100	-0.69834800	-1.43180800
H	7.33358200	0.25375000	-0.42773800
H	6.48854500	-1.14020300	0.26793300
C	-5.65891600	1.79604700	-0.68611200
H	-6.70555300	2.03867100	-0.51559200
H	-5.06666100	2.65281600	-0.35753600
H	-5.50522400	1.67169100	-1.76689700
C	-6.39416500	-0.29473100	0.42722900
H	-7.33358200	0.25374600	0.42773900
H	-6.48855200	-1.14015500	-0.26805000
H	-6.25027600	-0.69843900	1.43172800

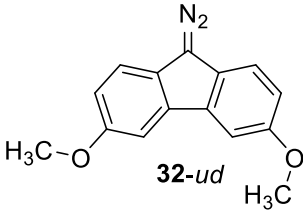
**26**

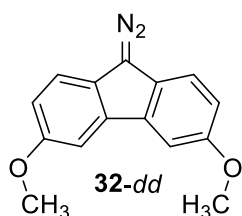
B3LYP/def2-TZVP
 E = -666.274068
 ZPVE = 0.212132

C	4.05938400	-1.47550500	0.16970100
C	2.84390000	-1.98533100	0.61354800
C	1.68850800	-1.21960800	0.54673100
C	1.71980100	0.08099500	0.02252600
C	2.95172200	0.58386500	-0.42343400
C	4.10408700	-0.18382000	-0.34519000
H	4.95871500	-2.07501200	0.22472800
H	2.79376400	-2.98588600	1.02517000
H	0.75568200	-1.62481000	0.91375200
H	3.00804200	1.58080700	-0.84297200
H	5.04179500	0.22763600	-0.69758300
C	-0.89158600	0.38134600	-0.02736100
C	-1.23859600	-0.77097500	-0.74233000
C	-1.91010100	1.04417900	0.66544500
C	-2.53833700	-1.24667400	-0.75253100
H	-0.47802000	-1.30030200	-1.30107400
C	-3.21599400	0.58344300	0.64519700
H	-1.67767000	1.93527500	1.23622000
C	-3.55476000	-0.57704300	-0.05969500
H	-2.77637000	-2.14008000	-1.31851800
H	-3.98297700	1.12278500	1.18907400
N	-4.87251700	-1.01904400	-0.12081500
C	0.49494400	0.88947500	-0.03303400
N	0.64010100	2.18439300	-0.09003600
N	0.76899900	3.31146900	-0.13020900
H	-5.47580700	-0.71125300	0.62497300
H	-5.00106600	-1.99296100	-0.34379500

 <p>S-16</p> <p>B3LYP/def2-TZVP E = -556.683592 ZPVE = 0.200861</p>	C	4.13382500	-0.84274000	-0.02165700
	C	3.09849500	-1.26967000	-0.84804700
	C	1.88772800	-0.59361000	-0.86105600
	C	1.69911500	0.58009000	-0.09134200
	C	2.78775500	1.02621300	0.69321700
	C	3.96339000	0.30052500	0.76075400
	H	5.07159000	-1.38331700	0.00096000
	H	3.23030500	-2.14678100	-1.47046800
	H	1.08245500	-0.93812700	-1.49728900
	H	2.67384400	1.94631200	1.25190700
	H	4.77052300	0.64372400	1.39657100
	C	0.50548600	1.36615200	-0.15019500
	C	-0.75549900	0.73212100	-0.05891000
	C	-1.90507300	1.44609300	-0.49142500
	C	-0.98424400	-0.56153900	0.49108500
	C	-3.16468600	0.90312700	-0.44335500
	H	-1.74965100	2.44360900	-0.88182400
	C	-2.24632000	-1.09214500	0.59763900
	H	-0.13916800	-1.12372600	0.86580600
	C	-3.36236100	-0.37724300	0.11481900
H	-4.01994500	1.46144000	-0.80649700	
H	-2.39704400	-2.06694300	1.04834100	
N	-4.61194500	-0.92120000	0.17515500	
H	-5.41474500	-0.34585800	-0.00892100	
H	-4.77020900	-1.74617200	0.72616400	
 <p>T-16</p> <p>B3LYP/def2-TZVP E = -556.686444 ZPVE = 0.199987</p>	C	4.41322700	-0.64225100	-0.11220400
	C	3.33376400	-1.37841400	-0.60377000
	C	2.05127500	-0.86676900	-0.55510000
	C	1.79748300	0.41566200	0.01016900
	C	2.91301200	1.14727800	0.49745100
	C	4.18974700	0.62337200	0.43322100
	H	5.41559700	-1.04783100	-0.15737000
	H	3.50141800	-2.35793300	-1.03537100
	H	1.22097500	-1.43482900	-0.95397400
	H	2.74337900	2.12708500	0.92490900
	H	5.02365500	1.20054800	0.81362400
	C	0.50698000	0.94296500	0.05884100
	C	-0.82956900	0.54680300	0.03784700
	C	-1.84880700	1.38394400	-0.48647500
	C	-1.24639900	-0.70107500	0.58024600
	C	-3.17113700	0.99931300	-0.48419100
	H	-1.56983200	2.34472500	-0.89945300
	C	-2.57001800	-1.08189200	0.57513600
	H	-0.50170000	-1.35893500	1.00884900
	C	-3.56251600	-0.24355000	0.04090200
H	-3.92410000	1.66380400	-0.89304400	
H	-2.85404700	-2.03947800	0.99758600	
N	-4.90060800	-0.60604500	0.08858800	
H	-5.51632700	-0.13737000	-0.55604900	
H	-5.09702600	-1.58978800	0.17774000	

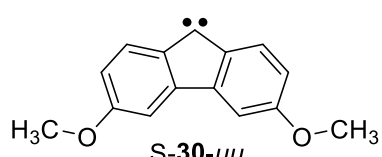
 <p>32-uu</p> <p>B3LYP/def2-TZVP E = -838.815679 ZPVE = 0.238571</p>	C	3.00663100	-1.02012400	-0.00000400
	C	3.45254600	0.30790600	-0.00000300
	C	2.53807600	1.35913800	-0.00000200
	C	1.18206900	1.07752300	0.00000000
	C	0.72957300	-0.26602600	0.00000100
	C	1.64032900	-1.30850800	-0.00000100
	H	4.50829800	0.53346100	-0.00000400
	H	2.89689200	2.38111800	-0.00000300
	H	1.32435600	-2.34342200	0.00000000
	C	0.00000000	1.92744800	0.00000000
	C	-1.18207000	1.07752400	0.00000100
	C	-2.53807600	1.35913900	0.00000000
	C	-3.45254700	0.30790700	0.00000200
	C	-3.00663100	-1.02012300	0.00000600
	C	-1.64033000	-1.30850800	0.00000600
	C	-0.72957400	-0.26602500	0.00000400
	H	-2.89689200	2.38111900	-0.00000200
	H	-4.50829900	0.53346200	-0.00000100
	H	-1.32435800	-2.34342100	0.00000700
	N	0.00000100	3.22335900	0.00000000
	N	0.00000600	4.35785900	0.00000000
	O	-3.83434600	-2.10437400	0.00000300
	O	3.83434400	-2.10437600	-0.00000200
	C	5.23594500	-1.89450900	0.00000200
	H	5.68701600	-2.88438000	0.00000800
H	5.56157400	-1.35040700	-0.89255700	
H	5.56156800	-1.35040000	0.89255900	
C	-5.23594600	-1.89450700	-0.00000800	
H	-5.56156400	-1.35040000	-0.89256900	
H	-5.68701800	-2.88437700	-0.00001200	
H	-5.56157900	-1.35040100	0.89254700	

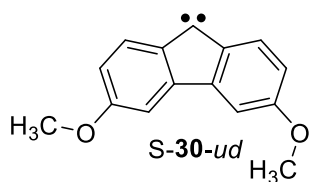
 <p> B3LYP/def2-TZVP E = -838.816241 ZPVE = 0.238602 </p>	C	3.14587500	-0.80347600	0.00000700
	C	3.53647400	0.54587100	0.00000200
	C	2.59500100	1.55973400	0.00000000
	C	1.24415500	1.22334400	0.00000200
	C	0.84615600	-0.13027300	0.00000600
	C	1.79661900	-1.14952600	0.00000900
	H	4.59500800	0.76842200	0.00000000
	H	2.91380900	2.59482600	-0.00000400
	H	1.47827100	-2.18160800	0.00001500
	C	0.03211600	2.02867400	-0.00000100
	C	-1.11681200	1.13540000	0.00000400
	C	-2.48270500	1.36320000	0.00000300
	C	-3.35523000	0.27686000	0.00000700
	C	-2.85695900	-1.03253900	0.00001200
	C	-1.48057100	-1.26696500	0.00001000
	C	-0.61051900	-0.18954700	0.00000700
	H	-2.88151600	2.37026200	0.00000000
	H	-4.41901300	0.46063600	0.00000600
	H	-1.12582700	-2.28933700	0.00001200
	N	-0.01694100	3.32420000	-0.00000800
	N	-0.06192200	4.45732700	-0.00001300
	O	-3.64147800	-2.14886600	0.00001100
	O	4.17084600	-1.70246200	0.00001200
	C	3.85927900	-3.08513900	-0.00002400
H	4.81305900	-3.60807800	-0.00004700	
H	3.29201000	-3.36896600	0.89245500	
H	3.29199300	-3.36891600	-0.89250800	
C	-5.05029000	-1.99401800	-0.00002200	
H	-5.39691300	-1.46306400	-0.89256100	
H	-5.46235400	-3.00077200	-0.00003500	
H	-5.39695400	-1.46307000	0.89250400	



B3LYP/def2-TZVP
 E = -838.816569
 ZPVE = 0.238620

C	-3.00100900	-0.82551000	0.00000000
C	-3.44462100	0.50735600	0.00000000
C	-2.54330100	1.55712200	0.00000000
C	-1.18055900	1.27391600	0.00000000
C	-0.72837500	-0.06342200	0.00000000
C	-1.63941600	-1.11888100	0.00000100
H	-4.51103900	0.68814800	0.00000000
H	-2.90225700	2.57900100	0.00000100
H	-1.28287100	-2.13847500	0.00000100
C	-0.00000100	2.12356600	0.00000000
C	1.18055800	1.27391700	0.00000000
C	2.54330000	1.55712500	0.00000000
C	3.44462100	0.50736000	-0.00000100
C	3.00101100	-0.82550700	-0.00000300
C	1.63941700	-1.11888000	-0.00000200
C	0.72837500	-0.06342100	-0.00000100
H	2.90225500	2.57900400	0.00000000
H	4.51103900	0.68815300	-0.00000100
H	1.28287400	-2.13847300	-0.00000100
N	-0.00000300	3.42062300	0.00000000
N	-0.00000700	4.55409700	0.00000100
O	3.99044900	-1.76406800	0.00000000
O	-3.99044600	-1.76407200	0.00000000
C	-3.62588400	-3.13315000	-0.00000100
H	-4.55860700	-3.69283300	-0.00000300
H	-3.04810000	-3.39506800	-0.89259200
H	-3.04810400	-3.39507100	0.89259200
C	3.62588800	-3.13314600	0.00000200
H	3.04810700	-3.39506800	-0.89258900
H	4.55861200	-3.69282900	0.00000400
H	3.04810500	-3.39506500	0.89259400

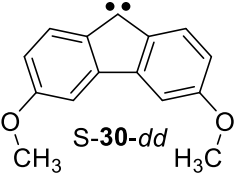
 <p>S-30-uu</p> <p>B3LYP/def2-TZVP E = -729.211344 ZPVE = 0.227908</p>	C	3.02991100	-0.55981800	-0.00000300
	C	3.44038400	0.77375800	0.00001000
	C	2.48281500	1.79246800	0.00000800
	C	1.13099300	1.48316600	-0.00000800
	C	0.73874400	0.11142400	-0.00002500
	C	1.65471200	-0.90188500	-0.00002000
	H	4.48984800	1.02655800	0.00002400
	H	2.78953200	2.83109200	0.00001300
	H	1.38318600	-1.95005900	-0.00003500
	C	0.00000100	2.40382200	0.00000500
	C	-1.13099200	1.48316700	-0.00000800
	C	-2.48281400	1.79247000	0.00000700
	C	-3.44038400	0.77376000	0.00000900
	C	-3.02991200	-0.55981600	-0.00000100
	C	-1.65471300	-0.90188400	-0.00001900
	C	-0.73874400	0.11142500	-0.00002500
	H	-2.78953000	2.83109400	0.00001100
	H	-4.48984700	1.02656100	0.00001900
	H	-1.38318700	-1.95005800	-0.00003500
	O	-3.87075000	-1.61692300	0.00000800
O	3.87074900	-1.61692400	0.00001000	
C	-5.27490800	-1.38794300	0.00001500	
H	-5.73590500	-2.37251900	0.00002600	
H	-5.58642400	-0.83909900	0.89299200	
H	-5.58643800	-0.83911200	-0.89296400	
C	5.27490700	-1.38794100	0.00001400	
H	5.73590600	-2.37251700	0.00002700	
H	5.58643400	-0.83911300	-0.89296800	
H	5.58642300	-0.83909300	0.89298900	

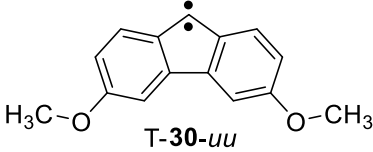


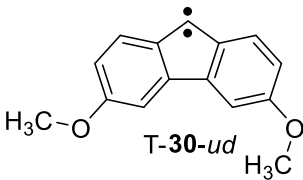
B3LYP/def2-TZVP
 E = -729.210134
 ZPVE = 0.227792

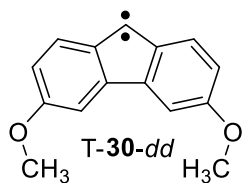
C	-2.88912100	-0.55967600	-0.00000200
C	-3.35304900	0.75427300	-0.00000900
C	-2.43592600	1.81241300	-0.00000800
C	-1.07462900	1.55824500	0.00000000
C	-0.62639500	0.20450600	0.00000100
C	-1.49919000	-0.84492900	0.00000000
H	-4.41174900	0.96494500	-0.00001900
H	-2.78500100	2.83758400	-0.00001100
H	-1.18643300	-1.88171900	0.00000300
C	0.02212900	2.52257800	0.00000900
C	1.18835300	1.64649500	0.00000400
C	2.53434600	2.00825000	-0.00000300
C	3.51548700	1.02588400	-0.00000400
C	3.16032300	-0.32726400	0.00000500
C	1.80323100	-0.72286300	0.00000400
C	0.85138700	0.26760900	0.00000400
H	2.80288800	3.05721000	-0.00000700
H	4.56816600	1.27440600	-0.00001200
H	1.52414100	-1.76694600	-0.00000200
O	4.19139300	-1.20085400	0.00001500
O	-3.68422300	-1.65205200	-0.00000400
C	3.92695500	-2.59847700	-0.00001500
H	4.90007700	-3.08327200	-0.00000700
H	3.37237900	-2.89888000	0.89334800
H	3.37239400	-2.89884300	-0.89339700
C	-5.09667500	-1.48136500	0.00000900
H	-5.51686100	-2.48404200	0.00005100
H	-5.43034900	-0.94560700	0.89293000
H	-5.43037400	-0.94566400	-0.89293600

10. Appendix

 <p>S-30-dd</p> <p>B3LYP/def2-TZVP E = -729.208471 ZPVE = 0.227611</p>	C	3.02469900	0.33744100	0.00000600
	C	3.43366100	-0.99841700	-0.00000300
	C	2.49116900	-2.02063900	-0.00000500
	C	1.13376200	-1.71329900	0.00000000
	C	0.74071200	-0.35029100	0.00000100
	C	1.65074400	0.67745100	0.00000400
	H	4.49529100	-1.20516800	-0.00000600
	H	2.80204400	-3.05785100	-0.00000700
	H	1.33091900	1.70994300	0.00000100
	C	0.00000400	-2.63449900	0.00000900
	C	-1.13375600	-1.71330100	-0.00000200
	C	-2.49116100	-2.02064400	0.00000200
	C	-3.43365500	-0.99842300	-0.00000300
	C	-3.02469700	0.33743600	-0.00000800
	C	-1.65074200	0.67744800	-0.00000100
	C	-0.74070800	-0.35029300	-0.00000300
	H	-2.80203500	-3.05785600	0.00000500
	H	-4.49528500	-1.20517700	-0.00000200
	H	-1.33091800	1.70994000	0.00001300
	O	-4.01864300	1.25401200	0.00000100
O	4.01864000	1.25402100	0.00000100	
C	-3.69692900	2.63895900	0.00000200	
H	-4.64913700	3.16370300	0.00000700	
H	-3.13068600	2.91678500	0.89351800	
H	-3.13069600	2.91678100	-0.89352200	
C	3.69691100	2.63896300	-0.00000300	
H	4.64911300	3.16371900	-0.00001700	
H	3.13065800	2.91677800	-0.89351600	
H	3.13068000	2.91678400	0.89352400	

 <p>T-30-uu</p> <p>B3LYP/def2-TZVP E = -729.210231 ZPVE = 0.227543</p>	C	3.01722300	-0.56435300	-0.00000100
	C	3.45564700	0.76747100	0.00000000
	C	2.53687100	1.81109700	0.00000100
	C	1.17173800	1.53009000	0.00000200
	C	0.73148700	0.15992200	-0.00000200
	C	1.64718200	-0.86763200	-0.00000200
	H	4.51062800	0.99681200	-0.00000300
	H	2.88512900	2.83585300	-0.00000300
	H	1.34528400	-1.90733200	-0.00000200
	C	0.00000100	2.32037500	0.00000400
	C	-1.17173700	1.53009100	0.00000100
	C	-2.53686900	1.81109900	-0.00000100
	C	-3.45564600	0.76747300	-0.00000300
	C	-3.01722400	-0.56435100	-0.00000100
	C	-1.64718300	-0.86763100	-0.00000300
	C	-0.73148700	0.15992300	-0.00000200
	H	-2.88512700	2.83585600	-0.00000600
	H	-4.51062700	0.99681600	-0.00000800
	H	-1.34528500	-1.90733100	-0.00000200
	O	-3.84765900	-1.64240600	-0.00000200
	O	3.84765900	-1.64240700	0.00000100
C	-5.25016300	-1.42971800	0.00000500	
H	-5.70237800	-2.41891500	0.00000000	
H	-5.57287800	-0.88480100	0.89262600	
H	-5.57288300	-0.88478900	-0.89260700	
C	5.25016200	-1.42971600	0.00000200	
H	5.70238000	-2.41891200	-0.00001100	
H	5.57287500	-0.88478200	-0.89260900	
H	5.57287900	-0.88480200	0.89262400	

 <p>T-30-ud</p> <p>B3LYP/def2-TZVP E = -729.210320 ZPVE = 0.227585</p>	C	-2.87536300	-0.55740500	0.00000600
	C	-3.36312600	0.75656300	0.00001700
	C	-2.48256700	1.83356900	0.00001800
	C	-1.10909500	1.60335400	0.00001000
	C	-0.61700000	0.25077600	0.00000200
	C	-1.49462900	-0.80973400	0.00000000
	H	-4.42576100	0.94698200	0.00002800
	H	-2.86841600	2.84480300	0.00002500
	H	-1.15626200	-1.83825200	-0.00000600
	C	0.03494700	2.43463300	0.00000700
	C	1.23279700	1.68555300	-0.00000100
	C	2.59330300	2.01780200	-0.00000800
	C	3.53551500	1.00908000	-0.00001500
	C	3.14875700	-0.34360800	-0.00001600
	C	1.79607500	-0.70051500	-0.00001000
	C	0.84429400	0.30666900	-0.00000100
	H	2.90428800	3.05440900	-0.00000600
	H	4.59398400	1.23199500	-0.00002000
	H	1.48778500	-1.73621100	-0.00001300
	O	4.17394700	-1.23736300	-0.00002700
O	-3.66458400	-1.66613100	0.00001400	
C	3.87376700	-2.62383200	0.00003800	
H	4.83237300	-3.13760100	0.00007200	
H	3.30952000	-2.91145200	0.89275800	
H	3.30953600	-2.91153800	-0.89266500	
C	-5.07419100	-1.50583200	-0.00003500	
H	-5.48932200	-2.51115700	-0.00006300	
H	-5.41680400	-0.97323800	0.89255400	
H	-5.41673900	-0.97321300	-0.89263300	

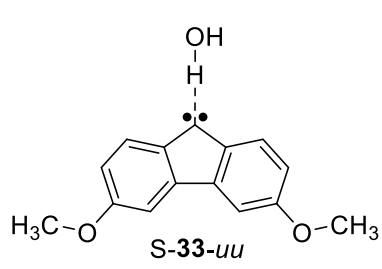


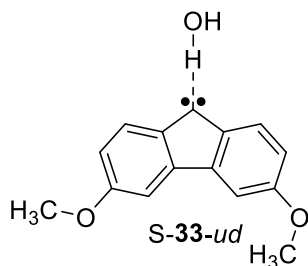
B3LYP/def2-TZVP

E = -729.210091

ZPVE = 0.227592

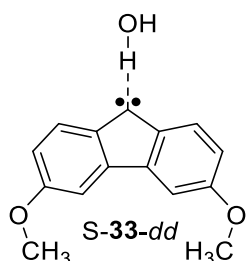
C	3.01123600	0.34595200	0.00000000
C	3.44788900	-0.99064300	0.00000300
C	2.54230900	-2.03340900	0.00000600
C	1.17173800	-1.75140800	0.00000400
C	0.73113700	-0.38823200	-0.00000100
C	1.64572700	0.65298000	-0.00000400
H	4.51373500	-1.17468700	0.00000400
H	2.89102600	-3.05796400	0.00000700
H	1.30137900	1.67733700	-0.00001000
C	0.00000000	-2.54229900	0.00000200
C	-1.17173700	-1.75140800	-0.00000100
C	-2.54230800	-2.03340900	-0.00000400
C	-3.44788900	-0.99064300	-0.00000500
C	-3.01123600	0.34595100	-0.00000300
C	-1.64572700	0.65298000	0.00000100
C	-0.73113700	-0.38823200	0.00000100
H	-2.89102500	-3.05796500	-0.00000300
H	-4.51373500	-1.17468700	-0.00000600
H	-1.30137900	1.67733700	0.00000400
O	-4.00233200	1.27773100	-0.00000300
O	4.00233100	1.27773100	-0.00000400
C	-3.65156800	2.65178400	0.00000900
H	-4.59056600	3.20059800	0.00000700
H	-3.07729100	2.91880700	0.89286200
H	-3.07728100	2.91881900	-0.89283500
C	3.65156700	2.65178400	-0.00000200
H	4.59056500	3.20059900	-0.00000300
H	3.07728400	2.91881300	-0.89285100
H	3.07728500	2.91881300	0.89284700

 <p style="text-align: center;">S-33-uu</p> <p>B3LYP/def2-TZVP E = -805.670687 ZPVE = 0.252300</p>	C	2.84858800	-1.16171400	-0.00257600
	C	3.35885200	0.13765600	-0.00693400
	C	2.48490900	1.22723600	-0.01188300
	C	1.11199900	1.01063100	-0.01240600
	C	0.61253700	-0.32601700	-0.00771600
	C	1.44981500	-1.40327000	-0.00310700
	H	4.42447800	0.30963800	-0.00506400
	H	2.85859100	2.24471200	-0.01452000
	H	1.10326600	-2.42889600	0.00125100
	C	0.05572200	2.00129300	-0.01367700
	C	-1.14728100	1.18858300	-0.00997200
	C	-2.47022000	1.60479100	-0.00700300
	C	-3.50424800	0.66462100	-0.00207200
	C	-3.19946500	-0.69719800	0.00034400
	C	-1.85445100	-1.14666700	-0.00197300
	C	-0.86134000	-0.21016300	-0.00705200
	H	-2.69626400	2.66383000	-0.00683600
	H	-4.53047800	0.99908600	0.00094700
	H	-1.66666600	-2.21285200	0.00143400
	O	3.60593800	-2.27728600	0.00276800
	O	-4.11907100	-1.68423600	0.00562200
	C	-5.50228900	-1.34779900	0.01078900
	H	-5.77377800	-0.77891100	-0.88253100
	H	-6.03706500	-2.29416000	0.01523200
	H	-5.76605200	-0.77485900	0.90380900
	C	5.02497600	-2.15679000	0.00795000
H	5.37282900	-1.62996300	0.90035200	
H	5.40790300	-3.17410400	0.01339000	
H	5.38002700	-1.63692000	-0.88574000	
O	1.65154600	4.41787700	0.10274300	
H	0.94468800	3.72032900	0.07504800	
H	1.42257200	5.03107200	-0.60211000	



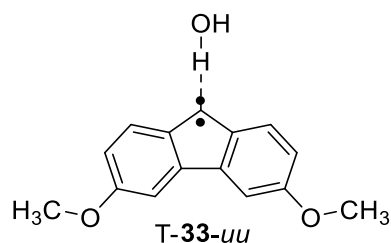
B3LYP/def2-TZVP
 E = -805.669437
 ZPVE = 0.252163

C	-3.33108400	-0.35319500	-0.00055300
C	-3.53525000	1.03106200	0.00349200
C	-2.45238700	1.89918400	0.00882400
C	-1.15497100	1.38968700	0.01104700
C	-0.96959500	-0.01865800	0.00686600
C	-2.02497200	-0.89636500	0.00076200
H	-4.55396500	1.39414800	0.00108400
H	-2.60567200	2.97100300	0.00974500
H	-1.86310900	-1.96474100	-0.00367100
C	0.10271000	2.11529100	0.01502000
C	1.08875100	1.05168300	0.01416100
C	2.47176200	1.16817100	0.01501100
C	3.26594000	0.01635900	0.00965000
C	2.66336300	-1.24063400	0.00340400
C	1.24881100	-1.37896000	0.00261800
C	0.49326900	-0.24409500	0.00790600
H	2.91910300	2.15545600	0.01935900
H	4.34114400	0.11129100	0.00899100
H	0.82960600	-2.37727000	-0.00315000
O	-4.45050800	-1.10732500	-0.00626800
O	3.33516900	-2.41021100	-0.00262400
C	4.75922800	-2.39429100	-0.00651100
H	5.15051000	-1.90257200	0.88799400
H	5.06675900	-3.43688200	-0.01279300
H	5.14544000	-1.89319000	-0.89796900
C	-4.34318100	-2.52651900	-0.01295000
H	-3.82789700	-2.89038600	0.88015300
H	-5.36428200	-2.89938300	-0.01731100
H	-3.82348500	-2.88157200	-0.90702600
O	1.87798800	4.40124100	-0.10610600
H	1.11702900	3.76371100	-0.07367600
H	1.67327300	5.06843600	0.55576900



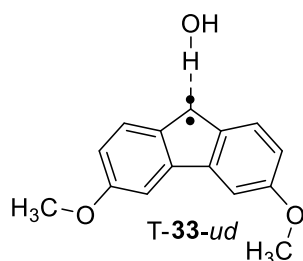
B3LYP/def2-TZVP
 E = -805.667335
 ZPVE = 0.251964

C	-3.20855000	-0.23272400	-0.00001100
C	-3.39943700	1.15141400	0.00426000
C	-2.30645100	2.01005800	0.00947400
C	-1.01601500	1.48850900	0.01134100
C	-0.84304400	0.07953700	0.00701100
C	-1.90544600	-0.78804100	0.00096700
H	-4.41430900	1.52497900	0.00210800
H	-2.44978500	3.08326000	0.01048600
H	-1.75499700	-1.85822900	-0.00368900
C	0.25186400	2.20053600	0.01490500
C	1.22683500	1.12615800	0.01355400
C	2.61785700	1.22699300	0.01426300
C	3.38454500	0.06815900	0.00971500
C	2.77094200	-1.18756000	0.00420300
C	1.35859600	-1.31197600	0.00287200
C	0.62054500	-0.15670400	0.00774200
H	3.07713900	2.20860600	0.01751900
H	4.46543700	0.10492300	0.00880600
H	0.88370700	-2.28276200	-0.00233700
O	-4.33426800	-0.97851000	-0.00558300
O	3.60749600	-2.24695600	0.00002700
C	3.07645900	-3.56667200	-0.00860800
H	2.47577900	-3.74814900	-0.90418100
H	3.93704900	-4.23085200	-0.01175500
H	2.47381000	-3.75916000	0.88336500
C	-4.23919800	-2.39799900	-0.01266300
H	-3.72721500	-2.76704300	0.88037400
H	-5.26342100	-2.76228100	-0.01688500
H	-3.72313600	-2.75778200	-0.90711000
O	2.04463000	4.47713700	-0.11029200
H	1.28089200	3.84420300	-0.07650800
H	1.85917600	5.12879500	0.57244000



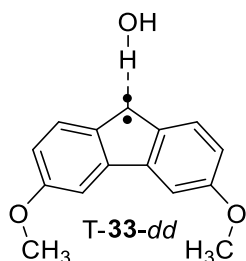
B3LYP/def2-TZVP
 E = -805.658073
 ZPVE = 0.250619

C	2.82715400	-1.18350200	-0.00179200
C	3.37119700	0.10902000	0.02187800
C	2.54129700	1.22376400	0.03671100
C	1.15796300	1.04867500	0.02841900
C	0.60587300	-0.28026200	0.00626500
C	1.43668400	-1.37703800	-0.00942200
H	4.44115500	0.25254200	0.03054100
H	2.96047200	2.22142500	0.06013300
H	1.05312800	-2.38926000	-0.02688600
C	0.05137200	1.92677700	0.03775900
C	-1.18258300	1.23979900	0.02658500
C	-2.52010000	1.63060900	0.03159200
C	-3.51996300	0.66479100	0.01545100
C	-3.19035700	-0.69790700	-0.00599400
C	-1.84883900	-1.11076100	-0.01116400
C	-0.85278300	-0.16157300	0.00544000
H	-2.78480400	2.67993000	0.04886000
H	-4.55287900	0.97858600	0.02015900
H	-1.63190100	-2.17127000	-0.02758900
O	3.56754800	-2.32353100	-0.01794600
O	-4.10398300	-1.70464500	-0.02297100
C	-5.48570100	-1.38080100	-0.01764900
H	-5.76351600	-0.79766400	-0.90103200
H	-6.01487300	-2.33080700	-0.03307200
H	-5.76341000	-0.82668600	0.88423300
C	4.98352800	-2.22525000	-0.00826200
H	5.34351200	-1.72347800	0.89506200
H	5.35349900	-3.24783500	-0.02350000
H	5.35367600	-1.69327300	-0.88998100
O	1.68279900	4.54083300	-0.00703100
H	1.02853400	3.93514700	0.37012900
H	1.55804100	4.45334900	-0.95838400



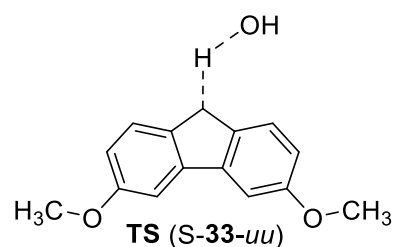
B3LYP/def2-TZVP
 E = -805.658136
 ZPVE = 0.250647

C	-3.32367100	-0.36150100	0.00161300
C	-3.55429300	1.02631900	-0.01523300
C	-2.50366500	1.92124800	-0.02737700
C	-1.19023200	1.43599400	-0.02291200
C	-0.95956800	0.02158300	-0.00658700
C	-2.01993600	-0.86984000	0.00617200
H	-4.58043400	1.36822000	-0.01883400
H	-2.69522100	2.98634500	-0.04105000
H	-1.83132700	-1.93373900	0.01890000
C	0.08695300	2.03778900	-0.03069800
C	1.13170600	1.08562700	-0.02338500
C	2.52287000	1.16310700	-0.02974900
C	3.27335600	-0.00754300	-0.01826100
C	2.63954800	-1.25788800	0.00008300
C	1.23845900	-1.35311400	0.00582000
C	0.48628400	-0.20076000	-0.00660000
H	3.01082100	2.12911400	-0.04891300
H	4.35069700	0.06074700	-0.02534000
H	0.78633100	-2.33680000	0.01932000
O	-4.44270000	-1.13250900	0.01259900
O	3.29687800	-2.44794500	0.01261500
C	4.71640300	-2.45009300	0.00436300
H	5.12219600	-1.94885100	0.88834900
H	5.01317400	-3.49632400	0.01595700
H	5.11172500	-1.97153100	-0.89672600
C	-4.30289000	-2.54466600	0.02763800
H	-3.77417800	-2.88479200	0.92351100
H	-5.31398100	-2.94507200	0.03333100
H	-3.77658100	-2.90399500	-0.86211100
O	1.91490000	4.52490900	0.00369300
H	1.21510700	3.97733900	-0.37997500
H	1.76111800	4.46613700	0.95300800



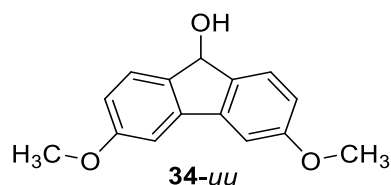
B3LYP/def2-TZVP
 E = -805.657740
 ZPVE = 0.250596

C	-3.20002200	-0.21900600	0.00181700
C	-3.40667300	1.17174900	-0.01567100
C	-2.33930300	2.04786700	-0.02987300
C	-1.03588400	1.53966400	-0.02687000
C	-0.82849400	0.12165300	-0.00987800
C	-1.90480100	-0.75051500	0.00497200
H	-4.42647500	1.53191700	-0.01811200
H	-2.51181500	3.11622800	-0.04399800
H	-1.73699700	-1.81796100	0.01821600
C	0.25361300	2.11666400	-0.03688400
C	1.27904000	1.14458300	-0.03047200
C	2.67798200	1.19801200	-0.03834800
C	3.39416300	0.01770700	-0.02596400
C	2.73984900	-1.22718400	-0.00545200
C	1.34158600	-1.30268600	0.00143100
C	0.61358800	-0.12407000	-0.01167500
H	3.18303400	2.15509600	-0.05914500
H	4.47572600	0.02037400	-0.03337900
H	0.83147600	-2.25522400	0.01640800
O	-4.33203800	-0.97114300	0.01489300
O	3.56008800	-2.31069900	0.00578700
C	2.98603900	-3.60783200	0.02203800
H	2.37281700	-3.78537500	-0.86705200
H	3.82114400	-4.30445700	0.02702100
H	2.37864400	-3.76570100	0.91883800
C	-4.21734900	-2.38510900	0.03069800
H	-3.69374600	-2.73424400	0.92623500
H	-5.23533000	-2.76766800	0.03803400
H	-3.69892800	-2.75457900	-0.85965700
O	2.11406300	4.57786800	0.02198900
H	1.40221300	4.04289600	-0.35719500
H	1.98132500	4.50152200	0.97321200



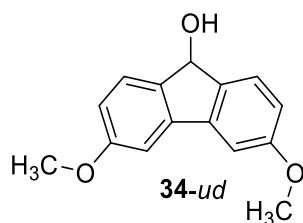
B3LYP/def2-TZVP
 E = -805.660966
 ZPVE = 0.247742

C	-3.03573700	-0.87537100	0.02071800
C	-3.44808700	0.45244100	-0.12799700
C	-2.49700300	1.46011300	-0.28663300
C	-1.14588700	1.14532400	-0.27091900
C	-0.74358500	-0.20975500	-0.09706700
C	-1.66388100	-1.21521500	0.02870300
H	-4.49730100	0.70544800	-0.13143300
H	-2.81222600	2.48815700	-0.41507600
H	-1.38907000	-2.25641700	0.13681000
C	0.00466700	1.99554300	-0.48267500
C	1.14413700	1.13400000	-0.28251400
C	2.49694900	1.44329800	-0.28695900
C	3.43887800	0.42818700	-0.12847500
C	3.01761800	-0.89772600	0.01591900
C	1.64365500	-1.22896100	0.02461400
C	0.73172500	-0.21612400	-0.10385200
H	2.81260200	2.47321000	-0.39184500
H	4.48969600	0.67446100	-0.12152200
H	1.36156200	-2.26747100	0.13961000
O	0.17370100	4.00280400	0.75339900
H	0.03563900	3.24097400	-0.21803600
H	-0.63975500	3.94213000	1.27020800
O	3.85252300	-1.94979400	0.15837400
O	-3.87749600	-1.92189100	0.16227700
C	5.25814500	-1.72722900	0.16637800
H	5.55193600	-1.08141100	0.99830400
H	5.71222700	-2.70715100	0.29018100
H	5.59432700	-1.28568500	-0.77573600
C	-5.28170500	-1.69111500	0.16458600
H	-5.74205800	-2.66794200	0.28939800
H	-5.57481100	-1.04139400	0.99379300
H	-5.61192500	-1.25032400	-0.78001800



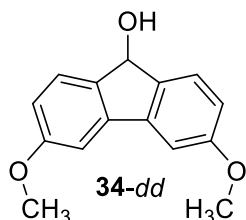
B3LYP/def2-TZVP
 E = -805.754215
 ZPVE = 0.256144

C	-3.00291400	-0.84748700	-0.00331900
C	-3.44922600	0.47601500	-0.05521700
C	-2.52583300	1.52144600	-0.14496200
C	-1.17744800	1.24073600	-0.17530000
C	-0.73432300	-0.08973000	-0.10536300
C	-1.63393200	-1.13652900	-0.02780500
H	-4.50409700	0.70411600	-0.02493100
H	-2.87853900	2.54523600	-0.17721200
H	-1.31593000	-2.16947900	0.02455800
C	0.00000100	2.18812500	-0.28684800
H	0.00000200	2.65792700	-1.27891900
C	1.17744900	1.24073500	-0.17529800
C	2.52583400	1.52144400	-0.14495700
C	3.44922600	0.47601300	-0.05521000
C	3.00291300	-0.84748900	-0.00331700
C	1.63393100	-1.13653000	-0.02780200
C	0.73432300	-0.08973100	-0.10536100
H	2.87854000	2.54523400	-0.17720300
H	4.50409700	0.70411300	-0.02491700
H	1.31592900	-2.16948000	0.02456000
O	0.00000200	3.21256800	0.71475900
H	-0.00001200	4.07059300	0.28302100
O	-3.82593900	-1.93052000	0.07880400
O	3.82593800	-1.93052100	0.07880900
C	5.22749900	-1.72213900	0.12027900
H	5.52071900	-1.13469900	0.99624900
H	5.67558600	-2.71122400	0.18558800
H	5.58655200	-1.22253000	-0.78525400
C	-5.22750000	-1.72214000	0.12028900
H	-5.67558500	-2.71122600	0.18559400
H	-5.52071600	-1.13470800	0.99626500
H	-5.58655900	-1.22252500	-0.78523700



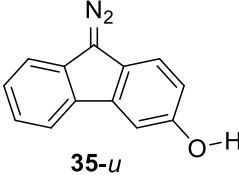
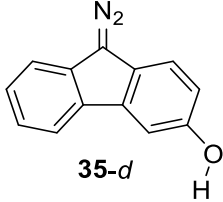
B3LYP/def2-TZVP
 E = -805.755270
 ZPVE = 0.256409

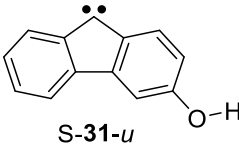
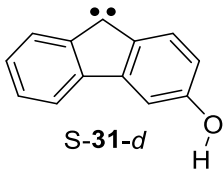
C	-3.13788800	-0.63514000	-0.01442200
C	-3.53533600	0.70544100	-0.09628200
C	-2.58808100	1.71695100	-0.18443000
C	-1.24159900	1.39163800	-0.17983900
C	-0.84786700	0.05351500	-0.09414600
C	-1.78297200	-0.97338900	-0.01539900
H	-4.59448800	0.92520900	-0.09216600
H	-2.91545000	2.74841500	-0.25492800
H	-1.45728600	-2.00131600	0.04645100
C	-0.02877300	2.29895800	-0.26954600
H	-0.01256800	2.81233400	-1.24224100
C	1.11055900	1.31176800	-0.17962400
C	2.46805100	1.54462500	-0.16739700
C	3.35322200	0.46595900	-0.08096600
C	2.85992300	-0.83969500	-0.01345600
C	1.48102200	-1.07922600	-0.02126700
C	0.61913400	-0.00099100	-0.09687800
H	2.85435700	2.55513600	-0.21182000
H	4.41597100	0.65560200	-0.06639700
H	1.12801100	-2.10037400	0.03930100
O	0.08162900	3.26896000	0.77681500
H	-0.67249700	3.86609600	0.71888400
O	-4.15261700	-1.54030800	0.06262500
O	3.64363300	-1.95178900	0.06694200
C	5.05250000	-1.79417100	0.09029200
H	5.37711600	-1.21115400	0.95801800
H	5.46515600	-2.79838500	0.15819700
H	5.41833800	-1.31473500	-0.82330200
C	-3.82971600	-2.91816600	0.15400000
H	-4.77948900	-3.44562900	0.20711600
H	-3.27577500	-3.25999800	-0.72617400
H	-3.24562800	-3.13457400	1.05416800

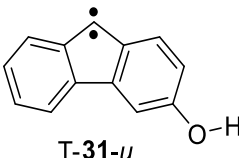
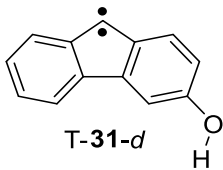


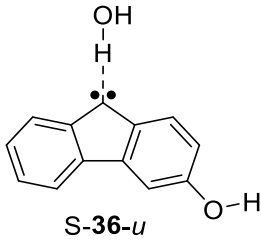
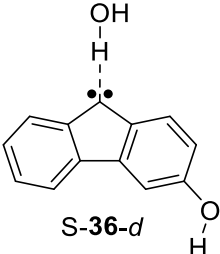
B3LYP/def2-TZVP
 E = -805.754381
 ZPVE = 0.256148

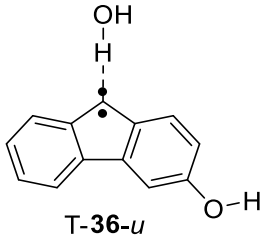
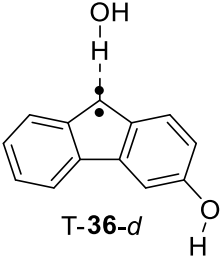
C	-2.99789100	-0.64688800	-0.01369800
C	-3.44209500	0.68078800	-0.05459300
C	-2.53241800	1.72691400	-0.13193800
C	-1.17719500	1.44584300	-0.16214700
C	-0.73442000	0.12214800	-0.10486800
C	-1.63230500	-0.93870000	-0.03829700
H	-4.50786300	0.86332900	-0.02240200
H	-2.88596400	2.75050700	-0.15523900
H	-1.27222000	-1.95623800	0.00194500
C	0.00000100	2.39405400	-0.26455800
H	0.00000000	2.86945500	-1.25419700
C	1.17719800	1.44584200	-0.16214900
C	2.53242100	1.72691100	-0.13194500
C	3.44209700	0.68078400	-0.05460000
C	2.99789200	-0.64689100	-0.01369700
C	1.63230500	-0.93870200	-0.03829600
C	0.73442100	0.12214700	-0.10486800
H	2.88596900	2.75050300	-0.15525000
H	4.50786600	0.86332400	-0.02241300
H	1.27222000	-1.95624000	0.00194500
O	-0.00000100	3.41016700	0.74418500
H	0.00003300	4.27193000	0.31998100
O	-3.98040100	-1.58880300	0.05521900
O	3.98039900	-1.58880700	0.05522000
C	3.60975800	-2.95552900	0.11165200
H	3.05422500	-3.25869100	-0.78184800
H	4.54000900	-3.51705100	0.16263400
H	3.00853200	-3.17235300	1.00061900
C	-3.60976600	-2.95552700	0.11164400
H	-4.54001900	-3.51704500	0.16263200
H	-3.05424400	-3.25869000	-0.78186200
H	-3.00853200	-3.17235400	1.00060500

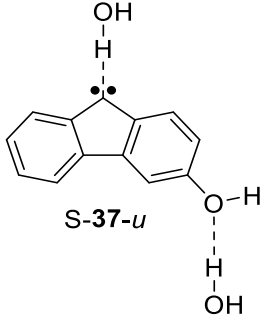
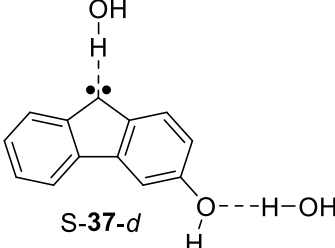
 <p>35-u</p> <p>B3LYP/def2-TZVP E = -684.986306 ZPVE = 0.177770</p>	C	-3.00852200	-0.63289600	0.00000400
	C	-3.06130400	0.76577300	-0.00000200
	C	-1.89312900	1.51918500	-0.00000500
	C	-0.67225100	0.86036400	-0.00000100
	C	-0.61737500	-0.55508800	0.00000200
	C	-1.78781500	-1.30094300	0.00000400
	H	-4.02427400	1.26411400	-0.00000400
	H	-1.94736600	2.60080500	-0.00000900
	H	-1.77686700	-2.38278600	0.00000300
	C	0.70274800	1.33834500	0.00000100
	C	1.59646700	0.19157600	-0.00000200
	C	2.98271400	0.09299000	-0.00000500
	C	3.55540300	-1.17381300	-0.00000300
	C	2.75900400	-2.32261000	0.00000100
	C	1.37223900	-2.22547000	0.00000200
	C	0.78103000	-0.96687000	0.00000100
	H	3.60569500	0.97907300	-0.00000700
	H	4.63353200	-1.27141100	-0.00000300
	H	3.22905900	-3.29758500	0.00000200
	H	0.76012700	-3.11886800	0.00000300
N	1.07444000	2.58154300	0.00000200	
N	1.39734900	3.66716500	0.00000600	
O	-4.13969800	-1.40248600	0.00000200	
H	-4.92009700	-0.83766900	-0.00003200	
 <p>35-d</p> <p>B3LYP/def2-TZVP E = -684.986300 ZPVE = 0.177832</p>	C	-3.01744300	-0.60769600	0.00000600
	C	-3.06167900	0.79144200	-0.00000600
	C	-1.88976800	1.53275600	-0.00000800
	C	-0.66985200	0.86621500	-0.00000300
	C	-0.62154100	-0.54670600	0.00000300
	C	-1.80120400	-1.28393200	0.00000800
	H	-4.02838300	1.27629000	-0.00001100
	H	-1.93536000	2.61484200	-0.00001400
	H	-1.77709800	-2.36829300	0.00001200
	C	0.70726000	1.33743600	0.00000200
	C	1.59542800	0.18696700	0.00000100
	C	2.98105700	0.08085000	0.00000000
	C	3.54752200	-1.18874600	-0.00000200
	C	2.74518500	-2.33341600	-0.00000200
	C	1.35896400	-2.22897400	-0.00000300
	C	0.77344500	-0.96749500	0.00000000
	H	3.60855200	0.96373900	-0.00000100
	H	4.62510700	-1.29183800	-0.00000200
	H	3.21020900	-3.31081300	-0.00000200
	H	0.74360600	-3.12033200	-0.00000300
H	0.74360600	-3.12033200	-0.00000300	
N	1.08577800	2.57895800	0.00000100	
N	1.41548600	3.66217400	0.00000500	
O	-4.22037200	-1.25900100	0.00000400	
H	-4.07675100	-2.21172500	-0.00003000	

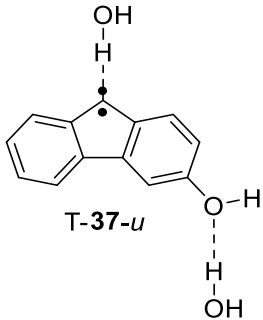
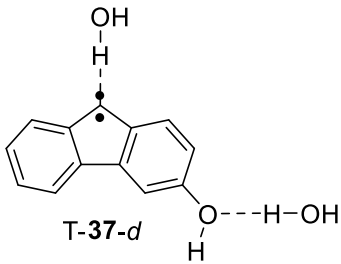
 <p>S-31-u</p> <p>B3LYP/def2-TZVP E = -575.375537 ZPVE = 0.166963</p>	C	2.78276300	-0.54832500	0.00000100
	C	3.00852100	0.82861500	-0.00002000
	C	1.92719300	1.70602900	-0.00001400
	C	0.62872500	1.20591400	-0.00001300
	C	0.42758100	-0.20711500	-0.00001400
	C	1.47612300	-1.08585400	0.00001100
	H	4.02598600	1.20295300	-0.00002700
	H	2.08329200	2.77747700	-0.00001900
	H	1.35390600	-2.16141100	0.00004000
	C	-0.60860800	1.96089800	0.00004000
	C	-1.61631200	0.88156700	0.00001200
	C	-2.99490300	1.01654700	0.00000600
	C	-3.79490500	-0.13540600	-0.00001500
	C	-3.21128100	-1.39319200	-0.00001200
	C	-1.81191000	-1.54804100	0.00000300
	C	-1.03581700	-0.41403700	0.00000400
	H	-3.43541000	2.00564200	0.00001600
	H	-4.87364700	-0.04554600	-0.00002700
	H	-3.84130000	-2.27415400	-0.00001900
	H	-1.37415300	-2.53922000	0.00001000
O	3.79408700	-1.44726000	0.00001400	
H	4.64561500	-0.99326700	-0.00002900	
 <p>S-31-d</p> <p>B3LYP/def2-TZVP E = -575.374839 ZPVE = 0.166876</p>	C	2.79197400	-0.53222900	-0.00000200
	C	3.01406300	0.84454300	0.00001200
	C	1.93024000	1.71485200	0.00001300
	C	0.62954100	1.21274100	0.00000800
	C	0.43045900	-0.19847400	0.00000300
	C	1.48523000	-1.07225600	-0.00001000
	H	4.03427000	1.20271200	0.00001500
	H	2.08265300	2.78680200	0.00001400
	H	1.34521300	-2.14878000	-0.00002500
	C	-0.60922800	1.96383600	-0.00003100
	C	-1.61616400	0.88157200	-0.00000700
	C	-2.99416500	1.01272900	-0.00000200
	C	-3.79173100	-0.14207600	0.00001000
	C	-3.20539600	-1.39775000	0.00000800
	C	-1.80484500	-1.54811700	0.00000000
	C	-1.03226300	-0.41221000	-0.00000100
	H	-3.43757200	2.00050800	-0.00000900
	H	-4.87065900	-0.05464700	0.00001800
	H	-3.83277100	-2.28055600	0.00001100
	H	-1.36538900	-2.53875400	-0.00000700
O	3.88245100	-1.33360300	0.00000200	
H	3.61835800	-2.26141900	-0.00004100	

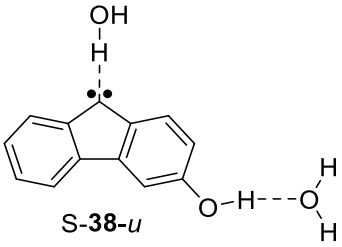
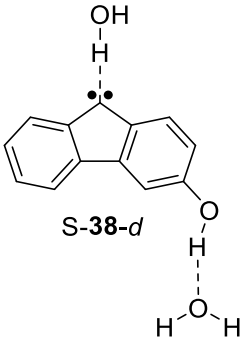
 <p>T-31-u</p> <p>B3LYP/def2-TZVP E = -575.379113 ZPVE = 0.166739</p>	C	2.77774100	-0.56018100	0.00001200
	C	3.02535200	0.81904000	-0.00000400
	C	1.97515300	1.72436700	-0.00000500
	C	0.66273700	1.24690800	-0.00000300
	C	0.41904200	-0.17086300	0.00000000
	C	1.47126100	-1.06162000	0.00000900
	H	4.04933300	1.17561200	-0.00001800
	H	2.17251700	2.78832900	-0.00001300
	H	1.31980200	-2.13337100	0.00001400
	C	-0.60698900	1.86213300	0.00000100
	C	-1.65985100	0.91199300	0.00000400
	C	-3.05177900	1.01342400	0.00000500
	C	-3.80751300	-0.15322800	0.00000000
	C	-3.19331000	-1.40822000	-0.00000500
	C	-1.80140800	-1.52476400	-0.00000600
	C	-1.02963600	-0.37741700	0.00000000
	H	-3.53079900	1.98391300	0.00000800
	H	-4.88820700	-0.08976100	0.00000100
	H	-3.80424700	-2.30174400	-0.00000900
	H	-1.33578100	-2.50313000	-0.00000900
O	3.78661500	-1.47755400	-0.00000900	
H	4.63966600	-1.02884800	0.00003600	
 <p>T-31-d</p> <p>B3LYP/def2-TZVP E = -575.378848 ZPVE = 0.166776</p>	C	2.78623900	-0.54513600	0.00000900
	C	3.02998300	0.83497600	0.00000100
	C	1.97724300	1.73230800	-0.00000300
	C	0.66314700	1.25156600	0.00000100
	C	0.42181200	-0.16399800	0.00000400
	C	1.48131900	-1.05064000	0.00000400
	H	4.05669200	1.17459000	-0.00000100
	H	2.16955200	2.79723500	-0.00000500
	H	1.31272100	-2.12269800	-0.00000300
	C	-0.60749200	1.86416900	-0.00000100
	C	-1.65924800	0.91190900	0.00000000
	C	-3.05081200	1.01012300	0.00000200
	C	-3.80456000	-0.15833300	0.00000100
	C	-3.18778200	-1.41163700	-0.00000100
	C	-1.79536400	-1.52480100	-0.00000400
	C	-1.02580100	-0.37597400	-0.00000400
	H	-3.53193500	1.97956400	0.00000200
	H	-4.88534200	-0.09700300	0.00000300
	H	-3.79661000	-2.30660300	0.00000000
	H	-1.32896100	-2.50298500	-0.00000300
O	3.87876200	-1.36067500	-0.00000900	
H	3.60168100	-2.28390100	0.00002800	

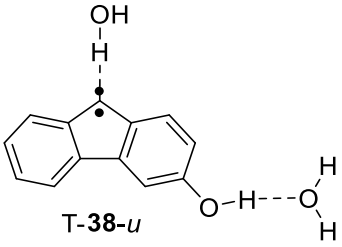
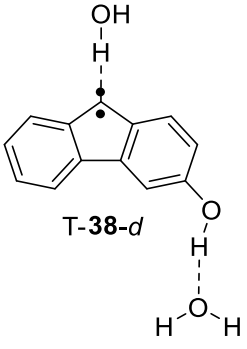
 <p>S-36-u</p> <p>B3LYP/def2-TZVP E = -651.834362 ZPVE = 0.191418</p>	C	-2.67752200	-1.16157300	0.00000500
	C	-2.99067500	0.19878400	0.01210700
	C	-1.97135100	1.14519600	0.02079300
	C	-0.64291100	0.71815800	0.01706400
	C	-0.34791700	-0.67914700	0.00471900
	C	-1.33849100	-1.62000500	-0.00381600
	H	-4.03020900	0.50649100	0.01347000
	H	-2.18470500	2.20780800	0.03009100
	H	-1.15192100	-2.68606600	-0.01420400
	C	0.54038900	1.53685000	0.01992100
	C	1.62272700	0.54140800	0.01080100
	C	2.98889000	0.76865700	0.00861300
	C	3.86285200	-0.32825900	-0.00161000
	C	3.36317600	-1.62124600	-0.01008600
	C	1.97649000	-1.86831500	-0.00873000
	C	1.12674000	-0.78938300	0.00200500
	H	3.36527300	1.78380600	0.01327800
	H	4.93313600	-0.16721900	-0.00380400
	H	4.04964200	-2.45878700	-0.01858800
	H	1.60540500	-2.88609600	-0.01661100
O	-3.62813900	-2.12097300	-0.00890400	
H	-4.50744800	-1.72262600	-0.00823900	
O	-0.71082800	4.14721800	-0.10094300	
H	-0.35085000	4.79230900	0.51489400	
H	-0.09095500	3.37366100	-0.06223300	
 <p>S-36-d</p> <p>B3LYP/def2-TZVP E = -651.833238 ZPVE = 0.191308</p>	C	-2.69121400	-1.14364300	0.00025800
	C	-2.99882600	0.21723600	0.01200100
	C	-1.97492100	1.15539300	0.02020600
	C	-0.64487500	0.72462800	0.01667800
	C	-0.35405700	-0.67159600	0.00435000
	C	-1.35244000	-1.60635300	-0.00395500
	H	-4.03959300	0.51017400	0.01314500
	H	-2.18270000	2.21910800	0.02855300
	H	-1.14930200	-2.67251400	-0.01409600
	C	0.54131200	1.53780900	0.02053200
	C	1.62156600	0.53770900	0.01118200
	C	2.98767900	0.75920800	0.00922200
	C	3.85788000	-0.34196700	-0.00131100
	C	3.35357300	-1.63229400	-0.01022000
	C	1.96505000	-1.87301100	-0.00907800
	C	1.12022200	-0.79075400	0.00188200
	H	3.36839600	1.77271600	0.01419700
	H	4.92873000	-0.18482700	-0.00337700
	H	4.03632700	-2.47281600	-0.01890400
	H	1.59082300	-2.88982900	-0.01733300
O	-3.72799900	-2.00961400	-0.00714200	
H	-3.40937900	-2.92029700	-0.01674500	
O	-0.68560700	4.16409500	-0.10485100	
H	-0.34383100	4.78514200	0.54518800	
H	-0.07632600	3.38308200	-0.06516700	

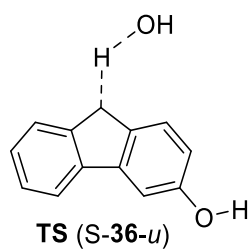
 <p>T-36-u</p> <p>B3LYP/def2-TZVP E = -651.826719 ZPVE = 0.189819</p>	C	-2.66747600	-1.18863700	0.00259100
	C	-3.00600100	0.17146700	-0.01670900
	C	-2.02033500	1.14550300	-0.02698500
	C	-0.67950600	0.75125800	-0.01835600
	C	-0.33918400	-0.64663200	-0.00033500
	C	-1.33043400	-1.60406700	0.01083200
	H	-4.05146500	0.45888700	-0.02508100
	H	-2.27524700	2.19708700	-0.04641000
	H	-1.10938700	-2.66351600	0.02519900
	C	0.54776600	1.44511000	-0.02395500
	C	1.66496500	0.57235100	-0.01375900
	C	3.04651200	0.76680900	-0.01659300
	C	3.87832500	-0.34691000	-0.00231600
	C	3.34877800	-1.63946000	0.01457800
	C	1.96763500	-1.84850600	0.01708400
	C	1.12051900	-0.75593500	0.00256800
	H	3.46042100	1.76675300	-0.03042200
	H	4.95227900	-0.21151500	-0.00469800
	H	4.01765100	-2.49033300	0.02546400
	H	1.56828400	-2.85559200	0.02984700
O	-3.61247500	-2.16987700	0.01355300	
H	-4.49371400	-1.77917300	0.00337100	
O	-0.71345900	4.27017100	-0.02229400	
H	-0.52582200	4.23850100	0.92222900	
H	-0.12490300	3.60244000	-0.40144100	
 <p>T-36-d</p> <p>B3LYP/def2-TZVP E = -651.826246 ZPVE = 0.189799</p>	C	-2.68233000	-1.16813500	0.00290600
	C	-3.01356800	0.19391900	-0.02175500
	C	-2.02217500	1.15760800	-0.03567300
	C	-0.68053800	0.75677200	-0.02518600
	C	-0.34639800	-0.63996000	-0.00184600
	C	-1.34762100	-1.59110700	0.01272700
	H	-4.05990000	0.46694200	-0.03109400
	H	-2.26975400	2.21091500	-0.05941300
	H	-1.11206300	-2.65022700	0.03132600
	C	0.54960300	1.44474000	-0.03225100
	C	1.66354400	0.56692700	-0.01821300
	C	3.04541300	0.75462100	-0.02072300
	C	3.87245800	-0.36314400	-0.00204400
	C	3.33688200	-1.65271500	0.01890200
	C	1.95444900	-1.85484900	0.02117600
	C	1.11232700	-0.75851500	0.00231400
	H	3.46404000	1.75253800	-0.03765400
	H	4.94698300	-0.23266300	-0.00413700
	H	4.00152100	-2.50685000	0.03317700
	H	1.55170400	-2.86071000	0.03714000
O	-3.71981400	-2.05061100	0.01604000	
H	-3.38610500	-2.95490100	0.02931100	
O	-0.67665600	4.28401100	-0.00984400	
H	-0.52224400	4.22001400	0.93903800	
H	-0.09470900	3.61077600	-0.38925700	

 <p>S-37-u</p> <p>B3LYP/def2-TZVP E = -728.282259 ZPVE = 0.214974</p>	C	2.48103900	0.64915800	-0.07527900
	C	2.04499700	1.97231200	-0.05454800
	C	0.68063700	2.25075600	-0.02763600
	C	-0.22780300	1.19362200	-0.02258500
	C	0.24872400	-0.15078300	-0.04647600
	C	1.58435500	-0.44303300	-0.07287600
	H	2.77230000	2.77639700	-0.05710600
	H	0.31022800	3.26912200	-0.00989500
	H	1.97880800	-1.45112800	-0.09004500
	C	-1.66806600	1.27322600	0.00994700
	C	-2.06932700	-0.13930500	-0.00077500
	C	-3.35313000	-0.66017600	0.01866800
	C	-3.52406700	-2.05182000	0.00311600
	C	-2.42159900	-2.89208000	-0.03045200
	C	-1.11005500	-2.37844500	-0.04955900
	C	-0.95107100	-1.01451500	-0.03453300
	H	-4.20453000	0.00809500	0.04637700
	H	-4.52016100	-2.47485900	0.01777300
	H	-2.56895000	-3.96491500	-0.04227200
	H	-0.26059000	-3.05010600	-0.07548500
O	3.80540400	0.33521100	-0.09910700	
H	4.34220300	1.13671600	-0.12196000	
O	4.12409600	-2.62006400	0.12380600	
H	4.29559500	-1.67299100	0.03649000	
H	4.42020900	-2.85391300	1.00910400	
O	-1.94887500	4.15015000	0.20235400	
H	-2.61652800	4.53273600	-0.37454900	
H	-2.08138700	3.16897200	0.14308500	
 <p>S-37-d</p> <p>B3LYP/def2-TZVP E = -728.280205 ZPVE = 0.214679</p>	C	2.53544300	-0.58246100	-0.05472600
	C	2.57725700	0.80931300	-0.08014200
	C	1.38277700	1.52257500	-0.07541200
	C	0.16399800	0.84734200	-0.04904500
	C	0.15342600	-0.57802600	-0.02712700
	C	1.31799800	-1.29843100	-0.02873000
	H	3.53995300	1.30237300	-0.10468400
	H	1.39083300	2.60499200	-0.09317600
	H	1.32656100	-2.38360400	-0.00912800
	C	-1.16673200	1.40879400	-0.03676600
	C	-2.02164800	0.21589700	-0.00969500
	C	-3.40730600	0.17367800	0.01002500
	C	-4.04114800	-1.07861300	0.03800900
	C	-3.29340100	-2.24498300	0.04543300
	C	-1.88344100	-2.21284400	0.02579400
	C	-1.26748000	-0.98695100	-0.00156700
	H	-3.96928700	1.10018100	0.00397800
	H	-5.12181800	-1.13537600	0.05473100
	H	-3.79852800	-3.20276200	0.06721700
	H	-1.31959300	-3.13810800	0.03275900
O	3.72651800	-1.24212800	-0.05343800	
H	3.58901800	-2.19666800	-0.06500500	
O	5.98594200	0.70058600	0.06625000	
H	6.22851500	0.77234300	0.99484200	
H	5.43795800	-0.09264700	0.00546400	
O	-3.22582800	3.45166200	0.11377600	
H	-2.38624700	2.92914100	0.05839700	
H	-3.10887900	4.18745100	-0.49440900	

 <p>T-37-u</p> <p>B3LYP/def2-TZVP E = -728.275326 ZPVE = 0.213524</p>	C	2.48703800	0.62026900	-0.08013900
	C	2.07536100	1.95629800	-0.02771000
	C	0.72643200	2.27578500	0.01760200
	C	-0.21160100	1.24087800	0.01107100
	C	0.22476400	-0.12835300	-0.04230000
	C	1.56830600	-0.43408600	-0.08939500
	H	2.81939500	2.74501600	-0.02009900
	H	0.39769000	3.30576600	0.06264000
	H	1.92958600	-1.45395600	-0.13289400
	C	-1.62178500	1.19274300	0.04741300
	C	-2.11999400	-0.13402600	0.02271800
	C	-3.39990100	-0.68949600	0.04273600
	C	-3.52788100	-2.07316600	0.00334000
	C	-2.40210800	-2.89826200	-0.05531700
	C	-1.11470500	-2.35600500	-0.07529200
	C	-0.96363800	-0.98252700	-0.03563700
	H	-4.27446200	-0.05353900	0.08827200
	H	-4.51423300	-2.51878400	0.01816900
	H	-2.52893900	-3.97269500	-0.08619500
	H	-0.24786100	-3.00422700	-0.12152700
O	3.81652700	0.28127200	-0.12308600	
H	4.36406500	1.07382900	-0.14825200	
O	4.12958800	-2.64061400	0.13139500	
H	4.24613400	-1.68940200	-0.00116900	
H	4.25386600	-2.77906900	1.07562300	
O	-1.99764200	4.26499100	0.13495400	
H	-2.19731400	4.18267000	-0.80403100	
H	-2.15743200	3.37888600	0.48881200	
 <p>T-37-d</p> <p>B3LYP/def2-TZVP E = -728.274236 ZPVE = 0.213366</p>	C	2.54168900	-0.55044300	-0.07786500
	C	2.58491900	0.84841000	-0.06850200
	C	1.40763100	1.57596700	-0.03534900
	C	0.18169900	0.90362300	-0.01359100
	C	0.15108400	-0.53210000	-0.02519900
	C	1.33144000	-1.24920900	-0.05728800
	H	3.54931800	1.33845500	-0.09092100
	H	1.43952300	2.65757100	-0.02895600
	H	1.32591000	-2.33428700	-0.06535400
	C	-1.16763500	1.31450700	0.01837300
	C	-2.06884700	0.21943600	0.03134100
	C	-3.45988700	0.11498500	0.06377800
	C	-4.02952300	-1.15361400	0.06570600
	C	-3.23368300	-2.30095600	0.03546200
	C	-1.83964100	-2.20769300	0.00385600
	C	-1.24883900	-0.95800600	0.00223000
	H	-4.06910500	1.00910300	0.09110400
	H	-5.10695200	-1.25398500	0.09199800
	H	-3.70272300	-3.27644900	0.03751300
	H	-1.23443200	-3.10627900	-0.01886300
O	3.74607800	-1.20688000	-0.10597700	
H	3.61075800	-2.15984700	-0.15186900	
O	6.02998700	0.65061600	0.09328300	
H	6.15390300	0.71036600	1.04578200	
H	5.42190200	-0.09046300	-0.03443200	
O	-3.34512100	3.52138700	0.01468800	
H	-2.55126200	3.11242900	0.38604800	
H	-3.18683500	3.52296000	-0.93571700	

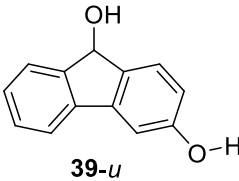
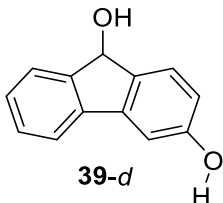
 <p>S-38-u</p> <p>B3LYP/def2-TZVP E = -728.289676 ZPVE = 0.215399</p>	C	2.22889100	-0.86281700	0.01392900
	C	2.40511800	0.52774200	0.02385400
	C	1.29834500	1.36567200	0.02612200
	C	0.01350200	0.81406700	0.01910100
	C	-0.14275500	-0.60716300	0.01040800
	C	0.93440100	-1.44506500	0.00781800
	H	3.41046700	0.92828200	0.02912500
	H	1.40558500	2.44437500	0.03278700
	H	0.85248300	-2.52450000	-0.00030600
	C	-1.23778900	1.51199300	0.01470800
	C	-2.22251500	0.41511800	0.00504700
	C	-3.60362800	0.50752500	-0.00299800
	C	-4.36693500	-0.66970000	-0.01246400
	C	-3.74449600	-1.90814100	-0.01440500
	C	-2.34049300	-2.01776700	-0.00708700
	C	-1.59965900	-0.86087600	0.00283500
	H	-4.07768400	1.48101900	-0.00354400
	H	-5.44792100	-0.61310600	-0.01922200
	H	-4.34613900	-2.80864300	-0.02238900
	H	-1.87081200	-2.99415100	-0.00993800
O	3.26064800	-1.71665900	0.00915700	
H	4.11611100	-1.24050600	0.00441800	
O	5.68912800	-0.36816300	-0.02650300	
H	6.30595400	-0.45067100	0.70887400	
H	6.21920100	-0.36920300	-0.83101100	
O	-0.29943500	4.25123100	-0.09848200	
H	-0.80792500	3.39787300	-0.07375100	
H	-0.69396900	4.79442600	0.59038700	
 <p>S-38-d</p> <p>B3LYP/def2-TZVP E = -728.288604 ZPVE = 0.215558</p>	C	-2.45528600	-0.68653200	0.01162700
	C	-1.98222800	-2.00403900	0.01538500
	C	-0.61847800	-2.25213600	0.01631600
	C	0.27984000	-1.17777200	0.01399400
	C	-0.22316100	0.15885600	0.01024600
	C	-1.56401900	0.42075000	0.00895900
	H	-2.70691500	-2.80670700	0.01563300
	H	-0.22606100	-3.26258600	0.01740300
	H	-1.96577600	1.42697600	0.00552200
	C	1.71120500	-1.23312200	0.01140700
	C	2.09318300	0.19203700	0.00676200
	C	3.36548300	0.73552500	0.00148700
	C	3.51220900	2.13164500	-0.00307000
	C	2.39654200	2.95323400	-0.00277900
	C	1.09518300	2.41362400	0.00182900
	C	0.95984000	1.04682100	0.00677100
	H	4.22948800	0.08293400	-0.00079000
	H	4.50152200	2.57097000	-0.00768700
	H	2.52457300	4.02866700	-0.00683600
	H	0.23358200	3.07085200	0.00082700
O	-3.78269200	-0.50544800	0.01036800	
H	-4.01341400	0.44512100	0.00259900	
O	-4.46729700	2.19688200	-0.02557900	
H	-4.96154300	2.53574700	0.72926400	
H	-4.92371000	2.51469600	-0.81275800	
O	2.12672100	-4.10176200	-0.11677900	
H	2.68352700	-4.40613900	0.60616600	
H	2.18898800	-3.11125900	-0.08703500	

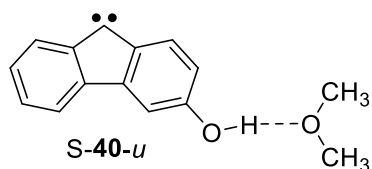
 <p>T-38-u</p> <p>B3LYP/def2-TZVP E = -728.279974 ZPVE = 0.213818</p>	C	2.53840000	-0.49950700	0.02122600
	C	2.54709000	0.90574300	-0.02371400
	C	1.35953300	1.61707200	-0.05798400
	C	0.14368800	0.92659700	-0.04780000
	C	0.14172800	-0.51261200	-0.00218400
	C	1.32920200	-1.21015800	0.03249600
	H	3.49794900	1.42321200	-0.03126200
	H	1.37388500	2.69888200	-0.09307600
	H	1.35991000	-2.29176100	0.06734600
	C	-1.20977500	1.31114800	-0.07230200
	C	-2.09265600	0.20048400	-0.04890600
	C	-3.48192900	0.07028600	-0.06176900
	C	-4.02951400	-1.20728100	-0.02709100
	C	-3.21302400	-2.34006900	0.02001400
	C	-1.82108500	-2.22133900	0.03223800
	C	-1.25156500	-0.96171600	-0.00225800
	H	-4.10952600	0.95128800	-0.10308100
	H	-5.10543200	-1.32670900	-0.03814600
	H	-3.66490400	-3.32339600	0.04614400
	H	-1.19786200	-3.10701800	0.06784500
O	3.67949000	-1.22518600	0.05540400	
H	4.46105300	-0.64185000	0.03926300	
O	5.95322000	0.43043900	-0.00354700	
H	6.54222100	0.39209500	0.75803800	
H	6.51467300	0.35917200	-0.78339000	
O	-3.33301100	3.53722200	0.05056100	
H	-2.57063500	3.06893500	-0.31995400	
H	-3.25949100	3.38545900	0.99913100	
 <p>T-38-d</p> <p>B3LYP/def2-TZVP E = -728.279901 ZPVE = 0.213956</p>	C	-2.46054700	-0.69571400	-0.00763500
	C	-1.99413500	-2.02085700	-0.03915100
	C	-0.63995900	-2.29451400	-0.05565300
	C	0.27227000	-1.23077100	-0.04077900
	C	-0.20750100	0.12404700	-0.01009600
	C	-1.56269300	0.38374500	0.00691100
	H	-2.72549000	-2.81766000	-0.05196800
	H	-0.27895300	-3.31458700	-0.08508800
	H	-1.94367300	1.39772000	0.03102800
	C	1.67670500	-1.14025400	-0.04816300
	C	2.13646000	0.20200900	-0.02747900
	C	3.39831000	0.79555700	-0.02737500
	C	3.48547800	2.18331400	-0.00148600
	C	2.33513800	2.97513100	0.02408400
	C	1.06501900	2.39336800	0.02388200
	C	0.95342900	1.01527000	-0.00213200
	H	4.29211200	0.18540200	-0.04778900
	H	4.45870100	2.65738500	-0.00147400
	H	2.42933300	4.05333500	0.04399200
	H	0.17899900	3.01705100	0.04352800
O	-3.80071900	-0.51333600	0.00713600	
H	-4.01872000	0.43706000	0.02176700	
O	-4.43556800	2.23279900	0.03276900	
H	-4.92891200	2.55522000	0.79515800	
H	-4.89567600	2.56469600	-0.74620600	
O	2.25259500	-4.16739000	0.03326900	
H	2.22866700	-4.01606800	0.98446700	
H	2.32530000	-3.27811800	-0.34237600	



B3LYP/def2-TZVP
 E = -651.825635
 ZPVE = 0.187071

C	-2.96966800	-1.98206600	0.15921300
C	-3.66226700	-0.79285900	-0.03729700
C	-2.97014700	0.40161400	-0.25722600
C	-1.58360100	0.38279800	-0.25090700
C	-0.88615900	-0.83081000	-0.02796300
C	-1.56691700	-2.01418400	0.15854700
H	-4.74451200	-0.79606000	-0.03051700
H	-3.50277000	1.32882200	-0.42857300
H	-1.04266200	-2.95031300	0.30634800
C	-0.64069400	1.46680500	-0.52628500
C	0.65624900	0.89323800	-0.28743800
C	1.90929200	1.49738500	-0.32693500
C	3.04553500	0.72112100	-0.13832700
C	2.92573500	-0.65750800	0.06286800
C	1.66832200	-1.28941700	0.10143500
C	0.55228300	-0.50583200	-0.05065500
H	1.98897500	2.56522800	-0.48335600
H	4.03010300	1.17440500	-0.15249100
H	1.62346000	-2.35957800	0.25479700
O	-0.97855300	3.37164300	0.72806100
H	-0.91737600	2.70896500	-0.27395400
H	-1.80698300	3.12671800	1.16048800
O	4.00462400	-1.45902600	0.23062600
H	-3.52147700	-2.90087400	0.31319600
H	4.81690100	-0.93997000	0.19037400

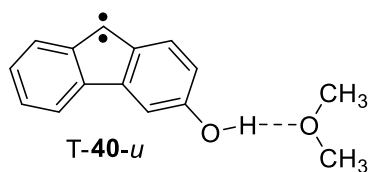
 <p>39-u</p> <p>B3LYP/def2-TZVP E = -651.924483 ZPVE = 0.195617</p>	C	2.99444200	-1.88351500	-0.09467200
	C	3.69083100	-0.68296400	0.02396000
	C	3.00155000	0.52321800	0.16172700
	C	1.61992000	0.50591300	0.16767700
	C	0.91727400	-0.70108200	0.04162800
	C	1.60142200	-1.90320900	-0.08509700
	H	4.77335800	-0.68692000	0.01247300
	H	3.55038700	1.45322900	0.26169300
	H	1.06560300	-2.83959600	-0.17898000
	C	0.65030300	1.66741900	0.30802600
	H	0.75917800	2.12245700	1.30357300
	C	-0.68833900	0.97962800	0.19172700
	C	-1.95386700	1.53095900	0.20172600
	C	-3.06098300	0.69153600	0.08738000
	C	-2.88907400	-0.68939000	-0.02933000
	C	-1.61337300	-1.25227900	-0.04438800
	C	-0.52056800	-0.40632100	0.05967600
	H	-2.08973200	2.60177500	0.28432600
	H	-4.06226900	1.10807600	0.08795700
	H	-1.50847700	-2.32447000	-0.14364800
O	0.77262700	2.67987000	-0.69309200	
H	1.63593700	3.09828600	-0.60168500	
O	-3.94657400	-1.54840600	-0.13748700	
H	-4.77265600	-1.05258500	-0.12478600	
H	3.54302400	-2.81144400	-0.19653500	
 <p>39-d</p> <p>B3LYP/def2-TZVP E = -651.924258 ZPVE = 0.195629</p>	C	2.98605100	-1.89033300	-0.09278800
	C	3.68643100	-0.69225700	0.02443000
	C	3.00093000	0.51649200	0.16094900
	C	1.61955300	0.50416700	0.16723700
	C	0.91238300	-0.70054500	0.04188500
	C	1.59274000	-1.90492800	-0.08333200
	H	4.76890800	-0.69982200	0.01270000
	H	3.55277400	1.44482300	0.25941400
	H	1.05503600	-2.84050900	-0.17633300
	C	0.65301200	1.66860800	0.30633500
	H	0.76200000	2.12260600	1.30235400
	C	-0.68772800	0.98498900	0.18952200
	C	-1.95426300	1.54110800	0.20003100
	C	-3.06461600	0.71075700	0.08800700
	C	-2.89823800	-0.67073800	-0.02793700
	C	-1.62447700	-1.23903900	-0.04342700
	C	-0.52374400	-0.39866900	0.05925600
	H	-2.08398100	2.61274100	0.28230200
	H	-4.06901100	1.11203300	0.08736200
	H	-1.50402700	-2.31261700	-0.14083800
O	0.77982700	2.68027100	-0.69435800	
H	1.63611900	3.10976500	-0.58969500	
O	-4.03417300	-1.42410200	-0.12744800	
H	-3.80260000	-2.35573500	-0.21020700	
H	3.53134900	-2.82031400	-0.19363300	



B3LYP/def2-TZVP
 E = -730.408834
 ZPVE = 0.248393

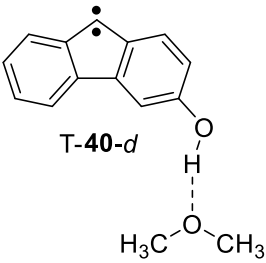
C	-1.33314800	-0.46977700	0.10909200
C	-1.52007900	0.91796900	0.16889900
C	-0.41772800	1.76448700	0.16455300
C	0.87144400	1.23689900	0.10273900
C	1.03515700	-0.18149400	0.04662100
C	-0.03411200	-1.03255700	0.04893600
H	-2.52771300	1.30880300	0.22569700
H	-0.54576200	2.83906500	0.21059300
H	0.06157000	-2.11020400	0.00541400
C	2.12099000	1.95947700	0.08722400
C	3.10483800	0.85557900	0.01741800
C	4.48514500	0.95583500	-0.02262600
C	5.25534800	-0.21497900	-0.08867700
C	4.64070300	-1.45750900	-0.11375300
C	3.23862800	-1.57667400	-0.07368000
C	2.49205600	-0.42440600	-0.00869800
H	4.95132300	1.93300700	-0.00249500
H	6.33563800	-0.15111400	-0.12043900
H	5.24764800	-2.35316300	-0.16501700
H	2.77456900	-2.55575900	-0.09403600
O	-2.35920600	-1.33251600	0.10433900
H	-3.22123700	-0.85900300	0.11595900
O	-4.74116100	-0.02009800	0.01314900
C	-5.77892500	-0.33997000	0.93015300
H	-5.31213500	-0.50105700	1.90014600
H	-6.49622800	0.48404400	1.00528000
C	-5.20004200	0.20998900	-1.31303700
H	-5.69960000	-0.67767000	-1.71647900
H	-5.89318000	1.05712700	-1.34104500
H	-6.30789700	-1.24982000	0.62528400
H	-4.32570600	0.43944900	-1.91975300

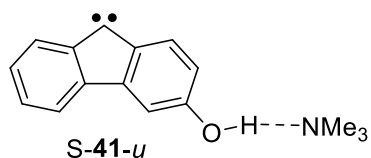
<p>S-40-d</p> <p>B3LYP/def2-TZVP E = -730.408383 ZPVE = 0.248347</p>	C	1.47214300	1.51123900	0.03256200
	C	0.88589100	2.78152000	0.00068400
	C	-0.49577700	2.90668500	-0.02347700
	C	-1.30416800	1.76761000	-0.01567000
	C	-0.68367200	0.48297000	0.01878100
	C	0.67630100	0.33604500	0.04315000
	H	1.53722700	3.64486900	-0.00542000
	H	-0.96262900	3.88356000	-0.04893300
	H	1.16052300	-0.63288600	0.07251900
	C	-2.74560900	1.70666100	-0.03789000
	C	-2.98533900	0.24437000	-0.01354300
	C	-4.20316000	-0.41269200	-0.02028200
	C	-4.22503800	-1.81601900	0.00722800
	C	-3.04046200	-2.53467800	0.04088200
	C	-1.79337300	-1.88064200	0.04805000
	C	-1.78188200	-0.50671900	0.02072400
	H	-5.12088800	0.16147300	-0.04640800
	H	-5.17104000	-2.34248600	0.00244400
	H	-3.07214000	-3.61716900	0.06222700
	H	-0.87631900	-2.45782200	0.07498600
O	2.81118800	1.44413200	0.05240600	
H	3.12120000	0.51141700	0.05939200	
O	3.69069400	-1.13518900	0.01523600	
C	4.47112300	-1.58736600	1.11451900	
H	4.46983900	-2.68118400	1.16577500	
H	5.50465500	-1.23245700	1.03635900	
C	4.17254100	-1.57708800	-1.24779200	
H	4.15830900	-2.67040000	-1.30630000	
H	5.19275900	-1.22040900	-1.42687500	
H	3.50846400	-1.16628300	-2.00627000	
H	4.01786600	-1.18313300	2.01781600	



B3LYP/def2-TZVP
 E = -730.410663
 ZPVE = 0.248265

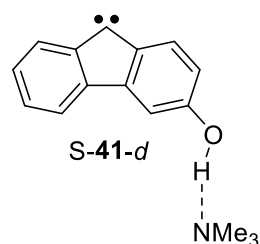
C	-1.33444200	-0.46807900	0.20880800
C	-1.53504000	0.92239100	0.27534300
C	-0.45835500	1.79352100	0.24503400
C	0.83903700	1.28109200	0.14992400
C	1.03718600	-0.14297700	0.08750500
C	-0.04072800	-1.00117300	0.11686400
H	-2.54560400	1.30092000	0.36148900
H	-0.62135100	2.86237600	0.29826700
H	0.07814700	-2.07624200	0.06931500
C	2.12351300	1.85786500	0.09682400
C	3.14564000	0.87806300	0.00278800
C	4.53761700	0.93811600	-0.07511400
C	5.25575900	-0.24932800	-0.15903900
C	4.60381600	-1.48519600	-0.16577600
C	3.21126800	-1.56036300	-0.08831500
C	2.47628700	-0.39180200	-0.00419900
H	5.04624100	1.89355600	-0.06993300
H	6.33624000	-0.21717500	-0.21994800
H	5.18556700	-2.39572500	-0.23171100
H	2.71554900	-2.52391800	-0.09404000
O	-2.36488500	-1.34459800	0.23049400
H	-3.22093600	-0.86946200	0.23465900
O	-4.75478400	0.00723600	0.00500500
C	-5.90985700	-0.40714300	0.71956600
H	-5.60706800	-0.57343000	1.75181800
H	-6.68407800	0.36735600	0.68937900
C	-4.99649100	0.25277900	-1.37406400
H	-5.36211100	-0.64936700	-1.87725700
H	-5.72824700	1.05756600	-1.50269100
H	-6.31805700	-1.33680500	0.30673200
H	-4.04820000	0.55265700	-1.81696600

 <p>T-40-d</p> <p>B3LYP/def2-TZVP E = -730.410714 ZPVE = 0.248334</p>	C	1.51033600	1.51344500	0.15243100
	C	0.94886700	2.79348900	0.01064200
	C	-0.41918800	2.95754300	-0.10041100
	C	-1.25271100	1.83236600	-0.07159900
	C	-0.67425500	0.52561300	0.07817500
	C	0.69315100	0.37257100	0.19114400
	H	1.61816100	3.64296900	-0.01126700
	H	-0.84257300	3.94764300	-0.21012300
	H	1.14335200	-0.60467100	0.31759500
	C	-2.64515500	1.63638400	-0.15737100
	C	-2.99822500	0.26406900	-0.06956100
	C	-4.20980800	-0.42660800	-0.10094800
	C	-4.19495100	-1.81226600	0.01604400
	C	-2.99271600	-2.50855500	0.16298200
	C	-1.77217500	-1.82985500	0.19583800
	C	-1.76303300	-0.45164100	0.08069100
	H	-5.14348300	0.10916900	-0.21395300
	H	-5.12833400	-2.36037400	-0.00636300
	H	-3.00770300	-3.58723600	0.25328800
	H	-0.84531000	-2.37951800	0.31186600
O	2.85748500	1.43472300	0.24887000	
H	3.14439400	0.49909900	0.27136600	
O	3.61389700	-1.21121100	0.05030400	
C	4.71100200	-1.74134300	0.77975400	
H	4.70921900	-2.83625400	0.74322300	
H	5.66423900	-1.37224500	0.38433600	
C	3.63253400	-1.54881600	-1.33068000	
H	3.58232800	-2.63459700	-1.46551200	
H	4.53692000	-1.16738600	-1.81767800	
H	2.75723300	-1.08762600	-1.78517700	
H	4.59846100	-1.41544500	1.81223200	



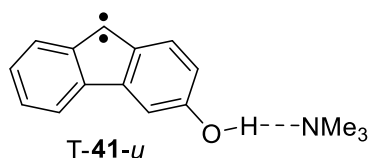
B3LYP/def2-TZVP
 E = -749.827720
 ZPVE = 0.288976

C	1.03073700	-0.37143800	0.00000700
C	1.16881700	1.02617700	-0.00000900
C	0.04327000	1.83933700	-0.00002000
C	-1.23119900	1.27265300	-0.00001600
C	-1.35089600	-0.15215600	0.00000000
C	-0.25679100	-0.96974500	0.00001200
H	2.16089100	1.45639600	-0.00001200
H	0.13962800	2.91831300	-0.00003200
H	-0.32119200	-2.05064500	0.00002400
C	-2.50044300	1.95567700	-0.00002600
C	-3.45183400	0.82035400	-0.00001400
C	-4.83514200	0.87691400	-0.00001800
C	-5.56973400	-0.31840100	-0.00000500
C	-4.91766400	-1.54204200	0.00001000
C	-3.51213400	-1.61677800	0.00001300
C	-2.80049200	-0.44063900	0.00000100
H	-5.33123900	1.83947000	-0.00002900
H	-6.65200100	-0.28839200	-0.00000700
H	-5.49751700	-2.45691400	0.00002000
H	-3.01799800	-2.58128100	0.00002500
O	2.07572300	-1.19715700	0.00001800
H	2.96113200	-0.71052100	0.00001300
N	4.57498700	-0.16640500	0.00000800
C	5.31835200	-1.42830500	0.00002600
H	5.05198100	-2.00904700	0.88326600
H	5.05198300	-2.00907200	-0.88319900
C	4.84621100	0.60971100	-1.20999100
H	4.24664500	1.52022100	-1.20844900
H	5.90591800	0.89190900	-1.28974400
C	4.84620800	0.60974400	1.20998600
H	4.24664200	1.52025400	1.20841700
H	5.90591600	0.89194500	1.28973200
H	4.57463100	0.02432900	-2.08867100
H	6.40564900	-1.26563300	0.00002500
H	4.57462700	0.02438600	2.08868100



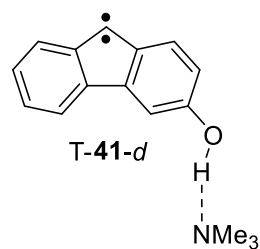
B3LYP/def2-TZVP
 E = -749.827153
 ZPVE = 0.288867

C	1.17963600	1.56647400	-0.00003400
C	0.57203200	2.83063400	-0.00001400
C	-0.80964800	2.94097100	0.00000800
C	-1.60825600	1.79335300	0.00000800
C	-0.97218300	0.51533400	-0.00001600
C	0.38859300	0.38512700	-0.00003700
H	1.21336600	3.70151100	-0.00001300
H	-1.28698500	3.91320600	0.00002600
H	0.87432700	-0.58243000	-0.00005600
C	-3.04654500	1.71637200	0.00003100
C	-3.27025800	0.24972200	0.00001600
C	-4.47976300	-0.42188300	0.00002600
C	-4.48475500	-1.82592200	0.00000800
C	-3.29197200	-2.53136900	-0.00001900
C	-2.05312400	-1.86191200	-0.00002900
C	-2.05804000	-0.48766500	-0.00001200
H	-5.40467000	0.14125100	0.00004700
H	-5.42466300	-2.36326200	0.00001500
H	-3.31065900	-3.61434600	-0.00003300
H	-1.12922000	-2.42914700	-0.00005000
O	2.51053200	1.51306800	-0.00005200
H	2.86573400	0.56871000	-0.00004500
N	3.74543600	-0.89579700	0.00000900
C	5.12575400	-0.40541700	-0.00000900
H	5.29420300	0.21094100	-0.88315200
H	5.85484100	-1.22823100	0.00003900
C	3.45552700	-1.66497500	1.20990800
H	3.62279200	-1.04196600	2.08872400
H	2.41133000	-1.97892300	1.20873100
C	3.45554200	-1.66510400	-1.20981100
H	2.41134700	-1.97905600	-1.20861300
H	4.08686000	-2.56181900	-1.28960200
H	3.62281600	-1.04218900	-2.08869200
H	4.08684100	-2.56168200	1.28980100
H	5.29419300	0.21103400	0.88307200



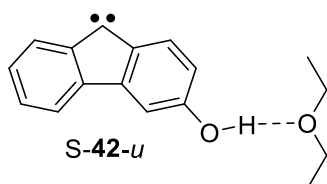
B3LYP/def2-TZVP
 E = -749.828880
 ZPVE = 0.288830

C	1.01842000	-0.37220900	-0.00001000
C	1.17466500	1.02734900	0.00003100
C	0.07455000	1.86827600	0.00005600
C	-1.21100900	1.31845000	0.00004100
C	-1.36899100	-0.11251800	0.00000000
C	-0.26668100	-0.93879000	-0.00002500
H	2.17331600	1.44308600	0.00004200
H	0.20951500	2.94243400	0.00008800
H	-0.35740100	-2.01769800	-0.00005700
C	-2.51226700	1.85683100	0.00005800
C	-3.50838900	0.84605900	0.00002900
C	-4.90376500	0.86425600	0.00003000
C	-5.58967100	-0.34495000	-0.00000500
C	-4.90258700	-1.56178500	-0.00004000
C	-3.50640000	-1.59512400	-0.00004200
C	-2.80290500	-0.40420300	-0.00000800
H	-5.43972200	1.80467400	0.00005700
H	-6.67237100	-0.34507600	-0.00000400
H	-5.45973200	-2.48993400	-0.00006700
H	-2.98304400	-2.54398500	-0.00007000
O	2.06756000	-1.21471900	-0.00003600
H	2.94172600	-0.72922700	-0.00002200
N	4.60131300	-0.16982400	-0.00001100
C	5.33197200	-1.43726200	-0.00005100
H	5.05967400	-2.01591900	0.88283800
H	5.05966400	-2.01586900	-0.88297000
C	4.87526100	0.60333300	-1.20914500
H	4.28024500	1.51709600	-1.20750100
H	5.93676400	0.88097100	-1.29217000
C	4.87527300	0.60326400	1.20916400
H	4.28025700	1.51702800	1.20757700
H	5.93677700	0.88089700	1.29219500
H	4.59900300	0.01946900	-2.08749000
H	6.42177400	-1.28663200	-0.00005300
H	4.59902300	0.01935000	2.08747800



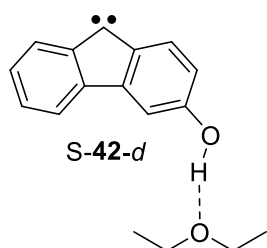
B3LYP/def2-TZVP
 E = -749.828979
 ZPVE = 0.288822

C	1.17960100	1.58987200	-0.02378700
C	0.57675300	2.86174200	-0.00801100
C	-0.79781900	2.99811700	0.00701400
C	-1.60559500	1.85306200	0.00654100
C	-0.99029600	0.55465300	-0.01043000
C	0.38413300	0.43139000	-0.02571900
H	1.22457000	3.72804500	-0.00751300
H	-1.24792600	3.98251100	0.01932400
H	0.85417200	-0.54359200	-0.04028300
C	-2.99515300	1.62737300	0.01919100
C	-3.31222600	0.24318200	0.01108600
C	-4.50776500	-0.47535700	0.01761700
C	-4.45555400	-1.86504500	0.00539600
C	-3.23168300	-2.53856200	-0.01314600
C	-2.02698600	-1.83165500	-0.01980800
C	-2.05460300	-0.44881800	-0.00783200
H	-5.45826200	0.04228400	0.03189800
H	-5.37642400	-2.43435400	0.01023400
H	-3.21743500	-3.62098200	-0.02254100
H	-1.08321700	-2.36468000	-0.03435800
O	2.52371700	1.53968500	-0.03723600
H	2.86316700	0.59907200	-0.03294400
N	3.72893900	-0.92378600	0.00580900
C	5.11746500	-0.46276400	-0.00355400
H	5.30414000	0.11628000	-0.90818700
H	5.83134500	-1.29902000	0.03268000
C	3.41338500	-1.63847900	1.24075700
H	3.59013400	-0.98644000	2.09645700
H	2.36150100	-1.92585400	1.24467900
C	3.42680400	-1.72838900	-1.17576300
H	2.37522200	-2.01704200	-1.16952200
H	4.03626500	-2.64336700	-1.22108700
H	3.61274600	-1.14204700	-2.07592300
H	5.29339600	0.18381400	0.85635500
H	4.02153300	-2.54754400	1.36064000



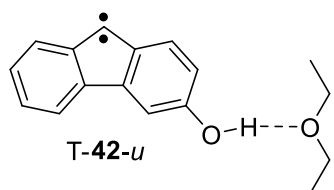
B3LYP/def2-TZVP
 E = -809.024048
 ZPVE = 0.305270

C	0.73606100	-0.30315600	0.08106200
C	0.85939800	1.01785800	-0.37105100
C	-0.28112700	1.76835100	-0.63019800
C	-1.54561300	1.21132900	-0.44144200
C	-1.64409700	-0.13724200	0.02049500
C	-0.53624800	-0.89378900	0.28140600
H	1.84910700	1.43295000	-0.50900500
H	-0.20256700	2.79047200	-0.97999900
H	-0.58243800	-1.91721300	0.63204100
C	-2.82747300	1.83823200	-0.65821800
C	-3.76021100	0.75010100	-0.28672900
C	-5.14422200	0.78277000	-0.29989600
C	-5.86018500	-0.35903200	0.09029400
C	-5.18883700	-1.50631900	0.48428700
C	-3.78210900	-1.55583700	0.50325400
C	-3.08895700	-0.43265200	0.11945600
H	-5.65506700	1.68580100	-0.61002100
H	-6.94275400	-0.34719000	0.08471300
H	-5.75422400	-2.38057700	0.78299700
H	-3.27327900	-2.46077800	0.81401900
O	1.80192700	-1.07134000	0.34597600
H	2.64233900	-0.58148000	0.18314700
O	4.12734100	0.22368400	-0.14035500
C	4.77012700	-0.24314100	-1.33261400
H	4.04377400	-0.07452300	-2.12902900
H	5.64327100	0.38687800	-1.53693900
C	4.98722200	0.46535500	0.97773100
H	5.47852400	-0.46387800	1.28538100
H	5.76635800	1.17542100	0.67544000
C	4.14890400	1.02540800	2.10722400
H	3.38075900	0.31256800	2.41027100
H	4.78007000	1.23684100	2.97174200
H	3.65887800	1.95023100	1.80091700
C	5.15418800	-1.71264500	-1.26784800
H	5.56229900	-2.03011400	-2.22953300
H	5.91155900	-1.90263800	-0.50640800
H	4.27830900	-2.32507000	-1.04798500



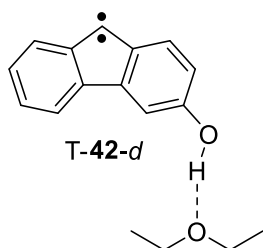
B3LYP/def2-TZVP
 E = -809.025940
 ZPVE = 0.305298

C	0.96991200	1.69415700	-0.00000200
C	0.30788500	2.92707000	0.00000400
C	-1.07908600	2.96937200	0.00000600
C	-1.81749600	1.78364200	0.00000200
C	-1.12015300	0.53867300	-0.00000500
C	0.24612000	0.47328200	-0.00000800
H	0.90610200	3.82810600	0.00000800
H	-1.60394900	3.91669600	0.00001200
H	0.78833000	-0.46390100	-0.00001500
C	-3.25282300	1.63570700	0.00000200
C	-3.40328400	0.16118300	-0.00000400
C	-4.57890200	-0.56874900	-0.00000500
C	-4.51505600	-1.97109900	-0.00001100
C	-3.28869600	-2.61678000	-0.00001600
C	-2.08368000	-1.88809700	-0.00001500
C	-2.15614300	-0.51575800	-0.00000900
H	-5.53014600	-0.05133900	-0.00000100
H	-5.42732500	-2.55408600	-0.00001200
H	-3.25433700	-3.69939800	-0.00002100
H	-1.13285000	-2.40855400	-0.00002000
O	2.31042100	1.70689700	-0.00000400
H	2.67576300	0.79337300	-0.00000100
O	3.33690500	-0.82155400	0.00000600
C	3.97036900	-1.26835900	1.20099600
H	3.98890300	-2.36508400	1.20648400
H	5.00952100	-0.91606600	1.21729800
C	3.97041800	-1.26835500	-1.20095900
H	3.98894600	-2.36507900	-1.20645400
H	5.00957400	-0.91606800	-1.21721200
C	3.19697400	-0.73306900	2.38730400
H	3.65547000	-1.07554100	3.31613200
H	3.19162300	0.35758900	2.38935700
H	2.16384500	-1.08206100	2.36424100
C	3.19707900	-0.73305000	-2.38729600
H	3.19173500	0.35760800	-2.38934000
H	3.65561200	-1.07551800	-3.31610800
H	2.16394600	-1.08203600	-2.36427900



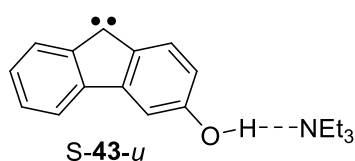
B3LYP/def2-TZVP
 E = -809.025891
 ZPVE = 0.305125

C	0.73239800	-0.28668000	0.06600500
C	0.86473000	1.03325600	-0.40124700
C	-0.25537700	1.80190100	-0.67090600
C	-1.52813300	1.25650700	-0.47521200
C	-1.65581300	-0.09467700	0.00312800
C	-0.53482400	-0.85137500	0.26856800
H	1.85822400	1.43823200	-0.54466900
H	-0.14529000	2.81712700	-1.03018300
H	-0.60052600	-1.87009000	0.62935700
C	-2.84152400	1.73816500	-0.64293900
C	-3.81557100	0.76584000	-0.29698000
C	-5.21091200	0.75539900	-0.29064700
C	-5.87050500	-0.39804100	0.11857800
C	-5.15709200	-1.53111100	0.51802200
C	-3.76033600	-1.53485000	0.51671000
C	-3.08301000	-0.39845200	0.11344900
H	-5.76706100	1.63117400	-0.59940100
H	-6.95292400	-0.41971100	0.12826900
H	-5.69386100	-2.41705800	0.83241200
H	-3.21666100	-2.41889500	0.82836500
O	1.80780100	-1.06119400	0.33828000
H	2.63970900	-0.56894200	0.16836000
O	4.16298500	0.24268200	-0.16033400
C	4.81945700	-0.30076200	-1.31058800
H	4.13752600	-0.11008700	-2.14061900
H	5.74078300	0.26334500	-1.49746100
C	4.99262800	0.45865500	0.98396600
H	5.41305400	-0.49074500	1.33308000
H	5.82655600	1.11181800	0.69851300
C	4.14726500	1.09613600	2.06640600
H	3.32390100	0.43943800	2.35040000
H	4.75521900	1.28808500	2.95199500
H	3.72910700	2.04203800	1.72030500
C	5.10144500	-1.79027300	-1.19030800
H	5.52330500	-2.16295300	-2.12600600
H	5.81522600	-2.00678300	-0.39452000
H	4.17846900	-2.33574900	-0.98779300



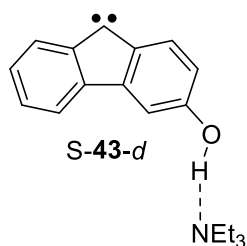
B3LYP/def2-TZVP
 E = -809.028381
 ZPVE = 0.305165

C	0.97380800	1.71425700	-0.00002200
C	0.31747000	2.95629400	-0.00001400
C	-1.06320900	3.02707600	-0.00000500
C	-1.81351800	1.84441700	-0.00000400
C	-1.13713200	0.57658000	-0.00001200
C	0.24169300	0.51659700	-0.00002100
H	0.92375300	3.85215700	-0.00001600
H	-1.56007100	3.98870400	0.00000000
H	0.76710400	-0.42999600	-0.00002700
C	-3.19169900	1.55249900	0.00000400
C	-3.44214400	0.15491400	0.00000200
C	-4.60222800	-0.61981400	0.00000700
C	-4.48329200	-2.00541900	0.00000100
C	-3.22837500	-2.61943000	-0.00001000
C	-2.05846300	-1.85605000	-0.00001500
C	-2.15290500	-0.47624600	-0.00000900
H	-5.57646000	-0.14815000	0.00001500
H	-5.37581300	-2.61823700	0.00000500
H	-3.16233200	-3.69998000	-0.00001400
H	-1.08972100	-2.34213800	-0.00002300
O	2.32660600	1.72730700	-0.00003000
H	2.67911600	0.81294700	-0.00002000
O	3.31147800	-0.84999600	0.00001500
C	3.94626200	-1.29246500	1.20007700
H	3.97147200	-2.38941600	1.20800400
H	4.98386400	-0.93464300	1.21786400
C	3.94630900	-1.29250600	-1.20000700
H	3.97150400	-2.38945700	-1.20790400
H	4.98391600	-0.93469900	-1.21775800
C	3.16843300	-0.75925100	2.38465200
H	3.62920700	-1.09415500	3.31525200
H	3.15338200	0.33128300	2.38055000
H	2.13808400	-1.11624100	2.36153500
C	3.16853900	-0.75931300	-2.38463000
H	3.15350300	0.33122100	-2.38055900
H	3.62934800	-1.09424900	-3.31520100
H	2.13818400	-1.11628900	-2.36154800



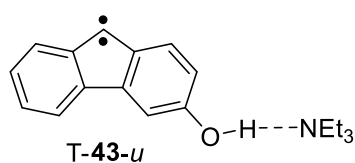
B3LYP/def2-TZVP
 E = -867.738654
 ZPVE = 0.374612

C	0.22521600	-0.27462800	-0.00001100
C	0.31140200	1.12740800	-0.00001400
C	-0.84340200	1.89843300	-0.00001200
C	-2.09631100	1.28542600	-0.00000800
C	-2.16344900	-0.14302700	-0.00000600
C	-1.04006000	-0.91958800	-0.00000700
H	1.28658800	1.59392800	-0.00001900
H	-0.78666500	2.98023200	-0.00001500
H	-1.06449000	-2.00215600	-0.00000500
C	-3.38965300	1.92113800	-0.00000400
C	-4.29873200	0.75147800	0.00000000
C	-5.68319100	0.75692300	0.00000500
C	-6.37320100	-0.46466800	0.00000800
C	-5.67649600	-1.66348700	0.00000700
C	-4.26920500	-1.68628400	0.00000200
C	-3.60141000	-0.48466900	-0.00000100
H	-6.21449500	1.70050900	0.00000500
H	-7.45584600	-0.47457200	0.00001100
H	-6.22224000	-2.59911100	0.00000900
H	-3.73973900	-2.63186500	0.00000200
O	1.29929600	-1.06010200	-0.00001100
H	2.17279100	-0.54006600	-0.00000800
N	3.74773400	0.05439100	0.00000200
C	4.49678200	-1.22015700	0.00001400
H	4.16520300	-1.79033600	0.86745200
H	4.16521600	-1.79034500	-0.86742300
C	6.02159900	-1.11388200	0.00002500
H	6.39494400	-0.59309400	0.88303500
H	6.45569400	-2.11513700	0.00003300
H	6.39495700	-0.59310300	-0.88298500
C	3.95876400	0.87064400	-1.21033100
H	3.33170500	1.75808900	-1.10061500
H	4.99472300	1.23322100	-1.26345400
C	3.58469700	0.16221100	-2.50567400
H	2.58022000	-0.25955300	-2.44515700
H	3.60376800	0.87781100	-3.32871800
H	4.27921300	-0.64052500	-2.75523100
C	3.95874600	0.87065600	1.21033100
H	3.33169200	1.75810200	1.10059500
H	4.994705	1.233229	1.263468
C	3.584653	0.162238	2.505675
H	3.603713	0.877846	3.328712
H	2.580175	-0.259521	2.445144
H	4.279161	-0.640498	2.755251



B3LYP/def2-TZVP
 E = -867.737815
 ZPVE = 0.374671

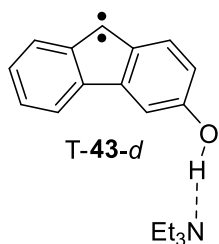
C	-0.39436900	1.75884300	-0.05335200
C	0.29175500	2.98156000	-0.10807100
C	1.67701900	3.00475300	-0.14301700
C	2.40256000	1.80951200	-0.12259500
C	1.68775400	0.57530800	-0.06738700
C	0.32196300	0.53051300	-0.03442000
H	-0.29376600	3.89085400	-0.12063300
H	2.21374600	3.94457800	-0.18535600
H	-0.22097400	-0.40452800	0.00403800
C	3.83266800	1.64124700	-0.15253600
C	3.96367800	0.16383200	-0.10808500
C	5.12790500	-0.58346500	-0.11090500
C	5.04393500	-1.98427200	-0.06357900
C	3.80926800	-2.61167400	-0.01466300
C	2.61557500	-1.86466500	-0.01113500
C	2.70772500	-0.49431700	-0.05770700
H	6.08642100	-0.08111500	-0.14937200
H	5.94773100	-2.58037000	-0.06521500
H	3.75949800	-3.69307000	0.02151900
H	1.65761400	-2.37081000	0.02759300
O	-1.72426100	1.78941100	-0.01830100
H	-2.14635000	0.86823800	0.04414200
N	-3.09204900	-0.53139000	0.11584300
C	-4.44187200	0.00196200	0.39427500
H	-4.39169200	0.50325500	1.36051600
H	-5.16354800	-0.81963500	0.50451200
C	-4.94105600	0.99926400	-0.64400500
H	-5.86922100	1.45077000	-0.29066500
H	-4.21498400	1.79705500	-0.80399400
H	-5.15365600	0.52678600	-1.60361700
C	-2.95946300	-1.15583400	-1.21596100
H	-3.13122900	-0.38152100	-1.96415000
H	-1.91299800	-1.44944800	-1.32373400
C	-3.85989500	-2.35860200	-1.49847900
H	-4.91705900	-2.09143200	-1.46477100
H	-3.64960500	-2.74564200	-2.49694800
H	-3.69159400	-3.16818800	-0.78682700
C	-2.63040700	-1.42222200	1.19874100
H	-1.75898100	-1.96392500	0.82433400
H	-3.391723	-2.180413	1.427908
C	-2.240419	-0.681677	2.473373
H	-3.089059	-0.176383	2.934252
H	-1.848641	-1.392725	3.202574
H	-1.46744	0.061705	2.276444



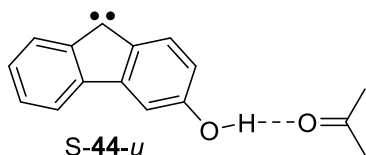
B3LYP/def2-TZVP
 E = -867.739693
 ZPVE = 0.374559

C	0.21034000	-0.27653000	0.00002300
C	0.31529800	1.12785100	0.00004500
C	-0.81493500	1.92800100	0.00004900
C	-2.07959200	1.33176900	0.00003100
C	-2.18525300	-0.10412000	0.00001200
C	-1.05356100	-0.88944300	0.00000800
H	1.29769400	1.57985400	0.00006100
H	-0.71907300	3.00635600	0.00006400
H	-1.10472200	-1.97096800	-0.00000800
C	-3.39969000	1.82217300	0.00002800
C	-4.35822800	0.77566000	0.00000800
C	-5.75335500	0.74275900	-0.00000200
C	-6.39455700	-0.49073500	-0.00002300
C	-5.66344400	-1.68164700	-0.00003200
C	-4.26697800	-1.66386700	-0.00002200
C	-3.60754900	-0.44799600	-0.00000200
H	-6.32338400	1.66292400	0.00000500
H	-7.47652900	-0.53046200	-0.00003100
H	-6.18627400	-2.62955100	-0.00004800
H	-3.70919400	-2.59291800	-0.00003000
O	1.28922000	-1.07945300	0.00001600
H	2.14973600	-0.56153600	0.00001800
N	3.77242100	0.05521300	-0.00000100
C	4.51196200	-1.22266100	-0.00005700
H	4.17705100	-1.79148800	0.86703100
H	4.17700900	-1.79143500	-0.86716300
C	6.03818600	-1.12689300	-0.00009100
H	6.41468300	-0.60801200	0.88284600
H	6.46649400	-2.13075800	-0.00013100
H	6.41464000	-0.60795900	-0.88301500
C	3.98242600	0.86856300	-1.20987500
H	3.35987500	1.75925000	-1.09848600
H	5.02011000	1.22740900	-1.27066100
C	3.59755700	0.16080000	-2.50274300
H	2.59255400	-0.25830500	-2.43328200
H	3.61337900	0.87540800	-3.32690700
H	4.28800300	-0.64437500	-2.75607700
C	3.98248300	0.86849200	1.20991100
H	3.35991800	1.75918100	1.09860700
H	5.020167	1.227343	1.270664
C	3.597685	0.160649	2.502756
H	3.613543	0.875208	3.326962
H	2.592682	-0.258459	2.43332
H	4.28815	-0.644536	2.756008

	C	-0.39017700	1.78839200	-0.08471600
	C	0.29640600	3.01682300	-0.12646400
	C	1.67688700	3.06151900	-0.14691600
	C	2.40706000	1.86555700	-0.12395200
	C	1.70657800	0.61191900	-0.08210700
	C	0.32710000	0.57986100	-0.06473800
	H	-0.29238600	3.92419200	-0.14084900
	H	2.19115200	4.01351700	-0.17910400
	H	-0.20473700	-0.36181300	-0.03797900
	C	3.77848800	1.54715400	-0.13276400
	C	4.00214300	0.14508300	-0.09825200
	C	5.14659000	-0.65230200	-0.09069100
	C	5.00088200	-2.03486400	-0.05141600
	C	3.73450600	-2.62406500	-0.01965200
	C	2.58008400	-1.83772900	-0.02667600
	C	2.70099300	-0.46045500	-0.06595000
	H	6.12980500	-0.20030500	-0.11499000
	H	5.88135000	-2.66484600	-0.04523100
	H	3.64755500	-3.70269400	0.01085000
	H	1.60237900	-2.30518300	-0.00166800
	O	-1.73371700	1.82742200	-0.06412900
	H	-2.14103700	0.91217700	0.01114600
	N	-3.08385600	-0.54392400	0.12216100
	C	-4.43666100	-0.02546100	0.40286800
	H	-4.38649600	0.49082100	1.36125300
	H	-5.14924500	-0.85340200	0.53058800
	C	-4.95521100	0.95126400	-0.64573100
	H	-5.88615100	1.39756900	-0.29270600
	H	-4.23830000	1.75397400	-0.82217100
	H	-5.16880400	0.46252100	-1.59707500
	C	-2.95176400	-1.19098500	-1.19672100
	H	-3.14462200	-0.43552500	-1.95902500
	H	-1.90102800	-1.46729200	-1.30933000
	C	-3.83189900	-2.41645300	-1.44763500
	H	-4.89363600	-2.16821700	-1.40971500
	H	-3.62305600	-2.82062800	-2.43973800
	H	-3.64266800	-3.20749300	-0.72038200
	C	-2.59327600	-1.39985800	1.21803900
	H	-1.71712700	-1.93500900	0.84502800
	H	-3.337278	-2.166488	1.477354
	C	-2.19792	-0.621935	2.468813
	H	-3.048856	-0.119909	2.929343
	H	-1.783491	-1.308064	3.209499
	H	-1.44145	0.129397	2.240777

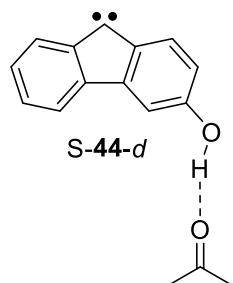


B3LYP/def2-TZVP
 E = -867.739600
 ZPVE = 0.374692



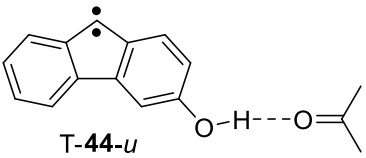
B3LYP/def2-TZVP
 E = -768.551696
 ZPVE = 0.252411

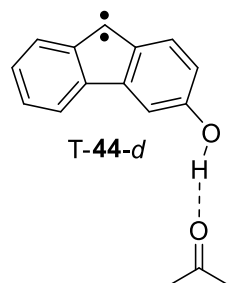
C	-1.05884200	-0.65971300	-0.71423800
C	-1.31323400	0.71475500	-0.82283900
C	-0.27906000	1.62630200	-0.64518900
C	1.01057300	1.17751100	-0.36433300
C	1.24744900	-0.22865600	-0.27209700
C	0.24512000	-1.14238200	-0.43981200
H	-2.31536500	1.04584000	-1.06039000
H	-0.46036500	2.69112200	-0.72676400
H	0.39593500	-2.21232000	-0.36985600
C	2.19365300	1.97435200	-0.14144700
C	3.21780000	0.93159600	0.09125300
C	4.56478300	1.11481200	0.35435200
C	5.38333200	-0.00771100	0.54959800
C	4.84881000	-1.28519000	0.48095200
C	3.48158900	-1.48865500	0.21460800
C	2.68743800	-0.38324500	0.02317200
H	4.96825200	2.11839600	0.40533100
H	6.43842200	0.12100100	0.75524300
H	5.49237800	-2.14280900	0.63414600
H	3.08054100	-2.49408700	0.16361300
O	-2.01957000	-1.58203600	-0.85600900
H	-2.90729000	-1.16301700	-0.93495200
C	-4.82524900	-0.03927500	0.40841100
C	-3.96468900	-0.28933600	1.61935700
H	-4.56845400	-0.49052500	2.50478000
H	-3.26609400	-1.10315800	1.43843600
H	-3.38680100	0.61913300	1.81697800
C	-6.12630600	0.68396000	0.62387200
H	-6.80456800	0.03797900	1.18882700
H	-5.96802000	1.57984400	1.22907600
H	-6.58079700	0.94422800	-0.32899100
O	-4.48002700	-0.38626100	-0.70764000



B3LYP/def2-TZVP
 E = -768.551251
 ZPVE = 0.252390

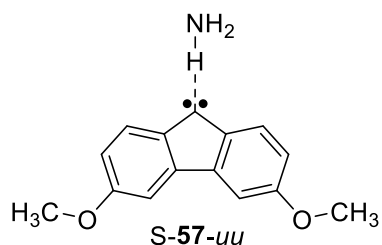
C	-1.24469100	1.76637700	-0.47924600
C	-0.63879200	2.94273000	-0.02296900
C	0.69926500	2.93692500	0.34447900
C	1.44607800	1.75958900	0.25836000
C	0.81150900	0.57594200	-0.22349600
C	-0.50581800	0.55931200	-0.59201700
H	-1.24335600	3.83739900	0.03837000
H	1.17815600	3.83920700	0.70424900
H	-0.99314100	-0.32922800	-0.97395900
C	2.83416200	1.56521100	0.60182200
C	3.02516000	0.13061600	0.28254700
C	4.18204500	-0.61750800	0.41194200
C	4.16535300	-1.97376900	0.04988600
C	3.00380000	-2.55630300	-0.43193900
C	1.81829700	-1.80849200	-0.56878700
C	1.84405900	-0.48191200	-0.21092500
H	5.08307200	-0.14917300	0.78790600
H	5.06403200	-2.56995200	0.14471600
H	3.00613200	-3.60302600	-0.71041400
H	0.91980700	-2.27844400	-0.95206600
O	-2.54427600	1.81928300	-0.80064400
H	-2.90344500	0.91991900	-0.97389600
C	-3.68832300	-1.26357200	0.21529300
C	-3.36235700	-0.53908500	1.49519900
H	-2.34454900	-0.81521400	1.78936600
H	-3.39242000	0.53855300	1.35088700
H	-4.02791800	-0.83731100	2.30563900
C	-4.17566900	-2.68188200	0.33033100
H	-5.16904400	-2.68185700	0.78823800
H	-4.22708100	-3.14902300	-0.65020500
H	-3.52384300	-3.25552900	0.99372300
O	-3.54458500	-0.73820700	-0.87503600

 <p>T-44-u</p> <p>B3LYP/def2-TZVP E = -768.553597 ZPVE = 0.252271</p>	C	1.07565300	-0.64073400	0.81321000
	C	1.34052200	0.73675000	0.91744900
	C	0.33494700	1.66776300	0.71361000
	C	-0.95635900	1.22951400	0.40522400
	C	-1.22326200	-0.18149200	0.31003500
	C	-0.21510200	-1.09916600	0.51197700
	H	2.34095100	1.05881800	1.17509800
	H	0.54693100	2.72583000	0.80031900
	H	-0.38597800	-2.16608300	0.44326800
	C	-2.17966600	1.87806000	0.14349700
	C	-3.22729400	0.95721500	-0.11725300
	C	-4.58221400	1.09586600	-0.42104200
	C	-5.34432000	-0.04946500	-0.62137300
	C	-4.77241100	-1.32047100	-0.52192000
	C	-3.41778100	-1.47425700	-0.21836900
	C	-2.64011300	-0.34869300	-0.01557200
	H	-5.02906300	2.07870800	-0.49783600
	H	-6.39686100	0.04358100	-0.85723800
	H	-5.38737800	-2.19692800	-0.68140800
	H	-2.98453500	-2.46455700	-0.14230800
	O	2.03669100	-1.57462800	0.99430300
	H	2.92090600	-1.15521200	1.04604300
	C	4.74707700	-0.05259000	-0.48078700
	C	3.80301000	-0.40281600	-1.60212400
	H	4.33717500	-0.59836800	-2.53223200
	H	3.17722300	-1.24991200	-1.33020600
	H	3.14839700	0.45821600	-1.77130500
	C	5.99964300	0.69912600	-0.84400300
	H	6.65227100	0.04543800	-1.42983600
	H	5.75839400	1.55456800	-1.47977600
	H	6.52141300	1.02695500	0.05194100
	O	4.50408000	-0.34146000	0.67696200



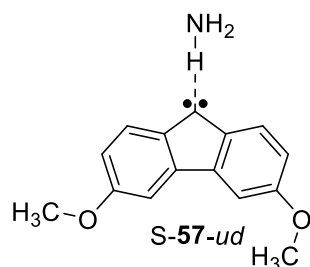
B3LYP/def2-TZVP
 E = -768.553807
 ZPVE = 0.252348

C	-1.31022500	1.75075800	0.50661000
C	-0.75005500	2.93809200	0.00573100
C	0.57317800	2.98456000	-0.39183000
C	1.36240800	1.83145800	-0.29594000
C	0.78849400	0.62201200	0.22598200
C	-0.53209200	0.58830200	0.62655000
H	-1.38586600	3.81055200	-0.06248400
H	0.99471200	3.90388600	-0.77746500
H	-0.97235700	-0.31115300	1.03843700
C	2.70238800	1.52633800	-0.60608600
C	3.02557500	0.17597800	-0.30949600
C	4.18486600	-0.59021100	-0.43180500
C	4.15369700	-1.92191100	-0.03225700
C	2.98693000	-2.49061700	0.48446400
C	1.81876000	-1.73527400	0.61243900
C	1.82639400	-0.40910100	0.21975800
H	5.09156200	-0.15298600	-0.82963000
H	5.04692100	-2.52721700	-0.12069800
H	2.98930200	-3.52857200	0.79190900
H	0.92048800	-2.18489900	1.01959100
O	-2.61543700	1.78106200	0.85790800
H	-2.94509700	0.87466300	1.03046000
C	-3.55834500	-1.35347900	-0.23730200
C	-3.25276000	-0.55807800	-1.47997100
H	-2.19978100	-0.72001800	-1.73221100
H	-3.84943900	-0.89317300	-2.32879000
H	-3.39542000	0.50562800	-1.30339500
C	-3.90907000	-2.80607500	-0.41857200
H	-4.87597600	-2.88127400	-0.92428600
H	-3.17663400	-3.29513500	-1.06557800
H	-3.96115100	-3.30910900	0.54408300
O	-3.50232800	-0.85702300	0.87339500



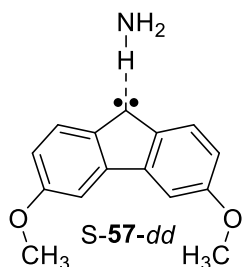
B3LYP/def2-TZVP
 E = -785.772216
 ZPVE = 0.264679

C	2.78285400	-1.25881900	0.00000000
C	3.33022100	0.02451800	-0.00000600
C	2.48940800	1.14112500	-0.00000600
C	1.10989700	0.96848800	-0.00000700
C	0.57390100	-0.35488500	-0.00000700
C	1.37831700	-1.45746900	-0.00000300
H	4.40052400	0.16561200	-0.00001000
H	2.89887000	2.14539000	-0.00001200
H	0.99988300	-2.47189900	-0.00000200
C	0.08036200	1.99341100	-0.00001000
C	-1.14339500	1.20443600	-0.00001000
C	-2.45487900	1.65417200	-0.00000800
C	-3.51398100	0.74131200	-0.00000800
C	-3.24525000	-0.62775300	-0.00000600
C	-1.91309300	-1.11180400	-0.00000500
C	-0.89568900	-0.20074700	-0.00000900
H	-2.65244000	2.71898800	-0.00000900
H	-4.53110500	1.10278700	-0.00000800
H	-1.75277200	-2.18257900	0.00000000
N	2.12891500	4.51119500	0.00001900
H	2.06998500	5.11285800	-0.81458900
H	1.29471100	3.91456000	0.00000800
H	2.06997900	5.11283200	0.81464500
O	3.50760500	-2.39759000	-0.00000100
O	-4.19174500	-1.59113600	-0.00000100
C	-5.56439500	-1.21688200	0.00002400
H	-5.81685300	-0.63855700	-0.89299000
H	-6.12559600	-2.14796200	0.00003500
H	-5.81682300	-0.63855400	0.89304400
C	4.92871900	-2.31730100	0.00001300
H	5.29552600	-1.80393400	0.89287100
H	5.28330600	-3.34498100	0.00001500
H	5.29554000	-1.80393100	-0.89283700



B3LYP/def2-TZVP
 E = -785.770664
 ZPVE = 0.264528

C	-3.12080100	-0.54870100	0.00000200
C	-3.39722800	0.81690500	0.00000200
C	-2.34139200	1.73688300	0.00000300
C	-1.02930200	1.29486400	0.00000200
C	-0.77295600	-0.10802900	0.00000000
C	-1.78381600	-1.02478300	0.00000100
H	-4.41614300	1.17320300	0.00000000
H	-2.54541700	2.80048500	0.00000600
H	-1.61857100	-2.09497300	0.00000300
C	0.19368800	2.08874900	0.00000600
C	1.22777000	1.06771600	0.00000100
C	2.61364600	1.24477000	0.00000100
C	3.44343200	0.13164700	0.00000000
C	2.90330400	-1.15869800	0.00000000
C	1.50315300	-1.36346100	0.00000000
C	0.69940900	-0.25106400	0.00000000
H	3.02099200	2.24970900	0.00000300
H	4.52064200	0.23015200	-0.00000100
H	1.08212900	-2.35876100	0.00000400
N	2.23033900	4.62021600	-0.00000500
H	2.16996600	5.22139500	-0.81479100
H	1.39899200	4.02028800	0.00001100
H	2.16998500	5.22142400	0.81476100
O	-4.05983800	-1.51975300	0.00000000
O	3.80113300	-2.16770700	-0.00000100
C	3.34536600	-3.51525300	-0.00000100
H	2.75466100	-3.73580400	-0.89343900
H	4.24194600	-4.13014400	0.00000300
H	2.75465700	-3.73580300	0.89343500
C	-5.43500100	-1.15459300	-0.00000600
H	-5.69096000	-0.57775100	-0.89297900
H	-5.99028900	-2.08921300	-0.00000800
H	-5.69096900	-0.57775200	0.89296700

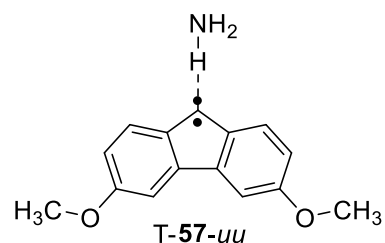


B3LYP/def2-TZVP

E = -785.769019

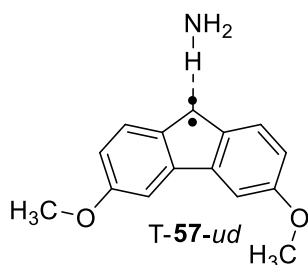
ZPVE = 0.264348

C	-2.66325000	-1.36075700	-0.00001200
C	-3.34952700	-0.14412200	-0.00005400
C	-2.65400800	1.05985800	-0.00008000
C	-1.25898700	1.04541700	-0.00006800
C	-0.57971800	-0.20123700	-0.00002000
C	-1.24689700	-1.39945400	0.00000500
H	-4.43085500	-0.17121000	-0.00006400
H	-3.17617000	2.01026800	-0.00010100
H	-0.71343700	-2.33947700	0.00003800
C	-0.34729800	2.17995600	-0.00010800
C	0.95944600	1.53234100	-0.00006600
C	2.21854800	2.12471200	-0.00007900
C	3.35883700	1.32894700	-0.00004000
C	3.24640100	-0.06346300	0.00001300
C	1.97722700	-0.69070600	0.00002400
C	0.86740200	0.11663000	-0.00001600
H	2.30053800	3.20442800	-0.00012200
H	4.35110500	1.75919700	-0.00005100
H	1.88667200	-1.76773700	0.00006500
N	-2.67007900	4.45370300	0.00017700
H	-2.68286400	5.05775000	0.81498000
H	-1.77220000	3.95915600	0.00008100
H	-2.68291200	5.05796400	-0.81446700
O	-3.43554100	-2.46967700	0.00000700
O	4.41373100	-0.74517300	0.00005200
C	4.39704300	-2.16708200	0.00006100
H	3.90372000	-2.55989300	-0.89349100
H	5.43975200	-2.47491100	0.00006300
H	3.90372200	-2.55988200	0.89361900
C	-2.82450100	-3.75360000	0.00003800
H	-2.21205000	-3.90367800	0.89363100
H	-3.64226700	-4.47003300	0.00003300
H	-2.21201600	-3.90370600	-0.89352600



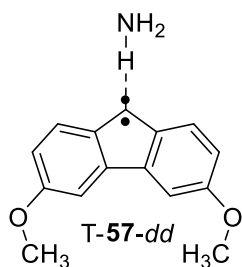
B3LYP/def2-TZVP
 E = -785.765870
 ZPVE = 0.263107

C	3.24627900	-0.61148200	0.00001400
C	3.53107400	0.76120000	-0.00003300
C	2.49949500	1.69390800	-0.00007300
C	1.17536300	1.26010800	-0.00006500
C	0.89252300	-0.15145900	-0.00001600
C	1.91939700	-1.06792300	0.00002300
H	4.55317300	1.10887400	-0.00004000
H	2.73012000	2.75148300	-0.00011000
H	1.73712000	-2.13511900	0.00006000
C	-0.08034000	1.90851500	-0.00009600
C	-1.15676100	0.99300300	-0.00007100
C	-2.54589000	1.12231200	-0.00008400
C	-3.33621400	-0.02125400	-0.00004900
C	-2.74963100	-1.29507700	-0.00000100
C	-1.35411300	-1.44229200	0.00001400
C	-0.56115100	-0.31720700	-0.00002000
H	-2.99626300	2.10689700	-0.00011800
H	-4.41058300	0.08622600	-0.00006000
H	-0.93632900	-2.44108800	0.00005300
N	-2.25505900	4.56302200	0.00013300
H	-2.27800700	5.16240700	0.81748300
H	-1.35620400	4.08953600	0.00003700
H	-2.27795900	5.16284000	-0.81690000
O	4.19366700	-1.58878100	0.00005500
O	-3.45252700	-2.46050600	0.00003500
C	-4.87017300	-2.40764700	0.00002500
H	-5.25236100	-1.90248700	-0.89241800
H	-5.20759800	-3.44170800	0.00006100
H	-5.25237100	-1.90242100	0.89242700
C	5.56275800	-1.21836500	0.00005100
H	5.82169300	-0.64023900	0.89262500
H	6.12445900	-2.14979000	0.00008900
H	5.82170600	-0.64030500	-0.89256300



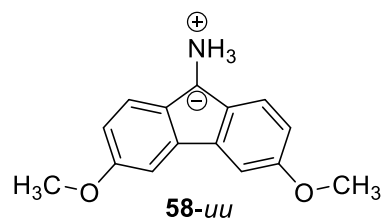
B3LYP/def2-TZVP
 E = -785.765804
 ZPVE = 0.263114

C	3.12385300	-0.50964400	0.00002100
C	3.40471800	0.86324100	-0.00003200
C	2.36901200	1.79254400	-0.00008000
C	1.04741700	1.35470400	-0.00007500
C	0.76768200	-0.05759700	-0.00002000
C	1.79799500	-0.97041100	0.00002600
H	4.42555000	1.21442400	-0.00003600
H	2.59611500	2.85091400	-0.00012100
H	1.62106300	-2.03861100	0.00006700
C	-0.21250300	1.99692600	-0.00011500
C	-1.28328100	1.07565200	-0.00009100
C	-2.67961400	1.20039900	-0.00011200
C	-3.45183600	0.05645200	-0.00007200
C	-2.86211600	-1.22109100	-0.00001100
C	-1.47068700	-1.36769100	0.00001000
C	-0.68506900	-0.22618300	-0.00003000
H	-3.13315900	2.18349300	-0.00015700
H	-4.53216400	0.11328700	-0.00008800
H	-1.00710500	-2.34381600	0.00005600
N	-2.40200400	4.64154900	0.00016700
H	-2.44069100	5.23960300	0.81782900
H	-1.49201000	4.19022000	-0.00003500
H	-2.44067200	5.24039400	-0.81691600
O	4.07361600	-1.48477400	0.00007200
O	-3.73764300	-2.26215400	0.00002600
C	-3.22826800	-3.58576800	0.00006000
H	-2.62643800	-3.78361500	0.89272000
H	-4.09653400	-4.24084200	0.00006900
H	-2.62642400	-3.78365400	-0.89258200
C	5.44181100	-1.11048400	0.00004400
H	5.69892500	-0.53157300	0.89258300
H	6.00620300	-2.04028400	0.00007900
H	5.69890800	-0.53164900	-0.89254900



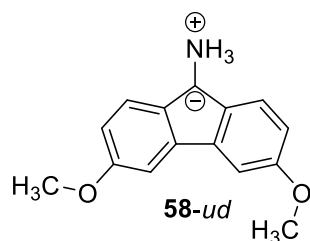
B3LYP/def2-TZVP
 E = -785.765622
 ZPVE = 0.263130

C	3.24489100	-0.01517200	0.00000200
C	3.35665400	1.38621700	-0.00001300
C	2.23162500	2.18787600	-0.00002600
C	0.96550400	1.59307900	-0.00002500
C	0.85569300	0.16430500	-0.00001000
C	1.98906200	-0.63314900	0.00000300
H	4.34968200	1.81490500	-0.00001400
H	2.33161800	3.26564200	-0.00003800
H	1.89383400	-1.70963600	0.00001500
C	-0.36038500	2.08355400	-0.00003500
C	-1.31643000	1.04255800	-0.00002800
C	-2.71650000	1.00057200	-0.00003200
C	-3.34815000	-0.22751300	-0.00002200
C	-2.61047600	-1.42475800	-0.00000600
C	-1.21083300	-1.40471000	-0.00000100
C	-0.56612100	-0.17798800	-0.00001200
H	-3.28338200	1.92303600	-0.00004400
H	-4.42751900	-0.29941800	-0.00002500
H	-0.63603000	-2.31987900	0.00001100
N	-2.85525200	4.44733600	0.00005900
H	-2.97174400	5.03550500	0.81752100
H	-1.89399000	4.11922100	-0.00008400
H	-2.97187500	5.03585300	-0.81713400
O	4.42671100	-0.68949200	0.00001400
O	-3.35515400	-2.56342800	0.00000400
C	-2.69214200	-3.81661900	0.00001700
H	-2.07109400	-3.94178400	0.89280100
H	-3.47616100	-4.57051600	0.00002200
H	-2.07108900	-3.94180000	-0.89276100
C	4.40652200	-2.10739000	0.00003200
H	3.91043000	-2.50124200	-0.89276300
H	5.44772400	-2.42183000	0.00004000
H	3.91042300	-2.50121900	0.89283300



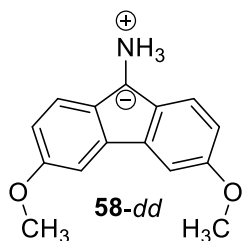
B3LYP/def2-TZVP
 E = -785.797811
 ZPVE = 0.268345

C	3.00711600	-0.87138200	-0.00009000
C	3.44334300	0.46189600	0.02516200
C	2.52707300	1.50720600	-0.04718900
C	1.16012100	1.23363800	-0.13315100
C	0.72291600	-0.13203500	-0.10865400
C	1.64892000	-1.16634400	-0.06773500
H	4.49629500	0.69339000	0.09221100
H	2.90263800	2.52685300	-0.05121000
H	1.34058500	-2.20437100	-0.06820700
C	0.00000000	2.05370400	-0.27042500
C	-1.16012000	1.23363800	-0.13315100
C	-2.52707200	1.50720700	-0.04718800
C	-3.44334200	0.46189700	0.02516500
C	-3.00711500	-0.87138100	-0.00008800
C	-1.64892000	-1.16634400	-0.06773400
C	-0.72291600	-0.13203500	-0.10865400
H	-2.90263500	2.52685400	-0.05120700
H	-4.49629400	0.69339200	0.09221400
H	-1.34058600	-2.20437100	-0.06820500
O	3.85083800	-1.95619900	0.04770400
O	-3.85083800	-1.95619800	0.04771000
C	-5.24246300	-1.72620200	0.10867500
H	-5.60317700	-1.17601300	-0.76809400
H	-5.71154000	-2.70836400	0.12936000
H	-5.52585500	-1.17634500	1.01375400
C	5.24246200	-1.72619900	0.10868100
H	5.52584500	-1.17634300	1.01376400
H	5.71154200	-2.70836000	0.12936700
H	5.60318200	-1.17600700	-0.76808300
N	-0.00000300	3.43030100	0.24793400
H	-0.00002600	3.50972700	1.28660800
H	-0.82001600	3.93173200	-0.09145200
H	0.82003300	3.93171900	-0.09141600



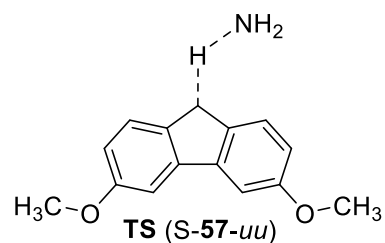
B3LYP/def2-TZVP
 E = -785.799147
 ZPVE = 0.268454

C	3.14342900	-0.65328900	0.01568600
C	3.52483500	0.70108900	0.03690300
C	2.58179300	1.70866700	-0.03459700
C	1.21973600	1.38087600	-0.11510700
C	0.83629800	0.00473000	-0.09073100
C	1.80276000	-1.00589300	-0.05068000
H	4.58085600	0.92924100	0.10045200
H	2.91810300	2.74202800	-0.03848600
H	1.49257000	-2.04126200	-0.05545200
C	0.03140800	2.15626700	-0.25183000
C	-1.09739400	1.29621400	-0.12544900
C	-2.47482900	1.51665400	-0.04868600
C	-3.35003300	0.43727600	0.01721900
C	-2.86132600	-0.87889300	-0.00466900
C	-1.49349300	-1.12164900	-0.06298600
C	-0.60508100	-0.05252300	-0.09735400
H	-2.88909200	2.52124100	-0.05341000
H	-4.41159100	0.62751300	0.07715900
H	-1.14749700	-2.14787600	-0.06248700
O	4.18477300	-1.54792300	0.06994100
O	-3.66399100	-1.99538200	0.03767400
C	-5.06376600	-1.81843200	0.08729200
H	-5.43818700	-1.28252100	-0.79255500
H	-5.49539300	-2.81772900	0.10461200
H	-5.37534600	-1.27973000	0.98979200
C	3.87689100	-2.92687200	0.06014200
H	3.35000800	-3.21765300	-0.85579700
H	4.82948800	-3.45160500	0.10627400
H	3.26704700	-3.21208300	0.92498100
N	-0.02334600	3.54219900	0.23484700
H	-0.05575600	3.64384500	1.27010700
H	-0.84732900	4.01288200	-0.13815800
H	0.79192000	4.05942700	-0.09280000



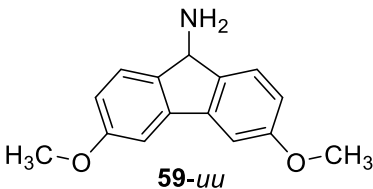
B3LYP/def2-TZVP
 E = -785.800390
 ZPVE = 0.268558

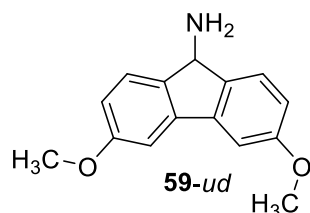
C	3.00230900	-0.67036200	0.00897400
C	3.43700600	0.66895500	0.02728800
C	2.53330300	1.71160100	-0.03582600
C	1.15873700	1.43644100	-0.10598600
C	0.71956300	0.07465400	-0.07926700
C	1.64972600	-0.97199400	-0.04677200
H	4.50155100	0.85555100	0.08274100
H	2.90860600	2.73150100	-0.03940400
H	1.30235900	-1.99560300	-0.05039100
C	0.00000000	2.25204000	-0.22942600
C	-1.15873700	1.43644000	-0.10598800
C	-2.53330300	1.71160100	-0.03582700
C	-3.43700600	0.66895400	0.02728500
C	-3.00230900	-0.67036300	0.00897000
C	-1.64972600	-0.97199500	-0.04677600
C	-0.71956200	0.07465300	-0.07926900
H	-2.90860400	2.73150200	-0.03940400
H	-4.50155100	0.85555000	0.08274000
H	-1.30235900	-1.99560400	-0.05039500
O	4.01008700	-1.60389600	0.05487000
O	-4.01008700	-1.60389600	0.05486300
C	-3.65086300	-2.96976400	0.04747200
H	-3.03724700	-3.23227900	0.91701000
H	-4.58327000	-3.53021600	0.08637500
H	-3.10640600	-3.24057800	-0.86447600
C	3.65086300	-2.96976300	0.04746000
H	3.10640800	-3.24056600	-0.86449200
H	4.58327000	-3.53021600	0.08635900
H	3.03724500	-3.23229000	0.91699400
N	-0.00000100	3.65187300	0.21443500
H	-0.00002500	3.78590000	1.24538100
H	-0.82058700	4.13499800	-0.15092800
H	0.82061400	4.13498000	-0.15088800



B3LYP/def2-TZVP
 E = -785.762174
 ZPVE = 0.260606

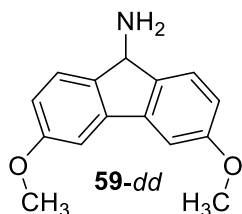
C	-3.01604000	-0.86205700	0.01865900
C	-3.44387900	0.45741000	-0.16779500
C	-2.50821200	1.47355000	-0.35743900
C	-1.15169400	1.18282900	-0.32702300
C	-0.73435200	-0.15830600	-0.11065400
C	-1.64629100	-1.17727600	0.03736400
H	-4.49638100	0.69702200	-0.18319900
H	-2.84433000	2.48926000	-0.52766300
H	-1.35177100	-2.21027100	0.17057800
C	-0.00000200	2.03768600	-0.58895100
C	1.15169200	1.18282600	-0.32704200
C	2.50821000	1.47354800	-0.35746300
C	3.44387800	0.45741000	-0.16780900
C	3.01604000	-0.86205400	0.01866600
C	1.64629100	-1.17727500	0.03736900
C	0.73435200	-0.15830700	-0.11066100
H	2.84432600	2.48925600	-0.52770000
H	4.49638000	0.69702000	-0.18323000
H	1.35177200	-2.21026900	0.17059000
H	0.00001300	3.29539700	-0.18208000
N	0.00000700	3.69950400	0.96456300
H	0.81582800	3.33770700	1.45231300
H	-0.81583100	3.33772600	1.45229600
O	3.85148400	-1.91801800	0.18618200
O	-3.85148600	-1.91802400	0.18615100
C	5.25440400	-1.69801600	0.16949600
H	5.56304500	-1.02729400	0.97695900
H	5.71069400	-2.67391800	0.31772600
H	5.58227600	-1.28619700	-0.78960200
C	-5.25440400	-1.69800900	0.16949800
H	-5.71069900	-2.67390800	0.31773800
H	-5.56302100	-1.02728500	0.97696800
H	-5.58229500	-1.28619000	-0.78959300

 <p>59-uu</p> <p>B3LYP/def2-TZVP E = -785.865284 ZPVE = 0.269130</p>	C	-3.00143900	-0.84755400	0.00257300
	C	-3.44986200	0.47063600	-0.11496000
	C	-2.52702800	1.51573900	-0.21820500
	C	-1.17585500	1.24356100	-0.19671300
	C	-0.73287000	-0.08401000	-0.07598000
	C	-1.63212400	-1.13061600	0.02061200
	H	-4.50575700	0.69550000	-0.12933700
	H	-2.89089500	2.53244700	-0.31416800
	H	-1.31157800	-2.16006700	0.11241200
	C	-0.00000200	2.19484400	-0.28868900
	H	-0.00000300	2.67823400	-1.27944100
	C	1.17585300	1.24356200	-0.19671500
	C	2.52702500	1.51574200	-0.21821000
	C	3.44986200	0.47064100	-0.11496700
	C	3.00144100	-0.84755000	0.00256800
	C	1.63212600	-1.13061300	0.02060900
	C	0.73287000	-0.08400900	-0.07598100
	H	2.89089000	2.53245100	-0.31417400
	H	4.50575600	0.69550700	-0.12934800
	H	1.31158200	-2.16006500	0.11241000
N	-0.00000200	3.17315200	0.81083100	
H	0.81512300	3.77290400	0.74492300	
H	-0.81512800	3.77290100	0.74492500	
O	-3.82362200	-1.93045400	0.10507300	
O	3.82362400	-1.93045100	0.10506500	
C	-5.22589000	-1.72545100	0.10077900	
H	-5.67349500	-2.71247000	0.19494100	
H	-5.54401500	-1.10342400	0.94369500	
H	-5.56233500	-1.26482400	-0.83376300	
C	5.22589300	-1.72545300	0.10079100	
H	5.54401100	-1.10343200	0.94371400	
H	5.67349300	-2.71247500	0.19495400	
H	5.56235100	-1.26482400	-0.83374500	



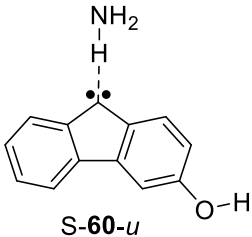
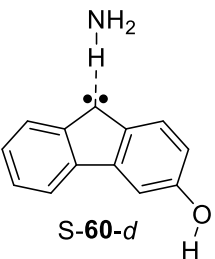
B3LYP/def2-TZVP
 E = -785.865604
 ZPVE = 0.269160

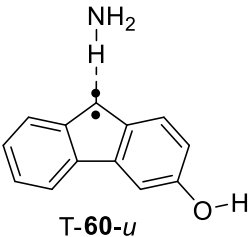
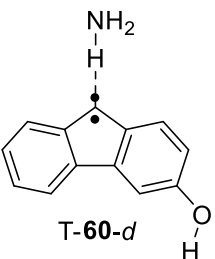
C	-3.13556700	-0.64132500	-0.02135100
C	-3.53428600	0.69764400	-0.12333100
C	-2.58910900	1.71059000	-0.21117700
C	-1.24106900	1.38952600	-0.19088500
C	-0.84677500	0.05299500	-0.08724700
C	-1.78118600	-0.97582100	-0.00422900
H	-4.59390400	0.91528700	-0.13334700
H	-2.91748500	2.74028100	-0.29443700
H	-1.45318200	-2.00194100	0.07369300
C	-0.03450300	2.30198700	-0.27051500
H	-0.01663800	2.79404400	-1.25701400
C	1.10867900	1.31119400	-0.18680700
C	2.46824500	1.53541100	-0.20071800
C	3.35355500	0.45674700	-0.10803900
C	2.85815500	-0.84564600	-0.00899000
C	1.47929900	-1.08009900	0.00136700
C	0.61772900	-0.00129800	-0.08406600
H	2.86824600	2.53970800	-0.28233900
H	4.41675600	0.64427400	-0.11607000
H	1.12384900	-2.09931100	0.07901900
N	-0.00465200	3.26903500	0.83815900
H	0.82810400	3.84457700	0.77779300
H	-0.80126200	3.89382000	0.77881200
O	-4.15050000	-1.54802400	0.05571700
O	3.64063000	-1.95887700	0.08222600
C	-3.82474000	-2.92301800	0.16820500
H	-4.77331500	-3.45314100	0.21807600
H	-3.26019700	-3.27481700	-0.70142700
H	-3.24936400	-3.12641300	1.07713300
C	5.04940000	-1.80380300	0.08539800
H	5.38598400	-1.20427300	0.93735800
H	5.46142500	-2.80720200	0.16831400
H	5.40553800	-1.34342800	-0.84190900

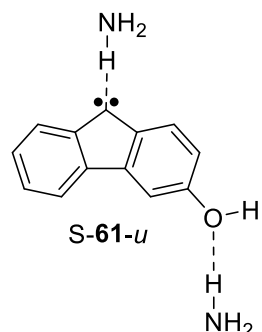


B3LYP/def2-TZVP
 E = -785.865646
 ZPVE = 0.269152

C	-2.99630900	-0.64792100	-0.02720900
C	-3.44238000	0.67649400	-0.11601800
C	-2.53319400	1.72298500	-0.19698200
C	-1.17519300	1.44944300	-0.18271400
C	-0.73276700	0.12672600	-0.09161100
C	-1.63060900	-0.93483400	-0.01603400
H	-4.50898400	0.85680300	-0.12139300
H	-2.89769000	2.74121500	-0.27007500
H	-1.26836600	-1.95017900	0.05184100
C	-0.00000200	2.40195100	-0.25773300
H	-0.00000100	2.89925700	-1.24195300
C	1.17519000	1.44944400	-0.18271200
C	2.53319100	1.72298800	-0.19697700
C	3.44237700	0.67649800	-0.11601300
C	2.99630800	-0.64791800	-0.02720600
C	1.63060900	-0.93483200	-0.01603200
C	0.73276500	0.12672700	-0.09161000
H	2.89768600	2.74121900	-0.27006900
H	4.50898100	0.85680800	-0.12138500
H	1.26836600	-1.95017700	0.05184400
N	-0.00000300	3.36299000	0.85615200
H	0.81500300	3.96380000	0.80002100
H	-0.81499200	3.96382200	0.80000100
O	-3.97856100	-1.59097400	0.04392800
O	3.97856300	-1.59096900	0.04393100
C	-3.60492700	-2.95418200	0.14335000
H	-4.53417100	-3.51778700	0.19037100
H	-3.03055900	-3.27859600	-0.73064700
H	-3.02077800	-3.14575600	1.04940500
C	3.60493500	-2.95418100	0.14333700
H	3.03057300	-3.27858900	-0.73066500
H	4.53418300	-3.51778200	0.19035600
H	3.02078400	-3.14576700	1.04938800

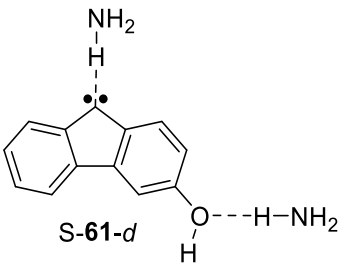
 <p>S-60-u</p> <p>B3LYP/def2-TZVP E = -631.936387 ZPVE = 0.203834</p>	C	2.55480600	-1.37158400	0.00000300
	C	2.96199700	-0.03725100	-0.00000100
	C	2.01230400	0.98056700	-0.00000100
	C	0.65617000	0.65143300	-0.00000500
	C	0.26605500	-0.72308500	-0.00000500
	C	1.18725200	-1.73275300	0.00000200
	H	4.02077500	0.19683500	-0.00000200
	H	2.30488200	2.02516700	-0.00000500
	H	0.92409000	-2.78270900	0.00000600
	C	-0.46948000	1.55532600	0.00000500
	C	-1.61540100	0.62754400	0.00000600
	C	-2.96323100	0.94579500	0.00001100
	C	-3.90995600	-0.08914600	0.00000200
	C	-3.49938200	-1.41332600	-0.00000600
	C	-2.13288200	-1.75325700	-0.00000800
	C	-1.21202300	-0.73359100	-0.00000100
	H	-3.26910500	1.98448000	0.00001700
	H	-4.96697800	0.14410200	0.00000400
	H	-1.83119300	-2.79389300	-0.00001600
	N	1.32007900	4.26901700	-0.00000700
H	1.21593800	4.86418500	-0.81475700	
H	0.53548700	3.60969300	-0.00000500	
H	1.21596100	4.86415500	0.81476700	
O	3.43656400	-2.39668100	0.00000400	
H	-4.24115500	-2.20245200	-0.00001200	
H	4.34085500	-2.05926900	0.00000000	
 <p>S-60-d</p> <p>B3LYP/def2-TZVP E = -631.935341 ZPVE = 0.203695</p>	C	2.56648800	-1.36033200	0.00000200
	C	2.97127200	-0.02609200	-0.00000500
	C	2.01862500	0.98598800	-0.00000500
	C	0.65985100	0.65641800	-0.00000300
	C	0.27083100	-0.71635300	-0.00000300
	C	1.19798800	-1.72254600	0.00000500
	H	4.03060400	0.19105700	-0.00000800
	H	2.30836300	2.03129500	-0.00000900
	H	0.91610100	-2.77087700	0.00001300
	C	-0.46714500	1.55757400	0.00001500
	C	-1.61334600	0.62760900	0.00000700
	C	-2.96085600	0.94309300	0.00000600
	C	-3.90639500	-0.09422400	-0.00000300
	C	-3.49392900	-1.41700900	-0.00000700
	C	-2.12593800	-1.75378200	-0.00000500
	C	-1.20748200	-0.73250000	0.00000100
	H	-3.26888900	1.98112000	0.00001200
	H	-4.96373900	0.13749200	-0.00000600
	H	-1.82336600	-2.79435600	-0.00000700
	N	1.31149900	4.28152300	-0.00000400
H	1.20657500	4.87618000	-0.81494500	
H	0.52945200	3.61975400	0.00001400	
H	1.20659100	4.87620300	0.81492200	
O	3.53764500	-2.30156300	0.00000200	
H	-4.23396800	-2.20771600	-0.00001300	
H	3.15083400	-3.18536400	0.00001100	

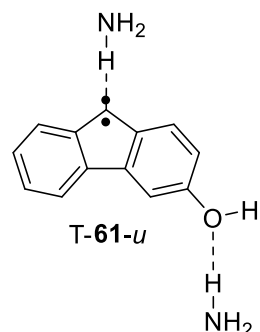
 <p>T-60-u</p> <p>B3LYP/def2-TZVP E = -631.934929 ZPVE = 0.202391</p>	C	2.51239000	-1.44116200	0.00000100
	C	2.96603000	-0.11507800	-0.00000900
	C	2.06929900	0.94184000	-0.00001500
	C	0.69910500	0.66341400	-0.00001100
	C	0.24041600	-0.70024900	-0.00000100
	C	1.14528200	-1.74049100	0.00000500
	H	4.03275700	0.08078900	-0.00001200
	H	2.41094700	1.96929900	-0.00002200
	H	0.83349900	-2.77702900	0.00001200
	C	-0.46377100	1.46145900	-0.00001500
	C	-1.65078300	0.68553200	-0.00000800
	C	-3.01095500	0.99702400	-0.00000900
	C	-3.93553900	-0.04111000	0.00000000
	C	-3.51899500	-1.37466600	0.00000900
	C	-2.16079200	-1.70103600	0.00001000
	C	-1.22299800	-0.68486100	0.00000100
	H	-3.33776000	2.02892000	-0.00001600
	H	-4.99402600	0.18598000	-0.00000100
	H	-1.84912200	-2.73877700	0.00001700
	N	1.47635600	4.31919000	0.00001700
H	1.48560500	4.91911100	-0.81719400	
H	0.58913500	3.82493200	0.00001300	
H	1.48562600	4.91905700	0.81726800	
O	3.37165400	-2.50024800	0.00000700	
H	-4.25845400	-2.16514700	0.00001500	
H	4.28192900	-2.18317700	0.00000200	
 <p>T-60-d</p> <p>B3LYP/def2-TZVP E = -631.934452 ZPVE = 0.202369</p>	C	-2.52153200	-1.43318200	-0.00000300
	C	-2.97408800	-0.10664000	-0.00000500
	C	-2.07519700	0.94458900	-0.00000500
	C	-0.70242500	0.66579100	-0.00000400
	C	-0.24383000	-0.69524800	-0.00000200
	C	-1.15459400	-1.73406200	-0.00000100
	H	-4.04107900	0.07039300	-0.00000600
	H	-2.41336300	1.97321500	-0.00000700
	H	-0.82401000	-2.76777200	0.00000100
	C	0.46028100	1.46358700	-0.00000600
	C	1.64794000	0.68747400	-0.00000200
	C	3.00767400	0.99825100	0.00000000
	C	3.93252400	-0.04024400	0.00000300
	C	3.51566500	-1.37330200	0.00000600
	C	2.15702700	-1.69894100	0.00000500
	C	1.21932200	-0.68269900	0.00000100
	H	3.33481000	2.03003800	-0.00000200
	H	4.99100200	0.18672200	0.00000400
	H	1.84649500	-2.73720000	0.00000700
	N	-1.47521100	4.32541200	0.00000800
H	-1.49724400	4.92459400	0.81743800	
H	-0.57885800	3.84830800	0.00001600	
H	-1.49722700	4.92459900	-0.81741800	
O	-3.47535200	-2.40775000	-0.00000200	
H	4.25473400	-2.16415300	0.00000900	
H	-3.05856600	-3.27687700	0.00000000	



B3LYP/def2-TZVP
 E = -688.492779
 ZPVE = 0.240025

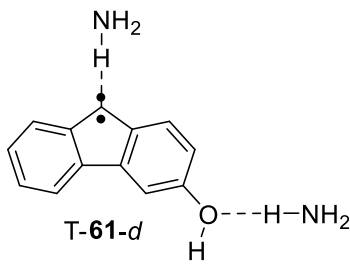
C	2.40796200	0.89396500	-0.00000100
C	1.83914600	2.16711500	-0.00001600
C	0.45361300	2.31016400	-0.00002500
C	-0.34897200	1.16918400	-0.00001800
C	0.26458500	-0.12015800	-0.00000300
C	1.62254300	-0.28095400	0.00000600
H	2.48265200	3.04017300	-0.00002100
H	-0.01266100	3.28949500	-0.00003500
H	2.11529200	-1.24594100	0.00001800
C	-1.79281400	1.10513500	-0.00002400
C	-2.04057000	-0.34789100	-0.00001200
C	-3.26251900	-1.00054500	-0.00001400
C	-3.28772200	-2.40278000	0.00000000
C	-2.10347600	-3.12459700	0.00001300
C	-0.85320900	-2.47696600	0.00001300
C	-0.83852600	-1.10301800	0.00000100
H	-4.17909700	-0.42395000	-0.00002400
H	-4.23477300	-2.92710800	0.00000000
H	0.06378900	-3.05391500	0.00002300
N	-2.24950400	4.32114300	0.00003100
H	-2.72570300	4.69349400	-0.81457100
H	-2.39218800	3.30595500	-0.00001400
H	-2.72559600	4.69340100	0.81473800
O	3.75489700	0.71243500	0.00000800
H	-2.13864500	-4.20715300	0.00002300
H	4.20283400	1.56712800	0.00001000
N	4.17877300	-2.54761700	0.00000700
H	4.57503800	-2.99803400	-0.81695100
H	4.57506400	-2.99803300	0.81695200
H	4.48969400	-1.58158800	0.00000100

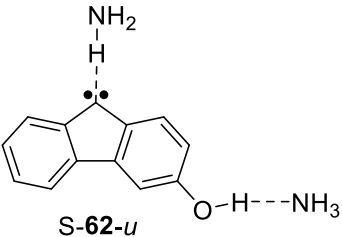
 <p>S-61-d</p> <p>B3LYP/def2-TZVP E = -688.490517 ZPVE = 0.239523</p>	C	-2.09835800	-1.12780200	-0.00000900
	C	-2.40569600	0.23109200	-0.00001300
	C	-1.37253200	1.16326600	-0.00001200
	C	-0.04287300	0.73056800	-0.00000800
	C	0.23996200	-0.66752600	-0.00000400
	C	-0.76339400	-1.59749800	-0.00000400
	H	-3.44718000	0.52753900	-0.00001600
	H	-1.58088000	2.22767100	-0.00001600
	H	-0.56398900	-2.66486400	0.00000200
	C	1.15093400	1.54192100	-0.00000200
	C	2.22229000	0.52629300	0.00000100
	C	3.59005100	0.73685700	0.00000500
	C	4.45296000	-0.37023600	0.00000700
	C	3.93953600	-1.65718600	0.00000700
	C	2.54962200	-1.88737200	0.00000400
	C	1.71246900	-0.79838000	0.00000100
	H	3.97706800	1.74812300	0.00000500
	H	5.52504700	-0.22076700	0.00000900
	H	2.16771100	-2.90155700	0.00000400
	N	-0.38497700	4.40832200	-0.00000200
H	-0.22525200	4.99043200	0.81506400	
H	0.33145300	3.67609300	-0.00002600	
H	-0.22523000	4.99051500	-0.81500300	
O	-3.13616300	-2.00553200	-0.00000800	
H	4.61636300	-2.50268700	0.00000900	
H	-2.80559300	-2.91162300	-0.00001700	
N	-5.83501100	-0.18613700	0.00002100	
H	-6.43363400	-0.17620000	-0.81752100	
H	-6.43360400	-0.17617800	0.81758400	
H	-5.32289100	-1.06152100	0.00002200	

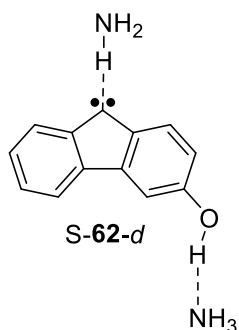


B3LYP/def2-TZVP
 E = -688.491354
 ZPVE = 0.238568

C	2.41226100	0.86718300	-0.00002700
C	1.86127800	2.15461100	-0.00008600
C	0.48633600	2.33727800	-0.00011700
C	-0.34087300	1.21047800	-0.00009000
C	0.23777500	-0.10638200	-0.00002700
C	1.60596700	-0.27591900	0.00000400
H	2.52054000	3.01606100	-0.00010600
H	0.05128500	3.32869800	-0.00015600
H	2.06956000	-1.25501900	0.00005000
C	-1.73881100	1.01669600	-0.00010900
C	-2.09342400	-0.35662600	-0.00006100
C	-3.30765000	-1.04459500	-0.00005700
C	-3.28867100	-2.43477500	-0.00000100
C	-2.08114000	-3.13793900	0.00005100
C	-0.85796600	-2.46303200	0.00004800
C	-0.85390700	-1.08039600	-0.00000800
H	-4.24547400	-0.50403000	-0.00009800
H	-4.22305600	-2.98162100	0.00000300
H	0.07482000	-3.01432700	0.00008800
N	-2.24594300	4.42282900	0.00018300
H	-2.66066500	4.85685400	-0.81682400
H	-2.53213000	3.44818700	0.00013800
H	-2.66027800	4.85666100	0.81748800
O	3.76877400	0.66766500	0.00000400
H	-2.09387900	-4.22036700	0.00009500
H	4.22220400	1.51800100	-0.00002400
N	4.17060300	-2.56015500	0.00009300
H	4.59277300	-2.98601300	-0.81695400
H	4.59279700	-2.98599200	0.81713900
H	4.42164700	-1.57661800	0.00007600

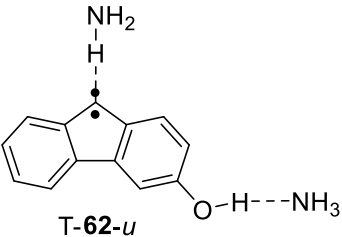
 <p>T-61-d</p> <p>B3LYP/def2-TZVP E = -688.489911 ZPVE = 0.238229</p>	C	-2.09161900	-1.11477200	0.00000600
	C	-2.40663800	0.25020900	0.00002300
	C	-1.39595100	1.19604200	0.00003100
	C	-0.06062700	0.77268700	0.00002200
	C	0.25104900	-0.62872700	0.00000400
	C	-0.76660600	-1.56306500	-0.00000400
	H	-3.44949900	0.54084700	0.00002900
	H	-1.62191100	2.25494700	0.00004200
	H	-0.54916500	-2.62655300	-0.00001700
	C	1.18119700	1.44187900	0.00002700
	C	2.27952700	0.54368300	0.00001300
	C	3.66458200	0.70766500	0.00001200
	C	4.47366500	-0.42352700	-0.00000500
	C	3.91700700	-1.70442800	-0.00002000
	C	2.53122100	-1.88329100	-0.00001800
	C	1.70718600	-0.77300100	-0.00000200
	H	4.09980100	1.69873900	0.00002300
	H	5.55031400	-0.31064600	-0.00000600
	H	2.11181100	-2.88258300	-0.00003000
	N	-0.40994900	4.49551600	-0.00002900
H	-0.36608700	5.09314100	0.81757500	
H	0.42734900	3.92120600	-0.00004700	
H	-0.36615500	5.09309300	-0.81767200	
O	-3.14130600	-1.99585500	0.00000000	
H	4.56749700	-2.56963900	-0.00003200	
H	-2.80928600	-2.90050300	-0.00001200	
N	-5.87378300	-0.27964900	-0.00001500	
H	-6.46821600	-0.35400800	-0.81733900	
H	-6.46825900	-0.35403700	0.81727600	
H	-5.24557000	-1.07636400	-0.00001200	

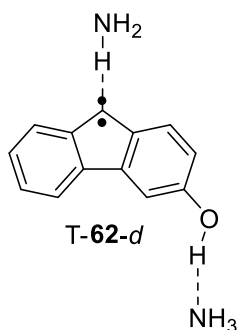
 <p>S-62-u</p> <p>B3LYP/def2-TZVP E = -688.505505 ZPVE = 0.241006</p>	C	-2.19342100	-0.89431900	0.00000300
	C	-2.37063400	0.49822800	-0.00000700
	C	-1.27080500	1.34520800	-0.00001400
	C	0.01955400	0.80553500	-0.00000800
	C	0.17995600	-0.61668900	0.00000200
	C	-0.89104400	-1.46220600	0.00000800
	H	-3.37506100	0.90023900	-0.00001400
	H	-1.39116500	2.42318800	-0.00002000
	H	-0.79995200	-2.54110100	0.00001700
	C	1.26873700	1.51334900	-0.00001500
	C	2.25466900	0.41151400	-0.00001000
	C	3.63565800	0.50625000	-0.00001300
	C	4.40251400	-0.66875000	-0.00000400
	C	3.78389100	-1.90939900	0.00000800
	C	2.38065300	-2.02206100	0.00001100
	C	1.63688400	-0.86627700	0.00000100
	H	4.10665900	1.48135600	-0.00002000
	H	5.48351300	-0.60914900	-0.00000700
	H	1.91284300	-2.99950800	0.00002100
	N	-0.00374500	4.49551900	0.00001900
H	0.22582200	5.05538400	0.81436300	
H	0.62759600	3.68656500	-0.00001900	
H	0.22583000	5.05548500	-0.81425300	
O	-3.21519700	-1.75064300	0.00001000	
H	4.38817100	-2.80826600	0.00001400	
H	-4.09618300	-1.28688800	0.00001000	
N	-5.75383900	-0.60496000	-0.00000500	
H	-5.93634700	-0.03357700	-0.81841200	
H	-5.93636000	-0.03356100	0.81838800	
H	-6.43039700	-1.36123000	-0.00001000	



B3LYP/def2-TZVP
 E = -688.504143
 ZPVE = 0.240856

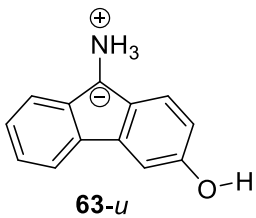
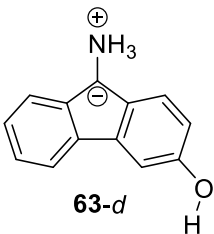
C	2.41519800	0.70256300	0.00000000
C	1.90509600	2.00808900	-0.00000700
C	0.53662700	2.22638900	-0.00001200
C	-0.34206400	1.13405200	-0.00001600
C	0.19553200	-0.19021200	-0.00000800
C	1.54193800	-0.42100900	0.00000100
H	2.61050000	2.82799700	-0.00000500
H	0.12697900	3.23064000	-0.00001300
H	1.95852900	-1.42100900	0.00000900
C	-1.77678700	1.15737500	-0.00001600
C	-2.11673600	-0.28375300	-0.00000600
C	-3.37353700	-0.86145400	-0.00000200
C	-3.48454400	-2.26117800	0.00000400
C	-2.34836900	-3.05416600	0.00000700
C	-1.06242900	-2.47975400	0.00000300
C	-0.96276800	-1.10933000	-0.00000300
H	-4.25401000	-0.23107400	-0.00000400
H	-4.46234500	-2.72591600	0.00000700
H	-0.18403700	-3.11494300	0.00000500
N	-2.09036500	4.38710900	0.00002200
H	-2.55540700	4.77309200	-0.81469000
H	-2.26269100	3.37623300	0.00001000
H	-2.55542700	4.77307500	0.81473100
O	3.74023900	0.55258800	0.00000600
H	-2.44841200	-4.13264500	0.00001100
H	4.01647100	-0.40192800	0.00001500
N	4.74288700	-2.05110700	0.00000600
H	5.75078200	-1.93173200	0.00002900
H	4.50329900	-2.60007500	-0.81888500
H	4.50326500	-2.60010400	0.81886800

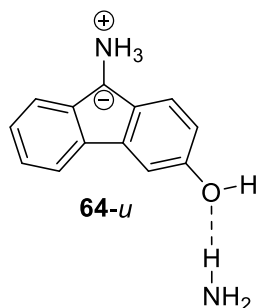
 <p>T-62-u</p> <p>B3LYP/def2-TZVP E = -688.501455 ZPVE = 0.239488</p>	C	-2.18613300	-0.90533800	-0.00000900
	C	-2.38055200	0.48948100	-0.00000900
	C	-1.30582200	1.36191700	-0.00000600
	C	-0.00652700	0.84099100	-0.00000200
	C	0.19235200	-0.58523000	-0.00000100
	C	-0.88761500	-1.44027200	-0.00000400
	H	-3.39104800	0.87707700	-0.00001100
	H	-1.45677600	2.43418400	-0.00000600
	H	-0.76933800	-2.51650300	-0.00000300
	C	1.28085300	1.41013500	0.00000400
	C	2.30636100	0.42966300	0.00000100
	C	3.70048700	0.48507400	-0.00000100
	C	4.41872100	-0.70537300	0.00000200
	C	3.76421400	-1.93986900	0.00000600
	C	2.36931600	-2.01022100	0.00000700
	C	1.63359400	-0.83896500	0.00000400
	H	4.21180400	1.43924400	-0.00000200
	H	5.50103600	-0.67647100	0.00000200
	H	1.87134500	-2.97264000	0.00000800
	N	-0.00252100	4.58006200	0.00001800
H	0.18545000	5.15053000	0.81690300	
H	0.67791000	3.82516000	0.00000500	
H	0.18546000	5.15056900	-0.81683700	
O	-3.21251200	-1.77786100	-0.00000900	
H	4.34573800	-2.85294200	0.00000800	
H	-4.08600300	-1.31519600	-0.00000900	
N	-5.79084800	-0.62965000	-0.00000600	
H	-5.98312600	-0.06256300	-0.81874200	
H	-5.98312400	-0.06256500	0.81873100	
H	-6.45114500	-1.39982500	-0.00000700	



B3LYP/def2-TZVP
 E = -688.500974
 ZPVE = 0.239452

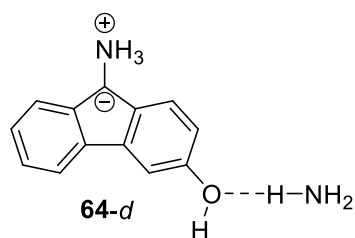
C	2.41526500	0.71650800	0.00001800
C	1.90587000	2.02850000	0.00001600
C	0.54575700	2.26728000	0.00000600
C	-0.33846900	1.17816900	-0.00000200
C	0.17950900	-0.16272300	0.00000200
C	1.54194300	-0.38466500	0.00001200
H	2.61516700	2.84535600	0.00002300
H	0.15410400	3.27675300	0.00000400
H	1.94392700	-1.39048000	0.00001500
C	-1.73967200	1.05008100	-0.00001200
C	-2.16002300	-0.30586400	-0.00001700
C	-3.40449300	-0.93528200	-0.00002700
C	-3.45393100	-2.32523200	-0.00002700
C	-2.28213600	-3.08564800	-0.00001700
C	-1.02916400	-2.46803400	-0.00000600
C	-0.95494100	-1.08685100	-0.00000600
H	-4.31524600	-0.35013800	-0.00003500
H	-4.41388000	-2.82588000	-0.00003500
H	-0.12663600	-3.06832400	0.00000200
N	-2.14995100	4.44838900	-0.00001500
H	-2.57138000	4.87524300	-0.81731800
H	-2.41906500	3.46874700	-0.00001600
H	-2.57139100	4.87524300	0.81728200
O	3.75452800	0.57346300	0.00003100
H	-2.34636600	-4.16631800	-0.00001700
H	4.02120100	-0.37782500	0.00003000
N	4.71976300	-2.08141000	0.00002800
H	5.73066800	-1.99497000	0.00004300
H	4.46046400	-2.62069000	-0.81899200
H	4.46044100	-2.62070000	0.81903400

 <p>63-u</p> <p>B3LYP/def2-TZVP E = -631.972009 ZPVE = 0.207451</p>	C	2.91106800	-0.68111200	0.02146100
	C	3.05115900	0.71411800	0.02257000
	C	1.93712200	1.54094500	-0.03875000
	C	0.66013600	0.97188800	-0.09209800
	C	0.52403500	-0.45650100	-0.05523800
	C	1.65572700	-1.26829800	-0.01809800
	H	4.04409400	1.14947100	0.06750900
	H	2.08182500	2.61757900	-0.04992900
	H	1.57857500	-2.34815500	-0.00555900
	C	-0.65177500	1.50995700	-0.20356100
	C	-1.60942600	0.47547000	-0.08313800
	C	-3.01228800	0.46075000	-0.01180300
	C	-3.67299000	-0.75492900	0.05576400
	C	-2.96663400	-1.96854300	0.05023700
	C	-1.57978000	-1.97261000	-0.00294200
	C	-0.88488400	-0.76573600	-0.05002800
	H	-3.59013900	1.38176500	-0.01694100
	H	-4.75493100	-0.77069000	0.11068000
	H	-1.03758100	-2.91122800	0.00658400
	O	4.00477000	-1.51979300	0.06871200
N	-0.95755300	2.90127800	0.13782600	
H	-0.91755200	3.12210100	1.15160200	
H	-1.89725400	3.13500800	-0.18428300	
H	-0.31099100	3.53711800	-0.33111100	
H	-3.51017400	-2.90348500	0.09430900	
H	4.81001200	-0.99250100	0.07641200	
 <p>63-d</p> <p>B3LYP/def2-TZVP E = -631.972668 ZPVE = 0.207655</p>	C	2.92032700	-0.66063400	0.02043900
	C	3.05418000	0.73546600	0.02134600
	C	1.93616500	1.55105800	-0.03539000
	C	0.65890400	0.97608400	-0.08473600
	C	0.52704700	-0.45050100	-0.05034900
	C	1.66836700	-1.25486500	-0.01619000
	H	4.05031000	1.15608700	0.06188800
	H	2.07325600	2.62890600	-0.04433000
	H	1.57803100	-2.33672200	-0.00492100
	C	-0.65449000	1.50937100	-0.19036100
	C	-1.60913800	0.47348000	-0.07715700
	C	-3.01243700	0.45298200	-0.01008800
	C	-3.66889400	-0.76486100	0.05186700
	C	-2.95774700	-1.97627500	0.04558700
	C	-1.57111400	-1.97527600	-0.00362500
	C	-0.87887400	-0.76601600	-0.04598400
	H	-3.59329700	1.37207700	-0.01263900
	H	-4.75089200	-0.78483500	0.10352600
	H	-1.02710800	-2.91312100	0.00448300
	O	4.08924500	-1.39015900	0.06446600
N	-0.96421000	2.90474500	0.12755900	
H	-0.94019400	3.13890000	1.13815800	
H	-1.89805100	3.13647900	-0.21302300	
H	-0.30799000	3.53261600	-0.33921300	
H	-3.49815200	-2.91323600	0.08574600	
H	3.87582700	-2.32917300	0.05952200	



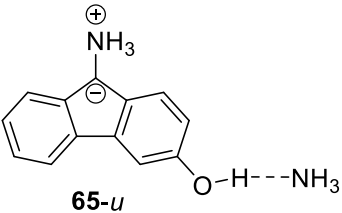
B3LYP/def2-TZVP
 E = -688.527956
 ZPVE = 0.243505

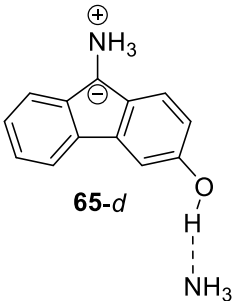
C	-2.53972700	-0.75474200	0.01313700
C	-2.13874500	-2.09700800	0.01994200
C	-0.79259600	-2.43566300	-0.03705500
C	0.16837600	-1.42023500	-0.09213600
C	-0.25538800	-0.04907300	-0.06054900
C	-1.61021200	0.27269100	-0.02724200
H	-2.89001300	-2.87884100	0.06636100
H	-0.51445300	-3.48576700	-0.04404200
H	-1.94991400	1.30092800	-0.01794400
C	1.58641700	-1.41218600	-0.20126600
C	2.07192200	-0.08738500	-0.08257800
C	3.36037900	0.46691200	-0.00952700
C	3.50019900	1.84400200	0.05471200
C	2.38039200	2.69103200	0.04417000
C	1.09886800	2.16050300	-0.01087200
C	0.92584900	0.77867400	-0.05487000
H	4.24895100	-0.15981000	-0.01094500
H	4.49219100	2.27619200	0.11101000
H	0.23434200	2.81422600	-0.00488200
O	-3.88047600	-0.40491100	0.05745300
N	2.40392500	-2.57585200	0.15092000
H	2.45269200	-2.78558200	1.16687800
H	3.36109600	-2.43313400	-0.17285500
H	2.05127500	-3.41554100	-0.31010300
H	2.52130400	3.76340600	0.08600900
H	-4.41835200	-1.20281500	0.05844100
N	-4.08234600	2.79358500	0.02250000
H	-4.52500000	3.17118700	-0.80725000
H	-4.53757500	3.21011000	0.82638600
H	-4.26819100	1.79547600	0.04416600

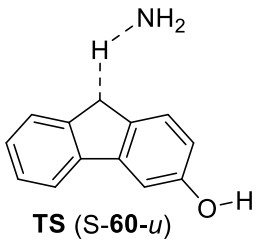
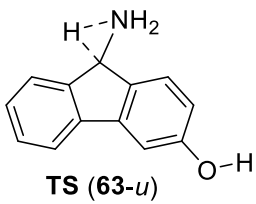


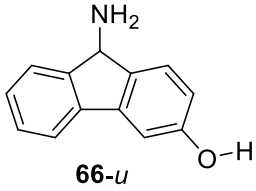
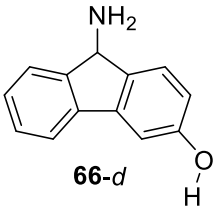
B3LYP/def2-TZVP
 E = -688.528961
 ZPVE = 0.243631

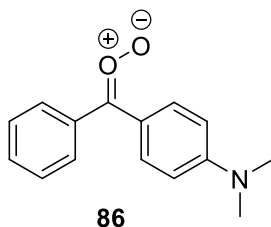
C	2.30566800	-0.77404700	0.00256200
C	2.49412700	0.61553400	0.00346400
C	1.40151400	1.46501700	-0.04549200
C	0.10476400	0.93403300	-0.08768200
C	-0.07759000	-0.48691400	-0.05401300
C	1.03685500	-1.32872800	-0.02658900
H	3.50366600	1.00437500	0.03840600
H	1.57510800	2.53764800	-0.05297800
H	0.91114000	-2.40719300	-0.01516800
C	-1.18904100	1.51243600	-0.18321400
C	-2.17986800	0.51201900	-0.06971700
C	-3.58290100	0.54113200	0.00103100
C	-4.28189200	-0.65279900	0.06299100
C	-3.61402900	-1.88862500	0.05365200
C	-2.22832300	-1.93674300	0.00042000
C	-1.49341500	-0.75296700	-0.04314500
H	-4.13048100	1.48039800	0.00257800
H	-5.36378300	-0.63455400	0.11762400
H	-1.71809900	-2.89345600	0.00584900
O	3.44949000	-1.55496200	0.03908900
N	-1.44600500	2.92164700	0.11815900
H	-1.42265800	3.16459400	1.12626700
H	-2.36576600	3.18899100	-0.23474700
H	-0.75857000	3.51654000	-0.34728900
H	-4.18714800	-2.80592600	0.09461400
H	3.19890400	-2.48446400	0.03416100
N	6.06274300	0.27649700	0.04544700
H	6.68488800	0.12693600	0.83150500
H	6.61285200	0.17053000	-0.79926800
H	5.37165500	-0.46782400	0.05487500

 <p>65-u</p> <p>B3LYP/def2-TZVP E = -688.534704 ZPVE = 0.244595</p>	C	2.34729600	-0.62961900	0.16476100
	C	2.45567800	0.77302400	0.16471800
	C	1.33090000	1.57906600	0.04147700
	C	0.06701800	0.99023800	-0.06381200
	C	-0.04505300	-0.43706500	-0.01544700
	C	1.09674700	-1.22991800	0.07357600
	H	3.43553700	1.22373100	0.26535600
	H	1.45680500	2.65866700	0.02501500
	H	1.03527200	-2.31100600	0.08932200
	C	-1.24981500	1.51128900	-0.24376600
	C	-2.19251000	0.45817200	-0.13195100
	C	-3.59561500	0.42092400	-0.09690500
	C	-4.23970800	-0.80465500	-0.03020300
	C	-3.51418900	-2.00582800	-0.00320400
	C	-2.12561000	-1.98719900	-0.01842900
	C	-1.44995100	-0.76990600	-0.05888700
	H	-4.18775700	1.33219600	-0.13539100
	H	-5.32244300	-0.83699100	-0.00381800
	H	-1.56831500	-2.91629300	0.01889800
	O	3.44053900	-1.43953300	0.27411300
N	-1.58705300	2.88030500	0.16523200	
H	-1.56337900	3.04812400	1.19150600	
H	-2.52597400	3.11326300	-0.15760300	
H	-0.94606300	3.54993700	-0.26033100	
H	-4.04324800	-2.94939200	0.03659000	
H	4.26754600	-0.92422500	0.16397200	
N	5.92798200	-0.12396900	-0.29112700	
H	6.58025000	-0.87264700	-0.49686400	
H	6.35814300	0.47953900	0.40032400	
H	5.80167400	0.41586700	-1.14018700	

 <p>65-d</p> <p>B3LYP/def2-TZVP E = -688.536052 ZPVE = 0.244723</p>	C	-2.53052200	-0.69170300	0.06790900
	C	-2.13011200	-2.03956200	0.03996200
	C	-0.79262300	-2.38741400	-0.05187200
	C	0.18316000	-1.38359000	-0.10659200
	C	-0.21963500	-0.01310600	-0.03877200
	C	-1.57472000	0.31831200	0.02889100
	H	-2.90057400	-2.79851100	0.08406100
	H	-0.52445400	-3.44020500	-0.08729000
	H	-1.88410600	1.35582700	0.06948900
	C	1.60202900	-1.39799800	-0.24786000
	C	2.10814200	-0.08433800	-0.10390700
	C	3.40514500	0.45015500	-0.03391100
	C	3.56920600	1.82281500	0.06074100
	C	2.46263300	2.68700100	0.08294500
	C	1.17277100	2.17542800	0.03317800
	C	0.97342700	0.79826700	-0.03748900
	H	4.28353500	-0.19011800	-0.06403800
	H	4.56865700	2.23780000	0.11423100
	H	0.32139300	2.84639000	0.06612900
	O	-3.86997800	-0.44676600	0.14460900
N	2.39709100	-2.57723500	0.10987700	
H	2.43466900	-2.78707300	1.12708300	
H	3.35810800	-2.45461900	-0.20932500	
H	2.02879900	-3.40964300	-0.35143200	
H	2.62042100	3.75614000	0.14590700	
H	-4.04892500	0.51753800	0.09698300	
N	-4.51687100	2.34048700	-0.09263800	
H	-5.52277700	2.44230200	-0.16953700	
H	-4.10350300	2.71286100	-0.94055300	
H	-4.20636600	2.91708100	0.68141800	

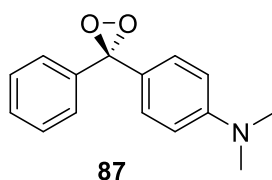
 <p>TS (S-60-<i>u</i>)</p> <p>B3LYP/def2-TZVP E = -631.929376 ZPVE = 0.200037</p>	C	-2.97603200	-1.93408200	0.16790400
	C	-3.66886600	-0.74372400	-0.04818000
	C	-2.98079900	0.44366700	-0.29437600
	C	-1.59122200	0.43079500	-0.28930200
	C	-0.89428700	-0.77715200	-0.03848500
	C	-1.57939100	-1.96221300	0.16480600
	H	-4.75139500	-0.74677000	-0.04088800
	H	-3.51909900	1.36286200	-0.49198000
	H	-1.05069400	-2.89385200	0.32601500
	C	-0.63862100	1.49675700	-0.61605200
	C	0.66525600	0.92629500	-0.31719700
	C	1.93125700	1.49986900	-0.37483300
	C	3.05336200	0.70786400	-0.16132200
	C	2.91270800	-0.66525000	0.06680600
	C	1.64937100	-1.26689900	0.10853700
	C	0.53951800	-0.46447200	-0.05589800
	H	2.04425200	2.55679100	-0.58336700
	H	4.04517900	1.14501700	-0.19113300
	H	1.57955900	-2.33468600	0.26998200
	H	-0.93026700	2.77297800	-0.27041500
N	-1.02690200	3.14760600	0.84228400	
H	-0.16096000	2.99103000	1.34938800	
H	-1.76345600	2.64476300	1.32833600	
O	3.98593900	-1.48208100	0.25092200	
H	-3.52852800	-2.84994100	0.33611200	
H	4.80270300	-0.97352700	0.19014300	
 <p>TS (63-<i>u</i>)</p> <p>B3LYP/def2-TZVP E = -631.934010 ZPVE = 0.201658</p>	C	2.91051000	-0.67539300	0.03911000
	C	3.05149800	0.71656500	0.02161200
	C	1.93532800	1.54053800	-0.08438700
	C	0.66839200	0.96967400	-0.14601200
	C	0.53117200	-0.44582900	-0.08843100
	C	1.65226800	-1.26372600	-0.01972500
	H	4.04288200	1.15346600	0.07562500
	H	2.07388300	2.61522800	-0.13721300
	H	1.57219500	-2.34277500	0.00804200
	C	-0.65464100	1.53283300	-0.30413400
	C	-1.61038400	0.46692300	-0.13760400
	C	-3.00240500	0.46178600	-0.04131800
	C	-3.66507000	-0.75433800	0.07935100
	C	-2.95867500	-1.96158200	0.08888200
	C	-1.57062500	-1.96775400	0.00651300
	C	-0.88812300	-0.75917400	-0.08186300
	H	-3.57153600	1.38457900	-0.08414100
	H	-4.74535400	-0.76835900	0.15535000
	H	-1.02617800	-2.90424600	0.03223000
	O	3.99398300	-1.51534100	0.11881400
N	-0.99685500	2.94560200	0.28244800	
H	-1.80193900	2.93663700	0.90473600	
H	-1.03766900	2.75503600	-0.86170000	
H	-0.18113200	3.40264700	0.67518600	
H	-3.49855300	-2.89653900	0.16712600	
H	4.80405100	-0.99530300	0.14513900	

 <p>66-u</p> <p>B3LYP/def2-TZVP E = -632.035033 ZPVE = 0.208344</p>	C	-2.98682800	-1.89576100	0.09355600
	C	-3.68636700	-0.69921200	-0.05030300
	C	-3.00183600	0.50863400	-0.19022500
	C	-1.61929200	0.49988800	-0.17720000
	C	-0.91428200	-0.70331900	-0.02937600
	C	-1.59479500	-1.90783400	0.10403600
	H	-4.76899400	-0.70814300	-0.05551600
	H	-3.55325200	1.43457900	-0.30712100
	H	-1.05501900	-2.83989400	0.21695800
	C	-0.65955500	1.66631100	-0.30934400
	H	-0.76472600	2.10221900	-1.31659100
	C	0.68533200	0.97804000	-0.20130800
	C	1.95396300	1.52206800	-0.24216500
	C	3.06292800	0.68492900	-0.12109600
	C	2.89083300	-0.69182100	0.03245800
	C	1.61469900	-1.25074900	0.07054400
	C	0.52064400	-0.40659900	-0.04411100
	H	2.10316700	2.58840800	-0.36665600
	H	4.06428300	1.10036100	-0.14826900
	H	1.50880000	-2.32077900	0.19063600
N	-0.85866400	2.65861700	0.75730600	
H	-0.17510200	3.40289800	0.67512300	
H	-1.77448700	3.08588100	0.67355100	
O	3.94883800	-1.55026800	0.15094700	
H	-3.53266500	-2.82495800	0.19881400	
H	4.77527700	-1.05620300	0.11755700	
 <p>66-d</p> <p>B3LYP/def2-TZVP E = -632.035009 ZPVE = 0.208381</p>	C	-2.97919200	-1.90150800	0.09189500
	C	-3.68232100	-0.70718700	-0.05086200
	C	-3.00119500	0.50292900	-0.18981000
	C	-1.61888300	0.49872800	-0.17705900
	C	-0.90977900	-0.70250700	-0.02990900
	C	-1.58692900	-1.90900900	0.10240600
	H	-4.76488800	-0.71937400	-0.05595300
	H	-3.55535200	1.42733000	-0.30558800
	H	-1.04560100	-2.84044900	0.21462100
	C	-0.66199200	1.66764200	-0.30776000
	H	-0.76799100	2.10423400	-1.31465500
	C	0.68462900	0.98302300	-0.20052400
	C	1.95432500	1.53167600	-0.24229000
	C	3.06631500	0.70361700	-0.12307800
	C	2.89959800	-0.67364200	0.03036000
	C	1.62539000	-1.23788100	0.06898300
	C	0.52349000	-0.39920500	-0.04450300
	H	2.09742600	2.59890200	-0.36683000
	H	4.07085100	1.10371600	-0.14861100
	H	1.50391000	-2.30925800	0.18789500
N	-0.86330100	2.65786900	0.76015600	
H	-0.17186700	3.39585800	0.68804400	
H	-1.77419100	3.09398600	0.66886100	
O	4.03612400	-1.42653900	0.13778300	
H	-3.52207400	-2.83253400	0.19635100	
H	3.80315500	-2.35523800	0.24541300	



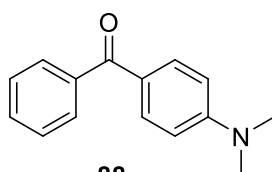
B3LYP/def2-TZVP
 E = -785.746014
 ZPVE = 0.267118

C	4.56584600	-1.75353500	0.16516200
C	3.41928800	-1.99101600	0.91592100
C	2.35044800	-1.10775500	0.85593500
C	2.41598400	0.03035200	0.04374300
C	3.57889800	0.26702800	-0.69966800
C	4.64203100	-0.62164400	-0.64096200
H	5.39744000	-2.44527800	0.21038200
H	3.35979300	-2.86177800	1.55641900
H	1.46713700	-1.28627900	1.45399400
H	3.63479000	1.14797000	-1.32424700
H	5.53180800	-0.43242300	-1.22781900
C	-0.08335500	0.61400500	-0.01163300
C	-1.12561700	1.46445900	0.41392400
C	-0.44992000	-0.66988300	-0.46525500
C	-2.43611200	1.04186100	0.42129500
H	-0.87567500	2.46260500	0.73288300
C	-1.75969300	-1.08957200	-0.48779700
H	0.31072000	-1.34371900	-0.83396000
C	-2.80158500	-0.24673800	-0.03164900
H	-3.19017200	1.73185500	0.76801300
H	-1.97794900	-2.07492900	-0.87001600
N	-4.10483000	-0.65907900	-0.03854400
C	-4.45824600	-1.96651300	-0.56144700
H	-5.53158900	-2.11036200	-0.47134100
H	-4.18991600	-2.06918800	-1.61830200
H	-3.96429600	-2.76867500	-0.00501400
C	-5.15977800	0.23977500	0.39627400
H	-6.11557000	-0.27366200	0.33455700
H	-5.01413000	0.55617000	1.43311600
H	-5.21410700	1.13673200	-0.22934800
C	1.30547100	1.00148600	-0.00127700
O	1.74304600	2.21155400	-0.03888600
O	0.89239900	3.28477600	-0.15047800



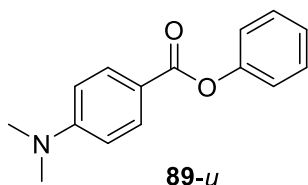
B3LYP/def2-TZVP
 E = -785.762733
 ZPVE = 0.266834

C	4.50693200	-1.69774300	0.19289400
C	3.45848600	-1.75179200	1.10600700
C	2.40918600	-0.84683200	1.01488600
C	2.40608400	0.12792600	0.01681900
C	3.46132600	0.18521300	-0.88950900
C	4.50502500	-0.72932500	-0.80444100
H	5.32235300	-2.40691200	0.26027700
H	3.45714600	-2.50005600	1.88848700
H	1.58844700	-0.89473700	1.71898800
H	3.46215000	0.95122400	-1.65237400
H	5.31913300	-0.68225400	-1.51666400
C	-0.11774900	0.64486100	0.00514100
C	-1.14264200	1.50518700	0.40314800
C	-0.46977000	-0.63782000	-0.41134100
C	-2.46274100	1.09903000	0.40803400
H	-0.89256300	2.51104800	0.71174700
C	-1.78922200	-1.05852200	-0.42027900
H	0.29577200	-1.32574100	-0.74479000
C	-2.82711800	-0.20479700	0.00505400
H	-3.21560800	1.80402400	0.72602200
H	-2.00615400	-2.05887700	-0.76220100
N	-4.13965400	-0.62406800	0.03135600
C	-4.49726000	-1.90180900	-0.55323600
H	-5.56302300	-2.07115400	-0.41946100
H	-4.27424700	-1.94946200	-1.62699900
H	-3.96912500	-2.72279000	-0.06169500
C	-5.19598900	0.33250100	0.30096700
H	-6.15343200	-0.18300600	0.30194400
H	-5.06986600	0.79422500	1.28335800
H	-5.23829500	1.13365500	-0.44802300
C	1.29194200	1.13214900	-0.04305200
O	1.52556400	2.25506400	-0.86096900
O	1.56142900	2.34242800	0.62788600



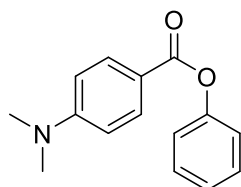
B3LYP/def2-TZVP
 E = -710.631272
 ZPVE = 0.263876

C	4.75458500	-1.34993200	0.15331000
C	3.61709400	-1.66415200	0.88820800
C	2.49231600	-0.85071700	0.81297800
C	2.50178500	0.29594400	0.01580700
C	3.65846600	0.61731800	-0.69881900
C	4.77240500	-0.20714100	-0.64232500
H	5.62728400	-1.98900700	0.20486500
H	3.60552200	-2.54168400	1.52248100
H	1.61226400	-1.09367700	1.39349400
H	3.66614000	1.52314800	-1.29047000
H	5.65877400	0.04291500	-1.21180900
C	-0.04455000	0.73368500	-0.00848000
C	-1.07720800	1.59988900	0.37199600
C	-0.40205100	-0.55625600	-0.41431600
C	-2.39513600	1.19710600	0.38233100
H	-0.81805200	2.60965700	0.66222300
C	-1.72039400	-0.97248800	-0.42986800
H	0.36020100	-1.24348900	-0.75595600
C	-2.75915000	-0.11154200	-0.01376300
H	-3.14937500	1.90294000	0.69556100
H	-1.94141200	-1.97081700	-0.77540800
N	-4.06842000	-0.52465800	0.00397600
C	-4.42391800	-1.83525700	-0.50527600
H	-5.49208300	-1.99192300	-0.37777300
H	-4.18741700	-1.94501400	-1.57055800
H	-3.90437800	-2.62782500	0.04027600
C	-5.12576600	0.41903300	0.31490000
H	-6.08278400	-0.09617000	0.29423500
H	-4.99905300	0.84447800	1.31417700
H	-5.16756800	1.24603100	-0.40371500
C	1.34436200	1.25105400	-0.04001100
O	1.56672900	2.45047300	-0.11118600



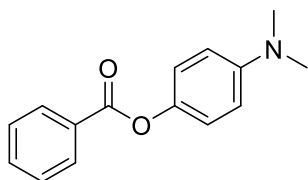
B3LYP/def2-TZVP
 E = -785.895257
 ZPVE = 0.267758

C	-0.58455800	-0.41085000	-0.09141600
C	-1.50699400	-1.43672700	-0.31876600
C	-1.07707200	0.86574900	0.19542300
C	-2.86560000	-1.20726500	-0.26357400
H	-1.13370200	-2.42717700	-0.54302900
C	-2.43433600	1.11213100	0.25562000
H	-0.38426300	1.67589200	0.37357400
C	-3.37339100	0.07997100	0.02921200
H	-3.53706700	-2.03162200	-0.44889700
H	-2.76658500	2.11416500	0.47997800
N	-4.72246200	0.31688000	0.09135800
C	-5.21849300	1.65313200	0.35987800
H	-6.30517700	1.63642400	0.37387400
H	-4.87611700	2.02336500	1.33145000
H	-4.90106000	2.36856000	-0.40668200
C	-5.66577900	-0.75194100	-0.17714900
H	-6.67841700	-0.37132600	-0.07203100
H	-5.55678100	-1.14773900	-1.19280300
H	-5.54512700	-1.58277800	0.52513900
C	0.85091900	-0.72918600	-0.16565300
O	1.31482100	-1.81702700	-0.39621500
C	3.01154700	0.28627600	0.05274200
C	3.68780900	-0.61394700	0.86594700
C	3.69981100	1.18920000	-0.74462000
C	5.07710000	-0.60378800	0.87084500
H	3.13207700	-1.31558300	1.46986800
C	5.08981600	1.19322000	-0.72821200
H	3.13996100	1.87708300	-1.36415900
C	5.78200700	0.29636500	0.07769700
H	5.61057300	-1.30544800	1.49951200
H	5.62978800	1.89757600	-1.34820700
H	6.86431700	0.29775800	0.08813100
O	1.62619200	0.38435800	0.05708100

**89-d**

B3LYP/def2-TZVP
 E = -785.886184
 ZPVE = 0.267628

C	-0.17778700	1.22286600	-0.21317100
C	-1.26551500	1.75080800	0.49093300
C	-0.34656400	-0.00998900	-0.85056100
C	-2.46376200	1.07502300	0.57828500
H	-1.15183600	2.71338100	0.97173200
C	-1.54332800	-0.69384600	-0.78467000
H	0.46548800	-0.43991700	-1.41912800
C	-2.63915100	-0.17727200	-0.05607200
H	-3.27011600	1.52278300	1.13863500
H	-1.62664400	-1.63564700	-1.30477900
N	-3.82365200	-0.86060800	0.03072800
C	-3.99477100	-2.11867600	-0.67149700
H	-4.98526500	-2.51419900	-0.46229400
H	-3.89891000	-1.99963100	-1.75659000
H	-3.26165400	-2.86246500	-0.34550500
C	-4.95451900	-0.27771700	0.72862400
H	-5.79173000	-0.96996700	0.69524900
H	-4.72155700	-0.08470300	1.78012200
H	-5.27551600	0.66547200	0.27287100
C	1.05817400	2.02167300	-0.29145900
O	1.13354400	3.19304800	-0.04035100
C	2.65720000	0.20694300	-0.21343000
C	2.48845300	-0.09483300	1.13440400
C	3.36136300	-0.65365600	-1.04910200
C	3.01330400	-1.27972300	1.63649300
H	1.95496900	0.59017000	1.77938100
C	3.88861700	-1.82984200	-0.53263800
H	3.48659300	-0.38592200	-2.08987400
C	3.71240000	-2.15212800	0.80968300
H	2.87945400	-1.51547100	2.68473400
H	4.43796300	-2.49792600	-1.18400700
H	4.12231100	-3.07065400	1.20866900
O	2.19612400	1.37834800	-0.76955300

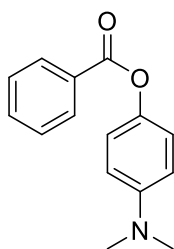
**90-u**

B3LYP/def2-TZVP

E = -785.889664

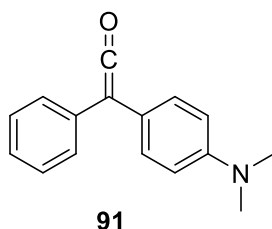
ZPVE = 0.267839

C	3.08668900	0.15570500	-0.07781100
C	4.06819700	1.03086800	-0.54760900
C	3.46378000	-1.03274700	0.55147100
C	5.41112800	0.72108700	-0.39149400
H	3.75799600	1.94685400	-1.03181200
C	4.80929400	-1.33856500	0.70700600
H	2.70382400	-1.70887900	0.91534400
C	5.78361300	-0.46406500	0.23638400
H	6.16817100	1.40243200	-0.75822700
H	5.09830700	-2.26020800	1.19587900
C	1.66184000	0.54177400	-0.27499400
O	1.29769700	1.56478900	-0.79392900
C	-0.56705600	-0.23054500	0.10588000
C	-1.21245300	0.87332100	0.63895100
C	-1.30191100	-1.24931700	-0.47325500
C	-2.59415600	0.96113900	0.58060500
H	-0.63765000	1.66820800	1.09150400
C	-2.68549400	-1.16896800	-0.53137900
H	-0.78660600	-2.11282400	-0.87314500
C	-3.37103500	-0.05049000	-0.01936600
H	-3.06479900	1.83349800	1.00707500
H	-3.22538700	-1.98658500	-0.98337500
O	0.81558700	-0.40907100	0.20680600
N	-4.75104100	0.05647600	-0.10981100
C	-5.52326300	-1.10400000	-0.50631200
H	-5.40418200	-1.95093100	0.18412200
H	-6.57734100	-0.83735600	-0.54055500
H	-5.23982800	-1.44127400	-1.50588600
C	-5.43017700	1.08866600	0.64820900
H	-5.09268600	2.08303300	0.34763900
H	-6.49812400	1.03426300	0.44848100
H	-5.27676600	0.99117200	1.73210700
H	6.83209600	-0.70566100	0.35879800

**90-d**

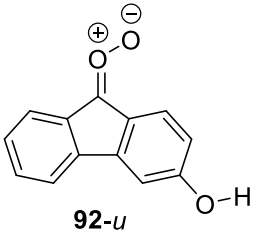
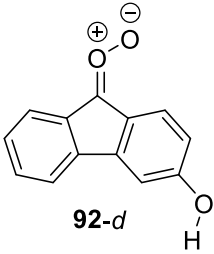
B3LYP/def2-TZVP
 E = -785.880115
 ZPVE = 0.267694

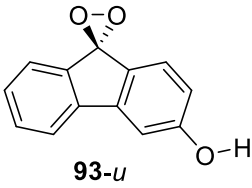
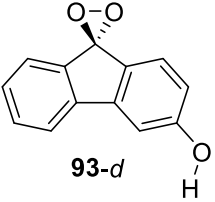
C	2.51169400	-0.12473700	-0.04482100
C	3.43944100	0.50780600	0.78420800
C	1.93108500	0.58507500	-1.09691100
C	3.76168100	1.84207700	0.58186900
H	3.90204900	-0.06192800	1.57884500
C	2.27270000	1.91344100	-1.31095700
H	1.22022200	0.10126700	-1.75070400
C	3.17934200	2.54679000	-0.46720100
H	4.47245800	2.33031700	1.23626300
H	1.82774900	2.45555000	-2.13546000
C	2.25363900	-1.57803600	0.19070200
O	3.08771200	-2.32451200	0.62367200
C	-0.14526900	-1.36229800	-0.06669300
C	-0.46214800	-0.61143900	1.05456400
C	-1.05831000	-1.46606700	-1.10313100
C	-1.67078900	0.06466800	1.12310100
H	0.23527600	-0.55280800	1.87976800
C	-2.27235100	-0.80005300	-1.03677800
H	-0.81410300	-2.07741700	-1.96214600
C	-2.60562200	0.00451800	0.07123000
H	-1.88170300	0.63673800	2.01333000
H	-2.96054200	-0.91319800	-1.86019600
O	1.03367100	-2.09372600	-0.15842800
N	-3.79982500	0.70916500	0.12165800
C	-4.83607300	0.40703900	-0.84632200
H	-5.17778400	-0.63611000	-0.79256200
H	-5.69086200	1.05586500	-0.66853700
H	-4.48958600	0.59701700	-1.86459500
C	-4.21081200	1.30767400	1.37656700
H	-3.47818500	2.04174800	1.71904900
H	-5.15218300	1.83278000	1.23032500
H	-4.34963600	0.56696300	2.17655500
H	3.43529300	3.58621400	-0.63004900

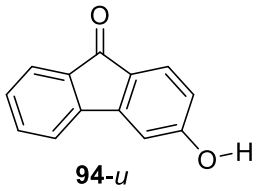
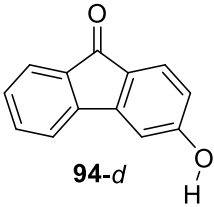


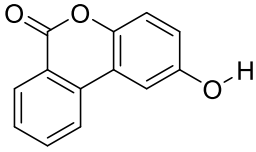
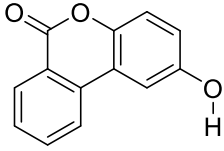
B3LYP/def2-TZVP
 E = -748.716979
 ZPVE = 0.268141

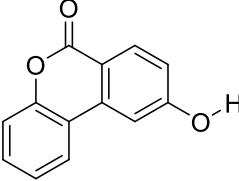
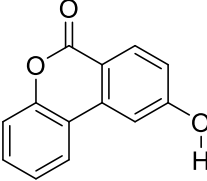
C	4.50965200	-1.87933100	0.33372200
C	3.22574100	-2.16796200	0.78232300
C	2.20180300	-1.24047600	0.63995500
C	2.43908300	-0.00078600	0.03392900
C	3.73485200	0.27450300	-0.42513100
C	4.75741000	-0.64946400	-0.26845900
H	5.30590900	-2.60363700	0.44706000
H	3.01779000	-3.12074300	1.25365100
H	1.20973600	-1.47372400	1.00249500
H	3.94129600	1.21624500	-0.92081500
H	5.75017200	-0.41260600	-0.63067600
C	-0.10059800	0.61430400	-0.07717800
C	-0.59287200	-0.38707200	-0.91869200
C	-1.01280900	1.24655300	0.76755400
C	-1.92902000	-0.74424500	-0.91693000
H	0.08934600	-0.90499100	-1.58116800
C	-2.35874000	0.91421300	0.76842900
H	-0.66135600	2.00960800	1.45180900
C	-2.86033900	-0.08862700	-0.08338100
H	-2.24821600	-1.53418900	-1.57976800
H	-3.01400000	1.43471600	1.45009400
N	-4.20369300	-0.41532900	-0.10605500
C	-5.08508000	0.12887700	0.90793700
H	-6.10069000	-0.21171300	0.71960900
H	-4.80176300	-0.17808200	1.92394500
H	-5.09448000	1.22088400	0.87562100
C	-4.63776400	-1.59844500	-0.82288700
H	-5.71860200	-1.68883400	-0.74224200
H	-4.39382500	-1.52757500	-1.88545400
H	-4.18543200	-2.51970000	-0.43142800
C	1.34302100	0.98168000	-0.09741000
C	1.62024900	2.26570900	-0.24170400
O	1.85030400	3.39813300	-0.36285100

 <p>92-u</p> <p>B3LYP/def2-TZVP E = -725.866966 ZPVE = 0.176624</p>	C	-2.87765400	-0.93976900	-0.00000300
	C	-3.06118000	0.44517100	0.00000100
	C	-1.96752200	1.30342900	0.00000500
	C	-0.69007600	0.75102600	0.00000700
	C	-0.50966700	-0.65802100	0.00000600
	C	-1.59257900	-1.50500500	-0.00000100
	H	-4.06676500	0.84998000	0.00000000
	H	-2.08378600	2.37545400	0.00000700
	H	-1.49069000	-2.58179800	-0.00000300
	C	0.62015200	1.34785600	0.00000100
	C	1.62369700	0.28563700	-0.00000200
	C	3.00750300	0.33866800	-0.00000500
	C	3.71078200	-0.86605500	-0.00000300
	C	3.03529800	-2.08440500	0.00000200
	C	1.63873700	-2.13457900	0.00000500
	C	0.93438400	-0.94463400	0.00000300
	H	3.52428300	1.28912400	-0.00000700
H	4.79286400	-0.85428800	-0.00000500	
H	3.60128100	-3.00712900	0.00000300	
H	1.12472500	-3.08736800	0.00000900	
O	-3.91840300	-1.80963800	-0.00000600	
H	-4.75502800	-1.32955000	-0.00001000	
O	-0.02615200	3.52342400	0.00000200	
O	0.95978800	2.57492100	-0.00000600	
 <p>92-d</p> <p>B3LYP/def2-TZVP E = -725.866050 ZPVE = 0.176568</p>	C	-2.88953800	-0.91736800	-0.00000300
	C	-3.06563500	0.46823500	0.00000000
	C	-1.96757200	1.31657700	0.00000800
	C	-0.68966300	0.75834200	0.00001500
	C	-0.51523500	-0.64896600	0.00001200
	C	-1.60673400	-1.48886400	0.00000100
	H	-4.07377200	0.85901300	0.00000000
	H	-2.07778600	2.38924700	0.00001500
	H	-1.48926400	-2.56683600	-0.00001000
	C	0.62391800	1.34811400	0.00000300
	C	1.62267600	0.28091300	-0.00000700
	C	3.00633000	0.32640100	-0.00001200
	C	3.70364300	-0.88222600	-0.00000700
	C	3.02197500	-2.09672700	0.00000500
	C	1.62487900	-2.13903600	0.00001000
	C	0.92663000	-0.94559800	0.00000100
	H	3.52811900	1.27410900	-0.00001800
H	4.78574900	-0.87597600	-0.00001100	
H	3.58291300	-3.02251800	0.00001000	
H	1.10709600	-3.08995000	0.00001900	
O	-4.01146200	-1.68010500	-0.00002400	
H	-3.78218000	-2.61675400	0.00005700	
O	-0.00496000	3.52863500	0.00000500	
O	0.97205900	2.57283100	-0.00001000	

 <p>93-u</p> <p>B3LYP/def2-TZVP E = -725.880923 ZPVE = 0.176268</p>	C	-2.98173000	-0.71334500	-0.00000600
	C	-3.08745700	0.67971300	-0.00001000
	C	-1.94022700	1.47040000	-0.00000900
	C	-0.70870100	0.84956000	-0.00001200
	C	-0.60168700	-0.54957500	-0.00000500
	C	-1.73316100	-1.34310000	0.00000000
	H	-4.06804900	1.14199100	-0.00001200
	H	-2.01294400	2.55015900	-0.00002000
	H	-1.68605800	-2.42372000	0.00000600
	C	0.66008800	1.44096400	-0.00000400
	C	1.58836000	0.26635500	-0.00000300
	C	2.96750100	0.24162100	-0.00000300
	C	3.60304500	-1.00148800	-0.00000300
	C	2.85639400	-2.17749600	0.00000200
	C	1.46128700	-2.14493000	0.00000200
	C	0.82854800	-0.91159700	-0.00000200
	H	3.53360600	1.16397100	-0.00001200
H	4.68411800	-1.05332700	-0.00000600	
H	3.36698800	-3.13226400	0.00000700	
H	0.89070400	-3.06500700	0.00000300	
O	-4.07596200	-1.52491600	0.00001200	
H	-4.88108200	-0.99490500	0.00002800	
O	0.95668100	2.58562900	-0.74813800	
O	0.95667500	2.58561200	0.74816700	
 <p>93-d</p> <p>B3LYP/def2-TZVP E = -725.880496 ZPVE = 0.176261</p>	C	-2.99087900	-0.69181700	-0.00000800
	C	-3.08983800	0.70159900	-0.00000900
	C	-1.93944900	1.48235100	-0.00000900
	C	-0.70756500	0.85579200	-0.00001200
	C	-0.60550000	-0.54082600	-0.00000700
	C	-1.74497700	-1.32762400	-0.00000200
	H	-4.07414100	1.14926500	-0.00001200
	H	-2.00556800	2.56254300	-0.00001900
	H	-1.68243300	-2.41020500	0.00000500
	C	0.66374700	1.44146200	-0.00000400
	C	1.58777800	0.26302700	-0.00000500
	C	2.96640700	0.23212400	-0.00000600
	C	3.59693400	-1.01393000	-0.00000300
	C	2.84532100	-2.18635300	0.00000300
	C	1.45005200	-2.14729300	0.00000300
	C	0.82248800	-0.91148000	-0.00000200
	H	3.53643500	1.15205100	-0.00001500
H	4.67775000	-1.07035300	-0.00000600	
H	3.35157400	-3.14343000	0.00000900	
H	0.87671200	-3.06582800	0.00000500	
O	-4.16017400	-1.39101400	0.00001600	
H	-3.98078000	-2.33798900	0.00001800	
O	0.96592300	2.58437600	-0.74809700	
O	0.96591700	2.58435800	0.74812900	

 <p>94-u</p> <p>B3LYP/def2-TZVP E = -650.749592 ZPVE = 0.173404</p>	C	-2.87455100	-0.67159000	0.00000600
	C	-3.05940900	0.71381800	0.00000200
	C	-1.95730400	1.56432000	0.00000400
	C	-0.69021000	1.01340300	0.00000300
	C	-0.50797500	-0.38067500	0.00000100
	C	-1.59115600	-1.23434600	0.00000200
	H	-4.06503100	1.11899800	-0.00000100
	H	-2.08382400	2.63955200	0.00000300
	H	-1.48803000	-2.31118000	-0.00000100
	C	0.63926200	1.68136100	-0.00000200
	C	1.63350900	0.55815600	-0.00000300
	C	3.01305400	0.60951200	-0.00000200
	C	3.71911000	-0.59548800	-0.00000100
	C	3.03876000	-1.81052000	0.00000200
	C	1.64164700	-1.85792600	0.00000200
	C	0.94292800	-0.66338700	-0.00000300
	H	3.52216800	1.56501000	-0.00000400
	H	4.80148600	-0.58796300	0.00000000
	H	3.60180200	-2.73546700	0.00000400
	H	1.12614100	-2.81011200	0.00000400
O	-3.91948000	-1.54194000	-0.00000500	
H	-4.75393800	-1.05890600	-0.00002000	
O	0.87613400	2.86947000	-0.00000200	
 <p>94-d</p> <p>B3LYP/def2-TZVP E = -650.749108 ZPVE = 0.173380</p>	C	2.88355100	-0.65383800	0.00000000
	C	3.06350900	0.73189700	0.00000100
	C	1.95863200	1.57413400	0.00000300
	C	0.69008400	1.01936100	0.00000200
	C	0.51110800	-0.37243900	0.00000100
	C	1.60149200	-1.22091900	0.00000000
	H	4.07236400	1.12120100	0.00000100
	H	2.08021300	2.64991900	0.00000300
	H	1.48149800	-2.29883300	-0.00000300
	C	-0.64134500	1.68305700	0.00000000
	C	-1.63327300	0.55656900	0.00000000
	C	-3.01245800	0.60331200	0.00000100
	C	-3.71504800	-0.60427200	-0.00000100
	C	-3.03096100	-1.81668800	0.00000000
	C	-1.63328600	-1.85904600	0.00000100
	C	-0.93843100	-0.66248100	0.00000000
	H	-3.52463000	1.55717700	0.00000000
	H	-4.79741800	-0.60010000	-0.00000100
	H	-3.59077300	-2.74358900	0.00000000
	H	-1.11591200	-2.81039700	0.00000100
O	4.00786200	-1.41901100	-0.00000500	
H	3.77446100	-2.35437200	0.00001800	
O	-0.88301700	2.86990000	-0.00000300	

 <p>95-u</p> <p>B3LYP/def2-TZVP E = -726.017170 ZPVE = 0.178255</p>	C	-0.76322400	-0.68388200	0.00000200
	C	-1.76821100	0.29989000	-0.00000100
	C	-3.11922900	-0.05905900	-0.00000100
	C	-3.48487000	-1.39119000	0.00000200
	C	-2.49486300	-2.37613400	0.00000300
	C	-1.15602300	-2.02976800	0.00000200
	C	0.63174000	-0.25203500	0.00000200
	C	0.89246300	1.12243000	0.00000700
	C	2.19135100	1.61199900	0.00000600
	C	3.25925700	0.73188900	0.00000300
	C	3.02323000	-0.64498800	-0.00000300
	C	1.72499500	-1.12641400	-0.00000400
	H	-3.85880100	0.72970100	-0.00000400
	H	-4.53047100	-1.66960800	0.00000700
	H	-2.77479400	-3.42210500	0.00000300
	H	-0.41052000	-2.81212700	0.00000000
	H	2.34508800	2.68231000	0.00001000
	H	4.27448100	1.11161300	0.00000600
	H	1.58316200	-2.19720400	-0.00000900
	O	-0.10739900	2.06345000	0.00001100
C	-1.43835100	1.73786300	-0.00000300	
O	-2.23969300	2.63381400	-0.00001500	
O	4.03396500	-1.56570500	-0.00000500	
H	4.88728100	-1.11866500	-0.00002700	
 <p>95-d</p> <p>B3LYP/def2-TZVP E = -726.016954 ZPVE = 0.178245</p>	C	-0.75856400	-0.68290300	0.00000300
	C	-1.76656300	0.29821300	-0.00000100
	C	-3.11661500	-0.06408900	-0.00000300
	C	-3.47977500	-1.39688500	0.00000100
	C	-2.48746700	-2.37942900	0.00000400
	C	-1.14957500	-2.02960700	0.00000400
	C	0.63410200	-0.24637600	0.00000300
	C	0.89147900	1.12595400	0.00000700
	C	2.19168800	1.62053500	0.00000700
	C	3.26198500	0.74885400	0.00000100
	C	3.03111000	-0.62963700	-0.00000400
	C	1.73536400	-1.11699800	-0.00000200
	H	-3.85773700	0.72323500	-0.00000700
	H	-4.52471900	-1.67760800	0.00000400
	H	-2.76499800	-3.42606200	0.00000500
	H	-0.40370000	-2.81182400	0.00000400
	H	2.33952100	2.69174200	0.00001100
	H	4.28055000	1.11175900	0.00000100
	H	1.57668800	-2.18788200	-0.00000500
	O	-0.11010300	2.06467200	0.00001200
C	-1.44030100	1.73692700	-0.00000400	
O	-2.24402400	2.63072500	-0.00001600	
O	4.13070200	-1.44100400	-0.00000700	
H	3.86058900	-2.36585600	-0.00002900	

 <p>96-u</p> <p>B3LYP/def2-TZVP E = -726.021259 ZPVE = 0.178404</p>	C	-0.46655200	-0.34926000	-0.00000400
	C	-0.89842800	0.99134800	0.00000000
	C	-2.26433500	1.28891600	0.00000300
	C	-3.20428900	0.28138100	0.00000400
	C	-2.77787700	-1.05298300	0.00000000
	C	-1.42628500	-1.36335500	-0.00000400
	C	0.97013500	-0.60977100	-0.00000500
	C	1.83900900	0.48787300	0.00000000
	C	3.22099000	0.32854300	0.00000800
	C	3.75939700	-0.94588400	0.00000700
	C	2.91834200	-2.05956600	-0.00000100
	C	1.54633700	-1.88866700	-0.00000700
	H	-2.56321400	2.32809000	0.00000600
	H	-4.26292700	0.51429100	0.00000400
	H	-1.14857700	-2.40696300	-0.00000600
	H	3.84375800	1.21265500	0.00001500
	H	4.83395800	-1.07459600	0.00001500
	H	0.90802200	-2.76115500	-0.00001500
	O	1.38906300	1.78010400	-0.00000500
	C	0.05203400	2.10894100	-0.00000200
O	-0.23651900	3.27598100	-0.00000200	
H	3.33713400	-3.05713600	-0.00000500	
O	-3.65250800	-2.09293500	0.00000600	
H	-4.55930400	-1.76547400	-0.00000300	
 <p>96-d</p> <p>B3LYP/def2-TZVP E = -726.021003 ZPVE = 0.178379</p>	C	-0.46962900	-0.34313400	-0.00000600
	C	-0.90071500	0.99519600	-0.00000100
	C	-2.26927500	1.29412000	0.00000700
	C	-3.21155000	0.29200000	0.00000900
	C	-2.78692200	-1.04255000	0.00000000
	C	-1.43522000	-1.35551600	-0.00000500
	C	0.96605000	-0.60750600	-0.00000800
	C	1.83684900	0.48897900	0.00000100
	C	3.21874000	0.32708100	0.00001500
	C	3.75565700	-0.94783300	0.00001300
	C	2.91302700	-2.06032300	-0.00000400
	C	1.54135800	-1.88688800	-0.00001400
	H	-2.56527800	2.33409200	0.00001200
	H	-4.27129100	0.50619800	0.00001600
	H	-1.13902300	-2.39669300	-0.00000600
	H	3.84262400	1.21040300	0.00002700
	H	4.83000600	-1.07803500	0.00002500
	H	0.90341700	-2.75985300	-0.00003000
	O	1.38890900	1.78048100	-0.00000500
	C	0.05085800	2.11131700	-0.00000500
O	-0.23486700	3.27863200	-0.00000900	
H	3.33038700	-3.05850100	-0.00001000	
O	-3.75685200	-1.99329800	0.00000500	
H	-3.36372900	-2.87380000	0.00000900	